



PROCEEDINGS OF THE

24th International Symposium
on Analytical and Environmental Problems

Szeged, Hungary
October 8-9, 2018



University of Szeged

Edited by:
Tünde Alapi
István Ilisz

Publisher:
University of Szeged, H-6720 Szeged, Dugonics tér 13,
Hungary

ISBN 978-963-306-623-2

2018.
Szeged, Hungary

***The 24th International Symposium
on Analytical and Environmental Problems***

Organized by:

SZAB Kémiai Szakbizottság Analitikai és Környezetvédelmi Munkabizottsága

Supporting Organizations

*Institute of Pharmaceutical Analysis, University of Szeged
Department of Inorganic and Analytical Chemistry, University of Szeged
Institute of Environmental Science and Technology, University of Szeged
Hungarian Academy of Sciences*

Symposium Chairman:

István Ilisz, PhD

Honorary Chairman:

Zoltán Galbács, PhD

Organizing Committee:

István Ilisz, PhD

associate professor

University of Szeged, Institute of Pharmaceutical Analysis

ilisz@pharm.u-szeged.hu

Tünde Alapi, PhD

assistant professor

University of Szeged, Department of Inorganic and Analytical Chemistry

alapi@chem.u-szeged.hu

Lecture Proceedings

EXERGY LIFE CYCLE ASSESSMENT OF NI-BASED CATALYST SYNTHESIS PROCESSES

Boris Agarski¹, Vesna Nikolić², Zeljko Kamberović³, Zoran Andić⁴, Borut Kosec⁵, Igor Budak¹

¹ Faculty of Technical Sciences, University of Novi Sad, 6 Trg Dositeja Obradovića, 21000, Novi Sad, Serbia

² Innovation Center of the Faculty of Technology and Metallurgy, University of Belgrade, 4 Karnegijeva Street, 11120, Belgrade, Serbia

³ Faculty of Technology and Metallurgy, University of Belgrade, 4 Karnegijeva Street, 11120, Belgrade, Serbia

⁴ Innovation Center of the Faculty of Chemistry, University of Belgrade, 12-16 Studentski Trg, 11000, Belgrade, Serbia

⁵ Faculty of Natural Sciences and Engineering, University of Ljubljana, 12 Aškerčeva Street, 1000, Ljubljana, Slovenia

Corresponding author e-mail: agarski@uns.ac.rs

Abstract

Within the life cycle assessment, exergy analysis is one of the specific approaches to evaluate impacts on the environment through the quality of energy which is degraded during the production process [1]. Exergy can be described as a measure of resources depletion and it can be used to evaluate the process efficiency. Comparative assessment of product and processes through life cycle assessment is often used to identify the differences and environmental hotspots. This research applies exergy life cycle assessment to compare different Ni-based catalysts synthesis processes. In previous research [2,3] the authors compared novel Ni-Pd/Al₂O₃ catalyst synthesis processes with other ones from environmental and performance point of view. Idea of this research is to calculate the impacts on the environment by the total exergy consumption of Ni-based catalyst processes and to compare these results with the results from previous research. Compared with other Ni-based catalyst synthesis processes, the assessment results confirm the previous findings that the novel Ni-Pd/Al₂O₃ catalyst synthesis process has the smallest environmental impact. Furthermore, exergy life cycle assessment provided insight into impacts on the non-renewable and renewable resources.

References

- [1] Milanovic, B., Agarski, B., Vukelic, Dj., Budak, I., Kiss, F. (2017). Comparative exergy-based life cycle assessment of conventional and hybrid base transmitter stations. *Journal of Cleaner Production* 167, 610-618.
- [2] Agarski, B., Nikolić, V., Kamberović, Ž., Andić, Z., Kosec, B., Budak, I. (2017). Comparative life cycle assessment of Ni-based catalyst synthesis processes. *Journal of Cleaner Production* 162, 7-15.
- [3] Nikolić, V., Agarski, B., Kamberović, Ž., Andić, Z., Kosec, B., Budak, I. (2016). Multi-criteria analysis of synthesis methods for Ni-based catalysts. *Materials and technology* 50 (2016) 4, 553–558.

PROMPT LEAD EXPOSURE OF AQUEOUS ENVIRONMENT BIOMONITORED BY PHOTOSYNTHETIC BACTERIA

Mariann Kis, Sa'ed Al-Atawneh and Péter Maróti

*Department of Medical Physics and Informatics, University of Szeged, H-6720 Szeged,
Rerrich Béla sqr. 1., Hungary
e-mail: pmaroti@sol.cc.u-szeged.hu*

Abstract

Anthropogenic activities including industrialization, urbanization and growth of population have significantly increased concerns about detrimental effects of pollutants on health and environment. Among the heavy metal ions, lead (II) ions are especially toxic and hazardous. Here, we report the application of purple photosynthetic bacteria in biomonitoring of lead pollution in aqueous habitats. The monitoring method is based on light absorption and fluorescence responses of living microorganism to prompt appearance of lead ions in the solution. The Pb(II) ions penetrate the cell membrane immediately, attack and (in few mM external concentration) destroy the light harvesting system together with the reaction center protein. As these bacteria may act as bioaccumulators of lead, they can be also used for bioremediation of contaminated cultures. The advantages using photosynthetic bacteria for monitoring and accumulating Pb(II) pollution in aqueous environmental compartments are presented in the paper.

Introduction

The release of highly toxic and hazardous heavy metal ions (mercury, lead and cadmium) of anthropomorphic origin into the biosphere has increased today to alarming levels [1]. Out of these non-biodegradable pollutants, lead(II) ions have special significance because of their wide use in various human activities including the glass and metal industries. They are employed in batteries, paints, pigments and ammunition, cables, alloys and steels, plastics, and are still used in petrol as an anti-knocking agent. Water from industrial effluents, vehicular traffic and mixing of roadside run-offs is heavily contaminated by lead and its compounds. Due to different physiological disorders and toxicological effects caused to humans, the permissible level of lead contamination in drinking water (World Health Organization limit) is as low as $10 \mu\text{g/l} \approx 50 \text{ nM}$.

Large efforts have been undertaken to investigate the behavior of lead in different ecosystems (particularly water, due to industrial wastewater pollution) and to work out strategies for its control, abatement and removal. Several analytical techniques have been applied to the assay of lead [2]. Voltammetry provided a reliable and cost-effective technique for its monitoring, especially in drinking water [3]. Different chemical methods including reduction and precipitation, ion-exchange, electrolysis and adsorption have been used for the removal of lead ions from water. In addition to the chemical methods, biological techniques are also available to detect and to remove the toxic heavy metal pollutants [4]. Photosynthetic bacteria were successfully used to monitor the level of mercury(II) ions in aqueous habitats [5-7].

The present study was carried out to demonstrate the possibility of detection (biomonitoring) of Pb(II) ions by purple photosynthetic bacteria in aqueous solutions and to assess the potential of these microorganisms to concentrate and to remove (bioremediate) lead contamination from the aqueous environment.

Experimental

Bacterial strains and growth conditions

The photosynthetic purple bacterium *Rubrivivax (Rvx.) gelatinosus* were grown in Siström's medium either in completely filled screw top vessels without oxygen (photoheterotrophic and anaerobic growth). The medium was inoculated from a dense batch culture (1:100) and was illuminated by tungsten lamps that assured 13 W m^{-2} irradiance on the surface of the vessel as described earlier [8].

Chemicals

The cells were harvested at the exponential phase of the growth and bubbled by nitrogen for 15 min before measurements. Variable amounts of $\text{Pb}(\text{CH}_3\text{COO})_2 \cdot 3\text{H}_2\text{O}$ (Pb(II)-acetate) were added to the bacterial culture for heavy metal ion treatment [4]. These chemicals are highly soluble in aqueous solution under physiological conditions. 100 mM $\text{Pb}(\text{CH}_3\text{COO})_2 \cdot 3\text{H}_2\text{O}$ stock solution was prepared freshly before the experiment. The durations of the Pb(II)-acetate treatments were prompt.

Optical assays

Steady-state absorption spectrum. The absorption spectra of intact cells were measured by dual beam spectrophotometer with reference of scattering suspension of sand of similar size ($\sim 5 \mu\text{m}$) and concentration ($\sim 1 \cdot 10^8$ particles/mL) as those of the bacteria.

Flash-induced absorption change kinetics. The kinetics of absorption changes of the whole cells induced by Xe flash were detected by a home-constructed spectrophotometer [8]. The electrochromic shift (ECS) of the carotenoids in the photosynthetic membrane were detected at 530 nm wavelength with reference to 510 nm wavelength.

Induction and relaxation of bacteriochlorophyll (BChl) fluorescence. The induction and subsequent decay of the BChl a fluorescence of intact cells were measured by a home built fluorometer [5]. The light source was a laser diode (808-nm wavelength and 2W light power) that produced rectangular shape of illumination and matched the 800 nm absorption band of the LH2 peripheral antenna of the cells. The BChl a fluorescence (centered at 900 nm in mature cells) was detected in the direction perpendicular to the actinic light beam, with a near infrared sensitive, large area (diameter 10 mm) and high gain Si-avalanche photodiode (APD; model 394-70-72-581; Advanced Photonix, Inc., USA) protected with an 850-nm high-pass filter (RG-850) from the scattered light of the laser. The usually very small deviation of the kinetics of the excitation from the rectangular shape was corrected by detection of the kinetics of extracted BChl a in organic solvent. The induction of fluorescence rise was measured during the actinic laser light and the subsequent dark-relaxation was tested by attenuated short ($3 \mu\text{s}$) laser pulses distributed according to geometrical series in time.

Results and discussion

The physiological properties of purple photosynthetic bacterium *Rubrivivax gelatinosus* show abrupt changes upon addition of Pb(II) acetate pollutant to the culture. While the I_{50} values (half lethal dose) of bacteria exposed to prolonged heavy metal ion contamination are low (e.g. $I_{50} = 2 \mu\text{M}$ for Hg^{2+}), prompt addition of lead to the culture evokes much (about 10^3 times) less changes due to slow kinetics of lead uptake through the cell wall (Fig. 1). Both red absorption bands characteristic of the peripheral (800 nm) and core (860 nm) antenna complexes demonstrate prompt decomposition after treatment with lead acetate in the few mM concentration range. The lead(II) ions can pass the cell wall of the bacteria in the short time range of exposure, and attack immediately the essential protein-pigment complexes including the peripheral and core light harvesting complexes. There is no preferential damage of the macromolecules as the observed rates of BChl degradation due to Pb(II) contamination are the same for the two antenna complexes.

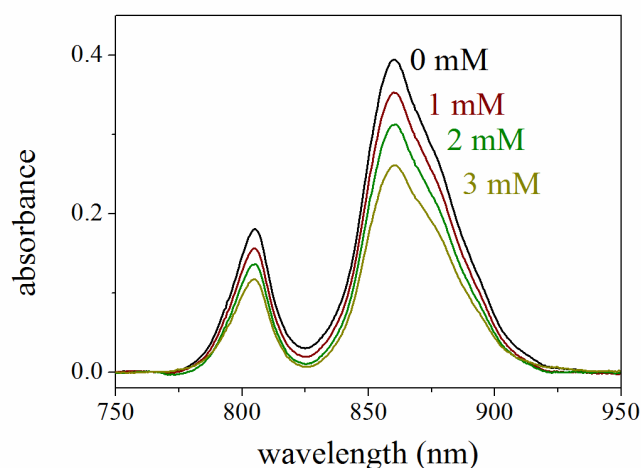


Fig. 1. Steady state red absorption spectra of intact cells of photosynthetic bacteria *Rubrivivax gelatinosus* after prompt addition of Pb(II) acetate to the culture.

The electrochromic signals due to absorption change of carotenoid pigments evoked by the membrane potential describe similar changes upon exposure to lead(II) ions (Fig. 2). The amplitude and not the kinetics of the flash-induced absorption change is sensitive to the Pb(II) treatment indicating that the magnitude of the membrane potential and not the pathways of disappearance of the initial charge pairs is primarily influenced by lead(II) ions.

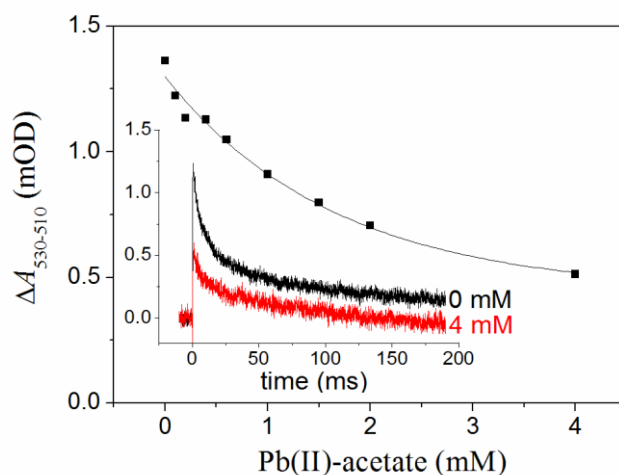


Fig. 2. Kinetics (inset) and lead(II)-dependent amplitude of flash-induced electrochromic response of the carotenoids in whole cells of *Rubrivivax gelatinosus* upon treatment with 0-4 mM Pb(II) measured by absorption change at 530 nm (vs. 510 nm).

The BChl fluorescence is especially sensitive to lead(II) contamination. Both the kinetics and the magnitude of fluorescence induction (F_{\max}) show major changes upon Pb(II) treatment (Fig. 3). The severe drops of F_{\max} and F_0 (the initial fluorescence) indicate substantial loss of BChl pigments together with decoupling of the light harvesting antenna systems from the reaction center.

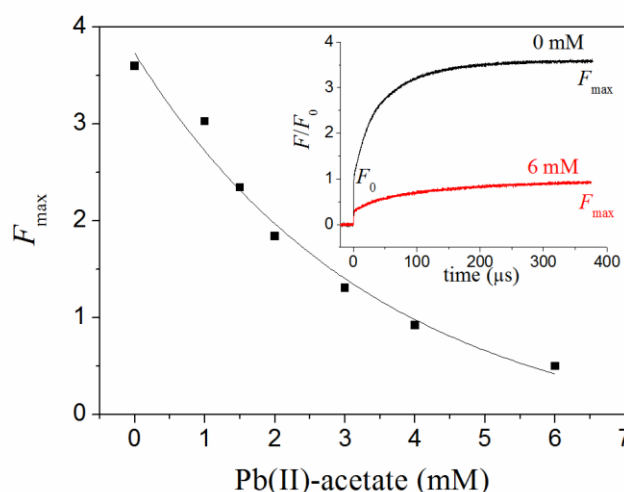


Fig. 3. BChl fluorescence (F) induction kinetics (inset) and lead-dependent changes of the maximum fluorescence (F_{\max}) in intact cells of photosynthetic bacteria *Rubrivivax gelatinosus* grown in the light upon addition of Pb(II) acetate to the culture. The kinetic traces are normalized to the initial F_0 fluorescence level of the untreated cells.

While the BChl fluorescence induction probes the intactness of the light harvesting system and primary photochemistry taking place in the reaction center protein, the relaxation of the BChl fluorescence gives information about the pathways of re-opening of the closed reaction centers in the dark (Fig. 4).

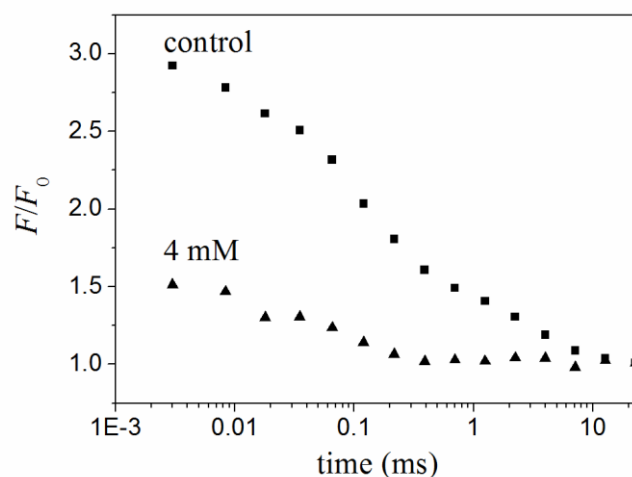


Fig. 4. Relaxation of the BChl fluorescence after flash excitation in intact cells of photosynthetic bacteria *Rubrivivax gelatinosus* grown in the light upon addition of Pb(II) acetate to the culture.

The prompt effect of lead(II) ions is expressed as significant decrease of the maximum fluorescence and minor acceleration of re-reduction of the oxidized BChl dimer in the

reaction center. This technique is also suited to track the diverse structural and functional changes in the photosynthetic apparatus of the intact cell caused by Pb(II) contamination.

Conclusion

Steady state absorption spectra and kinetics of flash-induced absorption changes and fluorescence of intact photosynthetic bacteria are sensitive bioindicators of lead(II) contamination of aqueous cultures. After fast penetration through the cell wall, the Pb(II) ions cause prompt and detectable physiological changes by disconnection and damage of the antenna pigments followed by graduate destruction of the photosynthetic machinery of the bacteria.

Acknowledgements

This work has been made at the University of Szeged, and supported by the European Union. Project identity numbers: EFOP-3.4.3-16-2016-00014 and 3.6.2-00005

References

- [1] Tchounwou PB, Yedjou CG, Patlolla AK, Sutton DJ (2012) Heavy Metal Toxicity and the Environment. In: Luch A. (eds) Molecular, Clinical and Environmental Toxicology. Experientia Supplementum, 101: 133–164. Springer, Basel.
- [2] Rose M, Knaggs M, Owen L, Baxter M (2001) A review of analytical methods for lead, cadmium, mercury, arsenic and tin determination used in proficiency testing, J. Anal. At. Spectrom., 16: 1101–1106.
- [3] Mouhamed N, Cheikhou K, Rokhy GEM, Bagha DM, Guèye MDC, Tzedakis Th (2018) Determination of Lead in Water by Linear Sweep Anodic Stripping Voltammetry (LSASV) at Unmodified Carbon Paste Electrode: Optimization of Operating Parameters, American Journal of Analytical Chemistry, 9: 171-186.
- [4] Giotta L, Agostiano A, Italiano F, Milano F, Trotta M (2006) Heavy metal ion influence on the photosynthetic growth of *Rhodobacter sphaeroides*, Chemosphere 62: 1490–1499.
- [5] Kocsis P, Asztalos E, Gingl Z, Maróti P (2010) Kinetic bacteriochlorophyll fluorometer, Photosynth Res 105:73–82.
- [6] Kis M, Sipka G, Maróti P (2017) Stoichiometry and kinetics of mercury uptake by photosynthetic bacteria, Photosynth Res 132(2): 197-209.
- [7] Sipka G, Kis M, Maróti P (2018) Characterization of mercury (II)-induced inhibition of photochemistry in the reaction center of photosynthetic bacteria, Photosynth Res 136 (3): 379-392.
- [8] Maróti P, Wraight C.A (1988) Flash-induced H^+ binding by bacterial photosynthetic reaction centers: comparison of spectrometric and conductometric methods, Biochim. Biophys. Acta 934: 314–328.

EXPERIMENTAL DETERMINATION OF RECYCLED AGGREGATES CONCRETE CARBONATION

**Remus Chendes¹, Liana Iures¹, Corneliu Bob¹, Sorin Dan¹,
Catalin Badea¹, Cristian Tănăsie²**

¹ Politehnica University Timisoara, Faculty of Construction , 2nd Traian Lalescu, 300223, Timisoara, Romania

² National Institute of Research & Development for Electrochemistry and Condensed Matter, 144th Dr. Aurel Paunescu Podeanu, 300569, Timisoara, Romania

remus.chendes@upt.com , liana.iures@upt.ro , cbob@mail.dnttm.ro , sorin.dan@upt.ro , catalin.badea@upt.ro, tase@incemc.ro

Abstract

The construction industry is one of the main sources of pollution, starting with the extraction of raw materials and the demolition of existing buildings, providing huge amounts of CDW (construction and demolition waste). Concretes with recycled aggregate have higher porosity than those achieved with natural aggregates, (20-30% higher) which can influence the carbonation depth. A typical C16 / 20 concrete class has been studied with natural aggregates, replacing the various granulometric fractions with recycled aggregates. The 100x100x100mm cube specimens were stored for 28 days in water, tested (physico-mechanical characteristics) and subjected to accelerated carbonation experiments. After being stored for 60 days under accelerated carbonation conditions, the specimens were cleaved to determine the carbonation depth after phenolphthalein testing of the faces in the splitting zone, measuring the minimum and maximum carbon dioxide penetration values. Correlation was made between the compressive strengths obtained for the studied specimens and the carbonation depth after the accelerated carbonation experiments in a protected environment - 50% carbon dioxide concentration, temperature 25 ° C and humidity 75-80%.

Introduction

In addition to its major benefits to civilization, the construction sector also has some negative contributions to the environment: it has an important contribution to global warming through CO₂-emitting processes and leads to the depletion of natural resources by over-exploiting them. At the same time, the uncontrolled disposal of waste resulting from construction and demolition processes also has a negative impact on the environment.

Eurostat estimates that in 2014 the total waste generated by economic and domestic waste for the 28 Member States at that time was 2598 million tones, being the highest value since 2004 and CDW representing 33.5% [1].

Reuse, recycling and waste reduction are considered to be the only ways to recover waste generated, but there is room for improvement in this direction [2].

Recycling is defined as the process that changes materials into new products for preventing the waste of potentially useful materials, reducing the consumption of fresh raw materials, the energy usage and the air and water pollution. Many of the large, existing buildings which don't have any historical importance, such as industrial type, office buildings or apartments, have a reinforced concrete structure, and in many cases the demolition is the economical option for them [3]. The resulted concrete is mainly used as coarse aggregate and filler in road construction industry. Another option, but not so often choose, for the concrete resulted from the demolition process is to be used as aggregates into a new concrete [4]. Using the RCA in construction field has begun immediately after the second world war, when

the concrete resulted from damaged roads, started to be used as support layer for new roads [5].

Results and discussions

An experimental study on the durability of recycled concrete was carried out, focusing on the probability that the RCA used in new concrete would influence the degree of carbonation over time.

The RCA used into the experimental program was obtained after an industrial building demolition, with a reinforced concrete structure as it can be seen in figure 1. The building was demolished using the top- down method, in a mechanical way, with excavators.



Figure 1. RCA after initial crushing

Recycled aggregate concretes are concretes with a higher porosity than those achieved with natural aggregates, with 20-30% which can influence the carbonation depth. It has been proposed, the usual concrete class C16 / 20 made with natural aggregate, replacing it on the different granulometric fractions, with the recycled aggregate.

Concrete Class	Mixture				Water/cement
	CEM I 42,5R [kg/m ³]	Mixture water [kg/m ³]	Admixture [kg/m ³]	Aggregate [kg/m ³]	
C16/20	292	205	1,46	1694	0,7

A typical C16 / 20 concrete class has been studied with natural aggregates, replacing the various granulometric fractions with recycled aggregates.

The 100x100x100mm cube specimens were stored for 28 days in water, tested (physic-mechanical characteristics) and subjected to accelerated carbonation experiments. After being stored for 60 days under accelerated carbonation conditions, the specimens were cleaved to determine the carbonation depth after phenolphthalein testing of the faces in the splitting zone, measuring the minimum and maximum carbon dioxide penetration values.

Correlation was made between the compressive strengths obtained for the studied specimens and the carbonation depth after the accelerated carbonation experiments in a protected environment - 50% carbon dioxide concentration, temperature 25 ° C and relative humidity 75-80%.



Figure 1. Experimental setup



Figure 2. Testo 350XL analyzer

The three parameters - carbon dioxide concentration, relative humidity and temperature - were measured with the Testo 350XL analyzer, shown in Figure 2.

After being stored for 60 days under accelerated carbonation conditions, the specimens were cleaved to determine the carbonation depth after phenolphthalein testing of the faces in the splitting zone, drawing the carbonated surface and measuring the minimum and maximum carbon dioxide penetration values (Figure 3).

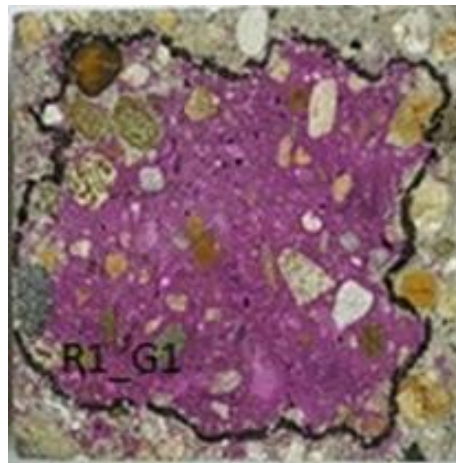


Figure 3. Phenolphthalein test - Carbonated surface

In the calculation of the average depth of theoretical carbonation, the developed C.Bob formula presented below [6] was used:

$$\bar{x}_{teoretic} = \frac{150 \cdot c \cdot k \cdot d}{f_c} \cdot \sqrt{t}$$

where:

\bar{x} - average carbonation depth [mm]

f_c - concrete compression strength [MPa]

t - time [years]

c, k, d - coefficients

Samples	Compression strength- f_c [Mpa]	c	k	d	Time [years]	x theoretic [mm]	x-min experimental [mm]	x-max experimental [mm]
M1 (100% natural) NAT: 0,0-16,0 mm	29	1	0,7	2,7	0,164	3,96	4,0	11,0
R1 (100% RCA) RCA: 0,0-16,0 mm	32,0	1	0,7	2,7	0,164	3,59	4,0	13,0
R2 (natural+RCA) NAT: 0,5-16,0 mm RCA: 0,0-0,5 mm	23,0	1	0,7	2,7	0,164	5,00	9,0	15,0

Conclusions

Experimental determinations have highlighted carbonation depth values for concretes with recycled aggregates higher than the theoretical values calculated using compression resistances.

For concretes with recycled aggregates, for higher strengths of tested concrete, the carbonation depth measured was lower.

Following the studies under accelerated carbonation conditions, a coefficient will be proposed in the carbonation depth calculation formula, which correlates with the concentration at which the concrete is exposed.

References

- [1] European Commission. Eurostat Waste statistics. [Interactiv] 2016. http://ec.europa.eu/eurostat/statistics-explained/index.php/Waste_statistics.
- [2] *Evaluations of existing waste recycling methods: A Hong Kong study*. Vivian W.Y. Tam, C.M. Tam. s.l. : Building and Environment, 2006, Vol. 41.
- [3] M. F. Prada, S. Brata, D. F. Tudor, D. E. Popescu, *Energy Saving in Europe and in the World – a Desideratum at the Beginning of the Millenium Case Study for Existing Buildings in Romania*, Proceedings of the 11th WSEAS International Conference on Sustainability in Science Engineering, pp246 – 251, ISBN: 978-960-474-080-2, Timisoara, Romania, May 27 - 29, 2009.
- [4] Catalin Badea, *The Time Behaviour of Self Compacting Concrete With Fly Ash*, 17th International Multidisciplinary Scientific GeoConference SGEM 2017, Energy and Clean Technologies, Issue 43, 27-29 November, pp. 259-265, Vienna, Austria, 2017
- [5] *Early Age Properties of Recycled Aggregate Concrete*. F.T., Olorusongo. Scotland, UK : Proceeding of the International Seminar on Exploiting Wastes in Concrete held at the University of Dundee, 1999.
- [6] Bob, Corneliu. *Verificarea calității siguranței și durabilității construcțiilor*. s.l. : Facla, 1989.

IMPROVEMENT OF OPTICAL PROPERTIES BY FLUORESC EIN COMPLEXATION WITH NANO-Pt- AND NANO-Ag -PORPHYRIN HYBRIDS

**Anca Lascu^{a*}, Luminita Salageanu^b, Diana Anghel^a, Nicoleta Plesu^a,
Eugenia Fagadar-Cosma^a**

^a *Institute of Chemistry Timisoara of Romanian Academy, M. Viteazul Ave. 24, 300223-Timisoara, Romania, Tel: +40256/491818; Fax: +40256/491824*

^b *Health Insurance House Timis, Corbului Street 4, 300239-Timisoara, Romania*
*email: *ancalascu@yahoo.com*

Abstract

Hybrid organic-inorganic nanomaterials based on Pt and Ag colloids, namely nano-Ag-5,10,15,20-tetrakis-(4-aminophenyl)-porphyrin-Zn(II) (**ZnTAPP-AgNPs**) and nano-Pt-5,10,15,20-tetrakis(*N*-methyl-4-pyridyl)porphyrin-Zn(II) tetrachloride (**ZnTMePyP-PtNPs**) were obtained and their capacity to form improved optically active complexes with fluorescein was investigated. By interaction with minute quantities of fluorescein the intensity of absorption of the plasmonic bands of the **ZnTAPP-AgNPs** and **ZnTMePyP-PtNPs** hybrids increases. **ZnTMePyP-PtNPs** hybrid will be further tested in clinical trials because it allows for a larger concentration domain of fluorescein complexation and more accurate dosage. All the sensitive materials are easy to prepare and respect the rules of sustainable chemistry.

Introduction

In recent years scientists were interested in obtaining more fluorescent molecules and hyperchromic optical effects in order to study the mechanisms of molecular interactions. For this purpose, porphyrins were complexed with fluorescein and novel dyads were obtained in various methods. For example, tetraphenylporphyrin was complexed with a fluorescein molecule via a flexible four carbon atoms linker [1]. The intramolecular interactions were studied for this heterodimer by means of absorption and fluorescence spectroscopy in various solvents. The prototropic equilibrium of fluorescein dyes as function of pH is extensively presented in literature [2]. The presence of color of the dyads containing fluorescein (structure in Figure 1) indicates the structural form having hydroxyl and carboxyl active groups.

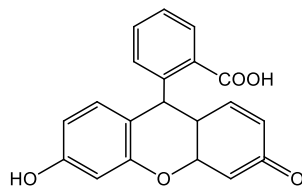


Figure 1. Fluorescein structure

Having hydroxyl and carboxyl active groups, the formation of the dyad can take place at different active sites [3]. The ester bond between the two chromophore molecules is performed in this case via a three carbon atoms flexible bridge. The same authors obtained Zn, Cu and Ni metal fluorescein-porphyrin dyads and analysed their photophysical properties [4]. They concluded that only the Zn^{2+} complex exhibits fluorescence emission and possesses a shorter fluorescence lifetime as compared to the free porphyrin dyad. They attributed this fact to the increase in electron density by the presence of Zn^{2+} ions in the complex.

A fluorescence strengthening was observed for the supramolecular system formed between 5-(p-hydroxyl-propanbrominephenyl)-10,15,20-triphenylporphyrin that was coupled with fluorescein and further complexed with copper(II) 5-(p-amino-phenyl)-10,15,20-triphenylporphyrin by hydroxyl-amino type hydrogen bonding [5].

Porphyrins tagged with fluorescein were obtained as dyads by linking the two molecules by a triazole bridge [6]. The intramolecular energy transfer was more efficient in DMSO as solvent than in chloroform.

The scope of our work was to obtain porphyrin-fluorescein complexes that exhibit better optical properties than the starting materials using a simple investigation tool like optical spectrophotometry. For this purpose, hybrid nanomaterials consisting of metalloporphyrins and noble metal Pt and Ag colloids, namely nano-Ag-5,10,15,20-tetrakis-(4-aminophenyl)-porphyrin-Zn(II) (**ZnTAPP-AgNPs**) and nano-Pt-5,10,15,20-tetrakis(*N*-methyl-4-pyridyl)porphyrin-Zn(II) tetrachloride (**ZnTMePyP-PtNPs**) were obtained and their capacity to form improved optically active complexes with fluorescein was investigated. Figure 2 a and b depicted the porphyrins structures.

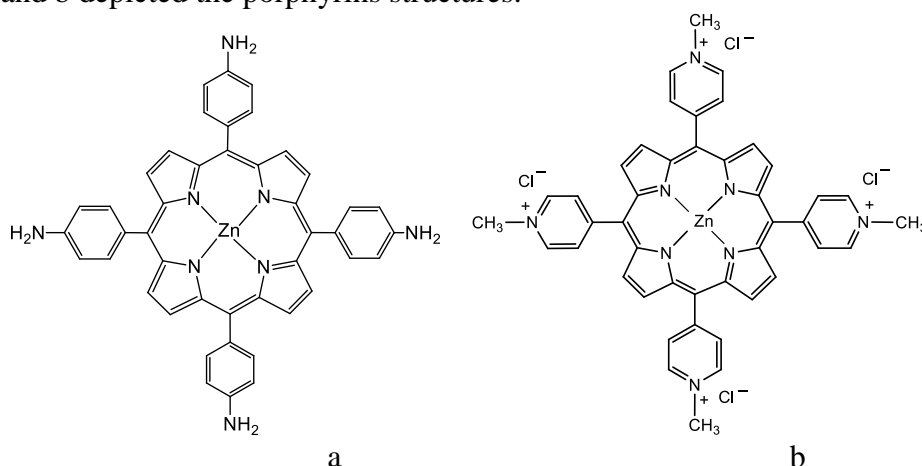


Figure 2. Structures of Zn-5,10,15,20-tetrakis-4-aminophenyl porphyrin (**ZnTAPP**)(a) and 5,10,15,20-tetrakis(*N*-methyl-4-pyridyl)porphyrin-Zn(II) tetrachloride (**ZnTMePyP**)(b)

Materials and methods

The metalloporphyrin 5,10,15,20-tetrakis(*N*-methyl-4-pyridyl)porphyrin-Zn(II) tetrachloride (**ZnTMePyP**) was obtained by our group and previously reported [7]. The metalloporphyrin 5,10,15,20-tetrakis-(4-aminophenyl)-porphyrin-Zn(II) (**ZnTAPP**) was purchased from Por-Lab GmbH (Germany). Fluorescein Standard (Free acid) was provided by Fluka. Solvents, DMSO and THF, were acquired from Merck and were used without further purification. The formation of the hybrid nanomaterial stabilized with polyethyleneglicole (PEG), **ZnTAPP-AgNPs** was previously reported [8] and the formation of the hybrid nanomaterial **ZnTMePyP-PtNPs**, was performed by adapting the procedures used in previous experiments already published by our group [7, 9]. A fluorescein solution having the concentration of 1.805×10^{-3} M in THF was used for the detection experiments.

Apparatus. A JASCO UV- V-650 spectrometer (Japan) was used for recording UV-visible spectra using standard 1 cm pass cells.

Results and Discussions

The UV-vis spectra of the starting materials are presented in Figures 3 and 4. The UV-vis spectrum of fluorescein (Figure 3a) does not have important peaks in the spectral domain of interest (350 – 550 nm). It can be seen that the interaction between the

metalloporphyrin and the silver colloidal nanoparticles leads to an enlargement of the plasmonic band ($\lambda_{\text{max}} = 437 \text{ nm}$ $I = 1.97$) (Figure 3d) of the silver colloid alone (Figure 3b) and also to an increase in intensity as compared to the Soret band of the Zn-metalloporphyrin ($\lambda_{\text{max}} = 428 \text{ nm}$ $I = 1.85$) (Figure 3c).

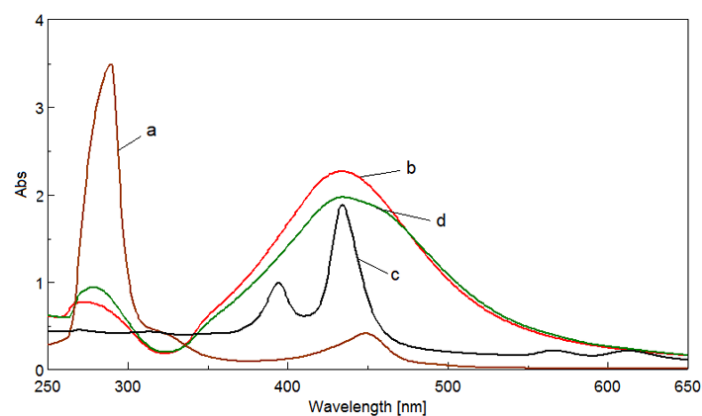


Figure 3. Overlapped UV-vis spectra of: fluorescein solution in THF (a); stabilized silver colloidal solution (b); **ZnTAPP** solution in THF (c) and the hybrid plasmonic nanomaterial **ZnTAPP-AgNPs** (d)

In the case of the hybrid nanomaterial formed between water soluble 5,10,15,20-tetrakis(*N*-methyl-4-pyridyl)porphyrin-Zn(II) tetrachloride (**ZnTMePyP**) and platinum colloid (Figure 4) it can be concluded that the intensity of absorption of the hybrid (Figure 4d) is decreased as compared both to the intensity of absorption of the porphyrin base (Figure 4c) and to the intensity of absorption of the nanoplatinum colloid (Figure 4b).

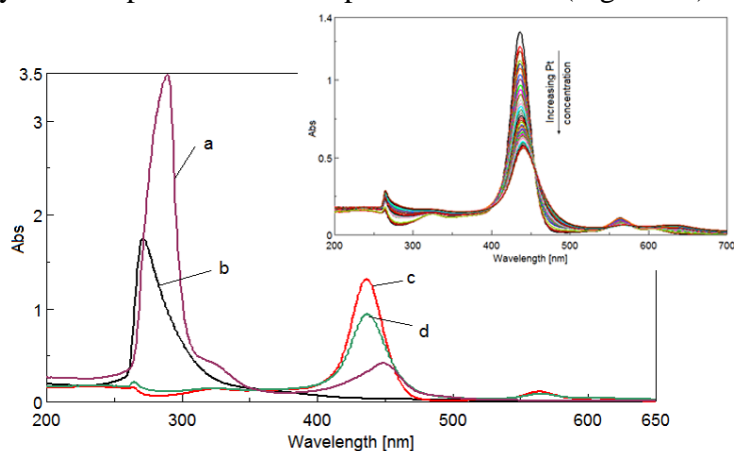


Figure 4. Overlapped UV-vis spectra of: fluorescein solution in THF (a); stabilized platinum colloidal solution (b); **ZnTMePyP** solution in water (c) and the hybrid plasmonic nanomaterial **ZnTMePyP-PtNPs** (d) presented also in detail by successive adding of Pt colloid

The fluorescein standard used in this experiment (Figure 1) has hydroxyl and carboxyl active groups and the interaction with the amino-substituted Zn-porphyrin and the silver colloidal nanoparticles leads to a dramatic increase in the intensity of absorption of the hybrid nanomaterial, as can be seen in Figure 5.

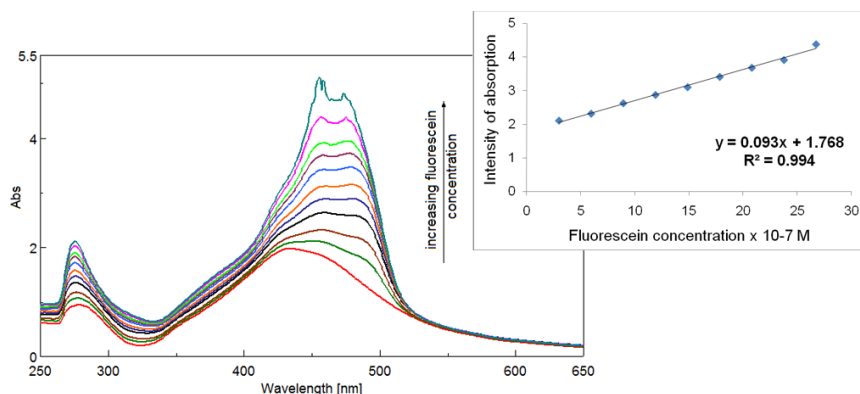


Figure 5. Overlapped UV-vis spectra after successive adding of fluorescein to **ZnTAPP-AgNPs** Dependence between the intensity of absorption at 457 nm and the fluorescein concentration

The concentration domain in which the dependence between the intensity of absorption of the plasmonic band and the concentration of fluorescein is linear spans from 2.97×10^{-7} M to 2.67×10^{-6} M (Figure 5 detail) and presents an excellent correlation coefficient of 99.4%

The demand for complexes with fluorescein used in smaller amounts justifies the experiment for obtaining fluorescein complexes with **ZnTMePyP-PtNPs** hybrid. The sequential adding of 0.001 mL fluorescein solution in THF ($c = 1.805 \times 10^{-3}$ M) to 3.2 mL of **ZnTMePyP-PtNPs** hybrid nanomaterial in water was performed. The solutions were stirred for 30 seconds on a sonication bath and the UV-vis spectra were recorded (Figure 6).

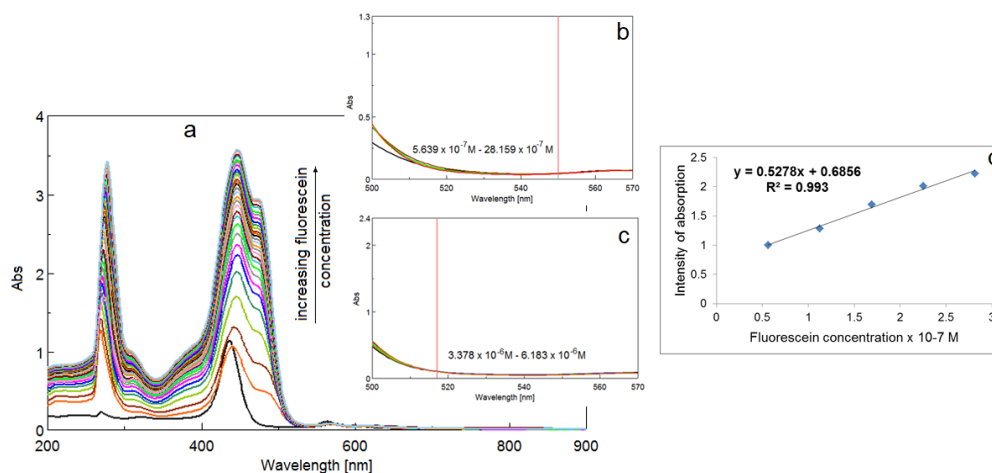


Figure 6. Overlapped UV-vis spectra for the sequential adding of fluorescein solution to the **ZnTMePyP-PtNPs** hybrid material. Details of the isosbestic points at 550 nm (b) and at 515 nm (c). Linear dependence between the intensity of absorption and the fluorescein concentration (d)

It can be observed that the intensity of absorption increases strongly and constantly after each fluorescein adding in the 250 – 650 nm wavelength domain. Another feature that confirms the formation of complexes between the **ZnTMePyP-PtNPs** hybrid material and fluorescein is the presence of two isosbestic points that appear, as a function of fluorescein concentration, at 550 nm and 515 nm respectively (Figure 6b and 6c). The increase in intensity of absorption is a linear function of the fluorescein concentration (Figure 6d).

Conclusion

Although the synthesis of dyads between porphyrins and fluorescein is known to require tedious workup and high temperatures and leads to a decreased intensity of absorption of the obtained material [4] by comparison to the initial porphyrin, in our case, the intensity of absorption of the plasmonic bands of the **ZnTAPP-AgNPs** and **ZnTMePyP-PtNPs** hybrids increase in intensity by interaction with fluorescein.

ZnTMePyP-PtNPs hybrid will be further tested in clinical trials because it allows for a larger concentration domain of fluorescein complexation and more accurate dosage.

All the sensitive materials are easy to prepare and require no high temperatures or purification steps.

Acknowledgements

The authors from Institute of Chemistry Timisoara of Romanian Academy are acknowledging UEFISCDI PN-III-P1-1.2-PCCDI-2017-1-Project **ECOTECH-GMP 76PCCDI/2018** and to Romanian Academy for financial support in the frame of Programme 3/2018 from ICT. This work is dedicated to the Centennial Anniversary of ROMANIA.

References

- [1] X. Yan, M. Weng, M. Z. T. Shen, *Dyes Pigm.* 35(2) (1997) 87-99.
- [2] N. A. Vodolazkaya, P. V. Shakhova, N. O. Mchedlov-Petrosyan, *Russ. J. Gen. Chem.* 79(7) (2009) 1437–1445.
- [3] X. Sun, D. Li, G. Chen, J. Zhang, *Dyes Pigm.* 71 (2006) 118-122.
- [4] X. Sun, G. Chen, J. Zhang, *Dyes Pigm.* 76 (2008) 499-501.
- [5] J.-Z. Lu, Y. Du, B. Wu, J.-W. Huang, J. Jiang, *Transition Met Chem* 35 (2010) 451–456.
- [6] O. Rezazgui, P. Trouillas, S. Qiu, B. Siegler, J. Gierschner, S. Leroy-Lhez, *New J. Chem.*, 40(4) (2016) 3843–3856.
- [7] A. Palade, A. Lascu, I. Fringu, L. Salageanu, D. Vlascici, M. Birdeanu, E. Fagadar-Cosma, *Farmacia* 66(3) (2018) 468 – 476.
- [8] L. Salageanu, A. Lascu, M. Birdeanu, E. Fagadar-Cosma,, *Dig. J. Nanomat. Bios.*, 13(3) (2018) 653 – 659.
- [9] A. Lascu, M. Birdeanu, B. Taranu, E. Fagadar-Cosma, *J. Chem. Hindawi* (2018), Article ID 5323561, 11 pages, doi: 10.1155/2018/5323561.

ION MOBILITY MASS SPECTROMETRY OF GANGLIOSIDES IN HUMAN BRAIN IN HEALTH AND DISEASE

Mirela Sarbu¹, Željka Vukelić², David E. Clemmer³, Alina D. Zamfir^{1,4}

¹National Institute for Research and Development in Electrochemistry and Condensed Matter, Timisoara, Romania; ²Department of Chemistry and Biochemistry, University of Zagreb Medical School, Zagreb, Croatia; ³Department of Chemistry, Indiana University, Bloomington, Indiana, United States of America; ⁴“Victor Babes” University of Medicine and Pharmacy, Timisoara, Romania
e-mail: mirela.sarbu86@yahoo.co.uk

Abstract

Gangliosides (GGs), a class of glycosphingolipids, are important biomarkers in early diagnosis of CNS pathologies, being in the focus of our research as potential therapeutic targets [1]. A series of neuropsychiatric disorders are characterized by amnesia and disorientation caused by hippocampal atrophy and diminished cholinergic activity. Based on ion mobility separation mass spectrometry (IMS MS) capability for a reliable glycopattern determination, and the occurrence of neuropsychiatric disorders [2,3], we report here on the improvement of novel and high performance IMS MS method for assessing the GG profile in a highly complex mixture extracted from an adult healthy brain region. The IMS separation of GGs based on charge state, carbohydrate chain length and degree of sialylation led to the detection and identification of over 100 species, the larger number of GGs ever reported before in this particular brain region. Moreover, the obtained data supports the concept of GGs cholinergic activity. Furthermore, by applying IMS MS/MS, novel GG species were structurally investigated in details.

Acknowledgements

This project was supported by the Romanian National Authority for Scientific Research, UEFISCDI through projects PN-III-P4-ID-PCE-2016-0073, PN-III-P1-1.2-PCCDI-2017-0046 granted to ADZ and PN-III-P1-1.1-PD-2016-0256 granted to MS.

References

- [1] R.L. Schnaar, R. Gerardy-Schahn, H. Hildebrandt, *Physiol. Rev.* 94 (2014) 461.
- [2] M. Sarbu, A.C. Robu, R.M. Ghiulai, Ž. Vukelić, D.E. Clemmer, A.D. Zamfir, *Anal. Chem.* 88, (2016) 5166.
- [3] M. Sarbu, Ž. Vukelić, D.E. Clemmer, A.D. Zamfir, *Biochimie* 139 (2017) 81.

GEOHERMAL ENERGY POTENTIAL IN PART OF PANNONIAN BASIN: HUNGARY, CROATIA, ROMANIA AND SERBIA- CURRENT SITUATION AND MUTUAL PERSPECTIVES

Momcilo Spasojevic¹, Dragana Strbac^{1*}

¹University of Novi Sad, Faculty of Technical Sciences, Trg Dositeja Obradovica 6, Novi Sad, Serbia

*draganastrbac@uns.ac.rs

Abstract

Hungary, Romania, Croatia and Serbia have a various tradition and current situation in geothermal usage, although their potential can roughly be estimated as similar. The reasons for insufficient usage of geothermal energy are dominated by legal regulations related to the obligation of reinjection, concession, as well as feed-in tariffs. All the facts support the need for joint projects, or at least for a common approach to increasing the use of geothermal energy. According to the geothermal water characteristics, the most efficient way to use geothermal water in the most of the Panonian Basin is cascade use, two-stage or multistage, which is proposed as a model for usage.

Introduction

Pannonian Basin has been recognised long time ago as a positive geothermal field. Hungary, Romania, Croatia and Serbia are countries with significant part of their territory in the Panonian Basin and have a various tradition and current situation in geothermal usage, although their potential can roughly be estimated as similar. The Pannonian Basin has a heat-flow density ranging from 50 to 130 mW/m², with a mean value of 90-100 mW/m² and a geothermal gradient of about 45 °C/km [1,2]

Hungarian Office for Mining and Geology reported, there are 1622 registered geothermal wells in Hungary with production of about 25 million m³ thermal water i.e. 2,509,519 GJ (data for year 2015.). The number, temperature and utilisation of geothermal wells vary greatly, as does the economic health of 19 provinces in which Hungary is administratively divided into (Figure 1(a)). As it has been previously published in [3], that from a geothermal point of view the most promising county is Csongrád, a province that has 282 geothermal wells and 9 abandoned hydrocarbon wells which are being evaluated for geothermal uses. The geothermal gradient is 37- 45 °C/km, with a county-wide heat flow of 90-106 mW/m² [1].

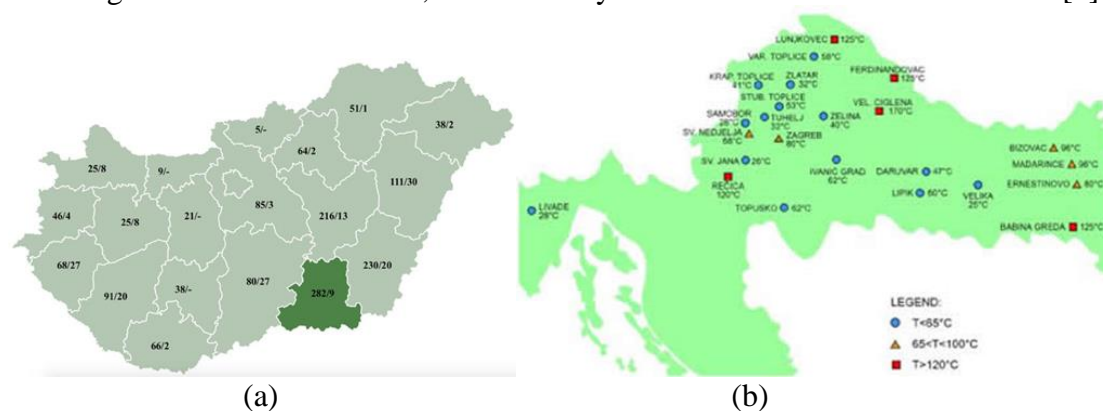


Figure 1. (a) Counties with the number of existed geothermal wells and the prosperous hydrocarbon wells in Hungary [3] and (b) Geothermal wells in Croatia [5]

Csongrad produces 25–30 million m³ of thermal water per year, or 1/6 of all Hungarian geothermal water production. Every town in the county has a geothermal heating system. The largest is in Hódmezővásárhely, with 8 producing and 2 injection wells. In addition to its highest geothermal potential in Hungary, it is important to emphasize here that Csongrad is a border country with Serbia and its position strongly encourages development of mutual bilateral and multilateral project.

As stated in the Geothermal Energy Utilization Potential in Croatia, the Field and Study Visits Report, published in June 2017 [4] there are 28 geothermal sites in total, of which 18 are in use. Panonian basin in Republic of Croatia have great properties from the viewpoint of geothermal potentials: the temperature gradient is 0.04 °C / m to 0.07 °C / m. The terrestrial welding flux is also high and ranges from 60 to over 100 mW / m².

Geothermal energy is used in the Republic of Croatia for 18 spas and recreational centers, and various medical therapies (Figure 1(b)). In 23 locations, shown in Figure 1(b), the direct use of the geothermal energy is the same as in the total installed power of about 75 MWt [5]. The yearly consumption of the total energy of all geothermal locations, calculated from a new factor of 0.27, could reach 650 TJ / year.

The main geothermal project, which is currently in the final phase, is Velika Ciglena, which is expected to be a crochet of Croatia, but also the largest European ORC geothermal power plant. There are 15 MW in the full production process of 15 MW is expected to be put into operation this year, 2018.

The main geothermal areas in Romania (Figure 2 (a)) are: Satu Mare, Tasnad, Acas, Marghita, Sacuieni, Salonta, Curtici-Macea-Dorobanti, Nadlac, Lovrin, Tomnatic, Sannicolau Mare, Jimbolia and Timisoara. The main purposes are: heating 10 hectares of greenhouse; district heating for about 2,500 apartments, obtaining sanitary hot water for 2,200 apartments, health and recreational bathing and fishing [6].

The Pannonian geothermal aquifer in Romania extends over an approximate surface of 2,500 km² along the western border of Romania, from Satu Mare to the north to Timisoara and Jimbolia in the south. The aquifer layer is located at a depth of 800 to 2,400 m. More than 100 geothermal wells were tested, of which 33 are currently exploited. The heat gradient is 45-55 °C / km. Boreholes are mainly used as artificial wells, and very few have installed pumps.

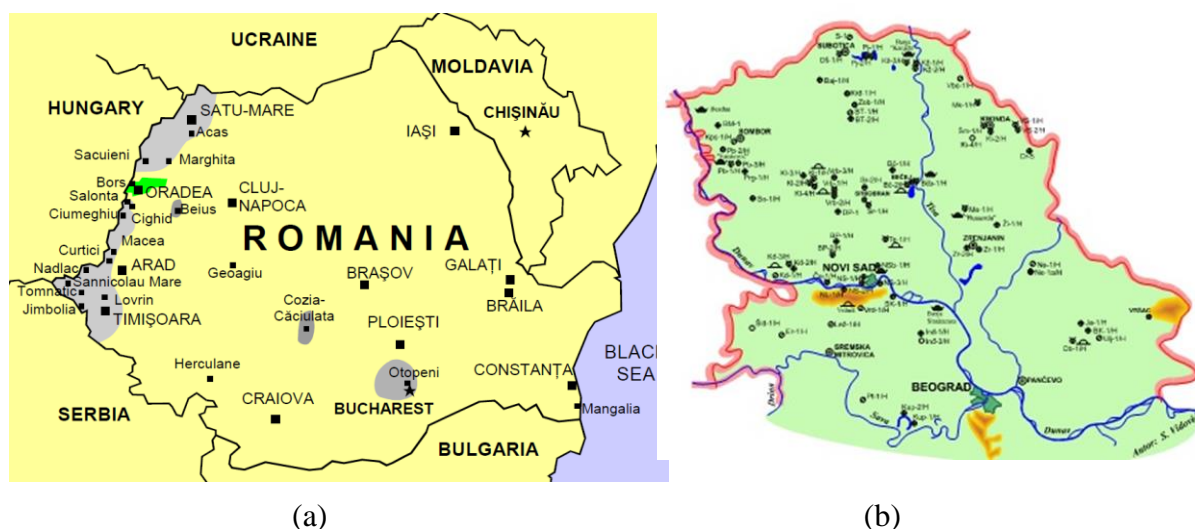


Figure 3. (a) Locations of main geothermal reservoirs in Romania [6]; (b) Geothermal potentials in Panonian Basin in Serbia

The main direct uses of geothermal heat are: central heating and individual space heating, balneology and recreation. In several places geothermal energy is used for heating greenhouses (about 10 ha), fish farming (several farms), industrial processes and drying.

In Panonian Basin in Serbia (province of Vojvodina), thermal waters usage are: spa and baths 43.6%, heating 38.8%, Industry 11.5%, recreation (outdoor and indoor swimming pools) 6.1%. The best application of geothermal water was realized in Kanjiža where hot water is used by multipurpose, cascade system, then in Bečej, even in Junaković near Apatin.

In Figure 2 (b). all objects of exploration and use of hydrothermal waters (drilled well drilling, wells in production, places of use, spa, sports-recreation centers etc.) in Vojvodina are shown. The total thermal energy of water and all drilled hydrothermal wells is about 55 [MW], and the power of all wells that were in production about 23 [MW]. The possible substitution of oil for drilling wells in production is about 10 000 [t per year].

The geothermal waters of the Pannonian Basin of Vojvodina, in terms of physical, chemical and geothermal characteristics, could be used in agriculture for heating greenhouses, livestock and horticulture for heating farms, industry as technical hot water, balneotherapy and sports and tourism centers, for heating of settlements and other facilities, supply of population with sanitary water, fishing, etc. It is important to mention that there is a low percentage of utilization (up to the 30%) of the potential of these hydrothermal wells is due to either unadjusted user installations or due to lower user needs compared to the potentials of the exploited well. In addition to the wells that are in operation, there are 11 hydrothermal wells on the territory of Vojvodina, with built hydrothermal systems, which are currently out of production and wells that have never been in production, which are promising both from the aspect of energy and the supply of drinking water to consumers.

Results and discussion

On a number of geothermal sources of interest there is a mixture of water and gas. This gas, by degassing process, should be separated and used in an environmentally friendly way, through cogeneration (coupled production of heat and electricity). After use, directly or indirectly, geothermal water should be returned to the wall mass, through geothermal sink. Those sinks are operated at an average distance of up to 300-500 m from the geothermal source. Figure 3 shows the use of water from the geothermal spring.

Thermal water from a geothermal source is pumped through a pump into a degasser where water and gas separation is carried out. The degassed water is gravitationally flowed into the underground tank of water tank while the gas goes into the above-ground gas tank. Degassed water is pumped through the pump line into the water line from which the consumers are supplied and the gas is transported by the compressor into the gas line from which the cogeneration plant is supplied. According to this scheme, the water will be return to the geothermal sink is relatively high temperature, about 28°C.

Pannonian Basin geothermal sources are more suitable for integrated use of the geothermal resource in multiple applications under the concept called cascade utilization for power generation and sequential use of geothermal heat for various direct uses, or by use of thermally activated technologies (Figure 4). In the first instance, through the heat exchanger, geothermal water would be used for underfloor heating, water treatment for swimming pools, etc. After that the geothermal water would go to second degree, again through a heat exchanger, into a heat pump. After that, the geothermal water would be returned to the geothermal sink.

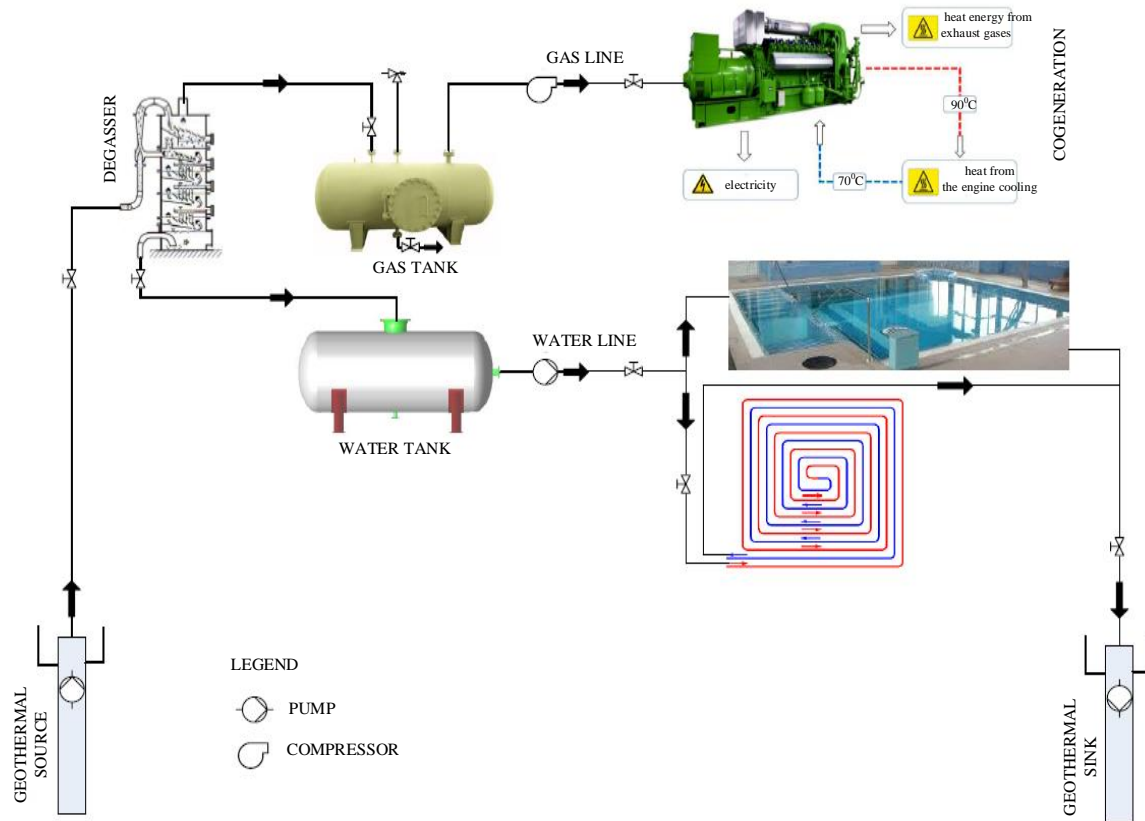


Figure 3. Scheme of usual geothermal energy utilisation

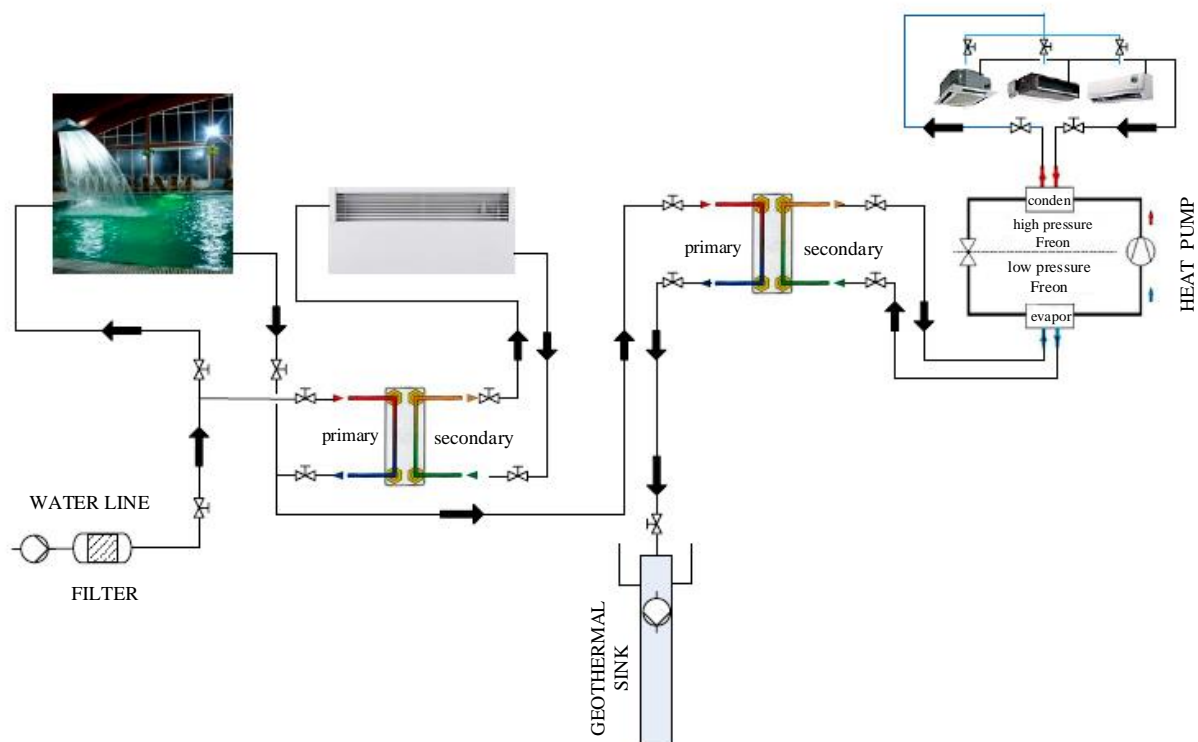


Figure 4. Cascade utilisation of geothermal energy

When using water from geothermal sources, special attention must be paid to the effect of temperature, as well as the quality of water on the equipment. The impact of corrosion on the heat exchanger has been thoroughly examined by the Oregon Institute and such experiences have led to the emergence of heat exchanger manufacturers specializing in geothermal water, or those who take into account the chemical composition of the fluid and determine, on the basis of it, materials that will be used in production.

In addition of the cascading use of geothermal energy mentioned above, cascade utilisation is also applied in agriculture (greenhouses, fishponds, etc.)

Conclusions

Geothermal resources in the Panonian part of Hungary, Croatia, Romania and Serbia are resources of medium and low enthalpy and therefore are suitable for cascade utilization. This is the integrated use of the geothermal resource in multiple applications for power generation and sequential use of geothermal heat for various direct uses. Cascading from power production provides water for direct uses, district heating, fishponds, greenhouses etc. Further projects (bilateral or multilateral) should be focused on investigation of the technical and economic feasibility to replace conventional boilers in the district heating network. The replacement should consider the direct utilization of geothermal heat in cascade to different temperature levels and the incorporation of a heat pumps.

References

- [1] Dövényi P., Horváth F., Liebe, P., Galfi, J., Erki I.: Geothermal conditions of Hungary, Geophys. Transactions, 29/1, 3–114, 1983
- [2] Dövényi P, Horváth F, Drahos D., Hungary. In: Hurter S, Haenel R (eds) Atlas of Geothermal Resources in Europe. Publication No. 17811 of the European Commission, Office for Official Publications of the European Communities. L-2985, Luxembourg. 36–38, 2002
- [3] Toth A. , Creating a Geothermal Atlas of Hungary, Proceedings. 42nd Workshop on Geothermal Reservoir Engineering, Stanford University. Stanford. California. February 13-15, 2017
- [4] Geothermal Energy Utilisation Potential in Croatia, Field and Study Visits' Report, Orkustofnun National Energy Authority, Island and Energy Institute Hrvoje Požar, Croatia, 2017
- [5] Kolbah, S., Živković, S., Golub, M., Škrlec, M., Croatia Country Update 2015 and On, Proceedings, World Geothermal Congress 2015, Melbourne, Australia, 2015
- [6] Rosca, M., Bendea, C, Cucueteanu, D., Geothermal Energy Use, Country Update for Romania, Proceedings, European Geothermal Congress 2013, Pisa, Italy, 2013

SYNTHESIS OF NOVEL Pt COMPLEXES WITH α -GLYOXIMES, SCHIFF BASES, AND THEIR PHYSICAL-CHEMICAL AND BIOLOGICAL STUDY

Csaba Várhelyi jr.¹, Roland Szalay², György Pokol^{3,5}, Firuța Goga¹, Judit Papp⁴, Pál Szabó⁵, Péter Huszthy³, Ligia-Mirabela Golban¹, Melinda Várhelyi¹, Laura Lang¹

¹ Faculty of Chemistry and Chemical Engineering, "Babeş-Bolyai" University, RO-400 028 Cluj-N., Arany János str. 11, Romania

² Institute of Chemistry, "Eötvös Loránd" University, H-1117 Budapest, Pázmány Péter str. 1/a, Hungary

³ Faculty of Chemical Technology and Biotechnology, Budapest University of Technology and Economics, H-1111 Budapest, Műegyetem rkp. 3, Hungary

⁴ Faculty of Biology and Geology, "Babeş-Bolyai" University, RO-400 015 Cluj-Napoca, Gheorghe Bîlaşcu str. 44, Romania

⁵ Hungarian Academy of Sciences - Research Centre for Natural Sciences, H-1117 Budapest, Magyar tudósok körútja 2, Hungary
e-mail: vcaba@chem.ubbcluj.ro

Abstract

Platinum-complexes permanently play an important role in the medical treatment of tumor cells. Since Pt has a soft-type Lewis acidic character, it forms the most stable complexes with S, P, N and I donor atoms, resulting planar (cisplatin) or octahedral (satraplatine) arrangement of ligands.

In our research, new platinum complexes were synthesized with α -glyoximes, such as $[\text{Pt}(\text{diethyl-glyoxH})_2(\text{amine})_2]$, where glyoxH = mono deprotonated glyoxime, amine = imidazole, 2-amino-pyrimidine or 3-hydroxy-aniline, and with Schiff bases, such as $[\text{Pt}(3\text{-heptanone})_2(\text{en})]$, $[\text{Pt}(3\text{-heptanone})_2(1,2\text{-pn})]$, $[\text{Pt}(3\text{-heptanone})_2(1,3\text{-pn})]$ (en = ethylenediamine, pn = propylenediamine). The Schiff bases were obtained with the condensation reaction between 3-heptanone and the corresponding diamines.

The molecular structure of our products has been investigated by IR, UV–VIS and NMR spectroscopy, MS, thermoanalytical measurements (TG-DTG-DTA), and powder XRD. The biological activity study of compounds revealed their possible application in medical point of view since some of them proved to act as antibacterial agents and potential anticancer drugs. On the other hand, some members of the family of complexes can play catalytic role in organic chemistry transformations.

Introduction

After cisplatin was discovered by Barnett Rosenberg due to its anti-tumor effect, and was introduced to the market as drug in 1978, beside the second generation Pt-drugs, as carboplatin, oxaliplatin [1, 2], it became the most important agent in cancer treatment.

During the study of relationships between the activity and the structure of Pt-complexes by Cleare and Hoeschele, they noted that the prerequisite of the metal complex to be an efficient drug is the ability of the platinum center to coordinate a bidentate amine ligand in cis position, or alternatively, two amine components containing minimum one NH group. Furthermore, the complexes must also contain two medium bonded leaving groups (e.g. chloride, sulfate, citrate, oxalate) [3].

The anti-tumor effect of cisplatin can be explained by the platinum coordination to the DNA, which makes a distortion in the helicoidal structure, resulting to the inhibition of

replication and transcription of DNA. Finally, this process leads to the cell circuit stop and apoptosis [4].

It is also worth mentioning that Schiff bases are used in many fields, as in paint industry, however, due to their biological activity, they deserve more interest as antibacterial, antiviral, and anti-inflammatory agents. Some derivatives have anti-tumor effect, too.

Experimental

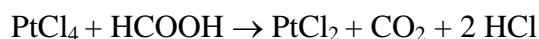
Used materials: PtCl_4 , MeOH, EtOH, HCOOH, 3,4-hexanedione, hydroxylamine-hydrochloride, KOH, 3-heptanone, ethylenediamine, 1,2-propylene-diamine, 1,3-propylene-diamine, imidazole, 2-amino-pyrimidine, 3-hydroxy-aniline.

Methods: - *Preparation of diethyl-glyoxime*

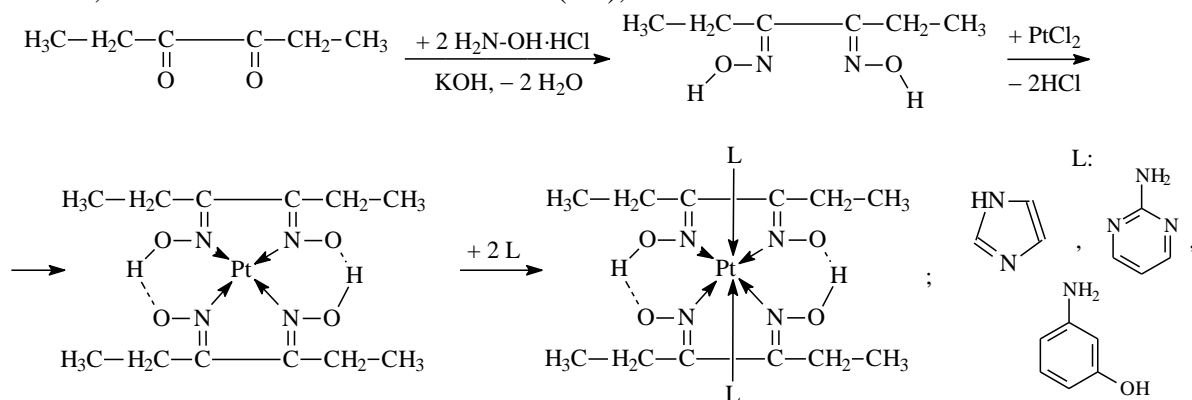
In the first step 3,4-hexanedione was reacted with hydroxylamine-hydrochloride dissolved in water. To the hydroxylamine-hydrochloride solution equimolar amount of KOH was added in order to liberate the free amine from its salt. The reaction mixture was heated for 2–3 hours, and then the precipitated product was filtered off. After recrystallization from EtOH or MeOH, it was dried on air.

- *Synthesis of $[\text{Pt}(\text{diethyl-glyoxH})_2(\text{amine})_2]$ complexes*

The platinum salt was reduced with formic acid before its use in the complex synthesis:



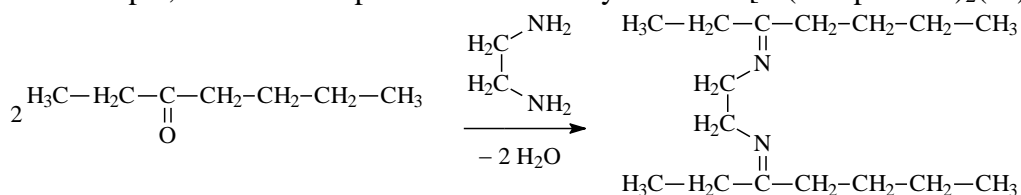
Diethyl-glyoxime was dissolved in EtOH or MeOH, than added to the aqueous solution of the reduced platinum salt (PtCl_2). The mixture was heated for 2–3 hours. After cooling, the formed $[\text{Pt}(\text{diethyl-glyoxH})_2]$ was filtered, washed with EtOH–water mixture (1:1), and dried on air. For the synthesis of complexes, the reaction mixture of the diethyl-glyoxime and PtCl_2 was heated for 1 hour, than the corresponding amine (imidazole, 2-amino-pyrimidine, 3-hydroxy-aniline) was added, and heated further for 2 hours. After cooling the product was filtered, washed with EtOH–water mixture (1:1), and then dried on air. The reactions:

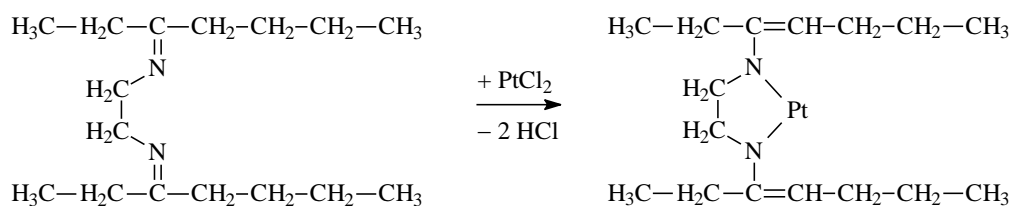


- *Synthesis of $[\text{Pt}(3\text{-heptanone})_2(\text{A})]$ ($\text{A} = \text{en}, 1,2\text{-pn}, 1,3\text{-pn}$) complexes*

The Schiff bases were prepared by the condensation reaction between 3-heptanone and the corresponding diamine (ethylenediamine, 1,2- and 1,3-propylenediamine) in EtOH solution. The mixture was heated at 70–80 °C for 2–3 hours. The solution obtained was directly used for the complex syntheses by adding the reduced platinum salt (PtCl_2) dissolved in water. The product was filtered, washed with EtOH–water mixture (1:1), and then dried on air.

For example, the reactions performed for the synthesis of $[\text{Pt}(3\text{-heptanone})_2(\text{en})]$ are:





Results and discussion

Microscopic characterization and the yield of prepared complexes are presented in Table 1.

Table 1. Microscopic characterization, calculated molecular weight and the yield of prepared complexes.

Nr.	Compound	Calc. mol. weight	Yield (%)	Microscopic characterization
1.	[Pt(diethyl-glyoxH) ₂]	481.41	59	Brown, triangle-based prisms
2.	[Pt(diethyl-glyoxH) ₂ (imidazole) ₂]	617.56	56	Brown, square-based long crystals
3.	[Pt(diethyl-glyoxH) ₂ (2-amino-pyrimidine) ₂]	671.61	54	Brown, long needles, triangle-based prisms
4.	[Pt(diethyl-glyoxH) ₂ (3-hydroxy-aniline) ₂]	699.66	42	Black, shining, triangle-based prisms
5.	[Pt(3-heptanone) ₂ (en)]	445.50	5	Black, irregular microcrystals
6.	[Pt(3-heptanone) ₂ (1,2-pn)]	459.53	18	Black, triangle-based crystals
7.	[Pt(3-heptanone) ₂ (1,3-pn)]	459.53	13	Black, irregular microcrystals

Infrared spectroscopic study

The mid-IR spectra were recorded with a Bruker Alpha FTIR spectrometer (Platinum single reflection diamond ATR), at room temperature, in the wavenumber range of 4000–400 cm⁻¹, and the far-IR range of 650–150 cm⁻¹, respectively, on a Perkin-Elmer System 2000 FTIR spectrometer, operating with a resolution of 4 cm⁻¹. The samples were measured in solid state (in powder form), respectively, in polyethylene pellets. The most important IR values for the selected complexes are presented in Table 2.

Table 2. IR data of the selected complexes.

Comp. cm ⁻¹	[Pt(diEt-glyoxH) ₂]	[Pt(diEt-glyoxH) ₂ (imidazole) ₂]	[Pt(diEt-glyoxH) ₂ (2-am.-pyrimid.) ₂]	[Pt(diEt-glyoxH) ₂ (3-HO-aniline) ₂]
$\nu_{\text{C-H}}$	2975, 2938, 2876 m	2975, 2938, 2876 m	2975, 2937, 2875 m	2974, 2937, 2876 w
$\nu_{\text{C=N}}$	1535 s	1532 vs	1535 s	1534 s
δ_{CH_2}	1459 s	1447 s	1459 s	1448 s
δ_{CH_3}	1360 m	1360 s	1359 m	1358 w
$\nu_{\text{N-O}}$	1241 vs	1242 vs	1241 vs	1240 vs
$\nu_{\text{N-OH}}$	1107 s	1110 s	1106 s	1106 s
$\tau_{\text{O-H}}$	916 vs	918 vs	916 vs	915 vs
$\gamma_{\text{C-H}}$	712 s	715 s	712 s	710 s
$\nu_{\text{Pt-N}}$	518 s	515, 512, 509 s	518, 515 s	516, 513, 501 s
$\delta_{\text{N-Pt-N}}$	358 vs	356 vs	328 vs	324 vs

(Abbreviations: vs = very strong, s = strong, m = medium, w = weak)

Mass spectrometry

Mass spectra of the samples were recorded by an Agilent/Technologies 6320 Mass Spectrometer using electrospray ionization (ESI). The samples were dissolved in MeOH. In the spectra we could detect the molecular ions and some decomposition fragments.

Thermoanalytical measurements (TG-DTG-DTA)

Thermal measurements were performed with a 951 TG and 910 DSC calorimeter (DuPont Instruments), in Ar or N₂ at a heating rate of 10 Kmin⁻¹ (sample mass 4–10 mg).

In the case of [Pt(diethyl-glyoxH)₂(amine)₂] complexes the first decomposition steps are belonging to the leaving amine groups up to 300 °C. Subsequently the decomposition of

glyoxime groups begins, which is accompanied by a big exothermic peak. This behavior can be explained with the presence of oxygen in the molecule as shown, for example, in Figure 1. The general decomposition mechanism is the following:

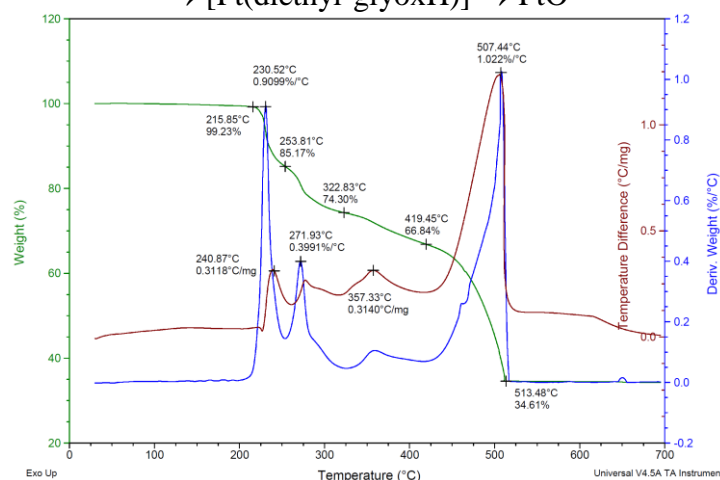
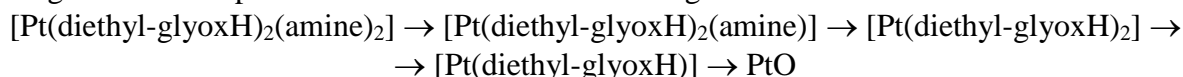


Figure 1. Thermal decomposition of $[\text{Pt}(\text{diethyl-glyoxH})_2(\text{imidazole})_2]$

NMR spectroscopic study

The NMR spectra (^1H and ^{13}C NMR) were recorded in DMSO-d_6 in 5mm tubes at RT on a Bruker DRX 500 spectrometer at 500 MHz, using TMS as internal reference. In the ^1H NMR spectra the aliphatic protons appear at 1.1–2.8 ppm in all complexes, the aromatic protons appear between 7.7–8.3 ppm. In the ^{13}C NMR spectra the aliphatic carbons appear at 10–20 ppm, and the double bonded carbons appear at 158 ppm.

Powder X-ray diffraction measurements

Powder XRD measurements were carried out on PANalytical X'pert Pro MPD X-ray diffractometer. The crystal structure of the complexes was studied with this method. As being new compounds their diffractograms are not deposited in the Cambridge database.

UV–VIS spectroscopy

The electronic spectra were recorded with Jasco V-670 Spectrophotometer in 10% EtOH/water solutions containing substrate in 10^{-4} mol/l concentration. For a few complexes the characteristic wavelengths are the followings: $[\text{Pt}(\text{diethyl-glyoxH})_2]$ – 271 nm, 320 nm, 470 nm; $[\text{Pt}(\text{diethyl-glyoxH})_2(2\text{-amino-pyrimidine})_2]$ – 198 nm, 286 nm. Using Britton-Robinson buffer solutions the electronic spectra were also recorded as a function of pH, and then the acidity constants were calculated with the formula below:

$$K_a = 10^{-\text{p}K_a}, \text{p}K_a = \text{pH} + \lg \frac{A - A_{\max}}{A_{\min} - A}, \text{ where } A \text{ is the absorbance.}$$

The obtained values are listed in Table 3.

Table 3. The acidity constants for selected complexes.

Compound	λ	pH	A	A _{max}	A _{min}	pK _a	K _a
[Pt(diethyl-glyoxH) ₂]	448	10.48	0.020123	0.0282773	0.0143296	10.63068	2.34·10 ⁻¹¹
	323	10.48	0.108823	0.112591	0.0803457	9.604606	2.49·10 ⁻¹⁰
	273	9.71	0.31477	0.339324	0.285667	9.638467	2.3·10 ⁻¹⁰
[Pt(diEt-glyoxH) ₂ (2-am.-pyrimid.) ₂]	268	10.48	0.458324	0.475482	0.290584	9.48983	3.24·10 ⁻¹⁰
	195	11.31	2.51446	2.63318	2.31618	11.08724	8.18·10 ⁻¹²

Biological study

The antimicrobial effects of complexes were studied for Gram-negative and Gram-positive (especially *B. Subtilis*) germs. The observation was made with the disk method. Filtering paper disks were impregnated with a concentrate probe solution, and sterilized (with UV-radiation or in autoclave), then putted on the germ substrate. After a 24 hour-incubation we investigated whether the studied compound blocked the growth of the germ substrate. When there was no growth of germ substrate around the disks, the case was called as inhibition zone. The Gram staining [5] is an empirical solution for dividing the germs into two parts (Gram-negative and Gram-positive) in accordance with the physical and chemical properties of the cell-wall. The results are included in Table 4. The complexes were dissolved in DMSO in 2 mmol/l concentration.

The results are included in table 4. The complexes were solved in DMSO, and the concentration was 2 mmol/l.

Table 4. The inhibition zone dimension as a function of the quantity of complexes.

Compound	5 μ l	10 μ l	20 μ l	30 μ l
[Pt(diethyl-glyoxH) ₂ (imidazole) ₂]	-	9 mm	12,7 mm	16,33 mm
[Pt(diethyl-glyoxH) ₂ (3-hydroxy-aniline) ₂]	-	7,83 mm	13,66 mm	14,66 mm

Conclusion

In this work new platinum complexes were synthesized and their physico-chemical properties were studied. Decomposition mechanism was determined with the thermoanalytical method. The antibacterial effect of compounds was investigated, and in the future we propose to study their anti-tumor effect, too.

Acknowledgement

The authors wish to express their thankfulness to the “Domus Hungarica Foundation” of Hungary for the several fellowships provided to Csaba Várhelyi jr.

References

- [1] T. Lazarević, A. Rilak, *European Journal of Medicinal Chemistry* 142 (2017) 1
- [2] N.J. Wheate, S. Walker, *Dalton Transactions* 39 (2010) 8097
- [3] M.J. Cleare, J.D. Hoeschele, *Bioinorganic Chemistry* 2 (1973) 187
- [4] P. Ruiz-Sanchez, *J. Biol. Inorg. Chem.* 16 (2011) 33
- [5] T.J. Beveridge, *Biotech. Histochem.* 76(3) (2001) 111

POLYANILINE – MORPHOLOGY AND SENSING PROPERTIES

Nicoleta Pleșu^{1*}, Andrea Kellenberger², Cornelia Crasmarean¹

¹ *Institute of Chemistry Timisoara of Romanian Academy, 24 Mihai Viteazul Blv., 300223 Timisoara, Romania,*

² *University “Politehnica” of Timisoara, Faculty of Industrial Chemistry and Environmental Engineering, P-ta Victoriei 2, 300006 Timisoara, Romania*

E-mail: plesu_nicole@yahoo.com

Abstract

The adsorption process of dye on polyaniline films electrodeposited on niobium has been investigated using electrochemical impedance spectroscopy. The negative $\Delta G_{\text{ads}}^{\circ}$ value ($-35.802 \text{ kJ mol}^{-1}$) and high value of K_{ads} obtained in our measurements indicate that Amino Black 10 dye adsorption process is spontaneous with the formation of a stable adsorbed dye layer on the polyaniline surface. The adsorption takes place via a combination of physical and chemical adsorption.

Keywords: PANI, dye, EIS

Introduction

In the last years Polyaniline (PANI) benefit from special attention due to its special properties and practical applications. It is an inimitable polymer because presents many oxidation forms (the polymer is in fact a mixture of different oxidation states: leucoemeraldine- pale yellow, emeraldine-green and conductive, pernigraniline- dark violet) and its conducting form is stable in air or water.

PANI properties depend on the synthesis conditions and can be obtained in different morphologies such as plate-like and leaf-like structures nanoflakes, nanofibers, nanotubular, nanospheres. The tendency of PANI to aggregate depends on the experimental conditions. Microstructures such as flower-like and leaf-like structures at pH 7, rod-like and granular-like morphologies at pH 3 and 1 or mushroom-like morphology were reported in literature. Also, 3D structures composed of nanosheets, nanorods based microspheres or nanorods based microrods have been observed in alkaline solution synthesis. The electrochemical method allows a more rigorous control of synthesis parameters and offers a very convenient way to study the electrochemical properties of PANI nanofibers [1-3]. Electrochemical impedance spectroscopy (EIS) is a noninvasive method for determining the fractional coverage of the adsorbed monolayer and investigates the nature of adsorption of some analytes on the PANI surface.

The scope of our work was to investigate the nature of adsorption of Amino Black 10 dye (AB10) on the PANI. EIS was chosen as measurement technique to investigate the interaction between the dye and the PANI surface.

Material and Methods

Aniline was freshly distilled under reduced pressure and stored in dark at low temperature. Double distilled water and analytical grade sulphuric acid were used to prepare the electrolyte solutions.

PANI films were obtained by electrochemical polymerization of aniline on niobium substrate from H_2SO_4 solution as reported [3]. The potentiodynamic polymerization was performed in a

standard three-electrode electrochemical cell connected to an Autolab PGSTAT 302N. The working electrode was a Nb disc ($A = 1 \text{ cm}^2$), two graphite rods were used as counter-electrodes and a saturated calomel electrode (SCE) as reference electrode.

EIS measurements were carried out using the FRA Module of Autolab 302N, in the frequency range from 10^6 Hz to 1 Hz and AC voltage amplitude of 10 mV . For each spectrum 60 points were collected, with a logarithmic distribution of 10 points per decade. The experimental electrochemical impedance data were fitted to the electrical equivalent circuit by a CNLS Levenberg–Marquardt procedure using the ZView-Scribner Associates Inc. software.

Adsorption studies

The adsorptions kinetics of AB10 dye was investigated using EIS technique. Adsorption of dye was studied under OCP condition and the adsorption profile was investigated. A dye stock solution of $3 \times 10^{-3} \text{ M}$ was prepared by dissolving the dye in distilled water followed by necessary dilutions of this stock solution. The values of surface coverage θ , corresponding to different concentrations of dye have been used to get best linearity isotherm [3, 4]. The values of surface coverage θ were obtained from impedance measurements according to equation (1):

$$\Theta = (C_o - C_i) / C_o \quad (1)$$

where C_o is the capacitance at time $t = 0$, C_i is the capacitance at any time.

Results and discussion

For adsorption studies four PANI films were prepared in the same conditions. The deposition of PANI on Nb electrode takes place only after substrate passivation, when Nb is covered by a passivating layer of niobium oxide [17]. The deposition charge Q was calculated for each PANI film to verify that they have similar masses and thicknesses. Values of 98, 95, 100 and 98 mC have been obtained for the four PANI films, showing a good reproducibility. The thickness of four PANI films deposited was estimated to be $5.25 \pm 0.35 \text{ }\mu\text{m}$ using an average density value for polyaniline of 1.4 g cm^{-3} [3]. The spectra of polymer obtained on Nb present the C=C stretching deformation of the quinoid and benzoid rings at 1570 cm^{-1} and 1482 cm^{-1} , the C–N stretching of the secondary aromatic amine at 1293 cm^{-1} [3]. The band at 1372 cm^{-1} present was attributed to the C–N stretching mode in the neighborhood of a quinoid ring. The band at 1232 cm^{-1} is assigned to C–N⁺ stretching in polaron lattice structure for Pani-Nb. The bands found in the structure of Pani-Nb at 1467, 1448 and 1414 cm^{-1} , was attributed to presence of the phenazine units and the aromatic C–H in-plane bending at 1128 cm^{-1} and the C–H out-of-plane bending at 815 cm^{-1} to the 1,4-substitution of the benzene ring. The vibrations at 780, 725 and 699 cm^{-1} present in the spectra is also a proof of the presence of multi-substituted benzene rings, associated with the formation of branched polymer structures and/or the presence of phenazine-like units. The symmetric stretching vibration of the sulfonate group is observed as a broad band at 1040 cm^{-1} only for Pani-Nb doped state [3]. The morfology of PANI deposited on Nb confirm the formation of network of nanofibers on the surface. The adsorption profile of AB10 dye was investigated by EIS under OCP condition.

The Nyquist plots (Figure 1a) contain depressed semicircles with the center under the real axis. The behavior is characteristic for solid electrodes and is often referred to a frequency dispersion attributed to roughness of the solid surfaces and physical phenomena such adsorption.

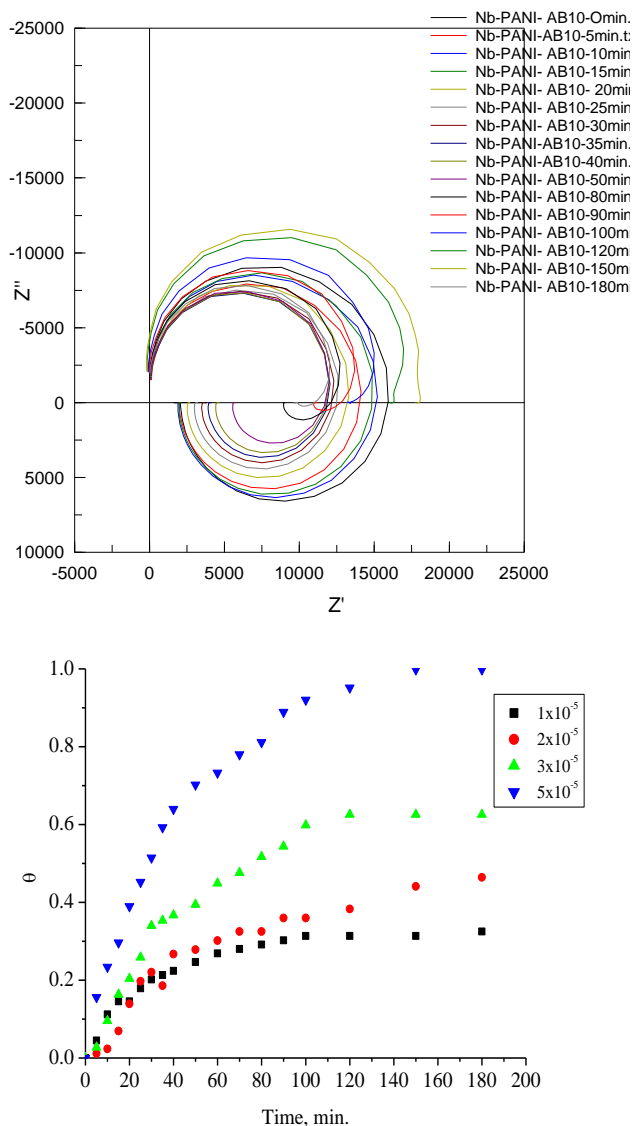


Figure 1. a) Nyquist plots for PANI/Nb electrode immersed in $1 \times 10^{-5} \text{ mol L}^{-1}$ dye solution at different moment of immersion and b) the variation of electrode surface coverage in time for all AB10 dye solution concentrations.

The electrochemical electric circuit (EEC) used to model the EIS data include a resistor (R_s is the solution resistance between the reference electrode and working electrode) in series with a parallel connection between a capacitor (double layer capacitance), C_{dl} expressed as a constant phase element CPE_{dl} (used instead a pure capacitance to account for the non-ideal capacitive response from the interface) and a resistance (R_{ct} is the charge transfer resistance). In EIS spectra the inductive loop appeared at low-frequency values (LF) was attributed to the relaxation process of dye species adsorbed on the PANI electrode surface and was modeled by elements R_L (is the inductive resistance) and L (is the inductance) [5, 6]. The C_{dl} values result after fitting of EIS data show an increase with increase of the concentration of dye in solution. The adsorption lead to a decrease in the local dielectric constant and/or to an increase in the thickness of the electrical double layer as water molecules present at the PANI-electrode interface are replaced through adsorption phenomena. [6]. When adsorption becomes significant the disappearance of the inductive loop is observed (Figure 1a) also R_L was observe to be proportional to the surface coverage of

PANI with AB 10 molecules. The value of L was found to decrease as a consequence of the accumulation of dye molecules in the porous PANI layer. The values of θ were obtained using capacity values determined by fitting EIS data with EEC and calculating according to equation (1). The evolution of surface coverage of PANI in time is presented in Figure 1b. In the first minute the adsorption is rapid, 85-90% of PANI surface is covered by the dye molecules. After 60 minutes the adsorption became slower and reaches a plateau. The rate of absorption process was evaluated from the decay of electrode capacitance in the first moments when an irreversible layer of dye is considered to be form on the PANI surface. The proper model for adsorption kinetics was establish to be the Langmuir model (equation 2) which gave a better fit for the representation of $\ln(1 - \theta)$ against time.

$$\Theta(t) = [1 - e^{-k_a t}] \quad (2)$$

The k_a was $18.21 \pm 2.56 \times 10^{-3} \text{ s}^{-1}$. These results are similar with the results reported for the azo red dye adsorbed on PANI surface [6].

The Langmuir adsorption isotherm fit the experimental data (equation 3a) and the K_{ads} was found to be $34005.21 \text{ mol}^{-1}$.

$$\frac{C}{\theta} = \frac{1}{K_{ads}} + C \quad (3a) \quad R_L = \frac{1}{1 + K_{ads} C} \quad (3b)$$

where θ is the surface coverage, C is the dye concentration, K_{ads} is the adsorption equilibrium constant. The values obtained for slopes in the Langmuir model were less than unity and indicate the existence of interactions between the adsorbed dye molecules and PANI surface. The dimensionless separation factor, $R_{Langmuir}$ are less than unity for all concentrations, confirming that the adsorption processes on PANI are favorable. Based on the value obtained for K_{ads} the free energy of adsorption (ΔG^0_{ads}), was calculated using the equation (4):

$$\Delta G^0 = -RT \ln(55.5 K_{ads}) \quad (4)$$

where R is the universal gas constant ($8.314 \text{ J mol}^{-1} \text{ K}^{-1}$) and T is the absolute temperature in Kelvin, K_{ads} is the adsorption equilibrium constant, ΔG^0_{ads} is the standard free energy of adsorption, 55.5 is the concentration of water in the solution in mol dm^{-3} .

The negative ΔG^0_{ads} value ($\Delta G^0_{ads} = -35.802 \text{ kJ mol}^{-1}$) and high value of K_{ads} obtained indicate that adsorption process is spontaneous with the formation of a stable adsorbed of AB10 dye layer on the PANI surface. The adsorption takes place via a combination of physical and chemical adsorption but mainly due to physical adsorption. The ΔG^0_{ads} value for the adsorption of AB10 dye on PANI/Nb is closer to the value reported for the adsorption process of red azo dye onto PANI/Nb (ΔG^0_{ads} of $-36.381 \text{ kJ mol}^{-1}$) [6].

Conclusion

The PANI film deposited electrochemically on Nb surface present a high specific surface and presents dye retaining capacity. The proper model for AB10 dye adsorption kinetics was establish to be the Langmuir model and k_a was $18.21 \pm 2.56 \times 10^{-3} \text{ s}^{-1}$. The Langmuir isotherm describes well the adsorption phenomena. The change of Gibbs energy evaluated for the adsorption of AB 10 dye onto PANI/ Nb electrode presents a negative value ($-35.802 \text{ kJ mol}^{-1}$). The $\Delta G_{\text{ads}}^{\circ}$ value and the high value of K_{ads} propose that adsorption process is spontaneous with the formation of a stable adsorbed dye layer on the PANI surface. The adsorption of AB10 dye takes place via a combination of physical and chemical adsorption.

Acknowledgements

The authors from Institute of Chemistry Timisoara of Romanian Academy are acknowledging Romanian Academy for financial support in the frame of Programme 2/2018 from ICT. This work is dedicated to the Centennial Anniversary of ROMANIA.

References

- [1] H.H. Zhou, S.Q. Jiao, J.H. Chen, W.Z. Wei, Y.F. Kuang, Thin Solid Films 450 (2004) 233–239.
- [2] H. Zhou, J. Wen, X. Ning, C. Fu, J. Chen, Y. Kuang, Synth. Met. 157 (2007) 98–103.
- [3] A. Kellenberger, N.Plesu, N., M. Tara-Lunga Mihali, N.Vaszilcsin, Polymer 54(13) (2013) 3166-3174.
- [4] S.John, K M. Ali, A. Joseph, Bull. Mater. Sci., 34(6) (2011) 1245–1256.
- [5] M. Lebrini, F. Robert, P.A. Blandinières, C. Roos, Int. J. Electrochem. Sci., 6 (2011) 2443 – 2460.
- [6]. M. Tara -Lunga-Mihali, N Plesu, A. Kellenberger, G. Ilia, Int. J. Electrochem. Sci., 10 (2015) 7643-7659.

PERCEPTION OF CORPORATE SOCIAL RESPONSIBILITY IN HUNGARY

Zita Varga¹, László Berényi²

¹*Faculty of Economics, University of Miskolc, H-3515 Miskolc-Egyetemváros, Hungary*

²*Institute of Management Science, University of Miskolc, H-3515 Miskolc-Egyetemváros, Hungary*

e-mail: szvblaci@uni-miskolc.hu

Abstract

Corporate social responsibility (CSR) does not have an exclusive definition. It can be understood as an umbrella that covers both theoretical and practical attempts as well as achievements to put a new basis of cooperation between corporations and their environment. Since corporations are core elements of the societal environment, a comprehensive is required. Our research contributes to this field by exploring the personal opinions and attitudes. The paper is an enhanced extract of a Scientific Students' Associations research. The non-representative research sample consists of the responses of 267 Hungarians. Results of the statistical analysis show that there is a general lack of information about the topic and there is a correlation between CSR knowledge level and the judgment on CSR. Surprisingly, a higher level of knowledge does not necessarily coincide a higher trust in CSR.

Introduction

Nowadays corporate strategies may include an approach to social responsibility. There are several application models available, due to the diversity of the influencing factors of the effective solutions. CSR initiations may give the frame of the related endeavors.

There is a conceptual diversity about defining CSR [1] but a common core is to discover:

- Bowen [2] stated that CSR “refers to the obligations of businessmen to pursue those policies, to make those decisions, or to follow those lines of action which are desirable in terms of the objectives and values of our society”.
- Friedman’s approach to responsibility, from profit-maximization to following the wishes of stakeholders [3] determine the thinking on the topic even nowadays.
- European Commission defines CSR as “a concept whereby companies decide voluntarily to contribute to a better society and a cleaner environment” [4].
- The definition of ‘social responsibility’ in the ISO 26000 standard embraces the essentials as “responsibility of an organization for the impacts of its decisions and activities on society and the environment, through transparent and ethical behavior...” [5]. The definition includes a contribution to sustainable development, health and the welfare of society, stakeholder-oriented thinking and compliance with the law and other norms. The scope of application covers both internal and external relations.
- Carroll’s model [6] [7] of corporate social responsibility (CSR) shows the feasible levels beyond economic interest. Economical and legal levels are marked as required by the society. Ethical responsibilities are marked as expected and philanthropic level as desired.

The practical and scientific interest led to various conceptual models and industrial applications. Farcane and Bureana [8] summarizes that the simple concepts of the 1950s were developed to the phenomenon, and it has been extended in the 1960s and 1970. Later, in the 1980s new concepts have been appeared such as corporate social performance, stakeholders’ theory and business ethics theory. Madрахimova [9] investigates also next eras. The 1990s can be labeled with the acceleration of globalization, and reports were released in this era.

Reporting was significantly developed in the 2000s. A comprehensive summary is presented in Figure 1.

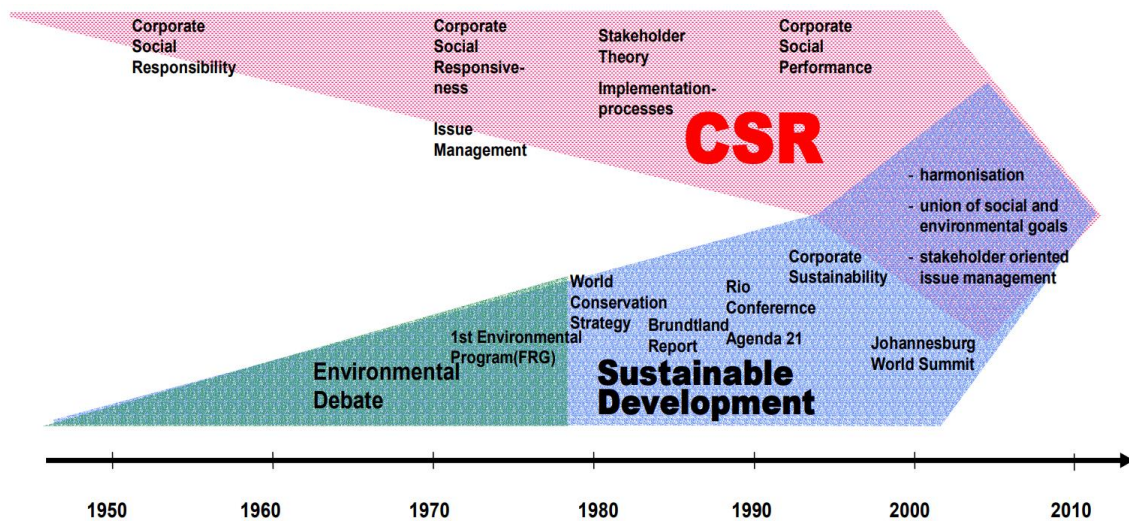


Figure 1. Historical development of CSR and sustainability debate [10]

Nowadays there is a literature diversity in the field that analyzes of the sectoral characteristics, related tools or the strategic integration possibilities. There are both theoretical achievement and case studies about the successful applications.

According to the opinion of Dempsey [11], an early representative of the topic, we agree that CSR cannot be interpreted in different ways for various corporations, citizens or the government, there is one and only one community. However, corporations have an extensive impact on the processes including both causing and solving the problems, the ultimate goal is improving the welfare of the society. Based on this approach, we think that initiatives and tools can be more successful if those are acceptable on an individual level. Turning the thought away, new initiatives should consider personal opinions and attitudes in the field. Our research aims to contribute to this challenge.

Experimental

The research uses a survey including 11 questions. There are questions about preliminary CSR studies, personal shopping habits as well as workplace CSR practices. The target group of our survey was the Hungarian citizens from various territorial locations and social situations. Data collection used the snowball method, the research sample is not representative.

The research sample consists of 267 responses. Data analysis was conducted by the support of IBM SPSS Statistics 22. The sample characteristics are as follows:

- 182 females (68.2%) and 85 males (31.8%) answered the questions,
- According to occupation and working activities, 33% are manual workers, 52% brain workers, 5% not working and 10% others.
- 73.4% of the respondents belong to the Generation Y (who were born between 1980 and 1994 [12]).

There are 4 research hypotheses formulated for the analysis presented in this paper:

- H1: There is a huge lack of knowledge about CSR in the society.
- H2: There is a difference of opinions about CSR by occupations.
- H3: The level of CSR studies has an impact on the opinions on the topic.

- H4: CSR awareness is at a higher level among brain workers than among physical ones.

Results and discussion

51.3% of the respondents have never learned about CSR, 40.5% has a superficial knowledge, and 8.2% has a detailed knowledge about the topic. Cross-tabulation shows significant differences by age categories (Chi-square=24.200, $d_f=9$, sig.=0.004), the youngsters learn more about the subject.

The survey asked whether the employers of the respondents have any activities that can be considered as CSR ones (note: the introduction of the questionnaire clarified the definition and content of CSR). 31% of the respondents found that CSR-related actions are entirely missing. 20.6% marked that social and local issues are considered, and 19.9% marked that environmental issues are also managed. The results show significant differences by the types of occupations (cross-tabulation Chi-square=108.632, $d_f=12$, sig.=0.000). 31% of brain workers and 39% of physical workers marked that their employers do not have CSR activities. However, the textual remarks attached to the responses show that there is a relevant information gap.

The satisfaction of the respondents with the corporate CSR activities shows a medium value based on a 5 point scale evaluation. Results are analyzed by cross tabulation, using various grouping factors. Based on the level of CSR studies, respondents without knowledge marked significantly lower values, i.e. more dissatisfaction (Chi-square=22.159, $d_f=12$, sig.=0.036) than the other groups. Respondents with superficial knowledge have the highest level of satisfaction.

The survey includes some statements about the content of CSR, partly using of a former survey [13], and asks the respondents to mark the level of agreement on a 5-point Likert-scale (a higher value mean a higher level of agreement):

- Helps to achieve the goals of sustainable development: 42.3% of the respondents marked rather (4) or fully (5) agreeing with the statement, while, only 4 answers of 267 shows a complete disagreement.
- Helps to coordinate corporate efforts: 38.6% marked the middle value (3) followed by rather agree (4) answers, i.e. the respondents do not have a clear trust in the proper strategic coordination role of CSR.
- CSR is a tool for influencing partners: 41.9% marked the middle (3) and 28.8% the rather agree (4) value.
- CSR is an excellent marketing communication tool: 37.8% marked the middle and 56.6% of the fully agree (5) options. However, the survey did not ask whether CSR as a marketing communication tool was welcome or harmful, the results show that people believe in its viability.
- Corporate CSR reports are authentic; CSR is just a corporate tool for increasing profit; CSR implementation is expensive: respondents are skeptical, marking of middle values (3) is the most common.
- CSR can be successful only for a large corporation: 48.7% of the respondent marked full or rather disagreement with this statement while 23.2% agrees or rather agrees.

Due to the scattered picture of the responses, we used the grouping factors for exploring more homogeneous opinions. ANOVA analysis shows significant differences by the level of CSR knowledge in case of the statements CSR is a tool for influencing partners ($F=8.373$ sig.=0.004) and CSR is an excellent marketing communication tool ($F=6.888$, sig.=0.009).

Respondents who did learn about CSR consider it a more relevant influencing tool, and they keep CSR a less excellent marketing communication tool.

Results by gender are checked by cross-tabulation, significant differences are summarized in Table 1. Females have a greater confidence in the authenticity of the CSR reports and they believe that CSR can be successful not only for the large corporations.

		Gender		Total
		Male	Female	
<i>Corporate CSR reports are authentic</i> Chi-square sig=0,027	1	12	8	20
	2	19	38	57
	3	37	82	119
	4	12	46	58
	5	5	8	13
<i>CSR can be successful only for large companies</i> Chi-square sig=0,027	1	21	33	54
	2	22	54	76
	3	15	60	75
	4	16	24	40
	5	11	11	22
<i>CSR implementation is expensive</i> Chi-square sig=0,011	1	8	3	11
	2	11	13	24
	3	33	69	102
	4	21	62	83
	5	12	35	47

Table 1: Significant results in cross-tabulation of judgment on CSR by gender (own edition)

Conclusion

However, corporate social responsibility is presented as a success story, empirical studies highlight that perception and individual opinions may be opposed to the theoretical intent and corporate interest. Our survey among Hungarians highlights the lack of knowledge. The results confirm that the level of knowledge about the CSR significantly influences the attitudes.

There were 4 hypotheses formulated for this paper. Considering the limitations of the sample and the content of the research, the analysis confirmed H1, H2 (partly) and H3. We rejected H4.

- H1: The lack of knowledge is presented in the low ratio of respondents who did learn about CSR. However, CSR is voluntary, most of the respondents bring this characteristic into question; it is hard to distinguish the interests behind the initiations.
- H2: The confirmation of the hypothesis is partial. The statistical analysis shows the higher sensitivity of females in social issues and higher trustfulness in CSR.
- H3: Statistical analysis confirmed that the level of CSR studies has an impact on the individual opinions. Nevertheless, wider knowledge does not mean a higher confidence in CSR.
- H4: However, employers of the brain worker respondents rather deal with CSR than physical workers, the hypothesis must be rejected since there is no significant difference.

A general experience of the research is that there is a need for comprehensive education actions about CSR. Next generations can benefit from the increasing attention by the higher

education institutions but for those who are already working, special methods must be developed. Both the literature review and the experiences of the research show that multinational corporations can play a key role in the diffusion of the CSR approach.

Acknowledgments

It has to be noted that the research giving the background of this paper is a Scientific Students' Associations essay by Zita Varga [14], supervised by László Berényi. The paper is an enhanced extract of the results.

References

- [1] A. B. Carroll, Corporate Social Responsibility: Evolution of a Definitional Construct, *Business & Society*. 38(3) (1999) 268-295.
- [2] H.R. Bowen, *Social Responsibility of the Businessman*, New York University Press, 1953.
- [3] T. Carson, Friedman's Theory of Corporate Social Responsibility, *Business & Professional Ethics Journal*. 12(1) (1993) 3-32.
- [4] European Commission, *Green Paper: Promoting a European framework for corporate social responsibility*, COM. 366, Brussels, European Commission, 2001.
- [5] ISO 26000:2010 -- Guidance on social responsibility p.3.
- [6] A.B. Carroll, A Three-Dimensional Conceptual Model of Corporate Performance, *The Academy of Management Review*. 4(4) (1979) 497-505.
- [7] A.B. Carroll, Carroll's pyramid of CSR: taking another look, *International Journal of Corporate Social Responsibility*, 1 (2016), doi:10.1186/s40991-016-0004-6
- [8] N. Farcane, E. Bureana, History of "Corporate Social Responsibility" Concept, *Annales Universitatis Apulensis Series Oeconomica*. 17(2) (2015) 31-48.
- [9] F. Madрахimova, History of Development of Corporate Social Responsibility, *Journal of Business and Economics*. 4(6) (2013) 509-520.
- [10] T. Loew, K. Ankele, S. Braun, J. Clausen, *Bedeutung der Internationalen CSR-Diskussion für Nachhaltigkeit und die sich daraus ergebenden Anforderungen an Unternehmen mit Fokus Berichterstattung*, Institut für ökologische Wirtschaftsforschung (IÖW) gGmbH, Berlin, 2004. p.12.
- [11] B.W. Dempsey, 'The Roots of Business Responsibility,' *Harvard Business Review*, Vol. 27, pp. 393–404, 1949
- [12] M. McCrindle, E. Wolfinger, *The ABC of XYZ: Understanding the Global Generations*, University of New South Wales Press, Sydney, 2010.
- [13] N. Deutsch, L. Berényi, Personal approach to sustainability of future decision makers: a Hungarian case, *Environment Development and Sustainability*. 20(1) (2018) 271-303.
- [14] Z. Varga, *Vélemények a CSR-ról Magyarországon (Reviews of CSR in Hungary)*, Scientific Students' Associations essay, Institute of Management Sciences, University of Miskolc, Miskolc, 2017.

SEPARATION OF AFLATOXINS BY CENTRIFUGAL PARTITION CHROMATOGRAPHY

Gábor Endre^{1,2}, Zsófia Hegedüs^{1,2}, Mónika Varga¹, Csaba Vágvolgyi¹, András Szekeres¹

¹*University of Szeged, Faculty of Science and Informatics, Department of Microbiology,
Közép fasor 52. Szeged H-6726*

²*Doctoral School in Biology, Faculty of Science and Informatics, University of Szeged,
Szeged, Hungary
egabcy@gmail.com, andras.j.szekeres@gmail.com*

Abstract

Aflatoxins are mycotoxins, produced by several species of filamentous fungi. For this group of toxins, there are very low, ppb-level limits in the EU in food and feed products, thus as reference standards relatively high amounts of pure aflatoxins are required. One of the promising methods for their purifications, the centrifugal partition chromatography could be used successfully. Herein this study, the development of a liquid-liquid chromatographic method for the separation of both the aflatoxins and the impurities was involved.

Introduction

Mycotoxins are the secondary metabolites produced by certain filamentous fungi. Within these toxic compounds, aflatoxins are playing an outstanding role due to their high level toxicity, which cause remarkable problems in food industry and agriculture [1,2]. Plenty of methods are available for monitoring or measuring these compounds from various matrixes [3,4], which requires relatively high amounts of pure aflatoxins. Liquid-liquid chromatography, which is based on a distribution of components between two phases in a biphasic solvent system, could serve solutions in their purifications. One of the technical implementation of this technique is the Centrifugal Partiton Chromatography (CPC) [5], which was applied in our work for the separation of aflatoxins from the fermentation product.

Experimental

Aspergillus parasiticus (SZMC 2473) was cultivated on liquid media for 7 days in dark at room temperature containing malt extract. The produced aflatoxins were extracted three times using dichloromethane and the pooled crude extract was dispensed into 1.5 ml vials and were evaporated to dryness for the solvent system testing. Each examined solvent system was mixed in 10 ml test tube. Than equal amounts of both saturated phases were added into same vial, containing the dried extract. Aflatoxins and the impurities were distributed between the two phases, and their concentrations in the upper- and lower phases were measured by HPLC-UV technique. The partition coefficients (P) and separation factors (α) were calculated, and the best system was selected for the purification of aflatoxins.

Results and discussion

At the beginning of our work, the aflatoxins were extracted from the culture media of *A. parasiticus* (SZMC 2473). The extraction of the desired compounds was carried out and the examination of ternary systems was started. The constructed ternary systems are based on the *best solvent method*. For these purposes, a solvent, which is best to dissolve the aflatoxins, is selected as core component of the solvent system. Beside this bridge solvent, two other solvents are also selected including both a more polar- and less polar solvents, compared to the best one. Applying these solvents in different ratios to solve the crude extract, the valuable component and the impurities could be shifted from one phase into the other. For the best

solvents, chloroform, acetone and acetic acid were selected initially and altogether 108 systems were created. The most promising system possessed 0.25, 0.53, 0.79 and 1.8 partition coefficient values for aflatoxin B1, B2, G1 and G2, respectively. After the calculation of separation factors this system was applied for the instrumental optimization and purification. , the preparative separation of aflatoxins was carried out. At the end of our work the purity of our products were measured.

Conclusion

In our study, a liquid-liquid chromatographic separation of four aflatoxins was accomplished using a cost-effective Centrifugal Partition separation method. Based on the results of our examinations the developed procedures will be proper for the large scale production of these type of mycotoxins in high purity.

Acknowledgements

This work was supported by the Hungarian Scientific Research Fund by grants NKFI K-115690 and this work was connected to the project GINOP-2.3.2-15-2016-00012.

References

- [1] J. W. Bennett, M. Klich, Mycotoxins. Clin. Microbiol. Rev. 16 (2003) 497.
- [2] D. L. Eaton, E. P. Gallagher, Ann. Rev. Pharmacol. Toxicol. 34 (1994) 135.
- [3] F. Hepsag, O. Golge, B. Kabak, Food Control 38 (2014) 75.
- [4] O. Golge, F. Hepsag, B. Kabak, Food Control 59 (2016) 731.
- [5] A. P. Foucalult, Centrifugal Partition Chromatography, New York: Marcel Dekker

ELIMINATION OF 4-NITROPHENOL FROM WATER BY OIL SHALE

Miklós Molnár¹, Ottó Horváth², Rita Földényi^{1*}

¹*Soós Ernő Water Technology Research Center, University of Pannonia Faculty of Engineering, 8200 Veszprém, Egyetem u. 10, Hungary*

²*Institute of Chemistry, University of Pannonia, 8200 Veszprém, Egyetem u. 10, Hungary
e-mail: foldenyi@almos.uni-pannon.hu*

Abstract

In this work, oil shale was used for elimination of a model potential anthropogenic pollutant, 4-nitrophenol. Sorption experiments were utilized under various different conditions; oil shale was pretreated with sodium azide to inhibit the microorganisms' activity, and the results were compared to those without pretreatment of oil shale. After a 24-hour equilibration time, in the presence of sodium azide pretreated oil shale, the concentration of 4-nitrophenol was higher than in the case of unpretreated oil shale, which indicates that during the sorption process not only sorption, but also decay of 4-nitrophenol took place. Desorption isotherm was also determined. Degradation experiments were applied to investigate how this persistent molecule transforms in the presence of oil shale. Sodium azide pretreated oil shale and MnCl₂ additive were also used to examine the effect of microorganisms and manganese(II) ion on the transformation of 4-nitrophenol. It was found that the presence of manganese(II) ion speeded up, while the sodium azide slowed down the transformation of the model molecule.

Introduction

Oil shale is a lamellar, sedimentary rock, its organic content can slightly be extracted by generally used organic solvents, but heat convection promotes this organic content to transform to oil. It consists of fossil algae biomass, clay mouldered from trap-tuff, volcanic wreckage and organic materials [1]. Application of oil shale is diverse: 1. in agriculture it is used as soil-ameliorating agent, starter fertilizer; 2. its curative power is utilized at some rheumatic diseases; 3. its considerable sorption ability can be applied for elimination of chemical compounds. Oil shale has already been used for acceleration of the degradation process of persistent molecules [2]. Distinguishing the location of formation of oil shale, two types occur in Hungary: laguna- and maar type.

4-nitrophenol can be utilized in multitudinous sectors in the industry as a precursor or intermediate of explosives, dyes, pesticides, pharmaceutical drugs. Since 4-nitrophenol is persistent, it can accumulate in soils and waters. It is listed as a priority pollutant material by Superfund sites. Only advanced chemical procedures and some bacteria can be used for degradation of 4-nitrophenol, such as Fenton, ozonation, electrochemical, photocatalysis, various nanoparticles and *Pseudomonas* bacteria [3-4]. In this work a simple procedure is presented, wherewith 4-nitrophenol can be easily eliminated, using Hungarian oil shale, a low-cost material.

Experimental

Maar type oil shale (collected from Pula, Hungary) was used. It was ground to the size of $\varnothing < 800 \mu\text{m}$. 4-nitrophenol and manganese(II) chloride tetrahydrate were purchased from Reanal Laborvegyszer Kft., calcium chloride dehydrate and sodium azide were obtained from Lach-Ner s.r.o. and Merck Darmstadt, respectively. All chemicals were used without further purification. Concentration measurement of 4-nitrophenol was performed by Merck Hitachi HPLC with UV detector at 317 nm. A mixture of 30% methanol and 70% water (pH was set

by acetic acid to 4.6 value) was used as eluent at a flow rate of 1 mL/min. Radelkis combination pH electrode was used for pH measurement.

Sorption on oil shale powder

Sorption experiments were performed using 250 mL stoppered Erlenmeyer flasks, wherein 5 g of oil shale were weighed. 5 mL distilled water or solution of sodium azide (10 g/L) was poured on the oil shale and was left to swell overnight. Solution of various concentrations of 4-nitrophenol (10 µmol/L to 20 mmol/L) were prepared, using 0.01 mol/L calcium chloride solution (pH=7.6). 50-50 mL of solutions were transferred to the swollen oil shale samples, and these suspensions were shaken and left to stand for 24 hours, until the equilibrium obtained. In order to separate the liquid and solid phases, approximately 2 mL of supernatant was sampled into an Eppendorf tube and centrifuged at 15000 rpm for 20 minutes. After centrifugation, concentration of 4-nitrophenol was measured by HPLC-UV.

Desorption on oil shale powder

The initial steps of desorption procedure were identical with the above mentioned method. Starting concentration range of 4-nitrophenol was 10 µmol/L to 500 µmol/L, solution of sodium azide was used for swelling of oil shale. After sorption equilibrating time (24 hours), the supernatant and oil shale were separated by centrifugation at 6000 rpm for 20 minutes. The removed supernatant (approximately 42 mL) was refilled by 0.01 mol/L calcium chloride solution. This suspension was shaken and left to stand another 24 hours. The supernatant was sampled and concentration of 4-nitrophenol was determined by HPLC-UV. The previous steps were repeated after 48 hours, the desorption process was completed.

Degradation in the presence of oil shale powder

25 g of oil shale powder was weighed into stoppered, 720 mL-glass flasks, and the oil shale was swollen by 25 mL of distillate water or solution of sodium azide (using 5, 10, 20 or 40 g/L concentration) or solution of manganese(II) chloride (30.4 g/L). Onto these swollen oil shale, 500 µmol/L of 4-nitrophenol in 0.01 mol/L calcium chloride solution was added. This suspension was shaken and left to stand for 24 hours. After equilibration, a small amount of supernatant was sampled, centrifuged at 15000 rpm for 20 minutes, and the concentration of 4-nitrophenol was determined by HPLC-UV. The remained sampled supernatant was added to the original system. The degradation process was considered from this point. Samples were taken periodically and the concentration of 4-nitrophenol was measured.

In all cases, blank sample was applied and all samples were in triplicate.

Results and discussion

Adsorption and desorption isotherms were analyzed in terms of Langmuir or Freundlich isotherm equation, whichever fits on the data better.

$$\text{Langmuir isotherm: } q_e = Q \cdot \frac{K_L \cdot c_e}{1 + K_L \cdot c_e}$$

$$\text{Freundlich isotherm: } q_e = K_F \cdot c_e^n$$

where q_e is the adsorption capacity at equilibrium (mol/g); c_e is the equilibrium solution concentration (mol/L); Q is the maximum amount of solute adsorbed for monolayer coverage of the surface (mol/g); K_L is the Langmuir constant (L/mol); K_F ($\text{L}^n/(\text{mol}^{(n-1)} \cdot \text{g})$) and n are the Freundlich constants.

Degradation curves were constructed as zero or first order kinetics, whichever fits on the data better.

A comparison of adsorption isotherms of 4-nitrophenol on oil shale with and without pretreatment of sodium azide can be seen in Figure 1. In the case of oil shale pretreated with sodium azide, the extent of adsorption is slightly lower than for that without pretreatment. Sodium azide inhibits the microorganisms' activity in the oil shale, thus it can be concluded that in the case of oil shale without sodium azide, microorganisms in the oil shale trigger a small degree of degradation of 4-nitrophenol during the one-day sorption process.

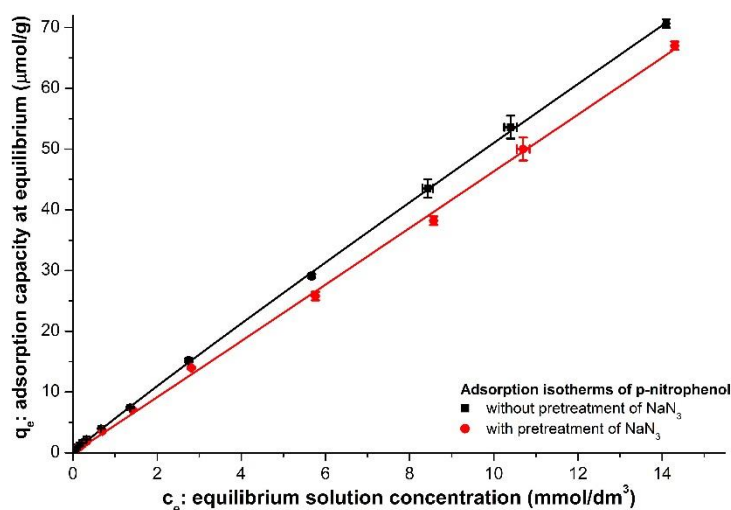


Figure 1. Adsorption isotherms of 4-nitrophenol

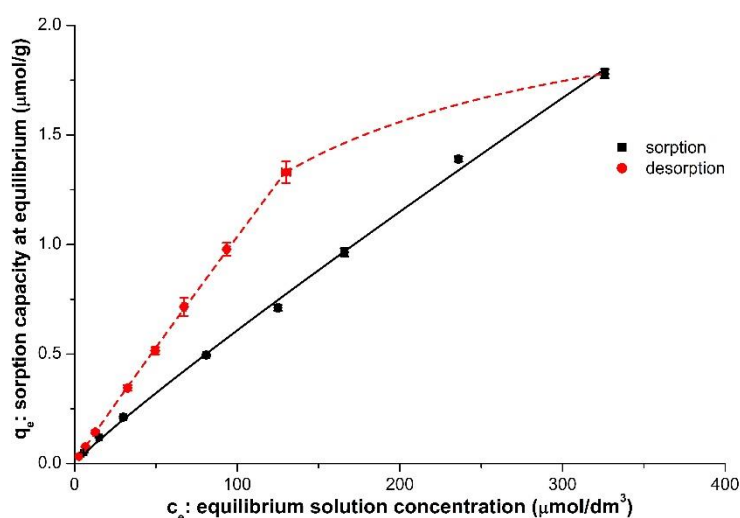


Figure 2. Adsorption-desorption isotherms of 4-nitrophenol

The hysteresis of adsorption-desorption isotherms can be seen in Figure 2. The nanoporous structure of oil shale containing kerogen caused a slow and reduced degree of desorption of 4-nitrophenol compared to the adsorption. After sorption of solute in kerogen, the desorption process was slow and retarded.

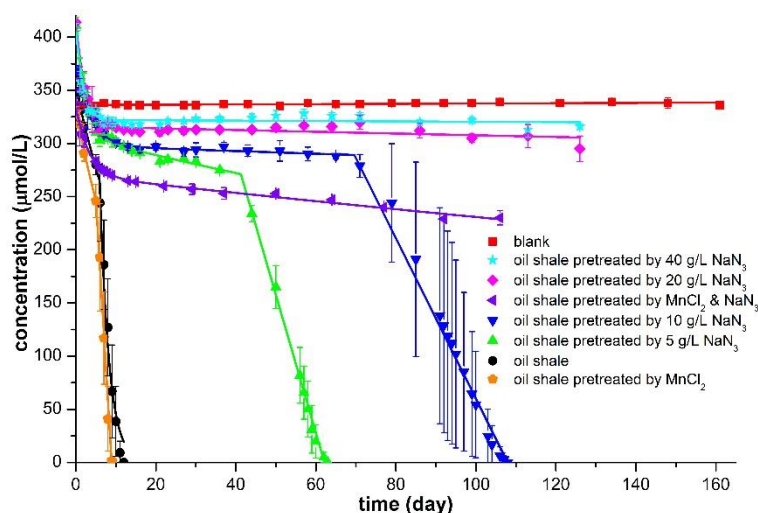


Figure 3. Degradation of 4-nitrophenol under various conditions

Figure 3. demonstrates the degradation of 4-nitrophenol. In the presence of oil shale, 4-nitrophenol transformed completely within 12 days. When oil shale was pretreated with sodium azide used in various concentrations, the time of degradation considerably increased because the microorganisms' activity was inhibited in the oil shale. When concentration of 5 g/l of sodium azide solution had been used, the transformation time of 4-nitrophenol was 63 days. In the case of 10 g/l, the transformation time changed to 108 days. When the concentration of sodium azide solution was increased to 20 and 40 g/l, the transformation time was much more than 130 days. These results highlight the importance of microorganisms' activity in the degradation process.

The effect of manganese(II) ions addition to the oil shale was the opposite, the time of the degradation of 4-nitrophenol decreased to 9 days. The difference between 9 and 12 days is not too large, but somehow the manganese(II) ions stimulate the microorganisms in the oil shale. It is proved by the experiment when the degradation of 4-nitrophenol was investigated in the presence of sodium azide pretreated oil shale, which contained manganese(II) ions. In this case, the time of the degradation of 4-nitrophenol was much more than 12 days, thus without microorganisms' activity, the effect of manganese(II) ions on degradation of the model compound was not favorable. A reasonable explanation can be given after the accurate identification of microorganisms.

We can notice breakpoints on the curves, which means that at least two consecutive processes are responsible for the transformation.

The analysis of the degradation product(s) of 4-nitrophenol is in progress.

Conclusion

Oil shale, a low-price rock is a suitable material for elimination of environmental pollutants, such as 4-nitrophenol, utilizing its good sorption capacity and capability of degrading molecules, even if they are persistent. The importance of microorganisms content of oil shale at degradation process was denoted, and improvement of this process could be achieved by adding manganese(II) ions to the oil shale. Further investigation is necessary to thoroughly understand the mechanism of the transformation.

Acknowledgements

We are thankful to Judit Szauer for her valuable work.

References

- [1] M. Hetényi, Maar-típusú olajpalák Magyarországon, Szeged, 1996.
- [2] R. Rauch, R. Földényi, Journal of Environmental Science and Health, Part B 47 (2012) 670.
- [3] S. Zhang et al., BMC Microbiology, 12 (2012) 27.
- [4] X. Chen, M. Murugananthan, Y. Zhang, Chemical Engineering Journal, 283 (2016) 1357.

ANTIBACTERIAL EFFECTS OF UNIFLORAL HONEYS AND PROPOLIS IN THE CONTEXT OF THEIR ANTIOXIDANT CAPACITY AND COLOUR

Kata Dorina Szűcs^{1,2}, Mónika Kovács¹, Éva Stefanovits-Bányai²

¹*Department of Microbiology and Biotechnology, Szent István University, H-1118 Budapest, Somlói street 14-16., Hungary*

²*Department of Applied Chemistry, Szent István University, H-1118 Budapest, Villányi street 29-43., Hungary*
e-mail: szucs.katad@gmail.com

Abstract

There is a huge potential for honey's therapeutic use, so it becomes increasingly important to examine its antibacterial effects and the factors influencing it. During the work the total polyphenol content and antioxidant capacity of 10 honeys and a propolis sample were examined with respect to their antibacterial effects. Based on this, there is a statistically significant correlation between the total polyphenol content and the antioxidant capacity, and between these properties and antibacterial activity. For the purpose of exploring the connection between the colour of honey and its properties, the colour of 6 honeys and the propolis were examined. Based on the results, dark-coloured honeydew honeys and light-coloured nectar honeys are sharply separated according to their antibacterial and antioxidant capacity.

Introduction

The healing effects of honey have been discovered by ancient cultures. Nowadays the medical community is once again discovering its healing potential, finding that its antibacterial and antioxidant effects can serve human healing in a number of ways [1].

This sweet product can be divided into two main types by its origin: nectar and honeydew. In the latter case, the honey is not harvested from flowers, but from the secretions of evergreens or the excretions of insects that feed on them. The two types show differences in colour, aroma, specific composition and characteristics [2].

Manuka honey comes to the front when it comes to therapeutic use – beside nectar honey. Experiments show that this type has a variety of phytochemical ingredients from several plant sources, and several flavonoids and terpenoids that make it different. In contrast to other honeys which contain hydrogen-peroxide, the activity of Manuka honey was due to the light and heat resistant methylglyoxal [3], [4].

Propolis is another important bee product which is a building material and a protective substance for the honeybee colony. Propolis, because of its considerable biological activity, has been used as a remedy in traditional medicine in treating burns, wounds, sore throats, and stomach ulcers for quite some time. Not unlike honey, propolis also has a potential to be used in the field of medicine and the food industry [5].

Numerous degenerative or chronic diseases such as diabetes mellitus, Alzheimer's disease, and heart disease are caused by oxidative stress. Experimental results show that honey due to its bioactive compounds has favourable effects against oxidative damage and degenerative diseases. The phytochemicals such as flavonoids, aromatic acids, phenolic antioxidants contribute the antibacterial properties of honey [5].

Experimental

Materials: 9 honeys were used in this study. Three of them (acacia, buckwheat, forest) were purchased from Golden Nectar Co. Ltd, the three Manuka honeys (Manuka UMF 15+, Manuka UMF 20+, Manuka UMF 22+) were imported from New Zealand. Three of

them (phacelia, pine, rape) were purchased from a local market, these originated from local beekeepers. Another bee product, propolis, (a Propolis Plus EPID Gocce Alcoholfree Propolis Drop) was analysed too. *Escherichia coli*; *Pseudomonas aeruginosa*; *Enterococcus faecalis*; *Listeria monocytogenes*; *Listeria innocua*; *Staphylococcus aureus* were used for the microbial analysis.

Preparation of samples for the analytical methods: Honey solutions in 250 mg/ml concentration were used for the analytical methods stored at -32 °C until analysis.

Total phenolic content (TPC): Total phenolic content was determined by the method put forward by Singleton and Rossi (1965) using a spectrophotometer at 765 nm wave length with the chemical of Folin-Ciocalteu. Gallic acid was used as the standard solution, so the results were specified in mg gallic acid equivalent/ 100 g dm. All measurements were performed three times in parallel.

Antioxidant capacity: The antioxidant capacity was determined by FRAP (*Ferric Reducing Ability of Plasma*) method. The reducing ability of ferric tripyridyltriazine complex was used for assessing total antioxidant capacity, which was measured with a spectrophotometer at a 593 wave length. Ferric reducing antioxidant power assay (FRAP) was defined in ascorbic acid equivalent (μg ascorbic acid equivalent/ 100 g dm).

Agar well diffusion method for inhibitory effect measurement: The hundredfold dilution of the 0.5 McFarland density test microorganism suspension was spread onto the TGE agar plate surface. Then, a 7 mm hole was punched aseptically with a sterile cork borer, and 4 drops of preheated sample was pipetted into the well. Plates were incubated for 24 hours at 25 °C. As time progressed the antimicrobial agent diffused in the agar medium and inhibited the growth of the sensitive microbial strain. The inhibition zones were measured by a ruler. The measurements were only repeated in cases where complications arose with the growth of the microorganisms.

Colour parameters: Colour parameters (L^* , a^* , b^*) were established in the CIE system using a Konica Minolta CR-300 Chroma-meter. The L^* value represents the brightness, the a^* is a red-green coordinate, and the b^* is the yellow-blue coordinate. The instrument was calibrated with a white reference tile.

Statistical analysis: Microsoft Excel 2016 was used to calculate averages, deviations and to create the tables and the diagram. The main statistical analysis was performed using IBM Statistics SPSS 22 software. The normal distribution of the measurement data were analysed by Shapiro-Wilk test, and after that the nonparametric Spearman's rank correlation coefficients (r_s) or the Pearson correlation coefficients (r) were calculated in order to determine the correlation between the particular parameters. Significance was set at $p < 0.05$.

Results and discussion

High variation was observed for the antioxidant activity among the samples (Table 1.). FRAP was expressed in μg AAE/100 g dm, ranged from 21.454 to 205.451. The FRAP value of the phacelia was the lowest, and the Manuka UMF 15+ was the highest. This value in the case of propolis was extremely high (1002.468 μg AAE/100 g dm) which is almost five-times higher than the highest value of the other honeys. The average deviation in FRAP values was low, 1.91 μg AAE/100 g dm. In the case of total phenolic content, the same pattern was observed. Polyphenols as antioxidant agents can explain the statistically significant correlation between ($r_s = 0.806$) the antioxidant capacity and the total phenolic content. In the case of Manuka honeys and propolis the total phenolic content and the antioxidant capacity were both extremely high. Beside these samples just the buckwheat, forest, and pine honeys have similar results. The results demonstrate that the darkest honeys contain the most phenolic compounds which in turn influence the antioxidant property of honeys. The average deviation in total phenolic content was 11.16 mg GAE/ 100 g dm.

1. Table: Total phenolic content and antioxidant capacity of honey samples and propolis

Honeys	Antioxidant capacity ($\mu\text{g AAE}/100\text{g dm}$)	Total phenolic content ($\text{mg GAE}/100\text{g dm}$)
Acacia	41.92	125.72
Buckwheat	151.92	662.78
Forest	179.83	432.72
Manuka UMF 15+	205.45	712.88
Manuka UMF 20+	123.18	551.54
Manuka UMF 22+	169.69	830.52
Phacelia	21.45	179.92
Pine	162.48	238.97
Rape	36.78	185.71
Propolis	1002.47	2984.29

The inhibition zone radii [(the diameter of the zone of inhibition - the diameter of the hole) /2)] around the pure honeys and the propolis sample varied in a wide range of samples (0.0-13.5 mm) (Table 2.). Propolis (6.75-12.25 mm), forest honey (4-12.25 mm), Manuka UMF 20+ (6.5-13 mm) had the highest antibacterial activity. Acacia (0.0-2.5 mm) honey showed to be the least effective against bacteria. The effectiveness of the samples was different for each of the strains. The largest zone was observed against *S. aureus* (2-13 mm) while *E. coli* (0.5-7 mm) turned out to be the most resistant. Different honey properties affected the microorganisms in different ways, but there was a significant correlation between inhibition radii and total phenolic content, and also between the antibacterial effect and antioxidant capacity. This suggests that the components contributing the antioxidant effect of honeys and propolis also have a role in the inhibition of microorganisms.

The antibacterial activity of Manuka honeys is considered to be due to the presence of methylglyoxal. Unique Manuka Factor (UMF) describes the amount of this non-peroxide component and it refers to the measure of antibacterial effect. Manuka honeys with 15+, 20+ and 22+ UMF were tested, but their efficiency were not in direct correlation with their UMF factors. The Manuka UMF 20+ honey had the highest antibacterial activity, but the zones of inhibition of Manuka UMF 22+ were similar to the zones of Manuka UMF 15+ (Table 2.). These samples were effective, but their activities were not remarkable. Only Manuka UMF 20+ honey had a significant effectivity as propolis, against *E. coli*. Antibacterial activity of most honeys is due to the presence of hydrogen peroxide, and while the Manuka honeys do not contain this component they still showed remarkable inhibitory effects. This raises the question that the presence of hydrogen peroxide might not play as an important role as we had thought previously, but this hypothesis needs further studies to prove.

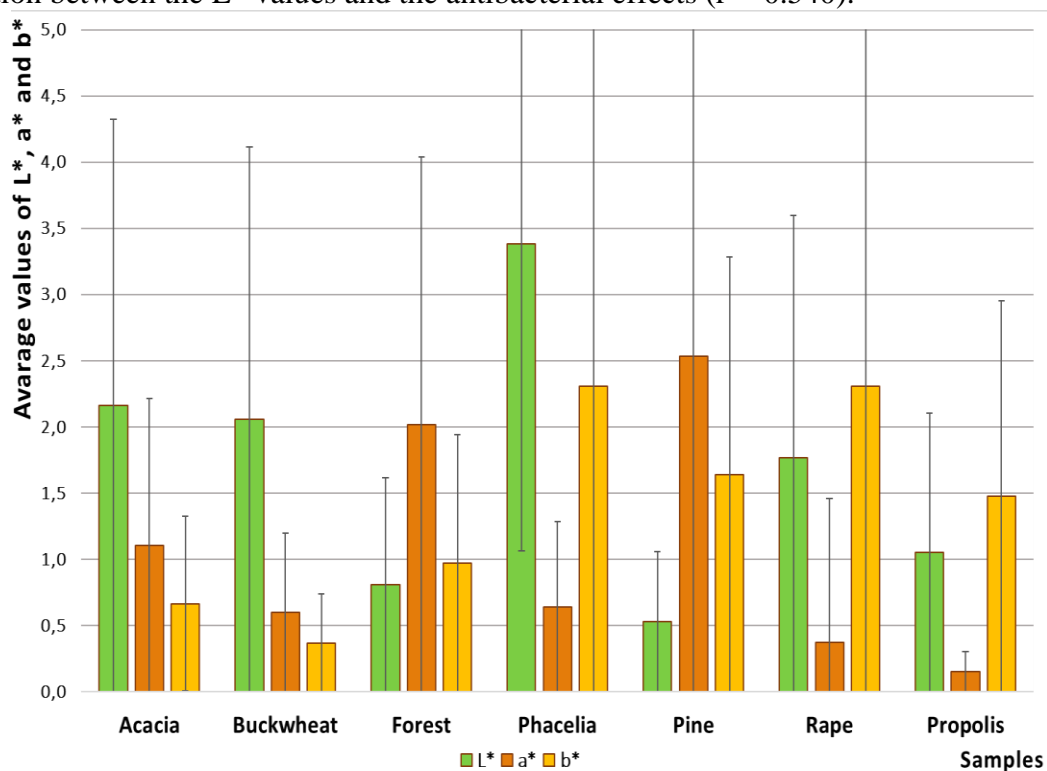
Propolis had a significant antibacterial effect (Table 2) against all strains, but its efficacy was not as pronounced compared to the honey samples, as its total polyphenol content and antioxidant capacity would have suggested. A possible explanation for this phenomenon is that the antibacterial property of propolis is only provoked by its polyphenol content and antioxidant capacity, while in honey there might be another factors that were not analysed in this study.

2. Table: Inhibition zone radii (mm)

Honeys	<i>E. coli</i>	<i>E. faecalis</i>	<i>P. aeruginosa</i>	<i>S. aureus</i>	<i>L. monocytogenes</i>	<i>L. innocua</i>
Acacia	0.5	0	2.25	2	2.5	1.5
Buckwheat	4	7.5	8	8.5	10	9.25
Forest	4	8.5	8.5	12.25	8.5	11.5
Manuka UMF 15+	5.5	5	6.5	9	6	7.5
Manuka UMF 20+	7	6.5	8.5	13	7.5	9.5
Manuka UMF 22+	6.5	5.5	7	12	6.5	7.5
Phacelia	2.25	4.5	5.25	5.5	5.5	7
Pine	3	6.5	7.5	7.25	7	9
Rape	2.5	4.75	6.75	6	6.25	6.5
Propolis	6.75	9.75	12.25	10.5	11.5	12

Generally, it can be said that darker coloured, honeydew honeys contain more phenolic compounds with antioxidant properties, and they are more effective against most microorganisms.

The colours of the honey samples (except Manuka honeys), and the propolis sample were analysed to find correlation between colour and other properties. The L^* value describes the brightness, and it shows that the honeydew honeys are much darker than the nectar honeys. According to the values of a^* and b^* there are red compounds in the samples, but yellow pigments are dominant. After propolis and the Manuka honeys, the commercially available darker coloured buckwheat (662.781 mg GAE/100g dm) and forest honey (432.717 mg GAE/100g dm) had the highest polyphenolic content; still no statistically significant correlation could be determined between colour and polyphenol amount. Furthermore, the dark coloured pine honey showed similar results as lighter honeys. There is significant correlation between the L^* values and the antibacterial effects ($r = -0.540$).

1. Figure: The L^* , a^* , b^* values of samples

Conclusion

The propolis sample and the Manuka honeys had a remarkable antioxidant capacity and high total phenolic content. While there is a significant correlation between these properties and antibacterial efficacy, these samples still failed to produce the effectiveness that the results would have suggested. Comparison of nectar and honeydew honeys have shown, that the dark coloured honeydew samples have greater antioxidant capacity and antibacterial effect. Significant correlation was determined between the L* value and the antimicrobial effect.

Acknowledgements

This study would not have been possible without the generous work of the employees from the Department of Microbiology and Biotechnology, the Department of Applied Chemistry, and the Department of Food Preservation in Szent István University.

References

- [1] S. Bogdanov, T. Jurendic, R. Sieber, and P. Gallmann, 'Honey for Nutrition and Health: A Review', *J. Am. Coll. Nutr.*, vol. 27, no. 6, pp. 677–689, Dec. 2008.
- [2] C. Pita-Calvo and M. Vázquez, 'Differences between honeydew and blossom honeys: A review', *Trends Food Sci. Technol.*, vol. 59, pp. 79–87, Jan. 2017.
- [3] H. Lee, J. Churey, and R. Worobo, 'Antimicrobial activity of bacterial isolates from different floral sources of honey', *Int. J. Food Microbiol.*, vol. 126, no. 1–2, pp. 240–244, Aug. 2008.
- [4] N. G Vallianou, 'Honey and its Anti-Inflammatory, Anti-Bacterial and Anti-Oxidant Properties', *Gen. Med. Open Access*, vol. 02, no. 02, 2014.
- [5] S. M. Cardoso and A. M. S. Silva, *Chemistry, biology and potential applications of honeybee plant-derived products*. 2016.

HETEROGENEOUS PHOTOCATALYSIS OF COUMARIN AND 3-CARBOXYCOUMARINIC ACID EFFECT OF NaF AND METHANOL ON THE TRANSFORMATION RATE AND FORMATION RATE OF HYDROXYLATED PRODUCTS

Máté Náfrádi¹, Dóra Kiss¹, Tünde Alapi¹

¹*Department of Inorganic and Analytical Chemistry, University of Szeged, H-6720 Szeged,
Dóm tér 7, Hungary
e-mail: nafradim@chem.u-szeged.hu*

Abstract

Using heterogeneous photocatalysis, it is complicated to determine the formation rate of hydroxyl radical (HO•) and its relative contribution to the transformation of various target substances. In this work we compared the transformation rate of coumarin and 3-carboxycoumarinic acid (3CCA), and the formation rate of their fluorescent hydroxylated intermediates under various experimental conditions. The fluorescent spectroscopic methods were optimized. The effect of NaF and methanol as a radical scavenger were also investigated. Coumarin poorly adsorbs on the surface of TiO₂; addition of NaF has no effect on the adsorption capacity, while NaF significantly hinder the adsorption of 3CCA. NaF increases the transformation rate of both model compounds, while slightly decreases the formation of their hydroxylated intermediates. Methanol decreases the transformation rates, and this effect is less pronounced in the case of 3CCA, probably because of its favored adsorption on the TiO₂ surface.

Introduction

Heterogeneous photocatalysis is a widely researched process, due to its great potential to remove recalcitrant organic pollutants from various type waters, including drinking water. The most widely used commercial photocatalyst is TiO₂, due to its great activity under UV irradiation, good stability and low price. However several publication focuses on the preparation of new, highly reactive photocatalysts. The effectiveness of photocatalysts are often described by their ability to produce hydroxyl radicals (HO•), and the optimization of methods are usually include their improved HO•-production. However the determination of the formation rate of HO• is complicated. The detection of HO• by ESR or pulse-radiolysis are complicated processes, and usually very expensive. A more simple and available method is based on the detection of fluorescence intermediates forming during the reaction of aromatic compounds with HO•. This method is generally based on the formation of the hydroxylated intermediate of coumarin, which is the umbelliferone. Another, less investigated compound is 3-carboxycoumarinic acid (3CCA), and its hydroxylated intermediate, 7-OH-3-carboxycoumarinic acid (7OH-3CCA) (*Fig.1.*).

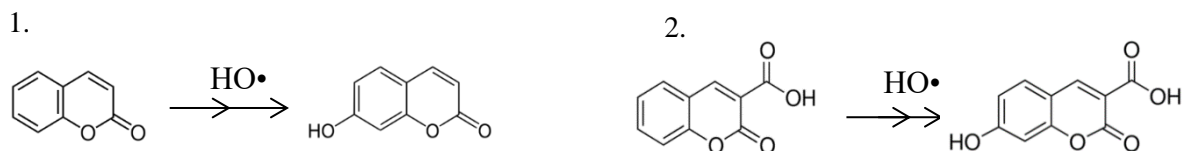


Figure 1. Coumarin and its fluorescent intermediate, umbelliferone (1.), and 3CCA and its fluorescent intermediate, 7OH-3CCA (2.) [1, 2]

Coumarin is also reported to react well with electrons ($k = 1,6 \times 10^{10} \text{ mol}^{-1} \text{ dm}^3 \text{ s}^{-1}$ [3]), therefore it may act as an electron scavenger. Transformation via direct charge transfer may be even more important using 3CCA, because of the affinity of carboxyl groups for metal oxide surfaces. The surface properties, especially the surface charge are highly important due to their influence on radical generation rate and adsorption of organic compounds. The $-\text{OH}$ groups of TiO_2 surface can be replaced by $-\text{F}$ groups via addition of NaF to the suspension. This is able to result in significant changes surface properties of the catalyst. [4]

The goal of our research is the determination and comparison of the transformation rates of two model compounds (coumarin and 3CCA), and the generation rates of formed hydroxylated intermediates. We have investigated the effect of methanol as a non-adsorbing $\text{HO}\cdot$ radical scavenger, and NaF, the surface changing agent on the transformation rate of both non-adsorbed coumarin and well adsorbed 3CCA and the formation rate of their hydroxylated intermediates.

Experimental

250 cm^3 aqueous solutions of coumarin and 3CCA ($1.0 \times 10^{-4} \text{ mol dm}^{-3}$) were irradiated in a reactor with a fluorescent mercury-vapor lamp emitting UV-light between 300 and 400 nm wavelengths. The TiO_2 containing suspension was circulated using a peristaltic pump with 330 $\text{cm}^3 \text{ min}^{-1}$ flow rate, thermostated at $25 \pm 1^\circ\text{C}$ and saturated with air. The TiO_2 photocatalyst (Aeroxide P25[®]) was added in 1.0 g dm^{-3} concentration, and dispersed by sonication. NaOH and HCl solutions were used to set the pH (measured with InoLab pH 730p) when needed. Methanol or NaF was added to the solutions in $5.0 \times 10^{-3} \text{ mol dm}^{-3}$ concentration. The samples were centrifuged and filtered using 0.22 μm syringe filters to remove the TiO_2 before analysis.

The transformation of coumarin ($\lambda_{\text{max}}=277 \text{ nm}$) and 3CCA ($\lambda_{\text{max}}=291 \text{ nm}$) were followed using spectrophotometry (Agilent 8453). Fluorescence spectroscopy (Hitachi F4500) was applied to determine the concentration of formed hydroxylated intermediates. The determination of formed umbelliferon concentration was based on the intensity of the emitted fluorescence light at 455 nm. The wavelength of excitation was 455 nm. The determination of 7OH-3CCA concentration was based on the intensity of the emitted fluorescence light at 447 nm at pH = 9.0. The wavelength of excitation was 387 nm.

Results and discussion

At first, the adsorbed amount of coumarin and 3CCA on TiO_2 surface was determined. While coumarin does not show significant affinity for the TiO_2 surface, 3CCA adsorbed well. Addition of NaF to the suspension hindered completely the adsorption of 3CCA on the TiO_2 surface, due to the changing the surface $-\text{OH}$ groups with $-\text{F}$ groups. Adsorption capacity of poorly adsorbed coumarin was not changed by this way. Desorption of 3CCA and 7OH-3CCA is necessary before the determination of their concentration, therefore we added 0.125 mol dm^{-3} NaF to each sample (recovery $\approx 98\text{-}100\%$) before analysis. Addition of NaF to the TiO_2 suspension changed the pH from 3.8 to 7.0, which effect is caused by the replacement of OH^- ions.

Due to the significant overlapping the absorption spectra of coumain and umbelliferon, 345 nm was choose as excitation wavelength, thus coumarin absorption does not disturb significantly the excitation of umbelliferon. We also investigated the pH-dependence of the fluorescence light intensity of umbelliferone, and finally set pH = 5.5 for each measurement. The concentration of coumarine was determined by spectrophotometric way (due to the absorption at 277 nm). The determination of formed umbelliferon concentration was based on the intensity of the emitted fluorescence light at 455 nm. The wavelength of excitation was

455 nm. Similar investigations were done for 3CCA, when pH was proved to be much more important factor. Deprotonated form of 3CCA emits intensive fluorescence light. Consequently pH has to be set 9.0, to avoid the emission and disturbing effect of this fluorescent light. 7OH-3CCA has an even stronger fluorescence, and its emission spectrum just slightly overlaps with its absorption spectrum and no overlapping with absorption spectrum of 3CCA. (Fig.2.) Thus the concentration of 3CCA was determined by spectrophotometric way (due to the absorption at 291 nm, pH = 3.8) The determination of formed 7OH-3CCA concentration was based on the intensity of the emitted fluorescence light at 447 nm at pH = 9.0. The wavelength of excitation was 387 nm.

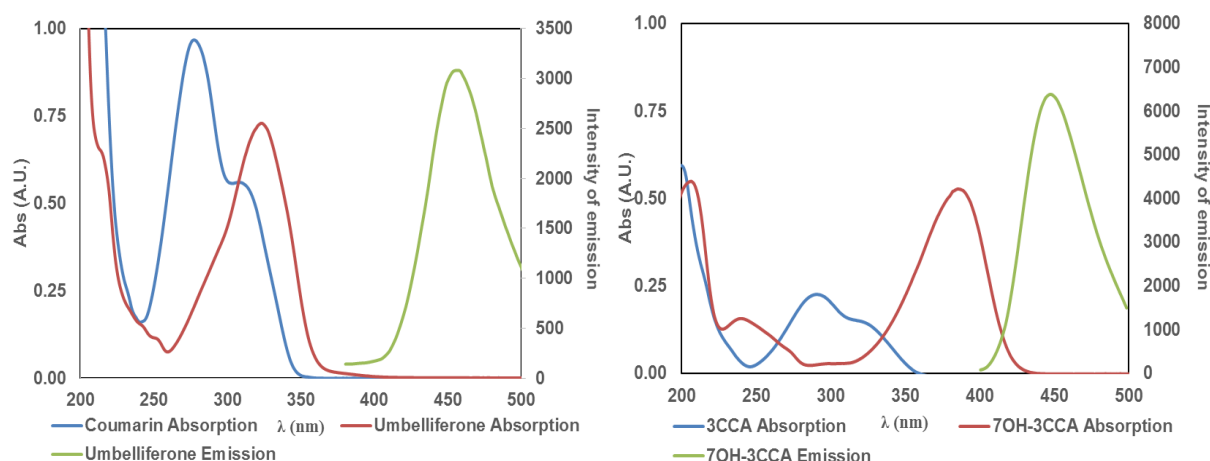


Figure 2. Absorption and emission spectra of coumain (pH = 5.5), 3CCA (pH = 9.0) and their hydroxylated intermediates

Addition of NaF significantly increased the transformation rate of coumarin, and slightly changed the formation rate of umbelliferone. However the maximum value of the concentration of formed umbelliferone and probably the transformation rate of this hydroxylated intermediate is significantly increased by NaF. Addition of methanol, as HO• scavenger reduced both the transformation rate of coumarin and formation rate of umbelliferone.

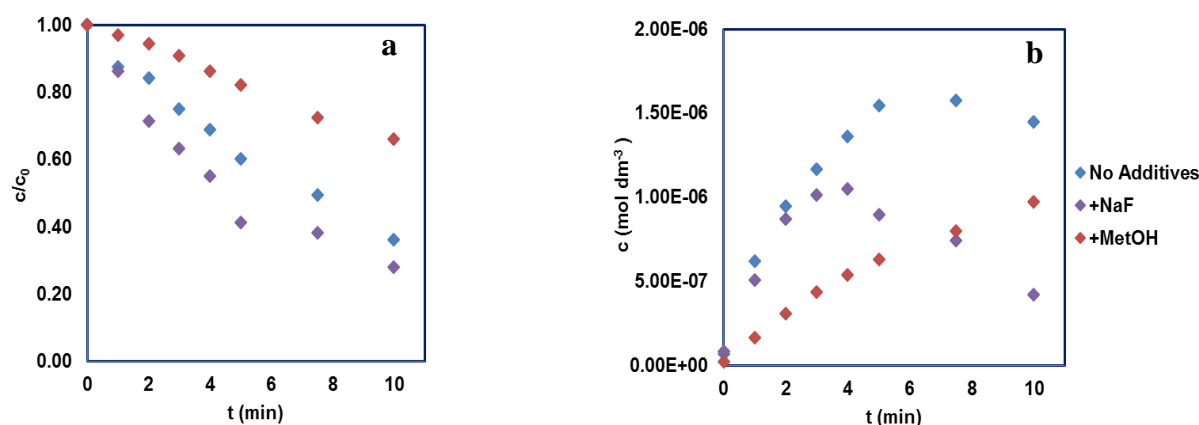


Figure 3. The relative concentration of coumarin (a), and the concentration of umbelliferone (b) as a function of time

Addition of $5.0 \times 10^{-3} \text{ mol dm}^{-3}$ NaF completely hinders the adsorption of 3CCA and 7OH-3CCA. Using 3CCA, which is well adsorbed on the surface of TiO_2 , experiments were done

with and without addition of NaF before filtration of treated samples. Addition of NaF is aimed to enhance the desorption of the 3CCA and 7OH-3CCA from the surface of the TiO₂ before determination of their concentration.

Addition of NaF increased the transformation rate of 3CCA in TiO₂ suspension under UV radiation, despite of that, the amount of adsorbed 3CCA was strongly decreased. At the same time the formation rate of 7OH-3CCA did not change. Methanol decreased both the transformation rate of 3CCA and formation rate of 7OH-CCA by scavenging HO•. We have to mention that, the effect of MeOH is much more pronounced in the case of coumarin than in the case of 3CCA most likely because of the different adsorption properties.

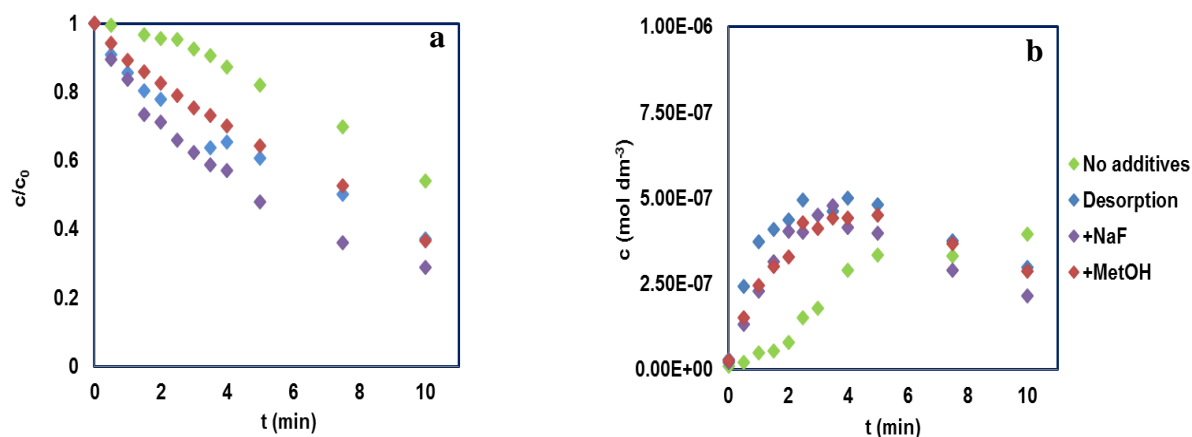


Figure 4. The relative concentration of 3CCA (a), and the concentration of 7OH-3CCA (b) as a function of time

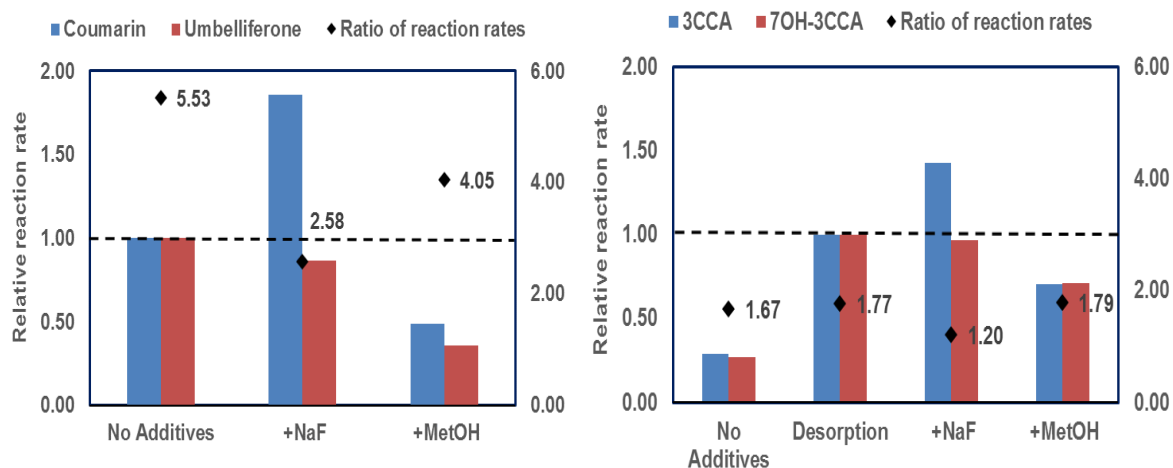


Figure 5. The relative reaction rates of the transformation of coumarin and 3CCA and formation of their hydroxylated intermediates, and the ratio of these values

The importance of HO• was proved by comparing the ratio of the transformation rate of the model compound and formation rate of the hydroxylated intermediate. In the case of coumarin, NaF significantly reduced this value (5.53→2.58), which probably indicates a change in the reaction mechanism. In the case of 3CCA this value changes to a lesser extent (1.77→1.20), which may indicate, that the influence of NaF via changing the adsorption properties is more important in this case. Addition of methanol slightly decreases these values (5.53→4.05 and 1.77→1.79). NaF is probably able to affect the transformation rate by two

different ways: changing the surface properties of TiO₂ the relative contribution of the direct charge transfer and HO• based reaction can change too. The most important effect of methanol is the decrease of the relative contribution of the HO• based reaction to the transformation of parent compounds (coumarin and 3CCA).

Conclusion

- Heterogeneous photocatalysis of coumarin and 3-Hydroxycoumarinic acid (3CCA) were investigate and compared in the presence of NaF and methanol.
- NaF strongly prevents the adsorption of 3CCA, while it has no effect on the adsorption of coumarin.
- NaF increases transformation rates for both model compounds, while reducing the formation of hydroxylated intermediates, possibly due to changes in their access to photogenerated charges and HO•.
- Methanol reduces the transformation rate of coumarin and 3CCA together with the formation rate of their hydroxylated intermediates by scavenging the HO•.

References

- [1] Y. Manevich, K.D. Heldt, J.E. Biaglow, *Radiation Research*. 148 (1997) 580-591.
- [2] Y. Nosaka, M. Nishikawa, A.Y. Nosaka, *Molecules*. 19 (2014) 18248-18267.
- [3] E.J. Land, T.G. Truscott, *Photochem. Photobiol.* 29 (1979) 861-866.
- [4] W. El-Alamia, D.G. Sousab, C. Fernández Rodríguez, O.G. Díaz, J.M.D. Rodríguez, M.El Azzouzia, J. Araña, J. *Photochem. Photobiol. A* 348 (2017) 139–149.

ENANTIOMER SEPARATION OF CHIRAL TETRAHYDROISOQUINOLINE ANALOGS BY SUPERCRITICAL FLUID CHROMATOGRAPHY AND HIGH-PERFORMANCE LIQUID CHROMATOGRAPHY

Attila Bajtai¹, Dániel Tanács¹, Tímea Orosz¹, Gyula Lajkó², István Szatmári², Ferenc Fülöp², Wolfgang Lindner³, István Ilisz¹, Antal Péter¹

¹*Institute of Pharmaceutical Analysis, University of Szeged, Somogyi utca 4, H-6720 Szeged, Hungary*

²*Institute of Pharmaceutical Chemistry, University of Szeged, Eötvös utca 6, H-6720 Szeged, Hungary*

³*Department of Analytical Chemistry, University of Vienna, Währinger Strasse 83, 1090 Vienna, Austria*

e-mail: bajtai@chem.u-szeged.hu

1,2,3,4-Tetrahydroisoquinoline and its analogs have received serious attention from synthetic and medicinal chemists lately. These compounds are core structural elements present in several peptide-based drugs and form an important part of various biologically active compounds. The optical purity of potential pharmacons has an immense importance during chiral drug development. Hence, there is a need for efficient separation methods of chiral 1,2,3,4-tetrahydroisoquinoline analogs. Selection of suitable chromatography technique is the first and the most difficult step in the method development. In our study we investigated the similarities and differences between liquid chromatography (LC) and supercritical fluid chromatography (SFC) methods on the bases of the separation of six 1,2,3,4-tetrahydroisoquinoline analogs and three structurally closely related enantiomer pairs.

Nine chiral stationary phases (CSPs) including quinidine- or quinine-based zwitterionic and polysaccharides based selectors were applied in HPLC and SFC mode to evaluate the chiral separation of the nine structurally related analogs. HPLC measurements were carried out in normal phase mode on seven polysaccharide-based CSPs and in polar ionic mode on the two zwitterionic CSPs. In normal phase LC mode, the effects of the composition of the bulk solvent and the natures of the alcohol and amine additives, while in SFC mode the effects of the content and natures of alcohol modifier, the counter-ion concentration and the structures of the analytes were investigated. The separations of the stereoisomers were optimized in both SFC and LC modes.

The effect of column temperature on the separation was also studied to gain deeper understanding of the complex thermodynamic processes taking part in the enantio-recognition. Thermodynamic parameters were calculated applying van't Hoff plots and the results showed that on the polysaccharide-based columns in both normal phase LC mode and in SFC mode mostly enthalpically-driven enantiomer separations were dominant. However, in some cases, entropically-driven separations were also observed.

The NP and SFC chromatographic mode exhibited different effectiveness in the separation of stereoisomers: separation was more efficient in SFC mode, however, sometimes very high resolutions were achieved in NP LC mode, which shows the different suitability of the SFC mode.

LABORATORY CHALLENGES OF DETECTING SYNTHETIC CANNABINOIDS IN URINE SAMPLES – A NEW SAMPLE PREPARATION METHOD

Boglárka Barna¹, Tímea Körmöczi¹, Éva Sija², Róbert Berkecz¹

¹*Department of Medical Chemistry, University of Szeged, H-6720 Szeged, Dóm tér 8, Hungary*

²*Institute of Forensic Medicine, University of Szeged, H-6724 Szeged, Kossuth Lajos sgt. 40, Hungary*

e-mail: berkecz.robert@med.u-szeged.hu

Abstract

Synthetic cannabinoids (SCs) put the spotlight on the designer drugs' market due to their dangerous – in some cases lethal – biological effects and easy accessibility. They are more potent than the well-known Δ^9 -tetrahydrocannabinol (THC) thanks to their special pharmacodynamic properties. The number of novel SCs on the market and of their users is growing which urges the forensic laboratories to use precise SCs detection methods routinely. Our aim was to develop a new sample preparation method for the newest 24 SCs analysis in urine samples achieving high recovery of SCs. Ethyl acetate was used instead of the traditional acetonitrile, and the targeted analysis of SCs was performed by use of liquid chromatography-electrospray ionization-tandem mass spectrometry (LC-MS/MS) method. The related matrix effect and process efficiency of sample preparation method were taken in consideration as well in our study.

Introduction

'Designer drug' is an almost 40-year-old term to describe those pharmaceuticals which trigger the same biological effect as well-known and banned substances of abuse do such as THC. Synthetic cannabinoids are a new subtype of the designer drug class which are aiming to mimic the recreational effects of marijuana by binding to the endogen cannabinoid receptors (CB₁ and CB₂), and they go by the street name of 'K2' or 'Spice'. Although SCs are often claimed to be the 'legal' and 'safe' analogues of marijuana it is far from the truth. As soon as the exact structure of a SCs is identified, it is immediately put on the illegal list of drugs, moreover, compared to marijuana, SCs have much stronger effect on the human body, because they are full (super) agonists of CB receptors while marijuana is a partial agonist [1]. This pharmacodynamic property of SCs is the key to understand why these are extremely dangerous. A hundred times lower concentration of SC is enough to trigger the same effect as can be obtained by using marijuana. [2] (*Figure 1*)

On the top of that, the endocannabinoid system crosses all over the human body and affects many different physiological functions; CB₁ receptors mainly can be found in the central nervous system (CNS) and on adipocytes – these receptors are involved in lipid metabolism, hence SCs originally were developed to treat obesity [3], while CB₂ receptors prominently play a role in immune modulation [4]. Clinical symptoms of acute SC intoxication are agitation, hallucinations, psychosis, anxiety, seizures and panic attacks [5]. Additionally, cardiovascular adverse effects are often present as well such as chest pain, hypertension and EKG abnormalities. [6] Lethal overdoses of SC are mostly linked to these cardiovascular effects. The pathophysiology behind its effects still remains unclear, but it is most likely linked to β -receptor activation in the heart. [7]

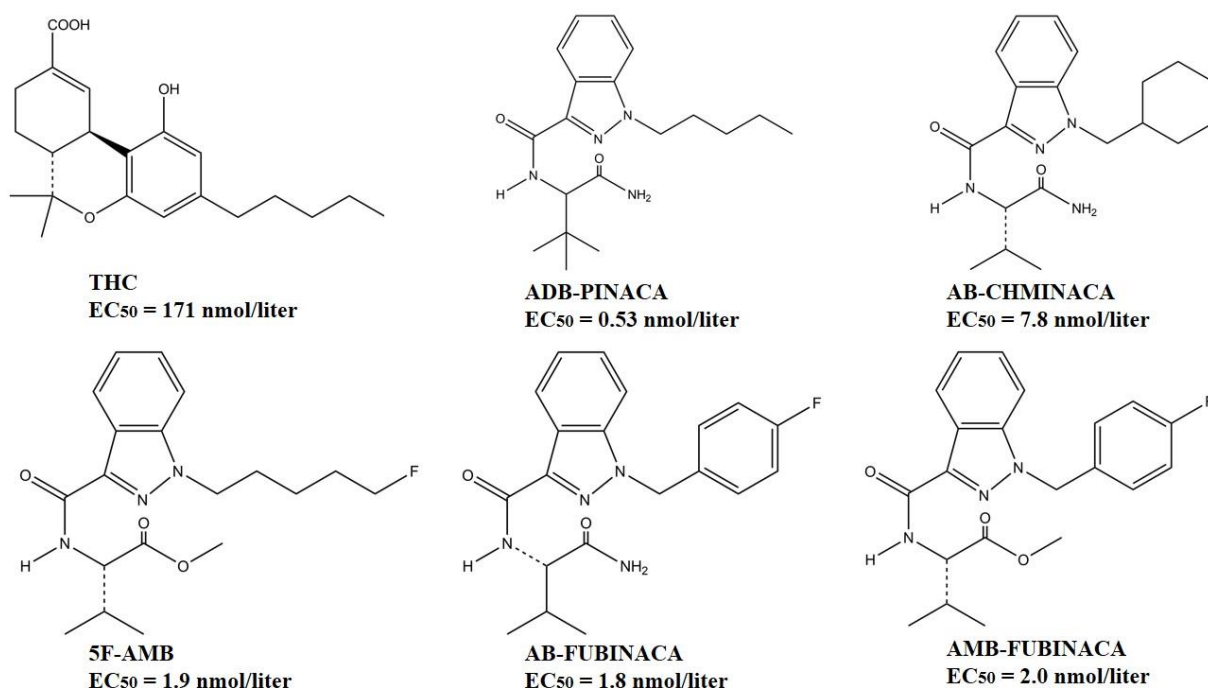


Figure 1 In vitro effective concentration required for 50% maximal response (EC_{50}) and the molecular structure of SC are shown.

The number of SC users has been grown in the last decade [8], and it lead to a demand towards forensic laboratories to be able to analyze the newest SCs in low concentration accurately from biological samples. Sample preparation method using acetonitrile (ACN) became widespread in laboratory practice. Our aim was to challenge this method and try to develop a more effective sample preparation way to maximize the recovery of SCs from urine samples.

Experimental

Sample preparation

During sample preparation control urine with no drug or drug metabolite content was used. The mixture of 24 SCs was added to the samples in known concentration (**Fig. 2**). Three series of samples were prepared and measured in this study, one series was prepared with the use of the original method and two were prepared with the newly developed method. The original method uses ACN as organic solvent and ammonium sulphate for saturation of aqueous phase to obtain two phases, while the new method applies ethyl acetate (EtOAc) as solvent and ammonia for pH level setting (**Fig. 2**). In order to determine the proper volume of EtOAc, 2, 4, 6, 8 and 10 mL were tested and no significant change was found over 4 mL in the recovery of SCs, therefore 4 mL was chosen for practical reasons. All other steps and the used chemicals were the same in both methods. After 1 min mixing, upon 5 min of incubation at room temperature, the sample was centrifuged at 2500 rpm for 8 min. In case of original method, 2 mL of the upper phase, while at new methods, 3 mL of top layer was collected. For double extraction procedure, the lower aqueous phase was re-extracted with 3 mL of EtOAc and 3 mL of upper phase was combined with the first 3 mL portion. The supernatants were dried by nitrogen stream at ambient temperature and the dried extracts were reconstituted in 200 μL ACN/water (1:1, v/v) containing 0.1 % formic acid mixture for LC-MS/MS measurement.

Determination of recovery, Matrix effect and process efficiency of methods were performed according to the protocol as described by Helga Trufelli and co- workers. [9]

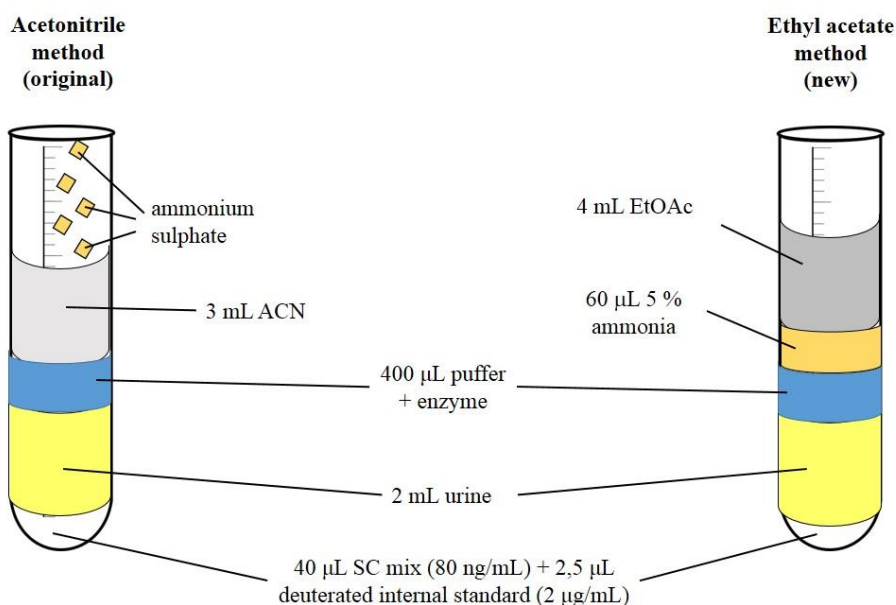


Figure 2 Comparison of the sample preparation methods

LC-MS/MS analysis

Separation was performed using an Agilent 1100 series HPLC system with Kinetex C18 column (100 x 2.1 mm, 2.6 µm) combined with a 50 x 2.1 mm guard column from Phenomenex. Injection volume was 20 µL. Elution was achieved within 6 min with a mobile phase composed of 0.1% FA in water (A) and 0.1% FA in ACN (B) at a flow rate of 0.4 mL/min. The gradient started with 50% B, ramped to 100% B within 4 min, held for 2 min. Autosampler and column oven temperatures were setting to 16 and 50 °C, respectively. The LC effluent was directed through the Agilent diverge valve to a Finnigan ESI interface on a Finnigan TSQ 7000 triple quadrupole mass spectrometer. The instrument was operated in the positive mode with a scan time of 0.3 s. The capillary heater was set at 250°C. The spray voltage was fixed at 4.5 kV. The collision gas (argon) pressure was set to 2.0 mTorr; the collision energy was optimized to two MS/MS transitions (quantifier, qualifier ions) per analyte. An electron multiplier voltage of 1900 V was used.

Results and discussion

The original acetonitrile method resulted in mean recovery of 66.3% for SCs, while the ethyl acetate method with single extraction improved to 75.2%, and the double extraction provided 91.8 % (Fig. 3).

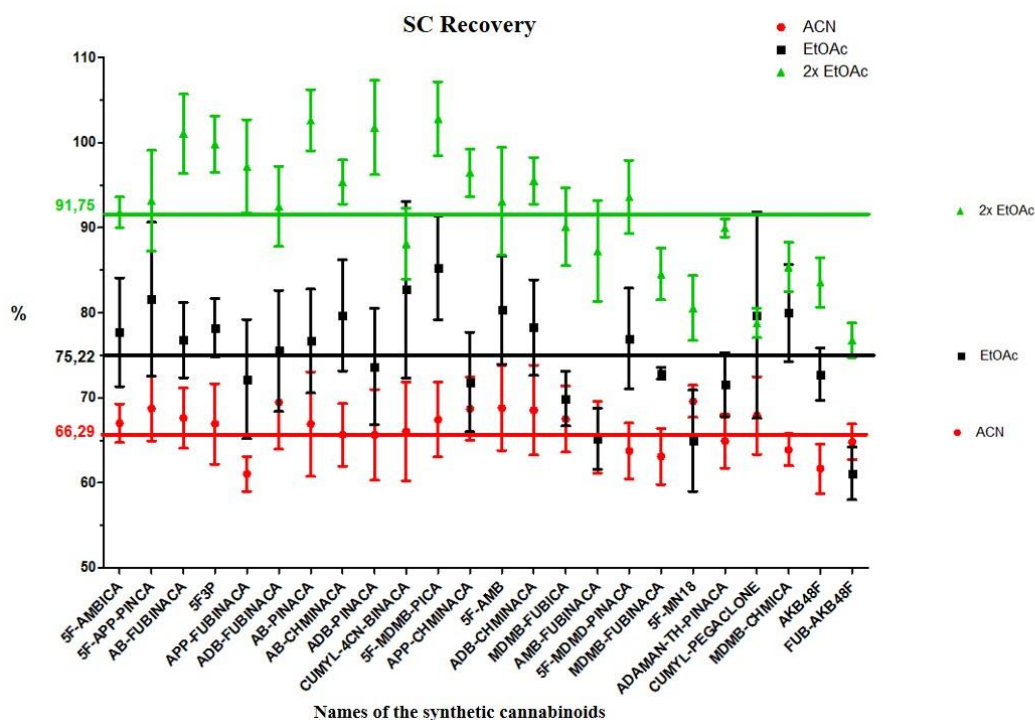


Figure 3 Recovery of 24 SCs with the acetonitrile and the single and double extraction ethyl acetate method

It was also evaluated if the matrix effect altered the recovery results. Matrix effects are caused by co-eluting matrix components (endogenous, exogenous) that alter the ionization of target analytes as well as the chromatographic behavior of target analytes, leading to reduced or increased sensitivity of the analysis. [10]

It was found that the matrix effect may cause more or less effective detection if each SC is evaluated individually. For example, the matrix effect decreased the peak area of MDMB-CHMICA, CUMYL-PEGACLONE, 5F-MDMB-PINACA, and 5F-AMBICA, especially with the ethyl acetate method, while it had a positive effect on the AMB-FUBINACA, 5F-AMB, CUMYL-4CM-BINACA, and 5F-MDMB-PICA. In some cases, the use of different solvents (ACN and EtOAc) resulted in opposite-signed matrix effect, e.g. the matrix effect with the use of ethyl acetate decrease the peak area of MDMB-FUBINACA and AB-PINACA, while the use of acetonitrile increased it. However, if the matrix effect was projected to the whole sample, meaning that all 24 SCs were considered together, it did not influence the effectiveness of the detection significantly.

The process efficiency was also measured. The mean process efficiency with the original acetonitrile method was 69.61%, with ethyl acetate, single extraction was 75.90%, and with ethyl acetate, double extraction was 89.10%.

Conclusion

Using double extraction with ethyl acetate solvent provided the highest recovery of SCs, and it is unambiguously more effective than the original ACN method in case of urine samples. Additionally, the new method is easier to conduct in the forensic laboratory environment. As a result of these two beneficial properties of the new sample preparation method, it has been introduced to everyday forensic laboratory practice in the Department of Forensic Medicine, University of Szeged.

New versions of SCs may appear any day on the market, this is why forensic laboratories should always use the best available sample preparation and detection methods, unless they will be unprepared for the challenges set by the designer drug market.

Acknowledgements

This study is supported by the ID number: *EFOP-3.6.1-16-2016-00008* EU project.

References

- [1] *Pharmacological and Toxicological Effects of Synthetic Cannabinoids and Their Metabolites*. **Fantegrossi, Sherrica Tai and William E.** 2017, *Curr Top Behav Neurosci.*, pp. 32: 249–262.
- [2] *“Zombie” Outbreak Caused by the Synthetic Cannabinoid AMB-FUBINACA in New York*. **Axel J. Adams, B.S., Samuel D. Banister, Ph.D., Lisandro Irizarry, M.D., Jordan Trecki, Ph.D., Michael Schwartz, M.D., M.P.H., and Roy Gerona, Ph.D.** *New England Journal of Medicine* : s.n., 2017, Vols. 376:235-242.
- [3] *Cannabis in fat: high hopes to treat obesity*. **Melody N. Hawkins, Tamas L. Horvath.** *The Journal of Clinical Investigation* : s.n., 2017, Vols. Volume 127, Issue 11.
- [4] *Is lipid signaling through cannabinoid 2 receptors part of a protective system?* **P.Pachera, R.Mechoulamb.** Pages 193-211, *Progress in Lipid Research* : s.n., 2011, Vols. 50, Issue 2.
- [5] *Toxicological Findings of Synthetic Cannabinoids in Recreational Users*. **Robert Kronstrand, Markus Roman, Mikael Andersson, Arne Eklund.** *Journal of Analytical Toxicology* : s.n., 2013, Vols. Volume 37, Issue 8, Pages 534–541.
- [6] *Cardiotoxicity associated with the synthetic cannabinoid, K9, with laboratory confirmation*. **Young AC, Schwarz E, Medina G, Obafemi A, Feng SY, Kane C, Kleinschmidt K.** *American Journal of Emergency Medicine* : s.n., 2012, Vols. 1320.e5-7.
- [7] *Receptors and Channels Targeted by Synthetic Cannabinoid Receptor Agonists and Antagonists*. **Pertwee, R.G.** *Curr Med Chem* : s.n., 2011, Vols. 17(14): 1360–1381.
- [8] *A Survey of Synthetic Cannabinoid Consumption by Current Cannabis Users*. **Erik W. Gunderson, MD, Heather M. Haughey, PhD, Nassima Ait-Daoud, MD, Amruta S. Joshi, MS, and Carl L. Hart, PhD.** *Subst Abus.* : s.n., 2014, Vols. 35(2): 184–189.
- [9] *An overview of matrix effects in liquid chromatography-mass spectrometry*. **Trufelli H, Palma P, Famiglini G, Cappiello A.** *Mass Spectrom Rev.* 2011, pp. 30(3):491-509.
- [10] *Biological Matrix Effects in Quantitative Tandem Mass Spectrometry-Based Analytical Methods: Advancing Biomonitoring*. **Parinya Panuwet, 1,* Ronald E. Hunter, Jr.,1,3 Priya E. D’Souza,1 Xianyu Chen,1,2 Samantha A. Radford,1,2 Jordan R. Cohen,1 M. Elizabeth Marder, Kostya Kartavenka, P. Barry Ryan, and Dana Boyd Barr.** *Crit Rev Anal Chem.* : s.n., 2016, Vols. 46(2): 93–105.

Poster Proceedings

EMISSIONS OF TOTAL VOLATILE ORGANIC COMPOUNDS DURING THE DIGITAL PRINTING PROCESS

Savka Adamović¹, Aleksandra Mihailović¹, Dragan Adamović¹

¹University of Novi Sad, Faculty of Technical Sciences, Trg Dositeja Obradovića 6,
21000 Novi Sad, Serbia
e-mail: adamovicsavka@uns.ac.rs

Abstract

The impact of the type of digital machine on increasing of total volatile organic compounds (TVOCs) in the ambient air of the digital printing office was analysed in this study. For that purpose, the TVOCs concentrations in gas samples were measured by mobile gas chromatograph Voyager-Photovac. The cumulative concentrations values of TVOCs for the single-color digital machine were in the range from 0.56 to 5.90 ppm and almost 4 and 25 times below compared to the same values for the four-color digital machine (14.01 - 24.84 ppm). The obtained results could be useful for the future risk assessment of indoor exposure of TVOCs, and for the creation of printing indoor air quality guidelines of the Republic of Serbia.

Key words: Digital printing process, total volatile organic compounds, indoor air quality

Introduction

Indoor air quality contaminants consist of the following compounds: CO, CO₂, NO₂, H₂S, SO₂, NH₃, formaldehyde, volatile organic compounds (VOCs), ozone, radon, and microorganisms, which are considered harmful [1].

VOCs are a class of organic compounds which have the following characteristics: boiling temperatures less than 50-260°C at standard atmospheric pressure and melting points below room temperature [2]. VOCs are the most common chemical harmful pollutants in the indoor air that we breathe and exposure to them can induce health problems such as asthma, nervous system impairment and cancers [3]. These pollutants can be classified into the following groups: aliphatic, aromatic, halogenated, and oxygenated, including, for instance, benzene, trichloroethylene, toluene, alcohols, acrolein, and polycyclic aromatic hydrocarbons [1].

The sources of VOCs in indoor environments can be divided into external (vehicular traffic and industry which emitted gas streams) and indoor [4]. Indoor sources of VOCs include building materials (floor and insulation), decorative materials (paints, furnishings, and carpet), cleaning compounds, cosmetics products, combustion products, tobacco smoke, insecticides, and copying and printing machines [1,4]. Also, gas streams contaminated VOCs produce variety industrial and commercial processes, such as printing, metal decorating, oil supplying, dry cleaning, metal degreasing, manufacturing of organic compounds and polymers, food processing, etc. [5].

The use of digital printing equipments (laser printers and photocopiers) has grown exponentially over the last decade as one of the major technologies for printing a document [6,7], a wide range of market application (decoration of porcelain, glass, ceramic tile products, etc.) [8] and the textile industry products [9]. The digital printing CMYK (i.e., cyan, magenta, yellow and black) inks, which are called toners, are a composite of polymer, colourant, and other additives that are essential for printing process [7].

As the sum of all individual VOCs in the target gas stream, the TVOCs often were used for evaluating the air indoor quality. It is important to note that currently there are no TVOCs emission standards that prescribe indoor TVOCs concentration levels [10].

The objective of this study was to evaluate the impact of the type of digital machine on increasing of TVOCs concentrations in the ambient air of the digital printing office. The quantification of the concentration levels of TVOCs in the ambient air of the digital printing office was conducted over ten working days.

Experimental

Digital printing office

Digital printing processes (electrophotographic procedure) were performed on single-color Xerox D95A and the four-color Xerox DocuColor 252 printing machines during ten days of monitoring of TVOCs concentrations. The offset paper ($G = 80 \text{ g/m}^2$) and cyan, magenta, yellow and black (CMYK) digital toners (manufactured by Xerox), were used as the graphic material. There are two employees in the digital printing office, but as the printing office is used for student education, from two to five students were present in practice during the monitoring of TVOCs concentrations.

Measurement of TVOCs concentrations

The TVOCs concentrations have been analysed in gas samples by Perkin Elmer Photovac Voyager-mobil GC chromatograph. The Voyager-mobil GC uses the principles of gas chromatography (GC) to separate and identify volatile organic compounds.

Mobile gas chromatograph Voyager-Photovac is a device with in-situ and online, on a short time interval, qualitatively and quantitatively and very precisely (with a detection limit of 1 ppb) determines the composition of the components of the gaseous samples. The standard for each component is stored in the Voyager database as retention time, peak area and concentration. In each analysis of an unknown gaseous sample, the retention time of the peak was compared with the retention times from the "base". The Site Chart software package is used to quickly and accurately processing the obtained results [11].

The operational parameters of ambient air during analysis of TVOCs concentrations by mobile gas chromatograph Voyager-Photovac are temperature (25 - 34°C), pressure (1005 - 1010 mbar) and relative humidity (21.5 - 33.7%). Parameters of ambient air were measured by the RH520A, manufactured by Extech Instruments, USA.

The time required for sampling, analysis and data processing by the gas chromatograph Voyager-Photovac is 40 minutes. For this reason, the monitoring of TVOCs concentrations was carried out every hour. Daily eight-time values of TVOCs concentrations are calculated by a cumulative compilation of one-hour data updated every hour. Also, concentration levels of TVOCs were measured one-hour before the start of the operations of digital machines during sampling.

Results and discussion

Detected concentrations of TVOCs before operation of digital machines (zero values) during monitoring were in the range from 0.04 to 0.10 ppm for single-color and from 0.07 to 0.12 ppm for four-color digital machine. The detected concentrations of TVOCs during the eight-hour operation for the tested machines were reduced by the zero value to obtain real TVOCs concentrations.

The statistical overview of minimum and maximum concentrations, their cumulative and mean values of TVOCs during ten days of monitoring for single-color and four-color digital machines are shown in Table 1.

Table 1. A statistical overview of TVOCs data for single-color and four-color digital machines for ten days of monitoring

Data	Single-color digital machine	Four-color digital machine
Total number of measurements	80	80
MIN C_{TVOCs} (ppm)	0.10	1.11
MAX C_{TVOCs} (ppm)	1.06	4.66
MIN cumulative value of C_{TVOCs} (ppm)	0.56	14.01
MAX cumulative value of C_{TVOCs} (ppm)	5.90	24.84
MIN mean value of C_{TVOCs} (ppm)	0.07	1.75
MAX mean value of C_{TVOCs} (ppm)	0.74	3.11

The lowest concentration of TVOCs (0.10 ppm) in addition to a single-color printing machine was measured during the eighth hour of the sixth day of monitoring. The highest individual concentration of TVOCs (1.06 ppm) was measured during the fourth hour of the first day of monitoring. In the case of the four-color digital machine results for ten working days shows that the highest concentration of TVOCs of 4.66 ppm was measured during the fifth hour of the fourth day, while the lowest concentration level of TVOCs (1.11 ppm) was measured at eight hours on the tenth day.

Analyzing the influence of the type of digital machine on increasing the concentrations of TVOCs in the ambient air of the digital printing office, it has been found that the significant contribution has four-color (Figure 1a) than the single-color digital machine (Figure 1b). The cumulative and mean values of TVOCs concentrations for the single-color digital machine were in the range: from 0.56 to 5.90 ppm and from 0.07 to 0.74 ppm, respectively (Table 1). For a four-color digital machine cumulative and mean values are almost 4.2 to 25 times higher compared to the same value for the single-color machine.

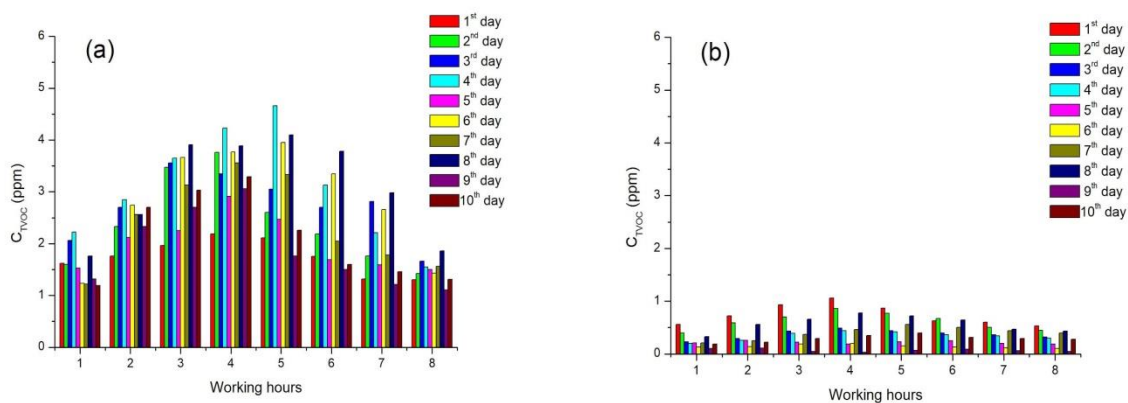


Figure 1. Concentrations of TVOCs for eight-hour operation during ten days of monitoring in addition to a) four-color Xerox DocuColor 252 and b) single-color Xerox D95A printing machines

According to the manufacturer, Xerox toners broadcast minimal quantities of VOCs concentrations because they consist mainly of pigments, polymers (styrene-acrylic, styrene-butadiene or polyester polymers) and small amounts of functional additives [12]. However, the conducted ten-day monitoring showed that the digital printing process broadcasts the cumulative value of TVOCs concentrations for eight-hour working hours at intervals from almost 0.5 to 6 ppm and 14 to 25 ppm for a single-color and four-color digital machine, respectively.

The Occupational Safety and Health Administration (OSHA) prescribes Permissible Exposure Limits (PEL) and the Short-Term Exposure Limit (STEL) for individual VOC, but not for TVOCs [13]. Also, Regulation on the conditions for monitoring and air quality requirements of the Republic of Serbia [14] does not prescribe emission limit values for TVOCs. Therefore, it is necessary to carry out long-term monitoring in digital as well as in other printing techniques and include increasing number of production printing facilities (which vary in size, type of machine they use, variety of printing materials, etc.) in order to obtain relevant data to complement legal regulations of the Republic of Serbia.

Conclusion

The conducted ten-day monitoring showed that the digital printing process contributes to the quality of ambient air through the emission of TVOCs. The results of the TVOCs concentrations control indicate that the highest concentration levels of 1.06 ppm and 4.66 ppm were detected during a one-hour of measurement for a single-color and four-color digital machine, respectively.

Analyzing the increase in the concentration of TVOCs in the ambient air of the digital printing office, it has been found that a more significant contribution has a four-color than a single-color machine. The cumulative and mean values for the four-color digital machine are in the range from 14.01 to 24.84 ppm and from 1.75 to 3.11 ppm, respectively. For the single-color digital machine, the cumulative (0.56 - 5.90 ppm) and mean (0.07 - 0.74 ppm) values are lower almost 4.2 to 25 times compared to the same value for the single-color machine.

References

- [1] A. Al-Hemoud, L. Al-Awadi, A. Al-Khayat, W. Behbahan, *Build. Environ.* 137 (2018) 127.
- [2] X. Zhang, Z. Xue, H. Li, L. Yan, Y. Yang, Y. Wang, J. Duan, L. Li, F. Chai, M. Cheng, W. Zhang, *J. Environ. Sci.* 55 (2017) 69.
- [3] D.H. Do, C. Walgraeve, A.N. Amare, K.R. Barai, A.E. Parao, K. Demeestere, H. van Langenhove, *Atmos. Environ.* 119 (2015) 330.
- [4] A. Cincinelli, T. Martellini, A. Amore, L. Dei, G. Marrazza, E. Carretti, F. Belosi, F. Ravegnani, P. Leva, *Sci. Total Environ.* 572 (2016) 333.
- [5] J.G. Watson, J.C. Chow, E.M. Fujita, *Atmos. Environ.* 35 (2001) 1567.
- [6] S.V. Pirela, G. Pyrgiotakis, D. Bello, T. Thomas, V. Castranova, P. Demokritou, *Inhal. Toxicol.*, 26 (2014) 400.
- [7] M. Ataefard, F. Nourmohammadian, *J. Lumin.* 167 (2015) 254.
- [8] J.-H. Lee, J.-W. Kweon, W.-S. Cho, J.-H. Kim, K.-T. Hwang, H.-J. Hwang, K.-S. Han, *Ceram. Int.* 44 (2018) 14151.
- [9] W. Ye, J. Lin, R. Borrego, D. Chen, A. Sotto, P. Luis, M. Liu, S. Zhao, C.Y. Tang, B. Van der Bruggen, *Sep. Purif. Technol.* 197 (2018) 27.
- [10] Y. Yang, L. Li, *J. Clean. Prod.*, 170 (2018) 1268.
- [11] D. Adamović, J. Dorić, M. Vojinović Miloradov, S. Adamović, S. Pap, J. Radonić, M. Turk Sekulić, *Sci. Total Environ.* 639 (2018) 339.
- [12] Xerox Corporation (2017) The Safety of Xerox Products, URL: https://www.xerox.com/downloads/usa/en/e/environment_safetyfacts.pdf.
- [13] OSHA, Occupational Safety and Health Administration (n.d.), Table Z-1-Limits for Air Contaminants, URL: https://www.osha.gov/pls/oshaweb/owadisp.show_document?p_table=STANDARDS&p_id=9992.
- [14] Official Gazette the Republic of Serbia. No. 11/2010, 75/2010 and 63/2013, Regulation on the conditions for monitoring and air quality requirements of the Republic of Serbia, 2013 (In Serbian).URL: <http://demo.paragraf.rs/WebParagrafDemo/?actid=107025>.

Mn-TETRATOLYLPORPHYRIN-NANO-Au COMPLEX SENSITIVE TO 4-AMINOSALICYLIC ACID

Anca Lascu^a, Diana Anghel^a, Bogdan Taranu^b, Luminita Salageanu^c

^a Institute of Chemistry Timisoara of Romanian Academy, M. Viteazul Ave. 24, 300223-Timisoara, Romania, Tel: +40256/491818; Fax: +40256/491824

^b National Institute for Research and Development in Electrochemistry and Condensed Matter, 1

Plautius Andronescu Street, 300569 Timisoara, Romania

^c Health Insurance House Timis, Corbului Street 4, 300239-Timisoara, Romania

Abstract

Porphyrins and metalloporphyrins provide recognition sites for amino acids both through their cationic central metal ion and due to various functional groups at the four *meso*- and the eight β -positions of pyrroles. Immobilized metallo-phenylporphyrins can be used as sensitive and selective sensors for different analytes as they provide two ways of interaction via the metallic center of porphyrin and between the π electrons of the macrocycles and the solute [1].

The purpose of this study was to establish an easy way to determine low concentrations of 4-aminosalicylic acid (**PAS**) using hybrid materials obtained from porphyrins, namely: Mn(III)-tetratolylporphyrin chloride (**MnTTPCl**) and gold nanoparticles (**n-Au**).

During the adding of 4-aminosalicylic acid to the **MnTTPCl-nAu** hybrid it can be observed that the intensity of the plasmonic band is continuously decreasing with the increase in 4-aminosalicylic acid concentration. Another notable feature is the bathochromic shift of the major peak to higher wavelengths from 619 nm to 622 nm. Equilibria processes are involved and accompanied by an isosbestic point around 725 nm. The dependence between the absorption intensity of the plasmonic complex and the concentration of 4-aminosalicylic acid is linear, with an excellent correlation coefficient of 99.31% in a wide range of 4-aminosalicylic acid concentrations: $2.88 \times 10^{-5} \text{ M}$ - $8.89 \times 10^{-4} \text{ M}$.

Introduction

Aminosalicylic acid is known to perform bacteriostatic activity against *Mycobacterium tuberculosis*, being involved in suppression of reproduction of bacteria, leading finally to cell death. This compound was also used as drug against tuberculosis (**TB**) but it has debilitating side effects such as anorexia, epigastria distress, nausea so that it is currently used only in the severe cases of multi-drug resistant **TB** and only by targeted release [1]. The detection of PAS in urine is necessary in order to monitor and avoid the toxic doses intake of PAS, due to its side effects [2]. The detection of amino acids is affected by the changes of pH [3]. A detector for amino acids at pH 7 should have a receptor that is sensitive to both the deprotonated carboxyl group and protonated amino group.

Spectrophotometric techniques are also applied in detection of **PAS**, based on the changes in the color of different dyes such as p-dimethylaminobenzaldehyde (DAB), and p-dimethylaminocinnamaldehyde (DAC) [4] upon interaction with amino acids.

Another type of analyses were capillary zone electrophoresis and flow injection analysis that was used for the determination of both p-aminosalicylic acid (PAS) and its metabolite N-acetyl-p-aminosalicylic acid (N-acetyl-PAS) in urine without any sample pretreatment [5, 6].

Porphyrins and metalloporphyrins might provide recognition sites for amino acids and by two avenues of interaction: via the metallic center of porphyrin [7] and between the π electrons of the macrocycles and the solute [3].

The aim of this work was to establish an easy spectrophotometric way to determine low concentrations of 4-aminosalicylic acid using hybrid materials obtained from porphyrins, namely: Mn(III)-tetratolylporphyrin chloride (structure in Figure 1) and gold nanoparticles.

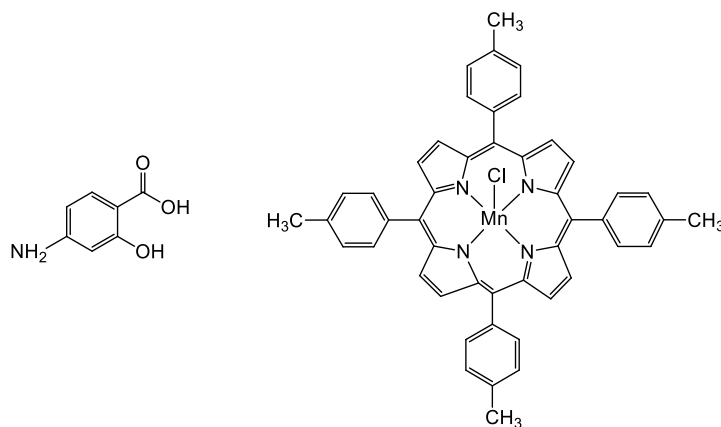


Figure 1: The Structure of *PAS* and *MnTTPCl*

Materials and methods

The solvents and PAS were purchased from Merck (THF, 4-aminosalicylic acid). 5,10,15,20-tetra(4-methyl-phenyl)porphyrinato manganese (III) chloride (MnTTPCl) was prepared from the porphyrin base previously synthesized and characterized [8] using modified Adler's method [9, 10] and the gold colloid was synthesized in an environmentally friendly manner [11].

Apparatus

A JASCO model V-650 spectrometer was used for the UV-vis measurements in 1 cm quartz cuvettes at room temperature. A Titan G2 80-200 TEM/STEM microscope (FEI Company, The Netherlands) was used to record the TEM and STEM images. Samples were prepared by drop-casting the nanomaterials with and without 4-aminosalicylic acid from THF-water mixtures on 200 mesh TEM copper grids coated with continuous carbon film. The images were registered at 200 kV using TEM Imaging & Analysis v. 4.7 software.

Method for obtaining of gold-porphyrin hybrid material

To 3.5 mL gold colloid solution in water ($c=4.58 \times 10^{-4}$ M) a solution of *MnTTPCl* in THF ($c=1.1 \times 10^{-6}$ M) was added and the mixture was stirred for five minutes. This mixture is selected because it produces the widest and most intense plasmonic band.

Results and discussions

In order to detect PAS, portions of 4-aminosalicylic acid solution ($c=4.353 \times 10^{-3}$ M) in distilled water were gradually added to 3 mL of the gold-porphyrin hybrid material as follows: 20 μ L for the first 16 steps, 50 μ L for the next 3 steps and 100 μ L for the last 3 steps. After each adding of 4-aminosalicylic acid solution the mixture was stirred and the UV-vis spectrum of the sample was recorded.

From the superposed UV-vis spectra (Figure 2) registered during the adding of 4-aminosalicylic acid to the *MnTTPCl-nAu* hybrid it can be observed that the intensity of the plasmonic band is steadily decreasing with the increase in 4-aminosalicylic acid concentration.

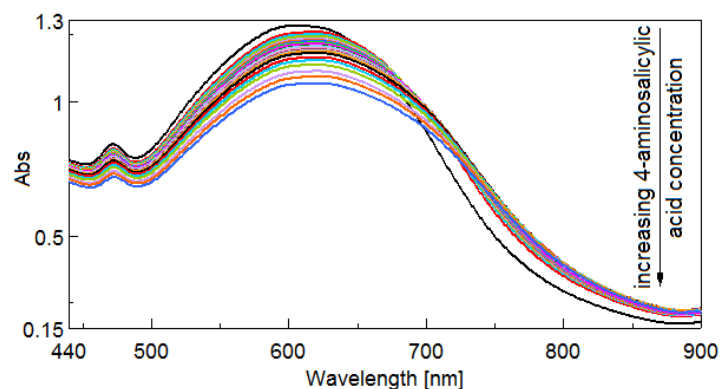


Figure 2: The overlapped UV-vis spectra registered during the adding of *PAS* solution to the *MnTTPCl-nAu* hybrid solution

Another notable feature is that the shift of the peak is moving to higher wavelengths (from $2.88 \times 10^{-5} \text{ M}$ which is the lowest recorded concentration producing the peak at 619 nm to the $8.89 \times 10^{-4} \text{ M}$ which is the highest *PAS* concentration that is located at 622 nm). An isosbestic point around 725 nm is the proof for the equilibrium process that accompanies the *PAS* recognition and mechanism of detection.

The dependence between the absorption intensity of the *MnTTPCl-nAu* hybrid and the concentration of *PAS* (Figure 3) is linear in a wide range of *PAS* concentrations: $2.88 \times 10^{-5} \text{ M}$ - $8.89 \times 10^{-4} \text{ M}$ characterized by an excellent correlation coefficient of 99.31% .

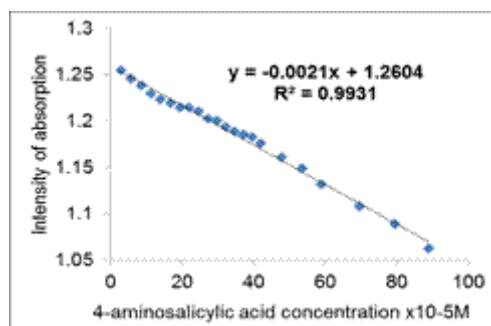


Figure 3: The dependence between the absorption intensity of the *MnTTPCl-nAu* hybrid and the concentration of 4-aminosalicylic acid

In order to prove the efficiency of the hybrid material as compared to the bare Mn-porphyrin alone, the experiment of adding a dilute solution of 4-aminosalicylic acid to a solution of *MnTTPCl* alone was performed. So, a solution of 2.5 mL *MnTTPCl* in THF ($c = 1.1 \times 10^{-6} \text{ M}$) is treated with portions of 20 μL of a solution of 4-aminosalicylic acid in water ($c = 4.353 \times 10^{-3} \text{ M}$). The mixture is stirred and the UV-vis spectra are recorded for each step.

As can be observed in Figure 4, the intensity of the Soret band of the porphyrin is behaving unevenly as the concentration of 4-aminosalicylic acid is continuously increasing. A slow shift of the Soret band intensity toward lower wavelengths is also obvious ($\lambda = 476 \text{ nm}$ for the lowest 4-aminosalicylic concentration ($3.45 \times 10^{-5} \text{ M}$) and $\lambda = 469 \text{ nm}$ for highest 4-aminosalicylic concentration ($4.1 \times 10^{-4} \text{ M}$)). An increase of intensity of the Va and VI absorption bands that are characteristic for manganese porphyrins can be observed (Figure 4) as the concentration in 4-aminosalicylic acid is increasing, but the dependence is not linear. This data proves that the porphyrin alone is not able to provide a good detection for *PAS*.

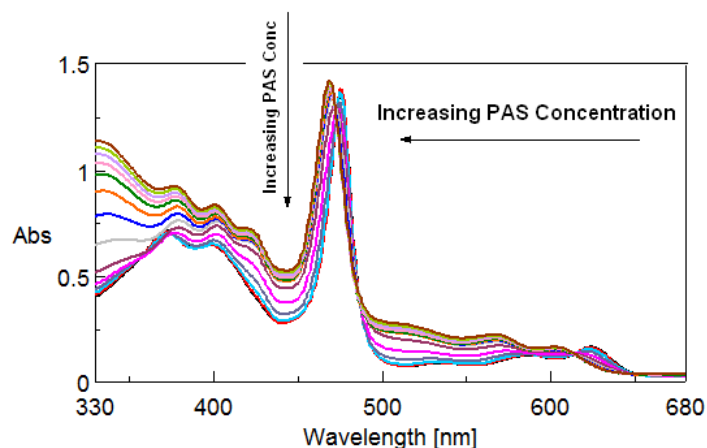


Figure 4: Superposed UV-vis spectra from adding 4-aminosalicylic acid solution to *MnTTPCl* solution in THF.

The proposed mechanism by which PAS chelates to Mn-porphyrin is based on the affinity of Mn to oxygen atoms of PAS, as illustrated in Figure 5, together with TEM images of *MnTTPCl-nAu* hybrid and of *MnTTPCl-nAu* hybrid after PAS detection.

From the chemistry point of view, PAS structure possesses a carboxyl group, along with hydroxyl group, providing an ideal chelating moiety for manganese, that is also capable to form Mn(V)=O bonds. This hypothesis is certified by the appearance in the UV-vis spectrum of the secondary Soret band (VI) located around 420 nm that is typical for porphyrin-Mn(V)=O species and also by the significant blue shift of the Q bands.

TEM images of *MnTTPCl-nAu* hybrid treated with PAS show globular assemblies of micellar type having different diameters, a completely different organization than in the *MnTTPCl-nAu* hybrid where they are cloudly organized. This type of spherical determined geometry is another proof for the proposed coordination.

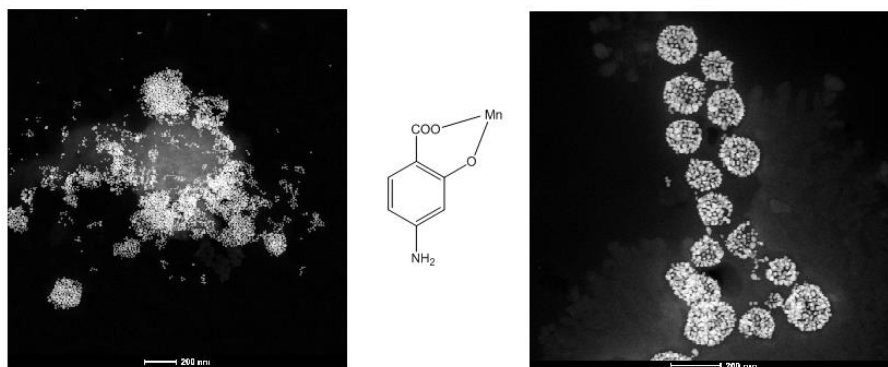


Figure 5: TEM images of *MnTTPCl-nAu* hybrid, type of PAS Coordination to Mn (V) and of *MnTTPCl-nAu* hybrid after PAS detection.

Although our experimental results imply a chelating action Mn(V) to PAS, the conclusive evidence might come only from *in vivo* urinary analysis of Mn following PAS treatment. Such a study may pave the way for future development of PAS detection in order to improve therapy using PAS [12].

Conclusions

A comparison between solely *MnTTPCl* and its *MnTTPCl-nAu* hybrid regarding the ability to recognize and detect PAS was performed.

MnTTPCl-nAu hybrid can detect 4-aminosalicylic acid with great accuracy in the range of concentrations from $2.88 \times 10^{-5} \text{M}$ to $8.89 \times 10^{-4} \text{M}$, that are relevant for analysis in medical trials of patients treated with PAS, following a linear dependence between the intensity of the bands in UV-vis spectra and the PAS concentration. *MnTTPCl* alone cannot be used for detection, its optical behavior being unlinear in the presence of increased PAS concentrations, but is able to recognize PAS molecules.

Acknowledgements

The authors from Institute of Chemistry Timisoara of Romanian Academy (ICT) are acknowledging Romanian Academy for financial support in the frame of Programme 3/2018 from ICT. This work is dedicated to the Centennial Anniversary of ROMANIA.

References

- [1] B. Saifullah, M. Z. Hussein, S. H. Hussein-Al-Ali, P. Arulselvan, S. Fakurazi, Chemistry Central Journal 7(72) (2013) doi: 10.1186/1752-153X-7-72.
- [2] A. Marreilha dos Santos, R.L. Lucas, V. Andrade, M. L. Mateus, D. Milatovic, M. Aschner, M. Batoreu, Toxicol. Appl. Pharmacol. 258 (2012) 394–402.
- [3] M. A. Awawdeh, J. A. Legako, H. J. Harmon, Sensors and Actuators B 91 (2003) 227–230.
- [4] M. G. H. Laghari, Y. Darwis, A. H. Memon, Trop. J. Pharm. Res. 13 (7) (2014) 1133–1139
- [5] C. L. Cummins, W. M. O'Neil, E. C. Soo, D. K. Lloyd, I. W. Wainer, J Chromatogr B Biomed Sci Appl. 697(1-2) (1997) 283-288.
- [6] M. I. Evgen'ev, S. Yu. Garmonov, L. Sh. Shakirova, J. Anal. Chem. 55(7) (2000) 696-702.
- [7] L. Salageanu, A. Lascu, M. Birdeanu, E. Fagadar-Cosma, Dig. J. Nanomat. Bios. 13(3) (2018) 653-659.
- [8] E. Fagadar-Cosma, C. Enache, I. Armeanu, D. Dascalu, G. Fagadar-Cosma, M. Vasile, I. Grozescu, Mater. Res. Bull. 44(2) (2009) 426-431.
- [9] A. D. Adler, F. R. Longo, F. Kampas, J. Kim, J. Inorg. Nucl. Chem. 32 (1970) 2443.
- [10] E. Fagadar-Cosma, M. C. Mirica, I. Balcu, C. Bucovicean, C. Cretu, I. Armeanu, G. Fagadar-Cosma, Molecules 14(4) (2009) 1370-1388.
- [11] P. Muthukumar, S. Abraham John, J. Coll. Interface Sci. 421 (2014) 78–84.
- [12] G. J. Patel, M. V. Hathi, S.V. Patel, J. Chem. 3(4) (2006) 319-326.

REMOVAL OF METHYLENE BLUE FROM WATER USING TiO₂ IMMOBILIZED ON A POLYMER SUPPORT

Nemanja Banić, Daniela Šojić, Nina Finčur, Branko Kordić, Ivana Jagodić, Biljana Abramović

*The University of Novi Sad, Faculty of Sciences, Department of Chemistry, Biochemistry and Environmental Protection, Trg D. Obradovića 3, 21000 Novi Sad, Serbia
e-mail: nemanja.banic@dh.uns.ac.rs*

Abstract

Among the water treatment technologies, advanced oxidation processes (AOPs) present great potential for treating a broad spectrum of contaminants. AOPs involve the *in-situ* generation of highly reactive oxygen species with low selectivity such as hydroxyl radicals, hydrogen peroxide, ozone, and superoxide anion radicals, providing complete mineralization to CO₂, H₂O, and inorganic ions or acids [1]. Titanium dioxide (TiO₂) is the best-known photocatalyst, and it was examined in a tremendous number of studies. The TiO₂ can be either immobilized or suspended in the reactor. Although the suspended system has the advantage of a larger surface area as compared to the immobilized system, the necessary separation of the catalyst particles is expensive and constitutes the main disadvantage in the commercialization of this system [2]. Adding polymer as support has been widely used in immobilized TiO₂ preparation to produce photocatalyst with improved mechanical strength, adsorption capability, and surface morphology [3]. The present study aimed to investigate the efficiency of three materials in which TiO₂ (Hombikat) was immobilized on polyvinyl chloride (PVC) support. For the preparation of the TiO₂/PVC materials, a patent-protected commercial formulation of PVC was used. TiO₂/PVC materials had a different mass ratio of TiO₂ to PVC (1, 2.5, and 5%) and were in the form of tablets (diameter of 5 mm and thickness of 2 mm). The efficiency of materials was tested for the removal of methylene blue ($c_0 = 2.45 \cdot 10^{-5}$ mol dm⁻³) under the influence of simulated solar radiation (SSR) ($I_{UV} = 0.223$ mW·cm⁻²; $I_{vis} = 208.5$ mW·cm⁻²). Experiments were also conducted in the dark to investigate the contribution of adsorption to the total removal efficiency. All of the TiO₂/PVC materials showed greater removal efficiency compared to direct photolysis. The optimal mass ratio TiO₂ towards PVC to total removal efficiency was 2.5%. For the most efficient system 2.5%TiO₂/PVC/SSR, the influence of the solution volume as well as the mixing rate was also examined. From the obtained results, it can be concluded that for an optimal volume of 30 cm³, the optimal mixing rate was 490 rpm. It was found that the optimal number of tablets was 29. The overall effectiveness of methylene blue removal for optimal reaction conditions and by using the most efficient system 2.5TiO₂/PVC/SSR was the highest at pH 4.6.

Acknowledgements

The authors acknowledge the financial support of the Ministry of Education and Science of the Republic of Serbia (Project No. ON172042).

References

- [1] O.K. Dalrymple, D.H. Yeh, M.A. Trotz, J. Chem. Technol. Biotechnol 82 (2007) 121.
- [2] M.F.J. Dijkstra, A. Michorius, H. Buwalda, H.J. Panneman, J.G.M. Winkelman, A.A.C.M. Beenackers, Catal. Today 66 (2001) 487.
- [3] S.K. Ain, M.S. Azami, R. Zaharudin, F. Bakar, W.I. Nawawi, Photocatalytic study of new immobilized TiO₂ technique towards degradation of Reactive Red 4 dye, MATEC Web of Conferences, 47 (2016) 05019.

ALLELOPATHIC EFFECT OF *Abutilon theophrasti* Med. EXTRACTS ON GERMINATION OF MAIZE SEED

Konstantinović Bojan¹, Samardžić Nataša^{1*}, Popov Milena¹, Šabović Strahinja¹

¹ University of Novi Sad, Faculty of Agriculture, Department of Environmental and Plant Protection, Trg Dositeja Obradovića 8, 21000 Novi Sad, Serbia
e-mail: natasam@polj.uns.ac.rs

Abstract

During 2014 allelopathic effects of *Abutilon theophrasti* Med. water extracts to germination and initial development of maize (*Zea mays* L.), were studied in laboratory conditions. In addition to the Water extracts out of dry mass of the tested weed species, the applied concentrations were 1 g/l, 2 g/l, 4 g/l of dry matter made out of weed species in the 3-4 leaf stage of development. Water solution of *A. theophrasti* showed inhibitory effect on maize seed epicotyls and hypocotyls length. The applied extracts made out of dry matter of the studied weed species *A. theophrasti* reduced maize seed germination for 9%-14% in comparison to the control in which it was 88%. After germination in a climate chamber, epicotyls' and hypocotyls' length of maize seeds was measured three, six and ten days following spraying by extracts.

Introduction

The term allelopathy has been used for the first time by Hans Molish, Vienna University in 1937. This term is constructed from two Greek words *allos* which means "one on another" and *pathos* which has two meanings suffering or „sensitivity“, and it's used to describe mutual impact of one organism on another [1]. Allelopathy can be defined as a biochemical interaction that has either a stimulative or a negative impact between plants (including microorganisms). Allelopathic effects are classified as weed on weed, weed on crop or weed on weed [2]. Soil and plant traits have a big impact on allelopathic effects. Growth inhibition that was caused by *Cyperus tuberosus* on some plants: tomato, bean, eggplant, had greater effect on light soils. Allelopathy has great role in spreading of invasive weed species. Some weed species of European origin *Centaurea maculosa* and *Centaurea diffusa*, are invasive species in North America. Allelochemicals that are produced by those two weeds, have been discovered in their native soil in Europe, but also in the soil of North America, where the concentration of their allelochemicals was far greater. So we can say that allelopathy depends on numerous factors [3]. Numerous experiments have shown that the allelopathic substances, which trigger biochemical interactions between plants are typical secondary metabolites. They have a low molecular weight, a simple structure and easily volatile [4]. Allelopathy is not only representing the effect of root exudates, but also the effect of toxic compounds which are the result of degradation organic matter in soil. Plants produce physiological active compounds (carbohydrates, ferments, organic and amino acids), they can have a positive or a negative effect on plants [5]. Johnson grass (*Sorghum halepense*) and wiregrass (*Cynodon dactylon*), are common weeds in corn and cotton fields that have an allelopathic effect. *Agrostema githago* has a positive effect on wheat growth. *Abutilon theophrasti* Med. is an annual weed with a high allelopathic potential, it can have negative effects on germination and growth of other crops and weeds [3]. The leaf of *Abutilon theophrasti* Med. produces mucous formations and they can severely damage the yield of soybean. The root produces various metabolic active compounds such as: organic acids, amino acids, carbohydrates, cinchon. Root mucus of some plants *Thymus serpyllum* prevents seed germination by getting in contact with other seeds. Remains of crops like: wheat,

sunflower, sugar beet, peas, can prevent the development monocotyledonous weeds from the *Poaceae* family, but not *Avena* spp [5]. The interaction between higher plants can be achieved through the impact of compounds, which are located in above ground plant organs. With the help of rain those compounds can get to surface of neighboring plants or in the soil. Young walnut leafs contain a high amount of juglon. Rye is a very active allelopathic plant [6]. A significant inhibitory effect is proven by aqueous extract of Jimson grass. The extract was made from different plant parts steam, root, leafs and it had the greatest effect on germination, primary root growth, and lower density of some weeds: *Ipomoea tribola*, *Echinochloa colonum*, *Rottboellia cochinchinensis*, *Rumex dentatus*, *Coronopus didymus*, *Convolvulus arvensis* and *Portulaca oleracea* [7]. Allelopathy is a phenomenon that can be used as an alternative mode to suppress weeds: allelochemicals as herbicides, in crops that are genetically modified. Lot of crops like rye or some plants from the families *Brassicaceae* and *Fabaceae* are recommended as cover crop to suppress weeds or to prevent erosion. Some crops have a positive effect in the crop rotation system, so in the next season there are less weed types in the field. In some countries secondary metabolites of microorganisms have been commercialized. These product are safe to use and have no negative impact on the environment [2].

Experimental

In 2011 and 2012, plant parts of *Abuthilon theophrasti* Med. were collected on two localities Bački Maglić and Kać. The collected plant matherial was split in two parts above-ground part of the plant (steam and leafs) and underground part (root). Above-ground and underground plant parts were together macerated. Velvetleaf water extracts of above-ground and underground were made in different concentrations: 1 g/l, 2 g/l and 4 g/l. Filter paper in Petri dishes (150 mm x 25 mm) with germinated seed of the assayed maize crop was saturated by 8 ml of the extracts. Control was moistened by distilled water. Each concetration was replicated four times. By extracts treated soybean and maize seed were germinated in climatic chamber [12] and seed surface was sterillized according to Elemaru and Filhou (2005) [8]. The assayes were set up according to the randomized block design with 4 replications. Each Petri dish contained 25 maize seeds, i.e. 100 seeds per treatment. All measurements were conducted third, sixth and tenth day after moistening of the studied crops seed. The existence of allelopathic activity of the studied weed species to the maize crops were established by measurement of the crops seed epicotyls (mm) and hypocotyls (mm) length and germination (%) [11].

Results and discussion

During the experiment that had the goal to prove alellopathic effects of *Abuthilon theophrasti* Med. water extracts on maize seed germanination. The following results have been obtained: Treatment that contained the extract concentration of 1 g/l had an average hypocotile length value 34.98mm, value of the control 67.90mm. Treatment that contained the extract concentration of 2 g/l had an average hypocotile length value 57.91mm, value of the control 67.90mm. Treatment that contained extract concentration of 4 g/l had an average hypocotile length value 58.63mm, value of the control 67.90mm, the results are presented in figure 1.

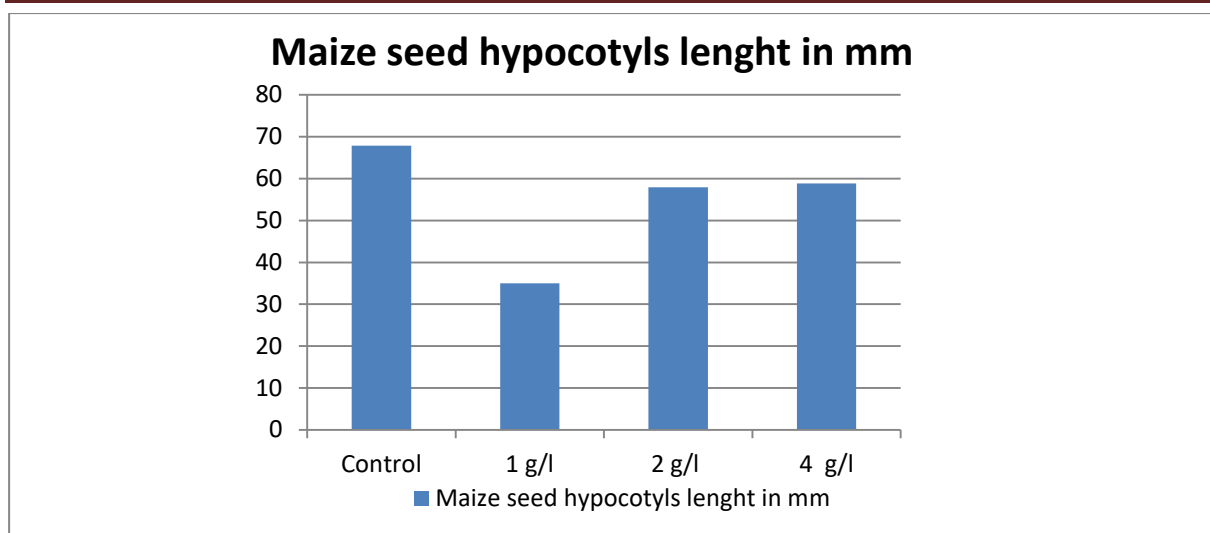


Figure 1 Measured values of maize seed hypocotyls after treatment with *Abutilon theophrasti* Med. extracts.

Average epicotyl length were for the extract concentration of 1 g/l 15.22mm compared to the control which was 54.42mm. Average epicotyl length were for the extract concentration of 2 g/l 18.95mm compared to the control which was 54.42mm. Average epicotyl length were for the extract concentration of 4 g/l 19.35mm compared to the control which was 54.42mm, the values of epicotyls length after treatment are shown in figure 2.

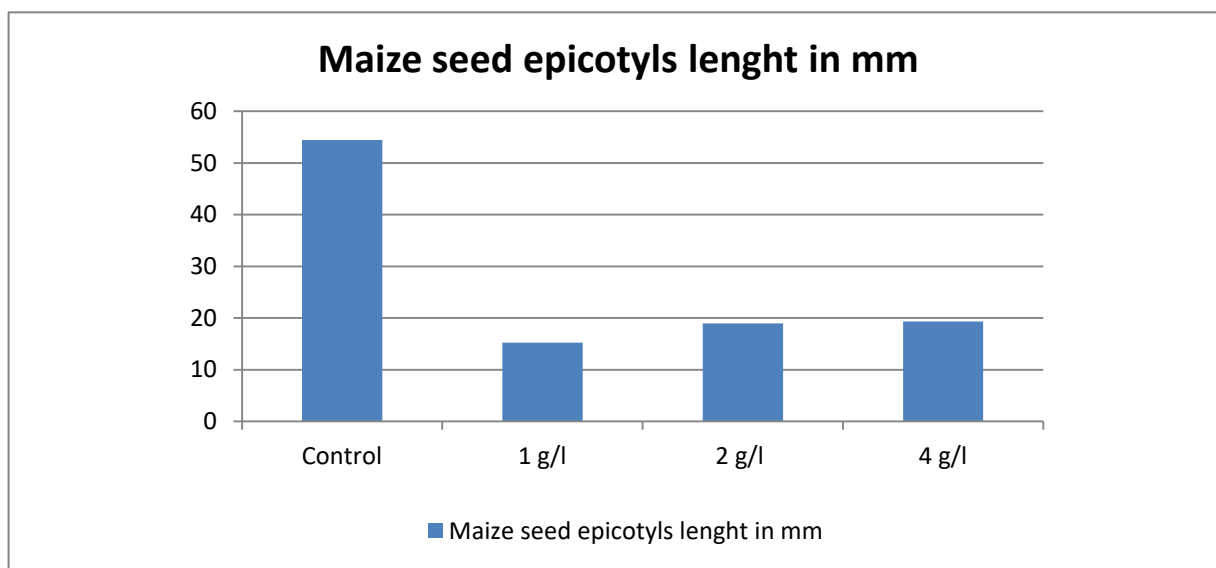


Figure 2 Measured values of maize seed epicotyls after treatment with *Abutilon theophrasti* Med. extracts.

Percentage of maize seed germination in the assay, has given different results: seeds that have been treated with the extract which had the concentration of 1 g/l 91%, compared to the control 88%. Seeds that have been treated with the extract which had the concentration of 2 g/l 91%, compared to the control 88%. Seeds that have been treated with the extract which had the concentration of 4 g/l 86%, compared to the control 88%. The results of seed germination percentage are shown in figure 3.

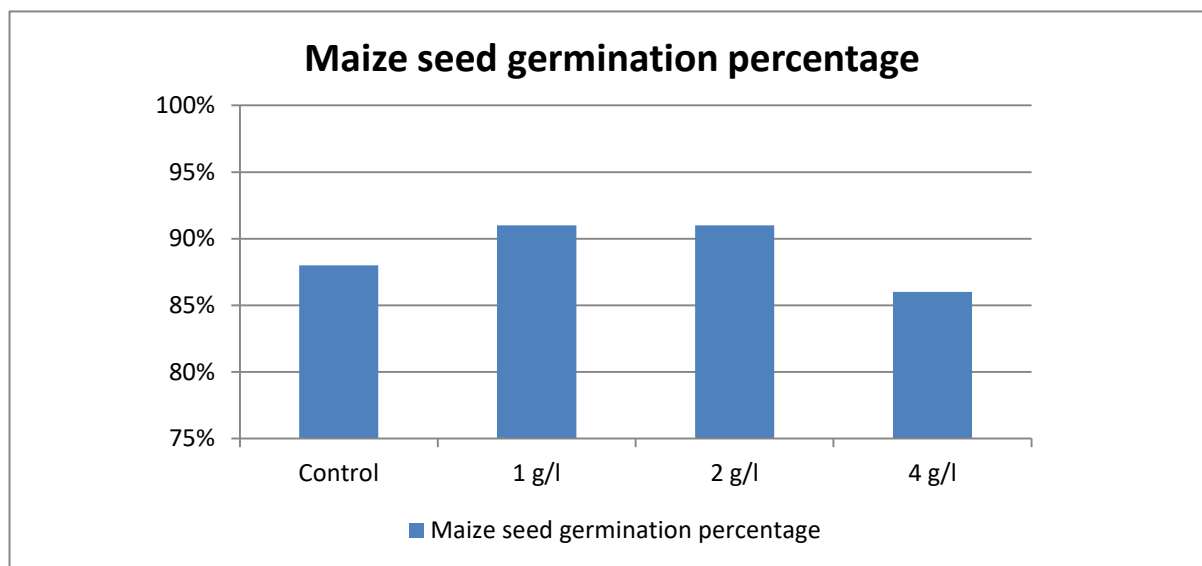


Figure 3 Seed germination of maize seeds after treatment with *Abuthilon theophrasti* Med. extracts.

Conclusion

Based on the results of the assays we can conclude, that the allelopathic effect of *Abuthilon theophrasti* Med. on maize seedlings has been detected. Water extract of *Abuthilon theophrasti* Med. had a greater impact on maize epicotyl length. Extracts of Velvetleaf had a stimulating effect on seed germination, but after the germination they shown negative effects on epicotyl and hypocotyl growth. The stimulating germination effect can be related to other factors. This research has been conducted under *in vitro* conditions, the allelopathic effects of *Abuthilon theophrasti* Med. have been proven. This indicates that further trials should be done also in the field and they should be continued *in vitro* in the next period. Allelochemicals of *Abuthilon theophrasti* Med. have shown an impact on seed germination, that trait could be used in future research to produce certain kinds of pesticides. Those allelochemicals need to be detected and their effect on crops and other weeds.

References

- [1] E. Gross, Allelopathy in benthic and littoral areas case studies on allelochemicals from benthic cyanobacteria and submerged macrophytes, 1999, Boca Raton, 179-199.
- [2] A. Uludag, I. Uremis, Mogućnost korišćenja alelopatskih useva za suzbijanje korova V kongres o zaštiti bilja, 2004, Zlatibor.
- [3] M. Simić, A. Uludag, Interakcije korov-gajena biljka: kompeticija i alelopatija, XIII Simpozijum sa savetovanjem o zaštiti bilja, 2007, Zlatibor.
- [4] V. Janjić, R. Stanković-Kalezić, L.J. Radivojević, Prirodni proizvodi sa alelopatskim, herbicidnim i toksičnim delovanjem, Acta herbologica, Vol. 17, No. 1, 2008, 1-22
- [5] B. Konstantinović, Korovi i njihovo suzbijanje, 2008, ABM ekonomik. Novi Sad.
- [6] R. Kastori, Fiziologija biljaka, 1998, Feljton, Novi Sad.
- [7] A. Ahmad, Z.A. Cheema, R. Ahmad, Evaluation of sorgaab as natural weed inhibitor in maize. JAPS 10, 2000, 141-146.
- [8] V. Elemar, V. Filho, Brazilian Society on Weed Science. Congress Xs 24, Svaio Pedro, BRESIL, 40(1), 2005, 217.

ANALYZING SOIL SEED BANK OF INVASIVE SPECIES IN SOIL IN NATURE PROTECTED AREA

Konstantinović Bojan¹, Samardžić Nataša^{1*}, Popov Milena¹, Šabović Strahinja¹

¹ University of Novi Sad, Faculty of Agriculture, Department of Environmental and Plant Protection, Trg Dositeja Obradovića 8, 21000 Novi Sad, Serbia
e-mail: natasam@polj.uns.ac.rs

Abstract

The aim of this research was to determinate the number from invasive weed seeds in two protected areas. Soil sampling was carried out in north of Serbia Landscape of Outstanding Features Nature Park "Palić" and Nature Reserve "Ludaško jezero". The depth at which samples were taken in each location was 0-10 cm. Weed seed bank from these two areas contained seeds of: *Lolium multiflorum*, *Amaranthus retroflexus*, *Celtis occidentalis*, *Galinsoga parviflora*, *Vicia articulata*, *Setaria italica*, *Datura stramonium*, *Asclepias syriaca*, *Matricaria discoidea*, *Portulacae oleraceae*, *Veronica persica*, *Iva xanthifolia* and *Echinochloa crus-galli*. *Amaranthus retroflexus*, *Celtis occidentalis*, *Portulaca oleracea* and *Setaria italic* were determined in very large numbers at each protected location. The sampling of soil was done at two locations, with a probe of the same volume. Identifying the seeds and determining their quantity was carried out with microscopes and determiners.

Introduction

Successful weed management in agroecosystems centers on manipulating the weed seed bank in soil, the source of annual weed infestations [1]. In the increasingly disturbed environment created by modern land use, soil seed banks are of growing importance in the management and restoration of vegetation [2]. The main source of annual weeds is the soil seed population [3]. The seed bank is the resting place of weed seeds and is an important component of the life cycle of weeds. Seed banks are the sole source of future weed populations of the weed species both annuals and perennials that reproduce only by seeds. For this reason, understanding fate of seeds in the seed bank can be an important component of overall weed control [4]. A seed bank is a reserve of mature viable seeds located in fruits (or cones) on the plant (aerial seed bank), on the soil surface or buried in soil, duff or litter. The formation of a non-aerial (soil) seed bank begins at seed dispersal and ends with germination or death of the seed. Traditionally, two broad types of soil seed banks have been designated: transient and persistent. Seeds of species with transient seed banks live for <1 year and those with persistent seed banks for more than 1 year. More recent classification schemes subdivide the transient and persistent seed-bank categories into 2 – 3 subtypes each, delineating them by 1 year to decades [5]. What has to be taken into account in the study of weed seed banks in soil is that they are only a part of a complex and dynamic system consisting of soil [6], plants, animals and microorganisms [7]. Seed banks have been described as the 'memory' of a population, because they may contain genotypes that have been eradicated from the growing plant portion of the population [8]. Seed bank enhances the survival of a species by buffering against harsh environmental conditions or highly effective control methods and allowing them to germinate over a period of many years. This ability slows the genetic shift of a weed population exposed to intense selection pressures by ensuring that all the seedlings that germinate in any one year are not all from similar genetic backgrounds [9]. Understanding the nature of seedbanks is a necessary prerequisite for studying plant population dynamics, or for setting up programs of weed control [10]. Invasion by non-native exotic species in alien environments poses a major threat to native plant communities and alters fundamental

structures and functions of ecosystems. It poses one of the most serious threats to biodiversity, causing major changes in vegetation at a global level [11]. Early detection of invasive plants when their spatial extent is small reduces the cost of control and increases the possibility of successful eradication [12].

Experimental

The aim was to determine number of seeds from invasive weeds in two protected areas. Soil sampling was carried out in locations of two protected areas in north of Serbia Landscape of Outstanding Features Nature Park ‘‘Palić’’ and Nature Reserve ‘‘Ludaško jezero’’. The depth at which samples were taken in each location was 0-10 cm. The sampling of soil was done at two locations, with a probe of the same volume. In the laboratory conditions, soil samples were sieved through sieves of various diameters. After that weed seeds separated in the sample from plant and other material and the identification of seeds was carried out. Identifying the seeds and determining their quantity was carried out with microscopes and determiners.

Results and discussion

The seeds of invasive weeds at the location of Nature Park ‘‘Palić’’ were identified: *Lolium multiflorum*, *Amaranthus retroflexus*, *Celtis occidentalis*, *Galinsoga parviflora*, *Vicia articulata*, *Setaria italica*, *Datura stramonium*, *Asclepias syriaca*, *Matricaria discoidea*, *Portulacae oleraceae*, *Veronica persica*. The average number of weeds at the location Nature Park ‘‘Palić’’ in the soil profil 0-10 cm is in the range of 159,51 to 5503,07 seeds per m² respectively. The weed seed bank contains several dominant species in all samples. *Amaranthus retroflexus* and *Celtis occidentalis* were one of the most numerous at the locality. *Celtis occidentalis* is the weed species with the highest number of selected seed from the samples (5503,07 seeds per m²), followed by *Amaranthus retroflexus* (2950,92 seeds per m²), *Datura stramonium* (2871,17 seeds per m²), *Setaria italica* (1515,34 seeds per m²), *Asclepias syriaca* (1196,32 seeds per m²), *Lolium multiflorum* (1116,56 seeds per m²), *Matricaria discoidea* (1036,81 seeds per m²), *Portulacae oleraceae* (877,30 seeds per m²) and *Galinsoga parviflora*, *Veronica persica*, *Vicia articulata* had same number of determinate weed seeds, (159,51 seeds per m²) (Table 1).

Weed seeds	SUM	No m ²
<i>Amaranthus retroflexus</i>	37	2950,92
<i>Asclepias syriaca</i>	15	1196,32
<i>Celtis occidentalis</i>	69	5503,07
<i>Datura stramonium</i>	36	2871,17
<i>Galinsoga parviflora</i>	2	159,51
<i>Lolium multiflorum</i>	14	1116,56
<i>Matricaria discoidea</i>	13	1036,81
<i>Portulacae oleraceae</i>	11	877,30
<i>Setaria italica</i>	19	1515,34
<i>Veronica persica</i>	2	159,51
<i>Vicia articulata</i>	2	159,51

Table 1: Determined invasive weed seeds at Nature Park ‘‘Palić’’

SUM- the total number of invasive weed seeds in 25 soil samples at 0-10 depth

NO m² - the total number of invasive weed seeds in all soil samples expressed per m²

The seeds of invasive weeds at the location of Nature Reserve ‘‘Ludaško jezero’’ were identified: *Amaranthus retroflexus*, *Portulaca oleracea*, *Setaria italica*, *Datura stramonium*,

Echinochloa crus-galli, *Iva xanthifolia*, *Celtis occidentalis*, *Ambrosia artemisiifolia* and *Lolium multiflorum*. The average number of weeds at the location Special at Nature Reserve „Ludasko jezero“ in the soil profil 0-10 cm is in the range of 79,75 to 43226,99 seeds per m² respectively. The weed seed bank contain several dominant species in all samples. *Amaranthus retroflexus* and *Portulaca oleracea* were one of the most numerous at the locality. *Amaranthus retroflexus* is the weed species with the highest number of selected seed from the samples (43226,99 seeds per m²), followed by *Portulaca oleracea* (38521,47 seeds per m²), *Datura stramonium* (3190,18 seeds per m²), *Setaria italica* (1674,85 seeds per m²), *Celtis occidentalis* (478,53 seeds per m²), *Echinochloa crus-galli* (398,77 seeds per m²), *Lolium multiflorum* (319,02 seeds per m²), *Ambrosia artemisiifolia* (159,51 seeds per m²) and *Iva xanthifolia* (79,75 seeds per m²) (Table 2).

Weed seeds	SUM	NO m ²
<i>Amaranthus retroflexus</i>	542	43226,99
<i>Ambrosia artemisiifolia</i>	2	159,51
<i>Celtis occidentalis</i>	6	478,53
<i>Datura stramonium</i>	40	3190,18
<i>Echinochloa crus-galli</i>	5	398,77
<i>Iva xanthifolia</i>	1	79,75
<i>Lolium multiflorum</i>	4	319,02
<i>Portulaca oleracea</i>	483	38521,47
<i>Setaria italica</i>	21	1674,85

Table 2: Determined invasive weed seeds at Special at Nature Reserve „Ludaško jezero“

SUM- the total number of invasive weed seeds in 25 soil samples at 0-10 depth

NO m² - the total number of invasive weed seeds in all soil samples expressed per m²

Conclusion

Analyzing deposited seed (seed bank) of invasive species in soil in nature protected area were conducted in the representative locations of four protected areas in the north of Serbia Landscape of Outstanding Features Nature Park „Palic“ and Special Nature Reserve „Ludasko jezero“. At the two protected location were determined 17 different seeds of invasive weed species. *Amaranthus retroflexus* and *Portulaca oleracea* were determined in every location. *Amaranthus retroflexus*, *Celtis occidentalis*, *Portulaca oleracea* and *Setaria italica* were determined in very large numbers at each protected location, while a smaller number of seeds remain determined invasive weed species. *Ambrosia artemisiifolia* was determinate in large numbers at Special Nature Reserve „Ludaško jezero“.

Acknowledgements

The results published in this paper are part of the research project “Nature Protection from Invasive Plant Species - PROTECT” HUSRB/1602/12/0132 – 5.7.3.

References

- [1] R.J. Kremer, Ecological Applications, Managment of Weed Seed Banks with Microorganisms, 3 (1) (1993) 42-52.
- [2] K. Thompson, S.R. Brand, J.G. Hodgson, Functional Ecology, Seed size and shape predict persistence in Soil, 7 (1993) 236-241.
- [3] J.P. Yenish, J.D. Doll, D.D. Buhler, Weed Science, Effects of Tillage on Vertical Distribution and Viability of Weed Seed in Soil, 40 (1992) 429-433.

- [4] M.M. Hossain, M. Begum, Journal of the Bangladesh Agricultural University, Soil weed seed bank: Importance and management for sustainable crop production, 13 (2) (2005) 221-228.
- [5] J.L. Walck, J.M. Baskin, C.C. Baskin, S.N. Hidayati, Seed Science Research, Defining transient and persistent seed banks in species with pronounced seasonal dormancy and germination patterns, 15 (2005) 189-196.
- [6] S. Otto, M.C. Zuin, G. Chiste, G. Zanin, Weed Research, A modeling approach using seed bank and soil properties to predict the relative weed density in organic fields of an Italian pre-alpine valley, 47 (2007) 311-326.
- [7] J.C. Chee-Sanford, M.M. Williams, A.S. Davis, K.G. Sims, Weed Science, Do Microorganisms Influence Seed-Bank Dynamics?, 54 (2006) 575-587.
- [8] P.B. Cavers, Canadian Journal of Soil Science, Seed banks: Memory in soil, 75 (1) (1995) 11-13.
- [9] R.H. Gulden, S.J. Shirtliffe, Weeds, Herbicides and Management, Weed Seed Banks: Biology and Management, 2 (2009) 46-52.
- [10] L.A. Ambrosio, L. Iglesias, C. Marin, J.P. Monte, Weed Research, Evaluation of sampling methods and assessment of the sample size to estimate the weed seedbank in soil, taking into account spatial variability, 44 (2004) 224-236.
- [11] R.K. Kohli, D.R. Batish, H.P. Singh, K.S. Dogra, Biological Invasions, Status invasiveness and environmental threats of three American invasive weeds (*Parthenium hysterophorus* L., *Ageratum conyzoides* L., *Lantana camara* L.) in India, 8 (2006) 1501-1510.
- [12] L.W. Lass, T.S. Prather, N.F. Glenn, K.T. Weber, J.T. Mundt, J. Pettingill, Weed Science, A review of remote sensing of invasive weeds and example of early detection of spotted knapweed (*Centaurea maculosa*) and babysbreath (*Gypsophila paniculata*) with a hyperspectral sensor, 53 (2005) 242-251.

EVALUATION OF TRANSFER AND BIOACCUMULATION FACTORS OF HEAVY METALS IN DIFFERENT PARSLEY SAMPLES

Despina -Maria Bordean^{1,2}, Ioan Caba^{*2}, Tiberiu Iancu^{*1}, Valentin Vladut², Petru Cardei², Diana Moigradean¹, Camelia Moldovan¹, Liana Alda¹, Luminita Pirvulescu^{*1}

¹Banat's University of Agricultural Sciences and Veterinary Medicine "King Mihai I of Romania" from Timisoara, 300645, 119, Calea Aradului, Timisoara, Romania

²National Institute of Research - Development for Machines and Installations designed to Agriculture and Food Industry – INMA, 013811, 6, Ion Ionescu de la Brad Blv., Sector 1, Bucharest, Romania

*Corresponding authors email: cabaioan@yahoo.com, iancutiberiu10@gmail.com, pirvulescu_l@yahoo.com

Abstract

Heavy metals transfer factors help to observe metals impact on agricultural products (vegetables and/or fruits) to evaluate different bioaccumulation scenarios to interpret available experimental results and for designing fingerprints or bioaccumulation maps. The aim of this study was to evaluate the transfer factors (TF) of some heavy metals (HMs) including (Fe, Mn, Zn, Cu, Ni, Pb and Cd) from soil to root and leaves of parsley samples cultivated on polluted and nonpolluted areas and to identify the fingerprint of transferred metals. The heavy metal (HM) content was analyzed using Flame Atomic Absorption Spectrometry (FAAS) technique. The bioaccumulation factor (BF) and TF in parsley samples were used for obtaining the fingerprints (HMs bioaccumulation maps) of parsley samples.

Introduction

The pollution at global level is continuously increasing and that is causing nutritional modifications. The plants have the capacity to sequester and/or to remove metals from the soil through roots and/or shoots. Plants heavy metals concentrations can be correlated with their surrounding environment (soil, air and water) [4]. Many plants can be used as biological indicators with specificity to heavy metals [6].

Metal toxicity presents noteworthy relationship with the characteristics, which are in control of the metal tolerance, including chemical interaction and ionic speciation [1].

The transfer (translocation) factor (TF), offers information about the capability of a plant to translocate the metal ions from roots through shoots and to leaves of a plant.

The bioaccumulation factor (BAF) from soil to plant expressed by the ratio of metal concentration in plant tissues divided by the heavy metal concentrations in soil and used as an indicator of the parsley accumulation behavior.

The aim of the study was to analyse the capacity of parsley roots and leaves to accumulate heavy metals and to generate the heavy metal fingerprints of parsley based on TF and BAF Values

Experimental

The parsley roots and leaves used for the study investigation were sampled in triplicate from ten different private vegetables farms. All the samples were washed with double distilled water, weighed, dried at 105 °C and grinded. The heavy metals concentrations were determined by flame atomic absorption spectrometry as described by Bordean et al, 2014 [3].

The transfer factors (TF) of Mn, Zn, Cu, Ni, Cd, Pb, from roots to leaves [1] were calculated using equation 1:

$$TF = \frac{C_{leafs}}{C_{root}} \quad (1)$$

TF = transfer or translocation factors of metals from roots to leaves

C_{leaf} = metal concentration in fresh weight plant tissue [mgKg^{-1}];

C_{root} = metal concentration in fresh plant tissue [mgKg^{-1}]

The bioaccumulation factors (BAF) were calculated as the ratio of metal concentration in the parsley plants (roots and shoots) to that of the soil [5], as specified in equation 2:

$$BAF = \frac{C_{plant}}{C_{soil}} \quad (2)$$

BAF = bioaccumulation factors of metals from soil to plant

C_{plant} = metal concentration in fresh weight plant tissue [mgKg^{-1}];

C_{soil} = metal concentration in dry soil [mgKg^{-1}].

Results and discussion

The heavy metals (manganese, zinc, copper, nickel, cadmium and lead) concentrations were determinate for all collected parsley samples, as well as of the soil samples were the plants were cultivated. All heavy metal analysis of soil, parsley roots and parsley leafs (table 1) were performed in triplicate and the values were used to calculate TF and BAF (table 2).

Table 1 Heavy metals concentrations of soil, parsley root and parsley leaf samples

Vegetables, soil/Me content ± Standard Deviation (SD)	Mn ± SD	Zn ± SD	Cu ± SD	Ni ± SD	Cd ± SD	Pb ± SD
Parsley Root	3.75 ± 0.87	3.92 ± 0.68	1.35 ± 0.47	0.22 ± 0.09	0.01 ± 0.00	0.11 ± 0.03
Parsley Leaf	6.98 ± 0.84	9.41 ± 1.75	1.27 ± 0.35	0.55 ± 0.17	0.04 ± 0.02	0.42 ± 0.11
Soil samples	1537.71±18.1 8	159.33± 8.57	27.83±6.23	12.22±1.08	0.19±0.05	27.15±4.89

Heavy metals concentrations in parsley root and leaves collected from 10 from investigated areas (mgKg^{-1} fresh weight, * $p < 0.05$); Heavy metals concentrations in soil samples collected from 10 from investigated areas (mgKg^{-1} dry weight, * $p < 0.05$)

Based on Baker and Brooks, 1989 studies, if TF presents values higher than 1, this shows that the plant transfers the metal from root to leaves [2].

As we can observe the translocation of heavy metals from roots to leaf in parsley is higher than 1 for Mn, Zn, Ni, Cd and Pb, but its lower than 1 for copper, which means it is not transferring copper, from roots to leaf.

Table 2 Presentation of translocation (transfer factors) and bioaccumulation factors of some heavy metals in parsley samples

Transfer and bioaccumulation factors	Heavy metals					
	Mn	Zn	Cu	Ni	Cd	Pb
TF	1.861	2.401	0.941	2.500	4.000	3.818
BAF	0.003	0.042	0.047	0.032	0.132	0.010

Legend: TF = transfer or translocation factor; BAF = bioaccumulation factor

At the same time, the bioaccumulation factors are lower than 1, which means that parsley can be an excluder of heavy metals (table 2). Based on the observations made by Radulescu et al, 2013, if the BAF is higher than 1, then the plants can be considered to behave like bioaccumulators of heavy metals and if the BAF is lower than 1, then the plant might be appreciated as an excluder of heavy metals [5].

The fingerprint of parsley samples based on TF and BAF for the studied heavy metals is presented in figure 1.

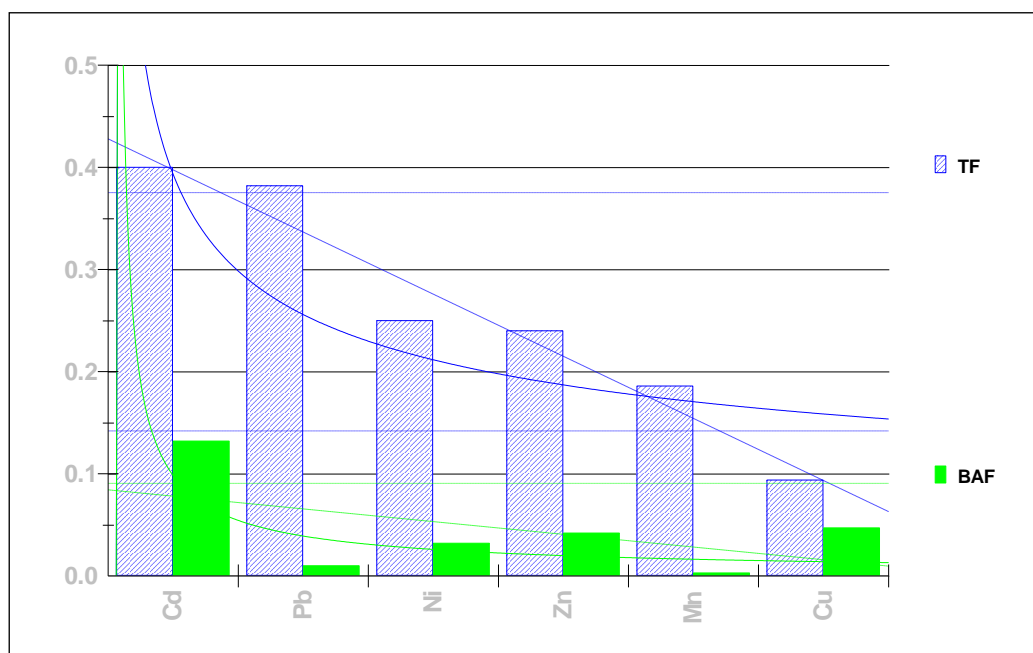


Figure 1. Heavy metals Fingerprint based on parsley TF and BAF, using Pareto Style

Legend: TF = transfer or translocation factor; BAF = bioaccumulation factor

Conclusion

The fingerprint presented can be used to identify the plants that are most suitable for nutrition, but also to reveal the best phytoremediators of soils. The obtained results explain why parsley and cilantro are used for heavy metals detoxification programs and are recommended in different detoxification diets for neurovegetative diseases like Alzheimer and Parkinson.

Acknowledgements

All authors have contributed equally to this paper. The present work was funded by the project "Study of synergic bioactivity of some antioxidant mixes fortification with the role to fortify patients with Parkinson's disease", No 47/12.11.2015, financed by Antiparkinson Association.

References

- [1]. Abdul H. Bu-Olayan and Bivin V. Thomas, Translocation and Bioaccumulation of Trace Metals in Desert Plants of Kuwait Governorates, 2009, Research Journal of Environmental Sciences, 3: 581-587, <http://docsdrive.com/pdfs/academicjournals/rjes/2009/581-587.pdf>;
- [2]. Baker, A.J.M. and R.R. Brooks,. Terrestrial higher plants which hyper accumulate metallic elements - A review of their distribution, ecology and phytochemistry, 1989, Biorecovery, 1: 81-126;
- [3]. Bordean, D. M., Nica, D. V., Harmanescu, M., Banatean-Dunea, I., Gergen, I. I., Soil Manganese enrichment from industrial inputs: a gastropod perspective, 2014, PloS one, 9(1), e85384;
- [4]. Keane, B., M.H. Collier, J.R. Shann and S.H. Rogstad, Metal contents of dandelion (*Taraxacum officinale*) leaves in relation to soil contamination and airborne particulate matter, 2001, Sci. Total Environ., 281: 63-78;
- [5]. Radulescu, L C., Stihi, C., Popescu, I.V., Dulama, I.D., Chelarescu, E.D., Chilian ,A., Heavy Metal Accumulation and Translocation in Different Parts of *Brassica Oleracea*, 2013, Rom. Journ. Phys., Vol. 58, Nos. 9–10, P. 1337–1354, http://www.nipne.ro/rjp/2013_58_9-10/1337_1354.pdf;
- [6]. Simon, L., H.W. Martin and D.C. Adriano, Chicory (*Cichorium intybus* L.) and Dandelion (*Taraxacum officinale* Web.) as phyto indicators of cadmium contamination, 1996, Water Air Soil Pollut., 91: 351-362;

ELECTRODEPOSITION AND CORROSION BEHAVIOR OF HYDROXYAPATITE ONTO TITANIUM

Bogdan Ovidiu Taranu, Alexandra Ioana Bucur^{*}, Iuliana Sebarchievici, Corina Orha

*National Institute for Research-Development in Electrochemistry and Condensed Matter, no
144 dr A. P. Podeanu, 300569 Timisoara, Romania
^{*}alexandra.i.bucur@gmail.com*

Abstract

The present study includes the results of the hydroxyapatite electrochemical deposition on titanium substrate from 3 solutions of different concentrations of precursors. The deposited HA layers and the substrate were studied by means of x-ray diffraction and scanning electron microscopy, and also corrosion resistance tests have been performed. Results confirmed the formation of low crystallinity hydroxyapatite coatings, displaying fine layers of feathery crystals and other structures resulted from agglomeration phenomena. Corrosion tests, performed in artificial saliva solution, showed that the corrosion resistance of the hydroxyapatite coated Ti sample obtained from 0.875M Ca and 0.525M P precursors solutions was higher than that of the other samples.

Introduction

Hydroxyapatite (HA) - chemical formula $\text{Ca}_{10}(\text{PO}_4)_6(\text{OH})_2$ - alone or deposited onto metallic substrates, is highly used in the biomedical field, due to undeniable advantages such as: biocompatibility, bioactivity and osseointegration [1,2]. One of the drawbacks of hydroxyapatite is its low mechanical resistance. The deposition of hydroxyapatite onto metallic substrates, such as titanium, provides the means to ensure the mechanical resistance of any implant, besides the mentioned biochemical advantages. Several methods have been developed regarding the deposition of HA coatings on metal substrates, including the electrochemical deposition method, having several advantages [3] such as: homogeneity, availability of deposition onto complex shape substrates, possibility to control the layer thickness on demand, etc.

Considering its long-term presence in the body, any implant should possess certain characteristics, including high corrosion resistance - as is the case with metal-hydroxyapatite implants [4].

This study aims to prepare HA coatings on titanium substrates by electro-deposition from precursors solutions having three different concentrations, and compare their corrosion behaviour by potentiodynamic polarization test in artificial saliva solution.

Experimental

The electrolyte solutions used for the electrochemical deposition were prepared from separate solutions of analytical grade $\text{Ca}(\text{NO}_3)_2 \cdot 2\text{H}_2\text{O}$ (Sigma Aldrich) and analytical grade $(\text{NH}_4)_2\text{HPO}_4$ (Merck) of different concentrations, as presented in Table 1.

Solutions were considered so as to preserve the Ca:P ratio of 10:6, as in natural hydroxyapatite. The pH level was kept in the 8.3-8.4 range, being adjusted with ammonia, after mixing the two precursor solutions.

Table 1. Details of the solutions concentrations used in the deposition process

Sample number	Ca and P precursors	
	Ca(NO ₃) ₂ ·2H ₂ O solution concentration (mM)	(NH ₄) ₂ HPO ₄ solution concentration (mM)
1	0.875	0.525
2	1.75	1.05
3	3.5	2.1

Before the electrochemical deposition, the Ti discs ($\phi = 1$ cm) were polished using SiC sandpaper of different grit sizes and felt, washed with acetone, placed in ethanol/acetone mixture 50:50 for 30 minutes in an ultrasonic bath, rinsed with bidistilled water and dried.

The electrochemical setup consisted in a PGZ 402 Voltalab potentiostat and a three-electrode glass cell with heating mantle. The working electrode was a titanium disc (used as the cathode), a platinum plate was used as counter electrode and the saturated calomel electrode (SCE) coupled to a salt-bridge junction was used as reference electrode. The electro-deposition took place at 80°C, at a constant potential of -1500 V, for 1h. After the deposition, the samples were dried at 40°C in an oven, and were investigated by x-ray diffraction (XRD), using a PANalytical X'Pert Pro MPD Diffractometer with Cu anode, working parameters 45 kV and 30 mA. Images of the samples surfaces were obtained using a Phillips Inspect S scanning electron microscope.

The Fusayama – Meyer simulated saliva solution (pH=5.8) of the following chemical composition [5]: NaCl (0.4 g/L); KCl (0.4 g/L); CaCl₂ (0.6 g/L); NaH₂PO₄·H₂O (0.79 g/L), urea (1 g/L) and Na₂S·9H₂O (0.005 g/L) was used as the testing electrolyte in corrosion studies at 37°C.

The electrochemical cell for corrosion tests included: a working electrode consisting in an uncoated or coated sample, a platinum wire as counter electrode and the SCE. Each sample was allowed to reach a steady open circuit potential (OCP) for 1h. Afterwards, a potentiodynamic polarization was initiated from -800 up to + 300 mV (vs. SCE), at a sweep rate of 1 mV/s.

Results and discussion

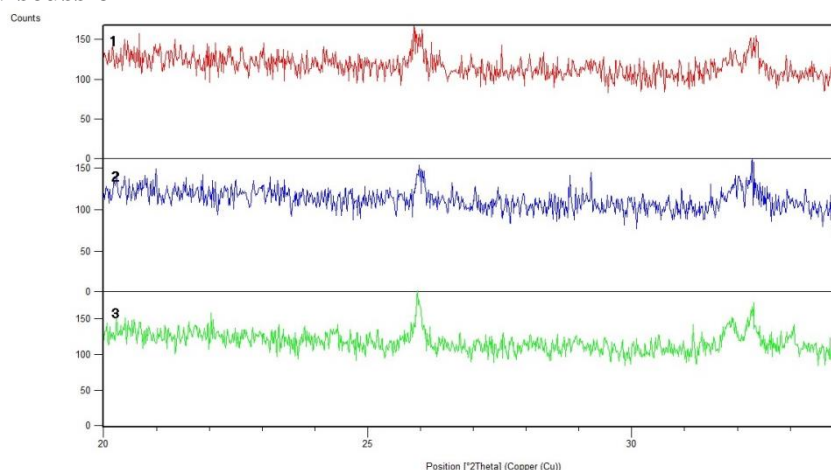


Figure 1. XRD patterns of the 3 deposited HA layers onto Ti, concentration order 1<2<3

The XRD results are presented in Figure 1, which confirm the hydroxyapatite formation, but with low crystallinity.

With increasing concentration (sample 3), the peaks resolution improves. The size of the peak at 25.96 2theta, representing the 002 crystallographic plane, is an indication of an elongated shape of the crystals.

Scanning electron microscopy (SEM) images are presented in Figure 2. For sample 1, with the smallest concentration used, the deposited layer is fairly uniform, with rare spherical arrangements of needle-shaped crystals. Increasing the concentration (sample 2) leads to extended areas of interconnected over-grown spherulites, while the substrate is covered with a uniform layer of feathery crystals. Increasing the concentration even more (sample 3) does not change the appearance of the deposition, but leads to an agglomeration of the crystals in the over-grown regions. In all cases the crystals are submicrometric in size, and all the substrates are covered with a fine layer of feathery crystals.

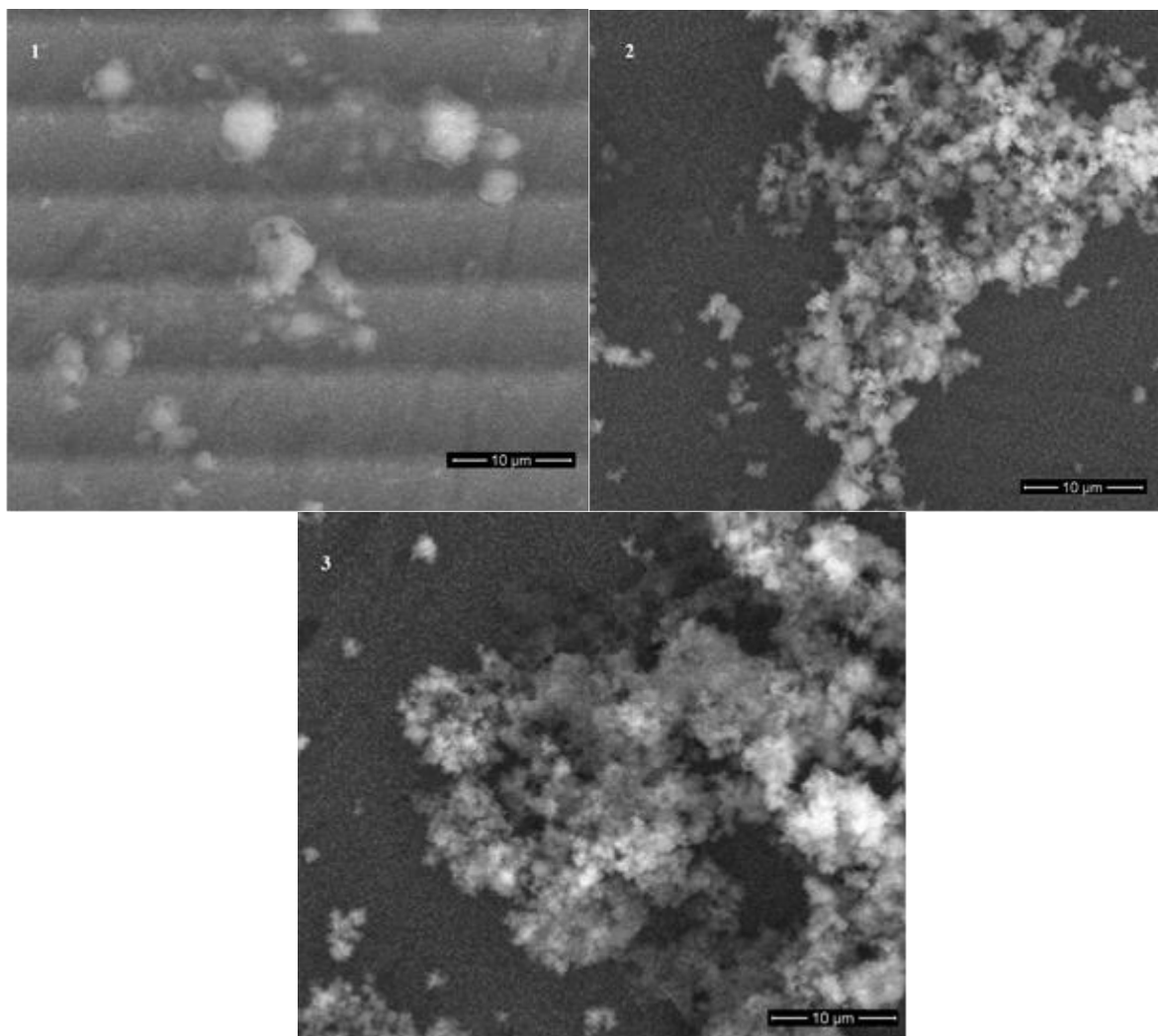


Figure 2. SEM images of the 3 deposited layers of HA onto Ti, concentration order $1 < 2 < 3$. The agglomeration increases in the order $1 < 2 < 3$ and is due to: on one side, the increase of concentration, and on the other side, to the alkaline pH where the deposition took place, favouring the existence of a large amount of available OH. All these findings indicate an accelerated nucleation and, as a consequence, a big number of small crystals and low growth rate.

The potentiodynamic polarization curves of the Ti samples, uncoated and coated with HA, in artificial saliva solution, at 37 °C, are shown in Figure 3.

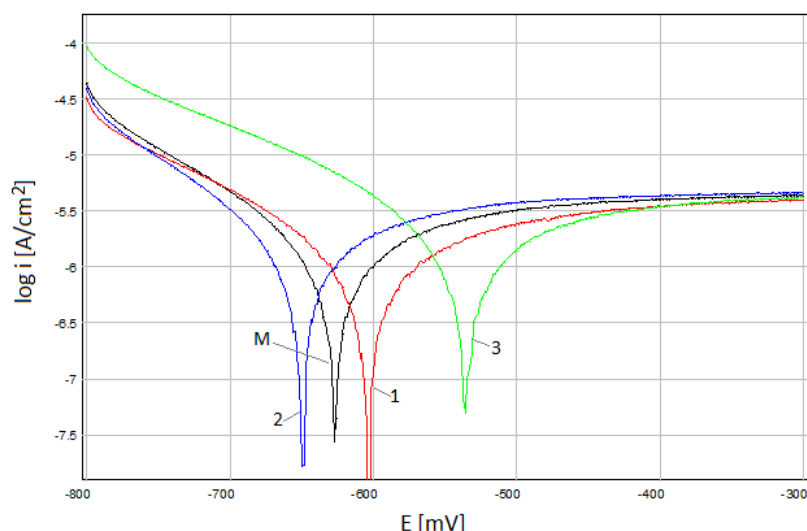


Figure 3. Potentiodynamic polarization curves for uncoated Ti (M) and coated with three different HA layers (1÷3).

Corrosion potential (E_{corr}) and corrosion current density (i_{corr}) determined by the Tafel extrapolation method and corrosion rate (v_{corr}) for each sample are shown in Table 2.

Table 2. Electrochemical parameters obtained from the Tafel extrapolation plots.

Sample	E_{corr} [mV]	i_{corr} [$\mu\text{A}/\text{cm}^2$]	v_{corr} [$\mu\text{m}/\text{year}$]
M	-628	1.17	10.20
1	-605	0.90	7.82
2	-651	1.30	11.28
3	-536	1.53	13.31

Sample 1 presents a lower value ($0.90 \mu\text{A}/\text{cm}^2$) for the i_{corr} parameter by comparison with both HA coated samples (2 and 3) and uncoated Ti discs (M). Also, the E_{corr} value is more electropositive than that of uncoated Ti, indicating that the corrosion resistance of Ti is improved by this HA coating.

Regarding *Sample 3* a different behaviour can be noticed, namely: it shows the most electropositive E_{corr} value (-536 mV), but the i_{corr} value is a little higher than the one obtained for uncoated Ti, indicating that the HA coating provides poor corrosion protection for Ti metal. The same conclusion can be drawn for *sample 2*, where the i_{corr} value was also higher than the one for uncoated specimen. The E_{corr} values are in good agreement with the values obtained from OCP measurements (not presented here).

Therefore, the corrosion behaviour of the *HA coating obtained using the smallest concentrations of precursors from this study* revealed a slower corrosion rate for Ti substrates ($7.82 \mu\text{m}/\text{year}$) than the other coatings (which act as corrosion activators).

These results indicate that the presence of the HA deposited from *diluted electrolyte solution* (the most uniform layer) can reduce the corrosion rate of Ti by acting as a barrier to the transport of ions and electrons between the substrate and the electrolyte, thus reducing the electrochemical reaction rate [6].

Conclusions

HA coatings were successfully formed on Ti substrate by electrochemical deposition, as confirmed by XRD studies. SEM micrographs revealed that all the substrates were covered

with a fine layer of feathery crystals and as the concentrations of the precursors increased, other structures were formed as a result of agglomeration phenomena.

The corrosion rate determined from polarization curves was high for samples 2 and 3, but for sample 1 it was lower than the other samples, including the uncoated Ti substrate. Thus, the electrochemical test, performed in artificial saliva solution, showed that the corrosion resistance of the HA coated Ti sample obtained from 0.875M Ca and 0.525M P precursors was higher than that of the bare Ti electrode.

Based on these results, it might be concluded that some HA coatings can moderately decrease the corrosion rate of Ti substrates in physiological environment, while others can accelerate it. Based on the SEM data, it seems that in the absence of significant agglomeration phenomena, the HA coating provides better corrosion protection.

The electrochemical synthesis parameters, in particular the concentration of the electrolyte, affect the crystallinity, morphology and corrosion protection of the resulting coatings.

References

- [1] A. I. Bucur, R. Bucur, T. Vlase, and N. Doca, "Thermal analysis and high-temperature X-ray diffraction of nano-tricalcium phosphate crystallization," *J. Therm. Anal. Calorim.*, vol. 107, no. 1, pp. 249–255, 2012.
- [2] A. I. Bucur, R. A. Bucur, Z. Szabadai, C. Mosoarca, and P. A. Linul, "Influence of small concentration addition of tartaric acid on the 220 °C hydrothermal synthesis of hydroxyapatite," *Mater. Charact.*, vol. 132, pp. 76–82, 2017.
- [3] D. T. M. Thanh *et al.*, "Controlling the electrodeposition, morphology and structure of hydroxyapatite coating on 316L stainless steel," *Mater. Sci. Eng. C*, vol. 33, no. 4, pp. 2037–2045, 2013.
- [4] B. Singh, Gurpreet; Singh, Hazoor; Singh Sidhu, "Characterisation and In Vitro Corrosion Resistance of Plasma-Sprayed Hydroxyapatite and Hydroxyapatite – Silicon Oxide Coatings on 316L SS," *Bull. Mater. Sci.*, vol. 37, no. 6, pp. 1519–1528, 2014.
- [5] J. Qiu, W. Q. Yu, F. Q. Ohang, R. J. Smales, Y. L. Ohang, and C. H. Lu, "Corrosion behaviour and surface analysis of a Co-Cr and two Ni-Cr dental alloys before and after simulated porcelain firing," *Eur. J. Oral Sci.*, vol. 119, no. 1, pp. 93–101, 2011.
- [6] Z. Chun-Yan, Z. Rong-Chang, L. Cheng-Long, and G. Jia-Cheng, "Comparison of calcium phosphate coatings on Mg-Al and Mg-Ca alloys and their corrosion behavior in Hank's solution," *Surf. Coatings Technol.*, vol. 204, no. 21–22, pp. 3636–3640, 2010.

CONCENTRATION INFLUENCE IN THE HYDROTHERMAL SYNTHESIS OF HYDROXYAPATITE AT 160 °C

Alexandra Ioana Bucur*, Raul Alin Bucur, Corina Orha

*National Institute for Research and Development in Electrochemistry and Condensed Matter
no 144 dr P. A Podeanu, Timisoara 300569, Romania
alexandra.i.bucur@gmail.com*

Abstract

The work presented here is the hydrothermal synthesis of hydroxyapatite (HA) at 160°C for 8h, starting from solutions of four different concentrations. The purpose of the study was to investigate the influence of the concentration on the morphology of the synthetic powder obtained. The identification of the synthesized compounds was performed by X-ray Diffraction, while the size and shape of the crystals was studied by means of Scanning Electron Microscopy. Results have showed that with raising the solution concentration, a secondary phase of CaHPO_4 appears and grows in direct relationship to solution concentration, while the hydroxyapatite morphology does not seem to have been influenced by concentration changes. Phase pure hydroxyapatite was obtained only for an initial solution concentration of 0.02 M, the smallest used in this study.

Introduction

Hydroxyapatite (HA), having the chemical formula $\text{Ca}_{10}(\text{PO}_4)_6(\text{OH})_2$, is a natural mineral present in the human hard tissues in large amounts. Given this reason, synthetic HA has been intensively investigated and used as a replacement material for damaged natural tissues, either alone or in combination with other substances, in the form of powders, cements, solid pieces, layers deposited onto metallic substrates, etc.

In a tight relationship to its uses, the properties of the synthetic HA are highly influenced by its morphological characteristics (such as size and shape of crystals) [1], so the method by which it was obtained has to be carefully chosen because each of the methods presents advantages as well as disadvantages. The hydrothermal technique is a facile and low-energy consuming method, which allows a good control over the properties of the desired material, such as crystallinity, morphology, size of particles, etc [2].

In the present study, hydrothermal technology has been used in a study meant to lead to pure-phase HA by running experiments at 160°C for 8h. Four different concentrations of the starting solutions have been used, in order to investigate the relationship between the concentration and the morphology of the final product.

Experimental

Analytical grade $\text{Ca}(\text{NO}_3)_2 \cdot 4\text{H}_2\text{O}$ (Sigma-Aldrich) was used as Ca precursor and the P precursor used was $(\text{NH}_4)_2\text{HPO}_4$ (Merck). Solutions of the 2 precursors were prepared with the following concentrations:

Sample name	Ca solution concentration (mol/L)	P solution concentration (mol/L)
1-S	0.02	0.02
2-S	0.05	0.05
3-S	0.1	0.1
4-S	0.2	0.2

After mixing the solutions with preservation of the Ca:P ions ratio of 10:6 under continuous stirring at room temperature, the solutions were transferred to Teflon liners and heated at 160°C for 8h. The initial pH was in the range 6.1-6.4 and the final pH was 4.3-4.9.

After cooling naturally to room temperature, the precipitates were extracted and washed with double-distilled water until pH returned to neutral. Then the powders were dried in the oven at 50°C for 6h.

The physico-chemical characterization of the powder samples was performed using a PANalytical X'Pert Pro MPD Diffractometer equipped with a Cu anode and PixCEL detector, powder samples supported on zero background silicone holders, working parameters: 45 kV, 30 mA and an Inspect S Scanning Electron Microscope (FEI Company), where the powder samples were supported on carbon tape.

Results and discussion

The X-ray diffraction results are presented in Figure 1. For the smallest concentration, of 0.02M, the sample consists in pure crystalline HA. With rising concentration, a secondary phase appears, of CaHPO_4 , whose amount is growing with concentration. The peaks which are not nominated with a or b in Figure 1 belong to either CaHPO_4 or its mixture with HA (many small peaks belonging to these two compounds have identical position reflexions).

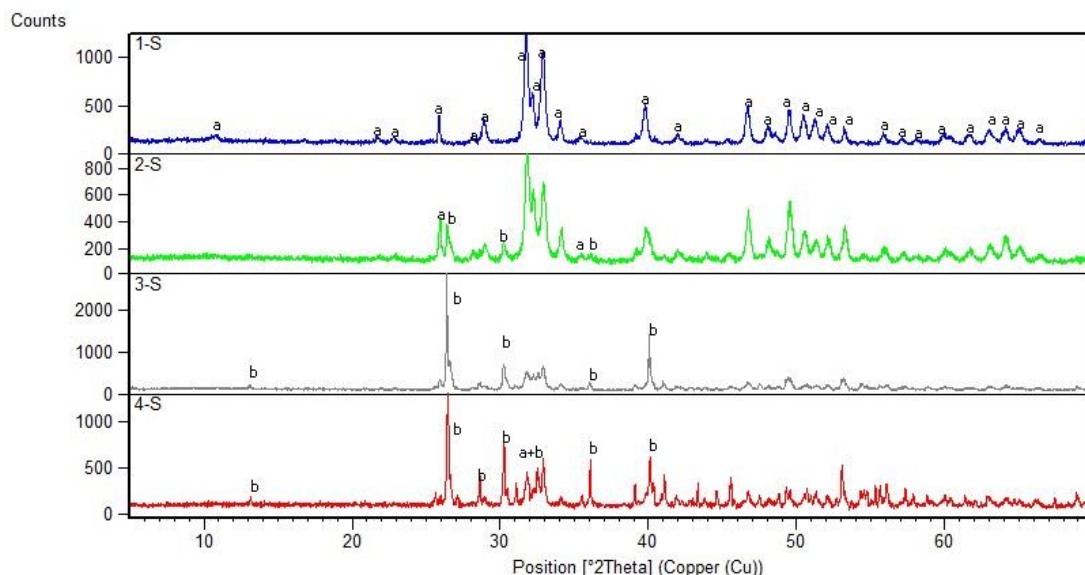


Figure 1. X-ray diffraction patterns of the four samples, where a=HA, b= CaHPO_4

Scanning electron microscopy images are presented in Figure 2. The morphology of sample 1-S is of submicronic acicular crystals, agglomerated in the shape of clews, typical for HA. When concentration increased (sample 2-S), the agglomerated formation of needles became less fluffy, because the HA crystals are combined with particles of CaHPO_4 . For samples 3-S and 4-S the CaHPO_4 crystals present a dramatic growth, while HA preserves its acicular

morphology and submicronic size. At the same time, the amount of HA is higher in the sample 3-S compared to the sample 4-S.

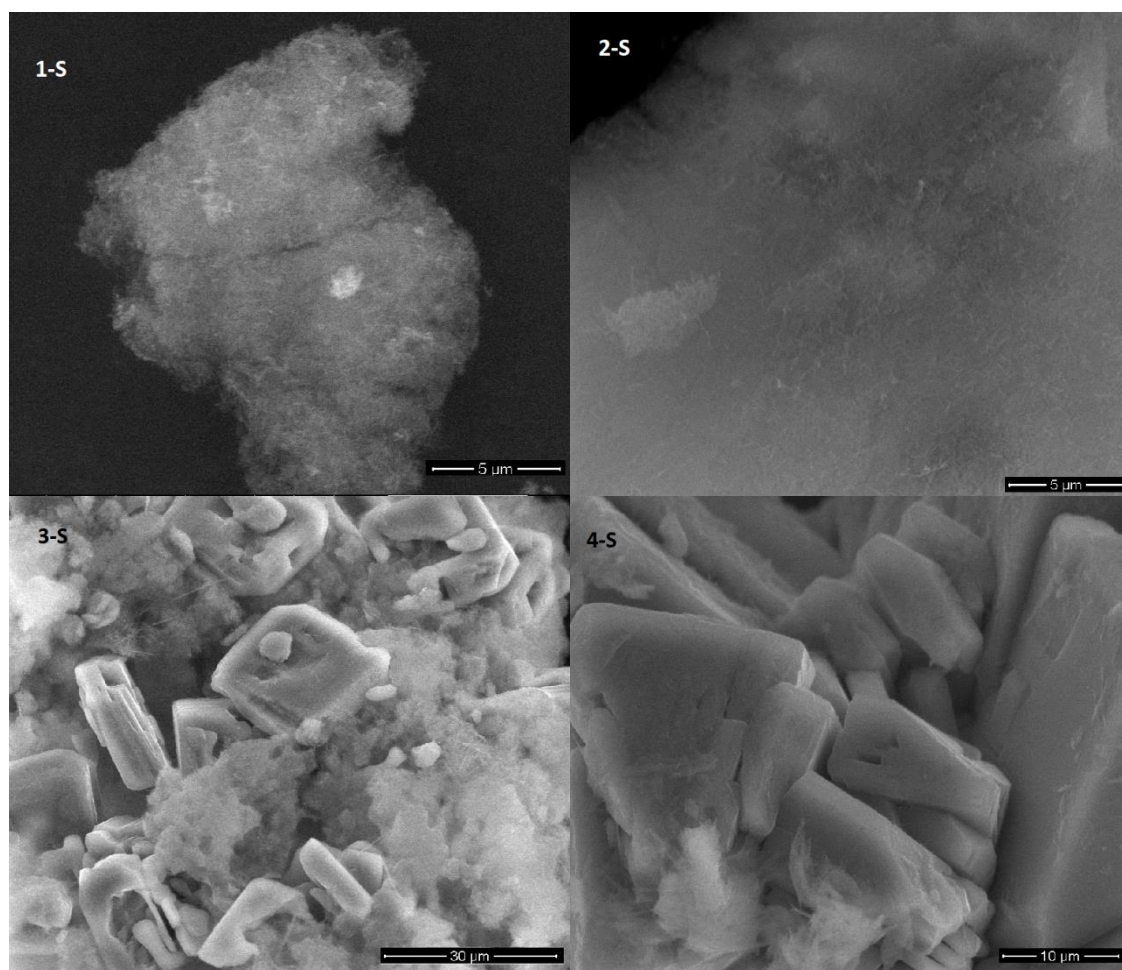
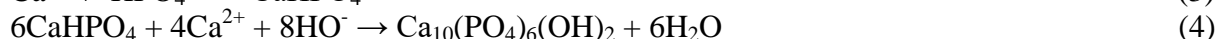


Figure 2 Scanning electron microscopy images

The chemical reactions implicated in the process are presumed to be:



First, the precursors are dissociated in their own solution, and then, when the two solutions are mixed, the ions interact according to eq (3) to form dicalcium phosphate (dihydrate or anhydrous). With rising temperature, the hydrolysis of CaHPO_4 starts and HA crystallizes, but the transformation is incomplete, probably due to either insufficient time or insufficient temperature.

The reactions sequence described by equations (1-4) is supported by the low pH values recorded at the end of the hydrothermal treatment, values located in the generally known pH region where dicalcium phosphate forms and HA is soluble. CaHPO_4 is recognized as an intermediate in the synthesis of HA [3, 4] during low pH. Due to the existence of the both phases in the final product (experimental results), we assume the reaction given by eq (4) is not complete in our case. Nevertheless, HO^- ions existence and number, vital for the formation of HA, is conditioned by the low pH, lowering the chances of formation of the

desired phase. HA morphology does not seem to have been influenced by the changes in the precursors concentration.

Conclusions

The hydrothermal synthesis at 160°C for 8h starting from pH values of 6.1-6.4 has led to the formation of a mixture of hydroxyapatite and dicalcium phosphate, the latter in direct proportional relationship to the concentrations of precursors solutions. Only when the starting concentration was as low as 0.02 (lowest in the present study), pure-phase HA was synthesized. The morphology or crystal size of hydroxyapatite was not influenced by the concentration changes. Time period allocated to the hydrothermal treatment needs to be increased and pH must be raised to alkaline domain, in order to obtain pure phase HA at higher concentrations.

References

- [1] H. Bin Zhang, K. C. Zhou, Z. Y. Li, and S. P. Huang, "Plate-like hydroxyapatite nanoparticles synthesized by the hydrothermal method," *J. Phys. Chem. Solids*, vol. 70, no. 1, pp. 243–248, 2009.
- [2] F. Nagata, Y. Yamauchi, M. Tomita, and K. Kato, "Hydrothermal synthesis of hydroxyapatite nanoparticles and their protein adsorption behavior," *J. Ceram. Soc. Japan*, vol. 121, no. 9, pp. 797–801, 2013.
- [3] M. Sadat-Shojai, M. T. Khorasani, and A. Jamshidi, "Hydrothermal processing of hydroxyapatite nanoparticles - A Taguchi experimental design approach," *J. Cryst. Growth*, vol. 361, no. 1, pp. 73–84, 2012.
- [4] A. I. Bucur, R. Bucur, T. Vlase, and N. Doca, "Thermal analysis and high-temperature X-ray diffraction of nano-tricalcium phosphate crystallization," *J. Therm. Anal. Calorim.*, vol. 107, no. 1, pp. 249–255, 2012.

ORTHORHOMBIC TO TETRAGONAL PHASE TRANSITIONS IN ENVIRONMENTAL FRIENDLY PIEZOCERAMICS

Bucur Raul Alin, Farkas Iuliana, Bucur Alexandra Ioana

National Institute for Research and Development in Electrochemistry and Condensed Matter,
Condensed Matter Department, No. 1 Plautius Andronescu, 300224 Timisoara, Romania.
e-mail: raul_alin_bucur@yahoo.com

Abstract

Nowadays, new environmentally friendly, lead-free piezoelectric materials have been developed to replace the classic lead-based materials, PZT. Presently, the family of lead-free ceramics showing the most promising piezoelectric properties is based on potassium sodium niobate: $K_{0.5}Na_{0.5}NbO_3$ (noted KNN) [1, 2]. Because of the toxicity of lead oxide, researches on lead-free piezoelectric ceramics focusing on substituting these toxic oxides have recently attracted much attention. Important developments were reported with $(K_{0.5}Na_{0.5})NbO_3$ (noted KNN) based ceramics, which showed that they are promising candidates for lead-free piezoelectric materials [3, 4].

The goal of this paper is to present some new results on $GdXO_3$ (where $X = Al, Co, Cr, Fe, Mn$) doped KNN ferroelectrics. Pure KNN and KNN doped with 1 mol% $GdXO_3$ were produced by the conventional solid state synthesis. The conventional processing steps have been chosen in order to obtain reproducible high quality samples without using complex techniques such as hot pressing or special powder handling. The variation of the real part of the dielectric constant and dielectric loss are presented (TEGAM model 3550). The ceramics obtained were structurally characterized using x-ray diffraction (PANalytical X'Pert Pro MPD), with emphasis on the shifting of orthorhombic to tetragonal crystal symmetry at room temperature. The more possible polarization states arising from the coexistence of two phases (orthorhombic and tetragonal) at room temperatures can improve the piezoelectric properties of KNN ceramics.

1. Matsubara, M., Yamaguchi, T., Sakamoto, W., Kikuta, K., Yogo, T. and Hirano, S., Processing and piezoelectric properties of lead-free $(K,Na)(Nb,Ta)O_3$ ceramics. J. Am. Ceram. Soc., 2005, 88, 1190–1196;
2. Saito, H. Takao, I. Tani, T. Nonoyama, K. Takatori, T. Homma et al., High performance lead-free piezoelectric materials, Nature 432, 84 (2004) ;
3. M.N. Palatnikova, V.A. Sandlerb, V.V. Efremova, N.V. Sidorova, V.T. Kalinnikova, Dielectric properties and electrical conductivity of $Li_{0.07}Na_{0.93}Ta_{0.1}Nb_{0.9}O_3$ and $Li_{0.07}Na_{0.93}Ta_{0.111}Nb_{0.889}O_3$ ferroelectric solid solutions, Inorganic Materials, , vol. 47, no. 11, pp. 1242–1248 (2011).
4. Y. Saito, H. Takao, T. Tani, T. Nonoyama, K. Takatori, T. Homma, T. Nagaya, M. Nakamura, Nature 432, 84–86, (2004).

REMOVAL OF ROSE BENGAL DYE BY HYDROPHOBIC CARBON QUANTUM DOTS AND POLYURETHANE NANOCOMPOSITES

Milica Budimir¹, Zoran Markovic^{1,2}, Zdenko Spitalsky², Dragana Jovanovic¹, Jovana Prekodravac¹, Dejan Kepic¹, Biljana Todorovic Markovic¹

¹*Vinča Institute of Nuclear Sciences, University of Belgrade, P.O.B. 522, 11001 Belgrade, Serbia*

²*Polymer Institute Slovak Academy of Sciences, Dúbravská cesta 9, 845 41 Bratislava, Slovak Republic*

e-mail: budimir@vin.bg.ac.rs

Abstract

In the present study we report the removal of Rose Bengal dye by gamma irradiated nanocomposites composed of hydrophobic carbon quantum dots incorporated in the matrix of polyurethane (hCQD-PU). It is assumed that the removal is caused by the combination of two different mechanisms. First mechanism suggested is a photocatalytic degradation by light-induced production of singlet oxygen and other reactive oxygen species by gamma irradiated hCQD and second mechanism is the adsorption of the remaining Rose Bengal dye from the solution, by polymer matrix. The removal efficiency of the dye reached up to 92% for 4 h of irradiation by visible lamp. We have investigated the effect of different parameters, such as the dose of gamma irradiation applied to the nanocomposite, as well as the exposure time of the sample to the blue lamp (470 nm). The proposed material has a potential in water purification systems.

LINURON RESIDUE FINDINGS IN CHAMOMILE FLOWERS

Vojislava Bursić^{1*}, Vuković Gorica², Marina Đukić², Bojana Špirović Trifunović³,
Martina Mezei¹, Predrag Markovljev¹, Milivoj Radojčin¹

¹University of Novi Sad, Faculty of Agriculture, Trg Dositeja Obradovića 8, Novi Sad, Serbia

²Institute of Public Health, Bulevar despota Stefana 54a, Belgrade, Serbia

³University of Belgrade, Faculty of Agriculture, Nemanjina 6, Zemun, Serbia

*Corresponding author: e-mail: bursicv@polj.uns.ac.rs

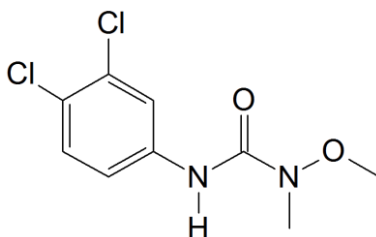
Abstract

The aim of this study was to highlight the influence of herbicide usage in agriculture on linuron residues in chamomile flower. It was collected six chamomile flower samples. The validated LC-MS/MS method according to SANTE/11813/2017 was applied in the quantitative analyses. Two samples were with no linuron detection, while all the other detected concentrations exceeded maximum residue limit of 0.1 mg/kg. The detected concentrations were in the range 0.89 to 1.90 mg/kg.

Introduction

Chamomile is a member of the Asteraceae/Compositae family, and is represented by two common varieties German chamomile (*Chamomilla recutita*) and Roman chamomile (*Chamaemelum nobile*) [1]. Nowadays, it is a highly favored and much used medicinal plant in folk and traditional medicine. Its multitherapeutic, cosmetic, and nutritional values have been established through years of traditional and scientific use and research [2]. Considered to be one of the most ancient and versatile medicinal herbs known to mankind, dried chamomile flowers have numerous, widespread health implications thanks to their high level of disease-fighting antioxidants like terpenoids and flavonoids. Throughout the world the flowers are used in the form of a simple tea (tisane) as a gentle medicine for colicky babies and for adults with mild upset stomach or symptoms of mild stress. Extracts of the flowers and also the essential oil distilled from them provide other formulations that extend the range of medicinal benefits through antioxidant, anti-inflammatory, antifungal, and antibacterial activities. Several studies have indicated that chamomile has potential anticancer activity. Other uses are in cosmetics and as a flavoring agent in foods, beverages, bakery products, ice cream, and tobacco [3].

The common practice in chamomile production involves weed control using herbicides. Weeds are the serious hygiene concern, since contaminants in the final product (flowers, oil or extract) will detract from the specified quality. Considering there are no authorized plant protection products for use in medicinal crops, there are no recommendations on concentration required for efficient weed control and crop safety. Linuron (phenylurea) (Figure 1) is used as a selective herbicide to control both annual and broadleaf weeds, perennial broadleaf weeds and grassy weeds. It can be applied as a pre-emergence treatment and a post-emergence treatment. Linuron hinders electron transport in photosystem II in the photochemical step in photosynthesis [4].

Figure 1. Structural formula of linuron

The LC-MS has been widely used for the analysis of pesticide residues in fruits, vegetable and other food samples. The coupling of LC with tandem mass spectrometry detection (MS/MS) has become significant for pesticide residue analysis [5]. Experience shows the chemicals to be useful, but none is registered for use on chamomile in Serbia [6]. That is why in this study the liquid chromatography tandem mass spectrometry (LC-MS/MS) was used for the determination of linuron residues in chamomile flowers, after the QuEChERS extraction. The determined concentrations were compared with the maximum residue levels (MRLs) for linuron in chamomile, which is 0.1 mg/kg [7].

Experimental

Chemicals and apparatus. All solvents used were of chromatography grade and were obtained from J.T. Baker (Netherlands). The certified pesticide analytical standard of linuron (99.5 %) was purchased from Dr. Ehrenstorfer (Augsburg, Germany) and the internal standard carbofuran-D3 was purchased from Sigma Aldrich (CAS Number 1007459-98-4). The linuron stock standard solution was in the concentration of 1 mg/mL, while the working standard has the final mass concentration of 1 µg/mL in acetonitrile. Magnesium sulphate, disodium hydrogencitrate sesquihydrate, trisodium citrate dihydrate, sodium chloride and formic acid, primary secondary amine and graphitized black carbon (GBC) were purchased from Fisher Scientific UK (Loughborough, UK). For LC analysis, an Agilent 1200 (Agilent Technologies, USA) HPLC system with a binary pump was used. This was equipped with a reversed-phase C18 analytical column of 50×4.6 mm and 1.8 µm particle size (Zorbax Eclipse XDB-C18, Agilent). The mobile phase was methanol (solvent A) and Milli-Q water (solvent B), both containing 0.1% formic acid in gradient mode, with the flow rate of 0.4 mL/min. The elution program was started with 90% B and held 2 min. It was linearly decreased to 20% B in 15 min, 10% B in 20 min, 5% B in 25 min and it held constantly for 3 min. The stop time was 28 min with the post run of 5 min. The injection volume was 5 µL. For the mass spectrometric analysis, an Agilent 6410 Triple-Quad LC/MS system was applied. Agilent MassHunter B.06.00 software was used for the data acquisition and processing. The analysis was performed in the positive ion modes. The ESI source values were as follows: drying gas (nitrogen) temperature 350 °C, drying gas flow rate 10 L/min, nebulizer pressure 40 psi and capillary voltage 3500 V. The detection was performed using the multiple reactions monitoring mode (MRM).

Validation parameters. The analytical method based on a simple QuEChERS solvent-based extraction was validated according to SANTE N° 11813/2017[8].

The LOD was estimated from the chromatogram of the lowest level of calibration using the Agilent MassHunter software (Agilent Technologies, B.06.00) for those concentrations that provide a signal to noise ratio of 3:1. The LOQ was defined as the lowest validated spike level

which meets the requirements of a recovery within the range of 70–120% and a $RSD \leq 20\%$. The LOQ was determined at 0.01 mg/kg in consideration of MRL (0.1 mg/kg). Recovery studies were done at two spiking levels (0.025 and 0.25 mg/kg). The method precision is expressed as the repeatability ($RSD\%$) based on recovery obtained values.

Sample preparation. The linuron was extracted from chamomile flower samples using an extraction procedure based on the QuEChERS methodology. For the chamomile extracton the 2 g of fine homogenised sample was mixed with 8 mL of water. It was followed by adding 100 μL of IS solution (10 $\mu\text{g}/\text{mL}$) and by the extraction with 10 mL of MeCN. After extracting on vortex mixer for 1 min, 6.0 g of magnesium sulfate anhydrous, 1.5 g of sodium chloride, 1.5 g of trisodium citrate dihydrate and 0.75 g of disodium hydrogencitrate sesquihydrate were added and the mixture was shaken vigorously for 1 min and after that centrifuged for 5 min at 4000 rpm. After the centrifugation 6 mL of supernatant was transferred into a clean-up tube containing 900 mg of MgSO_4 , 150 mg of PSA and 150 mg of GBC. After the centrifugation for 5 min at 4000 rpm, 5 μL of supernatant was injected into LC-MS/MS.

Results and discussion

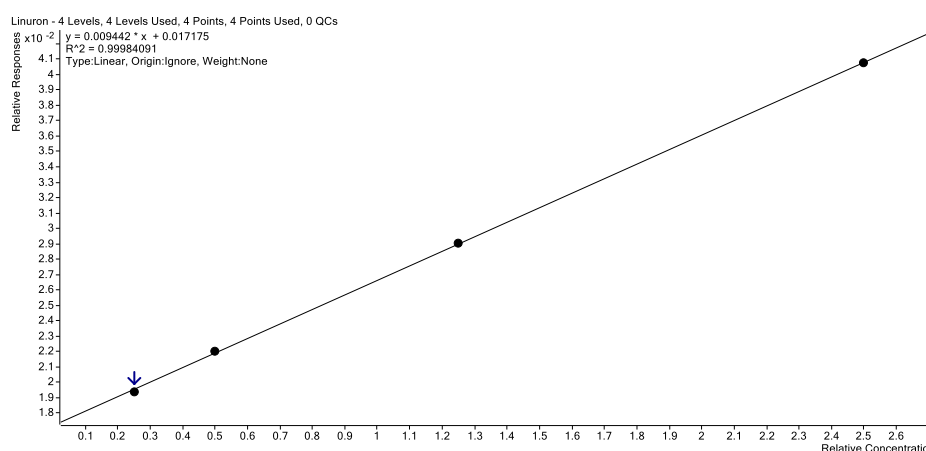
The summary of MRM transitions and LC-MS/MS operating parameters selected for the analysis of linuron and carbofuran-D3, as internal standard, in ESI positive mode are given in Table 1.

Table 1. MRM transitions of linuron and carbofuran-D3

Pesticide	Formula	Rt (min)	Precursor ion (m/z)	Product ion (m/z)	Frag (V)	CE (V)
Linuron	$\text{C}_9\text{H}_{10}\text{Cl}_2\text{N}_2\text{O}_2$	16.01	249	Q 182.3	100	8
			249	q 160.1	100	20
Carbofuran-D3	$\text{C}_{12}\text{H}_{12}\text{D}_3\text{NO}_3$	13.28	225.1	Q 165	94	10
			225.1	q 123.1	94	22

The previously developed LC-MS/MS method underwent a preliminary validation. The procedure exhibited an excellent linearity ($R^2=0.9998$) in the 5 – 50 ng/mL (corresponding 0.025–0.25 mg/kg) range with satisfactory precision expressed as relative standard deviation, $RSD=10.2\%$ (Figure 2).

Figure 2. Linuron calibration curve

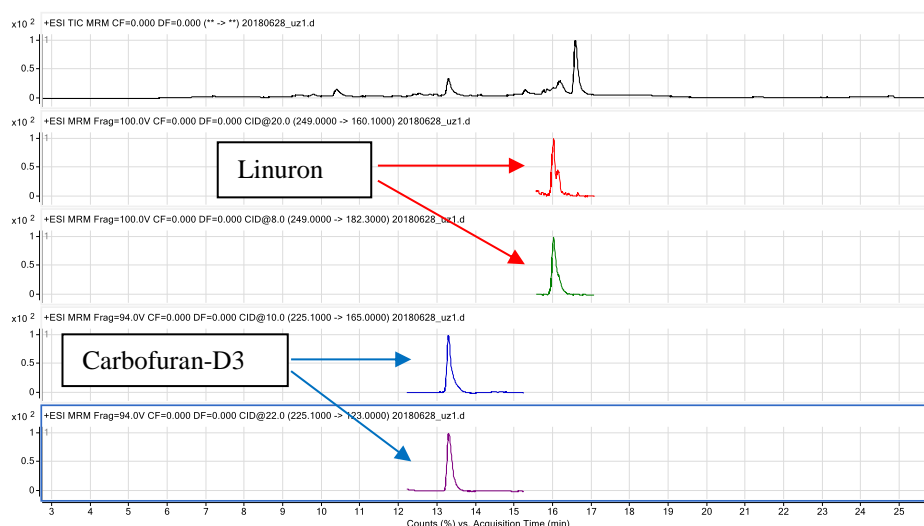


The accuracy and precision were determined via recovery experiments, spiking blank sample of chamomile at 0.025 and 0.25 mg/kg, at five replicates per level. The obtained recoveries

varied from 93.9% (RSDr=9.5%, level 0.25 mg/kg) to 99.9% (RSDr=3.8%, level 0.25 mg/kg) LOQ is experimentally set and confirmed at 0.025 mg/kg. These values are suitable for monitoring pesticides in plant material according to the EU Reg. 396/2005 [9] and National Regulation (Off. gazette RS 22/2018).

The analyses of six chamomile flower samples indicate that two samples were with no linuron detection, while the four samples were with the linuron detection above the MRL. The founding's were 0.89, 0.96, 1.09 to 1.90 mg/kg.

Figure 3. TIC chromatogram with MRM chromatograms of chamomile sample (linuron C=1.90 mg/kg)



Conclusion

An efficient, sensitive and specific method has been developed for the determination of linuron in chamomile flowers and stalks with LC-MS/MS, validated in accordance with SANTE/11813/2017 Document. This validated method was successfully applied for the analysis of linuron residues in six samples of chamomile flowers. No linuron residues were detected in 33.3% of investigated samples, while all the other detections were above MRL of 0.1 mg/kg. This indicates that linuron was applied during chamomile production, and implies that the constant monitoring of medical plants must be done.

Acknowledgements

The authors acknowledge the financial support of the Ministry of Education and Science, Republic of Serbia, Project Ref. TR31038.

References

- [1] K. Janmejai, K. Srivastava, E. Shankar, S. Gupta. Mol. Biol. Rep. (2010) 895.
- [2] O. Singh, Z. Khanam, N. Misra, M. K. Srivastava. Chamomile (*Matricaria chamomilla* L.), An overview. 2011, p. 82.
- [3] M. Das, M. Chamomile Medicinal, Biochemical, and Agricultural Aspects, Traditional Herbal Medicines for Modern Times, CRC Press, 2014.
- [4] M. Correia, F. Carvalho, Pl. Daninha (2017) 1.
- [5] B. Špirović-Trifunović, G. Vuković, K. Jovanović-Radovanov, V. Bursić, M. Meseldžija M. Pest. Phytomed. (2015) 115.
- [6] K. Jovanović-Radovanov, R. Radojević, D. Petrović, Proceedings of the 7th CMAPSEEC, 2012, p. 435.

- [7] Službeni glasnik RS broj 22/2018: Pravilnik o maksimalno dozvoljenim količinama ostataka sredstava za zaštitu bilja u hrani i hrani za životinje i o hrani za životinje za koju se utvrđuju maksimalno dozvoljene količine ostataka sredstava za zaštitu bilja.
- [8] SANTE/11813/2017: Method validation and quality control procedures for pesticide residues analysis in food and feed.
- [9] Regulation (EC) No 396/2005 of the European Parliament and of the Council of 23 February 2005 on maximum residue levels of pesticides in or on food and feed of plant and animal origin and amending Council Directive 91/414/EEC.

CHEMICAL RECYCLING OF PET WASTE BY ALKALINE HYDROLYSIS UNDER MICROWAVE IRRADIATION

Adina Căta¹, Mariana N. Ștefănuț¹, Marinela Miclău¹, Paula Șfirloagă¹, Ioana M.C. Ienașcu^{1,2}

¹ *National Institute of Research and Development for Electrochemistry and Condensed Matter, Dr. Aurel Păunescu Podeanu 144, 300569, Timișoara, Romania*

² *“Vasile Goldiș” Western University of Arad, Faculty of Pharmacy, Liviu Rebreanu 86, 310045, Arad, Romania
e-mail: adina.cata@yahoo.com*

Abstract

Hydrolytic depolymerization of polyethylene terephthalate (PET) waste in alkaline solution using microwave irradiation as heating technique was investigated in order to obtain pure terephthalic acid in high yields.

Introduction

PET has become one of the most valuable recyclable materials because of the wide range of applications [1]. Although PET is a non-toxic material, its non-biodegradability and the large amount of waste is a serious problem concerning environmental pollution [2]. Therefore, recycling processes are the best option to economically reduce the amount of PET waste.

Experimental

Colorless post-consumer PET bottles were manually cut into small flakes, then washed and dried. 1g PET waste flakes and aqueous solution of NaOH (5-10 mL) were charged in high-pressure teflon reactors without stirring. The following microwave program was used: step 1 (preheating): 160°C, 5 min.; step 2: 160-220° C, time in the range 2-120 min.

Results and discussion

The influence of reaction time, temperature and the amount of alkaline solution on the TPA yield have been determined in order to establish the optimum parameters at which the reaction is completed. The reaction products were analyzed by using FT-IR spectroscopy, X-ray diffraction, scanning electron microscopy and NMR.

Conclusion

The use of microwave offers extremely short reaction time for complete degradation of PET waste as compared to the conventional heating. PET depolymerization was carried out completely for PET: alkaline solution ratio (w/v) of 1:10 after 5 minutes of reaction at 220°C, 20 minutes at 210 and 200°C, and 30 minutes at 190°C. TPA yield reached more than 98%.

Acknowledgements

This work is part of the project PN 09-34 03 07/2009 “Studies regarding hydrolysis processes of polyethylene terephthalate waste”, carried out under NUCLEU Program funded by National Authority for Scientific Research (Romania).

References

- [1] F. Awaja, D. Pavel, Eur. Polym. J. 41 (2005) 1453.
- [2] H.K. Webb, J. Arnott, R.J. Crawford, E.P. Ivanova, Polymers 5 (2013) 1.

THE STUDY OF SOME ELECTRICAL AND MAGNETIC PROPERTIES FOR THE BULK AND SURFACE OF Fe_3O_4 AND OTHER BINARY COMPOUNDS BY *AB INITIO* METHODS

Marius Chirita , Mocanu Liviu

*National Institute for Research and Development in Electrochemistry and Condensed Matter,
Department of Condensed Matter, 1 Plautius Andronescu St., 300224 Timisoara, Romania
e-mail:mocanuliv@gmail.com*

Abstract

Development of computing power has allowed more close parallel between theoretical aspects of science of materials and experimental data, as well as their direct interpretation on the basis of the proposed models. *Ab initio* methods constitute some of the tools of quanto-chemical calculations for approaching of the crystalline structures.[1] This work is a first step in an attempt to justify the superparamagnetic behavior of particles of Fe_3O_4 micrometer-sized [2,3]. We also propose the study of some electronic and energetic properties and structure parameters both in volume and surface for ZnS and CdS, both belonging to the crystalline phase of the P 63mc space group. To this end we used the Hartree-Fock hamiltonian with GTF-Pople sets of base function for optimization of structures, as well as Kohn-Sham hamiltonian with different exchange-correlation functionals for DFT calculations. Given the large number of electrons involved in the primitive cell we was forced to use the effective core pseudopotentials (ECP) to model the inner layers electrons.

References

1. **Robert Evarestov** “ Quantum Chemistry of Solids : The LCAO First Principles Treatments of Crystals “ **Springer-Verlag Berlin Heidelberg 2007**
2. **Marius Chirita**, Radu Banica, Adrian Ieta, Ioan Grozescu, *Superparamagnetic unusual behavior of micrometric magnetite monodisperse monocystals synthesized by Fe-EDTA thermal decomposition*, **Particulate science and Technology**, **30**: 354–363, **2012**
3. M.L. Kiss, **M. Chirita**, C.A. Beljung, R. Polanek, C. Savii, A. Ieta, A. Ionut Mihaila Chirita, *Single Crystalline Micrometric Iron Oxide Particles with Superparamagnetic Behaviour for MRI Applications*, **Tech Connect World, Nanotech 2014 Vol. 1, Chapter 6: Nanoscale Materials Characterisation**, pp: 448-451.

PHYSICO-CHEMICAL CHARACTERISTICS FOR SOME GREEN PLANT JUICES ASSORTMENTS

Cozma Antoanela, Velciov Ariana, Petcu Mihaela, Stoin Daniela, Poiana Mariana
Moigradean Diana, Micula Lia, Popescu Sofia

*Banat's University of Agricultural Sciences and Veterinary Medicine „King Michael I of
Romania” Timisoara*
*Faculty of Food Processing Technology, Food Science Department, 300645 Timisoara, Calea
Aradului 119, Romania*
e-mail: antoanelacozma@yahoo.com

Abstract

Due to their nutritional and biological potential, natural juices from green fruits and vegetables are foods with multiple implications for the body's balance both physically, mentally and emotionally. Consumed moderately, as part of a balanced diet, green herbal juices offer properties that promote good health, reducing the risk of illness. With high vitamin, mineral, fiber and antioxidant content, green juices from vegetables and fruits are increasingly appreciated and recommended. The green juice made from apple (*Malus domestica*) cucumber (*Cucumis Sativus*) spinach (*Spinacia oleracea*) and parsley (*Petroselinum crispum*) has an antioxidant, detoxifying and alkalinizing role, contributes to improving the health of the body.

The purpose of this study was to analyze and compare some physico-chemical characteristics: pH, electrical conductivity, dynamic viscosity and refractive index in case of the juice samples obtained from apples, spinach, cucumber, parsley and lime each taken separately and in the mixture.

Keywords: green vegetables and fruits juices, physical-chemical characteristics

Introduction

Juice is a liquid obtained by squeezing, from fruits, vegetables, and sometimes from herbs [2]. The energizing, vitaminizing, refreshing drink, natural juices are prime for a balanced lifestyle. It is recommended, prophylactic and curative, as an adjuvant when the body accumulates large amounts of acids; which has repercussions such as diabetes, aging, gout [1].

The quality of the juices depends both on the quality of the processed raw materials and on the correctness of the technological process. Pressing fruits and vegetables gives raw juice as a result of centrifugation, filtration, enzymatic clarification, cleansing or freezing, being converted into clear juice. Top quality juices have flavor, color, taste and smell specific to the fruits of origin and are clear [3,4]. In fruits and vegetables there are small amounts of mineral substances, but their importance to the good functioning of the body is extremely high. Along with the vitamins and ferments, they guide all the chemical transformations which take place in the fruit and vegetables, as well as in the human body. The most common mineral substances are: calcium, potassium, magnesium, iron, sulfur, phosphorus, silicon, chlorine [6,8].

Apple belongs to the Rosaceae family, occupies the first place in the temperate climate of fruit trees species, due to its fruit value. Apples are rich in sugars, organic acids, ascorbic acid, protein substances, pectic substances, minerals, vitamins (C, A, B₁, B₂, PP). Apples have therapeutic effects in the following diseases: ischemic cardiopathy, diarrhea, hypertension, chronic hepatitis, constipation, insomnia, arthritis.

Cucumber is part of the family Cucurbitaceae, an annual plant. Cucumber fruits have a diversified content in nutritional principles containing: 96% water, dry substance 4-6%, 1.7% carbohydrates, 0.7-1.1% pectic substances, 0.44-0.57% mineral salts and vitamins (ascorbic acid, pantothenic acid, nicotinic acid, complex B) [5].

Parsley is a biennial plant of the Umbellifere family. The root and leaves are consumed both raw and prepared with indications in circulatory diseases, general and nervous stimulant with depurative effects, act in the control of pinworms, digestive tonic, remedy of kidney diseases, liver, heart [6].

Spinach is part of the family Chenopodiaceae and is native to Central Asia. The importance of spinach leaves food is reflected in 7 to 11.3% dry substance content, 1.5-3.5% sugars, protides 2 to 3.7%, 40-70 mg of C vitamin, B₁ 0.15 mg, B₂ 0.20 mg and mineral salts (K-520 mg, P-160 mg, Ca-130 mg, Fe-8mg); values reported on 100 mg of fresh product. For therapeutic purposes it is recommended in cases of anemia, rickets, senescence, physical and nervous asthenia, eczema, burns, scurvy [5].

Green juice is considered a miracle drink, being a combination of vegetables, herbs and even green fruits, which act as an intravenous infusion of vitamins, minerals and enzymes.

Because they are in the form of a juice, easily digested and assimilated, its components go directly into the system and fill the body with nutrients and energy in less than 20 minutes. Green juice has a great advantage because, unlike fruit juice, it contains less sugar and calories. Because the taste of such a "vitamin bomb" is not very pleasant, it can be sweetened by the addition of fruit [7].

Experimental

A green juice from vegetables and fruits was prepared for this work, because it provides the body with a complete set of active compounds, regulates the digestive system, alkalises, energizes, detoxifies the body and acts as a functional food.

The following recipe was used to prepare the mixed green juice: 2 green apples 250g, spinach baby 150g, cucumber 250g, parsley 50g, 1/2 green lime. Samples of fruits and vegetables were purchased from a local market in May 2018.

The green juice obtained is a 100% natural product, without additives or preservatives, made with the juicer by mastication that extracts, crushes and presses, contributing to the release of nutrients from fruits and vegetables used in the preparation.

Natural juices from green plants were prepared using a Centrifugal Juicer of fruit and vegetables. Five distinct samples of apple juice, cucumber, spinach, parsley, limes of about 200 ml, were prepared separately, and a mixed sample resulting from the mixture of the 5 ingredients.

The physicochemical characteristics were determined from fresh and clearly juice prepared using a fruit and vegetable press robot. The pH was measured using a pH meter mark OP-211/2 connected with combined electrode OP-0808P according to the AOAC methods. The total soluble solids (TSS) and the refractive index were obtained using the refractometry method, with the Abbe refractometer corrected to the equivalent reading at 20°C (AOAC, 1995). Electrical conductance was determined by conductometer OK 112 and viscosity using Ostwald-type viscometer.

Results and discussion

The purpose of this paper was to analyze and compare some physico-chemical characteristics: pH, electrical conductivity, dynamic viscosity, refractive index, in case of the juice samples obtained from apples, spinach, cucumber, parsley and lime taken separately and all in the mixture. The determination of the physico-chemical parameters (pH, G, n, η) is an important indicator in the investigation of the physico-chemical and nutritional properties of the green juices analyzed in this study.

The property of plant juices to drive the electric current is quantitatively evaluated by electrical conductivity, G. Electrical conductivity is one of the parameters that verifies the authenticity, freshness of a product. The electrical conductivity of a food product is a function of product characteristics (composition, sugar content and salts, pH, etc.), and is also influenced by the heating process, especially temperature.

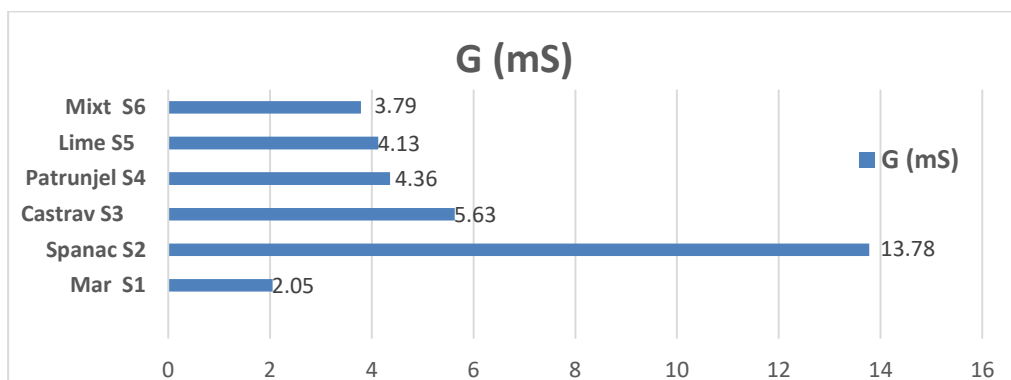


Figure 1. Determination of conductivity for different type of green juice samples

In terms of electrical conductivity, the highest value was obtained for natural spinach juice (13,78 mS) and the smallest of natural green apple juice (2,05mS). Natural juices contain a range of minerals, organic acids, fibers, salts and other bioactive substances.

Minerals are present in the form of electrolytes, so they are easily absorbable by the human body. It is known that the solution's conductivity increases with its content in dissolved substances. Conductivity varies with concentration and it grows with increasing electrolyte concentration. This increase depends both on the nature of the electrolyte and on the temperature.

Sugar (sucrose) is a carbohydrate that naturally occurs in fruits and vegetables. The high sugar concentration in fruit juices gives a high refractive index value. Regarding the refractive index, the smallest value (1.3439) was obtained in case of mixed natural juice with all ingredients and the highest value (1.3620) was obtained for the natural apple juice due to the soluble substance content, the sugar in the composition.

The acidity or alkalinity of a solution is expressed by physical size, pH. Being a measure of the acidic or basic character of a solution, pH is an important factor in the processing of fruit and vegetable products.

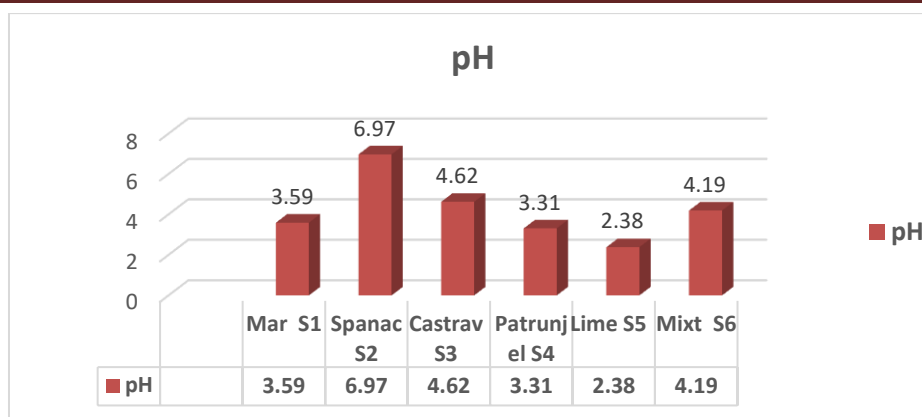


Figure 2. Determination of pH for different type of green juice samples

In case of the pH determination it was observed that the lowest value was obtained for lime juice (2.38) and the highest value for green spinach juice (6.97). Higher acidity (low pH) of preserved juices than fresh ones, recommends natural, fresh daily intake as a benefit in the treatment and prevention of many diseases. For example, most commercial drinking water has pH 7, beer has a pH of about 5, and juices between 5 and 6. Water and natural juices from fruits and vegetables have the role of compensating for a too acidic diet that can disrupt our metabolism. From the comparative analysis of pH determination results, this parameter is within the permissible limits for all the samples analyzed in this study.

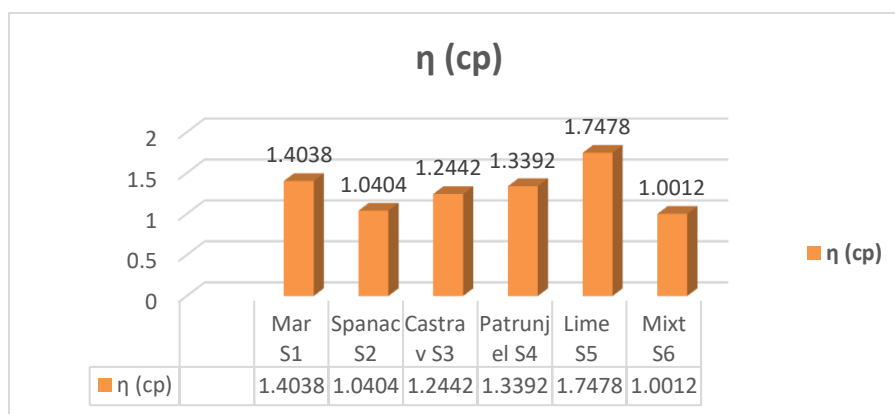


Figure 3. Determination of viscosity for different type of green juice samples

Viscosity is considered an important physical property for the quality of liquid foods. The increase in viscosity is the result of increased fiber, pectin and the amount of sugar present. If the natural herbal juices contain considerable amounts of pulp or are highly concentrated, they may have additional flow resistance represented by a higher stretching request. It has been found that the fresh juice viscosity is higher than the pasteurized ones due to the increased fiber content, pectin. For this reason, it is recommended to use freshly squeezed natural juices instead of pasteurized.

Conclusion

Green herbal juices have an important status in the modern diet due to their exceptional nutritional, functional and therapeutic qualities. Juices from green vegetables and fruits are an excellent source of water, natural sugar, vitamins, minerals, antioxidants, pigments, dietary fiber and other food ingredients.

From their analysis, for the natural juices considered (apples, spinach, cucumbers, parsley, and mixed) it can be noticed that their values differ from one category to another, but results are comparable to the data from the literature.

Due to its beneficial nutritional and antioxidant qualities, it is recommended to consume daily, succulent, freshly squeezed and immediately consumed over the pasteurized. Green vegetable and fruit juices acting as a functional food, is a simple affordable and effective alternative to cellular regeneration, health human body improvement.

References

- [1] Jianu I., Hădărugă Nicoleta, Natural extracts, flavors and flavoring compounds, T.P.A. Graduate guide in the specialization of extracts and natural food additives, 2000, Ed Eurostampa, Timișoara
- [2] Lascu Doina trad., Food Encyclopedia, 2008, Editura ALL
- [3] Pop Cecilia și Ioan Mircea, Food Merceology, 2006, Ed. Edict Production, Iași
- [4] Radu I. F., Treated fruit and vegetable technology, 1985, Ed. Scrisul Românesc, Craiova;
- [5] Poșta Gheorghe, Vegetable, 2008, Ed. Mirton, Timișoara
- [6] Coman Stelian, Preserving and processing fruits and vegetables, 1961, Ed. Agro-Silvica, București
- [7] <https://ligiapop.com/2009/04/24/the-importance-juice-green/>, 08.05.2018
- [8] Niac G., 2010, Nutrition, Nutrition, Food (Food science, culinary technologies), 2010, Ed. Emia

CHRONOPOTENTIOMETRIC DETERMINATION OF METAMITRON: COMPARING CLASSICAL AND BOX-BEHNKEN OPTIMIZATION APPROACHES

Ana Đurović¹, Zorica Stojanović¹, Snežana Kravić¹, Dušan Rakić¹, Nada Grahovac²

¹*University of Novi Sad, Faculty of Technology Novi Sad, Department of Applied and Engineering Chemistry, Bulevar cara Lazara 1, Novi Sad, Serbia*

²*Institute for Field and Vegetable Crops, Biotechnology Department, Maksima Gorkog 30, Novi Sad, Serbia*
e-mail: djurovic.ana@tf.uns.ac.rs

Abstract

This paper describes an optimization procedure for determination of the herbicide metamitron by chronopotentiometry. Two different working electrodes were used in the experiments: glassy carbon and thin film mercury electrode. The analytical signal of metamitron was the result of irreversible reduction on the working electrodes in Britton-Robinson buffer as the supporting electrolyte, and one reduction peak was obtained on both working electrodes. Operating conditions, involving several chemical and instrumental parameters such as: pH of Britton-Robinson buffer, initial potential and reduction current were optimized by the classical method, where one parameter is changing while others are constant, and by using Box-Behnken experimental design. In both optimization procedures, the maximum height of the metamitron analytical signal was requested. Obtained results from this study revealed that there were no differences between the two optimization methods.

Introduction

Metamitron (IUPAC: 4-amino-4,5-dihydro-3-methyl-6-phenyl-1,2,4-triazin-5-one, MTM) is a selective triazinone herbicide that is often used nowadays in agriculture for weed control in a variety of crops [1]. Like other pesticides, it can be toxic for humans, especially for aquatic organisms [2]. After application, the herbicide is predominantly absorbed by the roots, and also by leaves, and it acts as an inhibitor of photosystem II by induction chlorotic and necrotic symptoms in leaves [1, 3]. Depending on the environmental conditions: temperature, moisture, soil type, and application dose observed half-life for MTM in soil in the literature ranges from 6 to 90 days [3, 4]. High solubility in water (1.7 g/dm³) and weak sorption of MTM in soils with low organic matter content indicates the possibility of leaching and pollution of ground water sources [1, 5-7]. Hence, this herbicide was frequently detected in surface in ground water in concentrations up to 1.5 µg/dm³ [8-10].

Several methods have been reported in the literature for the determination of MTM such as chromatography [3, 8, 10-13] and spectroscopy [14]. These methods have proven to be sensitive and reliable, but also limited in the portability of sophisticated instrumentation, resulting in high cost and long detection time [15]. Nowadays, the use of electroanalytical procedures can be a suitable alternative, offering easy instrumental manipulation, low operating costs and accurate results with short analysis time. Square wave voltammetry [16, 17] and differential pulse voltammetry [18, 19] are the most frequently applied electroanalytical procedures for MTM determination.

The optimization procedure in most cases is carried out by monitoring the influence of one factor, while others are kept at constant level, in thus so called classical way. The major disadvantages of this kind optimization technique are increased number of experiments, and consumption of chemicals [20]. Also, this optimization technique does not consider the interactive effects among the studied parameters, which can lead to incorrect results. In past decade, response surface methodology with Box-Behnken experimental design has been

frequently applied in the optimization of analytical methods [21-23]. In this paper, glassy carbon electrode (GCE) and thin film mercury electrode (TFME) are used for chronopotentiometric determination of MTM. Results of two different optimization protocols using traditional and response surface methodology with Box-Behnken design are compared.

Experimental

All electrochemical measurements were carried out in a three-electrode system with M1 analyser for potentiometric and chronopotentiometric measurements constructed by our laboratory. GCE was used as the working electrode, or as an inert support for TFME. The auxiliary electrode was a platinum wire ($\varphi = 0.7$ mm, $l = 7$ mm), and the reference was an Ag/AgCl (3.5 mol/dm³ KCl) electrode. The GCE surface was polished with alumina slurry Al₂O₃ (0.5 μ m) and sonicated in mixture of ethanol and doubly distilled water for 10 min. TFME was prepared ex situ from the 0.02 mol/dm³ HCl solution containing 0.15 g/dm³ of Hg²⁺ ions at the potential of -0.4 V for 240 s, with stirring the solution.

Electrodes were immersed into the 20 dm³ of the supporting electrolyte, and the solution was purged with a nitrogen stream for 5 min before recording chronopotentiograms. Then, MTM standard solution was added to the supporting electrolyte and nitrogen stream was passed through the solution for additional 30 s. Afterwards, chronopotentiograms with the appropriate MTM reduction time were recorded.

MTM stock solution (0.01 mol/dm³) was prepared by dissolving of solid chemical (Dr Ehrenstorfer, Augsburg, Germany) in the HPLC grade acetonitrile (Kemika, Zagreb, Croatia). Working solution (0.04 mol/dm³) was prepared by appropriate dilution of the stock solution in doubly distilled water. Britton-Robinson (BR) buffers in the pH range from 2 to 12 are prepared by adding equal mols (0.04 mol) of boric, phosphoric and acetic acid. Sodium hydroxide (0.2 mol/dm³) was employed to adjust pH value of the buffer. All other reagents were of analytical grade.

Results and discussion

Classical optimization methodology

The effect of pH on the reduction time was investigated in BR buffer by applying pH values from 2 to 12, while the concentration of MTM was in the range from 2 mg/dm³ to 10 mg/dm³. Using the GCE as the working electrode, the best sensitivity was obtained from pH 2 to 4, with a significant decrease of reduction time from 2.15 s to 1.59 s (Table 1). In BR pH 5 only concentrations of herbicide higher than 2 mg/dm³ could be detected, therefore this value of pH is not included in further experiments. When MTM was investigated using TFME as a working electrode, the analytical signal is obtained in the range of pH of BR buffer from 2 to 10, while the best defined signals and highest sensitivity are accomplished in pH range from 5 to 9 (Table 1). As optimal pH values of BR buffer selected are those where the highest signal is obtained with best reproducibility and sensitivity. For GCE pH 2 was accepted as optimal, while for TFME pH 7 was proved as optimal.

The effect of initial potential on the MTM analytical signal using GCE was examined in the BR buffer pH 2 containing 10 mg/dm³ MTM, in the potential range from 0.01 V to -0.63 V. Change of initial potential from 0.01 V to -0.45 V did not significantly affect the height of the analytical signal, while at the initial potential of -0.63 V the analytical signal significantly decreased. As optimal value of the initial potential -0.31 V was accepted. Using TFME as a working electrode the influence of initial potential on the MTM analytical signal was investigated in BR pH 7 containing 10 mg/dm³ MTM in the potential range from 0 V to -0.51 V. In the investigated potential range MTM reduction time decreased from 0.95 s to 0.75 s, and the worst reproducibility is obtained at the value of -0.14 V. The highest and the most

reproductive analytical signal of MTM was obtained at the value of initial potential of 0 V ($\tau_{\text{red}} = 0.95$ s, RSD = 1.49%, Figure 1), and this value is accepted in all further experiments.

Table 1. The effect of pH of BR buffer on the MTM analytical signal, on GCE and TFME, concentration of MTM 10 mg/dm³

Working electrode	pH of BR buffer	Reduction time ± 2 SD (s) ^a
GCE	2	2.15 \pm 0.02
	3	1.75 \pm 0.03
	4	1.59 \pm 0.02
TFME	5	0.61 \pm 0.02
	6	0.65 \pm 0.04
	7	1.16 \pm 0.03
	8	1.13 \pm 0.03
	9	1.02 \pm 0.03

^a n = 3.

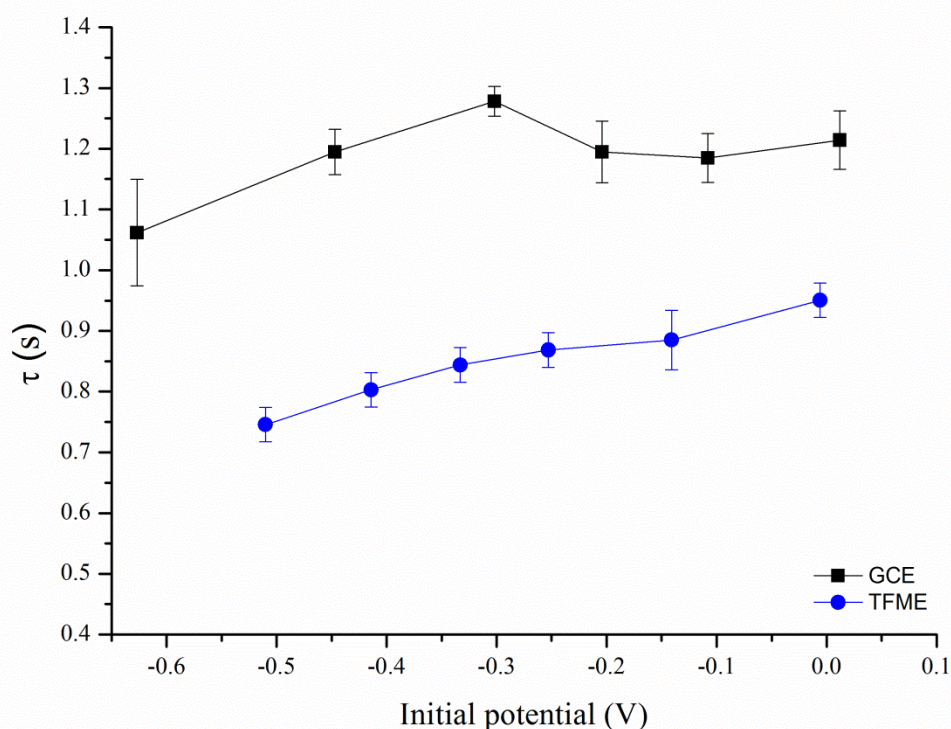


Figure 1. The effect of initial potential on the MTM analytical signal on GCE and TFME, concentration of MTM 10 mg/dm³, mean \pm 2SD, n = 3

In chronopotentiometry the reduction current represents the most important parameter of the analysis, as it heavily influences on the height and sharpness of the analytical signal. Studied ranges of reduction current for solutions containing 10 mg/dm³ MTM on GCE and TFME were from -1.9 μ A to -7.9 μ A, and from -3.5 μ A to -16 μ A, respectively. The MTM reduction time decreased exponentially with more negative values of reduction current for both working electrodes used in experiments. Obtained exponential functions for GCE and TFME were $\tau = 2.2576 e^{0.1182 i}$ $r = 0.9973$, and $\tau = 4.2113 e^{0.2597 i}$ $r = 0.9974$, respectively. Using the criterion of rectilinear sequence of dependence $I \tau_{\text{red}}^{1/2} = f(I)$, the appropriate intervals of reduction current that should be applied for MTM determination were from -1.9 to -7.9 μ A for GCE, and from -3.5 to -14.3 μ A for TFME.

Box-Behnken optimization method

Using the preliminary results of the classical optimization methodology, where a measurable signal of the analyte is obtained, a three-level three-factor Box-Behnken experimental design was used for optimization procedure. Chronopotentiometric experiments were performed in Britton-Robinson buffer using the reduction time of 10 mg/dm³ of MTM as the response of the system. The statistical analysis involves the significance of the parameters, and their interactions on the analytical signal has been described in detail elsewhere [24]. Based on the obtained results, the maximum analytical signals are obtained by the following combination of parameters: pH of BR buffer 2, initial potential -0.31 V, reduction current -2.3 μ A for GCE, and pH of BR buffer 7, initial potential 0 V, reduction current -3.5 μ A for TFME. By comparing the results of the classical optimization procedure with the results obtained using the experimental design, no differences in the optimal parameters of the analysis were observed.

Conclusion

This paper describes optimization procedures for chronopotentiometric determination of the herbicide MTM using GCE and TFME as working electrodes. In the first step, the optimization was performed in the classical way by changing one factor, while the others are maintained at a constant level. The results obtained using the classic optimization methodology, are compared with the results obtained on the basis of the Box-Behnken experimental design and the statistical analysis. In the light of findings from both optimization procedures, it can be concluded that they presenting similar results. The developed method could be applied for determination of the MTM content in real samples.

Acknowledgements

The authors are grateful to the Ministry of Education, Science and Technological Development of the Republic of Serbia for supporting this work by Grant III 46009.

References

- [1] T. R. Roberts, *Metabolic Pathways of Agrochemicals Part One: Herbicides and Plant Growth Regulators*, The Royal Society of Chemistry, Cambridge, UK, 1998, pp. 659.
- [2] EFSA (European Food Safety Authority) Scientific Report. Conclusion on the peer review of metanitrone, 185 (2008), <<http://onlinelibrary.wiley.com/doi/10.2903/j.efsa.2008.185r/epdf>, (Accessed 10 May 2018).
- [3] P. Janaki, S. Rathika, C. Chinnusamy, N. K. Prabhakaran, *Bull. Environ. Contam. Toxicol.* 90 (2013) 116.
- [4] P. Laitinen, K. Siimes, L. Eronen, S. Rämö, L. Welling, S. Oinonen, L. Mattsoff, M. Ruohonen-Lehto, *Pest. Manag. Sci.* 62 (2006) 473.
- [5] M. B. Matallo, S. D. B. Almeida, E. A. D. Da Costa, L. C. Luchini, M. A. F. Gomes, C. A. Spadotto, A. L. Cerdeira, M. A. M. Moura, D. A. S. Franco, *Embrapa Meio Ambiente* 18 (2008) 17.
- [6] S. Autio, K. Siimes, P. Laitinen, S. Rämö, S. Oinonen, L. Eronen, *Chemosphere* 55 (2004) 215.
- [7] Y. Coquet, *Pest. Manag. Sci.* 58 (2002) 69.
- [8] C. Moschet, E. L. M. Vermeirssen, H. Singer, C. Stamm, J. Hollender, *Water Res.* 71 (2015) 306.
- [9] A. E. Rosenbom, P. Olsen, F. Plauborg, R. Grant, R. K. Juhler, W. Brüsch, J. Kjær, *Environ. Pollut.* 201 (2015) 75.
- [10] J. J. Jiménez, J. L. Bernal, M. J. Del Nozal, J. M. Rivera, *J. Chromatogr. A* 778 (1997) 289.

- [11] J. Moros, S. Armenta, S. Garrigues, M. de la Guardia, *Anal. Chim. Acta.* 565 (2006) 255.
- [12] S. Kumar, S. Tandon, N. K. Sand, *Bull. Environ. Contam. Toxicol.* 92 (2014) 165.
- [13] J. Robles-Molina, B. Gilbert-López, J.F. García-Reyes, A. Molina-Díaz, *Sci. Total Environ.* 479–480 (2014) 247.
- [14] S. Tandon, S. Kumar, N. K. Sand, *Int. J. Anal. Chem.* 592763 (2015) 1.
- [15] X. Li, H. Zhou, C. Fu, F. Wang, Y. Ding, Y. Kuang, *Sens. Actuators B Chem.* 236 (2016) 144.
- [16] A.S. Arribas, E. Bermejo, M. Chicharro, A. Zapardiel, *Electroanalysis* 18 (2006) 2331.
- [17] A. Gómez-Caballero, N. Unceta, M. Aranzazu Goicolea, R. J. Barrio, *Electroanalysis* 19 (2007) 356.
- [18] A. Arranz, F.S. de Betoño, J.M. Moreda, A. Cid, J.F. Arranz, *Microchim. Acta.* 127 (1997) 273.
- [19] R. Šelešovská, L. Janíková, J. Chýlková, *Monatsh. Chem.* 146 (2015) 795.
- [20] S. L. C. Ferreira, R. E. Bruns, H. S. Ferreira, G.D. Matos, J.M. David, G. C. Brandão, E. G. P. da Silva, L. A. Portugal, P. S. dos Reis, A. S. Souza, W. N. L. dos Santos, *Anal. Chim. Acta* 597 (2007) 179.
- [21] M. Cuéllar, V. Pfaffen, P. I. Ortiz, *J. Electroanal. Chem.* 765 (2016) 37.
- [22] G. Zhao, H. Wang, G. Liu, Z. Wang, *Sens. Actuators B Chem.* 235 (2016) 67.
- [23] G. G. Honório, G. C. Azevedo, M. A. C. Matos, M. A. L. de Oliveira, R. C. Matos, *Food Control* 36 (2014) 42.
- [24] A. Đurović, Z. Stojanović, S. Kravić, D. Rakić, N. Grahovac, *Int. J. Environ. Anal. Chem.* 98 (4), 369.

INDUSTRIAL BY-PRODUCTS AS A SOURCES HIGH-VALUE POLISACCHARIDE COMPOUNDS

Tatjana Đorđević, Maja Milošević, Mirjana Antov

*University of Novi Sad, Faculty of Technology, Blvd. Cara Lazara 1, Novi Sad, Serbia
e-mail: tatjanadjordjevic@uns.ac.rs*

Abstract

Agricultural wastes and industrial by-products represent a major origin of carbohydrates. Obtaining hemicelluloses such as arabinoxylan and pectin from these sources presents attractive utilization of waste material. In additions, these polysaccharide products gained much attention because of their excellent biocompatibility, biodegradation and non-toxicity as well as extensive spectrum of their biological and functional properties. Polysaccharides with a molecular weight of about 20 kDa were isolated from the wheat chaff and sugar beet shreds. Obtained pectin produced gel coacervats with gelatin while arabinoxylan from wheat chaff formed a gel by mixing with β -glucan in the presence of laccase. Both of prepared gels under simulated gastric and intestinal conditions indicated a strong stability. Furthermore, biological investigation of extracted polysaccharides revealed good antioxidative activities.

Introduction

A large amount of waste is produced by agro-industrial sector but maximum benefit has not yet been attained from it [1]. Sugar beet shreds present an industrial by-product while wheat chaff is generated during harvest. They are usually used as animal feed rather than sources for extraction of valuable components for human use. Hence, there is a need for improved technologies that would be able to enhance utilization of all high-value components from such waste materials and reduce cost of processing. In this context, considerable interest has been focused during the last years on polysaccharides from agricultural and industrial by-products as desirable alternatives to conventional petroleum-based fuels. However, polysaccharides have a wide range of other features such as biological and functional activities. Therefore, the aim of this study was to investigate application of wheat chaff and sugar beet shreds as sources of antioxidant and functional carbohydrates.

Experimental

Arabinoxylan was isolated from wheat chaff by alkaline extraction, while pectin was isolated by hot acid extraction from sugar beet shreds. Following the extraction, polysaccharides were precipitated with ethanol and dried. Molecular mass of the isolated polysaccharides was determined viscosimetrically. Arabinoxylan gel was obtained by laccase crosslinking in 4% polysaccharide solution. Pectin gel was formed by coacervation of 0.5% pectin and 1.0% gelatin solution at pH 4. Prepared gels were dried at room temperature. The stability of dry gels was investigated in simulated gastrointestinal conditions. For 2 h gels were immersed in simulated gastric fluid (SGF) at pH 2, followed by 10 h in simulated intestinal fluid (SIF) at pH 7. The stability was monitored in defined time intervals as the amount of dissolved reducing sugars from the arabinoxylan gel or as the amount of dissolved gelatin from pectin based gel. ABTS method was applied to estimate antioxidant potential of extracted polysaccharides.

Results and discussion

Pectin was isolated from sugar beet shreds by acid extraction and subsequently precipitated with ethanol, washed in water, partially purified by ultrafiltration and dried with yield 202.5 mg/g while extraction yield of arabinoxylan from wheat chaff at alkaline conditions amounted 60 mg/g. The molecular weight of isolated polysaccharides was similar (Table 1). Both of obtained polysaccharides could form gel. Arabinoxylan formed gel using laccase for crosslinking of ferulic acid while the β -glucan was used for increase in gel stiffness [2]. Formation of pectins gel included interaction between negatively charged pectin polysaccharides and positively charged gelatin at acidic pH [3]. Both of formed gel structures showed good stability under simulated intestinal fluid while degradation in gastric fluid was more noticeable (Figure 1). In this study, ABTS *in vitro* assay was applied to evaluate antioxidant potential of polysaccharides extracted from wheat chaff and sugar beet shreds. As showed in Figure 2, arabinoxylan and pectin exhibited dose-dependent behavior of antioxidant activity.

Table 1. Yield and molecular weight of extracted polysaccharides

	Y(mg/g)	MW (g/mol)
Arabinoxylan	60.0	29,000
Pectin	202.5	22,200

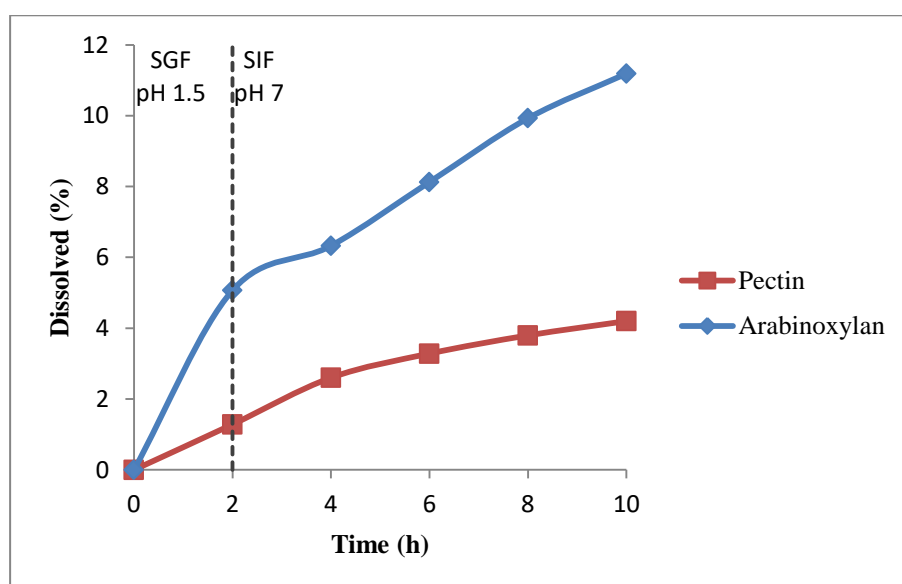


Figure 1. Stability of gels in gastrointestinal conditions

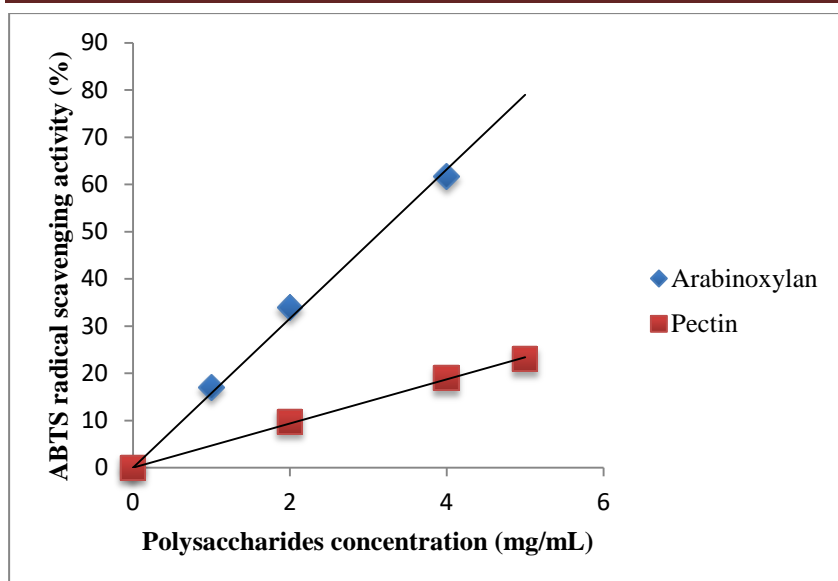


Figure 2. Antioxidant activity of extracted polysaccharides

Conclusion

Arabinoxylan and pectin could be novel bio-sources of gelling agents and antioxidants with potential added value when applied as functional food and for encapsulation of therapeutics.

Acknowledgements

Financial support from Ministry of Education, Science and Technological Development, Republic of Serbia (Grant No. III 46010 and III 45021) is gratefully acknowledged.

References

- [1] A. Fadel, A.M. Mahmoud, J.J.Ashworth, W. Li, Y.L. Ng, A. Plunkett, *Int J Biol Macromol.* 109 (2018) 819-831.
- [2] P. Lopez-Sanchez, D. Wang, Z. Zhang, B. Flanagan, M.J. Gidley, *Carbohydr Polym.* 151 (2016) 862-870.
- [3] M. Saravanan, K. Panduranga Rao, *Carbohydr Polym* 80 (2010) 808-816.

MICROWAVE-ASSISTED EXTRACTION OF CANNABIDIOL AND Δ^9 -TETRAHYDROCANNABINOL FROM CANNABIS AREAL PARTS AND PROCESS MODELING

Zorica Drinić,¹ Jelena Vladić,¹ Senka Vidović,¹ Anamarija Koren,¹ Biljana Kiprovska,² Tijana Zeremski²

¹ Department of Biotechnology and Pharmaceutical Engineering, Faculty of Technology, University of Novi Sad, 21000 Serbia

² Institute of Field and Vegetable Crops, Novi Sad, Serbia
e-mail: vladicjelena@gmail.com

Cannabis contains 66 cannabinoids which are divided into 10 subclasses: cannabigerol (CBG) type, cannabichromene (CBC) type, cannabidiol (CBD) type, Δ^9 -tetrahydrocannabinol (THC) type, Δ^8 -THC type, cannabicyclol (CBL) type, cannabielsoin (CBE) type, cannabinol (CBN) and cannabinodiol (CBND) types, cannabitrilol (CBT) type, and miscellaneous types subclass. In industrial cannabis, the allowed content of THC, which is the carrier of psychoactive activity, is different in different countries. According to the European Monitoring Centre for Drugs and Drug Addiction in the European Union countries, THC is allowed to be 0.2% expressed on dry matter, while in Serbia it is allowed to contain 0.3%. In most countries of the European Union, cannabis is legalized for medical purposes. Some countries allow its use only in the form of ready-made preparations containing isolated or chemically synthesized certain cannabinoids, while others allow the use of the extract.

The extraction of CBD and THC of industrial cannabis was carried out by a microwave-assisted technique, an emerging environmentally-friendly technology. The effects of different extraction parameters (ethanol concentration (30-70%), extraction time (10-30 min), and liquid/solid ratio (5-15 mL/mg)) on the extraction of CBD and THC were investigated using a response surface methodology. In obtained extracts content of CBD was in the range from 0.034 to 0.064 mg/mL, and content of THC was in the range from 0.224 to 1.842 mg/mL. Experimental results were described by the second order polynomial model. Model was estimated using analysis of variance (ANOVA). The optimization process carried out in order to obtain the most optimal content of desired types of cannabinoids.

SmCoO₃ DOPED (K.Na)NbO₃ LEAD FREE PIEZOELECTRIC CERAMICS

Farkas Iuliana¹, Bucur Alexandra Ioana¹, Bucur Raul Alin¹

¹ National Institute for Research and Development in Electrochemistry and Condensed Matter, Condensed Matter Department, No.1 Plautius Andronescu, 300224 Timisoara Romania.

e-mail: iulia_b24@yahoo.com

Abstract

(K_{0.5}Na_{0.5})NbO₃ (KNN) has been considered a promising material for lead-free piezoelectric ceramics because of its high Curie temperature (above 420 °C), good ferroelectric properties ($P_r = 33 \mu\text{C}/\text{cm}^2$), large piezoelectric longitudinal response ($d_{33} \sim 160 \text{ pC/N}$), and high planar coupling coefficient ($k_p \sim 46\%$). [1,2,3]

An environmental friendly piezoceramic material based on (K_{0.5}Na_{0.5})NbO₃ (noted KNN) was prepared by solid state synthesis. In order to increase the quality of the material we used SmCoO₃ as a dopant. Recently alkali oxide materials, including potassium sodium niobate, have been given attention in view of their ultrasonic application and also as promising candidates for a piezoelectric non lead-based system [4]. X-ray diffraction technique shows that the amount of SmCoO₃ changes the perovskite structure from orthorhombic to tetragonal, with small amount of impurities. The obtained materials were mixed with PVA and pressed into disks in order to examine the dielectric behavior. The dielectric measurements (from 100 Hz up to 5 MHz) were performed with a 42 Hz–5 MHz Programmable Impedance/LRC meter TEGAM model 3550, namely the variation of dielectric constant (ϵ_r) and dielectric loss ($\tan \delta$) at different frequencies. The dielectric constant generally decreases with the increase of frequency. The decreasing behavior of ϵ_r with the increase in frequency can be explained on the basis of dispersion of polarization with frequency. Dielectric polarization in the material is the sum of total different polarization mechanisms such as: electronic, ionic, dipolar and interfacial polarization [5,6]. The values that we measure for ϵ_r at 1 KHz are between 812 for low doped (1% SmCrO₃) material and 678 for KNN doped with 5% SmCrO₃ at room temperature conditions. In conclusion the addition of SmCoO₃ in KNN structure produce a phase transition at room temperature and enhance the value of the real part of the dielectric constant.

References

- [1] R.E. Jaeger, L. Egerton, J. Am. Ceram. Soc. 45 (1962) 209–213
- [2] K.-I. Kakimoto, I. Masuda, H. Ohsato, J. Eur. Ceram. Soc. 25 (2005) 2719–2722.
- [3] Manoon Sutapun, Chien-Chih Huang, David P. Cannb, Naratip Vittayakorn: Phase transitional behavior and dielectric properties of lead free (1-x)(K_{0.5}Na_{0.5})NbO₃-xBi(Zn_{0.5}Ti_{0.5})O₃ ceramics Journal of Alloys and Compounds 479 (2009) 462–466
- [4] Electrical properties of piezoelectric sodium-potassium niobate Author M. Ichiki, L. Zhang, M. Tanaka, R. Maeda, Journal of the European Ceramic Society Volume 24, Issue 6, 2004, Pages 1693-1697
- [5] Sridevi Swaina, Pawan Kumara, n, Dinesh K. Agrawalb, Sonia “Dielectric and ferroelectric study of KNN modified NBT ceramics synthesized by microwave processing technique, Ceramics International 39 (2013) 3205–3210
- [6] K. Singh, T.C. Goel, R.G. Mendiratta, O.P. Thakur, C. Prakash, Dielectric properties of Mn-substituted Ni–Zn ferrites, Journal of Applied Physics 91 (2002) 6626.

STRUCTURE–RHEOLOGY RELATIONSHIP IN POLYSULFONES WITH TRIPHENYLPHOSPHONIUM PENDANT GROUPS SYSTEMS FOR ENGINEERING APPLICATIONS

Anca Filimon¹, Adina Maria Dobos¹, Adriana Popa²

¹*Department of Physical Chemistry of Polymers, „Petru Poni“ Institute of Macromolecular Chemistry, Grigore Ghica Voda Alley 41A, 700487, Iassy, Romania*

²*Institute of Chemistry Timisoara of Romanian Academy, 24 Mihai Viteazul Blv., 300223, Timisoara, Romania*

e-mail: capataanca@yahoo.com; apopa_ro@yahoo.com

Abstract

Ionic polysulfones have received widespread attention for their promising roles in order to create new materials that can modulate the membrane properties. In this context, understanding of mechanisms developed in quaternized polysulfones with triphenylphosphonium pendant groups solutions, considering their specific interactions and the way in which these interactions affect their physical properties were evaluated by rheological investigations. Rheological behavior of this system, described by the non-linear flow curve, indicates the effect of the chemical structure of quaternized polysulfone, in order to facilitate the subsequently preparation of the active membranes. Thus, this study analyzes the processing-property relationship of solutions based on quaternized polysulfones and possibility of using it's, with expected future developments in the engineering fields.

Introduction

Polymeric materials are used for a wide range of industrial products making them more valuable to their users, namely, in separation technology, food processing, biological processes, medical devices and blood purification or hemodialysis [1,2]. In this context, it is known that polysulfones (PSFs), possessing superior properties, such as chemical, mechanical, and thermal resistance, represent the ideal candidates in the membrane industry. However, the use of these polymers is restricted by their hydrophobicity and may be improved by their modification through different processes [3-5]. Therefore, the introduction of reactive groups (e.g., ammonium, phosphonium) onto the polysulfone backbone affords the possibility to obtain polysulfones with improved properties. Thus, polymers carrying these groups have properties quite different from those of polysulfones and have a significant technological importance for the manufacture of commercial membranes with expanding the application area of the polysulfones, such as gas separation, pervaporation, hemodialysis, nano and ultrafiltration, cell culture, biological processes, or blood purification [6-8].

Particularly, functionalized polysulfones with triphenylphosphonium pendant groups, PSFPs, indicate some key characteristics generated by the phosphonium units, which should be underlined as compared to the ammonium or sulfonic units. Generally, PSFP shows a higher degree of hydrogen bonding and a lower water uptake, comparatively with their sulfonated compounds. Owing to the enhanced thermal stability of phosphonium versus ammonium cations, PSFPs have a greater technological importance as phase transfer catalysts, antistatic agents, biocides, humidity sensors, and water filtration membranes [9]. Consequently, the phosphonium cations may improve the thermal stability of polymers, being preferred for long-term use applications [10], for facilitating aggregation [11] or as an aid in matrix reinforcement of ionomers [12].

This study evaluates the effect of the chemical structure of quaternized polysulfone with triphenylphosphonium pendant groups (PSFP) on the rheological data for establishing its

processing-property relationships. The knowledge of the rheological parameters of PSFP solutions is very important for development of flow models for engineering applications, formulation of commercial production, design and process evaluation, quality control and storage stability. Therefore, these results are useful in future investigations concerning utilization of these polymers as semipermeable membranes in biomedical or industrial field.

Experimental

Commercial aromatic polysulfone (PSF, UDEL-3500) was used in the synthesis of chloromethylated polysulfones (CMPSFs) and subsequently, of polysulfones containing triphenylphosphonium pendant groups (PSFPs) [3,4,13]. Thus, a mixture of commercial paraformaldehyde with an equimolar amount of chlorotrimethylsilane (Me_3SiCl) as a chloromethylation agent, and stannic tetrachloride (SnCl_4) as a catalyst, was used for the chloromethylation reaction of polysulfone, at 50 °C [3,4]. The reaction time necessary to obtain chloromethylated polysulfones (CMPSF) was 72 h. Finally, the samples were dried under vacuum at 40 °C.

Polysulfone with triphenylphosphonium pendant groups, PSFP was synthesized by reacting chloromethylated polysulfone with triphenylphosphine (PPh_3) in the presence of dioxane [13]. The mixture was maintained under stirring, in nitrogen atmosphere, for 15 h at 90 °C. The viscous product thus obtained was filtered, washed with dioxane and ethyl ether, and finally dried.

The contents of ionic chlorine, Cl_i , and total chlorine, Cl_t , were determined by potentiometric titration (Titrator TTT1C Copenhagen), with 0.02N AgNO_3 aqueous solutions. The ratios between the ionic chlorine and the total chlorine contents show that the quaternization reaction of CMPSF occurs at a transformation degree around 72 %. The characteristics of the synthesized polysulfones are presented in Table 1.

Table 1. Total chlorine, ionic chlorine, and phosphorus contents, substitution and functionalization degrees and number-average molecular weights, \overline{M}_n , of polysulfone and functionalized polysulfones

Properties	PSF	CMPSF	PSFP
Cl (%)	-	8.68	5.85
Cl_i (%)	-	-	4.23
P (%)	-	-	3.11
Substitution degree (%)	-	98	72
Functionalization degree (mmol/g)	-	-	1.001
\overline{M}_n (g/mol)	39,000	29,000	28,000

Rheological properties of quaternary polysulfone with triphenylphosphonium pendant groups in N,N-dimethylformamide (DMF) were determined on a Bohlin CS50 rheometer, manufactured by Malvern Instruments (Worcestershire, United Kingdom). The measurements were performed by using a system presents cone-plate geometry with a cone angle of 4° and 40 mm diameter. Shear viscosities were registered in the range of 0.07–150 1/s shear rate domain, at several temperatures (25–45 °C) and concentrations in semi-dilute domain ranging from 5–12.5 g/dL. According to the amplitude sweep test performed at a frequency of 1 Hz, in the linear viscoelastic regime for shear stresses between 2 and 10 Pa, a shear stress of 2 Pa

was selected for all samples. Rheological tests were obtained with an accuracy of $\pm 5\%$, for different measurements.

Results and discussion

Dynamic rheology is one of the most effective tools to investigate the flow behavior and microstructural changes in the polymer materials. Thus, the flow behavior of PSFP in DMF at different concentrations, where a complex behavior appears under specific conditions, was evaluated from the dynamic viscosity - shear rate dependence (Figure 1a).

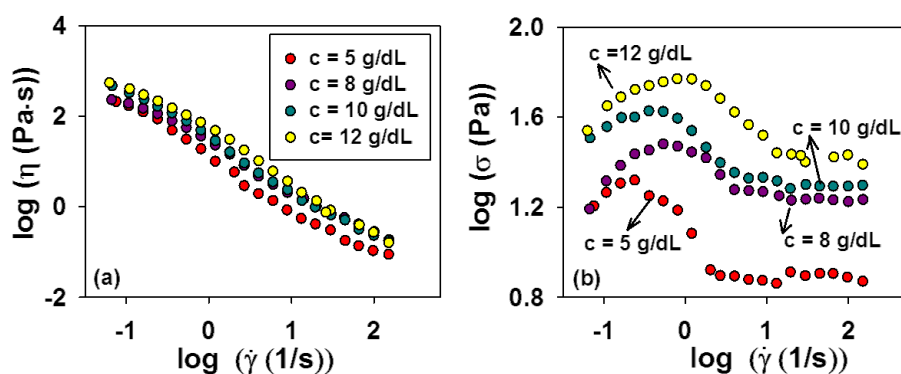


Figure 1. Variation of rheological parameters for solutions of PSFP in DMF at different concentrations and 25 °C: (a) Double logarithmic plot of dynamic viscosity (η) versus shear rate ($\dot{\gamma}$); (b) Logarithmic plot of shear stress (σ) as a function of shear rate ($\dot{\gamma}$).

According to literature data [14], examination of flow curves (Figure 1a) reveal that, the dynamic viscosity - shear rate dependence for PSFP solutions exhibit a shear thinning behavior in the shear rate range studied. Therefore, the investigated solutions present a dynamic viscosity that decreases with increasing of shear rate due to the destruction of the solutions microstructure at high shear, showing a pseudoplastic flow ("shear thinning"). In addition, increase of concentration led to an increase of dynamic viscosity on the shear rates domain. At the same time, it is observed that, as shear rate increases, the slope of curves decreases, and a Newtonian plateau tends to appears. In this context, one can conclude that these solutions possess properties of pseudoplastic materials, characterized by reduced entanglement density and enhanced number of oriented segments, as a result of increasing shear rates [15].

In our study, rheological tests were performed by increasing the shear rate at the different state of movement, in order to quantify flow behavior. Thus, this behavior illustrated in Figure 1a is also reflected in the variation of shear stress (σ) with shear rate ($\dot{\gamma}$) (Figure 1b). Concentrated solutions studied reveal a maximum on upward curve at very low shear rate, explained by Burgentzle et al. [16] as a consequence of the fact that a large shear stress must be applied to break the strongly network between polymer particles and to orient in the flow direction.

The solutions exhibit peculiar properties, namely they stop to flow abruptly below a critical stress and start to flow at a high velocity beyond a critical stress [17]. In accordance with literature [17], the rheological behavior of concentrated PSFP solutions is the result of the competition between the two processes which occur in these systems:

- "aging phenomena" which consists of a viscosity increase at rest due to the build-up of the microstructure and
- "shear rejuvenation" process associated with the decrease of the viscosity in time under shear due to the destruction of the microstructure.

Flow behavior illustrated in Figure 1a is also reflected in the values obtained for the flow behavior (n) and consistency (k) indices, evaluated from variation of shear stress (σ) with shear rate ($\dot{\gamma}$) according to the Ostwald-de Waele model [2]. The values of these parameters are indicative which can be explained by modification of the specific interactions from the system PSFP/DMF.

Consequence, this behavior can be explained by the balance between macromolecular mobility and specific interactions, reflecting the significant contribution of electrostatic interactions and, also suggesting the manifestation of an aggregation tendency as results of the long-range interactions between polymer chains.

Conclusion

Influence of the structural characteristics of polysulfone with triphenylphosphonium pendant groups, PSFP is reflected on the rheological properties, through dynamic viscosity and consistency indices. Therefore, the quantified results of parameters which describe the conformation properties of PSFP solutions determine a lower packing efficiency conducting to a shear thinning behavior in the shear rate range studied. Additionally, the rheological behavior of PSFP solutions is affected by specific interactions, including hydrogen-bonding and association phenomena.

The results of this study have demonstrated that PSFP solutions may provide some important advantages concerning to their specific applications. Thus, these results are useful in future investigations on engineering applications, and utilization of these polysulfones as membranes in this field.

References

- [1] J. Barzin, S.S. Madaeni, H. Mirzadeh, M. Mehrabzadeh, J. Appl. Polym. Sci. 92 (2004) 3804.
- [2] A. Filimon, R.M. Albu, I. Stoica, E. Avram, Composites Part B 93 (2016) 1.
- [3] E. Avram, E. Butuc, C. Luca, J. Macromol. Sci. Part A Pure Appl. Chem. 34 (1997) 1701.
- [4] C. Luca, E. Avram, I. Petrariu, J. Macromol. Sci. Part A 25 (1988) 345.
- [5] A. Filimon, E. Avram, I. Stoica, Polym. Int. 63 (2014) 1856.
- [6] Y.F. Zhao, L.P. Zhu, Z. Yi, B.K. Zhu, Y.Y. Xu, J. Membr. Sci. 440 (2013) 40.
- [7] L.J. Zhu, L.P. Zhu, J.H. Jiang, Z. Yi, Y.F. Zhao, B.K. Zhu, J. Membr. Sci. 451 (2014) 157.
- [8] A. Filimon, E. Avram, S. Dunca, Polym. Eng. Sci. 55 (2015) 2184.
- [9] S. Cheng, F.L. Beyer, B.D. Mather, R.B. Moore, T.E. Long, Macromolecules 44 (2011) 6509.
- [10] W. Xie, R. Xie, W. Pan, D. Hunter, B. Koene, L. Tan, R. Vaia, Chem. Mater. 14 (2002) 4837.
- [11] J.S. Parent, A. Penciu, S.A. Guillen-Castellanos, A. Liskova, R.A. Whitney, Macromolecules 37 (2004) 7477.
- [12] A. Eisenberg, B. Hird, R.B. Moore, Macromolecules 23 (1990) 4098.
- [13] A. Popa, C.M. Davidescu, R. Trif, Gh. Ilia, S. Iliescu, Gh. Dehelean, React. Funct. Polym. 55 (2003) 151.
- [14] H. Li, X. Shen, G. Gong, D. Wang, Carbohydr. Polym. 73 (2008) 191.
- [15] H. Watanabe, Prog. Polym. Sci. 24 (1999) 1253.
- [16] D. BURGENTZLE, J. DUCHET, J.F. GERARD, A. JUPIN, B. FILLON, J. Colloid Interface Sci. 278 (2004) 26.
- [17] P. Coussot, Q.D. Nguyen, H.T. Huynh, D. Bonn, J. Rheol., 46 (2002) 573.

EFFECTS OF TETRAETHYL ORTHOSILICATE INTRODUCING ON THE RHEOLOGICAL PROPERTIES OF CELULOSE ACETATE SOLUTION

Adina Maria Dobos¹, Anca Filimon¹, Adriana Popa²

¹Department of Physical Chemistry of Polymers, "Petru Poni" Institute of Macromolecular Chemistry, Aleea Grigore Ghica Voda 41 A, 700487 Iasi, Romania

²Institute of Chemistry Timisoara of Romanian Academy, Mihai Viteazul Blv. 300223 Timisoara, Romania

e-mail: capataanca@yahoo.com; apopa_ro@yahoo.com

Abstract

The rheological behavior of cellulose acetate (CA)/tetraethyl orthosilicate (TEOS) solution in N,N-dimethylacetamide (DMAc) has been investigated as a function of TEOS content for different shear rates and temperatures. The shear-thinning behavior or so called "pseudoplastic" behavior of the CA pure solution may be caused, on the one hand, by the destruction of the polymer chains as the shear rate increases, and on the other hand, by the increasing of the chains orientation in the flow direction during the rotational measurements. Also, for CA/TEOS blend solutions the curves shape varies from one content to another, a decrease in viscosity as the content of TEOS increases being observed. This tendency, of viscosity decreasing, is mainly due to the formation of hydrogen bonds between -OH groups and Si-OH, characteristic to TEOS, which means that increase in TEOS content tends to form a stable gel network. Furthermore, as temperature increases the viscosity varies irregularly, this being a consequence of the conformational transitions occurring in the system.

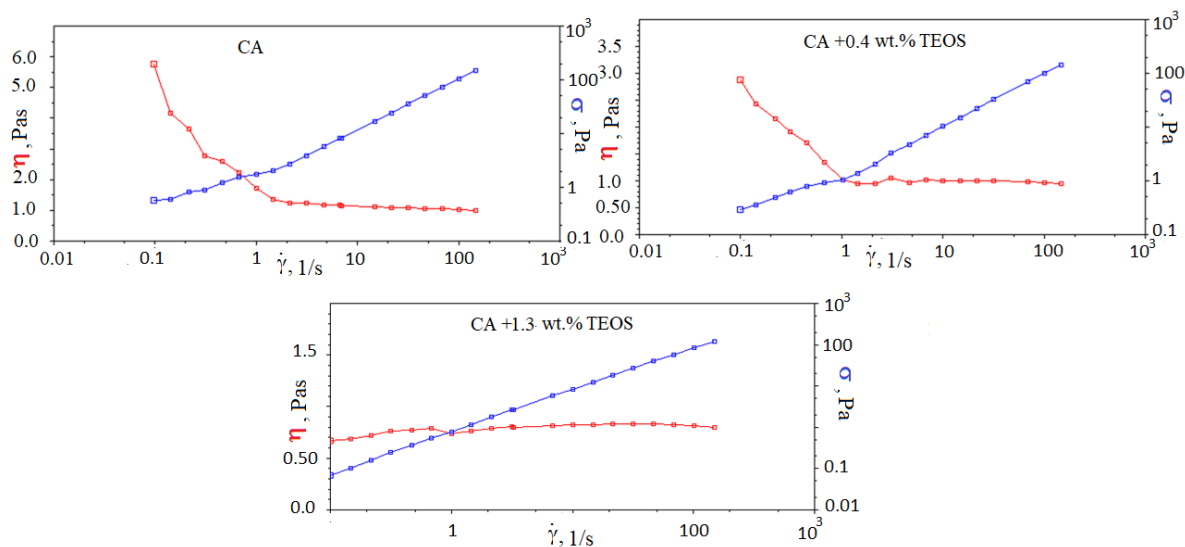


Figure 1. Plots of dynamic viscosity *versus* shear rate for CA/TEOS solutions at different content of TEOS.

The incorporation of TEOS in CA solution was described from rheological point view with the aim to produce chemically and mechanically resistant hybrid films with highly degree of dispersed metal particles. Consequently, the present study represents the basis for obtaining hybrid membranes with specific properties, which will find application both in industrial and bioengineering field.

DIRECT AND INDIRECT PHOTOLYSIS OF TRICYCLIC ANTIDEPRESSIVE DRUG

**Nina Finčur, Daniela Šojić Merkulov, Vesna Despotović, Nemanja Banić,
Biljana Abramović**

*University of Novi Sad, Faculty of Sciences, Department of Chemistry, Biochemistry and
Environmental Protection, Trg Dositeja Obradovića 3, 21000 Novi Sad, Serbia
e-mail: nina.fincur@dh.uns.ac.rs*

Abstract

Conventional systems for water purification cannot completely remove organic pollutants from wastewater and for this reason, it is necessary to find more efficient processes for their removal. Advanced oxidation processes (AOPs) are very important methods for the oxidation and removal of a wide range of organic pollutants from natural and wastewater [1]. AOPs are characterized by various radical reactions involving a combination of chemical agents (O_3 , H_2O_2 , transition metals, and metals oxides) and energy sources (UV-Vis irradiation, electricity, γ -irradiation, and ultrasound). In these processes, hydroxyl radicals represent primary oxidants [2]. Photolysis can be performed by a direct and indirect mechanism. Direct photolysis is a consequence of irradiation absorption, whereby the breakdown of chemical bonds in the molecule of the pollutant occurs in the case of overlapping of the absorption spectrum of pollutants with a wavelength of irradiation. On the other hand, indirect photolysis is performed in the presence of oxidants, resulting in a large number of reactive radicals, which then react with pollutants [3]. In recent years, great attention has been paid to drugs as potential bioactive substances in the environment. The high usage of antidepressants in the treatment of depression and anxiety disorders has led to the accumulation of active compounds of these drugs in the environment [4]. Amitriptyline is one of the most commonly used tricyclic antidepressant and since amitriptyline appears in the environment, it is necessary to well examine its stability and the possibility of elimination. In this paper, photodegradation of amitriptyline was studied using direct and indirect photolysis of amitriptyline under UV and simulated solar irradiation. Indirect photolysis was tested in the presence of H_2O_2 , $KBrO_3$, and $(NH_4)_2S_2O_8$. Besides, the effect of H_2O_2 concentration on the efficiency of the amitriptyline removal process was also observed.

Acknowledgments

The authors acknowledge financial support of the Ministry of Education, Science and Technological Development of the Republic of Serbia (Project No. 172042).

References

- [1] A.B.C. Alvares, C. Diaper, S.A. Parsons, *Environ. Technol.* 22 (2000) 409.
- [2] P.R. Gogate, A.B. Pandit, *Adv. Environ. Res.* 8 (2004) 501.
- [3] K. Sornalingam, A. McDonagh, J.L. Zhou, *Sci. Total Environ.* 550 (2016) 209.
- [4] L. Giebułtowicz, G. Nałęcz-Jawecki, *Ecotox. Environ. Safe.* 104 (2014) 103.

ADVANCED MASS SPECTROMETRY METHODS FOR THE DETERMINATION OF GANGLIOSIDES STRUCTURE AND FUNCTIONAL INTERACTIONS

Raluca Ica¹, Mirela Sarbu¹, Alina D. Zamfir^{1,2}

¹National Institute for Research and Development in Electrochemistry and Condensed Matter, Timisoara, Romania; ²“Victor Babes” University of Medicine and Pharmacy, Timisoara, Romania

e-mail: raluca.ica@gmail.com

Abstract

To address the issues of high biological relevance of gangliosides (GGs), mass spectrometry (MS) has lately become a method of choice due to its capability to detect minor species in complex mixtures and the unsurpassed sensitivity. GGs are localized in the cellular membrane, with the ceramide (Cer) rooted in the lipid bilayer and the oligosaccharide chain protruding freely outside the cell, acting as a receptor [1,2]. Here, a complex mixture of GGs extracted from adult human brain was first characterized by MS for a thorough mapping and a detailed structural characterization, and lately, the complex GG mixture was submitted to an interaction assay with the B subunit monomers of cholera toxin (Ctb5). Aliquots of the reaction products were collected after 10 and 30 min and also after 60 min and submitted to MS analysis. Multistage fragmentation by electron transfer dissociation (ETD) and collision-induced dissociation (CID) completed the assay and provided solid data on the noncovalent binding site at the monomer level.

Acknowledgements

This project was supported by the Romanian National Authority for Scientific Research, UEFISCDI through projects PN-III-P4-ID-PCE-2016-0073, PN-III-P1-1.2-PCCDI-2017-0046 granted to ADZ and PN-III-P1-1.1-PD-2016-0256 granted to MS.

References

- [1] K. Sandhoff, K. Harzer, J. Neurosci. 33 (2013) 10195.
- [2] J.M. Ryan, G.E. Rice, M.D. Mitchell, Nutr. Res. 33 (2013) 877.

IN VITRO TESTING OF SALICYLANILIDE DERIVATIVES AGAINST SOME FUNGAL AND BACTERIAL STRAINS

Ioana M.C. Ienaşcu^{1,2}, Diana Obistioiu³, Iuliana M. Popescu⁴, Mariana N. Ştefănuţ¹, Adina Căta¹

¹National Institute of Research and Development for Electrochemistry and Condensed Matter, 144 Dr. A. P. Podeanu, 300569, Timișoara, Romania

²“Vasile Goldiș” Western University of Arad, Faculty of Pharmacy, Department of Pharmaceutical Sciences, 86 Liviu Rebreanu, 310045, Arad, Romania

³Banat's Agricultural Science University, Faculty of Agriculture, Interdisciplinary Research Platform, 119 Calea Aradului, 300645, Timișoara, Romania

⁴Banat's Agricultural Science University, Faculty of Agriculture, Department of Chemistry and Biochemistry, 119 Calea Aradului, 300645, Timișoara, Romania
e-mail: imcienascu@yahoo.com

Abstract

Twelve N-(2-bromo-phenyl)-2-hydroxy-benzamide and N-(4-bromo-phenyl)-2-hydroxy-benzamide derivatives were tested for antimicrobial activity against 6 bacterial strains, *S. aureus* (ATCC 25923), *E. coli* (ATCC 25922), *P. aeruginosa* (ATCC 27853), *S. pyogenes* (ATCC 19615), *S. flexneri* (ATCC 12022), *S. typhimurium* (ATCC 14028) and 2 fungal strains, *C. albicans* (ATCC 10231), *C. parapsilopsis* (ATCC 22019), using the Disk diffusion method for susceptibility testing, according to the Standard Rules for Antimicrobial Susceptibility Testing using Impregnated Disks [1]. *In vitro* testing was performed in plates, containing microcomprimates with Nystatin for the antifungal activity and Gentamicin for the antimicrobial activity as positives controls, alongside blank filter papers impregnated with DMSO as negatives controls and filter papers impregnated with 10 µL of 20 g/L stock solution of each compound. A 10⁻² dilution of the fresh *Candida* cultures and a 10⁻² fresh bacteria culture was used to perform the assay, an inoculum equivalent to a 0.5 McFarland standard. The Petri plates so seeded and the respective specimens with the extract were incubated at 30 °C for *Candida* species and 37 °C in case of the bacterial strains, for 24-48 hours. Tests were performed in duplicate. Finally, the interpretation of the result, the ratio of the antimycotic and antibacterial effect of the tested compounds, was achieved by measuring the diameter of the analyzed culture inhibition zones (including the diameter of the disc – 5mm) in millimeters. The results are presented as the average of three determinations as well as the standard deviation and a percentage representation of the efficacy of the compounds in relation to the effectiveness of the positive control. The tested compounds presented no effect against *S. aureus*, *S. flexneri*, *S. typhimurium* and *C. parapsilopsis* at the tested concentration. The results indicated that the N-(2-bromo-phenyl)-2-hydroxy-benzamide derivatives were more active against the tested microbes, inhibition zones of 6-10 mm being obtained, although the most effective compound against *S. pyogenes* proved to be N-(4-bromo-phenyl)-2-hydroxy-benzamide (14 mm inhibition zone).

Key words: N-(2-bromo-phenyl)-2-hydroxy-benzamide derivatives, N-(4-bromo-phenyl)-2-hydroxy-benzamide derivatives, antibacterial effect, antimycotic effect, disk diffusion method

References

[1] I. Cavalieri, J. Stephen, in: M.B. Coyle (Coord. Editor), Manual of Antimicrobial Susceptibility Testing, American Society for Microbiology, 2005, pp. 39.

DEVELOPMENT OF GROUNDWATER MANAGEMENT BY USING ELECTROCOAGULATION FOR REMOVAL OF FLUORIDE AND COEXISTING ANIONS

Sorina Negrea¹, Monica Ihos¹, Mihaela Dragalina¹, Dorian Neidoni¹, Florica Manea²

¹*National Research and Development Institute for Industrial Ecology ECOIND, Timisoara Subsidiary, Street Bujorilor no. 115, code 300431, Timisoara, Romania*

²*Politehnica University of Timisoara, Faculty of Industrial Chemistry and Environmental Engineering, Bv. Vasile Pârvan Nr.6, 300223 Timisoara, Romania
e-mail: monica_ihos@yahoo.com*

Abstract

The electrocoagulation was applied to removal of fluoride and coexisting anions from simulated groundwater. The concentration of fluoride, chloride and sulfate was of 5 ppm, 347 ppm and 199 ppm, respectively. The influence of pH, current density, electrolysis time and sulfate presence were studied. Fluoride and sulfate removal efficiency, chloride concentration and specific energy consumption were calculated.

Introduction

Groundwater represents about 30% of world's fresh water. From the other 70%, nearly 69% is captured in the ice caps and mountain snow/glaciers and merely 1% is found in rivers and lakes. Groundwater counts in average for one third of the fresh water consumed by humans, but at some parts of the world, this percentage can reach up to 100% [1].

Taking into account the importance of groundwater as one of the main part of the existing freshwater resources and source of supply for drinking water, irrigation and industry, it is necessary to apply an appropriate groundwater management. Thus, the unadvised exploitation of groundwater and depletion of groundwater storages is avoided [2,3].

One of the important tools of groundwater management is represented by the technical aspects that suppose groundwater treatment technology especial for drinking purposes. The chemical characteristics of groundwater quality are responsible for the decision to treat the groundwater for drinking waters purposes. Among the challenges related to the groundwater quality, the presence of fluoride and coexisting anions above the limits allowed by the regulations in use require finding the technological solutions.

The processes and methods reported for removal of fluoride itself or along with coexisting anions from groundwater are various [4-12]: adsorption, membrane distillation, electrodialysis, micellar ultrafiltration, capacitive deionization, electrochemical processes and coagulation.

The aim of this study was to apply the electrocoagulation process for removal of fluoride and coexisting anions from a simulated groundwater in order to provide a reliable experimental model to developing an efficient groundwater management.

Experimental

The electrocoagulation experiments were carried out in a Plexiglas cell with horizontal electrodes. The sacrificial anode of 5.6 x 14 cm was made on aluminium and the cathode was a wire mesh grid made up of 3 mm diameter stainless steel wires. The distance between the electrodes was 5 mm.

Volumes of 500 ml working solutions were introduced in the cell, and the applied current densities were 10, 50, 100 and 150 A/m², respectively. Electrolysis duration was 60 minutes and samples were taken at every 15 minutes. The experiments were carried out with simulated

groundwater with concentration of 5 ppm fluoride, 347 ppm chloride and 199 ppm sulfate. All reagents were of analytical grade and the solutions were prepared with distilled water. The pH of initial solutions was adjusted to 5.3 and 7, respectively.

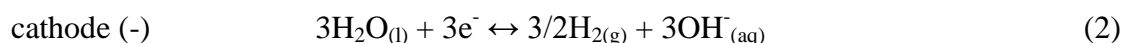
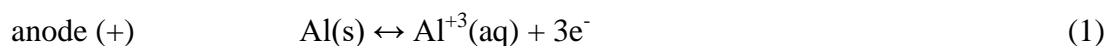
The fluoride concentration was determined by using a Thermo Scientific Orion fluoride ion selective electrode (range: from 0.02 ppm to concentration at saturation). TISAB II solution was used as a buffer to maintain the pH and background ion concentrations.

The chloride and sulfate concentration was carried in accordance with SR ISO 9297:2001, and EPA9038, respectively.

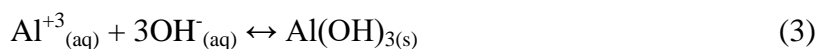
Results and discussion

For better understanding the experiments results some theoretical issues should be briefly presented.

When electrocoagulation is carried out with Al as sacrificial anode, the electrochemical reactions that occur at the electrodes are:



During the electrocoagulation the reaction between Al^{+3} and OH^- lead to various monomeric and polymeric species of hydrated aluminium, such as: $\text{Al}(\text{H}_2\text{O})_4(\text{OH})^{2+}$, $\text{Al}(\text{H}_2\text{O})_5(\text{OH})^{2+}$, $\text{Al}(\text{H}_2\text{O})_6^{3+}$, $\text{Al}(\text{OH})^{2+}$, $\text{Al}(\text{OH})_2^+$, $\text{Al}_2(\text{OH})_2^{4+}$, $\text{Al}(\text{OH})_4^-$, $\text{Al}_6(\text{OH})_{15}^{3+}$, $\text{Al}_7(\text{OH})_{17}^{4+}$, $\text{Al}_8(\text{OH})_{20}^{4+}$, $\text{Al}_{13}(\text{OH})_{34}^{5+}$, $\text{Al}_{13}\text{O}_4(\text{OH})_{24}^{7+}$ [13]. These species are further transformed into in amorphous $\text{Al}(\text{OH})_{3(\text{s})}$:



Near neutral pH the aluminium predominant species is $\text{Al}(\text{OH})_{3(\text{s})}$. The newly-formed precipitate of $\text{Al}(\text{OH})_{3(\text{s})}$ has a large surface that is beneficial to fast adsorption of soluble compounds and destabilization of colloidal particles.

Regarding the fluoride removal, one can notice that with the increase of the current density and the electrolysis time, at both initial pH, 5.3 and 7, the increase of removal efficiency of fluoride occurred (Figures 1 and 2).

The applied current density is an important parameter for pollutants removal because it determines the rate of dosing of the coagulant, the yielding of gas bubbles, the size and growth of the flocks what influences the removal efficiency by electrocoagulation.

In accordance with Faraday's law the amount of dissolved aluminium is directly proportional to the quantity of electricity passed through the solution during the electrocoagulation. Therefore, the higher the amount of electricity, the higher the amount of coagulant and gas bubbles. Thus, by increasing the current density the yielding rate of Al^{3+} and OH^- ions will increase which will accelerate the removal of pollutants.

The fluoride removal efficiency was higher at initial pH of 5.3 because the pH of electrolysed solutions ranged between 8.1 and 9.2 when the applied current densities ranged between 10-150 A/m^2 . The pH of electrolysed solutions of initial pH of 7 ranged between 8.6-9.5 when the applied current densities ranged between 10-100 A/m^2 . At higher pH of 8, the solubility of amorphous $\text{Al}(\text{OH})_{3(\text{s})}$ increases and thus the anions removal efficiency decreases.

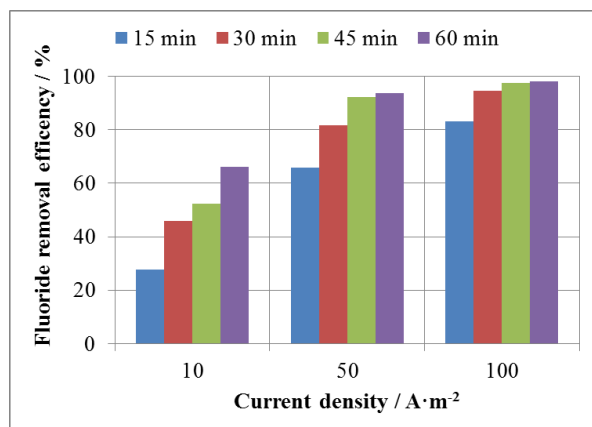


Figure 1. Fluoride removal efficiency by electrocoagulation at pH 5.3
 C_F^- : 5 ppm, C_{Cl^-} : 347 ppm

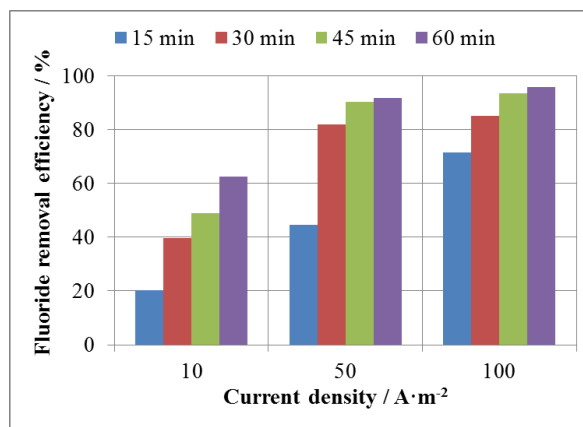


Figure 2. Fluoride removal efficiency by electrocoagulation at pH 7
 C_F^- : 5 ppm, C_{Cl^-} : 347 ppm

Regarding the chloride concentration, the data listed in Table 1 did not show significant changes along with the increasing of current density, pH and electrolysis time.

It should be noticed that the presence of chloride is beneficial because it facilitates the electrical charge transport by increasing the solution conductivity and also, eliminates the aluminium passivation due to the precipitation of $Al(OH)_3$ and Al_2O_3 [14]. Besides the repercussion of passivation to block the electrode activity another important aspect is given by increasing the cell voltage and thus, the energy consumption and the cost of electrocoagulation are higher.

Table 1. Working conditions and chloride concentration variation
initial concentration: 5 ppm F^- ; 347 ppm Cl^-

Current density / A/m ²	Cell voltage / V	Electrolysis time / min	Chloride concentration / ppm	
			pH 5.3	pH 7
10	1	15	333	333
		30	329	333
		45	329	333
		60	319	333
50	2.2	15	320	312
		30	320	312
		45	320	305
		60	305	298
100	3.7	15	319	305
		30	297	297
		45	287	279
		60	271	260

Examination of the data in Tables 2 and 3 showed that the presence of SO_4^{2-} ions led to a slight decrease of fluoride removal efficiency. This is probably due to a competitive adsorption effect.

Table 2. Working conditions and fluoride removal efficiency in presence of sulfate
initial concentration: 5 ppm F⁻, 347 ppm Cl⁻, 199 ppm SO₄⁻;
pH=5.3; current density: 100 A/m²

Electrolysis time / min	Cell voltage / V	Fluoride content / ppm	Fluoride removal efficiency / %	Chloride content / ppm	Sulfate content / ppm	Sulfate removal efficiency / %
15	2.9	0.97	80.6	312	149	25.1
30	2.9	0.40	92.0	294	140	29.6
45	2.9	0.21	95.8	276	142	28.6
60	2.9	0.12	97.6	259	124	37.7

Table 3. Working conditions and fluoride removal efficiency in presence of sulfate
initial concentration: 5 ppm F⁻, 347 ppm Cl⁻, 199 ppm SO₄⁻;
pH=7; current density: 150 A/m²

Electrolysis time / min	Cell voltage / V	Fluoride content / ppm	Fluoride removal efficiency / %	Chloride content / ppm	Sulfate content / ppm	Sulfate removal efficiency / %
15	4.0	0.59	88.2	301	142	28.6
30	4.2	0.28	94.4	266	133	33.2
45	4.2	0.19	96.2	245	122	38.7
60	4.2	0.06	98.8	239	119	40.2

The specific energy consumption is an important parameter in characterization of electrocoagulation performances regarding the removal of fluoride and coexisting anions from groundwater. This parameter was calculated according to equation (1) by using as working conditions: pH of 5.3, applied current density of 150 A/m² (1.17 A), electrolysis time of 45 minutes, cell voltage of 4.2 V, groundwater sample of 500 ml and it was of 7.4 kWh/m³.

$$Q = U \cdot I \cdot t \cdot 10^{-3} / V \cdot 3600 \quad (1)$$

where:

Q = specific energy consumption, kWh/m³; U = cell voltage, V; I = current intensity, A; t = electrolysis time, s; V = electrolyzed solution volume, m³

In the above conditions, the concentration of fluoride and chloride in the treated groundwater was under the threshold limits of 1.2 ppm and 250 ppm, respectively, stipulated in Romanian Law 458/2002 concerning the drinking water quality.

Conclusion

Electrocoagulation was applied to groundwater treatment for drinking water purposes and was focused on removal of fluoride and coexisting anions, chloride and sulfate. As a result, the fluoride concentration was 0.19 ppm and chloride concentration was 245 ppm in treated

simulated groundwater, that are values under the limits stipulated in Romanian Law 458/2002 concerning the drinking water quality. The presence of sulfate influenced slightly fluoride removal efficiency. The results of this study showed that electrocoagulation should be considered for the development of efficient groundwater management.

Acknowledgements

This work was carried out within the framework of a Core Program, managed by The Romanian Ministry of Research and Innovation, project code PN 18 05 03 02.

References

- [1] <https://www.un-igrac.org/> (accessed 16.09.2018)
- [2] Z. Şen, Practical and Applied Hydrogeology, Elsevier, Amsterdam, 2015, pp. 342.
- [3] M.N. Fienen, M. Arshad, in: A.J. Jakeman, O. Barreteau, R.J. Hunt, J.-D. Rinaudo, A. Ross (Eds.), Integrated Groundwater Management, SpringerLink.com, 2016, pp. 21
- [4] A. Iriel, S.P. Bruneel, N. Schenone, A. Fernández Cirelli, Ecotox. Environ. Safe., 149 (2018) 166.
- [5] G.J. Millar, S.J. Couperthwaite, L.A. Dawes, S. Thompson, J. Spencer, Sep. Purif. Technol., 187 (2017) 14.
- [6] J. Plattner, G. Naidu, T. Wintgens, S. Vigneswaran, C. Kazner, Sep. Purif. Technol., 180 (2017) 125.
- [7] C. Onorato, L.J. Banasiak, A.I. Schäfer, Sep. Purif. Technol., 187 (2017) 426.
- [8] M. Grzegorzec, K. Majewska-Nowak, Sep. Purif. Technol., 195 (2018) 1.
- [9] W. Tang, P. Kovalsky, B. Cao, T.D. Waite, Water Res. 99 (2016) 112.
- [10] A. Guzmán, J.L. Nava, O. Coreño, I. Rodríguez, S. Gutiérrez, Chemosphere 144 (2016) 2113.
- [11] J. Zhang, T.E. Brutus, J. Cheng, X. Meng, J. Environ. Sci. 57 (2017) 190.
- [12] S. Dubey, M. Agarwal, A.B. Gupta, J. Mol. Liq. 266 (2018) 349.
- [13] L.S. Thakur, P. Mondal, J. Environ. Manage., 190 (2017) 102.
- [14] M.A. Sandoval, R. Fuentes, J.L. Nava, I. Rodriguez, Sep. Purif. Technol., 134 (2014) 163.

PHOTOCATALYTIC EFFICIENCY OF TITANIUM OXIDE/MOLYBDITE OXIDE POWDER MIXTURE

Tamara Ivetić¹, Nina Finčur², Biljana Abramović², Predrag Vulić³, Ljubica Đaćanin Far¹, Svetlana Lukić-Petrović¹

¹*University of Novi Sad, Faculty of Sciences, Department of Physics, Trg Dositeja Obradovića 4, 21000 Novi Sad, Serbia*

²*University of Novi Sad, Faculty of Sciences, Department of Chemistry, Biochemistry and Environmental Protection, Trg Dositeja Obradovića 3, 21000 Novi Sad, Serbia*

³*University of Belgrade, Faculty of Mining and Geology, Đušina 7, 11000 Belgrade, Serbia
e-mail: tamara.ivetic@df.uns.ac.rs*

Abstract

Coupling TiO₂ with MoO₃ is one of many strategies for the enhancement of titanium oxide photoabsorption under the solar light irradiation. TiO₂ being a wide band-gap semiconductor with its unique properties (nontoxicity, photo and chemical stability, and low-cost) is a prominent material for the photocatalytic applications but only when excited by the UV light [1]. Here we report for the first time the photocatalytic efficiency of mixed 2TiO₂/MoO₃ powders prepared using a simple, mechanochemical solid-state chemistry procedure at a relatively low temperature of 700 °C. Materials structure was examined by means of X-ray diffraction that confirmed the presence of three phases, rutile TiO₂, anatase TiO₂ and molybdate MoO₃ [2]. A unique heterojunction structure with Ti-O-Mo bond between the TiO₂ and MoO₃ interfaces enables the solar light-driven photocatalytic reaction as well as more efficient separation of the photogenerated electrons and holes for the overall improvement of TiO₂ photocatalytic performance. The mixed titanium oxide/molybdate oxide photocatalytic activity was examined under simulated solar irradiation and the experimental photocatalytic kinetics showed that the obtained 2TiO₂/MoO₃ powder mixture has a good potential for Vis-activated degradation of ciprofloxacin, a widely used antibiotic for the treatment of a number of bacterial infections, which is the reason why it was continuously introduced into the environment through wastewaters, and therefore represents a potential risk for the living organisms.

Acknowledgments

The authors are grateful to the APV Provincial Secretariat for Higher Education and Scientific Research for partly financing this work (Project No. 142-451-2387/2018-01/02) and acknowledge the support of the Ministry of Education, Science and Technological Development of the Republic of Serbia (Project numbers: ON 171022 and ON 172042).

References

- [1] H. Liu, T. Lv, C. Zhu, Z. Zhu, Sol. Energ. Mat. Sol. C. 153 (2016) 1.
- [2] T.B. Ivetić, P.J. Vulić, I.O. Gúth, S.R. Lukić-Petrović, Structure and morphology characterization of Ti-Mo mixed oxide powder for photocatalytic applications, 55th Meeting of the Serbian Chemical Society, June 8-9, 2018, Novi Sad, Serbia, Book of Abstracts, p. 42.

PORE MICROSTRUCTURE CHARACTERIZATION OF Zn_2SnO_4 USING MERCURY INTRUSION POROSIMETRY

Tamara Ivetić¹, Jugoslav Krstić², Nina Finčur³, Biljana Abramović³, Svetlana Lukić-Petrović¹

¹*University of Novi Sad, Faculty of Sciences, Department of Physics, Trg Dositeja Obradovića 4, 21000 Novi Sad, Serbia*

²*University of Belgrade, Institute of Chemistry, Technology and Metallurgy, Department of Catalysis and Chemical Engineering, Njegoševa 12, 11000 Belgrade, Serbia*

³*University of Novi Sad, Faculty of Sciences, Department of Chemistry, Biochemistry and Environmental Protection, Trg Dositeja Obradovića 3, 21000 Novi Sad, Serbia*
e-mail: tamara.ivetic@df.uns.ac.rs

Abstract

The zinc stannate (Zn_2SnO_4) is marked as a promising semiconductor material to be used in a field of environmental protection and photocatalysis especially when its band gap is adjusted to enough narrow value to provide its applicability under the visible light irradiation. A traditional solid-state procedure was used to synthesize Zn_2SnO_4 when a stoichiometrical mixture of starting zinc oxide (ZnO) and tin oxide (SnO_2) powders were mechanochemically activated by grinding in a planetary ball mill for 160 min and additionally annealed at 1200°C for 2 h. In this paper, we investigate the most important textural features of the Zn_2SnO_4 powder for its usage in the photocatalytic degradation of the organic pollutants from wastewaters. Mercury intrusion porosimetry was combined with the scanning electron microscopy to study morphology and surface properties, like specific pore volume, specific surface area, apparent density, and total porosity.

Introduction

Ternary zinc-tin-oxide (Zn_2SnO_4) is a well-known *n*-type semiconductor with promising applications, like in gas sensors [1], dye-sensitized solar cells [2,3], lithium-ion batteries [4], and recently in the photocatalysis [5-9]. The photocatalytic activity of an oxide semiconductor is highly dependent on its particle size, morphology, and surface properties since photocatalytic reactions mainly occur on the catalyst surface [10]. Solid-state mechanochemistry is a simple, sustainable and economical/eco-friendly method that successfully competes against the most common multistep toxic-organic-solvent-based routes like sol-gel, hydrothermal, co-precipitation, for the synthesis of Zn_2SnO_4 [11,12]. In this work, we describe the characterization of the textural Zn_2SnO_4 powder features by mercury intrusion porosimetry assisted with the scanning electron microscopy (SEM) measurements. The results should indicate the size of the impact that surfaces' properties of the cubic Zn_2SnO_4 powder, synthesized by the mechanochemical solid-state method, have on the efficiency of Zn_2SnO_4 as a photocatalyst in the degradation of the organic compounds from wastewaters [13]. The mercury intrusion porosimetry (Fig. 1a-c) is a method very often used in powder characterization. This method is based on fact that a non-wetting liquids are not being adsorbed on the surface of solids or inside their pores [14], and thereby the volume of such liquids when forced into the pores with appropriate high pressures starting from vacuum (Fig. 1a), give a sufficient information on the materials' pore structure properties. In the beginning, basically, this type of materials characterization provides a curve called the intrusion curve, *i.e.*, the plot of the intruded volume of a non-wetting liquid (in this case mercury) per sample mass unit *vs.* the applied pressure in MPa. Using obtained intrusion curve and the appropriate theoretical model of intrusion porosimetry that takes into account

the surface tension, capillary forces and pressure, the following elementary information on the samples' textural properties could be obtained: total specific cumulative pore volume (V_{tot}), total specific surface area (SSA), average pore diameter (D_{av}), bulk density (ρ_{bl}), apparent (real) density (ρ_{ap}) and total porosity. Porosity is defined as the ratio of the volume of void-space and total (or bulk) volume of material, including the solid and void components. There are three categories of pores according to their size: micropores (pore diameter < 2 nm), mesopores (pore diameter 2 – 50 nm) and macropores (pore diameter > 50 nm) [14], and four according to their shape (Fig. 1d). The basic principle of the intrusion porosimetry states that the pressure required to force a non-wetting liquid (mercury is non-wetting to most solid materials) to enter a pore or capillary of circular cross-section is inversely proportional to the effective diameter of the capillary and directly proportional to the surface tension of the non-wetting liquid and angle of contact with the solid surface [15]. Essentially, if we assume that the pores or capillaries in the sample are cylindrical and circular in cross-section openings, the relationship between the applied pressure and the minimum pore size into which the non-wetting liquid will be forced to enter could be simply described by Washburn's equation [15]:

$$D = \frac{-4\gamma \cos \theta}{P} \quad (1)$$

where D is the diameter of the pore where non-wetting liquid intrudes, γ is the surface tension of the non-wetting liquid (for mercury generally 480 mN/m) and θ is the contact angle of the non-wetting liquid on the surface of a sample (for mercury generally 140 °). Therefore, the size of the pore where non-wetting liquid, like mercury, intrudes is inversely proportional to the applied pressure. Mercury intrusion porosimetry, in fact, measures the entrance towards a pore (Fig. 1e) and not the actual inner size of a pore [16], and that is the most important limitation of this technique. All this means that for any pressure it can be determined which pore sizes have been invaded by mercury and which size have not [15], so closed pores could not be analyzed since the mercury has no way of entering in. However, today's various software solutions based on different assumptions' and pore models provide an overview of how the cross-linking structure between pores looks like.

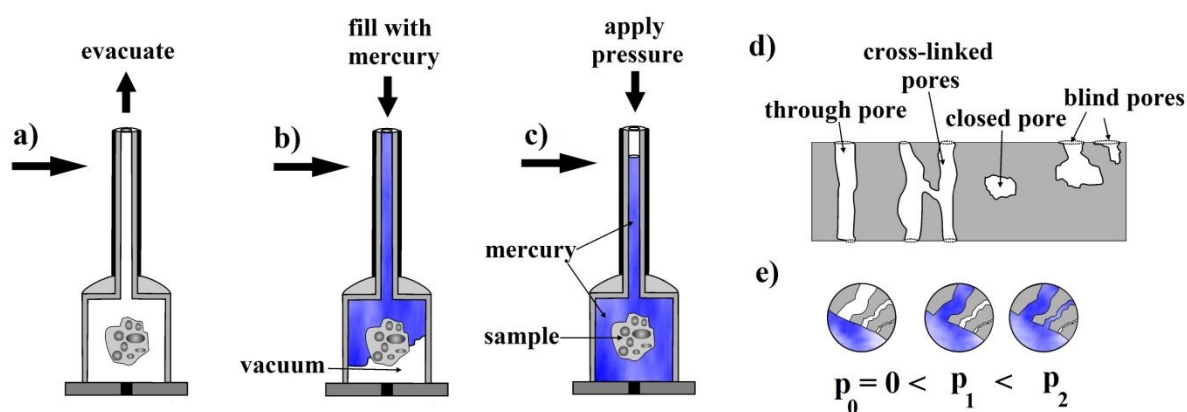


Figure 1. Schematic illustration of a)-c) mercury intrusion porosimetry principle, d) pore shape types, and e) pressures at which different pore size entrances are invaded by mercury

From the intrusion curve, the total pore volume is read as the total intruded volume of the mercury at the highest pressure determined because this property does not require Washburn's equation or a pore model. Dividing this value by mass of the sample gives the total

cumulative specific pore volume (V_{tot}) in units of volume per unit mass (cm^3/g). The total pore specific surface area is calculated by:

$$SSA = \frac{1}{\gamma |\cos \theta|} \int_0^{V_{tot}} p dV \quad (2)$$

and represents the area above the intrusion curve, while the average pore diameter (D_{av}) is then calculated as:

$$D_{av} = 4 \frac{V_{tot}}{S} \quad (3).$$

The D_{av} is an average pore diameter (more precisely, hydraulic pore diameter) which is calculated as the ratio of pore volume multiplied by four to pore area. Median pore diameter ($D_{50\%}$) is a diameter that corresponds to the 50% of total pore volume, i.e. the diameter for which one-half of the pore volume is found to be in larger pores and one-half is found to be in smaller pores. Apparent density (ρ_{ap}) is determined by a gas pycnometry as the difference between mercury pycnometry envelope density and amount of the helium uptake at the maximal uptake volume at the corresponding relative pressure.

Experimental

Zn_2SnO_4 powder sample was synthesized in the two-step solid-state processing, when starting materials, commercially available ZnO and SnO_2 (Sigma–Aldrich, purity 99.9%, particle size $\leq 1\mu\text{m}$) powders mixed in stoichiometrical ratio were first mechanically activated in high energy ball mill (Retsch GmbH PM100) using zirconium vial and zirconium balls of 10 mm diameter (ball to powder ratio = 10:1) in air for 160 min, and secondly annealed in furnace at 1200°C for 2 hours. X-ray diffraction was carried out using the Philips PW 1050 instrument, with $\text{Cu K}\alpha_{1,2}$ radiation, and a step scan mode of $0.02^\circ/\text{s}$ in an angular range $2\theta = 15\text{--}70^\circ$. SEM (JEOL JSM-6460LV) was used to investigate the morphology of the obtained sample. The textural properties, including total cumulative volume (V_{tot}) and total specific surface area (SSA), were obtained using Porosimeter 2000 (Fisons Instruments) within the pressure range from 1 to 2000 bar, while bulk density was obtained with Macropore Unit 120 (Fisons Instruments). All samples were dried in an oven at 110°C during 16 h and additionally evacuated from 90 min at room temperature prior to the analysis. Two intrusion-extrusion runs, denoted as Run1 and Run2, were conducted on the same powder specimen. The recordings of the intruded Hg volume vs. applied pressure were obtained through an interface Milestone 100 Software System for PC, while Pascal Ver. 1.05 software was used for calculations.

Results and discussion

The X-ray diffraction pattern of the obtained powder sample confirmed the formation of face-centered cubic spinel Zn_2SnO_4 (JCPDS card No. 74–2184) with an average crystallite size of about 40 nm, which was in detail shown elsewhere [13].

SEM image (Fig. 2a) show that agglomeration of particles exists in Zn_2SnO_4 powder sample. Likewise, the real origin of Zn_2SnO_4 particles microstructure complexity is more clearly visible in the SEM image with higher magnification (Fig. 2b) that shows octahedral shaped neck-associated and blinded Zn_2SnO_4 grains, with the sizes that vary in the range from 536 nm to $2.03\mu\text{m}$. This means that the real particle sizes are actually bigger than the values shown in Fig. 2b. This type of morphology is the result of reaction-sintering and grain-growth processes happening in the mechanochemically activated ZnO-SnO_2 system at such a high temperature (1200°C) of synthesis.

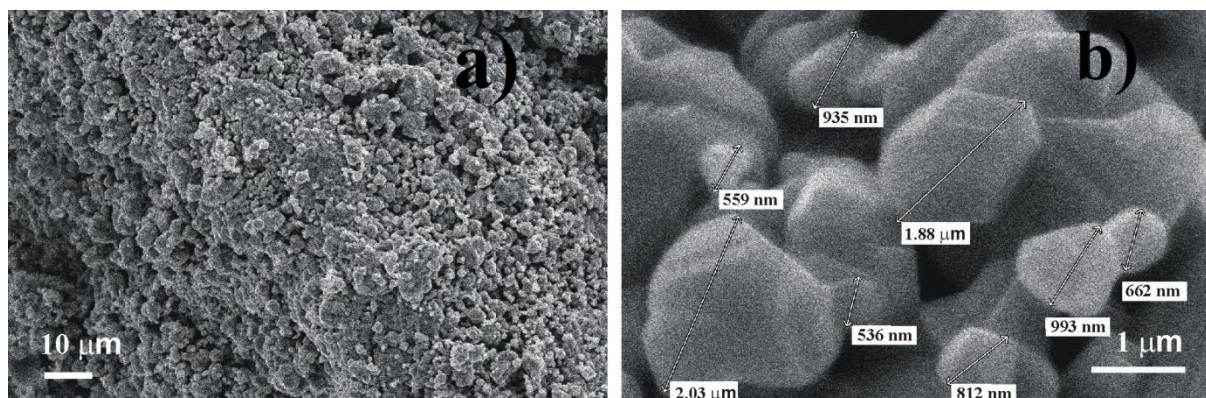


Figure 2. SEM images of Zn_2SnO_4 with different magnifications

Results obtained by the mercury intrusion porosimetry were summarized in Table 1 and revealed that the pores in Zn_2SnO_4 powder sample belong to the group of macropores (pore diameter > 50 nm). Most of the porosity comes from the intraparticle volume. The intraparticle porosity is probably a result of Zn_2SnO_4 solid-state synthesis mechanism. The expansion of the powders occurs during the solid-state reaction between the ZnO and SnO_2 particles as they are being separated when the reaction product (Zn_2SnO_4), that grows as the grain-neck region, is formed at the starting particles (ZnO and SnO_2) contact points. The voids (interparticle porosity) are only 23% of the total imprinted volume (37 mm^3 of 160 mm^3). Apparent density (ρ_{ap}) obtained from helium pycnometry is 6.13 g/cm^3 at the maximum of the applied intrusion pressure. Apparent density represents the actual density in the case of an idyllic non-porous specimen or sample with exclusively pore greater than 7.5 nm, which is the case with the obtained Zn_2SnO_4 powder sample.

Table 1. Results obtained from mercury intrusion porosimetry

Zn_2SnO_4	Run1	Run2
Total cumulative volume, V_{tot} (cm^3/g)	0.160	0.123
Total specific surface area, SSA (m^2/g)	0.31	0.27
Average pore diameter, D_{av} (μm)	2.04	1.83
Median pore diameter, $D_{50\%}$ (μm)	4.72	3.57
Total porosity (%)	49.6	43.0

The low specific surface area (Table 1) is mostly the result of mentioned Zn_2SnO_4 reaction-sintering mechanism and grain-growth at 1200°C that causes the formation of bigger and complex particles (Fig. 2b) but also the agglomeration is noticed as well (Fig. 2a). This all may be the main reason for the inefficient photocatalytic performance of the obtained Zn_2SnO_4 powder sample when used for degradation of alprazolam, short-acting anxiolytic of the benzodiazepine class of psychoactive drugs [13] because a large surface area is desirable for the efficient photocatalysis.

Conclusion

In this paper, we report the textural properties of the solid-state synthesized Zn_2SnO_4 powder using mercury intrusion porosimetry. The data obtained using this technique and combined with the SEM images pointed out that mechanism of the solid-state Zn_2SnO_4 reaction synthesis defines its textural properties and contributes to its poor photocatalytic performance in the degradation of some pharmaceutically active compounds from wastewaters.

Acknowledgments

The authors are grateful to the APV Provincial Secretariat for Higher Education and Scientific Research (Project number: 142-451-2387/2018-01/02) for partially financing this work and acknowledge the support of the Ministry of Education, Science and Technological Development of the Republic of Serbia (Project numbers: ON 171022, ON 172042 and III 45001).

References

- [1] W. Wang, H. Chai, X. Wang, X. Hu, X. Li, *Appl. Surf. Sci.* 341 (2015) 43.
- [2] B. Tan, E. Toman, Y. Li, Y. Wu, *J. Am. Chem. Soc.* 129 (2007) 4162.
- [3] K. Wang, Y. Shi, W. Guo, X. Yu, T. Ma, *Electrochim. Acta* 135 (2014) 242.
- [4] L. Qin, S. Liang, A. Pan, X. Tan, *Mater. Lett.* 141 (2015) 255.
- [5] M.B. Ali, F. Barka–Bouaifel, H. Elhouichet, B. Sieber, A. Addad, L. Boussekey, M. Férid, R. Boukherrab, *J. Colloid Interf. Sci.* 457 (2015) 360.
- [6] E.L. Foletto, J.M. Simões, M.A. Mazutti, S.L. Jahn, E.I. Muller, L.S.F. Pereira, E.M. de Morales Flores, *Ceram. Int.* 39 (2013) 4569.
- [7] L. Shi, Y. Dai, *J. Mater. Chem. A* 1 (2013) 12981.
- [8] T. Jia, J. Zhao, F. Fu, Z. Deng, W. Wang, Z. Fu, F. Meng, *Int. J. Photoenergy* 2014 (2014) 197824.
- [9] S. Baruah, J. Dutta, *Sci. Technol. Adv. Mater.* 12 (2011) 013004.
- [10] T.B. Ivetić, M.R. Dimitrievska, N.L. Finčur, Lj.R. Đačanin, I.O. Gúth, B.F. Abramović, S.R. Lukić–Petrović, *Ceram. Int.* 40 (2014) 1545.
- [11] K. Ralphs, C. Hardacre, S.L. James, *Chem. Soc. Rev.* 42 (2013) 7701.
- [12] V. Šepelák, S.M. Becker, I. Bergmann, S. Indris, M. Scheuermann, A. Feldhoff, C. Kübel, M. Bruns, N. Stürzl, A.S. Ulrich, M. Ghafari, H. Hahn, C.P. Grey, K.D. Becker, P. Heitjans, *J. Mater. Chem.* 22 (2012) 3117.
- [13] T.B. Ivetić, N.L. Finčur, Lj.R. Đačanin, B.F. Abramović, S.R. Lukić–Petrović, *Mater. Res. Bull.* 62 (2015) 114.
- [14] S. Westermarck, Use of Mercury porosimetry and nitrogen adsorption in characterization of the pore structure of mannitol and microcrystalline cellulose powders, granules and tablets, Academic Dissertation, Helsinki, 2000, p. 1-60.
- [15] P.A. Webb, An introduction to the physical characterization of materials by mercury intrusion porosimetry with emphasis on reduction and presentation of experimental data, Micrometrics Instrument Corp., Norcross, Georgia, 2001, p. 1-22.
- [16] H. Giesche, *Part. Part. Syst. Charact.* 23 (2006) 1.

ZINC ACCUMULATION IN WHOLE GRAIN OF DIPLOID, TETRAPLOID AND HEXAPLOID WHEAT

**Rudolf Kastori¹, Ivana Maksimović¹, Marina Putnik-Delić¹, Vojislava Momčilović²,
Srbislav Denčić²**

¹University of Novi Sad, Faculty of Agriculture, Trg Dositeja Obradovića 8, Novi Sad, Serbia

²Institute of Field and Vegetable Crops, Maksima Gorkog 30, Novi Sad, Serbia

e-mail: kastori@polj.uns.ac.rs

Abstract

Zinc (Zn) is an essential element for all leaving organisms. Plants are the most important source of Zn for humans and animals; therefore its accumulation in edible plant parts is of great importance.

Plant species, but also genotypes and specific varieties differ with respect to accumulation of mineral elements. During three years, accumulation of Zn in the grain of *Aegilops* and *Triticum* species, with different genomes (AA, BB, BBAA, BBAADD and DD), grown on calcareous, gleyic chernozem soil in temperate continental climate, was followed. Three-years average results allowed to establish the following order with respect to the concentration of Zn in the whole grain (mg kg⁻¹ DW): BB (36.24) > AA (30.86) > DD (28.98) > BBAA (25.43) > BBAADD (17.97). The analysis of variance revealed a highly significant effect of genome and year as well as of the interaction between genome and year.

Introduction

Zinc is present in low concentrations in all parts of the biosphere. It is essential element for all living organisms. Metabolic role of Zn is based on its tendency to form tetrahedral complexes with O-, N-, and especially S-ligands. Therefore, Zn has functional (catalytic) and structural role in enzymatic reactions [1]. Zinc is associated with more than fifty metalloenzymes which are involved in different processes, including synthesis of nucleic acids, specific proteins like hormones and their receptors [2]. Hence, Zn has a very important role in metabolism, growth and differentiation of cells.

Zinc enters human and animal organisms predominantly through food. Since its extreme importance for metabolic processes, Zn content in food is very important as well. Wheat is one of the most significant sources of nutrients for people in many parts of the world. Among three most important small grain crops wheat is grown on the largest surfaces (around 221 millions of ha). It is followed by maize (around 185 millions of ha) and rice (around 161 millions of ha). Wheat is grown mostly for food – about 54% of production in developed countries and 85% in developing countries. After [3] nearly one half of human population takes in insufficient amounts of Zn. The lack of Zn in food and feed may cause many diseases. Therefore, the aim of this work was to examine concentration of Zn in the whole grain of different kinds of wheat, since plant species but also genotypes within them often differ greatly with respect to the accumulation of mineral elements [4].

Experimental

Concentration of Zn was assessed in the grains of 20 genotypes of different levels of ploidy and of different origin: six diploid genotypes of wheat with different genome formulas (BB, AA or DD), five tetraploids (BBAA) and nine hexaploids (BBAADD). The names of the cultivars are given in Table 1. The wheat genotypes were sown in 2011, 2012 and 2013, on calcareous, gleyic chernozem. The soil was well-provided with total nitrogen and Zn, and rich in available phosphorus and potassium. The genotypes were harvested at crop maturity and all

hulled genotypes were manually de-hulled. After digestion of grain whole meal in the mixture of 10 mL HNO₃ (63%) and 2 mL of H₂O₂ (30%), the concentration of total Zn was determined by inductive coupled plasma emission spectrometer. Statistical analyses were done in Infostat, version 2016. More details about the experimental procedures are available in the paper [5].

Results and discussion

Plants belonging to family *Gramineae*, to which wheat belongs, are about average with respect to the accumulation of Zn. In wheat, Zn accumulates more in the grain than in the straw [6]. In the grains and seeds mineral elements, including Zn, are located predominantly in the protein [7]. High concentrations of Zn in the protein bodies of wheat scutellum (600 µg g⁻¹ DW) were found by [8]. Protein bodies are characterized by high content of phytine. Zn binds firmly to phytic acid, building in this way protein-Zn-phytic acid complex which is resistant to hydrolysis, which reduces bioavailability of Zn for monogastric animals and men. In the regions where molar ratio phytate: Zn in food is high, the danger of insufficient intake of Zn is much higher [3]. The grain of the majority of small grains is characterized by medium levels of Zn. In addition, the high phytine content in them reduces the concentration of absorbable Zn. Nevertheless, wheat grain, due to its high abundance in the diet, globally represents an important source of Zn for men and animals alike.

[9] states that average concentrations of Zn in wheat grains in different countries are similar and they are about 22-33 mg Zn kg⁻¹ of dry matter. However, inside one country large differences are present. [10] found significant differences in the Zn concentration in the grains of different wheat cultivars, and those differences were much higher in *T. durum* than in *T. aestivum* cultivars.

Concentration of Zn in the grain depends also on many ecological factors. [11] found that precipitations and soil type significantly affect concentration of Zn in wheat grains. Higher doses of phosphorus fertilizers reduce availability of P for plants. [12] concluded that concentration of Zn in wheat grain declined with application of phosphorus fertilizers.

During the three years long experiment, in *Aegilops* and *Triticum* species concentration of Zn in the whole grain, depending on the genotype and a year, ranged between 14.8 and 36.7 mg kg⁻¹ DW (Tab. 1). Significant differences in the concentration of Zn were found between different species (Tab. 1; Tab. 3) and genomes (Tab. 2; Tab. 4). In average, during three years, the highest concentration of Zn was found in the genome BB and the lowest in BBAADD. Contemporary hexaploid genotypes are also characterized by significant variations of the concentration of Zn in the whole grains (Fig. 1 and Fig. 2).

In our previous study we found that the concentration of tin [13], barium [14] and strontium [5] was also significantly the highest in the grains of *Aegilops speltoides* which is characterized by several times lower mass of 1000 grains (5.40 g) than the other examined genotypes. Mineral substances in wheat grains are concentrated in the peripheral part of the grain. Hence, the concentration of mineral substances in whole grains depends on the ratio of peripheral part and endosperm. The smaller the grain, the higher is the mass of the peripheral portion in the total mass of grain, which may contribute to higher concentrations of minerals in the grain as a whole. According to [15], there is a weak correlation between the mass of 1000 grains, and the concentrations of microelements, except in cultivars which differ significantly in the mass of 1000 grains, which is in line with our results. Further research is needed with the aim to find out whether only the small size of the grain or some other genetic characteristic besides the size of the grain contribute to much higher accumulation of Zn in the grains of *Aegilops speltoides* with respect to the other examined *Aegilops* and *Triticum* species.

Table 1. Concentration of Zn in the whole grain of *Aegilops* and *Triticum* species (mg kg⁻¹ DW)

No	Species and subspecies	Genome	Year			Average
			2011	2012	2013	
1	<i>Aegilops speltoides</i> subsp. <i>speltoides</i> 1	BB	45.8	23.9	40.5	36.7 ^a
2	<i>Aegilops speltoides</i> subsp. <i>speltoides</i> 2	BB	36.5	29.3	41.6	35.8 ^{ab}
3	<i>Triticum urartu</i>	AA	28.7	30.0	25.4	28.0 ^e
4	<i>Triticum monococcum</i> subsp. <i>egilopoides</i>	AA	37.7	27.4	37.3	34.1 ^{bc}
5	<i>Triticum monococcum</i> subsp. <i>monococcum</i>	AA	39.7	20.7	31.0	30.5 ^d
6	<i>Aegilops tauschii</i> subsp. <i>tauschii</i>	DD	47.1	16.0	23.9	29.0 ^{de}
7	<i>Triticum turgidum</i> subsp. <i>dicoccoides</i> (IPK)	BBAA	24.8	18.4	27.4	23.5 ^f
8	<i>Triticum turgidum</i> subsp. <i>dicoccoides</i> (IFVC)	BBAA	37.8	26.9	22.8	29.2 ^{de}
9	<i>Triticum turgidum</i> subsp. <i>dicoccon</i>	BBAA	24.0	14.9	20.6	19.8 ^{ghi}
10	<i>Triticum turgidum</i> subsp. <i>turgidum</i>	BBAA	32.3	30.2	36.3	32.9 ^c
11	<i>Triticum turgidum</i> subsp. <i>durum</i> (cv. Durumko)	BBAA	25.2	21.7	18.3	21.7 ^{fg}
12	<i>Triticum aestivum</i> subsp. <i>spelta</i> (cv. Nirvana)	BBAADD	20.7	18.0	23.3	20.7 ^{gh}
13	<i>Triticum aestivum</i> (cv. Panonnia)	BBAADD	14.0	15.8	16.2	15.3 ^{kl}
14	<i>Triticum aestivum</i> (cv. Bankut 1205)	BBAADD	17.4	21.3	21.8	20.2 ^{ghi}
15	<i>Triticum aestivum</i> (cv. Bezostaja 1)	BBAADD	15.0	17.0	19.5	17.1 ^{ijk}
16	<i>Triticum aestivum</i> (cv. Siete Cerros)	BBAADD	11.5	17.9	18.3	15.9 ^{kl}
17	<i>Triticum aestivum</i> (cv. Florida)	BBAADD	13.2	14.2	17.3	14.9 ^l
18	<i>Triticum aestivum</i> (cv. Renan)	BBAADD	19.0	12.4	23.7	18.4 ^{ij}
19	<i>Triticum aestivum</i> (cv. Condor)	BBAADD	15.3	22.4	21.8	19.8 ^{ghi}
20	<i>Triticum aestivum</i> (cv. Bolal)	BBAADD	11.7	22.2	24.8	19.5 ^{hi}
Average			25.9 ^a	21.0 ^b	25.6 ^a	

Different letters indicate significant difference at $P < 0.05$ level.

Table 2. Concentration of Zn in the whole grain of five genomes over 3 years (mg kg⁻¹ DW)

Genome	Year			Average
	2011	2012	2013	
AA	35.3	26.0	31.2	30.86 ^b
BB	41.1	26.6	41.1	36.24 ^a
BBAA	28.8	22.4	25.1	25.43 ^c
DD	47.1	16.0	23.9	28.98 ^b
BBAADD	15.3	17.9	20.7	17.97 ^d

Table 3. Analysis of variance of Zn concentrations of *Aegilops* and *Triticum* species

Source of variation	SS	df	MS	F	p-value
Year	886.24	2	443.12	285.71	<0.0001
Genotype	8825.58	19	464.5	299.5	<0.0001
Genotype*Year	4024.91	38	105.92	68.29	<0.0001
Error	186.11	120	1.55		

Table 4. Analysis of variance of Zn concentrations in five genomes

Source of variation	SS	df	MS	F	p-value
Year	886.24	2	443.12	41.86	<0.0001
Genome	7223.54	4	1805.88	170.59	<0.0001
Year*Genome	2623.15	8	327.89	30.97	<0.0001
Genome/Genome>Genotype	1602.05	15	106.8	10.09	<0.0001
Error	1587.88	150	10.59		

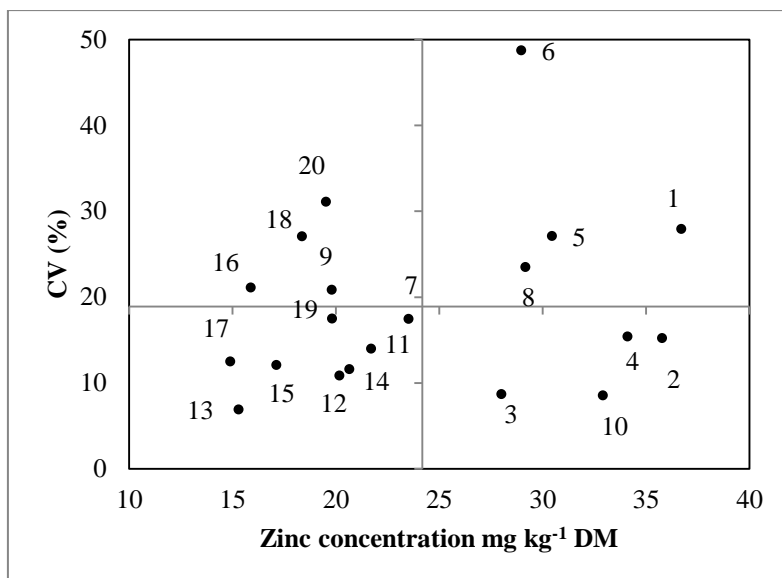


Figure 1. Coefficient of variation for zinc concentration in *Aegilops* and *Triticum* genotypes

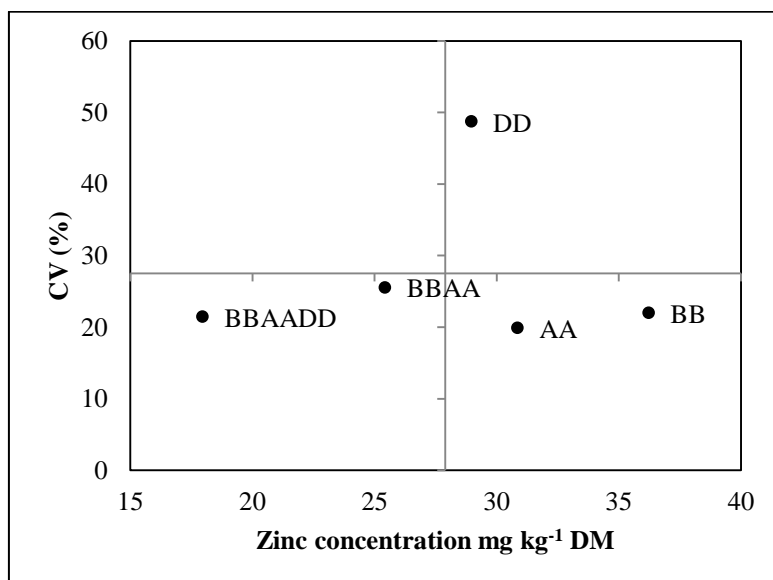


Figure 2. Coefficient of variation for zinc concentration in different genomes

Conclusion

Average concentration of Zn in the whole grains, in three-years period, ranged from 14.9 to 36.7 mg kg⁻¹ DW. Concentration of Zn differed significantly in different genomes (BB, AA, DD, BBAA, BBAADD). The highest concentration of Zn was found in wild diploid species *Aegilops speltoides*, which bares BB genome (36.24 mg kg⁻¹ DW), and the lowest in hexaploid wheat, baring genome BBAADD (17.97 mg kg⁻¹ DW). Concentration of Zn varied also between different experimental years. The results suggest that the grains of different *Triticum* and *Aegilops* genotypes, but also cultivars within them, due to differences in Zn concentrations, contribute to different levels to provision of humans and animals with Zn.

Acknowledgements

Help in chemical analysis of Prof. Dr. Imre Kádár, Research Institute for Soil Science and Agricultural Chemistry of the Hungarian Academy of Sciences, Budapest, Hungary, is kindly acknowledged.

References

- [1] B.L. Vallee, D.C. Auld, *Biochemistry* 29 (1990) 5647-5659.
- [2] R.J. Cousins, R.J. Zinc, in: E.E. Ziegler, E.E., Filer (Eds.) *Present knowledge in nutrition*. 7th ed. International Life Sciences Institute Press, Washington (1996) 293-306.
- [3] K.H. Brown, S.E. Wuehler, J.M. Pearson, *Food and Nutrition Bulletin* 22 (2001) 113-125.
- [4] R.B. Clark, *Plant Soil* 72 (1983) 175-196.
- [5] R. Kastori, I. Maksimović, S. Denčić, I. Kádár, M. Putnik-Delić, V. Momčilović, J. *Plant Nutr. Soil Sci.* 180 (2017) 212-219.
- [6] I. Kádár, A főbb szennyező mikroelemek környezeti hatása. Magyar Tudományos Akadémia ATK Talajtani és Agrokémiai Intézet, Budapest 2012. pp. 359.
- [7] H. Marschner, *Mineral Nutrition of Higher Plants*, Academic Press, London 1995. pp. 889.
- [8] A.P. Mazzolini, C.K. Pallaghy, G.J.F. Legge, *New Phytol.* 100 (1985) 483-509.
- [9] A. Kabata-Pendias, *Trace Elements in Soil and Plants*, 3rd ed. CRS press, Boca Raton, FL. USA 2000. pp. 413.
- [10] E.G. Zook, F.E. Greene, E.R. Morris, *Cerela Chemistry*. 47 (1970) 720-731.
- [11] C.L. White, A.D. Robson, H.M. Fisher, *Aust. J. Agric. Res.* 32 (1981) 47-59.
- [12] I. Kádár, Összefüggés a talaj termékenysége és tápanyag-ellátottsága között, MTA ATK Talajtani és Agrokémiai Intézet, Budapest 2015. pp. 389.
- [13] R. Kastori, S. Denčić, I. Kádár, I. Maksimović, M. Putnik-Delić, V. Momčilović, *The 20th Int. Symp. on Analytical and Environmental Problems, Szeged Hungary* (2014) 83-86.
- [14] S. Denčić, R. Kastori, I. Kádár, I. Maksimović, M. Putnik-Delić, V. Momčilović, *Matica Srpska J. Nat. Sci. Novi Sad* 129 (2015) 27-34.
- [15] Z. Svečnjak, *Agric. Food Sci.* 22 (2013) 445-451.

OPTIMIZATION OF HOMOGENOUS FENTON PROCESS USING DEFINITIVE SCREENING DESIGN APPLIED FOR FLEXOGRAPHIC PRINTING WASTEWATER

Vesna Kecić¹, Đurđa Kerkez², Miljana Prica¹, Milena Bečelić-Tomin², Aleksandra Kulić Mandić², Anita Leovac Maćerak², Božo Dalmacija²

¹*Department of Graphic Engineering and Design, University of Novi Sad, Faculty of Technical Sciences, Trg Dositeja Obradovića 6, 21000 Novi Sad, Serbia.*

²*Department of Chemistry, Biochemistry and Environmental Protection, University of Novi Sad, Faculty of Sciences, Trg Dositeja Obradovića 3, 21000 Novi Sad, Serbia.*

e-mail: kecic@uns.ac.rs

Abstract

The treatment of flexographic cyan dye synthetic solution and real printing effluent has been studied by using homogeneous Fenton process with the addition of $\text{FeSO}_4 \cdot 7\text{H}_2\text{O}$ as a catalyst. The study demonstrate that applied treatment could significantly reduce dye concentration in the examined aqueous solutions. Operating parameters, such as initial dye concentration, iron dosage, hydrogen peroxide concentration and pH were varied to investigate their influence on decolorization efficiency, as well as their mutual interactions. The optimal conditions, found with definitive screening design (DSD) statistical method, were: dye concentration = 123 mgL^{-1} , Fe concentration = 60 mgL^{-1} , H_2O_2 concentration = 5.44 mM and a pH value = 2. Under these conditions decolorization efficiency resulted with 87% and 37% for cyan synthetic solution and real printing effluent, respectively.

Introduction

Wastewater generated from printing industry presents a prominent source of aquatic contamination as it is enriched with high content of organic matter, heavy metals and various forms of dyes, followed with high pH value and low BOD/COD ratio [1, 2]. The conventional treatments, such as coagulation/flocculation, adsorption or membrane filtration are difficult to apply, especially in regards to color removal, due to the complex polyaromatic structure of the dyes. It has been demonstrated that these methods can only transfer pollutants from one phase to another, leaving the final environmental problem unsolved, such as the mineralization of the contaminants and toxicity reduction [3, 4]. Therefore, the key result of the present work is the application of advanced oxidation process (AOP) – homogeneous Fenton process. Fenton reaction has been proved as efficient treatment processes in terms of many hazardous organic pollutants from water due to the *in situ* generation of highly reactive and non-selective hydroxyl radical (HO^\bullet), as a product of reaction between hydrogen peroxide and ferrous ions [4]. In order to determine the best optimum conditions such as catalyst dosage, hydrogen peroxide concentration, initial dye concentration and pH value, definitive screening design (DSD) as adequate statistical tool was applied.

The main objectives of this study were to investigate the possibility of homogeneous Fenton process application for the water-based Cyan flexographic printing dye removal, as well as to apply DSD in order to optimize the Fenton process.

Experimental

Materials. All chemicals used in this work were of analytical grade and all sample analyzes were carried out directly, without pre-treatment. Hydrogen peroxide (30%) was obtained from NRK engineering, Serbia, NaOH (>98.8%) and $\text{FeSO}_4 \cdot 7\text{H}_2\text{O}$ were obtained from POCH, while ccH_2SO_4 (>96%) was produced by J.T. Baker. Deionized water was used for the

preparation of all working solutions within the desired concentrations. The Cyan wastewater and the sample of fresh Cyan dye used in the present study were obtained from flexographic printing facility located in Novi Sad, Serbia. Water-soluble Cyan flexographic dye (C.I.: PB15:3, chemical formula: $C_{32}H_{16}CuN_8$, molar mass: 576.07 g/mol) was produced from Flint Group.

Application of homogeneous Fenton process. All experiments were carried out in a glass beaker (250 ml) on JAR apparatus (FC6S Velp Scientific, Italy). The reaction suspension was prepared by adding a dye solution of various concentration ($20\text{--}180\text{ mgL}^{-1}$) and a catalyst in a form of $FeSO_4 \cdot 7H_2O$ ($0.75\text{--}60\text{ mgL}^{-1}$). After adjusting the pH (2–10) with NaOH or cH_2SO_4 , a H_2O_2 in various concentration (1–11 mM) was added to the mixture. Decolorization efficiency was calculated as follows (1):

$$E(\%) = A_0 - A / A_0 * 100 \quad (1)$$

where A_0 is absorbance of Cyan dye aqueous solution pretreatment, whereas A represents absorbance of Cyan dye aqueous solution after Fenton treatment. Decolorization efficiency was determined by measuring the absorbance of the aqueous solutions at 636 nm by using UV/VIS spectrophotometer (UV 1800 Shimadzu, Japan).

Statistical analysis. A statistical methodology DSD was adopted to optimize the Fenton process. In this study, the influence of four main factors has been investigated: concentration of dye (X_1), iron concentrations (X_2), pH value (X_3) and hydrogen peroxide concentration (X_4), (Table 1), while the decolorization efficiency was considered as dependent factor. The results were analyzed with 95% confidence intervals using the JMP13 (SAS Institute, USA). All experiments were conducted in duplicate with two extra central points, resulting with 28 total runs.

Table 1. Process variables with experimental levels

Variables	Unit	Symbol coded	Levels		
			-1	0	+1
Dye concentration	mgL^{-1}	X_1	20	100	180
Iron concentration	mgL^{-1}	X_2	0.75	30	60
pH	-	X_3	2	6	10
H_2O_2 concentration	mM	X_4	1	6	11

Results and discussion

The results of 28 experimental runs contributed to decolorization efficiency from 1.09 to 78.09%, confirming the assumption that dye removal process is exceptionally dependable on the applied experimental conditions, i.e. the individual parameters contribute to the efficiency of the Fenton process to a certain extent. In order to derive the regression model that best fits the obtained results, JMP's regression analysis was applied. The regression model includes the main factors, their square values and dual factor interactions. The summarized presentation of the adopted regression model, as well as the coefficients of significant main parameters, their quadratic members and dual factor interactions for the obtained model are shown in Tables 2 and 3.

Table 2. The adopted model statistics

Descriptive factor	Value
R^2	0.917
R^2 Adjusted	0.861
RMSE	9.652
Number of experiments	28

Table 3. Estimated significant main parameters, their square members and dual factor interactions

Factor	Estimated parameters	Standard error	<i>t</i> value	Probability > <i>t</i>
Dye concentration	4.242	2.158	1.97	0.0670
Iron concentration	11.858	2.158	5.49	<0.001
H ₂ O ₂ concentration	-1.261	2.158	-0.58	0.5672
pH	-22.182	2.158	-10.28	<0.001
Dye * H ₂ O ₂	-3.565	4.531	-0.79	0.443
H ₂ O ₂ * H ₂ O ₂	-10.107	5.778	-1.75	0.099
Fe * pH	7.510	4.889	1.54	0.144

The results of statistical analysis indicate a high significance of iron concentration, but also the pH value in the homogeneous Fenton process. Significant interactions of individual factors have not been established. Optimal process conditions for the removal of cyan dye using a homogeneous Fenton process are shown in Figure 1. The statistical model proposed a process efficiency of 87.85% for the following optimum values of the investigated factors: dye concentration of 123 mgL⁻¹, iron concentration 60 mgL⁻¹, H₂O₂ concentration of 5.44 mM and a pH value of 2.

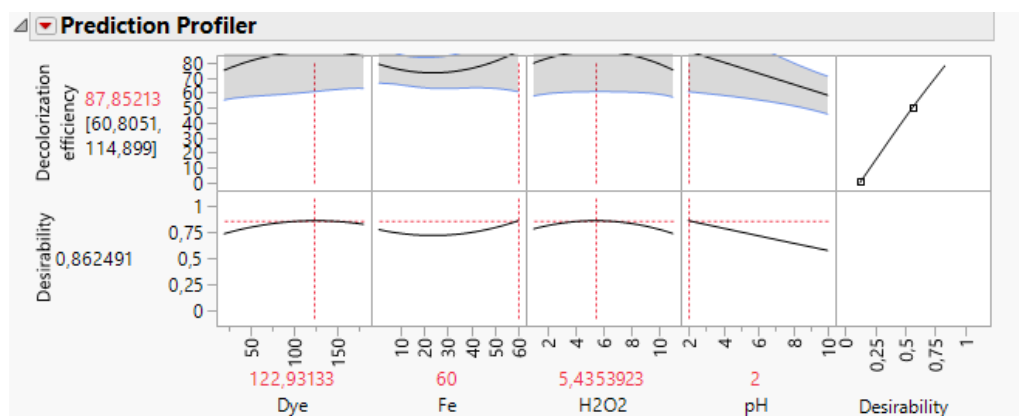


Figure 1. Optimal conditions for homogeneous Fenton process

Validation of the experiments was carried out with eight additional points under optimal conditions, yielding the following efficiency of the homogeneous Fenton process: 85.14; 86.43; 85.56; 86.03; 86.57; 87.29; 87.81; 87.20. The confidence interval [85.56 - 90.15%] confirms the adequacy of the selected model because the suggested efficiency of the homogeneous Fenton process of 87.85% enters the limits of the confidence interval.

In order to determine the possibility of using homogeneous Fenton process for real printing effluent treatment, wastewater generated after the printing process and colored with cyan dye was subjected to homogeneous Fenton process at optimal doses of the tested parameters. Dye

removal efficiency was monitored for a period of 120 minutes and the results are shown in Figure 2.

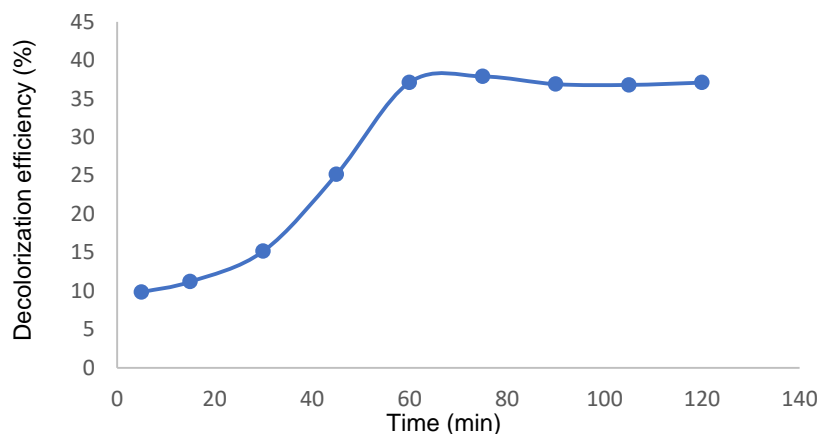


Figure 2. Dependence of the decolorization efficiency with the reaction time

Degradation efficiency after 60 minutes was 37.13% which is also the maximum efficiency. Compared to the treated synthetic dye solution, the process efficiency in the case of a real printing effluent was lower, due to the presence of compounds in the complex effluent matrix. Different organic and inorganic species can achieve an inhibitory effect on the dye degradation process, behaving as hydroxyl radical catchers, thereby achieving competition for active sites on the catalyst surface.

Conclusion

The paper examines the possibility of applying homogeneous Fenton process to the effective removal of the cyan dye from the synthetic dye solution and real effluent generated after the flexographic printing process. High decolorization efficiency, up to 78% is obtained in the case of synthetic dye solution, while a lower expected efficiency of 37% is achieved within the wastewater treatment. Definitive screening design, as a new three-level generation of experimental design, has enabled determination of the optimal conditions for the applied process in order to achieve maximum decolorization efficiency.

Acknowledgements

The authors acknowledge the financial support of the Ministry of Education, Science and Technological Development of the Republic of Serbia within the Projects No. TR 34014 and III43005.

References

- [1] A. Mukamin, N. Zen, A. Purwanto, K.A. Wicaksono, H. Vistanty, A.S. Alfauzi, J. Environ. Chem. Eng. 5 (2017) 5222.
- [2] V. Kecić, Đ. Kerkez, M. Prica, S. Rapajić, A. Leovac Maćerak, M. Bečelić-Tomin, D. Tomašević Pilipović, Journal of Graphic Engineering and Design 8 (2017) 35.
- [3] V. Kecić, Đ. Kerkez, M. Prica, O. Lužanin, M. Bečelić-Tomin, D. Tomašević Pilipović, B. Dalmacija, J. Clean. Prod. 202 (2018) 65-80.
- [4] R. Wang, X. Jin, Z. Wang, W. Gu, Z. Wei, Y. Huang, Z. Qiu, P. Jin, Bioresource Technol. 247 (2018) 1233.

GOLD NANOPARTICLES/EXFOLIATED GRAPHENE HYBRID OBTAINED BY GAMMA IRRADIATION

Dejan Kepić¹, Zoran Marković², Jovana Prekodravac¹, Milica Budimir¹, Biljana Todorović Marković¹

¹ *Vinča Institute of Nuclear Sciences, University of Belgrade, P.O.B. 522, 11001 Belgrade, Serbia*

² *Polymer Institute, Slovak Academy of Sciences, Dubravska cesta 9, 84541 Bratislava, Slovakia*

e-mail: d.kepic@vin.bg.ac.rs

Abstract

Gold nanoparticles decorated graphene sheets present a good surface-enhanced Raman spectroscopy (SERS) platform for the development of ultrasensitive analytical applications. Here, we prepared gold nanoparticles/exfoliated graphene hybrid by gamma irradiation of chloroauric acid as a precursor in the presence of electrochemically exfoliated highly oriented pyrolytic graphite (HOPG). The effects of various irradiation doses (1, 5, 10 and 20 kGy) on the size and shape of synthesized nanoparticles were studied. It was found that the presence of HOPG leads to the formation of gold nanoparticles of triangular, spherical, hexagonal, trapezoidal and rod-shape morphology. On the other hand, irradiation of chloroauric acid solution without HOPG results mainly in irregular shaped nanoparticles, however, certain amount of square shaped nanoparticles is observed. According to statistical analysis of gold nanoparticles/graphene hybrid, nearly half of the nanoparticles have sizes in the 11-20 nm range for all of the applied doses. The increase of irradiation dose results in the increase of the amount of smaller nanoparticles (up to 10 nm in size). Nevertheless, for the highest applied dose agglomeration of nanoparticles takes place leading to the formation of particles that exceed 100 nm in size. Presented synthetic route is fast, simple and low-cost since it does not require the use of a gold nanoparticle stabilizer.

ATTENUATION OF SELECTED PHARMACEUTICALS DURING RIVERBANK FILTRATION IN DANUBE RIVER ALLUVION

Srdan Kovačević¹, Milan Dimkić², Nevena Živančev¹, Veselin Bežanović¹, Aleksandar Čalenić²

¹*University of Novi Sad, Department of Environmental Engineering and Occupational Safety and Health, Trg Dositeja Obradovića 6, 21000 Novi Sad, Serbia*

²*Institute for Water Development „Jaroslav Černi“, 11226 Belgrade, Jaroslava Černog 80, Serbia*

e-mail: srdjankovacevic@uns.ac.rs

Abstract

The paper presents the results of the transport analysis for selected pharmaceuticals during riverbank filtration from the river Danube to the drainage wells at the specific site Kovin-Dubovac. In the Republic of Serbia the occurrence of pharmaceuticals in surface and groundwater was not sufficiently analyzed, so there is a need for research and testing of the occurrence and behavior of pharmaceuticals in order to better understand the flow of pharmaceuticals in the environment and transport of pharmaceuticals in groundwater during riverbank filtration. During the investigation period between 2009-2015, a total of 25 pharmaceuticals were analyzed in 52 samples, of which 13 samples of surface water and 39 samples of alluvial groundwater. A total of 7 pharmaceuticals in Danube River and 6 pharmaceuticals in alluvial groundwater were detected. Carbamazepine and metamazole metabolites N-acetyl-4-amino-antipyrine (4-AAA) and N-formyl-4-amino-antipyrine (4-FAA) have the highest frequency of occurrence in surface water and in groundwater samples, respectively. Results showed that riverbank filtration could significantly remove investigated pharmaceuticals. Percentage of removal during riverbank filtration was determined for carbamazepine (35%), trimethoprim (100%), 4-AAA (82%) and 4-FAA (43%). These results are extremely important for better understanding of self-purification potential of alluvial aquifers and protection from potential impacts of anthropogenic pollution to the groundwater sources in the Republic of Serbia.

Introduction

In the Republic of Serbia population growth is not present, but due to society urbanization and the increase of the average age of population [1], the use of pharmaceuticals is increasing in order to protect human health and improve the conditions and quality of life. In Serbia, the vast majority of cities and industrial systems directly discharge untreated water into natural or artificial recipients, leading to a cumulative occurrence of pharmaceuticals in surface and groundwaters. Also, there are many studies indicating that a large number of pharmaceuticals were not fully removed at the wastewater treatment plants [2,3,4,5]. As a result, pharmaceuticals occur in surface water and groundwater, according to several papers that present the results of studies conducted in Serbia [6,7,8,9]. Using the riverbank filtration (RBF), surface water is treated through filtration in the alluvial aquifer, which is a very important addition to the treatment of drinking water. Also, RBF can reduce the risk of accidental pollution. Due to these facts the knowledge of the processes that take place during the RBF in order to define the most optimal way of line treatment for drinking water and prevent possible occurrence of polluting substances in drinking water. The aim of our study was to obtain sufficient information about the occurrence of selected pharmaceuticals in surface water and groundwater, and to observe the removal of these pharmaceuticals through RBF, which is generally the method of choice for drinking water supply in Serbia.

Materials and methods

In the period 2009–2010 the water samples for pharmaceutical analysis were prepared applying the method of solid phase extraction (SPE) and extracts were analyzed using liquid chromatography tandem mass spectrometry method (LC-MS/MS). Detailed information about the used analytical procedure, instrumental parameters, SPE recoveries, calibration curves, accuracy, precision, detection limits, and quantification limits is described in the previously published study [10].

After the year 2010 samples were analyzed with the slightly modified methods previously published [10,11] in which 7 cardiovascular pharmaceuticals were added. The method was validated and the results are presented in the supplementary material of the published papers. Out of 19 investigated pharmaceuticals, 12 were analyzed continuously between 2009 and 2015: sulfamethoxazole, trimethoprim, erythromycin, azithromycin, doxycycline, diazepam, bromazepam, lorazepam, carbamazepine, diclofenac and two metamizole metabolites, N-formyl-4-amino-antipyrine (4-FAA) and N-acetyl-4-amino-antipyrine (4-AAA). In the period 2010 – 2015, additional group of seven cardiovascular pharmaceuticals were included into analysis: enalapril, cilazapril, atorvastatin, simvastatin, amlodipine, metoprolol, bisoprolol. Selected pharmaceuticals belong to different pharmaceutical classes and the selection was based on the application extent of pharmaceuticals in Serbia and the review of occurrence in surface water and groundwater [12]. Surface water and groundwater samples were sampled mainly in the spring and fall every year.

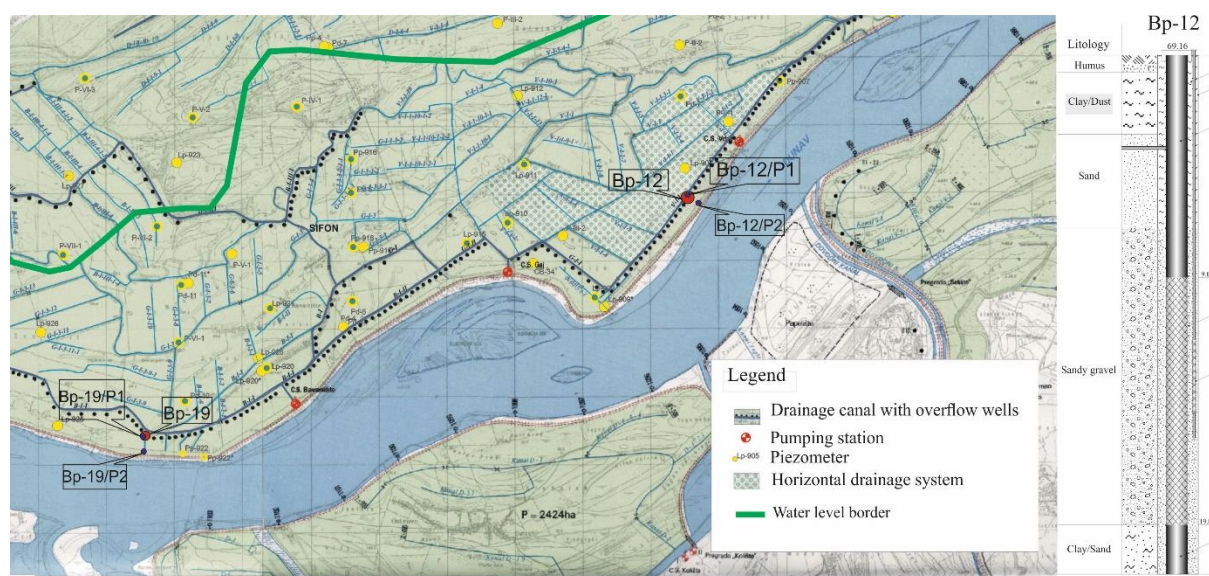


Figure 1. Research location and profile from one analysed drainage well Bp-12

Both, surface water and groundwater samples were taken at the same time during the investigation period. Surface water was sampled mid-stream, at a depth of about one meter. Groundwater samples (GW) were collected from wells in the immediate vicinity of the river Danube. In the case of free-flowing or pumped wells, measurements were conducted by submerging a peristaltic pump to the level of the well screen or horizontal collector, whereas in the case of observation wells the pump was submerged to the screen after removing a minimum of three water volumes from the observation wells with the use of a peristaltic pump.

Results and Discussion

Based on the results of analysis of the presence of selected pharmaceuticals into surface water and groundwater in the Danube River alluvion, it is evident that concentration in the groundwater was reduced as a result of the process of self-purification of groundwater during RBF. In Figure 2 there the average concentrations of detected pharmaceuticals in surface water and groundwater in the alluvium of the Danube River are shown.

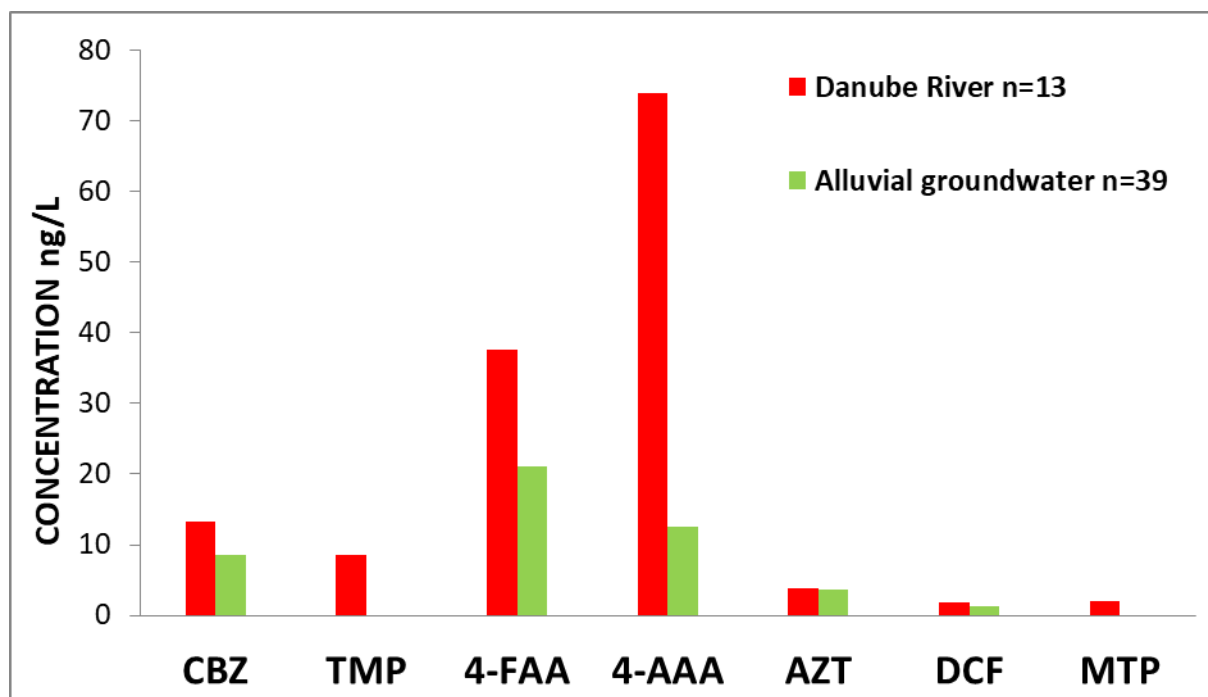


Figure 2. Average concentration of detected pharmaceuticals in the Danube River and corresponding wells of the drainage system Kovin-Dubovac (n - number of samples; $\frac{1}{2}$ LOD - half of the value of the limit of detection was adopted, where the pharmaceuticals were not detected in the selected samples)

The average concentration of carbamazepine (CBZ) in the groundwater was reduced by 35% compared to the average concentration in the Danube River. Carbamazepine was detected in a total of 8 samples of the Danube River while it is registered with the concentration range between 12-32 ng/l. Trimethoprim (TMP) has been completely removed during RBF, and it was detected in one sample of the Danube River with a concentration of 110 ng/l. The average concentration of diclofenac (DCF) in the alluvial groundwater was decreased by 30% compared to the concentration in the Danube River. Diclofenac has been registered in the one sample of the Danube River with concentrations of 18 ng/l and in one sample of the alluvial groundwater with concentration of 13 ng/l. At Kovin – Dubovac drainage system 4-FAA and 4-AAA were reduced by 43 % and by 82 % respectively. Metamizole metabolite 4-AAA was detected in 9 samples of the Danube River with concentration range of 31-260 ng/l, and in the alluvial groundwater 4-AAA was detected in a total of 14 samples with a concentration range of 12-105 ng/l. 4-FAA was detected in 9 samples of Danube River with concentration range between 28-144 ng/l, and in corresponding groundwater with the concentration range between 14-98 ng/l. Azithromycin (AZT) was detected in one sample of Danube River with concentration of 56 ng/l, and in two samples of corresponding groundwater 21-68 ng/l. Metoprolol (MTP) was detected in one sample in the Danube River with concentration of 35 ng/l, but it was not detected in alluvial groundwater. None of the other pharmaceuticals was detected in the surface water or groundwater samples. Because of the relatively small

percentage of removal at a relatively long path from the river to the well (approximately 400 meters) where carbamazepine was exposed to the process of self-purification can indicate that carbamazepine can be assessed as persistent pharmaceutical, as it was noted in previous studies [13,14]. Trimethoprim as readily degradable pharmaceutical was fully removed, because the degradation takes place relatively quickly [15]. Other pharmaceuticals were either not detected or the detection frequency was too low to quantify the rates of their removal through RBF.

Conclusion

Results clearly showed that concentration of selected pharmaceuticals could be reduced during RBF. In general, the concentrations detected in the Danube River were several times greater than those detected in the wells of Kovin – Dubovac drainage system. Removal of detected pharmaceuticals through RBF is evident in the area of the Kovin – Dubovac drainage system, with a relatively long path from the river to the well (approximately 400 meters). Carbamazepine was the most persistent pharmaceutical, and all other detected pharmaceutical were significantly attenuated or completely removed.

Acknowledgements

This research was supported by the Ministry of Education, Science and Technological Development, Republic of Serbia, under the Project No. TR 37014 and project III 46009.

References

- [1] Statistical Office of the Republic of Serbia, Statistical yearbook data 2016.
- [2] Jiang J, Zhou Z, Sharma V K (2013) Occurrence, transportation, monitoring and treatment of emerging micro-pollutants in waste water — A review from global views. *Microchemical Journal* 110: 292–300. doi: 10.1016/j.microc.2013.04.014.
- [3] Luo Y, Guo W, Hao H, Duc L, Ibney F, Zhang J, Liang S (2014) A review on the occurrence of micropollutants in the aquatic environment and their fate and removal during wastewater treatment. *Science of the Total Environment* 473-474: 619–641. doi: 10.1016/j.scitotenv.2013.12.065
- [4] Patrolecco L, Capri S, Ademollo N (2015) Occurrence of selected pharmaceuticals in the principal sewage treatment plants in Rome (Italy) and in the receiving surface waters. *Environmental Science and Pollution Research* 22: 5864–5876. doi: 10.1016/j.scitotenv.2013.08.079.
- [5] Papageorgiou P, Kosma C, Lambropoulou D (2016) Seasonal occurrence, removal, mass loading and environmental risk assessment of 55 pharmaceuticals and personal care products in a municipal wastewater treatment plant in Central Greece. *Science of the Total Environment* 543: 547-569. doi: 10.1016/j.scitotenv.2015.11.047.
- [6] Terzić S, Senta I, Ahel M, Gros M, Petrović M, Barcelo D, Müller J, Knepper T, Martí I, Ventura F, Jovančić P, Jabučar D (2008) Occurrence and fate of emerging wastewater contaminants in Western Balkan Region. *Science of the Total Environment* 399: 66-77. doi: 10.1016/j.scitotenv.2008.03.003
- [7] Radović T, Grujić S, Dujaković N, Radišić M, Vasiljević T, Petković A, Boreli-Zdravković Đ, Dimkić M, Laušević Mila (2012) Pharmaceutical residues in the Danube River Basin in Serbia - a two-year survey. *Water Science and Technology* 66 (2): 659-665 doi: 10.2166/wst.2012.225.

- [8] Petrović M, Škrbić B, Živančev J, Ferrando-Climent L, Barcelo D (2014) Determination of 81 pharmaceutical drugs by high performance liquid chromatography coupled to mass spectrometry with hybrid triple quadrupole–linear ion trap in different types of water in Serbia. *Science of the Total Environment* 468-469: 415-428. doi: 10.1016/j.scitotenv.2013.08.079.
- [9] Radović T, Grujić S, Petković A, Dimkić M, Laušević M (2015) Determination of pharmaceuticals and pesticides in river sediments and corresponding surface and ground water in the Danube River and tributaries in Serbia. *Environmental Monitoring and Assessment* 187:4092. doi: 10.1007/s10661-014-4092-z.
- [10] Grujić S, Vasiljević T, Laušević M (2009) Determination of multiple pharmaceutical classes in surface and ground waters by liquid chromatography-ion trap-tandem mass spectrometry. *Journal of Chromatography A*. 1216: 4989–5000. doi: 10.1016/j.chroma.2009.04.059.
- [11] Jauković Z, Grujić S, Vasiljević T, Petrović S, Laušević M (2014) Cardiovascular Drugs in Environmental Waters and Wastewaters: Method Optimization and Real Sample Analysis. *Journal of AOA C International* 97 (4): 1167-1174. doi: 10.5740/jaoacint.12-121.
- [12] Mompelat S, Le Bot B, Thomas O (2009) Occurrence and fate of pharmaceutical products and by-products, from resource to drinking water. *Environment International* 35: 803–814. doi: 10.1016/j.envint.2008.10.008.
- [13] Laws B, Dickenson E, Johnson T, Snyder D, Drewes J (2011) Attenuation of contaminants of emerging concern during surface-spreading aquifer recharge. *Science of The Total Environment* 409 (06): 1087–1094. doi: 10.1016/j.scitotenv.2010.11.021.
- [14] Hamann E, Stuyfzand P, Greskowiak J, Timmer H, Massmann G (2016) The fate of organic micropollutants during long-term/long-distance river bank filtration. *Science of the Total Environment* 545–546: 629–640. doi: 10.1016/j.scitotenv.2015.12.057.
- [15] Storck FR, Schmidt CK, Lange FT, Henson JW, Hahn K (2012) Factors controlling micropollutant removal during riverbank filtration. *Journal of American Water Works Association* 4 (12): 643–652. doi: 10.5942/jawwa.2012.104.0147.

ADSORPTION-DESORPTION PROCESSES ON DISCRETE SUBSTRATES – OPTIMIZATION OF MONOLAYER GROWTH

Ivana Lončarević¹, Ljuba Budinski-Petković¹, Slobodan Vrhovac², Zorica Jakšić²

¹*Faculty of Technical Sciences, University of Novi Sad, 21000 Novi Sad, Trg D. Obradovića
6, Serbia*

²*Institute of Physics, University of Belgrade, 11080 Zemun, Pregrevica 118, Serbia
e-mail: ivanalon@uns.ac.rs*

Abstract

Kinetics of the deposition process of dimers on a 1D lattice in the presence of desorption is studied by Monte Carlo method. The growth of the coverage $\theta(t)$ above the jamming limit to its steady-state value θ_∞ is analyzed when desorption probability P_{des} decreases both stepwise and linearly (continuously) over a certain time domain. We report a numerical evidence that the process of vibratory compaction of granular materials can be optimized by using a time dependent intensity of external excitations.

Introduction

In RSA processes particles are randomly, sequentially, and irreversibly deposited onto a substrate. The dominant effect in RSA is the blocking of the available substrate area since the particles are not allowed to overlap. The system is jammed in a nonequilibrium disordered state for which the limiting (jamming) coverage θ_{jam} is less than the corresponding density of the closest packing. The possibility of desorption makes the process reversible and the system ultimately reaches an equilibrium state when the rate of desorption events becomes comparable to the rate of adsorption events. The density of particles in the steady state depends only on the desorption or adsorption rate ratio [1,2].

Within the framework of the adsorption-desorption model it was shown in [3] that the increase of packing fraction can be accelerated by changing the desorption rate during the adsorption-desorption process. The aim of this work is to investigate how do various temporal dependencies of the desorption rate hasten or slow down the deposition process.

Simulation method

The Monte Carlo simulations of adsorption-desorption processes are performed on a one-dimensional lattice of size $L=10^5$ with a periodic boundary condition. The adsorbing objects are dimers covering two sites. The time t is counted by the number of adsorption attempts and scaled by the total number of lattice sites L . The data are averaged over 100 independent runs. At each Monte Carlo step adsorption is attempted with probability P_a and desorption with probability P_{des} . In the case of adsorption-desorption processes the kinetics is governed by the ratio of desorption to adsorption probability P_{des}/P_a [1,4,5]. Since we are interested in the ratio P_{des}/P_a , in order to save computer time, it is convenient to take the adsorption probability to be $P_a=1$. For each of these processes a lattice site is selected at random. In the case of adsorption, we try to place the dimer with the beginning at the selected site, i.e., we search whether adjacent site in a randomly chosen direction is unoccupied. If so, we place the dimer. Otherwise, we reject the deposition trial. When the attempted process is desorption, and if the selected site is occupied by a dimer, the object is removed from the lattice.

Results and discussion

Simulations of the adsorption-desorption processes of dimers were performed for a wide range of desorption probabilities $P_{\text{des}} = 0.001\text{--}0.050$. In Fig. 1 the coverage is plotted as a function of time for different values of P_{des} . Notice that the curves for different values of P_{des} always cross. This means that, for the reversible RSA model, the coverage is not always monotonic in P_{des} . In Fig.1, for example, the system with $P_{\text{des}} = 0.030$ has a higher coverage than the system with $P_{\text{des}} = 0.010$ for $15 \leq t \leq 500$; above $t \approx 500$ coverage is higher for the lower value of desorption probability, $P_{\text{des}} = 0.010$. As already discussed in the context of the parking lot model [3], the existence of a minimum in the insertion probability (the fraction of the substrate that is available for the insertion of a new particle) is a sufficient condition for this phenomenon. It follows that for a given finite time, the densification can be made more efficient by changing the desorption probability P_{des} during the deposition process.

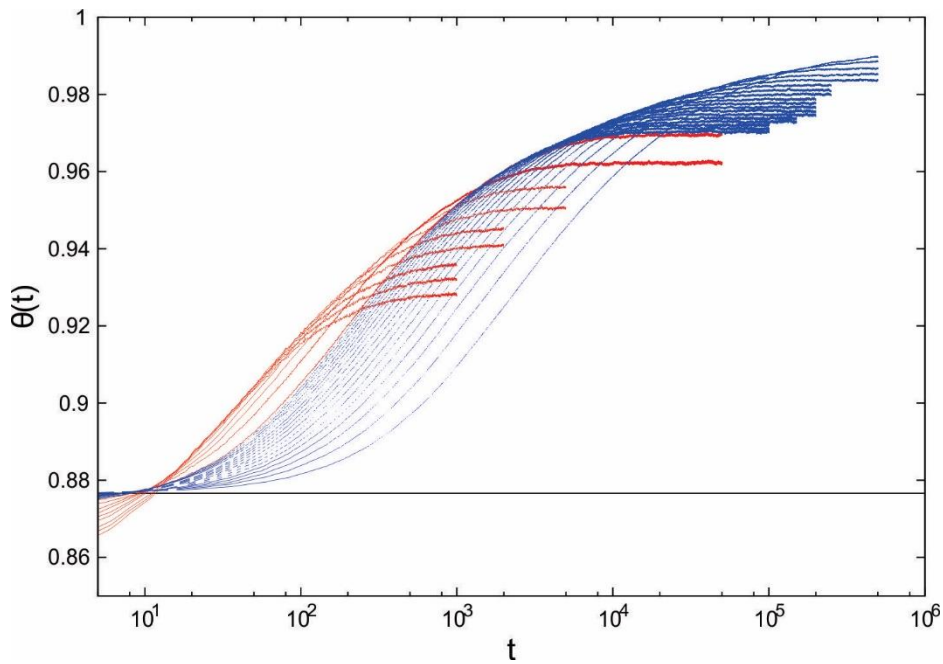


Figure 1. Temporal behavior of the coverage $\theta(t)$ for various desorption probabilities P_{des} . Red (solid) lines correspond to values $P_{\text{des}} = 0.010 + n \cdot 0.005$, $n = 0, 1, 2, \dots, 8$. Blue (dashed) lines correspond to values $P_{\text{des}} = 0.0010 + n \cdot 0.0005$, $n = 0, 1, 2, \dots, 17$. The equilibrium coverage θ_{eq} is found to decrease with the desorption probability P_{des} . The horizontal line represents the jamming coverage for dimers, $\theta_{\text{jam}} = 0.8766$.

The possibility to hasten the dynamics of reversible RSA is studied by decreasing the desorption probability from $P_{\text{des}}^{(I)} = 0.050$ to $P_{\text{des}}^{(F)} = 0.010$ in a stepwise manner. Starting from an empty lattice, the system evolves at fixed desorption probability $P_{\text{des}}^{(I)} = 0.050$ up to the coverage $\theta^{(I)}$ above the jamming coverage θ_{jam} . Then, the desorption probability is abruptly lowered at fixed time intervals t_c . Those time intervals follow each other directly without any gap. We always use an instantaneous drop of $P_{\text{des}} = 0.005$ for a change of the desorption probability P_{des} , so that the final probability of $P_{\text{des}}^{(F)} = 0.010$ is reached after eight abrupt changes of P_{des} . The final desorption probability $P_{\text{des}}^{(F)}$ does not change further in time. In Fig. 2, we demonstrate that the deposition process can be made much more efficient by decreasing the desorption probability P_{des} in time. Several horizontal arrows are inserted in Fig. 2 and

placed at certain values of the coverage θ in the range $[0.890, 0.955]$. These arrows show how much more time is needed for a system to reach a given coverage θ in the case when the desorption probability has the constant value $P_{\text{des}}^{\min}(\theta)$ in time.

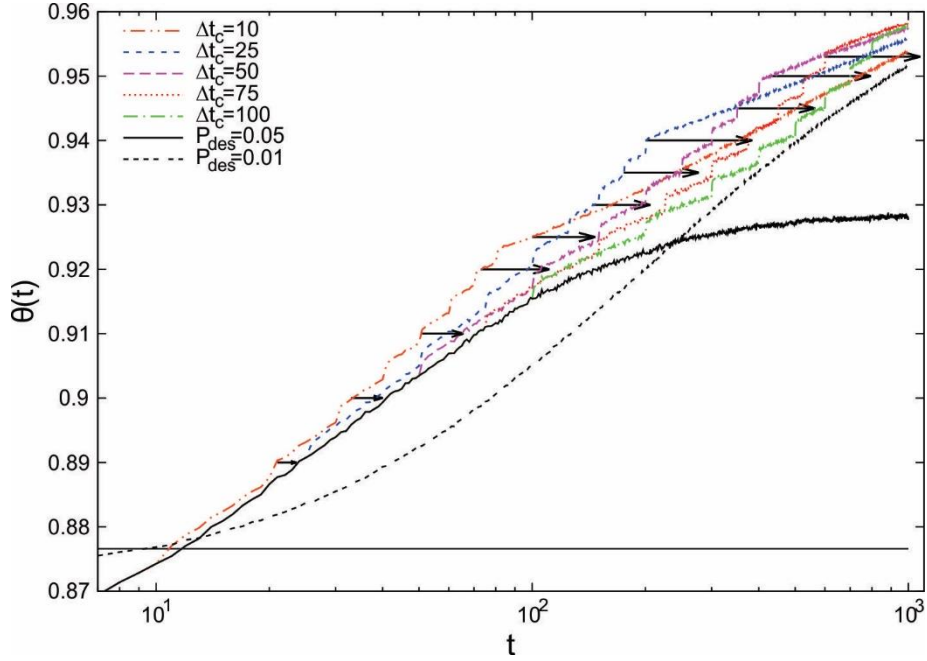


Figure 2. Temporal behavior of the coverage $\theta(t)$ when the desorption probability P_{des} decreases from $P_{\text{des}}^{(1)} = 0.050$ to $P_{\text{des}}^{(F)} = 0.010$ in a stepwise manner. The desorption probability is abruptly lowered by $\Delta P_{\text{des}} = 0.005$ at fixed time intervals $\Delta t_c = 10, 25, 50, 75, 100$, as indicated in the legend. Arrows show how much more time is needed for a system to reach the given coverage θ in the case when desorption probability has the constant value $P_{\text{des}}^{\min}(\theta)$ in time (e.g., see Fig. 1). The horizontal line represents the jamming coverage for dimers, $\theta_{\text{jam}} = 0.8766$.

It is important to consider the case when the desorption probability varies continuously over a certain time domain. Here we show that the linear decay in the desorption probability as a function of time may be used to hasten the deposition process. The system first evolves at a fixed desorption probability $P_{\text{des}}^{(1)}$, up to the intersection point of relaxation curves at time t_1 . Then, the desorption probability starts to decrease linearly with time according to $P_{\text{des}}(t) = K \cdot (t - t_1) + P_{\text{des}}^{(1)}$, where $t_1 < t < t_2$. The final probability of $P_{\text{des}}^{(2)}$, is reached during the time interval $\Delta t = t_2 - t_1$, so that the negative slope coefficient $K = -(P_{\text{des}}^{(1)} - P_{\text{des}}^{(2)}) / (t_2 - t_1) = -\Delta P_{\text{des}} / \Delta t$ depends on the time interval Δt .

In Fig. 3 the temporal dependence of coverage $\theta(t)$ is displayed for the fixed probabilities $P_{\text{des}}^{(1)} = 0.050$ and $P_{\text{des}}^{(2)} = 0.010$, and for different time intervals $\Delta t = 0, 10, 20, 40, 100, 200, 500, 10^3, 2 \times 10^3, 5 \times 10^3, 10^4, 2 \times 10^4$. Several horizontal arrows are placed at certain values of coverage θ in order to show that much more time is needed for a system to reach a given coverage θ in the case when the desorption probability has a constant value $P_{\text{des}}^{\min}(\theta)$ in time.

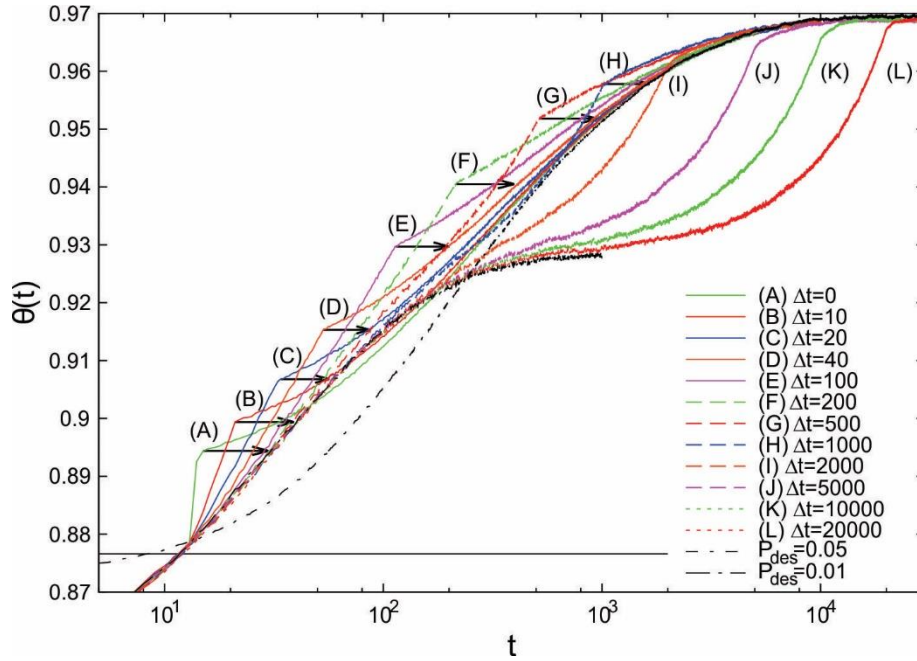


Figure3. Temporal behavior of the coverage $\theta(t)$ when the desorption probability P_{des} decreases linearly with time from $P_{\text{des}}^{(1)} = 0.050$ to $P_{\text{des}}^{(2)} = 0.010$. The final probability of $P_{\text{des}}^{(2)}$ is reached during the time interval Δt . Curves (A)–(L) correspond to various time intervals Δt ranging from 0 to 2×10^4 , as indicated in the legend. Arrows show how much more time is needed for a system to reach the given coverage θ in the case when desorption probability has the constant value $P_{\text{des}}^{\text{min}}(\theta)$ in time (e.g., see Fig.1). The horizontal line represents the jamming coverage for dimers, $\theta_{\text{jam}} = 0.8766$.

Conclusion

We have investigated numerically the kinetics of the deposition process of dimers on a 1D lattice in the presence of desorption. A systematic approach is made by examining deposition with various time dependencies of the desorption probability P_{des} . We focused on the time evolution of the coverage $\theta(t)$ in the whole postjamming time range $\theta(t) > \theta_{\text{jam}}$.

We have shown that the time needed for a system to reach a given coverage θ may be less if P_{des} decreases in time. We have considered the behavior of the system when the desorption probability P_{des} decreases both stepwise and linearly (continuously) over a certain time domain. Furthermore, the initial and final desorption probability do not have arbitrary values. If P_{des} is large enough, the system will not reach the jamming. In other words, there is an upper limit $P_{\text{des}}^{(B)}$ of the desorption probability, above which the steady-state coverage will be lower than the jamming limit. For our 1D system we use $P_{\text{des}}^{(B)} \approx 0.10$. The greatest impact on the deposition rate is obtained if the initial value of the desorption probability $P_{\text{des}}^{(I)}$ corresponds to the limiting value $P_{\text{des}}^{(B)}$. The final value of the desorption probability $P_{\text{des}}^{(F)}$ determines the maximal value of the coverage $\theta_{\infty}(P_{\text{des}}^{(F)})$ that can be achieved.

Since the time needed for a system to reach a given coverage θ can be significantly reduced if P_{des} decreases in time, we propose the application of an analog procedure to optimize the compaction process in weakly vibrated granular materials. Granular materials are complex systems exhibiting rich macroscopic phenomenology and showing many characteristic glassy behaviors. One of the striking features of granular materials are the memory effects observed by measuring the short-time response to an instantaneous change in tapping acceleration [6].

The short-term memory effects observed in granular materials are reflected in the fact that the future evolution of the packing fraction θ after time t_0 depends not only on the $\theta(t_0)$, but also on the previous tapping history. Response properties of granular media and the observation of short-term memory effects indicate that the change in tapping acceleration can affect the dynamics and efficiency of the compaction process.

Acknowledgements

This work was supported by the Ministry of Science of the Republic of Serbia, under Grant No. ON171017.

References

- [1] P. L. Krapivsky and E. Ben-Naim, J. Chem. Phys. 100 (1994) 6778.
- [2] Lj. Budinski-Petković and U. Kozmidis-Luburić, Physica A 301 (2001) 174.
- [3] J. Talbot, G. Tarjus, and P. Viot, Phys. Rev. E 61 (2000) 5429.
- [4] I. Lončarević, Lj. Budinski-Petković, S. B. Vrhovac, and A. Belić, Phys. Rev. E 80 (2000) 021115.
- [5] R. S. Ghaskadvi and M. Dennin, Phys. Rev. E 61 (2000) 1232.
- [6] C. Josserand, A. Tkachenko, D. M. Mueth, and H. M. Jaeger, Phys. Rev. Lett. 85 (2000) 3632.

SWOT ANALYSIS OF DECARBONIZATION THROUGH METHENIZATION PROCESS

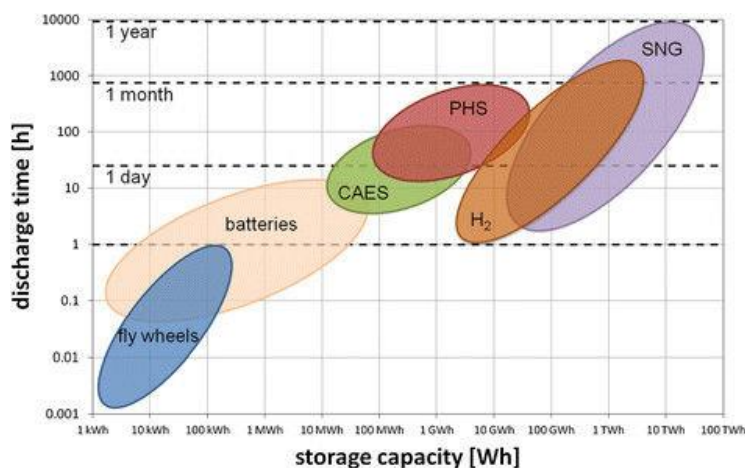
Corina Macarie, Ionel Balcu, Mirela Iorga, Paula Sfirloaga

National Institute for Research and Development in Electrochemistry and Condensed Matter,
144 Dr. A. Paunescu Podeanu, 300569, Timisoara, Romania, Tel.: +40 256 222119
e-mail address: mac_cora@yahoo.com

Abstract

Despite the exhaustion of natural resources, the needs of society which are on the rise, and environmental challenges the current economic system is based on intensive use of conventional energy sources. This requires a reconsideration of prevalent management approaches and the implementation of new management modes. The promising solution is decarbonization which implies the implementation and development of ecological economy policies. Until 2050, a percentage between 50% and 70% of electricity will be supplied by renewable energy sources. Decarbonation represents a trend in economic development, which involves an intense development of civil society based on alternative economic approaches [1].

A comparison of technologies in terms of storage capacity and their characteristic during charge / discharge is shown in follow figure:



Legend:

- ✓ CAES - Compressed Air Energy Storage;
- ✓ PHS - Pumped Hydro Storage;
- ✓ SNG - Substitute Natural Gas.

Charge/discharge period and storage capacity of different electricity storage systems.

An essential requirement for these technologies (energy storage from renewable sources) is high storage capacity combined with long charging / evacuation periods. Only secondary chemical carriers such as hydrogen and carbon-based fuels (SNGs) complies this requirement [2]. State-of-the-art technologies that implement the industrial ecology concept only make it to the market if environmental gains and economic benefits are significant [3].

This delivers results relevant to national and sectorial policy and decision making, by quantifying revenue opportunities.

It also informs the innovation, policy, and regulatory environment required to ensure market development and resilience of different streams.

Management uses SWOT analysis to make decisions about developing the overall strategy.

Acknowledgements

This work was supported by a grant of the Romanian Ministry of Research and Innovation CCCDI-UEFISCDI, project number PN-III-P1-1.2-PCCDI-2017-0404 / 31PCCDI/2018, within PNCDI III

References

- [1] E.G. Matugina, O. V. Pogarnitskaya, N.V. Dmitrieva, L.S. Grinkevich, J.O. Selenchuk, A.B. Strelnikova, Evaluating perspectives of economy “decarbonation” – environmental aspect IOP Conf. Series: Earth and Environmental Science 43 (2016) 012042
- [2] Tanja Schaaf, Jochen Grünig, Markus Roman Schuster, Tobias Rothenfluh, Andreas Orth Methanation of CO₂ - storage of renewable energy in a gas distribution system Energy, Sustainability and Society
- [3] Muhammad Salman, Maarten Dubois, Andrea Di Maria, Karel Van Acker, Koenraad Van Balen Construction Materials from Stainless Steel Slags: Technical Aspects, Environmental Benefits, and Economic Opportunities Journal Industrial Ecology

SUPPRESSED LEACHING OF A Pd(II) COMPLEX IMMOBILIZED ON HYDROPHILIC GRAPHITE OXIDE USED IN THE HECK COUPLING REACTION

Martin Hancsárik^{1,2}, Tamás Szabó², Ágnes Mastalir¹

¹Department of Organic Chemistry, University of Szeged, H-6720 Szeged, Dóm tér 8, Hungary

²Department of Physical Chemistry and Materials Science, University of Szeged, H-6720 Szeged, Rerrich Béla tér 1, Hungary
e-mail: mastalir@chem.u-szeged.hu

Abstract

Immobilization of homogeneous organic catalysts has fundamental environmental aspects. It is desirable that (i) the catalyst is prepared under benign conditions and (ii) it is not removed from the surface of the support under catalytic conditions. Graphene based supports such as graphite oxide (GO) seem to be feasible for the achievement of the above two requirements. In this study we heterogenized tetraamminepalladium(II) chloride monohydrate on hydrophilic GO. Two samples, with Pd contents of 2% and 5%, referred to as Pd2 and Pd5 were prepared and tested as catalysts in the Heck coupling reaction of styrene and bromobenzene. The Pd complexes heterogenized on graphene oxide platelets proved to be highly active and selective catalysts. Hot filtration tests revealed that the active Pd particles did not undergo any leaching in NMP and DMF solvents at 423 K.

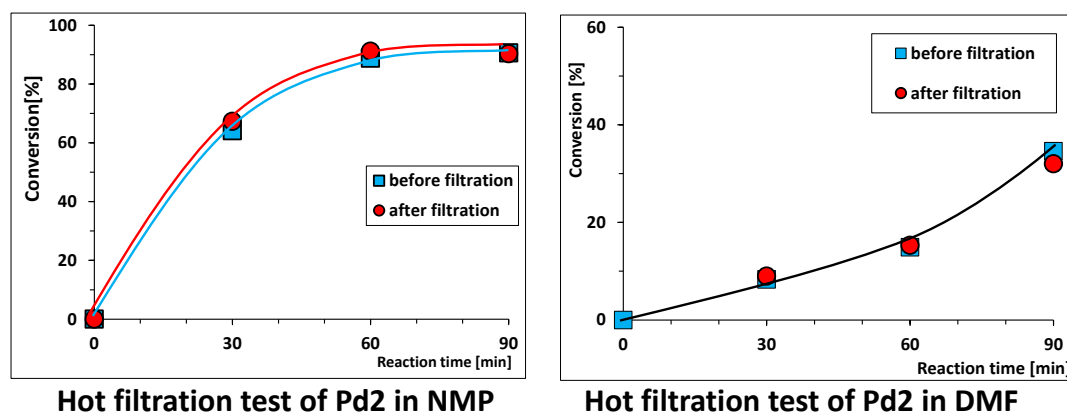


Figure 1. Conversions of the coupling reaction between styrene and bromobenzene in the presence of a catalyst containing 2 wt% Pd on GO as a function of reaction time in N-methyl pyrrolidone (left) and dimethyl formamide (right)

Acknowledgements

Project no. 124851 has been implemented with the support provided from the National Research, Development and Innovation Fund of Hungary, financed under the FK funding scheme.

References

- [1] F. Christoffel, T.R. Ward, Catal. Lett. 148 (2018) 489.
- [2] Á. Mastalir, M. Hancsárik, T. Szabó, Immobilization of a Pd(II) complex on hydrophilic graphite oxide and its catalytic investigation in the Heck coupling reaction, manuscript submitted to publication.

ENVIRONMENTAL AWARENESS AMONG THE CHILDREN IN NOVI SAD CITY

Jelena Mičić¹, Bogdana Vujić¹, Višnja Mihajlović¹, Una Marčeta¹

*¹Technical Faculty „Mihajlo Pupin“, University of Novi Sad, Đure Đakovića bb, Zrenjanin
e-mail: jelena.micic@tfzr.rs*

Abstract

Education on environmental protection must be realized throughout the entire education period, from pre-school age, in order to create a model of responsible behavior towards the environment. In order to assess the environmental awareness among children, a survey was conducted among children aged 6 to 12, who attend preschool and elementary schools at the territory of Novi Sad. The purpose of the work is to show wheather the children are aware of the problems of environmental and nature disorders and pollution, with which they most often associate the term "environment".

Introduction

Schools are a significant factor in developing awareness and behavior of children. It is important that from the beginning of children's education, to introduce to children and get them familiar with basic knowledge and concepts of environmental protection. Pre-school children are considered to accepted and adopting knowledge and behaviors of adult at the most, ie parents and teachers [1]. Particularly important issue in knowledge transfer is the teacher's commitment to children, from pre-school age. People involved in children's education, pre-school teachers, school teachers and trainers of children are responsible for shaping the children's attitudes, values and skills needed to develop environmental care [2]. The results of a survey conducted among teachers in the South-Backa District show that only 35% of teachers in preschool institutions have strong interest in implementing environmental activities, and as much as 54% think they are not sufficiently trained to carry out educational work in this field [3].

Environmental education has recently become a part of teaching system in Serbia. It is teach, depending on the age, as a separate course or educational content within the activities of pre-school institutions, or as part of courses like nature and/or society, or biology, chemistry, geography and physics, or vocational subjects in secondary schools [4]. Legal obligation for preschools is a program of rest and recreation, climate recovery and teaching in nature, in order to form positive attitudes towards nature and its protection [5]. In the curricula of elementary schools in the Republic of Serbia, from the first to the fourth grade, ecological and environmental contents are mostly represented in the subjects "The world around us" and "Nature and society". In the first and second grade, the share of "The World around Us" makes up about 10% of the total number of hours of regular education [6]. Knowledge of environmental protection is important in order to develop the correct ecological behavior and to undertake correct actions in order to protect the nature and environment. Promotion of ecological education is necessary as it seen as a key component in environmental education and a prerequisite for ecological behavior [7]. The aim of this paper is to examine the child's perception of environmental protection, as well as their behavior, which contribute to a minor disruption of the environment.

Experimental

Using random sample method, a questionnaire was conducted among children from 6 to 12 years. The research involved 25 respondents, and the research was conducted at the Festival of Science and Education in Novi Sad as a part of workshop organized at the Festival. Research was conducted using questionnaire in print form and in direct contact with respondents. The children responded to questions independently but in some situations when respondents was from pre-school, they need a help to read and understand certain questions. Questionnaire was used as tool to obtain the necessary data for research. Questionnaire had two parts, first one in which the respondents answer the standard questions on gender and age, and second part was questionnaire questions (Q):

- Q1: Do you turn off the tap while you brush your teeth?
- Q2: Do we need to re-use the used things?
- Q3: Do you turn off the light when you are not in the room?
- Q4: Do you play in the park and spend the time in nature?
- Q5: Do you use both sides of the paper when writing / drawing?
- Q6: Do we need to use pesticides (chemicals) in our gardens?
- Q7: Do you throw waste into the garbage bin?
- Q8: Do you study in school about how to protect the environment?
- Q9: Have you made objects/figures from recycled materials with a teacher/educator?
- Q10: Do you think we need do the most to protect the nature and environment?
- Q11: How do you protect the environment?
- Q12: When you think of environmental protection, what comes to your mind first?

Available answers to questionnaires from Q1 to Q7 were as follows: a) always, b) sometimes and c) never. Answers to Q8 and Q9 were: a) Yes, b) I do not know, and c) No, while for Q10, Q11 and Q12, respondents was free to write the answer.

Results and discussion

Structure of respondents based on age and gender is given in Figure 1 and Figure 2, respectively.

A total of 25 respondents took part in the survey, of which 14 boys and 11 girls. According to age, the structure of the respondents is as follows:

- children aged 6 and 7 years - 7 respondents,
- children aged 8 and 9 years - 10 examinees and
- children aged 10.11 and 12 years - 8 subjects.

The analysis was conducted by a random sample method and one can notice almost equal distribution of respondents both by sex and age.

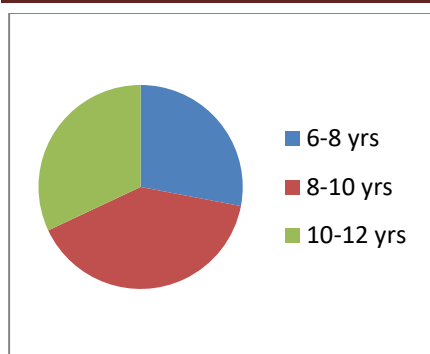


Figure 2. Respondents age

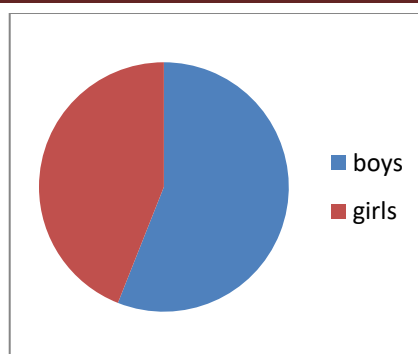


Figure 1. Respondents gender

In following tables, responses to questions were analyzed and presented as a percentage of total answers for each question (%).

Table 1. Distribution of answers from Q1 to Q7 (%)

Questionnaire question	Always	Rare	Never
Q1	16	28	56
Q2	36	52	12
Q3	92	8	0
Q4	52	44	4
Q5	40	40	20
Q6	4	36	60
Q7	92	4	4

Table 2. Distribution of answers for Q8 and Q9 (%)

Questionnaire question	Yes	I do not know	No
Q8	96	0	4
Q9	44	4	52

Questions related to environmental protection, Q1, whether you turn off the tap while you brush your teeth, 56% of the respondents gave a positive response. Majority of respondents (96%) turn-off the light when they do not stay in the room, and 60% think that we should never use chemicals in the gardens. Almost all surveyed children (96%) gave a positive answer to the question of whether they learned about how to protect the environment. At the same time, Q8 is an indicator how much attention do the children pay to this topic and their interest about environmental protection. However, more than half of respondents (52%) answered that they did not have recycling workshops in kindergarten / school, which implies the need for different trainings for teachers in the field of environmental protection and necessity to design workshops adapted to children of different ages. Q10 refers to increasing environmental care and 24 children responded that we should take more care of the environment. Reasons are mainly associated with waste pollution and excessive nature pollution. Children believe that taking care of the environment also concerns the health of people, and in the answers we can found that the children are familiar with the term “principle of environmental sustainability”, in the sense that nature should be preserved for future generations. Children’s contribution environmental protection is in most of the responses is related to the waste separation (68%). Also, they perceive water saving as an contribution to environmental protection as well as recycling, and planting. The first

association to environmental protection is nature and preservation of nature from pollution, as well as recycling and waste disposal.

Conclusion

The aim of this work was to obtain the data and information about the children's awareness regarding environmental protection. In order to do it, questionnaire with 10 questions was prepared to conduct the analysis and obtain the relevant data. A survey was conducted among pre-school children and younger primary school children which shows that the children are aware about the problem of environmental protection, namely aware of waste dumping and waste pollution. Their behavior is reflected in waste separation in designated places. There is also awareness of the need for saving water and electricity. Certain answers nevertheless indicate insufficient activity in kindergartens and schools, in terms of maintenance of recycling and other ecological workshops. This analysis showed that there is a need for additional plans and programs in our country in order to promote the environmental protection rise the awareness about the problem related to environmental pollution, from preschools to universities.

It can be noticed that there were no responses in children's free responses regarding the wastewater and water pollution, air pollution due to traffic and industry. This indicates the necessity of expanding theoretical and practical activities that would expand the awareness of children in that segment. Education on the environmental protection should take place throughout the life and should be implemented from the beginning of education, from preschool to higher levels of education including after college education. This could be done through the promotions of activities in environmental protection which need to be carried out continuously.

References

- [1] Grozdinska-Jurzak M, Stepska A, Nieszporek K, Bryda G. 2006. perception of Environmental problems among pre-school children in Poland, *International Research in Geographical and Environmental Education* Vol.15, No.1
- [2] Shobeiri S.M, Alihosseini S.H, Meiboudi H, Saradipour A. 2015. Preschool educators qualifications for environmental education of children in Iran, *Journal of Educational and Management studies*, 5(1):22-26
- [3] Aleksić D, Stepanov J, Čurčić Lj, Štrbac S. 2010. Edukacija o zaštiti životne sredine u predškolskim ustanovama, Šesta regionalna konferencija – Životna sredina ka Evropi EnE10
- [4] Skenderović I, Fetić M. 2014. Uloga ekološkog obrazovanja u zaštiti i unapređenju životne okoline, *Ekonomski izazovi*, Godina 3. broj 5, str.123-134
- [5] Pravilnik o osnovama programa odmora, rekreacije, klimatskog oporavka i nastave u prirodi („Sl.glasnik RS“, broj 52/95)
- [6] Skenderović I, Romelić J. 2013. Zaštita okoline u nastavnim planovima i programima osnovne škole u Republici Srbiji, *Ekonomski izazovi*, Godina 2, broj 3, str. 151-160
- [7] Otto S, Pensini P. 2017. Nature-based environmental education of children: Environmental knowledge and connectedness to nature, together are related to ecological behaviour, *Global Environmental Change* 47 (2017) 88-94
- [8] Jokić D, Marjanović R. 2009. Ekološko obrazovanje u funkciji zaštite životne sredine, 1st International Conference Ecological Safety in Post-Modern Environment, Banja Luka, BiH
- [9] Torkar G. 2014. Learning expiriences that produce environmentally active and informed minds, *NJAS – Wageningen Journal of Life Sciences* 69 (2014) 49-55

BIOACTIVE COMPOUNDS OF PUMPKIN JUICE ASSORTMENTS

Diana Moigradean^{*}, Mariana-Atena Poiana, Liana-Maria Alda, Daniela Stoin,
Antoanela Lena Cozma

*Faculty of Food Engineering, Banat's University of Agricultural Sciences and Veterinary
Medicine „King Michael I of Romania” from Timisoara, Calea Aradului 119, Timisoara,
RO 300645, Romania
e-mail: dimodean@yahoo.com*

Abstract

The purpose of this study was to obtain and characterize of some fresh pumpkin juices with addition of water, walnuts, honey, cinnamon and fresh peppermint leaves. Total soluble content, vitamin C by titration with a 2,6-dichlorophenolindophenol sodium, antioxidant capacity by FRAP assay and total phenolic content by Folin-Ciocalteu method were analyzed. Vitamin C content ranged from 0.09 to 0.15 mg/mL, with 0.13 mg/mL in individual pumpkin juice; the juice assortment without walnuts has the lower vitamin C content. Among the investigated juices, the pumpkin juice assortment with all ingredients have the higher amount total polyphenol content (4.19 mM GAE/mL) and the total antioxidant capacity (2.53 mM Fe²⁺/mL). We observed that the fresh pumpkin juice assortments are a real source of bioactive compounds.

Introduction

Pumpkin (*Cucurbita moschata*) is a species originating in either Central America or northern South America [17]. Pumpkin is highly nutritious and antioxidant-rich vegetable widely grown all over the world. The autumn star, pumpkin is a vegetable that grows for seeds, fruits and flowers. It has a rich content of phenolic compounds and vitamin A and a very low calorie level [9]. It is a rich source of vitamin C that is associated with the prevention of various degenerative, cardiovascular and neurological diseases. It has been used as a medicine in many countries in Central and North America [15]. Pumpkin is poor in taste and carbohydrates but high in antioxidants and it is mixed with fruit or vegetable to improve its nutritional and sensory properties [1]. Pumpkin is a fruit which is healthy and functional, being rich in phenolic compounds, flavonoids and vitamins, and has a low energy [5] showed that a pumpkin-rich diet could reduce blood glucose levels. The World Health Organisation (WHO) estimates that worldwide consumption of fruits and vegetables is only 20–50% of the recommended daily minimum of 400 g per person [16].

Experimental

Juice preparation

The pumpkin fruits and other ingredients were obtained from Timisoara, local markets. Was used linden honey and fresh peppermint leaves. Pumpkin was cut into pieces which were handily peeled and the seeds were discarded. The peeled pumpkin was squeeze immediately using a fruit and vegetable home scale juicer Myria MY4002, then analyzed immediately.

So, were prepared four juice assortments: PJ1 (control sample) - juice prepared of 100 g pumpkin with 100 mL water; PJ2 - juice prepared of 100 g pumpkin with 100 mL water, 10 g walnuts and 1 g honey; PJ3 - juice prepared of 100 g pumpkin with 100 mL water, 1 g honey and three peppermint leaves; PJ4 - juice prepared of 100 g pumpkin with 100 mL water, 10 g walnuts, 1 g honey, 0.5 g cinnamon and three peppermint leaves. Peppermint has a strong sweetish and fresh cooling taste and improves the pumpkin juices taste.

Chemical analysis

The fresh juices were analyzed in terms of total soluble substances (TSS), vitamin C, total antioxidant capacity (TAC) and total phenolic content (TP).

Total soluble substances (TSS) were determined with DR201-95 KRUSS digital handheld refractometer by Carl Zeiss Jena and the results were reported as °Brix at 20°C [2].

The **Vitamin C** evaluation in pumpkin juice has been carried out following 2,6-dichlorophenolindophenol sodium assay [10] and has been measured in pumpkin juices (mg/mL).

For determination the total antioxidant capacity and total phenolic compounds the samples were subjected to alcoholic extraction. So, 1 mL of each juice sample was added to 9 mL ethanol 45% (v/v) and after 1 h the solution was filtered.

The **total antioxidant capacity** (TAC) has been measured by FRAP (ferric reducing antioxidant power) assay (Benzie & Strain, 1996) [3]. 0.5 mL of hydroalcoholic extract diluted in the ratio 1:10 (v/v) in distilled water has been added to 2.5 mL FRAP reagent: 10 mM TPTZ (2,4,6-Tris(2-pyridyl)-s-triazine) solution - diluted in HCl 40 mM, 20 mM $\text{FeCl}_3 \cdot 6\text{H}_2\text{O}$ solution and 300 mM sodium acetate buffer at pH 3.6 in the ratio of 1:1:10. FRAP reagent was prepared freshly. Absorbance was read after 30 minutes at the wavelength of 593 nm using as standard FeSO_4 aqueous solution. Correlation coefficient (r^2) for calibration curve was 0.9890. Total antioxidant capacity was expressed as mM Fe^{2+} /mL.

Total phenolic content (TP) of juice samples were determined by the Folin-Ciocalteu method [14] using gallic acid as a standard for the calibration curve ($r^2 = 0.9980$). Briefly, 0.5 mL of hydroalcoholic extract samples diluted in the ratio 1:10 (v/v) in distilled water was mixed to 2.5 mL of Folin-Ciocalteu reagent diluted 1:10 (v/v) in distilled water. Then, was added 2.0 mL of 7.5% sodium carbonate solution. The results were read at 750 nm after 2 hours with the UV-VIS Spectrophotometer SPECORD 205 by Analytik Jena. The results were calculated and expressed in mM gallic acid equivalent (GAE)/mL.

All determinations were performed in triplicate.

Statistical analysis

Pearson correlation was conducted using Microsoft Office Excel 2010 for Windows.

Results and discussions

The values of some chemical characteristics of pumpkin juice assortments are presented in Table 1.

Table 1. The chemical characteristics of pumpkin juice assortments

Characteristics	Juice			
	PJ1	PJ2	PJ3	PJ4
TSS [°Bx]	11.42	12.54	11.86	14.22
Vitamin C [mg/mL]	0.13	0.15	0.09	0.14
TAC [mM Fe^{2+} /mL]	0.67	2.10	0.42	2.53
TP [mM GAE/mL]	2.57	3.51	2.42	4.19

As shown in Table 1, the highest content of TSS was found in PJ4. It can be seen that the level of TSS content varies directly proportional to the amount of ingredients added to the pumpkin juice, as follows: $\text{PJ4} > \text{PJ2} > \text{PJ3} > \text{PJ1}$. According to Romanian standard [12] the TSS values of juices varies from 5.20 to 11°Bx which is slightly larger than the results obtained in our study. After international standard [6] TSS value range between 10-20°Bx. Vitamin C and beta-carotene are present in abundance in pumpkin and impart high

antioxidant potential to it [9]. Vitamin C is highly sensitive to oxidation and leaching into water-soluble media during vegetables processing [4, 11]. The retention of ascorbic acid is often used as an estimate for the overall nutrient retention of food products [8, 11]. The vitamin C in the juice PJ2 (0.15 mg/mL) and PJ4 (0.14 mg/mL) has values close to those of natural pumpkin juice (0.13 mg/mL) whereas PJ3 show lower values (0.09 mg/mL) than PJ1. This is the only juice assortment that does not contain walnuts; the walnuts (*Juglans regia*) contain very large amounts of vitamin C – 1.3 to 1.7 mg/100g [13].

The phenolic composition of vegetables is dependent on commodity, cultivar, maturity stage and postharvest conditions. Since phenolic compounds are antioxidants, they are subject to oxidation during storage and processing of foods [11]. Phenolic constituents is very important in the plant because of their scavenging ability due to their hydroxyl groups. Phenolic compounds are powerful chain breaking antioxidants and has been reported are associated with antioxidant activity [15]. The content of polyphenols is influenced by the content of ingredients added to the pumpkin juice. The data indicated that the TP of fresh pumpkin juice PJ1 (2.57 mM GAE/mL) decreased to 2.42 mM GAE/mL in PJ3 and increased to 3.51 mM GAE/mL in PJ2 and to 4.19 mM GAE/mL in PJ4.

A similar trend was seen in TAC. FRAP value of PJ1 (0.67 mM Fe²⁺/mL) dropped to 0.42 mM Fe²⁺/mL in PJ3 and increased to 2.10 mM Fe²⁺/mL in PJ2 and to 2.53 mM Fe²⁺/mL in PJ4, as reported in Table 1.

Difference in TAC and TP values is attributed to ingredients mixed in each juice assortments, including walnut. As is known, walnut contains two times more antioxidants than other hard shell nuts [13].

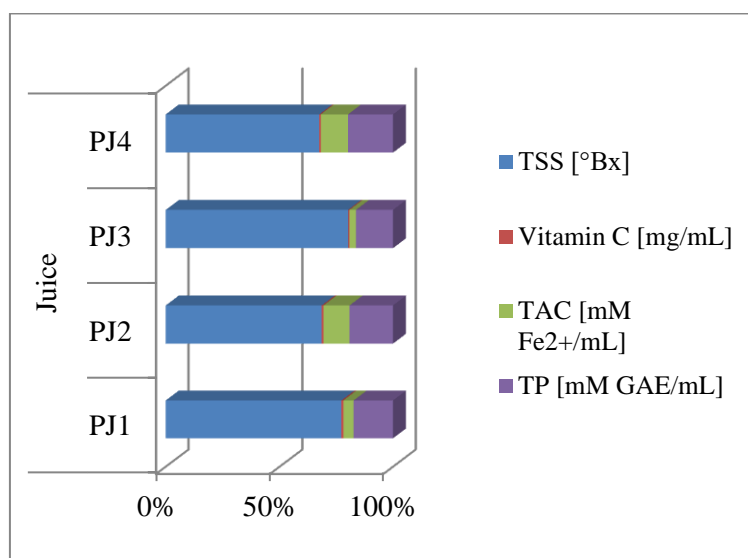


Figure 1. The percentage of chemical characteristics of pumpkin juice assortments

In the graphical representation of Figure 1, the TSS and vitamin C is a major percentage of the chemical characteristics of pumpkin juice assortments.

Full results of the statistical analysis methods used are reported in Table 2. The correlation of all chemical characteristics was positively [7]. Vitamin C are strong correlation with TAC ($r = 0.788$) and TP ($r = 0.716$). TAC has high correlation with TP ($r = 0.985$); it confirms, again, the strongly correlated between this two antioxidant compounds.

Table 2. The Pearson correlation among chemical characteristics of pumpkin juice assortments

	TSS [°Bx]	Vitamin C [mg/mL]	TAC [mM Fe ²⁺ /mL]	TP [mM GAE/mL]
TSS [°Bx]	1			
Vitamin C [mg/mL]	0.450	1		
TAC [mM Fe ²⁺ /mL]	0.881	0.788	1	
TP [mM GAE/mL]	0.943	0.716	0.985	1

Antioxidant activity has been attributed to total phenolic content which have been found to be strongly correlated [11].

Conclusion

The mixed vegetable juice prepared from pumpkin, water, walnuts, honey, cinnamon and peppermint leaves showed a high amount of antioxidant compounds.

I noticed that there is a close correlation between total antioxidant capacity and total phenolic content.

In conclusion, the fresh pumpkin juices are a real source of bioactive compounds.

References

- [1] A.A.M. Abou-Zaid, A.S. Nadir, M.T. Ramadan, J Appl Sci Res. 8 (5) (2012) 2632-2639.
- [2] A.O.A.C. Official Methods of Analysis. 17th Edition of The Association of Official Analytical Chemists. Food Analysis Gaithersburg M D. USA, 2000.
- [3] I.F.F Benzie, L. Strain, Anal Biochem. 239 (1996) 0-76.
- [4] A.A. Franke, L.J. Custer, C. Arakaki, S.P. Murphy, J Food Compos Anal 17 (2004) 1–35
- [5] C.L. Fu, H. Shi, Q.H. Li, Plant Foods Hum. Nutr. 61 (2006) 70-77.
- [6] R. Habib, M. Iqbal, A., LWT. 2(6) (2014) 83-91.
- [7] S. Iqbal, U. Younas, Sirajuddin, W.K. Chan, A.R. Sarfraz, K. Uddin, Int J Mol Sci. 13 (2012) 6651-6664.
- [8] M.A.Murcia, B. Lopez-Ayerra, M. Martinez-Tome, A.M. Vera, F. Garcia-Carmona J Sci Food Agric. 80 (2000) 1882–1886.
- [9] S. Muzzaffar, W.N. Baba, N. Nazir, F.A. Masoodi, M.M. Bhat, R. Bazaz, Cogent Food Agric. 2 (1) (2016), 1163650.
- [10] S.S Nielsen, Food Analysis Laboratory Manual 2010, pp. 55-6.
- [11] J.C. Rickman, D.M. Barrett, C.M. Bruhn, J Sci Food Agric 87 (2007) 930–944.
- [12] Romanian Order no.359/671/137/2002 modified by Order no.416/628/406/2005
- [13] S.M. Sen, T. Karadeniz, Journal of Hygienic Engineering and Design, 11 (2015) 68-71.
- [14] V.L. Singleton, R. Orthofer, R.M. Lamuela-Raventos, Methods Enzimol. 299 (1999) 152-178.
- [15] B.A. Sopan, D.N. Vasantrao, S.B. Ajit, Int J Pharm Sci Res. 5(5) (2014) 1903-1907.
- [16] <http://www.fao.org/ag/magazine/0606sp2.htm>.
- [17] https://en.wikipedia.org/wiki/Cucurbita_moschata.

IDENTIFICATION OF BIOACTIVE COMPOUNDS IN COMFREY ROOT EXTRACTS

Nataša Nastić¹, Jaroslava Švarc-Gajić¹, Antonio Segura-Carretero^{2,3}, Isabel Borrás-Linares³, Jesús Lozano-Sánchez²

¹*Faculty of Technology, University of Novi Sad, Bulevar cara Lazara 1, 21000 Novi Sad, Serbia*

²*Department of Analytical Chemistry, Faculty of Sciences, Avda. Fuentenueva s/n, 18071 Granada, Spain*

³*Functional Food Research and Development Centre (CIDAF), Health Science Technological Park, Avda. del Conocimiento s/n, Bioregion building, 18016 Granada, Spain.
e-mail: natasa.nastic@uns.ac.rs*

Abstract

In the present study bioactive compounds present in comfrey root extracts obtained by supercritical fluid (SFE) and pressurized liquid extraction (PLE) were identified. Chemical characterization of the extracts was carried out by high-performance liquid chromatography coupled to DAD and electrospray-ionization time-of-flight mass spectrometry (HPLC–ESI-TOF-MS) yielding in total of 23 identified compounds. PLE as a fast, green and innovative approach, seems to be the best choice for extracting wide variety of compounds with different polarities within the shortest extraction time being the fatty acids and their derivatives the most abundant. The present study also highlights the potential application of comfrey root extracts as constituents of new added-value formulations.

Introduction

Comfrey (*Symphytum officinale* L.) is a medicinal plant widely spread across Europe, but it can also be found in some parts of Asia and South America. Pyrrolizidine alkaloids in comfrey have been linked to cases of hepatotoxicity and carcinogenicity, and for this reason in traditional medicine comfrey roots are used topically, mostly for the treatment of wounds, joint disorders, and musculoskeletal injuries of all kinds [1,2]. The content of pyrrolizidine alkaloids is the highest in comfrey root [3,4]. Active compounds identified in comfrey root include allantoin, rosmarinic acid and other hydroxycinnamic acid derivatives, mucopolysaccharides, A, B and C vitamins, triterpenoid saponins, tannins, calcium, potassium and selenium [5,6]. Allantoin, as a principal compound identified in comfrey root, activates metabolic processes in subcutaneous tissue and stimulates the cell growth resulting in epithelization. It also strongly promotes the cell growth in bone cells and connective tissue [7].

In the literature only few papers deal with the extraction of bioactive compounds from comfrey root relying mostly on conventional solid/liquid extraction [8-11]. Conventional extraction techniques, however, are quite laborious, time- and solvent-consuming. The issues encountered in conventional extraction approaches can be overcome by application of modern extraction techniques.

In view of the fact that there is limited information available on the detailed chemical composition of comfrey root, present research was focused on the recovery of bioactive compounds using supercritical fluid (SFE) and pressurized liquid extraction (PLE). SFE and PLE have been compared in terms of their selectivity and efficiency to recover bioactive compounds from comfrey root. Major bioactive compounds in comfrey root were identified by high-performance liquid chromatography coupled to electro-spray time-of-flight mass spectrometry.

Experimental

The commercial samples of dry *S. officinale* roots were purchased from local healthy food retail store in Novi Sad, Serbia. The roots were finely grounded and kept at room temperature and darkness until use.

The PLE experiment was performed in a static mode (1500 psi and 20 min as the pressure and extraction time) with 85% ethanol at the temperature of 63°C. The dried comfrey root sample (3 g) was mixed with 6 g of sand and loaded into a stainless-steel extraction cell. After that, the extraction conditions described above were applied and the extract was collected in vials. The residual solvent was evaporated. Dried extract was stored at –20°C and protected from light until analysis.

SFE-CO₂ extraction was performed at 40°C in a dynamic mode with CO₂ plus ethanol (7%) and pressure of 150 bar. For extraction, 5 g of comfrey root powder were mixed with sea sand, placed in the extraction cell and pressurized with CO₂. The total extraction time was established at 120 min for each experiment. The collected extract was concentrated in a water-bath at 40°C using a rotary evaporator. Dried extract was stored at –20°C and protected from light until analysis.

Chemical profile of bioactive compounds from comfrey root extracts was defined using an Agilent 1200-HPLC system (Agilent Technologies, Palo Alto, CA, USA) of the Series Rapid Resolution coupled to an electro-spray time-of-flight mass spectrometer (HPLC-ESI-TOF-MS), previously described by García-Salas et al. [12] with some modifications.

Results and discussion

Comfrey root extracts obtained by SFE and PLE were characterized by means of HPLC–ESI–TOF–MS. The compounds were tentatively identified on the basis of their MS spectra and the molecular formula provided by the software together with data previously reported in literature. The resulting base peak chromatograms of a representative comfrey root extract are presented in Figure 1.

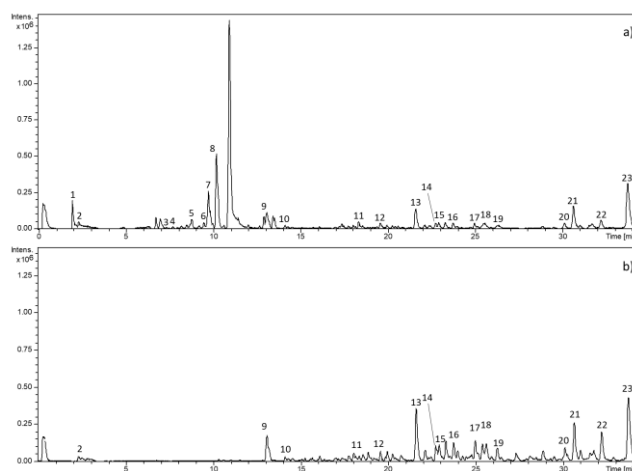


Figure 1. Base Peak chromatogram (BPC) of *S. officinale* root extracts obtained by: a) PLE and b) SFE. Peaks are numbered according to their elution order.

The chromatographic profile of *S. officinale* extract obtained by PLE (Figure 1a) showed the largest number of identified bioactive compounds, while the extract obtained by SFE (Figure 1b) showed the presence of more non-polar compounds as expected. A total of 23 compounds were identified in *S. officinale* root. Identified compounds belonged to different chemical

classes that included organic acids, phenolic compounds (simple phenols and anthraquinones), and fatty acids and derivatives.

Table 1. Characterized compounds in comfrey root extracts obtained by SFE and PLE using HPLC-ESI-TOF-MS.

Peak	Retention time (min)	<i>m/z</i> experimental	<i>m/z</i> calculated	(M-H) ⁻	Proposed compound
1	2.01	377.0873	377.0878	C ₁₈ H ₁₇ O ₉	caffeic acid derivative
2	2.39	191.0195	191.0197	C ₆ H ₇ O ₇	citric acid
3	7.53	137.0234	137.0244	C ₇ H ₅ O ₃	hydroxybenzoic acid
4	7.92	179.0328	179.035	C ₉ H ₇ O ₄	caffeic acid
5	8.72	537.1033	537.1038	C ₂₇ H ₂₁ O ₁₂	salvianolic acid H/I
6	9.52	717.1475	717.1461	C ₃₆ H ₂₉ O ₁₆	salvianolic acid B
7	9.65	311.0562	311.0561	C ₁₇ H ₁₁ O ₆	acetyl-monomethyl-trihydroxy anthraquinone
8	10.23	719.1624	719.1618	C ₃₆ H ₃₁ O ₁₆	sagerinic acid
9	13.09	329.2329	329.2333	C ₁₈ H ₃₃ O ₅	trihydroxy-octadecenoic acid isomer 1
10	13.99	329.2335	329.2333	C ₁₈ H ₃₃ O ₅	trihydroxy-octadecenoic acid isomer 2
11	18.55	311.2222	311.2228	C ₁₈ H ₃₁ O ₄	hydroperoxy-octadecadienoic acid
12	19.57	315.2551	315.2541	C ₁₈ H ₃₅ O ₄	dihydroxystearic acid
13	21.55	295.2283	295.2279	C ₁₈ H ₃₁ O ₃	hydroxy-octadecadienoic acid isomer 1
14	22.63	293.2125	293.2122	C ₁₈ H ₂₉ O ₃	oxo-octadecadienoic acid isomer 1
15	22.84	293.2126	293.2122	C ₁₈ H ₂₉ O ₃	oxo-octadecadienoic acid isomer 2
16	23.78	293.2125	293.2122	C ₁₈ H ₂₉ O ₃	oxo-octadecadienoic acid isomer 3
17	25.12	295.2275	295.2279	C ₁₈ H ₃₁ O ₃	hydroxy-octadecadienoic acid isomer 2
18	25.58	295.2289	295.2279	C ₁₈ H ₃₁ O ₃	hydroxy-octadecadienoic acid isomer 3
19	26.12	295.2271	295.2279	C ₁₈ H ₃₁ O ₃	hydroxy-octadecadienoic acid isomer 4
20	30.06	277.2176	277.2173	C ₁₈ H ₂₉ O ₂	linolenic acid isomer 1
21	30.59	277.2188	277.2173	C ₁₈ H ₂₉ O ₂	linolenic acid isomer 2
22	32.15	253.2177	253.2173	C ₁₆ H ₂₉ O ₂	palmitoleic acid
23	33.68	279.2339	279.233	C ₁₈ H ₃₁ O ₂	linoleic acid

Conclusion

The present study aimed to compare extraction of bioactive compounds from comfrey root using PLE and SFE for recovery of natural constituents with interest in food, pharmaceutical and cosmetic industries. A potent HPLC method coupled to DAD and TOF-MS has been used to characterize comfrey root extracts, allowing identification of 23 compounds. The main compounds detected in the extracts were identified as phenolic acids (mainly sagerinic acid), and fatty acids (especially linolenic and linoleic acid). The application of PLE proved to be more advantageous comparing to SFE allowing extraction of wide variety of compounds with different polarities within the shortest extraction time. The present study also highlights the potential application of *S. officinale* extracts as a source of diverse bioactive compounds to design new functional foods, nutraceuticals and cosmetic products.

Acknowledgements

This work was funded by project TR 31014 financially supported by the Serbian Ministry of Education, Science and Technological Development, the Andalusian Regional Government Council of Innovation and Science (project P11-CTS-7625) and the Spanish Ministry of Economy and Competitiveness (MINECO) (project AGL2015-67995-C3-2). The author IBL gratefully acknowledges the Spanish Ministry of Economy and Competitiveness (MINECO) in association with the European Social Fund (FSE) for the contract PTQ-13-06429 and JLS also thanks the Spanish Ministry of Economy and Competitiveness (MINECO) for the grant IJCI-2015-26789.

References

- [1] C. Weston, B. Cooper, J. Davies, D. Levine, Br. Med. J. Clin. Res. 295 (1987) 183.
- [2] N. Mei, L. Guo, P. Fu, J. Fuscoe, Y. Luan, T. Chen, J. Toxicol. Environ. Health 13 (2010) 509–526.
- [3] C.E. Couet, C. Crews, A.B. Hanley, Nat. Toxins 4 (1996) 163–167.
- [4] N.C. Kim, N.H. Oberlies, D.R. Brine, R.W. Handy, M.C. Wani, M.E. Wall, J. Nat. Prod. 64 (2001) 251–253.
- [5] P. Andres, R. Brenneisen, J.T. Clerc, Planta Med. 55 (1989) 66–67.
- [6] V.U. Ahmad, M. Noorwala, F.V. Mohammad, B. Sener, K. Aftab, Phytochemistry 32 (1993) 1003–1006.
- [7] R. Dennis, C. Dezelak, J. Grime, Acta Pharm. Hung. 57 (1987) 267–274.
- [8] G.P. Roman, E. Neagu, V. Moroeanu, G.L. Radu, Rom. Biotech. Lett. 13 (2008) 4008–4013.
- [9] I. Tahirovic, Z. Rimpapa, S. Cavar, S. Huseinovic, S. Muradic, M. Salihovic, E. Sofic, Planta Med. 76 (2010) 1265.
- [10] G. Paun, E. Neagu, S.C. Litescu, P. Rotinberg, G.L. Radu, J. Serb. Chem. Soc. 77 (2012) 1191–1203.
- [11] V. Savić, S. Savić, V. Nikolić, Lj. Nikolić, S. Najman, J. Lazarević, A. Đorđević, Hem. Ind. 69 (2014) 1–8.
- [12] P. García-Salas, A.M. Gómez-Caravaca, D. Arráez-Román, A. Segura-Carretero, E. Guerra-Hernández, B. García-Villanova, A. Fernández-Gutiérrez, Food Chem. 141 (2013) 869–878.

INFLUENCE OF PHOSPHORUS AND NITRATES ON THE SPECIES DEVELOPMENT OF *LEMNA MINOR* L.

Dorian-Gabriel Neidoni, Valeria Nicorescu, Ladislau Andres, Monica Ihos, Mihaela Dragalina, Iuliana Iordache, Izabela Siminic, Sorina-Claudia Negrea, Lidia Ani Diaconu

*National Research and Development Institute for Industrial Ecology- ECOIND
Timisoara Subsidiary, 115 Bujorilor Str., 300431, Timisoara, Romania
e-mail: neidoni_dorian94@yahoo.com*

Abstract

In this paper we wanted to determine the influence of phosphorus and nitrates in the development of *Lemna minor* L. To achieve this purpose, eight different growth variants were proposed, starting from the Hoagland culture medium, where the concentration of these two compounds varied. The growth rate in the eight experimental variants, ranges between 150% - 325%, with a minimum in the control sample and a maximum at the highest concentration of phosphorus in water.

Introduction

Duckweed (*Lemna minor* L.) is a widespread aquatic plant located in lakes, rivers, ponds and other bodies of water [1]. *L. minor* L. belongs to the family Araceae [2], being an aquatic (submerged) plant with free (floating) root, consisting of small leaves. The size of the leaves is between 0.5-1.0 cm and the root length is about 3.0-4.0 cm.

This plant has been reported in numerous phytoremediation studies to remove pesticides and heavy metals from water [3, 4] and it is therefore important to determine the optimum conditions for plant growth in order to ensure the plant material needed for these studies.

Aquatic plants absorb the organic and inorganic nutrients dissolved in the water column and these can be exhausted to the extent that the growth of aquatic plants is limited by nutrients [5]. Nitrogen compounds, including nitrates, along with phosphorus, are among the most important nutrients in crops, and are limiting factors in ontogenetic plant development.

Low levels of phosphate limit plant growth in both land and aquatic systems [6], however, excess nitrogen compounds and excess phosphorus in an aquatic environment stimulate excessive production of algae and phytoplankton, which leads to eutrophication [7, 8], therefore it is imperative to know and adapt the amounts of nutrients used in the growth of aquatic plants.

Experimental

Vegetal material and plant development variants

The plants were collected from a natural environment between March and April and were transferred to the laboratory, where they were thoroughly washed with distilled water to remove impurities, and then introduced into the Hoagland's culture medium, described by Cowgill & Milazzo in 1989 [9]. The Hoagland's culture medium is described in tables 1 and 2.

Table 1. Hoagland's culture medium preparation

Composition	Preparation stock solution	Quantity used
1. $\text{MgSO}_4 \cdot 7\text{H}_2\text{O}$	24.6 g/100 mL	1.0 ml/L
2. $\text{Ca}(\text{NO}_3)_2 \cdot 4\text{H}_2\text{O}$	23.6 g/100 mL	2.3 ml/L
3. KH_2PO_4	13.6 g/100 mL	0.5 ml/L
4. KNO_3	10.1 g/100 mL	2.5 ml/L
5. Micronutrients	See below (table 2)	0.5 ml/L

Table 2. Preparation of micronutrients solution

H_3BO_3	2.86 g/L
$\text{MnCl}_2 \cdot 4\text{H}_2\text{O}$	1.82 g/L
$\text{ZnSO}_4 \cdot 7\text{H}_2\text{O}$	0.22 g/L
$\text{Na}_2\text{MoO}_4 \cdot 2\text{H}_2\text{O}$	0.09 g/L
$\text{CuSO}_4 \cdot 5\text{H}_2\text{O}$	0.09 g/L

Experiments were performed on eight lot, using different reagent quantities (to determine the influence of nitrates and phosphorus on plant growth), presented in the Hoagland's culture medium, as follows: Lot 1: culture medium in which the phosphorus concentration was varied by the addition of 0.25 mL of dihydrogen phosphate; Lot 2: culture medium in which the phosphorus concentration was varied by the addition of 0.75 mL of dihydrogen phosphate; Lot 3: culture medium in which the phosphorus concentration was varied by the addition of 1.00 mL of dihydrogen phosphate; Lot 4: culture medium in which the nitrate concentration was varied by the addition of 1.20 mL of calcium nitrate and 1.25 mL of potassium nitrate; Lot 5: culture medium in which the nitrate concentration was varied by the addition of 3.5 mL of calcium nitrate and 3.75 mL of potassium nitrate; Lot 6: culture medium in which the nitrate concentration was varied by the addition of 4.6 mL of calcium nitrate and 5 mL of potassium nitrate; Lot 7: Hoagland's culture medium, according to tables 1 and 2; Lot 8: control sample. For the control sample, water from the natural environment (pond water) where the plants was harvested, was used.

Experimental conditions

Approximately 4 grams of plants were placed in plastic containers containing one of the growth variants shown above of size $L \times l \times h = 20 \times 16 \times 6$ cm. The experimental duration was 7 days at a temperature between 19°C - 25°C and a day / night cycle of 15/9. The culture media described in the above lots, was renewed on day 4 to support the growth rate and to compensate the deficiency of water compounds, vital compounds in plant growth. The plants were placed in the laboratory at the window leve, exposed directly to sunlight.

Calculating the growth rate of plants

Growth rate is the degree of growth and development of plants, over a period of time. The growth rate is calculated according to the initial plant weight used and the weight of the plants at the end of the experiments. The resulting value is expressed as a percentage (%).

$$\text{Growth rate}(\%) = \frac{\text{final biomass} - \text{initial biomass}}{\text{initial biomass}} \times 100$$

Results and discussion

All experiments data, presented in the present paper represent the average of three samples. In the following tables, the growth and development of plants at different concentrations of macro-nutrients and in particular of phosphorus and nitrogen compounds was pursued.

Interpreting the tables below, it can be observed the decisive influence of phosphorus on the rate of plant growth. The baseline recipe shows a 275% plant growth in the presence of 16 mg/L phosphorus and 369 mg/L nitrated in water (lot 7). Comparing lots 1, 2, 3 and 7, in which the phosphorus concentration in water varied (the rest of the elements remained approximately unchanged), the highest increase was found in lot 3 (at the highest concentration of phosphorus: 26.0 mg/L), the increase being 325%.

For lots 4, 5, 6 and 7 in which the nitrate concentration varied (the rest of the elements remained approximately unchanged), it can be said that their influence in the water is quite small, the growth rates being in the range of 200-275% with a maximum increase in the nitrate concentration in water of 369 mg/L. The lowest values of the growth rate (200% - lot 5 and 225% - lot 6) are observed at 644 mg/L and 846 mg/L nitrate respectively, whereby high concentrations of nitrates inhibit ontogenetic development of plants.

The control sample (lot 8), differs from the rest of the growth variants by the lowest proliferation of plants, with a growth rate of only 150%, demonstrating the influence and importance of micro and macro-nutrients and, in particular, of phosphorus compounds and nitrogen for an accelerated development of aquatic plants, especially *Lemna minor* L.

Table 1. Modified culture medium (with 0.25 mL dihydrogen phosphate) (lot 1)

pH	Phosphorus (mg/L)	Ammonium (mg/L)	Nitrates (mg/L)	Nitrites (mg/L)	Initial weight (g)	Final weight (g)
8,2	8,00	0,247	412	0,096	4	11
Growth rate (%)=175						

Table 2. Modified culture medium (with 0.75 mL of dihydrogen phosphate) (lot 2)

pH	Phosphorus (mg/L)	Ammonium (mg/L)	Nitrates (mg/L)	Nitrites (mg/L)	Initial weight (g)	Final weight (g)
7,9	22,0	0,241	388	0,080	4	15
Growth rate (%)= 275						

Table 3. Modified culture medium (with 1 mL dihydrogen phosphate) (lot 3)

pH	Phosphorus (mg/L)	Ammonium (mg/L)	Nitrates (mg/L)	Nitrites (mg/L)	Initial weight (g)	Final weight (g)
7,8	26,0	0,223	370	0,094	4	17
Growth rate (%)= 325						

Regarding the influence of pH on plant growth (in the above mentioned variants, a pH between 6.6-8.8 was determined), this is not a limiting factor according to the literature, in which many authors reported that the duckweed species resist at a wide range of pH, within the range 3.5-10 [4].

Table 4. Modified culture medium (with 1.2 mL of calcium nitrate and 1.25 mL of potassium nitrate) (lot 4)

pH	Phosphorus (mg/L)	Ammonium (mg/L)	Nitrates (mg/L)	Nitrites (mg/L)	Initial weight (g)	Final weight (g)
8,1	14,0	0,226	203	0,065	4	14
Growth rate (%)=250						

Table 5. Modified culture medium (with 3.5 mL of calcium nitrate and 3.75 mL of potassium nitrate) (lot 5)

pH	Phosphorus (mg/L)	Ammonium (mg/L)	Nitrates (mg/L)	Nitrites (mg/L)	Initial weight (g)	Final weight (g)
8,0	15,0	0,201	644	0,262	4	12
Growth rate (%)=200						

Table 6. Modified culture medium (with 4.6 mL of calcium nitrate and 5 mL of potassium nitrate) (lot 6)

pH	Phosphorus (mg/L)	Ammonium (mg/L)	Nitrates (mg/L)	Nitrites (mg/L)	Initial weight (g)	Final weight (g)
7,9	16,0	0,196	846	0,116	4	13
Growth rate (%)= 225						

Table 7. Hoagland's culture medium (lot 7)

pH	Phosphorus (mg/L)	Ammonium (mg/L)	Nitrates (mg/L)	Nitrites (mg/L)	Initial weight (g)	Final weight (g)
6,6	16,0	<0,025	369	<0,024	4	15
Growth rate (%)= 275						

Table 8. Control sample - pond water (lot 8)

pH	Phosphorus (mg/L)	Ammonium (mg/L)	Nitrates (mg/L)	Nitrites (mg/L)	Initial weight (g)	Final weight (g)
8,8	<0,017	<0,025	<0,074	<0,024	4	10
Growth rate (%)= 150						

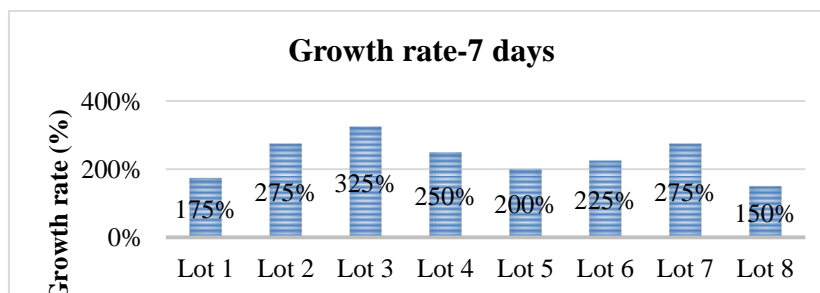


Figure 1. Synthetic presentation of growth rates after 7 days

Figure 1 shows the growth of the plant *Lemna minor* L., from which we can see that the greatest development of the plants we have in the lot number 3, and the lowest in the lot with number 8, the latter being control sample.

For the highest growth rates, ranging from 275% to 325%, the optimal conditions for growth/development of *Lemna minor* L. in terms of nutrient content in water are defined (Table 9).

Table 9. Optimum conditions for the development of the *Lemna minor* L. plant, in terms of nutrient content

pH	Phosphorus (mg/L)	Ammonium (mg/L)	Nitrates (mg/L)	Nitrites (mg/L)
6,6 - 7,9	16,0 -26,0	0,025- 0,241	approx. 369	0,024 -0,094

Conclusion

In experiments on the variation of the phosphorus concentration in water, it can be seen that the highest proliferation of the plant, of 325%, is in the presence of phosphorus concentration in the water of 26.0 mg/L.

In experiments in which nitrate concentration varied, we can mention that the maximum growth rate (275%) is observed at water nitrate concentrations of 369 mg/L.

High concentrations of phosphorus lead to plant proliferation, while high concentrations of nitrates inhibit their growth.

In the presented above, it is found that the greatest influence on the growth rate of *Lemna minor* L. is phosphorus, followed by nitrogen compounds, from where it results, in studies in which multiplication of the plant is desired, this aspect must be taken into account.

Acknowledgements

This work was carried out within the framework of a “Nucleu” Program, managed by The Romanian Ministry of Research and Innovation, project ELFIT, code PN 18 05 03 02

References

- [1] Q. Lu, T. Zhang, W. Zhang, C. Su, Y. Yang, D. Hu, Q. Xu, Ecotoxicol. Environ. Saf. 147 (2018) 500
- [2] <http://www.iucnredlist.org/details/164057/0>
- [3] N. Dirilgen, Ecotoxicol. Environ. Saf. 74 (2011) 48
- [4] R. Verma, S. Suthar, AEJ, 54 (2015) 1297
- [5] C. Angove, A. Norkko, C. Gustafsson, J. Exp. Mar. Biol. Ecol. 507 (2018) 23
- [6] M. Tarrago, M. Garcia-Valles, S. Martínez, D.R. Neuville, J. Environ. Manage. 220 (2018) 54
- [7] Md. Eshrat E. Alahi, S.C. Mukhopadhyay, Sens. Actuators, A 280 (2018) 210
- [8] K. Lin, J. Pei, P. Li, J. Ma, Q. Li, D. Yuan, Talanta. 185 (2018) 419
- [9] U.M. Cowgill, D.P. Milazzo, in: U.M. Cowgill, L.R. Williams (Eds.), The culturing and testing of two species of duckweed, American Society for Testing and materials, Philadelphia, 1989, pp. 379

CHITOSAN FOR FUNGAL DISEASES CONTROL

Ileana Nichita^{1*}, Aurelia Visa², Adriana Popa², Diana Obistioiu¹, Valentin Radu Gros¹

¹ „Banat” University of Agricultural Science and Veterinary Medicine, 119 Calea Aradului, 30465, Timisoara, Romania,

² Institute of Chemistry Timisoara of Romanian Academy, 24 Mihai Viteazul Blv., 300223 Timisoara, Romania,

E-mail: nichita_ileana@yahoo.com; apopa_ro@yahoo.com

Abstract

The use of chitosan is a promising alternative; it can be applied in many fields based on its biological activity and easy-to-obtain procedures. Such it was used in agriculture, environmental protection, pharmaceutical and biomedical applications. The fungicidal activity of the chitosan against *Fusarium graminearum*, *Penicillium chrysogenum* and *Aspergillus orizae* were done by using the plate growth rate method.

Key words: chitosan, fungicidal activity

Introduction

Chitosan; a linear polysaccharide is the second most abundant polysaccharide found in nature after cellulose. Chitosan has been found to be non-toxic, biodegradable, biofunctional, biocompatible and was reported by several researchers to have strong antimicrobial and antifungal activities [1, 2].

Chitosan possesses three types of reactive functional groups: an amino group at the C-2 position of each deacetylated unit, as well as primary and secondary hydroxyl groups at the C-6 and C-3 positions, respectively, of each repeat unit (Figure 1) [3].

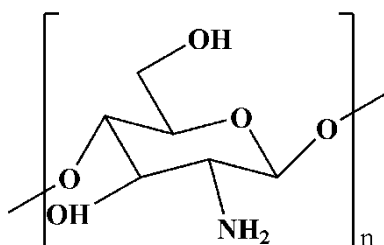


Figure 1. The structure of chitosan

Fresh vegetables and fruits with good quality have benefits for the health of human body due to their good flavor, and the contents in nutrients [4]. The safety of vegetables and fruits is related to its high decay rate and short shelf life period. The rot of vegetables and fruits could be observed because the loss of nutrients and the infection of microorganism during storage. Chitosan can inhibit several plant diseases because it has a fungicidal effect against various fungi. The article demonstrates that the aqueous acid solutions of chitosan presented fungicidal activity against different fungi species as follow: *Fusarium graminearum* - ATCC 46779m, *Penicillium chrysogenum* ATCC 9179 and *Aspergillus orizae* ATCC 10124.

Material and Methods

The chitosan solution was prepared in 2 % (v/v) acetic solution acid. This solution has been preserved at 37°C to maintain its fluidity. The solution of chitosan was prepared by weighing 0.5 grams of low molecular weight chitosan and adding to 100 ml of 2% acetic acid solution (2 ml of glacial acetic acid was added to 98 ml of distilled water).

The Erlenmayer containing the solution of chitosan acetic acid was sonicated for 2 hours for the complete dissolution of chitosan.

The antifungal activity of this chitosan acid aqueous solution was tested on strains of different fungi species as follow: *Fusarium graminearum* - ATCC 46779m, *Penicillium chrysogenum* ATCC 9179 and *Aspergillus orizae* ATCC 10124.

These standard fungi cultures were maintained in laboratory conditions, at 4°C, in tubes with yeast glucose agar (CYGA). From these species were obtained active cultures by inoculation on Petri dishes with melted chloramphenicol yeast glucose agar (CYGA). Antifungal tests against *Fusarium graminearum* (ATCC 46779m), *Penicillium chrysogenum* (ATCC 9179) and *Aspergillus orizae* (ATCC 10124) were performed by using the plate growth rate method [5-7].

Into each Petri plate was aseptically introduced 1 ml from the chitosan acid aqueous solution and after was added 15 ml of chloramphenicol yeast glucose agar (CYGA). The content of Petri plates was gently swirled to achieve uniform mixing of the content. The final concentration of the chitosan in each Petri plates was 0.33%. In the control plates was poured only 15 ml of chloramphenicol yeast glucose agar. After the solidification of the media discs with 5 mm diameter were extracted. Also inoculum discs of the test fungus species were obtained from the original cultures and these were inoculated on the solidified media.

In each plate were inoculated three inoculum discs. The plates were incubated at $25 \pm 2^\circ\text{C}$ and after seven days the radial growth of mycelium was measured. The results were compared with negative control. The mean of three readings was taken for calculations using equation:

Antifungal activity (%) = $(D_c - D_s) / D_c \times 100$; [5]

Where: D_c is the diameter of growth in control plate and D_s is the diameter of growth in the plate containing tested antifungal agent

Results and discussion

The FTIR spectra of chitosan is presented in Figure 1.

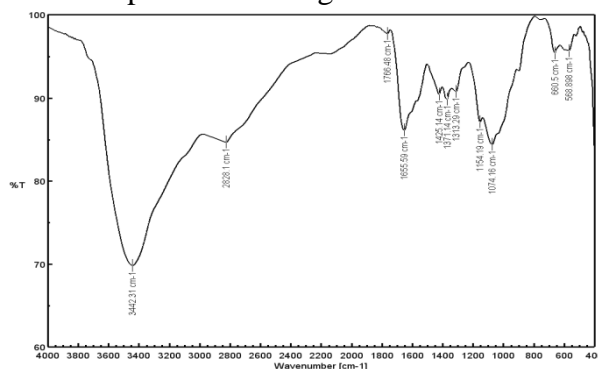


Figure 2. FTIR spectrum of Chitosan

The FTIR spectra shows characteristic absorption bands at approximately 1666 has been assigned as the $-\text{NH}$ bending of NH_2 group and at 3442 cm^{-1} has been assigned as the hydroxyl group. At 1371 cm^{-1} has been assigned as amide band. The skeletal vibrations involving the C-O-C stretching band was observed at 1074 cm^{-1} .

In the present article the elemental composition of chitosan was confirmed by energy dispersive analysis of X-rays (EDAX), see Figure 3.

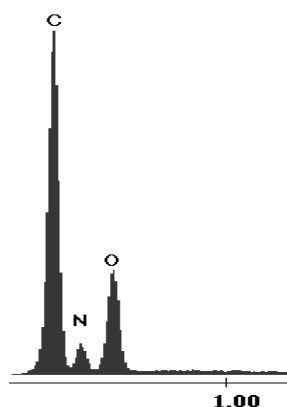


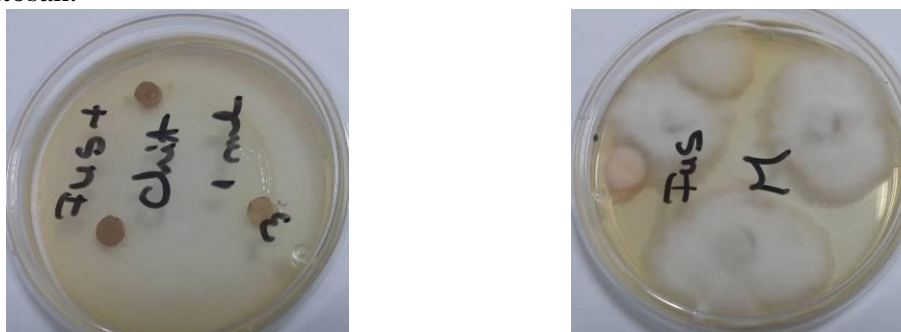
Figure 3. EDAX image for Chitosan

The results of the chitosan acid aqueous solutions on the fungi species tested are presented in Table 1.

Table 1. Antifungal activity of chitosan acid aqueous solution

Fungi specie	Diameter of grow (mm)								Antifungal activity (%)
	Control				Chitosan				
	1	2	3	M	1	2	3	M	
<i>Fusarium graminearum</i>	48	40	35	41	0	0	0	0	100
<i>Penicillium chrysogenum</i>	18	20	20	19.3	0	0	0	0	100
<i>Aspergillus orizae</i>	20	20	20	20	0	0	0	0	100

The efficacy of chitosan acid aqueous solution was 100% against all the fungi species tested. In Figure 4 are presented results with *Fusarium graminearum* of control sample (M) and sample with chitosan.


Figure 4. Images of the *Fusarium graminearum* (sample M and sample with chitosan)

Our results could be compared with others studies but there are not uniformity between these results due to different types of chitosan tested [8].

The effect of chitosan on fungal cell walls is dependant on the concentration, degree of acetylation and the pH. In a study on cultures of *Rizhopus solani* was observed that the fungus germination decreased with increasing the chitosan concentration in the medium. When the inhibition process occurs, the medium became alkaline and this reduces the effectiveness of the chitosan [9].

Inhibition rate in order of 80% against plant fungus such as *Phomopsis asparagi* and as high as 95% against *Fusarium oxysporum*, *Cucumernum owen*, *Rhizoctonia solani* and *Fusarium oxysporum* have been, however, known to occur with low chitosan concentration (20-150 mgL⁻¹) [10].

The inhibitory effect of chitosan depends also on the type of solvent. The best effect had chitosan dissolved in lactic acid compared to dissolve in formic acid and acetic acid [11].

Conclusion

The article shows the results of fungicidal activity of aqueous acid solutions of chitosan. This acid aqueous solution of chitosan had a good fungicidal activity against all the fungi species tested. Procedure of using of the aqueous acid solutions of chitosan as biopesticides is very effective and eco-friendly for the reason that, it is no-toxic, biodegradable and biocompatible. Much of study is still to be done in the field of biochemical mode of action of chitosan against fungi.

References

1. Jo, C., Lee, J. W., Lee, K. H., & Byun, M. W., Quality properties of pork sausage prepared with water-soluble chitosan oligomer. *Meat Science*, 2001, 59(4), 369–375.
2. Mohammed Aider, Chitosan application for active bio-based films production and potential in the food industry: Review, *LWT - Food Science and Technology* 2010, 43, 837–842.
3. Hafdani N., Sadeghinia N., A Review on Application of Chitosan as a Natural Antimicrobial *International Journal of Medical, Health, Biomedical, Bioengineering and Pharmaceutical Engineering* Vol:5, No:2, 2011, 46-50
4. Yage Xing, Qinglian Xu, Xingchen Li, Cunkun Chen, Li Ma, Shaohua Li, Zhenming Che, and Hongbin Lin, Chitosan-Based Coating with Antimicrobial Agents: Preparation, Property, Mechanism, and Application Effectiveness on Fruits and Vegetables, *International Journal of Polymer Science*, 2016, Article ID 4851730, 24 pages, <http://dx.doi.org/10.1155/2016/4851730>
5. Zhaoqian.F. , Yukun.Q., Song. L., Ronge. X., Huahua. Y., Xiaolin. C., Kecheng. L., Pengcheng. L., Synthesis, characterization, and antifungal evaluation of diethoxyphosphoryl polyaminoethyl chitosan derivatives, *Carbohydrate Polymers*, 2018, 190(15):1-11. doi.org/10.1016/j.carbpol.2018.02.056
6. xxx- Clinical Laboratory Standards Institute. 2006. Performance standards for antimicrobial disk susceptibility tests; Approved standard—9th ed. CLSI document M2-A9.26:1. Clinical Laboratory Standards Institute, Wayne, PA
7. Nichita, I., Popa, A., Tarziu, E., Gros, R.V., Seres, M., Sala, C., Studies on antimicrobial activity of aqueous acids solutions of chitosan. *Proceedings of the 21st International Symposium on Analytical and Environmental Problems*, 2015, 244-246
8. Balicka-Ramisz A., Wojtasz-Pajak B., Pilarczyk A., Ramisz L.L.. Antibacterial and antifungal activity of chitosan, 12th ISAH Congress on Animal Hygiene, Warsaw, 2005, 406
9. Goy R.C., Britto D., Assis O.B.G., A Review of the Antimicrobial Activity of Chitosan, *Polímeros: Ciência e Tecnologia*, 2009, 19(3), 241-247.
10. Zhang C., Ping Q., Zhang H., Shen J., Synthesis and characterization of water soluble O-succinyl chitosan. *European Polymer Journal*, 2003,39, 1629-1634.
11. Li Y.C., Sun X.J., Bi Y. , Ge Y.H., Wang Y., Antifungal activity of Chitosan on *Fusarium sulphureum* in relation to dry rot of potato tuber, *Agricultural Sciences China*, 2009, 8, 597-604.

ASSESSMENT OF WATER QUALITY FOR IRRIGATION IN THE AREA OF POMORAVLJE DISTRICT

Radmila Pivić¹, Aleksandra Stanojković-Sebić¹, Zoran Dinić¹, Magdalena Knežević¹, Jelena Maksimović¹

¹*Institute of Soil Science, Belgrade, Teodora Dradžera 7, Serbia
e-mail: drradmila@pivic.com*

Abstract

The assessment of the quality of water for irrigation in the Republic of Serbia is carried out using the traditional classifications by Stebler, Neiggebauer and the classification of the US Laboratory for saline soils and by the more recent FAO and RSC classifications. In twenty selected locations in the area of Pomoravlje area in 2016, samples of irrigation water were sampled within the existing irrigation systems or at the locations of agricultural areas where the installation of irrigation systems is planned.

The following parameters were analyzed in the samples: pH value-potentiometric; EC-electroconductivity-electrochemical; dry residue-thermogravimetric; ionic balance: CO_3^{2-} ; HCO_3^- ; Cl^- -volumetric. The acid-available fraction of heavy metals and other microelements (As, B, Cd, Cr, Cu, Fe, Ni, Pb, Zn) and SO_4^{2-} ; Ca^{2+} ; Mg^{2+} preparation and reading on the ICP-OES method EPA 200.7; Content K^+ , Na^+ -plamenphotometric; SAR (Sodium Adsorption Ratio)-calculating. The above analyzes were carried out to evaluate the above classifications. In all tested samples, the content of heavy metals and the tested microelements was within the limits of maximum permissible concentrations. Modern classifications require more detailed analysis of the chemical properties of the tested parameters than traditional ones, while they provide a more complex approach to the assessment of the usability of water and they should have priority in the application.

Key words: Irrigation, water, quality, classifications

Introduction

The sustainability of water resources depends to a large extent on the proper management and efficient use of available water resources. The testing of groundwater quality has become indispensable especially in developing countries where there is a growing shortage of surface waters [8]. In addition to the basic purpose, which allows the survival of life on earth, the use of water for agricultural purposes, primarily irrigation, is certainly invaluable. Irrigation aims to meet the ever-growing needs for food due to population growth [1]. Given that in many areas of the world [11] without irrigation, agricultural production would not be possible, it is necessary to pay special attention to the available water resources both on quantity and on their quality. Inadequate water quality for irrigation can significantly reduce the expected economic yield of agricultural production [4, 19]. Water quality is a element used to describe the physical, chemical and biological parameters of water characteristics and defines the suitability for a specific purpose and used in the decision-making process [7]. Water of inadequate quality can affect the salinization, alkalization and deterioration of water-physical soil properties. It is very important to estimate the risk of salinization of springs for irrigation of any agricultural area in order to maximize the yield of cultivated crops [18]. There are traditional and modern methods and classifications for assessing the quality of water for irrigation. None of them can be considered absolutely applicable to all conditions in plant production [16].

Description of the field of research and methodology of sampling

The Pomoravlje Administrative District, where research was conducted in 2016, ranges from 43°43'-44°19's north latitude and from 20° to 21°50's east longitude. The irrigation water sampling site coordinates are presented together with results of the analyzes in Table 1. At the sites where research was conducted, the drip irrigation system is applied at nine locations; in eight places plants are irrigated by artificial rain, and within the three parcels it is planned to use some of the irrigation methods in the following period. Water samples used for irrigation were taken from the well at eighteen locations, while from natural sources, river, water were sampled at two locations. Sampling was conducted in accordance with the procedure documented in the professional literature.

Research methods

In the irrigation water samples, the following parameters are determined: pH-potentiometric (SRPS H.Z1.111: 1987) [12], electrical conductivity (EC) - (SRPS EN 27888: 1993) - electrometric [5]; the total dissolved solids content (TDS) - gravimetric [9]; CO_3^{2-} ; HCO_3^- ; Cl^- - volumetric, K^+ ; Na^+ - plamenfotometric (APHA) [2]. The content of heavy metals and other toxic elements (As, B, Cd, Cr, Cu, Fe, Ni, Pb, Zn) and SO_4^{2-} ; Ca^{2+} ; Mg^{2+} are determined by EPA method 200.7, [13] on the ICAP 6300 ICP optical emission spectrometer (ICP-OES); (SAR) - calculating [17].

Results and discussion

In relation to the Stebler classification, based on the estimation of the irrigation coefficient determined by the content of Na^+ , Cl^- , SO_4^{2-} , all the tested irrigation water samples are of good quality, which means that it can be used without special measures to prevent the accumulation of harmful salts in the soil. Based on the Neiggebauer classification [14], which takes into account the total amount of salt in irrigation water in interaction with the concentration of Na^+ with Ca^{2+} and Mg^{2+} , the tested samples, 88.5% belong to the Ia class, in which the dry residue is smaller of 700 mg l^{-1} , and the ratio $(\text{Ca} + \text{Mg}) : (\text{Na} + \text{K})$ is > 3 and 11.5%, Ib class, where the dry residue is less than 700 mg l^{-1} , and the ratio $(\text{Ca} + \text{Mg}) : (\text{Na} + \text{K})$ is > 3 . These are impeccable water with ameliorative characteristics of flushing salt marsh.

Experts from the University of Riverside, USA [6] made the largest contribution to the study of irrigation water quality and its classification as regards the benefits of irrigation of agricultural crops, and it is applied worldwide. The basis for assessing the method is EC and SAR. In the tested water samples for irrigation, the C1-S1 class belongs to 7.7% of the tested samples with characteristic that $\text{EC} \leq 0.250 \text{ dS m}^{-1}$; SAR 0-10. These are waters where there is a small risk of dredging / alkalization, or water suitable for irrigation. 69.2% of the tested samples belong to the Class C2-S1 class of water, in which the EC values range from 0.250 to 0.750 dS m^{-1} and can be used for irrigation of plants with a mean salt tolerance. The remaining 23.1% of the tested samples belongs to the class C3-S1, in which the EC values range from 0.750 to 2.250 dS m^{-1} , and their use requires the application of special measures in the prevention of soil depletion.

Modified FAO classification [3], analyzes in detail the influence of dissolved salt in irrigation water and its impact on the water-physical properties of the soil, primarily on infiltration. It takes into account the risk of sedimentation, based on the amount of electrical conductivity (EC) and salt concentration in the test sample (TDS).

Table 1 shows the values of the parameters on the basis of which the irrigation water samples were estimated in relation to the above classification. It was found that 65.4% of the samples belong to the class of drinking water and irrigation ($\text{EC} < 0.7 \text{ dS m}^{-1}$, $\text{TDS} < 500 \text{ mg l}^{-1}$) and 34.6% water class for irrigation ($\text{EC}: 0.7\text{-}2 \text{ dS m}^{-1}$; $\text{TDS} 500\text{-}1500 \text{ mg l}^{-1}$). An additional estimate using the possible influence of some elements dissolved in irrigation water,

analyzing Na^+ effects through different relationships with other tested substances (Na_2CO_3) was determined on the basis of the RSC-Residual Sodium Carbonate classification [10]. Based on this classification, 92.3% of the tested irrigation water samples belong to the class of good water ($\text{RSC} < 1.25$) and 7.7% water class at the usability limit ($\text{RSC} = 1.25\text{--}2.50$).

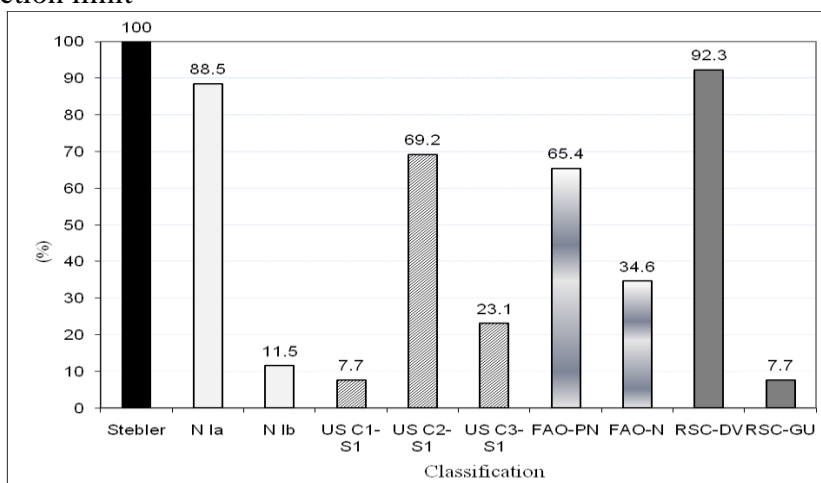
The obtained values of the content of the studied microelements and heavy metals are presented in Table 1. The interpretation was prepared on the basis of the limit values in the Ordinance on the permitted quantities of hazardous and harmful substances in soil and irrigation water [15] and by the data from literature [3] (*).

The content of trace elements and heavy metals in irrigation water samples in all tested irrigation water samples was below the maximum permissible concentration (MAC).

Table 1. Chemical and physical properties of water samples for irrigation

N°	Coordinate		pH	EC (dSm^{-1})	TDS (mg l^{-1})	SAR (mg l^{-1})	As	B	Cd	Cr	Cu	Fe	Ni	Pb	Zn
	X	Y													
1	518133	4867123	7.00	0.99	850	0.58	bdl	0.0772	bdl	0.001	0.006	0.0544	0.0021	0.0013	0.0198
2	522588	4868034	7.10	0.72	550	0.37	bdl	bdl	bdl	0.0047	0.0068	bdl	0.0026	bdl	0.3372
3	507682	4855615	7.50	0.56	500	0.37	bdl	bdl	bdl	0.0013	0.0126	bdl	0.0001	0.0012	0.141
4	519887	4866458	7.30	0.85	640	0.42	bdl	bdl	bdl	0.0254	0.0599	bdl	bdl	0.0078	0.0544
5	510021	4854678	7.40	0.57	570	0.58	bdl	0.0128	bdl	0.0019	0.0058	bdl	0.009	0.0023	bdl
6	529462	4867180	8.10	0.63	480	0.52	bdl	0.0213	bdl	0.0008	0.0072	bdl	0.0007	bdl	bdl
7	509624	4856500	8.40	1.12	920	0.48	bdl	0.0939	bdl	0.0038	0.0101	bdl	0.0053	0.0047	0.0044
8	532709	4861037	7.20	0.68	450	0.47	bdl	bdl	bdl	0.0015	0.0052	bdl	bdl	0.0051	0.0269
9	533345	4868033	7.10	1.4	110	0.63	bdl	bdl	bdl	0.0017	0.0059	bdl	0.0003	0.0003	bdl
10	532788	4870253	7.10	1.12	120	0.45	bdl	bdl	bdl	0.0139	0.0311	bdl	0.0047	0.0038	0.0401
11	542816	4881028	7.25	0.54	360	0.65	bdl	bdl	bdl	0.0005	0.0204	bdl	0.0404	0.0022	0.5134
12	542482	4883901	7.15	0.42	330	0.69	bdl	bdl	bdl	0.001	0.0121	bdl	bdl	0.0059	0.017
13	530215	4887712	7.20	0.21	180	0.45	bdl	bdl	bdl	0.0013	0.0069	bdl	bdl	bdl	bdl
14	528908	4886074	7.50	0.52	410	0.95	bdl	bdl	bdl	0.0008	0.0073	bdl	bdl	0.0046	bdl
15	515990	4896413	7.20	0.47	400	0.4	bdl	bdl	bdl	0.0019	0.0084	bdl	0.0006	bdl	0.0117
16	531727	4852202	7.40	0.56	50	0.49	bdl	bdl	bdl	0.0006	0.0065	bdl	0.0081	0.0073	bdl
17	530419	4856321	7.40	0.36	310	0.36	bdl	bdl	bdl	0.0011	0.0418	0.0348	0.0001	0.0049	bdl
18	517732	4898714	7.60	0.39	330	0.37	bdl	bdl	bdl	0.0009	0.0306	bdl	0.001	bdl	bdl
19	515714	4896532	7.30	0.72	630	0.31	bdl	bdl	bdl	0.0021	0.0063	bdl	0.0001	bdl	0.0365
20	533811	4851397	7.40	0.62	570	0.36	bdl	bdl	bdl	0.0111	0.0067	bdl	0.0053	0.0057	bdl
MAC							to 0.05	to 1.00	to 0.01	to 0.50	to 0.10	to 5*	to 0.10	to 0.10	to 1.00

bdl-below detection limit



N-Classification Neiggebauer [14]; US- Classification Laboratory for saline soil University Riverside[6]

Figure 3. Representation of tested samples according to the classifications of irrigation water

Conclusion

Based on the obtained and analyzed results of the quality study of irrigation water, it can be concluded that water from sampling sites can be used without restrictions to irrigate cultivated crops and there is no risk to have a negative impact on the structure of the soil on which it is applied. Nevertheless, the tests should be carried out periodically irrigation water and soil in order to prevent the creation of a rupture and breakdown of the structure.

Acknowledgment: This research was financially supported by the Ministry of Education, Science and Technological Development, Republic of Serbia [Project TP 37006].

References

- [1] Alemu, M.M., Desta F.Y. Irrigation water quality of River Kulfo and its implication in irrigated agriculture, South West Ethiopia. *Int J Water Resour Environ Eng*, 2017 9: 127–132.
- [2] APHA Standard methods for the examination of water and wastewater. In A.E. Greenberg, A.E., Clesceri, L.S. and Eato, A.D. (Eds.) American Public Health Association, 18th ed., Washington, U.S.A., 1992.
- [3] Ayers, R.S., Wescot, D.W. Water Quality for Agriculture, Irrigation and Drainage paper 29, Rev.1., 1994.
- [4] Capar, G., Dilcan, C.C., Aksit, C., Arslan, S., Celik, M., Kodai, S. Evaluation of irrigation water quality in Gölbaşı District. *Tarım Bilimleri Dergisi-J Agric Sci.*, 2016, 22:408–421.
- [5] Determination of electrical conductivity SRPS EN 27888:1993, 1993.
- [6] FAO, U.S. Salinity Laboratory Staff, 1954.
- [7] Farhad, M., Fatemeh, D., Mostafa, R., Baden M. Introducing a water quality index for assessing water for irrigation purposes: A case study of the Ghezel Ozan River. *Science of The Total Environment*, Volume 589, 2017, p.p.107-116.
- [8] Gidey, A. Geospatial distribution modeling and determining suitability of groundwater quality for irrigation purpose using geospatial methods and water quality index (WQI) in Northern Ethiopia. *Applied Water Science*, 2018, 8:82.
- [9] Greenberg, A.E., Clesceri, L.S., Eato, A.D. Standard Methods for the Examination of Water and Wastewater, American Public Health Association, 20th ed., Washington, U.S.A., 1998.
- [10] Joshi, D.M., Kumar, A., Agrawal, N. Assessment of the Irrigation Water Quality of River Ganga in Haridwar District India. *J. Chem.*, 2009, 2(2):285-292
- [11] Letey, J., Hoffman, G.J., Hopmans, J.W., Grattan, S.R. Suarez, D., Corwin, D.L., Oster, J.D., Wu, L., Amrhei, C. Evaluation of soil salinity leaching requirement guidelines *Agricultural Water Management*, Vol. 98(4):502-506. , 2011.
- [12] Measurement of pH - Potentiometric method SRPS H.Z1.111:1987, 1987.
- [13] Method 200.7: Determination of trace elements in water and wastes by inductively coupled plasma-atomic emission spectrometry, Revision 4.4, EMMC Version, Method for the determination of metals in environmental samples, Supplement I, EPA/600/R-94-111, US EPA, 1994.
- [14] Nejgebauer, V., 1949. Upotrebljivost površinskih i podzemnih voda za navodnjavanje i njihova klasifikacija u prirodnim prilikama Vojvodine. *Radovi poljoprivrednih naučnoistraživačkih ustanova*, I.
- [15] Official Gazette of Republic Serbia, 23/94, 1994.
- [16] Pivić, R., Jošić, D., Dinić, Z., Maksimović, J., Stanojković-Sebić, A. Assessment of water quality for irrigation in the Mačva region by using traditional and contemporary classifications. *ICA FOF Cesme-Izmir, Turkey*. 2018, p.p. 531-540.

- [17] Rhoades, J.D., Akandiah, A.M., Theuse, M., The use of saline waters for crop production. FAO Irrigation & Drainage Paper, 1992, No.48.
- [18] Shammi M., Rahman R., Rahman M.M., Moniruzzaman M., Bodrud-Doza M., Karmakar B., Uddin M.K. Assessment of salinity hazard in existing water resources for irrigation and potentiality of conjunctive uses: a case report from Gopalganj District, Bangladesh. Sustainable Water Res Manag, 2016, 2(4):369–378.
- [19] Towfiqul Islam, A.R.M., Shen, S., Bodrud-Doza, M.D., Safiur Rahman, M. Assessing irrigation water quality in Faridpur district of Bangladesh using several indices and statistical approaches Arabian Journal of Geosciences, October 2017, p.p.10:418.

ELECTROCHEMICAL CHARACTERIZATION OF PVC-Pt(II)PORPHYRIN-MEMBRANE

Nicoleta Plesu^{1*}, Gheorghe Fagadar-Cosma², Anca Lascu¹, Mihaela Petric¹, Manuela Crisan¹, Eugenia Fagadar-Cosma¹

¹*Institute of Chemistry-Timișoara of Romanian Academy, 24 M. Viteazul Ave, 300223 Timisoara, Romania*

²*Faculty of Industrial Chemistry and Environmental Engineering, Politehnica University Timisoara, Pta Victoriei 2, 300006 Timisoara, Romania*

**e-mail: plesu_nicole@yahoo.com*

Abstract

The maximum water volume fraction absorbed by membrane based on Pt(II)-5,10,15,20-tetra(4-methoxy-phenyl)-porphyrin (PtTMeOPP) in poly(vinyl)chloride (PVC) matrix applied on iron substrate is 0.3 % and the permeability is $7.6 \times 10^{-12} \text{ m}^2 \text{ s}^{-1}$. After 24 h immersion in the 0.5 M 4-morpholinoethanesulfonic acid (MES) solution of pH = 5.5, the Nyquist representation of impedance data shows diffusion into the membrane of electrolytes from the buffer solution, causing a decrease of the membrane electric resistance, but no delamination was observed for immersion longer than 48 h. Furthermore, the coating resistance is still close to $\sim 16000 \text{ ohm.cm}^{-2}$ after 25 hours. This recommends this membrane as good material in potentiometric sensors design.

Introduction

The incorporation of compounds with special recognition properties (i.e porphyrins and metalloporphyrins) in common polymers allowed the obtaining of membranes with tailored properties [1]. Structural features and the functionalization possibility recommend porphyrin derivatives as good and sensitive compounds for sensors design (to recognize ions, neutral molecules and biologically active substances). Platinum-porphyrins were reported in oxygen detection [2-5], anions determination (perchlorate, iodide) [6-9] and alcohol sensing [10].

In membrane preparation, barrier properties against water and ionic species present in solution are important and can define if the membrane can facilitate the migration of ions through the electrode coating and if a certain membrane can act as a sensitive material for analytes detection. Electrochemical characterization of PVC-PtTMeOPP porphyrin-membrane is presented in this paper.

Experimental

Reagents. Poly(vinyl)chloride (PVC), o-nitrophenyloctylether (NPOE), tetrahydrofuran (THF) were purchased from Fluka and Merck. All reagents (salts, acids and bases) were of purum analyticum grade. Double distilled water was used. The synthesis of PtTMeOPP was already reported by our group [9].

Electrode Membrane Preparation. The studied membranes have the composition 1% metalloporphyrin, 33% PVC, 66% NPOE (plasticizer) and the appropriate amount of THF was added under stirring to obtain a transparent solution, that was deposited onto a glass plate. The solvent was slowly evaporated at room temperature and a flexible membrane was obtained. A circular membrane of 8 mm diameter was cut and stucked on the Fluka electrode body (inox electrode with an active surface equal to 0.785 cm^2) by THF.

Apparatus and Electrodes. Autolab 302N EcoChemie equipped with the FRA2 impedance module were used for Electrochemical Impedance Spectroscopy (EIS) investigations,

performed at room temperature in a conventional three-electrode cell, equipped with two stainless steel counter electrodes and Ag/AgCl as reference electrode. The sinusoidal potential amplitude was 10 mV and the tested frequency range was in the range from 0.1 Hz to 100 kHz.

The performance of membrane was investigated by measuring impedance in the frequency range at different immersion times in 4-morpholinoethanesulfonic acid (MES) solution at pH = 5.5. The experimental data were fitted to the equivalent electrical circuit by a complex non-linear least squares method, using the ZView software - Scribner Associates Inc., Southern Pines, North Carolina, USA and Solartron Analytical, Oak Ridge, Tennessee, USA.

Results and discussion

The PtTMeOPP compound was obtained with a yield over 88% as brownish crystals after metalation of the porphyrin base, 5,10,15,20-tetra(4-methoxy-phenyl)-porphyrin, with large excess of $\text{PtCl}_2(\text{PhCN})_2$ in the presence of $\text{CH}_3\text{COONa} \times 3\text{H}_2\text{O}$ [9]. The metalloporphyrin was further characterized by UV-vis spectroscopy in different solvents, by FT-IR and $^1\text{H-NMR}$ to confirm the structure.

The UV-vis spectra of 10^{-5}M Pt-TMeOPP in various solvents: chlorobenzene, dichloromethane, THF, DMF and DMSO, presented in the order of increasing polarity, show that the solvent with the lowest polarity generates the spectrum with the highest intensity of absorption and with the highest red shift of both Soret and Q bands (Figure 2, Table 1).

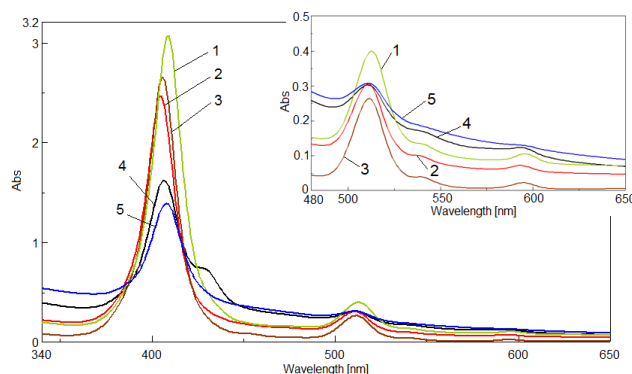


Figure 2. Overlapped UV-vis spectra of Pt-TMeOPP in various solvents (increasing polarity):

1-chlorobenzene, 2-dichloromethane; 3-THF; 4-DMF; 5-DMSO

Table 1: UV-vis parameters compared for Pt-TMeOPP in various solvents by increasing polarity:

Solvent	Soret		Q		Q	
	λ [nm]	I [u.a.]	λ [nm]	I [u.a.]	λ [nm]	I [u.a.]
chlorobenzene	409	3.062	513	0.398	596	0.1049
CH_2Cl_2	406	2.653	511	0.262	595	0.021
THF	405	2.462	511	0.304	593	0.071
DMF	407	1.613	511	0.301	593	0.122
DMSO	408	1.384	511	0.307	-	-

Electrochemical Characterization of the membranes. The Nyquist and the Bode diagrams recorded during immersion in MES solution are presented in Figure 5 and are similar with those reported in [9]. The Nyquist diagrams present one large semicircle followed by one more flat semicircle in low frequency region (Figure 5a). The modulus and the phase angle for the membrane during immersion presented in Figure 5b show a well-defined time constant at lower frequencies and a second incomplete peak at higher frequencies arising from

diffusion phenomena. The experimental data were fitted to the equivalent electrical circuit (EEC) presented in Figure 5c.

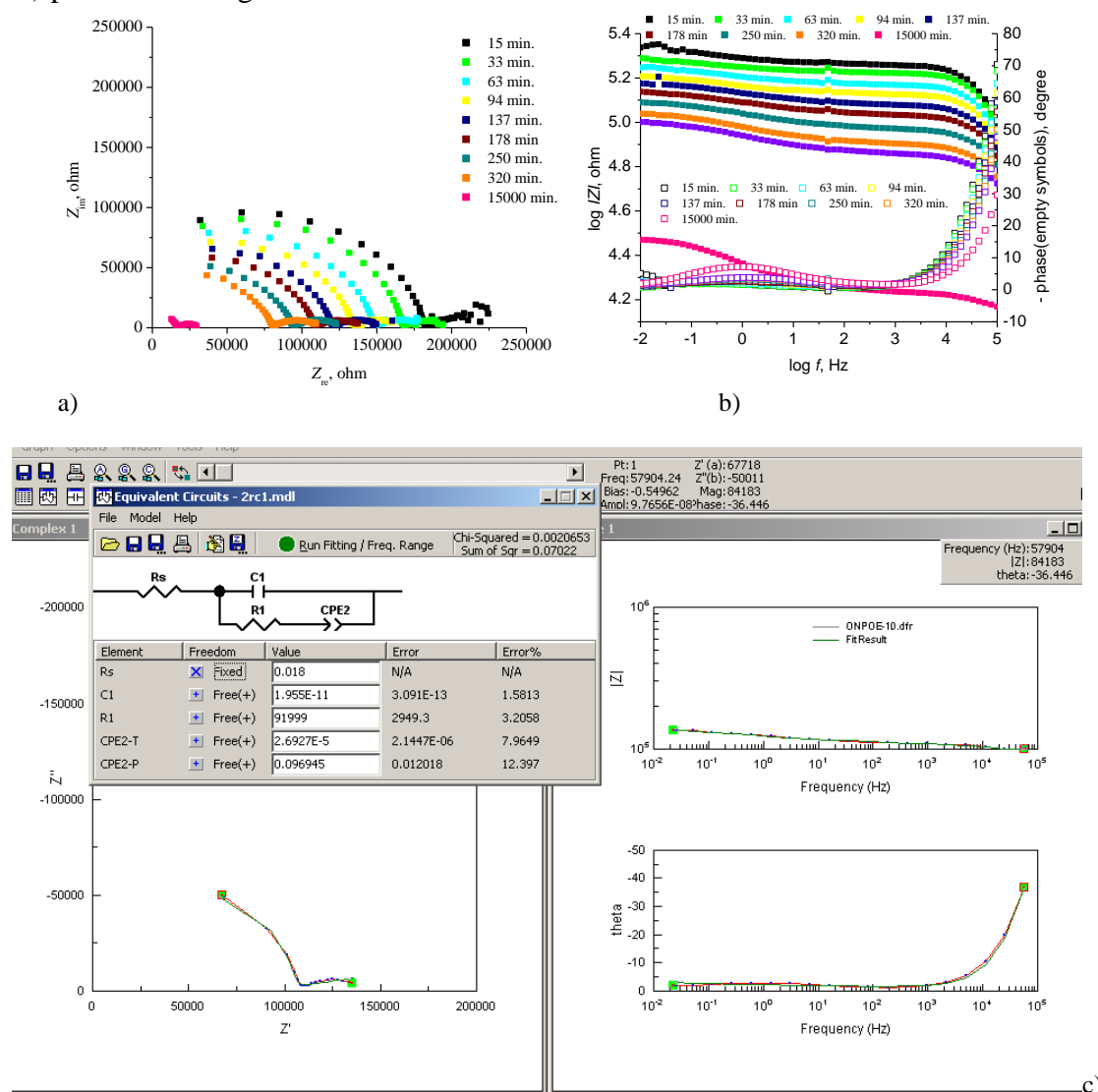


Figure 5. Nyquist (a) and Bode (b) diagrams in case of membrane at OCP in MES buffer solution, pH= 5.5 and schematic representation of the electric equivalent circuit for EIS data and a simulation example of Nyquist and Bode diagrams with the suggested model for 15 min. immersion time of the membrane (c).

The EEC includes the resistance of electrolyte R_s , in series with a parallel connexion of capacitance C_1 (representing the charge/discharge process that occurs at the substrate/electrolyte interface) and the polarization resistance R_1 . The concentration gradient appears as a result of ions transportation between the bulk and the interface and C_2 was used to model the diffusion phenomena. Constant phase element (CPE) was introduced to represent the double layer capacitance, for the reason of non-ideal behaviour. The impedance of a CPE can be expressed by $Z_{CPE} = [T(j\omega)^n]^{-1}$, where ω is the frequency, T is the CPE magnitude and the exponent n is between 0 and 1. The incertitude of parameters for the simulation is not higher than 16 % and the circuit was considered to model well the experimental data.

The film capacitance C_1 increases, and the resistance R_1 decreases with immersion time describing the penetration of water throw the pores and the swelling process of the membrane and possible formation of some ionically conducting paths across the membrane (Figure 6). The polarization resistance R_1 decreases with increasing immersion time. The

observed R_1 values are situated around $16000 \text{ ohm.cm}^{-2}$ after 25 hours of immersion and show a good integrity of this membrane. A slightly decrease of the diffusion capacitance C_2 (from $4.3 \times 10^{-5} \text{ F.cm}^{-2}$ in the first moment of immersion to $2.6 \times 10^{-5} \text{ F.cm}^{-2}$) becomes visible due to the low number of ions involved in diffusion process as the membrane became more swelled.

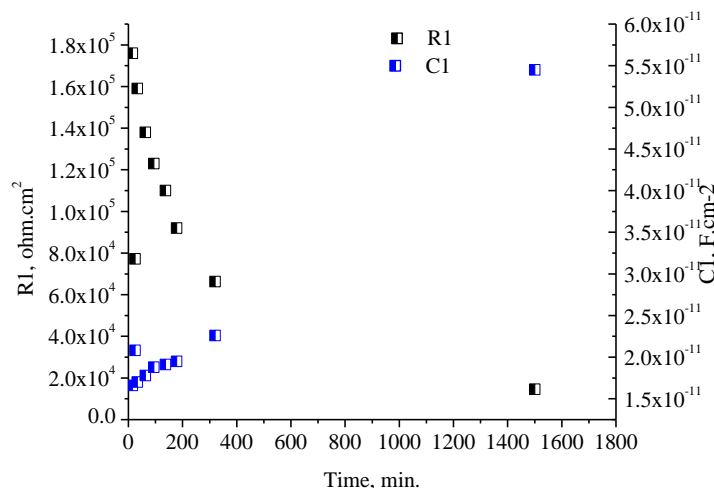


Figure 6. Variation of R_1 and C_1 with immersion time at OCP in MES buffer solution (pH= 5.5).

To estimate the volume fraction of water in membrane a uniform distribution of water was assumed. Relation (1) was used to calculate the water uptake of the membrane using the capacity obtained from EIS data (C_t at time t , C_0 at $t = 0$) and the dielectric constant of water ($\epsilon_{\text{H}_2\text{O}} = 80$). The maximum water uptake was $\sim 0.3\%$. The diffusion coefficient of water (D) was calculated with the half-life method, relation (2), where $t_{0.5}$ is the time when the water fraction reaches a half of the saturation value and l is the coating thickness [12]. The permeability, P of the coating is the product of the diffusion coefficient and the solubility, relation (3). The solubility of water in coatings was derived from the water volume fraction at saturation (W_s) and water density (ρ_w).

In Figure 6 the increase of the absorption of water and the decrease of R_f in time reveal that the water saturation is reached after 25 hours and the data emphasized the necessity to introduce a membrane conditioning step, before the any use in detection.

$$W = \frac{\log[C_t / C_0]}{\log 80} \quad (1) \quad D = \frac{0.04919x4l^2}{t_{0.5}} \quad (2) \quad P = DxS = DxW_s x \rho_w \quad (3)$$

For a 180 micron membrane the calculated diffusion coefficient is $D = 5.03 \times 10^{-11} \pm 0.22 \text{ m}^2 \text{ s}^{-1}$ and the permeability is $P = 1.45 \times 10^{-7} \text{ kg m}^{-1} \text{ s}^{-1}$. It was observed a considerably decreases of W by incorporation of Pt-TMeOPP salt, a lipophilic compound in plasticized or unplasticized PVC. The obtained value of the diffusion coefficient is close to the reported value for other PVC membrane ($1.3 \times 10^{-7} \text{ cm}^2 \cdot \text{s}^{-1}$) [13].

The values of the diffusion coefficient and the solubility are relatively comparable to some epoxy coatings where a diffusion coefficient close to $10^{-11} \text{ m}^2 \cdot \text{s}^{-1}$ and a water solubility value of about 40 kg m^{-3} was reported [14].

Conclusion

A Pt(II)-metalloporphyrin is characterized by UV-vis, FT-IR and $^1\text{H-NMR}$ and the electrochemical characterization of PVC- PtTMeOPP porphyrin-membrane is presented. The EIS estimation of the water uptake of membrane at saturation was possible for the prepared membranes applied on an electrochemically inert material (inox) in MES. On this electrode

no corrosion reaction was observed after the saturation process. The maximum volume fraction of the adsorbed water determined was 0.29 ± 0.015 , reached after ~ 1600 min. The electrical resistance of the membrane decreased with the increasing of the water absorption. The diffusion coefficient is $D = 5.03 \times 10^{-11} \pm 0.22 \text{ m}^2 \text{ s}^{-1}$ and the permeability is $P = 1.45 \times 10^{-7} \text{ kg m}^{-1} \text{ s}^{-1}$.

Acknowledgements

The authors from Institute of Chemistry Timisoara of Romanian Academy are acknowledging UEFISCDI PN-III-P1-1.2-PCCDI-2017-1-Project **ECOTECH-GMP 76PCCDI/2018** and to Romanian Academy for financial support in the frame of Programme 3/2018 from ICT. This work is dedicated to the Centennial Anniversary of ROMANIA.

References

- [1] R. Paolesse, S. Nardis, D. Monti, M. Stefanelli, C.D. Natale, Chem. Rev. 117 (2017) 2517.
- [2] Y. Amao, K. Asai, I. Okura, H. Shinohara, H. Nishide, Analyst 125 (2000) 1911.
- [3] C. Staudinger, S.M. Borisov, Methods Appl. Fluoresc. 3 (2015) 042005.
- [4] Y. Mao, Z. Meia, J. Wen, G. Li, Y. Tian, B. Zhou, Y. Tian, Sensor. Actuat. B-Chem. 257 (2018) 944.
- [5] E. Önal, S. Saß, J. Hurpin, K. Ertekin, T.S. Zehra, M.U. Kumke, C. Hirel, J. Fluoresc. 27 (2017) 861.
- [6] A. Soleymanpour, E.H. Asl, S.M. Nabavizadeh, Sensor. Actuat. B-Chem. 120 (2007) 447.
- [7] D. Masih, M. Shawkat, S.M. Aly, E. Alarousu, O.F. Mohammed, J. Mater. Chem. A 3 (2015) 6733.
- [8] C. Baker, S.E. Kahn, E.W. Bermes, Ann. Clin. Lab. Sci. 10 (1980) 523.
- [9] D. Vlascici, G. Fagadar-Cosma, N. Plesu, A. Lascu, M. Petric, M. Crisan, A. Belean, E. Fagadar-Cosma, Sensors 18 (2018) 2297.
- [10] S. Carturan, A. Quaranta, M. Tonezzer, A. Antonaci, G. Maggioni, R. Milan, IEEE Sens. 2008, 305.
- [11] R. Wysokinski, K. Hernik, R. Szostak, D. Michalska, Chem. Phys. 333 (2007) 37.
- [12] L.V.S. Philippe, S.B. Lyon, C. Sammon, J. Yarwood, Corros. Sci. 50 (2008) 887.
- [13] T. Lindfors, S. Suntfors, L. Hofler, P.E. Gyurcsanyi, Electroanal., 21 (2009) 1914.
- [14] S. Duval, Y. Camberlin, M. Glotin, M. Keddam, F. Ropital, H. Takenouti, Prog. Org. Coat. 39 (2000) 15.

DEGRADATION OF ORGANIC DYES UNDER VISIBLE LIGHT

**Jovana Prekodravac¹, Bojana Vasiljević², Dejan Kepić¹, Milica Budimir¹, Duška Kleut¹,
Biljana Todorović–Marković¹**

¹*Institute of nuclear sciences Viča, University of Belgrade, Belgrade, Serbia*

²*Department of Chemistry, Biochemistry and Environmental Protection, Faculty of Sciences,
University of Novi Sad, 21 000 Novi Sad, Serbia
e-mail: prekodravacj@gmail.com*

Abstract

We performed the “bottom-up” synthesis of N-doped CQDs *via* swift and easy one-step microwave-assisted method. The percentage of bound nitrogen in this short amount of time was about 11 at% in the form of pyridinc/NH₂, pyrrolic-N and graphitic-N. The synthesized N-doped CQDs showed good photocatalytic activity in organic dyes degradation after only 30 min of exposure to the visible light.

Introduction

The water pollution is one of the major problem of today. Industries discharge waste matter, containing organic dyes, into natural water resources without any treatment [1]. These organic dyes, such as rose bengal (RB) and methylene blue (MB) are extremely genotoxic, mutagenic and cytotoxic [2–6]. So far, various semiconductor materials have been used as photocatalysts for the removal of different dyes from aqueous solutions. Different parameters affect the rate of the dye degradation, such as pH, concentration and light intensity [1]. Here we performed the photocatalytic degradation of RB and MB in the presence of visible light.

Experimental

Synthesis of N-CQDs was performed from water solution of glucose in the presence of ammonia hydroxide (NH₄OH, 25%). Aqueous solution were irradiated in closed-vessel system of CEM Discover BenchMate single mode microwave reactor for only 1 minute, at fixed temperature (100 °C) and power (100 W, 200 W). After synthesis, the samples were dialized for 5 days and filtrated through filters from 450 nm to 10 nm. For the photocatalytic activity study, the N-CQD₁₀₀ or N-CQD₂₀₀ samples were dispersed in RB (0.03 mM) and MB (0.03M) water solutions and treated under visible light at different conditions.

Results and discussion

The Atomic force microscopy (AFM) was used for analysis of morphology and structure of synthesized N-CQDs (Fig 1.) showing that samples (N-CQD₁₀₀ and N-CQD₂₀₀) have good morphology with spherical like shapes. Taking into account the anomalies related to measurements of particles thickness [7] and diameter [8] we calculated the real particle diameter distribution by analysing 100 dots for each sample. The measured real particle diameters were in the range from 5 to 30 nm.

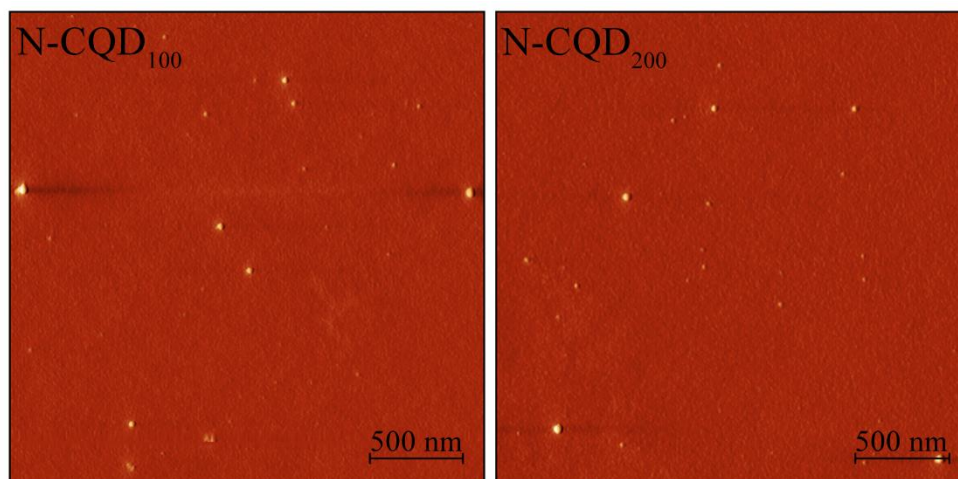


Figure 1. Top view AFM images of N-CQD₁₀₀ (left) and N-CQD₂₀₀ (right) samples.

Chemical analysis of the synthesized N-CQDs was performed with XPS measurements (Table 1). From the XPS results, we noticed that with increase in applied MW power there is the increase in C sp^3 comparing to the sp^2 domains. These results suggest that synthesized quantum dots are carbon nanodots consisting of sp^2 carbon domains in sp^3 carbon matrix. The XPS analysis also showed incorporation of relatively high atomic percentage (at%) up to 10 to 11 at% approximately, of N containing groups in the samples. The highest noticed N at% was in the form of pyridinic/ NH_2 . The detail analysis of the XPS spectra is presented in Table 1.

Table 1. Detail XPS analysis of the N-CQDs samples.

<i>Name</i>	Sample N-CQD₁₀₀		Sample N-CQD₂₀₀	
	<i>Peak BE (eV)</i>	<i>Atomic %</i>	<i>Peak BE (eV)</i>	<i>Atomic %</i>
C1s sp^2	284.5	18.9	284.5	18.8
C1s sp^3	285.1	22.7	285.1	28.2
N1s pyrrolic	400.4	23.4	400.4	20.8
N1s pyridinic/ NH_2	399.4	64.6	399.4	69.3
N1s graphitic/ NH_3^+	401.7	12.0	401.6	9.8

Photo degradation rate of RB and MB under visible light was examined by changing the catalyst concentration (0.25 mg/ml and 1 mg/ml) and irradiation time (30 min to 24h). Fig. 2 presents the photodegradation rate of RB (%) depending on catalyst concentration and irradiation time. From Fig 2 it can be seen that the degradation rate increases with increase in the catalyst concentration from 72–78 % at lower concentration to 92–93 % at higher catalyst concentration. The influence of the irradiation time was the most obvious after 30 min of exposure to the visible light while further prolongation of irradiation time did not had any significant effect on the dye degradation rate.

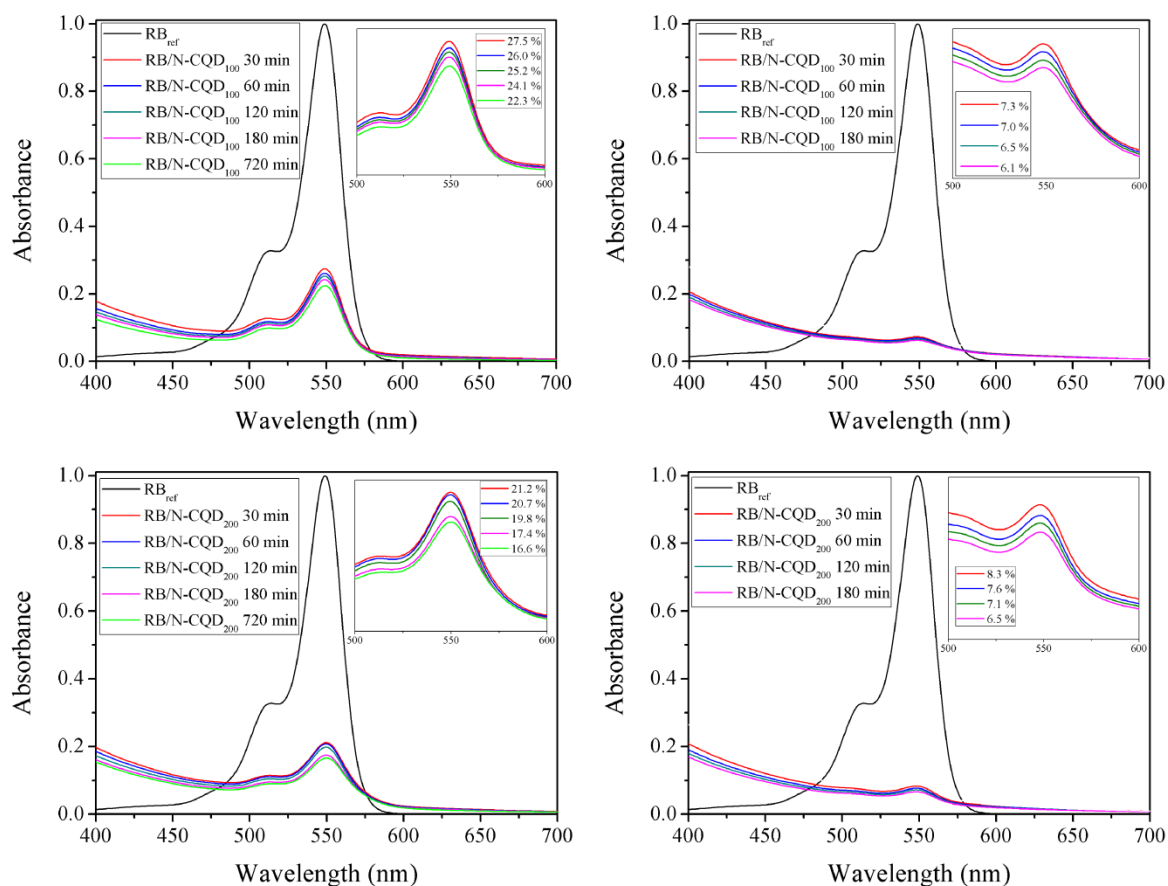


Fig 2. The dye degradation rate of RB (%) depending on the catalyst concentration of 0.25 mg/ml (left) and 1 mg/ml (right) and irradiation time (from 30 to 720 min).

Fig 3. presents the degradation rate of MB (%) after 4h and 24h of the exposure to the visible light.

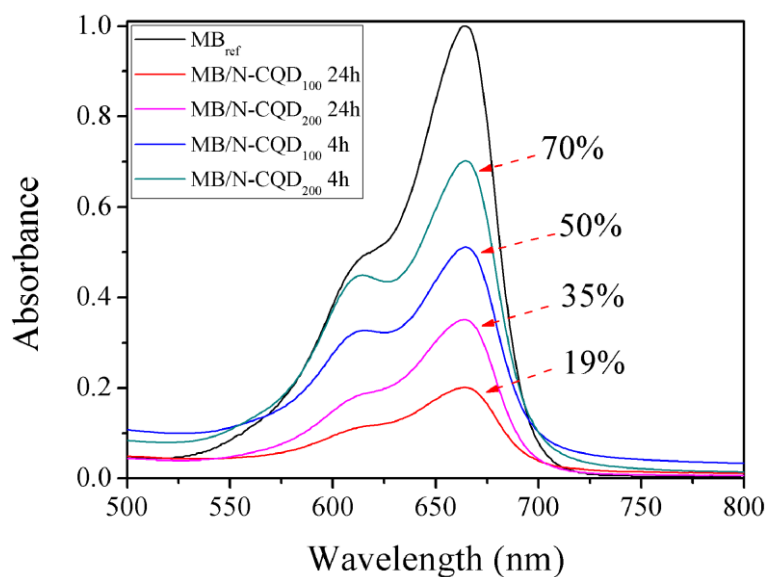


Fig 3. MB degradation rate (%) depending on irradiation time.

Here can be seen that the degradation rate is smaller comparing to the results obtained for RB degradation. After 4h of exposure to the visible light almost 50 to 70% of MB remain in the

samples, while after 24h of exposure the degradation rate was up to 70 to 80%. Smaller concentrations than 1 mg/ml were not examined since at this catalyst concentration results showed that at least 24h are necessary for significant degradation.

Conclusion

Here we demonstrated fast and easy one-step microwave assisted synthesis of N-doped carbon quantum dots with approximately 10–11 % of attached nitrogen. The photocatalytic activity of synthesized N-doped CQDs as catalyst was examined on the RB and MB toxic organic dyes. Very good degradation rate of RB up to 93 % was proven after only 30 min of exposure to the visible light irradiation, where further prolongation of irradiation time did not affect significantly on the RB degradation. By examining the effect of catalyst concentration, we noticed that the degree of RB degradation increases proportionately with increasing catalyst concentration. By analysing the degradation of MB we observed the significant degradation rate after 24h of exposure to the visible light. The obtained results indicate the possibility of using synthesized material for purification of textile industry wastewaters.

Acknowledgements

Financial support for this study was granted by the Ministry of Education, Science and Technological Development of Republic of Serbia (grants numbers 172003).

References

- [1] S. Sharma, R. Ameta, R.K. Malkani, S.C. Ameta, J. Serb. Chem. Soc. 78 (2013) 897–905.
- [2] F.M.D. Chequer, V. de P. Venâncio, M. de L.P. Bianchi, L.M.G. Antunes, Food Chem. Toxicol. 50 (2012) 3447.
- [3] W.K. Walthall, J.D. Stark, Environ. Pollut. 104 (1999) 207.
- [4] N.K. Tripathy, M.d.J. Nabi, G.P. Sahu, A.A. Kumar, Food Chem. Toxicol. 33 (1995) 923.
- [5] P. Mpountoukas, A. Pantazaki, E. Kostareli, P. Christodoulou, D. Kareli, S. Poliliou, S. Mourelatos, V. Lambropoulou, T. Lialiaris, Food Chem. Toxicol. 48 (2010) 2934.
- [6] E.E. Ritchie, J.I. Princz, P.Y. Robidoux, R.P. Scroggins, Chemosphere 90 (2013) 2129.
- [7] P. Nemes-Incze, Z. Osvath, K. Kamaras, L.P. Biro, CARBON 46 (2008) 1435-1442.
- [8] M. Rasa, B.W.M. Kuipers, A.P. Philipse, J. Colloid Interface Sci. 250 (2002) 303-315.
- [9] S.P. Jovanović, Z. Syrgiannis, Z.M. Marković, A. Bonasera, D.P. Kepić, M.D. Budimir, D.D. Milivojević, V.D. Spasojević, M.D. Damićanin, V.B. Pavlović, B.M. Todorović Marković, *ACS Appl. Mater. Interfaces* 7 (2015) 25865–25874.
- [10] J. Ju, R. Zhang, S. Heab, W. Chen, RSC Adv. 4 (2014) 52583.
- [11] F.A. Permatasari, A.H. Aimon, F. Iskandar, T. Ogi, K. Okuyama, Scientific Reports 6 (2016) 1–8.

MICRONUTRIENTS CONCENTRATION IN FIELD GROWN PEPPER (*Capsicum annum* L.) IN DIFFERENT FERTILIZATION SCHEMES

Marina Putnik-Delić, Ivana Maksimović, Rudolf Kastori, Žarko Ilin, Milena Daničić

University of Novi Sad, Faculty of Agriculture, Trg D. Obradovića 8, Novi Sad, 21000, SERBIA

e-mail: putnikdelic@polj.uns.ac.rs

Abstract

Pepper is used as vegetables, spice and medicine. It may be consumed fresh, preserved (turkish), dry or dry minced. Due to its wide use, quality of pepper fruit is very important and largely determined by the way of cultivation (fertilization). In this paper, 14 fertilizer schemes, including mineral and organic fertilizers, were applied to two varieties of peppers (Anita and Amfora). All the treatments were performed with and without mulch. The influence of fertilization and mulch on the concentration of micronutrients was analyzed. Concentrations of Cu, Fe, Mn and Zn were significantly changed under applied fertilization schemes as well as the application of the mulch.

Introduction

Cu, Fe Mn and Zn are essential micronutrients, which are necessary for the proper development of plants and are equally important in human diet. Essential trace minerals are necessary nutrients for normal functioning of human metabolism and health. It is widely accepted that these elements are significantly better exploited when introduced into the organism through food than through supplements. Therefore, their concentrations are important features of fruits, including pepper [1] and adjusting fertilization to attain better fruit quality in the sense of biofortification is permanent task.

Experiment was set in the field and the effect of different fertilization schemes (calculated on the basis of nitrogen input) and mulching on the concentration of Cu, Fe, Mn and Zn in fruits of two pepper cultivars was analyzed.

Experimental

Two cultivars of pepper, Anita and Amfora (NS SEME, Novi Sad, Serbia), were grown under 14 fertilization schemes (Table 1), each of which was conducted in two variants - unmulched and mulched with plastic foil. Total amount of added nitrogen was 240 kg/ha.

Table 1. Sources of nitrogen provided to pepper during cultivation (%). The same fertilization schemes were applied in production of Anita and Amfora, with and without mulching.

	Fertilization schemes													
	1	2	3	4	5	6	7	8	9	10	11	12	13	14
NPK	-	100	75	50	-	75	50	-	75	50	-	75	50	-
Cattle manure	-	-	25	50	100	-	-	-	-	-	-	-	-	-
Vermicompost	-	-	-	-	-	25	50	100	-	-	-	-	-	-
Fertor	-	-	-	-	-	-	-	-	25	50	100	-	-	-
Pig manure	-	-	-	-	-	-	-	-	-	-	-	25	50	100

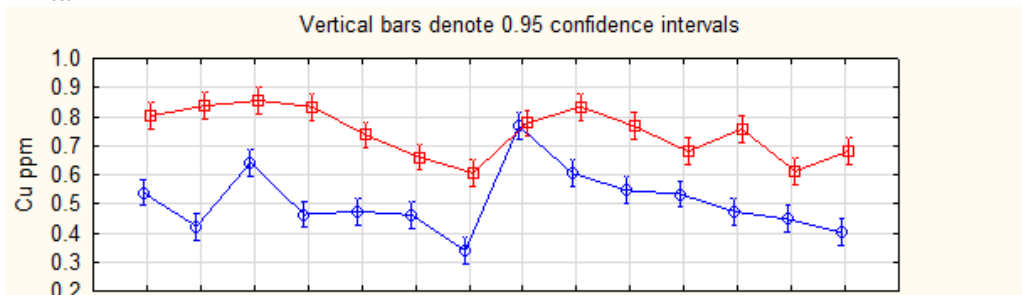
Pepper was planted on plots $P=17.5 \text{ m}^2$, 30 plants/plot, each variant in 4 replications.

Concentration of Cu, Fe, Mn and Zn were assessed at harvest, by AAS (Shimadzu 6300). Statistical analysis was performed using STATISTICA 13.3 (StatSoft, University Licence, University of Novi Sad, 2018).

Results and discussion

Mineral composition and concentrations of nutrients in leaf tissues depend of various factors, such as features of a plant (species, cultivar, type of leaves, age), soil, fertilizer, climate, cultivation practices, and pests and diseases [2]. In general, the absorption of nutrients in the majority of crops follows the pattern of the growth curve (accumulation of dry matter) [3]. In these two tested pepper varieties, Anita and Amfora, the Cu concentration was significantly changed in the presence of different fertilizers. Differences are also observed with respect to mulching (Figure 1). In Anita, concentration of Cu varied more due to applied fertilizers, while in Amfora mulching had significantly higher impact on the Cu concentration (in about 50% of applied fertilizers, a statistically significant increase in Cu in fruits was obtained). In Amfora the application of 100% NPK in combination with mulch resulted in the highest Cu concentration of all treatments and it was 42% higher than without mulch.

Anita



Amfora

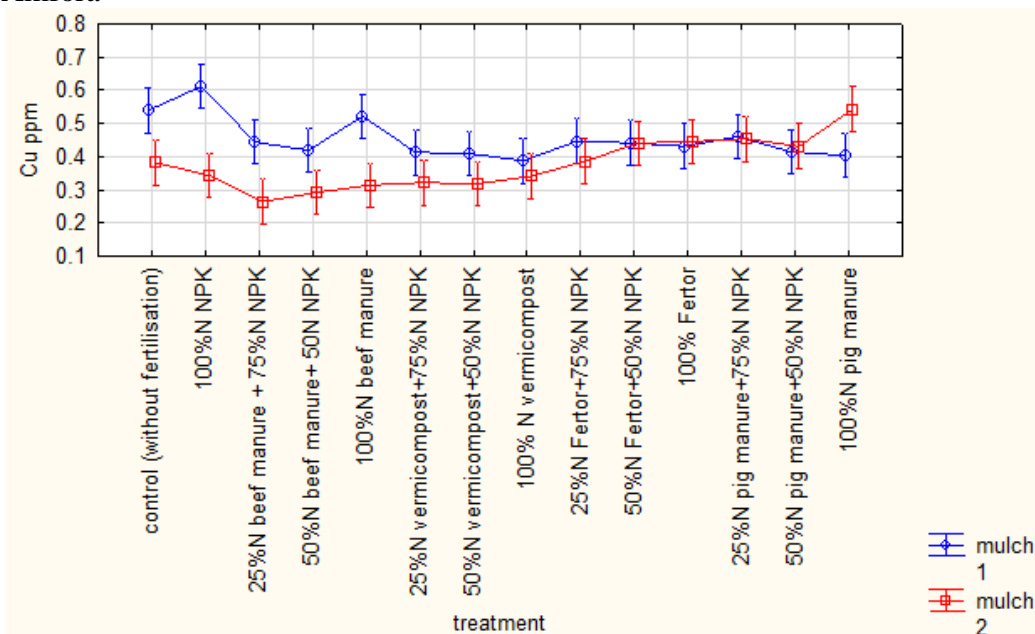
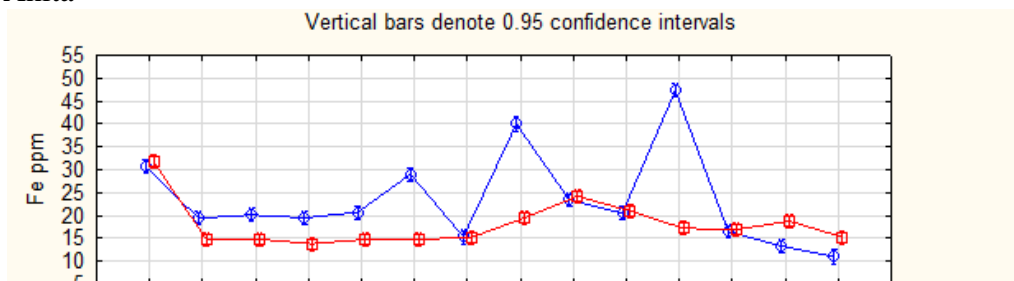


Figure 1. Concentration of Cu in fruits of two pepper cultivars produced under 14 fertilization schemes, with (mulch 1) or without (mulch2) mulching

The results show that mulching significantly reduced concentration of Fe in pepper (Figure 2). The significantly lower Fe concentrations were found at Amfora compared to Anita. It can

be observed that when applying [50%N Fertor + 50%N NPK] and [25%N pig manure + 75%N NPK], the Fe concentration didn't change regardless of the mulching. Accordingly, some authors conclude that accumulation of mineral nutrients in the leaves and the fruit of pepper were not significantly affected by plastic mulches [4].

Anita



Amfora

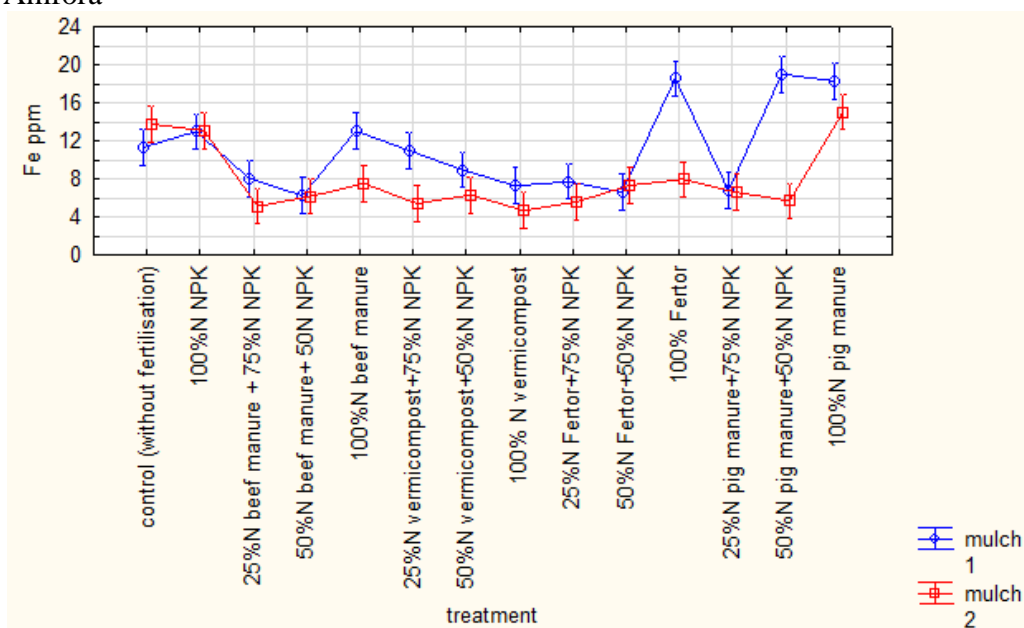
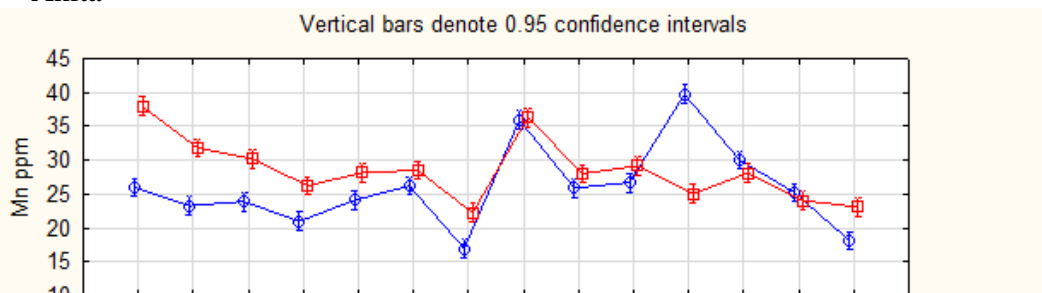


Figure 2. Concentration of Fe in fruits of two pepper cultivars produced under 14 fertilization schemes, with (mulch 1) or without (mulch2) mulching

The concentration of Mn was reduced by mulching (Figure 3). Applied fertilization regimes didn't cause a significant increase in the concentration of Mn in relation to non-fertilized control. In Amfora, there are particularly small variations in the Mn concentration.

There are statistically significant differences between Anita and Amfora with respect to the average concentration of Zn (Figure 4). Generally, in Anita significantly higher concentration of all analyzed elements was recorded. Concentration of Zn was strongly affected by the use of different fertilizers, whereas mulching had less pronounced effect. Certainly the kind of mulch can play an important role also. In potato, the use of colored mulches were found to be associated with differences in the concentrations of Cu and Zn in the leaves and the tubers [5].

Anita



Amfora

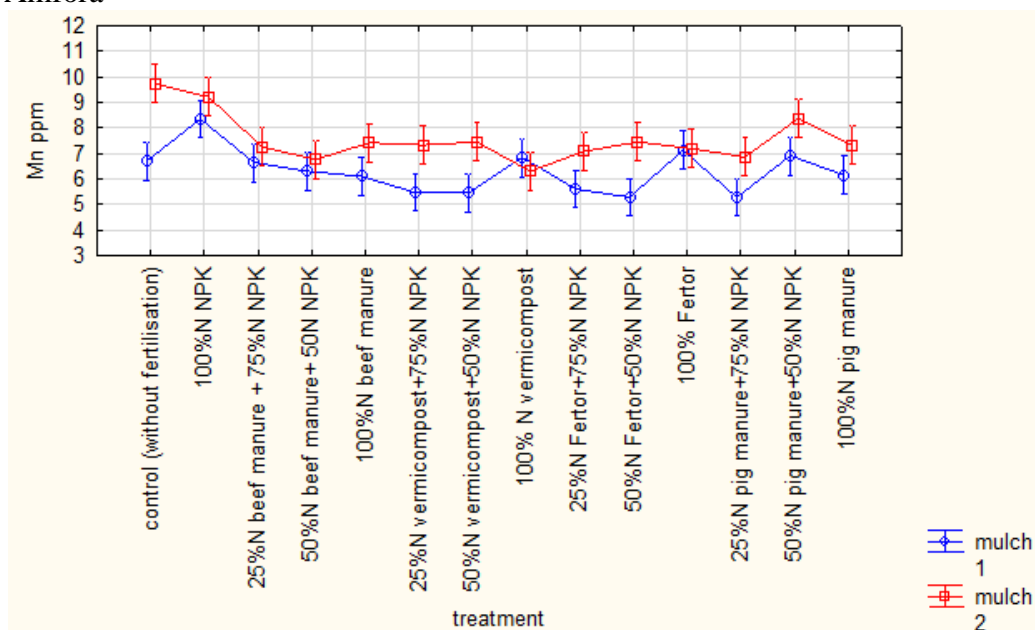
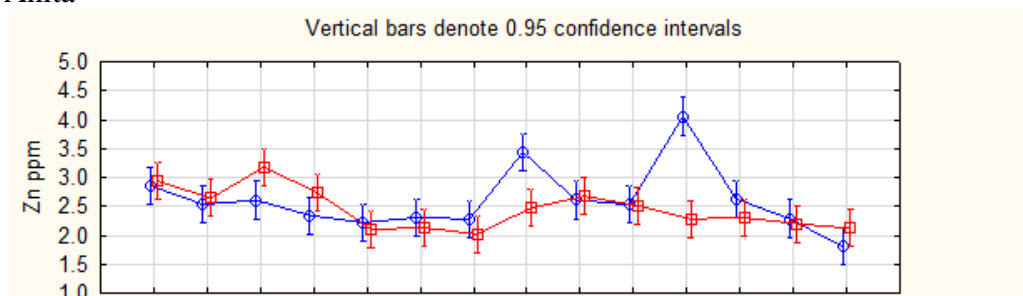


Figure 3. Concentration of Mn in fruits of two pepper cultivars produced under 14 fertilization schemes, with (mulch 1) or without (mulch2) mulching

Anita



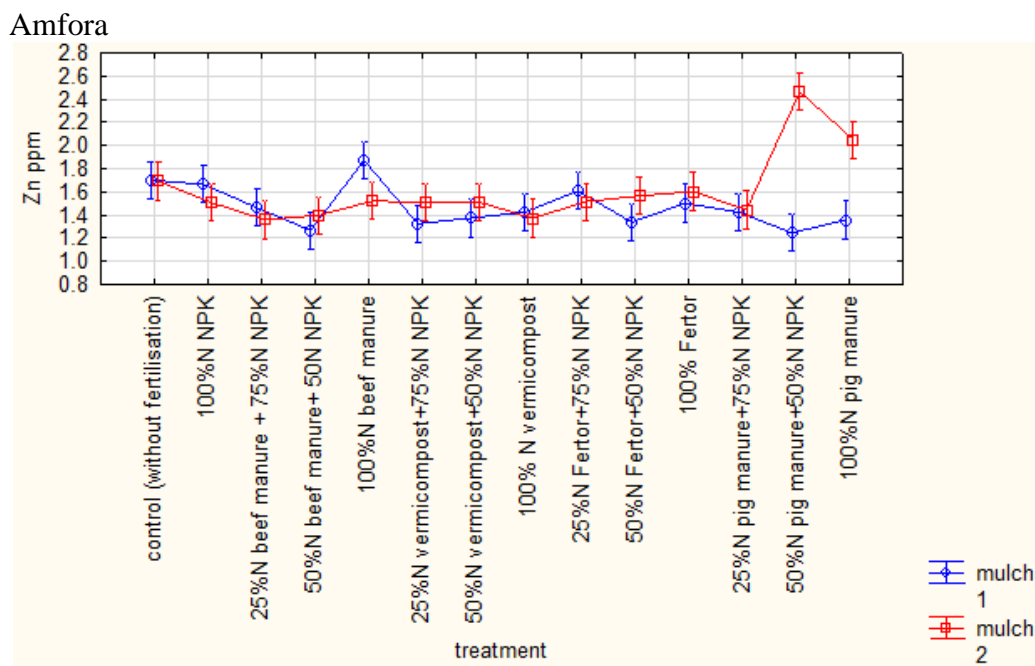


Figure 4. Concentration of Zn in fruits of two pepper cultivars produced under 14 fertilization schemes, with (mulch 1) or without (mulch2) mulching

Conclusions

Under applied fertilization schemes concentrations of Cu, Fe, Mn and Zn were significantly changed. Moreover, significant differences between two pepper cultivars (Anita and Amfora) were detected as well. Concentration of Cu was altered the most in response to on mulching, of the four analysed micronutrients.

Acknowledgements

We thank Ministry of Education, Science and Technological Development of the Republic of Serbia, TR 31036, for financial support.

References

- [1] A. Agarwal, S. Gupta, Z. Ahmed, *Acta Horticulturae*. 756 (2007) 309-314.
- [2] E. Malavolta, G.C. Vitti, S.A. Oliveira, *Avaliação do estado nutricional das plantas. Princípios e aplicações*. 2^a ed. Piracicaba: POTAFOS, (1997) 319p.
- [3] C. Hamilton César de O, O. Sueyde F de Vargas, P.F. Castoldi, R. Barbosa, J. Carlos, B. Leila T. *Horticultura Brasileira* 30 (2012), 125-131.
- [4] J.C. Díaz-Pérez, *Hort Science* 45 (2010) 1196–1204.
- [5] M. Baghour, D.A. Moreno, G. Villora, I. Lopez-Cantarero, J. Hernandez, N. Castilla, L. Romero, *Journal of Agricultural and Food Chemistry* 50 (2002) 140–146.

EMISSIONS IN ENVIRONMENT AND WASTEWATER TREATMENT IN SOME SUGAR FACTORIES IN SERBIA

Zita Šereš¹, Nikola Maravić¹, Szabolcs Kertesz², Ljubica Dokić¹, Dragana Šoronja Simović¹, Biljana Pajin¹, Žana Šaranović¹, Aleksandar Jokić¹

¹*Faculty of Technology, University of Novi Sad, 21000 Novi Sad, Bul. Cara Lazara 1, Serbia*

²*Faculty of Engineering, University of Szeged, H-6725 Szeged, Moszkva krt. 5-7, Hungary*

e-mail: zitas@tf.uns.ac.rs

Abstract

In a beet-sugar plant numerous sources of wastewaters exist. The cleanest water is from the evaporators (150% calculated on the sugar-beet), which contains ammonium and ammonium carbonate. The waste water used for cooling afterwards is used for beet washing (830% calculated on the sugar-beet). The third kind of waste water is used for washing beets soaked with dirt. This water contains some residues, suspended solids, organic compounds. The fourth group is fecal waste water, which is treated in a system designed for recycling the waste. This system is composed of two decanters. Calcium-carbonate, aluminium sulphate could be used as precipitating agents. Sugar factories that manipulate with 500 tonnes of sugar-beet need lagoons with an area of about 30-40ha. Since 2006 the sugar factory near Novi Sad has not been letting the effluent into the channel Bezdán-Vrbaš. The waste water which is let into the lagoons has about 3000mg/l BOD₅, and 4-5 months later the level of BOD₅ decreased for about 70%.

Introduction

The sugar industry is one of the largest polluters. In a beet-sugar plant numerous sources of emission exist, especially in water and air. Beside that there are huge amount of emission of sludge too. Although sugar factories are only working one hundred days a year, in that period several million m³ of highly contaminated wastewater (COD 5000-20000 mg/l) is generated [1,2].

If there would not be a regular practice in sugar industry that water recirculates, the water consumption would be very large. Thanks to the recirculation circuits, the water consumption is reduced to a far smaller value. For example, for total water consumption of 15 m³/t of processed beet, the consumption of fresh water is only 0.25 - 0.4 m³/t, and in modern factories even smaller, about 0.1 m³/t indicating that this technique achieved huge savings in the consumption of water and the amount of generated waste water, which is accompanied by adequate savings in the costs of providing fresh water and wastewater treatment costs [4,5,6]. Due to the nature of the raw materials used and the final products, the waste water derived from sugar plant is biodegradable. Auxiliary washing materials and disinfecting materials may be a problem if they are not degradable enough. The concentration and quantity of organic matter present in the wastewater depends on the ratio of the produced quantity of sugar to the amount of the generated wastewater [3,4,5].

The average COD / BOD ratio is about 1.5, indicating a high degree of biodegradability of the present substances. In addition to organic substances, technological wastewater is also loaded with suspended substances, and significantly increases during the sugar beet campaign. The ammonia content is about 12 mg/L and is not problematic for processing. Phosphorus from the wastewater originates from the used cleaning and disinfection agents. The concentrations vary, but generally the range is 0.25-6 mg/L. As with nitrogen, the phosphorus content depends on the amount of water and the type of detergent and disinfectant. The content of

heavy metals in wastewater is very low [4]. Waste water must not contain halogens derived from the use of chlorine or chlorine-releasing compounds, with the exception of chlorine dioxide in a warm water cycle [5,6]

Secondary products as a result of organic matter reduction appear in sugar wastewater. These products are gases of aerobic and anaerobic origin (methane, ethane, carbon dioxide, carbon monoxide, sulfur dioxide and others) dissolved in wastewater. In addition, pesticide and artificial fertilizers of agrochemicals occur in the wastewater of sugar. As regards microbiological contamination, it is expected not only in sanitary waters, but also as a result of favorable conditions (warm water, plenty of organic matter) for the development of microorganisms [4].

The wastewater in the sugar industry plant is usually purified in a process, which is divided in three parts. The first part is the water recycling circle from the sugar beet discharge, flooding and cleaning, which are connected through a decanter. The second part is transporting two types of sludge to the depositional fields (lagoons). The third part is the additional decanter where the decontaminated water settles.

Experimental

The basic characteristics of the wastewater of the sugar industry are determined in accordance with the methods prescribed by international standards for wastewater. The process of determining the COD is based on the principle of oxidation of organic substances in a sample with potassium bichromate in a sulfuric acid medium with silver sulfate as a catalyst. After completion of the oxidation process, the amount of spent bichromate is determined titrimetrically according to the HRN ISO 6060: 2003 method. The pH value is determined by the method of domestic standards SRPS H.Z1.111:1987. The water temperature is measured according to SRPS H.Z1.106:1970. NH_4^+ ion is measured using spectrophotometer by method SRPS ISO 7150-1:1992. The total nitrogen content is measured by method SRPS EN 12260:2008, using oxidation method, and the phosphorus is measured by SRPS EN ISO 6878:2008 [7,8,9,10,11].

Results and discussion

At the inhabitant's insistence on obeying the Law of about water cleanliness, high taxes and fines for using fresh water and letting the effluent out into running water, forces sugar factories to construct a system of cooling and recirculating barometric water as well as creating an additional 23ha of new lagoon. Sugar factories that manipulate with 400-500 tonnes of sugar-beet need lagoons with an area of about 30-40 ha. Since 2006 this sugar factory has not been letting the effluent into the channel Bezdan-Vrba [12].

In the Table 1. the average values of some physical characteristics of the wastewater in the lagoons during the campaign of the sugar plant are shown. Every month during the campaign in the sugar factory a samples of wastewater from each lagoons were examined.

Table 1. The physical characteristics of the wastewater in the lagoons during the campaign of the sugar plant

Sampling time	Air temperature (°C)	Water temperature (°C)	pH value
October	17	16	6.5
November	10	9	7.4
December	-2	3	6.2

Beside the physical characteristics, the main chemical characteristics of the sugar factory wastewater were examined too and the average result are shown in the table 2. In the table 2. could be seen that the wastewater which is let into the lagoons has about 3000mg/l COD at the

end of the sugar campaign but after 4-5 months later the level of COD decreased for about 70%.

Interesting is that at the end of the sugar campaign, the level of P_2O_5 increases almost twice [12].

Table 2. The chemical characteristics of the wastewater in the lagoons during the campaign of the sugar plant

Sampling time	Organic compounds $KMnO_4$ (mg/l)	NH^{4+} (mg/l)	N (mg/l)	COD (mg O_2 /l)	BOD_5 (mg O_2 /l)	P_2O_5 (mg/l)
October	1120	0	6	980	640	1.5
November	1820	10	7	1643	962	1.5
December	3110	0	30	2750	1860	2.5

Conclusion

Due to the recirculation circuits in the frame of the sugar technology, the water consumption is reduced to a far smaller value. For example, for total water consumption of $15 \text{ m}^3/\text{t}$ of processed beet, the consumption of fresh water is only $0.25 - 0.4 \text{ m}^3/\text{t}$. Sugar factories that manipulate with 400-500 tonnes of sugar-beet need lagoons with an area of about 30-40 ha and in that case they do not need to let the wastewater effluent into the channel Bezdan-Vrbas. The main conclusion is that the wastewater which is let into the lagoons at the end of campaign, in December, has about 3000 mg/l COD, but after 4-5 months later the level of COD decreased for about 70%.

Acknowledgements

Presented study was financially supported through bilateral project between the countries of Hungary and Serbia (HU project no. TÉT-16-1-2016-0138 financed under the NKFIH-1557-1/2017; SRB project number 451-03-02294/2015-09/4).

References

- [1] J.P. Kushwaha, A review on sugar industry wastewater: sources, treatment technologies, and reuse, *Desalination and Water Treatment*, 53 (2015) 309-318
- [2] S. Ahmad, T. A. Mahmoud, Wastewater from a sugar refining industry, *Water research*, 16 (1982) 345-355
- [3] S. Gluck, A. Soltan, Treating high sugar wastewater in the Food & Beverage sector with new biological technology. A case study, *Proceedings of the environment federation, WEFTEC 2017, Water Environment Federation, 2017*, 176-189
- [4] M. Asadi, *Beet sugar handbook*, John Wiley & Sons, Inc., New York, 2007
- [5] F. Léder, I. Németh, J. Lajos, F. Mohos, A. Zsigmond, I. Boros, L., Völgyi, Környezeti hatások felmérése a gabona-, malom-, sütő-, édes- és cukoriparban különös tekintettel a melléktermékek, hulladékok kérdésére és a vízminőségvédelemre, Budapest, 1997.
- [6] J. Saratlic, *Studija o proceni uticaja zatečenog stanja kompleksa "AD fabrika šećera TE – TO, Senta" na životnu sredinu – izmena i dopuna*, Senta, 2010.
- [7] M. Dalmacija, S. Maletić, B. Dalmacija, *Praktikum iz zaštite voda I deo*, PMF-Departman za hemiju, biohemiju i zaštitu životne sredine, Novi Sad, 2013

- [8] B. Dalmacija, S. Maletić, D. Krčmar, M. Dalmacija, D. Tomašević, S. Ugarčina Perović, V. Pešić, Praktikum iz zaštite voda II deo, PMF-Departman za hemiju, biohemiju i zaštitu životne sredine, Novi Sad, 2014
- [9] Pravilnik o štetnim i opasnim materijama u vodama - "Službeni glasnik RS" br. 31/82
- [10] Zakonom o vodama ("Službeni glasnik RS" br. 46/91, 53/93 – dr. zakon, 67/93 – dr. zakon, 48/94 – dr. zakon, 54/96 i 101/05 – dr. Zakon – odredbe od člana 81. do 96., a odredbe člana od 99. do 107. prestaju da važe 1.01.2011. god. i "Službeni glasnik RS" br. 30/2010, osim članova 150. do 195. koji stupaju na snagu 1.01.2011. god.)
- [11] Pravilniku o štetnim i opasnim materijama u vodama - "Službeni glasnik RS" br. 31/82
- [12] Y. Anjaneyulu, V. Manickam, Enviroment Impact Assessment Methodology, India, 2007.

ANALYSIS OF THE CRYSTALLINE STRUCTURE AND MORPHOLOGICAL FEATURES OF PEROVSKITE MATERIALS PERFORMED THROUGH DIFFERENT WAYS

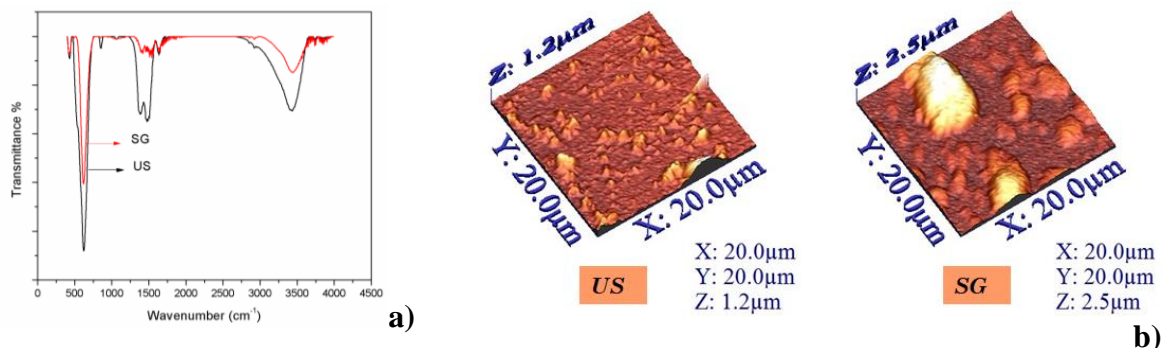
Paula Sfirloaga, Maria Poienar, Cristina Mosoarca, Paula Svera, Paulina Vlazan

*National Institute for Research and Development in Electrochemistry and Condensed Matter, Timisoara, P. Andronescu no.1, 300224, Romania
e-mail: paulasfirloaga@gmail.com*

Abstract

Manganites are mixed oxides of manganese whose broad stoichiometric formula is ABO_3 , where A is a lanthanide element and B is manganese, with possible oxygen non-stoichiometry. Usually the manganite compounds crystallize within perovskite structure, with the following possible space groups: ideal cubic structure $Pm\bar{3}m$, orthorhombic $Pbnm$ or rhombohedral $R\bar{3}CH$ [1, 2]. The phase purity and physico-chemical properties of perovskites depends upon the preparation methods, thus a variety of chemical methods have been developed to prepare lanthanum manganite nanoparticles at low cost and lower processing temperature [3].

In order to analyze the crystalline structure and morphological properties, $LaMnO_3$ materials were prepared by ultrasonic method with immersed sonotrode in the reaction medium (US) and the sol-gel technique (SG), followed by thermal treatment at low temperature. Structural characterization was performed by X-ray diffraction (XRD), Raman and Fourier transform infrared spectroscopy (FTIR), and morphological analysis was achieved using atomic force microscopy (AFM) and transmission electron microscopy (TEM).



FTIR spectra (a) and AFM images (b) of the $LaMnO_3$ materials obtained through different methods

Acknowledgements

The authors thank the X-ray Diffraction Laboratory from National Institute for Research and Development in Electrochemistry and Condensed Matter, Timisoara.

References

- [1] D. Varshney and N. Kaurav, Eur. Phys. J. B 37 (2004) 301.
- [2] S. Ghosh, A.D. Sharma, R.N. Basu, and H.S. Maiti, J. Am. Ceram. Soc. 3741 (2007) 3747.
- [3] G. Siquin, C. Petit, J.P. Hindermann, A. Kiennemann, Catal. Today **70**, 183–196 (2001).

HUMIC ACID REMOVAL FROM SURFACE WATER USING ULTRAFILTRATION MEMBRANE

Marjana Simonič¹

¹*Faculty of Chemistry and Chemical Engineering, University of Maribor, SI_2000 Maribor, Smetanova 17, Slovenia
e-mail: marjana.simonic@um.si*

Abstract

The main focus of research was to purify surface water with ultrafiltration, so it could be used as a source of drinking water. By measuring individual parameters and performing physical and chemical analysis, we determined the influence of natural organic matter (NOM) and checked the membrane fouling. The operation of the membrane was carried out at various transmembrane pressures (*TMP*) (2, 3 and 4 bar).

Purification with UF was carried out on the Memcell device with regenerated cellulose membrane type NADIR® PM UC030 with NMWCO of 30 kDa. With increasing pressure, the quality of the purified water increased. At 4 bars, the COD was totally removed from the Mura river sample.

Introduction

Characterisation and understanding of fouling layer, play most important role in the design of pre-treatment as well as impact the membrane cleaning protocol. [1] The UF membranes were studied for gathering drinking water from river water. UF with 300 to 2000 Da were tested. Removal of NOM depend on TMP, material, pore size of membrane, and Ca content. [2] COD_{Mn} was lowered by 31 to 42%, DOC from 42 to 47% by treating surface water. Coagulation was perfect for improvement of fouling and flux increase. [3]

The NOM removal from river water was studied. Certain analytical parameters were measured, such as concentration of humic acid, chemical oxygen demand (COD), temperature and conductivity, in river water and permeate.

Experimental

Membrane used was made from regenerated cellulose (NADIR® PM UC030) with NMWCO of 30 kDa, Support material was non-woven polyester. Characteristic pH range was 2-11 and temperature 5-55 C.

pH was determined by WTW pH meter and water conductivity was measured using WTW Conductometer. The concentration of humic acid was measured at 254 nm using spectrophotometer. The calibration curve is seen from Figure 1. The concentration of humic acid was calculated from presented curve.

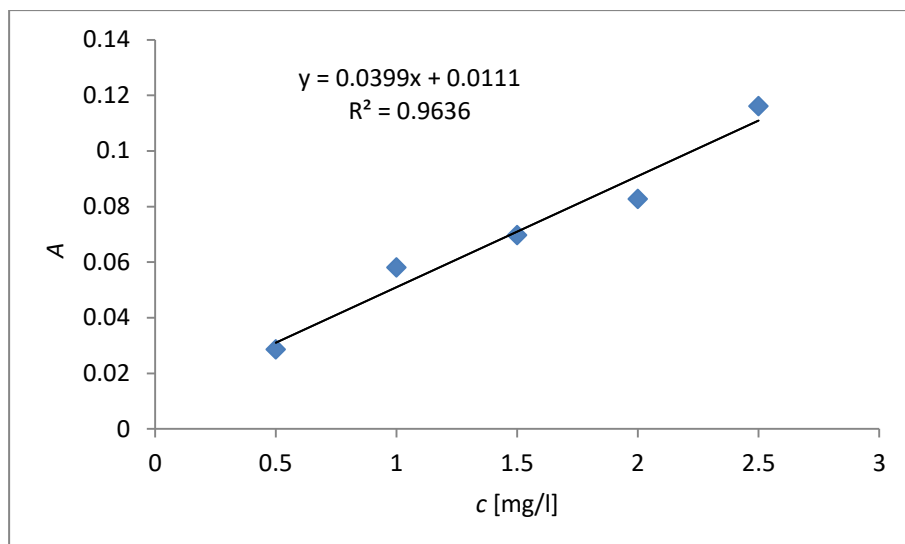


Figure 1: Calibration curve for humic acid determination

Filtration was performed on Memcell apparatus, shown in Figure 2. Water circulated through the system, permeate samples were taken and concentrate was recycled back into the feed reservoir.

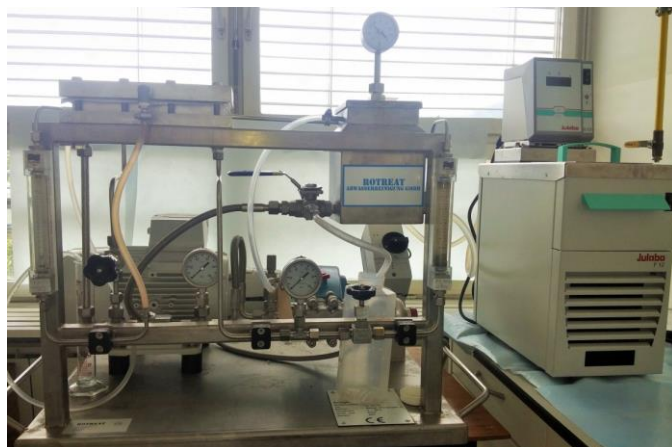


Figure 2: Memcell UF unit

Firstly, the permeability of membrane was determined. Then, four samples of surface water from the Mura and three from Drava river were taken. UF was performed at various transmembrane pressures (*TMP*) ranging from 2 to 4 bar at room temperature and original pH.

Results and discussion

The rate of water flow through the membrane was proportional to the TMP. Permeability was determined at 1.5 L/min.m².bar as seen from Figure 3. The flux was the same as the TMP was increased from 8 to 10 bars. However, producer recommendation for TMP was up to 6 bar, therefore TMPs from 2-4 bars were chosen for further analyses.

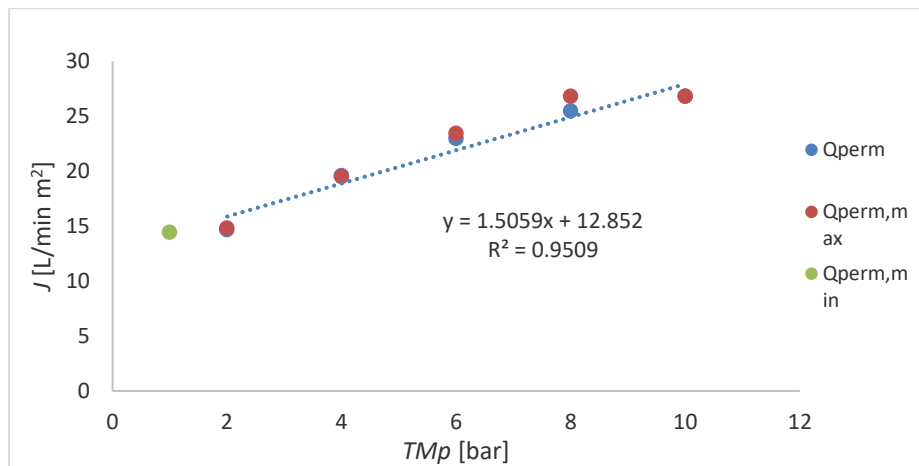


Figure 3: Membrane permeability

It was found that the pressure does not have an effect on the permeate flow, since during the UF process, regardless of the pressure, the decrease due to the formation of the filter cake, was similar. The results are presented in Figure 4. After half an hour of operation, the water flow reached the value around 11 ml/min for all tested water samples. The results at lower TMP were very similar, reaching steady state flow at 10 ml/min.

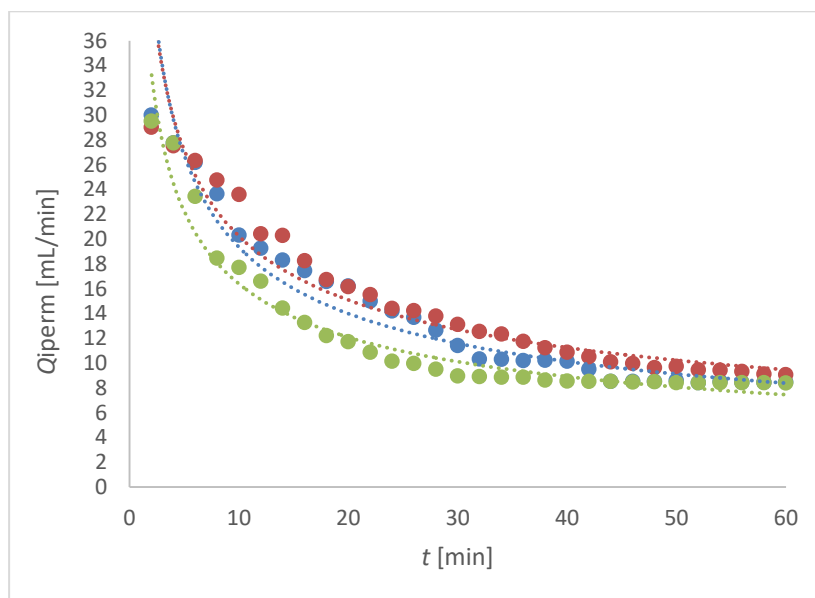


Figure 4: Water flux for Mura river permeate samples (different colour means different sample)

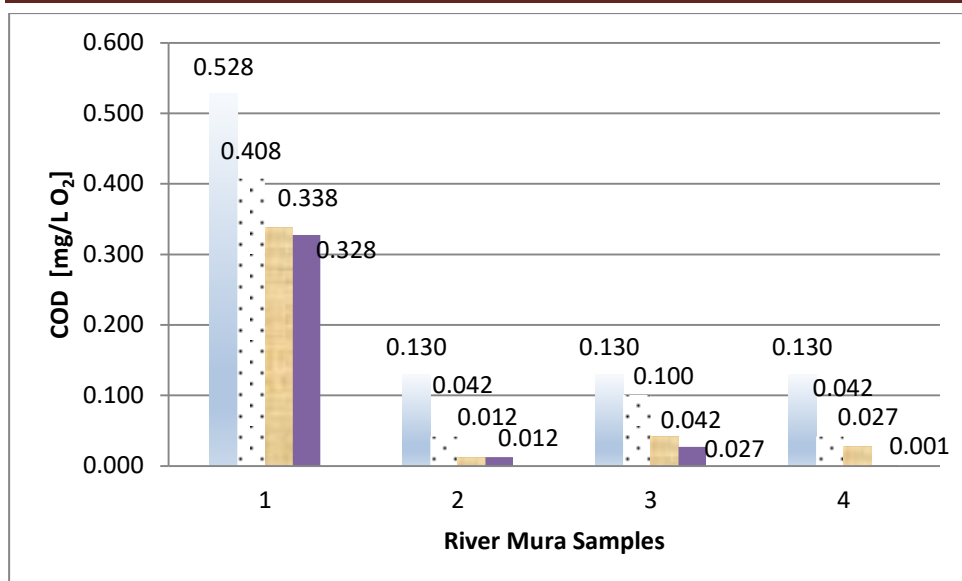


Figure 3: COD in Mura river samples: first column represents river water, second UF permeate at 2 bar, third after 3 bar and fourth after 4 bar

By increasing the pressure, the COD and the NOM content decreased. At the highest TMP at 4 bar, the highest decrease of COD was obtained, up to 99 % in case in the fourth sample. If the COD was higher in untreated water, the removal efficiency was lower.

Results of measurement of humic acid concentration showed the decrease at all TMPs. The optimal removal was 70 % in fourth sample at 4 bar. If the initial concentration of humic acid was higher, the removal was lower.

The limiting factor of UF systems is fouling which is defined as the precipitation of solutes in the form of a cake layer on the surface of the membrane. From Figure 4 it is seen that the cake layer forms in accordance with another study [4].

Conclusion

Tested membrane successfully removed humic acid from river water. The best removal was achieved in Mura river sample at 99 %. The limiting factor of UF systems is fouling which is defined as the precipitation of solutes in the form of a cake layer on the surface of the membrane. General parameters, such as pH, conductivity and temperature did not vary.

Acknowledgements

The research work was produced within the framework of the program P2-0032 Process System engineering and sustainable development, financially supported by Slovenian Research Agency.

References

- [1] M. Xie, W. Luo, S.R Gray, *Wat Res* 111 (2017) 375.
- [2] M. Alborzfar, C. Grøn, G. Jonsson, 20 (1994) 411.
- [3] S. Xia, X. Li, R. Liu, G. Li, *Desalination* 179 (2005) 369.
- [4] M. Kazemimoghadam, Z. Amiri-Rigi, J. Water Environ. Nanotechnol., 2 (2017) 311.

PHOTOCATALYTIC DEGRADATION OF MESOTRIONE IN THE PRESENCE OF TiO₂ HOMBİKAT MODIFIED WITH DIFFERENT Au NANOPARTICLES

Daniela Šojić Merkulov, Marina Lazarević, Aleksandar Djordjevic, Nina Finčur, Vesna Despotović, Nemanja Banić, Biljana Abramović

*University of Novi Sad, Faculty of Sciences, Department of Chemistry, Biochemistry and Environmental Protection, Trg Dositeja Obradovića 3, 21000 Novi Sad, Serbia
e-mail: daniela.sojic@dh.uns.ac.rs*

Abstract

Due to the harmful and toxic effects of organic pollutants scientists are searching for an effective method to remove these substances from the environment. One of the most efficient and environmentally friendly technologies for removing of organic water pollutants is photocatalytic degradation in the presence of various photocatalysts [1]. There are many metal-oxide photocatalysts which showed great photoactivity, but the most frequently used is TiO₂ [2]. Recently, great attention has been paid to Au nanoparticles because in the case of TiO₂ have showed extend of the spectral response to the visible light region in comparison with nonmodified TiO₂ [3], and efficiently suppress the e⁻-h⁺ recombination [4]. Mesotrione [2-(4-methylsulfonyl-2-nitrobenzoyl)-1,3-cyclohexanedione] is a selective herbicide for pre- and post-emergence control of broad-leaf and grassy weeds in corn. It was developed by the company Syngenta Crop Protection and it was registered in Europe in 2000, and in the United States in 2001. Beside good properties in control of weeds mesotrione has harmful and toxic effects on non-target organisms. Low sorption of mentioned herbicide may indicate the leaching potential in the groundwater from maize production fields [5], wherein its presence in environmental waters can lead to negative consequences on the aquatic ecosystem. In this paper, photocatalytic degradation of mesotrione using TiO₂ Hombikat modified with Au nanoparticles (nonmodified and modified with 2-mercaptoethanol, as well as with 2-mercaptoethanol and fullerenol nanoparticles) under simulated solar irradiation was investigated. Different volumes of various nanoparticles were added in suspension in order to enhance activity of commercial TiO₂ Hombikat under simulated sunlight.

Acknowledgments

The authors acknowledge financial support of the Ministry of Education, Science and Technological Development of the Republic of Serbia (Project No. 172042).

References

- [1] H. Dong, G. Zeng, L. Tang, C. Fan, C. Zhang, X. He, Y. He, Water Res. 79 (2015) 128.
- [2] J.-J. Chen, W.-K. Wang, W.-W. Li, D.-N. Pei, H.-Q. Yu, ACS Appl. Mater. Interfaces 7 (2015) 12671.
- [3] G. Wang, X. Wang, J. Liu, X. Sun, Chem. Eur. J. 18 (2012) 5361.
- [4] I. Bannat, K. Wessels, T. Oekermann, J. Rathousky, D. Bahnemann, M. Wark, Chem. Mater. 21 (2009) 1645.
- [5] K. Ferreira Mendes, M. Rodrigues dos Reis, M. Hiroko Inoue, R.F. Pimpinato, V.L. Tornisielo, Geoderma 280 (2016) 22.

HPLC-DAD DETECTION OF SOME PESTICIDE RESIDUES IN AGRICULTURAL PRODUCTS

Mariana N. Ștefănuț¹, Adina Căta¹, Fîruța Fițigău¹, Marius C. Dobrescu¹, Cristian Tănăsie¹, Dan Roșu¹, Ioana M.C. Ienașcu^{1,2}

¹ *National Institute of Research and Development for Electrochemistry and Condensed Matter, Dr. Aurel Păunescu Podeanu 144, 300569, Timișoara, Romania*

² *“Vasile Goldiș” Western University of Arad, Faculty of Pharmacy, Liviu Rebreanu 86, 310045, Arad, Romania*
e-mail: mariana.stefanut@gmail.com

Abstract

A rapid HPLC method for pesticide residues detection and monitoring in some vegetables, fruits and crops has been developed. The residual pesticide concentrations in samples were compared with MRLs authorized by EU laws.

Introduction

Productivity of fruits and vegetables has been greatly enhanced by developing techniques work, use of the best seeds and better water management, and also by the efficiency administration of pesticides. As pesticides are hazardous and toxic to human health [1], it is important to find any pesticide traces that can be ingested in order to increase and ensure the security in people nutrition.

Experimental

The pesticides extraction from food matrices was carried out using two methods: a) QuEChERS and b) ultrasonication in one step, in acetonitrile. After concentration and filtration, the extracts were subjected to HPLC-DAD analyses to identify and quantify the following pesticides: imidacloprid, deltamethrin, bromoxynil, and amidosulfuron.

Results and discussion

Deltamethrin was found in large quantities in tomatoes and potatoes, and bromoxynil in clementines. In the analyzed cereals, imidacloprid was found in larger quantities in wheat and maize.

Conclusion

The high sensibility and the short time of analyses recommend this method for pesticides monitoring at farmer's demand. Imidacloprin was found in almost all of the studied samples, in some samples exceeding the MRLs allowed of EU laws [2].

Acknowledgements

This work is part of the project PN 18-36 03 02/2018 “Determination of some pesticides from various foods by fast and modern physico-chemical methods”, carried out under NUCLEU Program funded by National Authority for Scientific Research (Romania).

References

- [1] K.H. Kim, E. Kabir, S.A. Jahan, Sci. Total Environ. 575 (2017) 525.
- [2] Commission Regulation (EU) 2017/1016 of 14 June 2017, OJ L 159, p. 1–47.

SUNFLOWER SEED CAKE AS A POTENTIAL BIORESOURCE FOR ISOLATION OF FLAVONOIDS

Zorica Stojanović¹, Snežana Kravić¹, Ana Đurović¹, Nada Grahovac², Ranko Romanić, Nada Hladni², Ana Marjanović Jeromela²

¹*University of Novi Sad, Faculty of Technology Novi Sad, Bulevar cara Lazara 1, Novi Sad, Serbia*

²*Institute for Field and Vegetable Crops, Maksima Gorkog 30, Novi Sad, Serbia
e-mail: zorica.stojanovic@uns.ac.rs*

Abstract

Sunflower seed cake is remaining after isolation of oil from sunflower seeds and practically represents a waste from production of cold pressed sunflower oils. This waste product is considered as a viable potential source of various natural compounds and can be exploited for the production of new products and isolation of valuable substances such as biologically active compounds and nutraceuticals. In addition, isolation of biologically active substances from food waste represents the way for recycling and may be economically attractive as well. Flavonoids represent a group of polyphenol compounds with a high antioxidant power. These phytochemicals are known to reduce many chronic diseases such as cardiovascular diseases, heart diseases, diabetes, obesity and certain cancer [1]. In this work we investigated the flavonoids content in seven sunflower seed cakes coming from cold pressed oil production. Flavonoids are extracted by using 80% ethanol and ultrasound-assisted extraction at 30°C for 10 minutes. Total flavonoid content is determined by a colorimetric method [2]. The results showed that sunflower seed cakes contained significant amounts of total flavonoids. The total flavonoids content is found to be in the range from 12.3 to 24.6 mg of catechin equivalent/g. The results proved that sunflower seed cakes obtained from cold pressed oil production represent valuable by-product and can be used as a raw material for isolation of bioactive flavonoids which could be further applied for development of various functional foods.

Acknowledgements

The authors are grateful to the Ministry of Education, Science and Technological Development of the Republic of Serbia for supporting this work by Projects TR31014 and III 46009.

References

- [1] S. Vijayalaxmi, S.K. Jayalakshmi, K. Sreeramulu, J. Food Sci. Technol. 52 (2015) 2761.
- [2] J.S. Bao, Y. Cai, M. Sun, G. Wang, H. Corke, J. Agric. Food Chem. 53 (2005) 2327.

INFLUENCE OF PHOTOCATALYSTS MASS ON PHOTOCATALYTIC DEGRADATION OF MIXTURE OF PHARMACEUTICALS BY OXIDE ZnO/TiO₂ NANOPOWDER

Dragana Strbac^{1*}, Senka Bubulj¹, Mladenka Novakovic¹, Goran Strbac², Ivana Mihajlovic¹

¹*University of Novi Sad, Faculty of Technical Sciences, Trg Dositeja Obradovica 6, Novi Sad, Serbia*

²*University of Novi Sad, Faculty of Science, Trg Dositeja Obradovica 4, Novi Sad, Serbia*

**draganastrbac@uns.ac.rs*

Abstract – In this paper, the efficiency of photocatalytic degradation of mixture of pharmaceuticals (naproxen, diclofenac, ketoprofen and ibuprofen) in the aqueous medium using nanoparticle photocatalysts powder ZnO/TiO₂, activated by UV radiation, has been examined. It has been shown that the degradation of diclofenac, ketoprofen and ibuprofen takes place efficiently regardless of the mass of the catalyst. Naproxen has proven to be the most resistant pharmaceutical and degradation constants are calculated for naproxen only, which may be used as guidelines in further research.

Keywords: photocatalysis, pharmaceuticals, naproxen, diclofenac, ketoprofe, ibuprofen, ZnO/TiO₂

Introduction

Emergent substances are a specific group of synthesized or natural compounds, identified as pollutants, which are predominantly produced in various industrial branches, especially in the chemical, petrochemical, metal and pharmaceutical industries, and through wastewater they are introduced and transported through all spheres of the environment. These substances are used in everyday anthropogenic activities, and can be from a group of chemical compounds of pharmaceuticals, disinfectants, products for personal and household hygiene, pesticides, wood preservatives and others. Continuous discharge of municipal and industrial wastewater with or without treatment into aquatic systems provokes the emergence of a new feature - pseudopersistence. Primary pathways that pharmaceuticals reach into surface waters include conventional wastewater treatment plants and systems for discharging untreated sanitary wastewater. Technological operations that are applied to the treatment of municipal and industrial wastewater are not able to isolate or remove pharmaceuticals from the outflow streams, and certain stages of treatment may induce degradation of pharmaceuticals to forms that have even more significant negative effects on the environment [1]. Additional concern is the fact that naproxen, diclofenac, ketoprofen, ibuprofen, as well as a large number of other pharmaceuticals, remain biologically active in aquatic matrix over a long period of time (more than a year and possibly activity up to several years), which causes accumulation and a harmful effect on organisms and the environment.

The path of distribution of pharmaceuticals and their metabolites, as well as the method of disposal of released pollutants depend on the physico-chemical properties and basic characteristics of the environment in which the pollutant is released, and they are directly dependent on the coefficient of sorption or retention in soil mass and sediment of surface waters [2]. Environmental risk assessments are mainly based on an active component, however, pharmaceuticals are present in the environment as a multi-component mixture, a chemical cocktail with a different ecotoxicological effect from the individual component, and

it is very important to investigate the processes for degradation of these pollutants under the presence conditions combined pharmaceuticals.

Among the methods that have been developed for water disinfection, advanced oxidation processes such as heterogeneous photocatalysis appears as an emerging technology for the decomposition of most of the organic pollutants [3]. While nanostructured TiO_2 is being the most explored material up until now ZnO appears as a strong rival to due to its considerably better photocatalytic activity (PC) [4]. Therefore, interest has also arisen on the photocatalytic properties of mixed oxide nanopowders, which could potentially combine the properties of the individual oxides.

Experiment

ZnO/TiO_2 mixed powder photocatalysts were prepared using a simple, low-cost, threeand three-step mechanochemical solid-state method. Starting precursors (ZnO and TiO_2 Sigma Aldrich, purity 99.9%) were grounded in an agate mortar for 10 min in molar ratio 2:1, annealed at 700°C in air for two hours and grounded again for 10 min. It has recently been reported that binary nanopowders based on ZnO exhibit photocatalytic activity which depends slightly on molar ratio, which is however maximized for ZnO -rich compositions [5].

The photocatalytic decompositions of chosen pharmaceuticals were carried out at ambient temperature in aqueous solution in batch mode. The aqueous solution was stirred for 1 h in the dark to establish adsorption-desorption equilibrium between the pharmaceutical and photocatalyst before being irradiated. The aqueous solutions were exposed under continuous UV irradiation. In order to investigate the change in composition of the investigated pollutant, aliquots were collected at certain time intervals (5, 10, 20, 30, 40, 50, and 60 minutes). Each sample was filtered through filter paper (diameter $0,45\ \mu\text{m}$ mm) in order to separate the nanoparticles from the solution. After the filtration step, 1 ml of sample was transferred into 1,5 ml vials. A HPLC (high performance liquid chromatography) with diode array detector (Agilent 1260 series) was used for the measurement of each specific pharmaceutical concentration after photocatalytic degradation.

Results and Discussion

Experiments have shown that the mixture of nanoparticle powder ZnO/TiO_2 possesses prominent photocatalytic abilities: after 5 minutes from the beginning of the experiment, the concentration of pharmaceuticals decreased almost to half, while diclofenac, ketoprofen and ibuprofen from the mixture have almost totally degraded after 60 minutes. According to the obtained experimental data, naproxen is the most resistant pharmaceutical pollutant, and the experimental data were processed depending on the effect of the mass of the catalyst (Figure 1). The degradation kinetics of naproxen was quantified by fitting the experimental data where the concentration change depends logarithmically on time:

$$\ln\left(\frac{C_0}{C}\right) = kt$$

where k is the rate constant and C_0 , C are the analyte concentrations before and after UV irradiation, respectively [6,7] (Figure 2). Diclofenac, ketoprofen and ibuprofen are so rapidly disintegrating that Langmuir-Hinshelwood's model cannot be applied, since this dependence no longer describes the approximate experimental data (The example of diclofenac is presented in Figure 3).

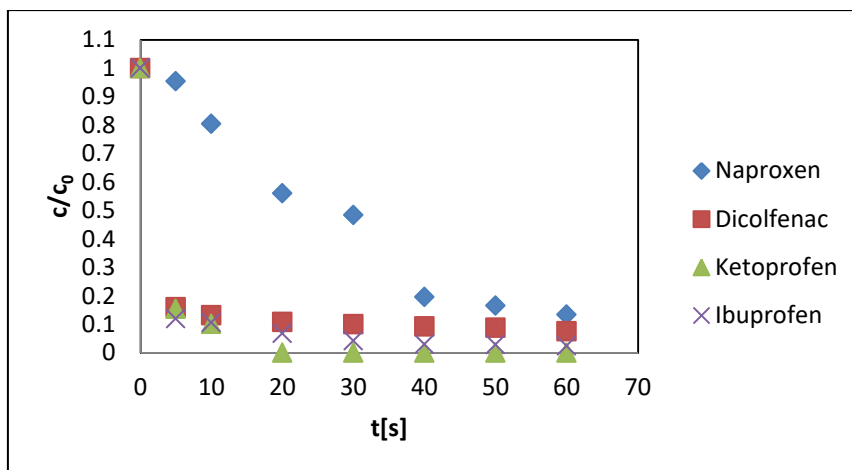


Figure 1. Photocatalytic degradation of a mixture of pharmaceuticals using ZnO/TiO₂ nanopowder

For the decomposition of naproxen, based on the calculated degradation constants, the weight of the 60 mg catalyst was best demonstrated (Figure 4).

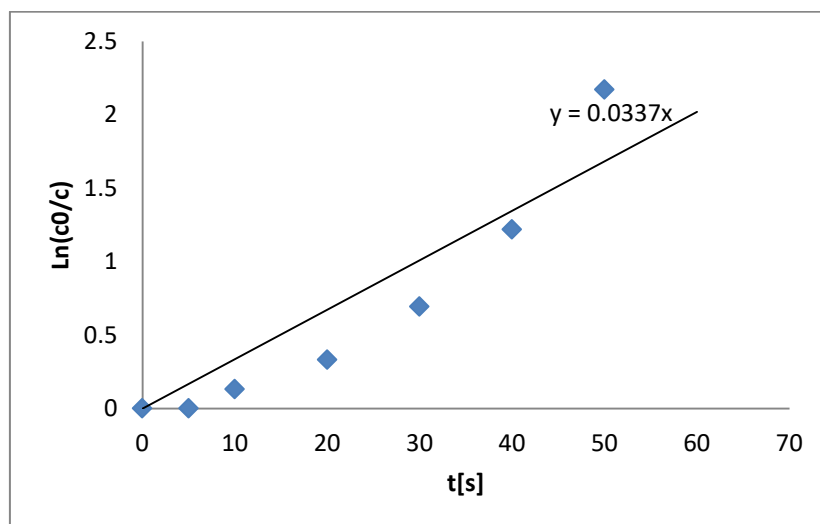


Figure 2. Kinetic of Naproxene photocatalytic degradation of in a mixture of pharmaceuticals using ZnO/TiO₂ nanopowder

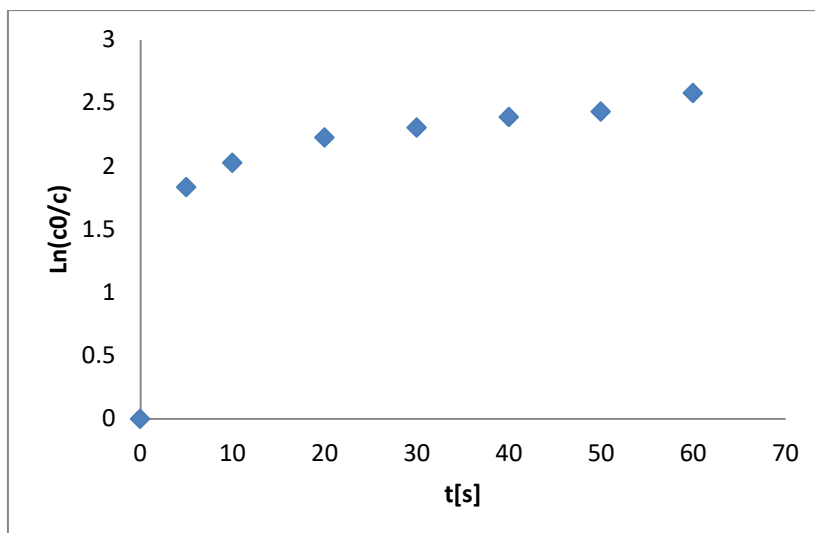


Figure 3. Deviation of kinetics of diclofenac photodegradation from Langmuir-Hinshelwood model

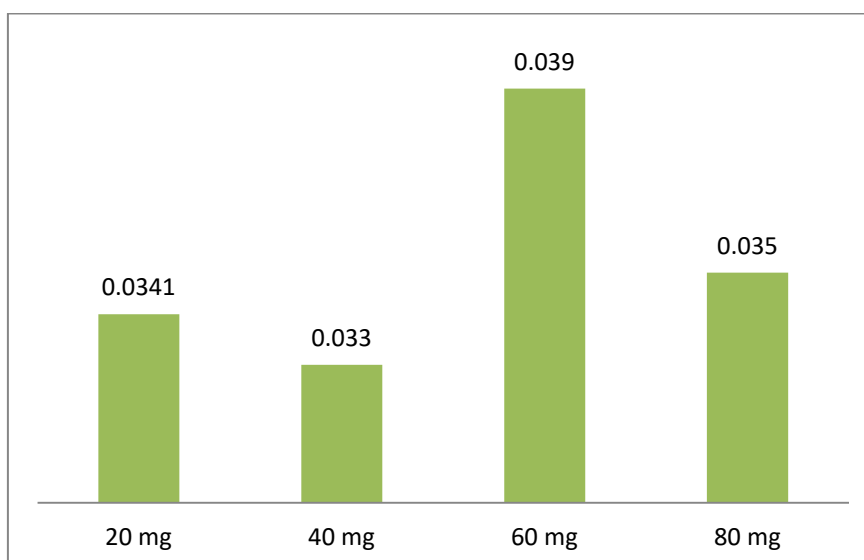


Figure 4. Degradation constants of Naproxene dependence on photo-catalysts mass

Conclusion

The mixture of nanoparticle powder ZnO/TiO₂ possesses distinctive photocatalytic abilities: after 5 minutes from the beginning of the experiment, the concentration of pharmaceuticals decreased almost to half, while diclofenac, ketoprofen and ibuprofen from the mixture were almost totally degraded after 60 minutes. According to the obtained experimental data, naproxen was the most resistant pharmaceutical pollutant, and experimental data were processed depending on the effect of the mass of the catalyst. Diclofenac, ketoprofen and ibuprofen are so rapidly degrading in the given experimental conditions, so Langmuir-Hinshelwood's model cannot be applied, since this dependence no longer describes the experimentally obtained data. On the basis of the calculated degradation constants, for the decomposition of naproxen the weight of the 60 mg catalyst was best revealed.

Acknowledgement

The presented research is partly financed within a project of the Government of Vojvodina “Synthesis and application of new nanostructured materials for the degradation of organic pollutants from municipal landfill leachate in Vojvodina” 142-451-2387/2018-01/02.

References

- [1] Ravina M, Campanella L, Kiwi J., Water Research 2002. 36(14), 3553-3560.
- [2] Boxall A.B.A, Kay P, Blackwell P.A, Fogg L.A. Fate of veterinary medicines applied to soils. In Pharmaceuticals in the Environment, 2004. ch.4, 165–180. Heidelberg, Germany: Springer.
- [3] Phillips R. Sources and Applications of Ultraviolet radiation. 1983. London, UK: Academic Press.
- [4] Aggelopoulos, C. A., Dimitropoulos, M., Govatsi, K., Sygellou, L., Tsakiroglou, C. D., Yannopoulos, S. N., Appl. Catal. B: Environ. 205, 2017. 292–301.
- [5] Ivetić T., Finčur N, Đaćanin Lj, Abramović B, Lukić-Petrović S. Materials Research Bulletin 2015. 62(1), 114–121.
- [6] Hinshelwood, C. N., The Kinetics of Chemical Change, first ed., 1940. Oxford Clarendon Press.
- [7] Langmuir, I., J. Am. Chem. Soc. 1918. 40, 1361–1403.

CHARACTERISATION OF COLLOIDAL GOLD SYSTEMS BY PHOTOMETRY, SPECTROPHOTOMETRY AND CHRONOPOTENTIOMETRIC STRIPPING ANALYSIS

Jaroslava Švarc-Gajić, Marijana Ačanski, Zorica Stojanović, Nataša Nastić

Faculty of Technology, University of Novi Sad, Bulevar cara Lazara 1, 21000 Novi Sad, Serbia

e-mail: jsgajic@gmail.com

Abstract

Colloidal systems of different metals attract lot of attention in scientific research due to their specific physico-chemical properties and possible application routes. In this respect particularly interesting is colloidal gold that has very broad application in different fields, including catalysis, biological and cancer research, electronics etc. Colloidal gold was generated by electric arc discharge method in a home-made generator. The generator consisted of a control system which maintained a constant distance between the electrodes (2 mm), a power supply system and amperometer which controlled the arc discharge parameters, halogen bulbs used as resistors, a glass container with deionized water and a magnetic stirrer. Generation technique consisted in adding 10 µl of 35% hydrochloric acid to 500 ml of distilled water, submerging gold (99.9999%) electrodes (d=1 mm) in the solution and initiating electric arc discharge. Initial voltage was set to 20-70 V and the current was maintained at 20 ± 5 A during entire generation process (30 min) by adjusting electrode distance. The influence of the initial voltage on optical characteristic of colloidal systems was examined by photometry and spectrophotometry, whereas the concentration of free gold ions was determined by chronopotentiometric stripping analysis at glassy carbon electrode. Photometric and spectrophotometric analyses were performed to characterise indirectly particle size distribution, since light absorption, reflection and transmission are highly affected by particle size. The size of gold nanoparticles, in return, affects strongly their properties and behavior in biological systems. By using both yellow-green and blue optical filters in photometric analysis, absorption increased almost linearly in the entire voltage range. Spectrophotometric analysis revealed absorption maximum in the range of 470-590 nm, depending on the initial voltage. Absorption maximum increased with initial voltage, indicating increase in the concentration of colloidal gold. Initial voltage also affected dominant particle size. Particle size distribution was determined by Zetasizer Nano ZS90. Dominant particle size was in the range from 5 nm (at 50 V) to 19 nm (at 30 V). The influence of generation potential on the concentration of free gold was evaluated by chronopotentiometric stripping analysis at glassy carbon electrode. As a supporting electrolyte 0.1 HCl was used. Electrolysis potential was -0.6 V. After 600 s of electrolysis dissolution current of 8.3 µA was applied to reach final potential of +1.25V. The concentration of free gold increased linearly with initial voltage ($y=0.01x+0.73$; $r^2=0.9849$) from 0.95 mg/l (at 20 V) to 1.3 mg/l (at 70 V).

SYNTHESIS, CHARACTERIZATION AND ANTICORROSIVE PROPERTIES OF PSEUDO-BINARY OXIDE NANOMATERIALS

Mihaela Birdeanu¹, Corina Orha¹

¹National Institute for Research and Development in Electrochemistry and Condensed Matter, Plautius Andronescu Street, 300224 Timisoara, Romania
e-mail: mihaelabirdeanu@gmail.com

Abstract

This paper presents some results of the study regarding the corrosion inhibition properties evaluated in 0.1 M NaCl environment of drop casting deposited on steel, using $\text{Zn}_3\text{Ta}_2\text{O}_8$ and $\text{Zn}_3\text{Nb}_2\text{O}_8$ nanomaterials.

$\text{Zn}_3\text{Ta}_2\text{O}_8$ and $\text{Zn}_3\text{Nb}_2\text{O}_8$ nanomaterials were obtained by hydrothermal method. The starting materials used during the synthesis were: tantalum (V) oxide - Ta_2O_5 (99.99%, Merck), niobium (V) oxide - Nb_2O_5 (99.99%, Merck) and zinc acetate dihydrate - $(\text{CH}_3\text{COO})_2\text{Zn} \times 2\text{H}_2\text{O}$ Merck, 99.5 %) while keeping the molar ratio at 1:3. The pH of the obtained mixtures was adjusted to 12 by using sodium hydroxide (NaOH) solution of 10 M concentration. The resulting suspensions were transferred into Teflon-lined stainless steel autoclaves and then these were introduced in an oven at 220 °C for 8 h long. The filling degree of the used autoclaves was set at 70%. The resulting white precipitates were filtrated, and then five times washed with distilled water and, finally, three times with ethylic alcohol. In the next stage, the precipitate was dried in an oven at 80 °C for 6 h [1-3].

The obtained materials were used for thin films depositions using the drop casting method. The depositions were realized on polished carbon steel electrode disks (10 mm diameter and 2 mm thick).

The surfaces of the thin films realized using the pseudo-binary oxides nanomaterials $\text{Zn}_3\text{Ta}_2\text{O}_8$ and $\text{Zn}_3\text{Nb}_2\text{O}_8$ on electrode steels were morphological and topographical investigated using the scanning electron microscopy (SEM – Model Inspect S) and the atomic force microscopy (AFM - Model Nanosurf[®] EasyScan 2 Advanced Research microscope) using the non-contact mode cantilever (scan size 2.3 μm x 2.3 μm).

From AFM measurements, according to equations from [4], were determined the topographical parameters S_a – the average roughness and S_q – the mean square root roughness for each drop casting deposition's surface on steel electrodes. The obtained values were calculated using the NanoSurf EasyScan 2 software.

The corrosion behaviour was studied using on Voltalab potentiostat Model PGZ 402 with single compartment three-electrode cell. Platinum wire was employed as counter electrode and the saturated calomel electrode (SCE) was the reference electrode. All potentials reported in this article were referenced to the standard hydrogen electrode (SHE). Bare and coated steel substrates were used as working electrodes. The potentiodynamic polarization curves were analyzed using VoltaMaster 4, v.7.09 software. This software performed the Tafel fitting and calculated the values of the corrosion potential (E_{corr}), corrosion current density (i_{corr}) and corrosion rate (v_{corr}). The measurements were performed by sweeping the potential between – 700 and 100 mV, in 0.1 M NaCl electrolyte solution, at a scan rate (v) of 1 mV/s. The degree of the corrosion inhibition efficiency IE (%) has been calculated [5] for each drop casting deposition.

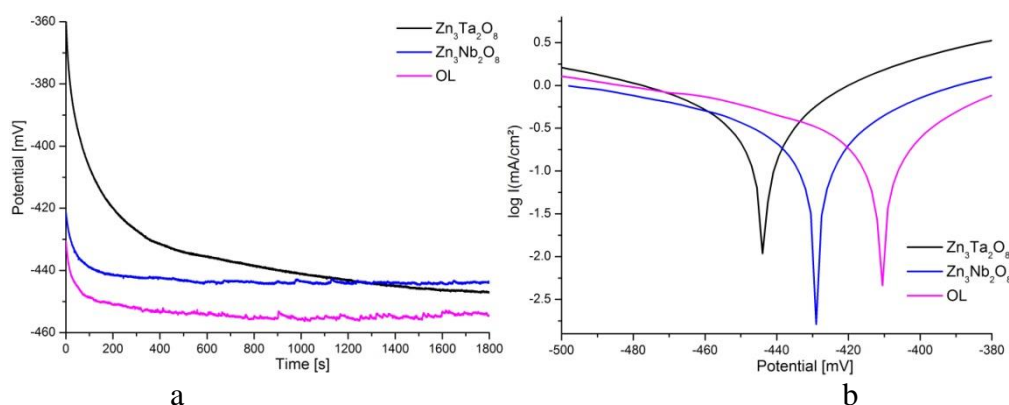


Figure 1 a) Evolution of open circuit potential with time for investigated electrodes, in 0.1 mol / L NaCl saline solution; b) Tafel representation of polarization curves recorded in 0.1 mol / L NaCl saline solution

The anticorrosive properties of the coatings were evidenced by electrochemical measurements taken in 0.1 NaCl acidic media. For all the drop casting depositions consisting in pseudo-binary oxide materials on carbon steel electrodes a degree of the inhibition efficiency over 70% was obtained.

Acknowledgements: The authors kindly acknowledge Romanian financing agency UEFISCDI- PN III No. 107 PED / 2017 project - CorOxiPor:

References

- [1] M. Bîrdeanu, A.-V. Bîrdeanu, A.S. Gruia, E. Fagadar-Cosma, C.N. Avram, J Alloy. Comp. 573 (2013) 53-57.
- [2] M. Bîrdeanu, M. Vaida, F. Peter, E. Fagadar-Cosma, 21th International Symposium on Analytical and Environmental Problems", Szeged, Hungary, 2015
- [3] M. Bîrdeanu, A.-V. Bîrdeanu, I. Popa, B. Taranu, F. Peter, I. Creanga, A. Palade, E. Fagadar-Cosma, Comparative research regarding corrosion protective effect of different sandwich type nanostructures obtained from porphyrins and pseudo-binary oxides by changing the deposition order, NANOCON 2014-6th International Conference on Nanomaterials, Nov 5th – 7th, Brno, Czech Republic, Conference ISI Proceedings, Ed. TANGER Ltd., Ostrava, Czech Republic, 2015, p. 262-268, ISBN 978-80-87294-53-6.
- [4] V. Kapaklis, P. Pouloupoulos, V. Karoutsos, Th. Manouras, C. Politis, Thin Solid Films, 2006, vol. 510, pp. 138.
- [5] Z. Ahmad, Principles of Corrosion Engineering and Corrosion Control, Butterworth-Heinemann / IChem Series, Elsevier 2006.

DEVELOPMENT OF FUNCTIONAL PRODUCTS BASED ON HOREHOUND USING INNOVATIVE EXTRACTION TECHNOLOGIES

Jelena Vladic, Aleksandra Gavaric, Natasa Nastic, Senka Vidovic

*Department of Biotechnology and Pharmaceutical Engineering, Faculty of Technology,
University of Novi Sad, 21000 Serbia*

Marrubium vulgare, which belongs to the genus *Lamiaceae*, has been present in pharmacopoeias for decades. *Marrubii herba* is a medicinal plant known for its diverse uses including inflammatory, gastroenterical, and respiratory disorders. In the past, white horehound was traditionally used especially in context of respiratory disorders. According to literature, this perennial herb is usually provided in the forms of herbal tea and liquid extract with ethanol. Dry powder extracts are more convenient than the liquid ones in terms of stability, reduced bulk size, and higher concentration of active compounds. Therefore, in order to obtain dry powders, spray drying of subcritical water extract of horehound was applied. Two samples (with addition of maltodextrin as carrier in concentrations 0% and 10%) were obtained and physical-chemical characteristics of powders were determined. In both powders, moisture content was lower than 5%. Powder obtained using 10% maltodextrin showed bulk density of 86.96 mg/mL and hygroscopicity of 19.83%. The powders also showed high antioxidant activity, that is, low IC_{50} (0.02 mg/mL) and EC_{50} values (0.07 mg/mL) which make them suitable for application as an ingredient of herbal products.

BISMUTH DOPING EFFECTS ON STRUCTURAL AND MORPHOLOGICAL PROPERTIES OF SODIUM TITANATE SYSTEM

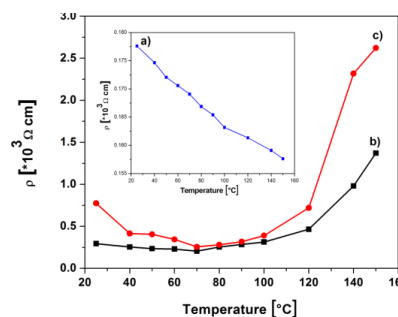
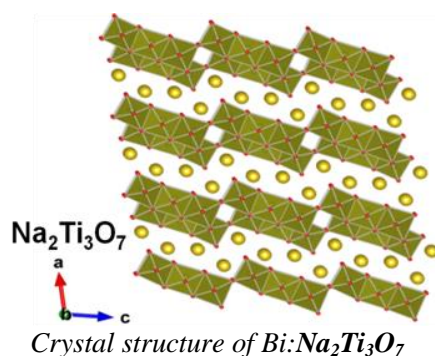
Paulina Vlazan, Paula Sfirloaga, Daniel Ursu, Mihaela Birdeanu, Maria Poienar, Rus Florina Stefania, Novaconi Stefan

*National Institute for Research and Development in Electrochemistry and Condensed Matter,
Department of Condensed Matter, 1 Plautius Andronescu St., 300224 Timisoara, Romania
e-mail: vlazanp@yahoo.com*

Abstract

Energy shortage and environmental pollution have become urgent problems that restrict social development and endanger the health of the planet. For sustainable development of society, the most effective route is the active development and utilization of clean and renewable energy sources [1]. In this regard, the sodium titanates are of great interest for possible applications such as photocatalysts [2], as fuel-cell electrolytes, [3] in the treatment of industrial wastewaters and contaminated groundwaters [4] and in a number of medical applications [5,6].

In this paper, we report the study of bismuth doping effects in the sodium titanate materials, synthesized by hydrothermal method. Moreover, the influences of the synthesis temperature and autoclaving time on the structural and morphological properties are presented. The structure and morphology of Bi-doped sodium titanate nanocrystals are studied in the context of their possible use for sensors application. These materials are prepared using hydrothermal method at 200°C for 12h followed by heat treatment at 600°C, 6 hours for a better crystallization. Characterization of the obtained compounds was achieved by X-ray diffraction (XRD), scanning electron microscopy (SEM), atomic force microscopy (AFM) and electrical behavior (ρ/T) was studied. The X-ray diffraction analysis showed that all samples are homogenous and crystallize in the monoclinic system with the P12/m space group. The obtained particles are as needle-like shape and their size decreases with increasing of dopant concentration.



Temperature dependence of the electrical resistivity in the Bi-doped Na₂Ti₃O₇: a)-Bi 1%, b)-Bi 2% and c) Bi 3%

Acknowledgement

This work was supported by a grant of the Romanian Ministry of Research and Innovation, CCCDI-UEFISCDI, project number PN-III-P1-1.2-PCCDI-2017-0391/CIA_CLIM-Smart buildings adaptable to the climate change effects, within PNCDI-III.

References

- [1] J. Shi, L. Guo, ABO₃-based photocatalysts for water splitting, *Progress in Natural Science: Materials International*, 22 (2012) 592–615.
- [2] J.H. Choy, H.C. Lee, H. Jung, S.J. Huang, A novel synthetic route to TiO₂-pillared layered titanate with enhanced photocatalytic activity, *J. Mater. Chem.*, 11 (2001) 2232-2234.
- [3] D.J.D. Corcoran, D.P. Tunstall, J.T.S. Irvine, Hydrogen titanates as potential proton conducting fuel cell electrolytes, *Solid State Ionics* 136/137 (2000) 297-303.
- [4] Elvington, M.C.; Click, D.R.; Hobbs, D.T. *Sep. Sci. Technol.*, 45 (2010) 66-72.
- [5] Hobbs, D. T.; Messer, R. L. W.; Lewis, J. B.; Click, D. R.; Lockwood, P. E.; Wataha, J. C.; *J. Biomed. Matls. Res. Part B: Appl. Biomats.*, 78 (2006) 296-301.
- [6] Davis, R.; Hobbs, D.T.; Lockwood, P. E.; Messer, R. L. W.; Prices, R.; Lewis, J. B.; Wataha, J. C.; *J. Biomed. Matls. Res. Part B: Appl. Biomats.*, 83B (2007) 505-511.

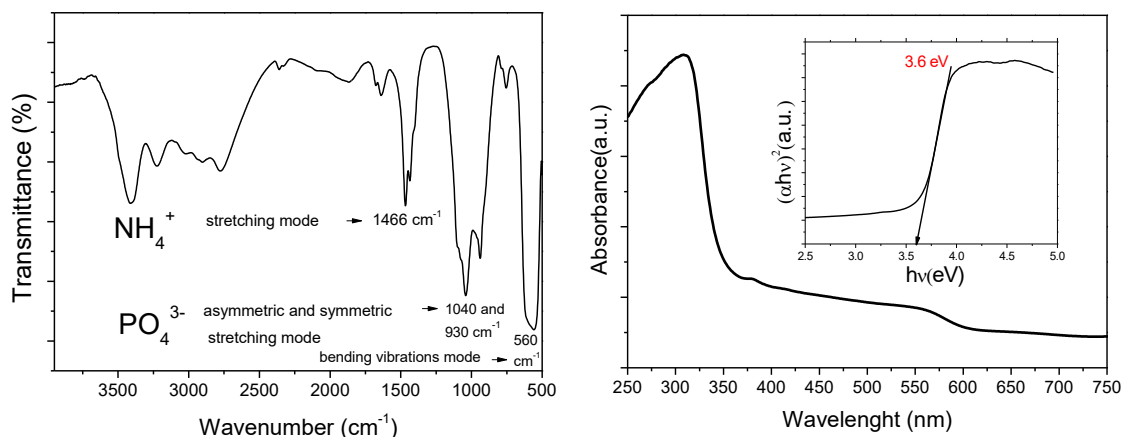
STRUCTURAL AND OPTICAL PROPERTIES OF LAYERED AMMONIUM-IRON (II) PHOSPHATE MONOHYDRATE

Maria Poienar, Paula Sfirloaga, Anamaria Dabici, Paulina Vlazan

*National Institute for Research and Development in Electrochemistry and Condensed Matter, Timisoara, P. Andronescu no.1, 300224, Romania
e-mail: maria_poienar@yahoo.com*

Abstract

Ammonium-iron phosphates phases have recently attracted more interest due to their promising applications as fertilizer [1] or as promising anode material for lithium-ion battery application [2], for example. In this context, $\text{NH}_4\text{FePO}_4 \cdot \text{H}_2\text{O}$ materials are obtained from FeCl_2 , Fe_2O_3 and $\text{NH}_4\text{H}_2\text{PO}_4$ as starting reagents and NH_4OH solution by one step hydrothermal method. The factors that affect the formation processes and the product morphologies: the pH and reaction time have been analysed. The as-synthesized compounds have been characterized by X-ray diffraction (XRD), scanning electron microscopy (SEM) and Fourier Transform infrared (FT-IR) spectroscopy. The optical properties of $\text{NH}_4\text{FePO}_4 \cdot \text{H}_2\text{O}$ were for the first time studied in this research work: the material displays p-type conductivity behaviour and the value for direct optical band gap E_G is estimated to be approximately ~ 3.6 eV. The results from this paper suggests that these phosphate materials could be suitable candidates for several applications as for example in photovoltaic technology.



FT-IR spectra (left) and optical absorption spectra (right) obtained at room temperature (insert: determination of the direct optical band gap E_G) of $\text{NH}_4\text{FePO}_4 \cdot \text{H}_2\text{O}$.

Acknowledgements

The authors thank E. Berei and D. Ursu for help during the materials characterisation.

References

- [1] N. Barros, C. Airoidi, J.A. Simoni, B. Ramajo, A. Espina, J.R. Garcia, *Thermochimica Acta* 441 (2006) 89–95.
- [2] T. Zhang, H. Wu, S. Wang, G. Zhang, C. Feng, H. Liu, *Materials Letters* 225 (2018) 69–72.

ENVIRONMENT BETWEEN POLLUTION AND THERAPY

Mirela Ahmadi¹, Cornelia Milovanov¹, Boldura Oana¹, Dorel Dronca², Narcisa Mederle¹, Ileana Nichita¹, Oprea Adrian², Tulcan Camelia¹

¹*Faculty of Veterinary Medicine, Banat's University of Agricultural Sciences and Veterinary Medicine „King Michael I of Romania“, Timisoara-300645, Calea Aradului 119, Romania*

²*Faculty of Bioengineering of Animal Production, Banat's University of Agricultural Sciences and Veterinary Medicine „King Michael I of Romania“, Timisoara-300645, Calea Aradului 119, Romania*

E-mail: ddronca@animalsci-tm.ro

Abstract

Environment is a critical complex index for quality of the habitat for humans, animals and plants. Ecosystems are communities of different species of plants and animals which lives together, depending one of another, being influenced by the pollution of air, water or soil. Some plants and animals are used as natural bioindicators of environmental quality, thus in pollution situations the specific organisms cannot live in the ecosystem. Then, environment was since ancient the source of the natural therapeutics products. But in case of pollution the plants used in curing do not have the same effect, or even cannot be used as therapy due to the pollutant contains. So, the environmental quality is very important not only for the ecosystems, but also for some applications of plants in natural products therapy.

Introduction

Environmental bioindicators could be represented by biological, physical or chemical indicators which can give information about the quality of the ecosystem. Biological bioindicators are plants, animals, microorganisms; physical and physic-chemical indicators are represented by the pH, the temperature, electrical conductivity, color, smell, texture and others; and chemical indicators are organic carbon content, total nitrogen, phosphorus, potassium, cation exchange capacity, oxygen compounds, dissolved oxygen, and other chemicals [Bending et al., 2004; Ahmad et al., 2006; Bianchi et al., 2013; Hannah et al., 2016; Turner and Montagna, 2016; Fusaro et al., 2018].

Bioindicators and environment quality

Bioindicators are living organisms which can screen the quality of an ecosystem, in terms of nutritional and pollution characteristics. Thus, for example, some plants can be nutrients for animals and some animal products can become nutritional facts for plants. But when pollutants concentrate too much, the plants nutrients are affected both in quantity and quality, and also further the animals are affected due to the quality and quantity of nutritional plants.

Experimental researches demonstrated that there are some specific organic entities, like plankton, which respond very quickly to the environmental changes, and due to this very important characteristic these organisms became bioindicator of water quality and pollution. This phenomenon is explained by the fact that some pollutants modify several water characteristics such as light transmission, temperature, chemical composition and pH, dissolved oxygen. The most important advantages are that these bioindicators could be used as early pollution diagnosis, can be used for evaluate the degree of contamination, being in the same time a very good economical option for environmental pollution evaluation [Khatri and Tyagi, 2015; Parmar et al., 2016].

Soil contaminants and bioindicators

Usually the bioindicator term is used for a group of biotic and abiotic reactions to environmental changes. Thus, different varieties of moss are used as natural monitoring bioindicators to heavy metals pollution. *Hylocomium splendens* was often used as heavy metal pollution indicator in tundra environment from northwest of Alaska. Very close to that geographical area is a mine from where are extracted large quantities of zinc, and this metal became in time an important contaminant of the soil, muss being affected very easily at any increase of zinc concentration. Not only this muss variety is used as bioindicator of metal contamination, but also different specific lichens [Parmar et al., 2016].

Heavy metals are the most common contaminants of the soil, along with the agriculture chemicals used in excess, which unfortunately cannot be broke down in metabolic pathways. Thereby, when metal concentration exceeds the optimal and tolerability range, the plant nutrition, development, and health is negatively affected. This can be explained due to metal property to inhibit the enzyme activity in the cellular structure, and oxidative stress is manifested. On the other hand, heavy metals replace some mineral essential nutrients from soil, affecting the plant normal biochemical pathways [Chibuike and Obiora, 2014].

Rice plant is reduced in height growth if the soil is contaminated with 1mgHg/kg [Kibra, 2008].

Experimental researches demonstrate that an association of plants and microbes reduced faster the heavy metal content of some polluted mercury soil [Weyens et al., 2009].

Air contaminants and bioindicators

Ozone is a chemical form of oxygen which is an aggressive stress factor for forest health. Due to its importance in the quality of air given by the forest quality and health, United States Department of Agriculture made some specific protocols of sampling and estimation of ozone pollution (U.S. Forest Service Forest Inventory and Analysis Program – FIA) and its impact on forest health [Smith et al., 2007].

Specific vascular plant species like tobacco (*Nicotiana tabacum* L.) are very sensitive to environmental ozone. Thus, when the concentration of ozone is increased the tobacco plant exhibits different foliar injuries symptoms. Also black cherry (*Prunus serotina*) is used as ozone uptake bioindicator in North America [Manning, 1998].

Other research reports presented a very good option to use lichens as bioindicators of air quality. Lichens inflorescence and specific anatomical parts of lichens are susceptible to ecosystem pollutants, and by monitoring and characterization of lichen species behavior to different contaminants the quality of air can be appreciated [Stolte et al., 1993].

The main characteristic of plants regarding pollution and contaminants is that these organisms “cannot run out of pollution”, like animals can do. Plants have to find biochemical mechanisms to filter the contaminants and intake the nutrients from the environment. Water content of soil and air, soil and air chemistry, temperature, pH, dissolved oxygen are only some of the characteristics very important for plants health. Plants can be used as environment alarms that react relatively quickly to any increase of the concentration of some components in the environment. Because the leaves are the plant “lungs”, first signs of pollution are the foliar symptoms and leaves composition, leaf being the anatomical part of the plants that concentrate especially the metals [Nouchi, 2002].

Water contaminants and bioindicators

Also some animals and microorganisms metabolism is influenced by the composition of nutrients and the contaminants of ecosystem. Oxidative stress is a biochemical state which can be unbalanced due to various factors, including contaminants. Thus, the oxidative stress is evaluated by the quantification of some specific enzymes (catalase, glutathione S-transferase,

glutathione peroxidase, reduced glutathione) and compounds (lipid peroxidation products) which very easily deviate from the normal range, with repercussions on the cellular activity and viability. This property was tested on *Anguilla Anguilla* L. (European eel) as a contamination response on the natural freshwater lake in Portugal. So, the concentration of oxidative stress enzymes increased in the case of heavy metals, agricultural chemicals and domestic polluted waters discharged into the lake, and the distribution of the pollution chemicals in different organs were also indicators of the degree of contamination [Ahmadi et al., 2006].

Therapy with plants and environment

Plants are used from ancient to different therapeutic treatments, for prevention and cure various diseases. The only drugs from old time were the herbs, and for all medical problems they knew which plant and which anatomical part to use to solve the medical problem. Tinctures, extractions (aqueous extractions; glyceric, hydro-glyceric, alcoholic, hydro-alcoholic extraction), infusions, teas, are the most used form of therapy. Oils, tinctures and gemmotherapeutic products are used for prevention and healing, but if these plants are contaminated with metals or different chemicals, the natural effect as drugs is diminished.

In agriculture it is important to know the agricultural aspects (planting time, the growth, the harvest time). Plants were used to obtain some nanomaterials, which can be used to proving the economical and biochemical safe, due to the interactions between NPs in plant. Nanomaterials are considered as waste or by-product of washing process, from where is accumulated in air, soil, and water. Some nanoparticles are very efficient to decontamination of the soil and water due to large specific surface area, available active sites on the surface, good optical and electrical properties, high stability and absorption capacity [Rai et al., 2018].

Lately, some plants extract are used as natural biopesticides in agriculture with very good results. Thus, saponin-rich plant extracts from plants like *Quillaja saponaria* and *Chenopodium quinoa* were used as ingredient in biopesticide [Jiang et al., 2018].

Traditional and Arabic plants were used in complementary and alternative treatment of different forms of cancer. According to new reports of World Human Organization, even advanced countries in the world accepted complementary treatment of cancer using herbal treatments. The benefic action of herb cancer therapy is given by some phytochemicals from plants, these herbal treatments having the advantages to have antitumoral effect with low side effects. Ethnopharmaceutical of Arabic and Islamic plants include acacia, different mushrooms, leak, onion, garlic, aloe, dill, celery, mustard, crown daisy, camphor, myrrh, saffron, chamomile, black seed, olive, Harmala Africa Rue, wheat, ginger, red-berry, grapes. Arabic and Islamic herbal medicine have long tradition, stimulates the immunologic system, and have antiviral, antibacterial, antiinflammatory, antioxidant, anticancer and antimutagenic effect [WHO, 2013-2014; Azaizeh and Arab, 2008].

Conclusion

Plants are part of ecosystem, being in relation with the other living organisms, and with the quality of the environment. Plants can be used as bioindicators of environmental pollution, and also can be used for decontamination of soil, water or even air.

Polluted environment is often the nutritional environment of different plants. As the plants cannot move from a side of another like animals, they became contaminated because of the polluted environment.

Due to the possibility of using plants therapy in cancer and many other diseases treatment, the environment of the plants used in herbal organic therapy has to be free of contaminant and to assure the optimal nutrients for development.

References

- [1] I. Ahmad, M. Pacheco, M.A. Santos, *Chemosphere*, 65 (2006), 952-962.
- [2] R. Ahmad, N. Ahmad, A.A. Naqvi, A. Shehzad, M. S. Al-Ghamdi, *Journal of traditional and complementary medicine*, 7 (2017), 195-204.
- [3] S.B.Azaizeh, H. Said, O. Arab, *Botanical Medicine in Clinical Practicies*, 4 (2008), p.31
- [4] G.D. Bending, M.K. Turner, F. Rayns, M.C. Marx, M. Wood, *Soil Biology and Biochemistry*, 36 (2004), 1785-1792.
- [5] F.J.J.A. Bianchi, V. Mikos, L. Brussaard, B. Delbaere, M.M. Pulleman, *environmental Science and Policy*, 27 (2013), 223-231.
- [6] G.U. Chibuike, S.C. Obiora, *Applied and Environmental Soil Science* (2014), 1-12..
- [7] S. Fusaro, A. Squartini, M.G. Paoletti, *Applied Soil Ecology*, 123 (2018), 699-708.
- [8] C. Hannah, A. Vezina, M.S. John, *Progress in Oceanography*, 84 (2016), 121-128.
- [9] X. Jiang, H.C.B. Hansen, B.W. Strobel, N. Cedergreen, *Environmental Pollution*, 236 (2018), 416-424.
- [10] N. Khatri, S., Tyagi, *Frontiers in Life Science*, 8 (2015), 23-39.
- [11] M.G. Kibra, *Soil and Environment*, 27 (2008), 23-28.
- [12] W.J. Manning (Editor), *The use of plants as bioindicators of ozone*, U.S. Forest Service – Caring for the land and serving people, Unites Stataes Department of Agriculture, Treereseach, Publication of General Technical Report, Pacific Southwest Research Station, 1998.
- [13] I. Nouchi, *Plants as Bioindicators of Air Pollution*, in *Air Pollution and Plant Biotechnology*, K. Omasa, H. Saji, S. Youssefian, N. Kondo (Editors), Springer, Tokyo, 2002, p 41-60.
- [14] T.K.Parmar, D. Rawtani, Y.K. Agrawal, *Frontiers in Life Science*, 9 (2016), 110-118.
- [15] P.K.Rai, V. Kumar, S.S. Lee, N. Raza, K.H. Kim, Y.S.Ok, D. C.W. Tsang, *Environment International*, 119, (2018), 1-19.
- [16] G.C. Smith, W. D. Smith, J.W. Coulston, *Ozone bioindicators sampling and estimation*, U.S. Forest Service – Caring for the land and serving people, Unites Stataes Department of Agriculture, Treereseach, Publication of General Technical Report, Northern Research Station, 2007, p.34.
- [17] K. Stolte, D. Mangis, R. Doty, K. Tonnessen, L.S. Huckaby, *Lichens as bioindicators of air quality*, U.S. Forest Service – Caring for the land and serving people, Unites Stataes Department of Agriculture, Treereseach, Publication of General Technical Report, Rocky Mountain Forest and Range Experiment Station, 1993, p.131.
- [18] E.L. Turner, P.A. Montagna, *Ecological Informatics*, 36 (2016), 118-125.
- [19] N. Weyens, D. Van der Lelie, S. Taghavi, L. Newman, J. Vangronsveld, *Trends in Biotechnology*, 27 (2009), 591-598.

CHRONOBIOLOGICAL CHANGES INDUCED BY THE GALLIUM COMPLEX C(24) IN SOME HEMATOLOGICAL PARAMETERS IN RATS

Gârban Z.^{1,2}, Ioniță Hortensia³, Gârban Gabriela^{2,4}, Baltă C.^{2,5}, Ahmadi-Vincu Mirela^{2,6}, Muselin F.^{2,6}, Lungu Camelia⁴, Acatincăi St.⁷, Ujhelyi R.P.^{2,8}, Simiz Eliza⁷, Boldura Oana⁶

1. Department of Biochemistry and Molecular Biology (former), Faculty of Food Products Technology, University of Agricultural Sciences and Veterinary Medicine of Banat "King Michael I of Romania" Timișoara, Calea Aradului No. 119, RO-300 645 Timișoara, Romania; 2. Working Group for Xenobiochemistry, Romanian Academy-Branch Timișoara; Bd. M. Viteazu No. 24, RO-300 223 Timișoara, Romania; 3. Clinic of Hematology-Oncology, Faculty of Medicine, "Dr. Victor Babeș" University of Medicine and Pharmacy, Str. G. Dima, Nr.5, 300 079 Timișoara, Romania; 4. Laboratory of Environment and Nutrition, National Institute of Public Health-Branch Timișoara, , Bd. Dr.V. Babeș Nr.16, 300 226 Timișoara Romania; 5. Faculty of Medicine, West University "Vasile Goldiș" Arad, Bd. Revoluției Nr. 94-96, 310 025 Arad, Romania; 6. Faculty of Veterinary Medicine, Departments of Biochemistry/Toxicology, University of Agricultural Sciences and Veterinary Medicine of Banat "King Michael I of Romania" Timișoara; 7. Faculty of Animal Sciences and Biotechnology, University of Agricultural Sciences and Veterinary Medicine of Banat "King Michael I of Romania", Timișoara, Romania; 8. Medical Department, S.C. CaliVita International, Timișoara, Romania
e-mail: zeno.garban@yahoo.com

ABSTRACT

In the present research the authors proposed to monitor possible chronobiological changes in some hematological parameters (erythrocytes, leukocytes and thrombocytes) of Wistar strain rats induced by the novel gallium complex - C(24). For this purpose a morning (m) and an evening (e) animal series were designed, each including a control (C_p) and an experimental (E) group. Animals of the control groups (C_p-m, C_p-e) were injected intraperitoneally with polyethylene glycol and those from the experimental groups (E-m, E-e) with the novel gallium complex in the morning and in the evening. At 48 hours after the administration of substances the animals were anesthetized and blood samples were collected for biochemical and hematological analysis.

Erythrocytes, leukocytes and thrombocytes parameters were determined. The resulted values showed an increase in most of erythrocytes parameters in E-m group and a slight decrease of all parameters in E-e group. As to leukocytes parameters an increase of most values both in E-m and E-e groups was recorded. Platelets parameters indicated decrease both in E-m and E-e groups, being more evident in case of platelets number.

Key words : gallium complex C(24), chronobiology, hematological parameters

INTRODUCTION

In chronobiology and chronobiochemistry one can distinguish three types of rhythms : a) ultradian - from some seconds to some hours; b) circadian - about 24 hours; c) infradian - from some days to months or year (Hayes et al., 1990; Schwob, 2007).

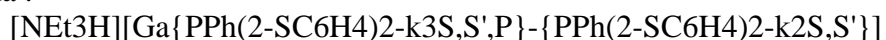
In the last period more and more experimental and clinical studies are dealing with the anticancer effects of various gallium salts and complexes (Haiduc and Silvestru, 1990; Chitambar, 2010). This trend is due to the fact that gallium is the second metallic element after platinum with evident anticancer effects (Bernstein, 2005).

The aim of the present paper was to evidence possible changes in some hematological parameters after a period of 48 hrs (including two circadian cycles) from the administration of

the gallium complex C(24) with the molecular weight 820 Da - synthesized at the Department of Inorganic Chemistry of the University "Babeş-Bolyai" Cluj-Napoca (Vălean et al., 2009).

MATERIALS AND METHODS

Experimental design. Wistar strain rats, divided into a morning series (administration time 7 a.m.) and an evening series (administration time 7 p.m.) were used. Afterwards each series were divided in two control groups, i.e. one morning (C_p-m) and one evening (C_p-e) - the animals receiving intraperitoneally (i.p.) a solution with Et-OH 40% : PEG 400 in the ratio of 1 : 1.5 (Gârban et al., 2012). It is to mention that polyethylene glycol (PEG) is suitable for solubilizing of various compounds of pharmaceutical and nutritional interest as well as xenobiotics (Milton, 1992; Smolinske, 1992; Gârban, 2007). Also, there were constituted the morning (E-m) and evening (E-e) experimental groups. Animals (E-m and E-e) were injected i.p. with 0.25 mg/mL of the compound C(24) in solution with Et-OH / PEG. A quantity of 1 mL / 100 g body weight (b.wt.), i.e. 2.5 mg/kg b.wt. was injected. Each animal group consisted of 3 males and 3 females. The administered compound noted C(24) was an *amonium gallium complex of phosphinobisthiolato P,S,S pincer ligand* with the formula :



The experiment lasted 48 hrs starting from the administered substances. At the end of the experiment blood samples were collected for analysis and the animals were euthanized by an Anesteran (purchased from Rompharm Co., Bucharest-Romania) overdose. Requirements for the protection of animals used in scientific or other experiments were respected according to Council Directive 86/609/EEC of 24 November 1986 and National Governmental Ordinance No.37/30.01.2002.

Hematological investigations: Using an automated „Abacus Junior Vet” type analyzer where a quantity of 25 µl whole blood was introduced we obtained data on parameters regarding: red blood cells (erythrocytes); white blood cells (leukocytes) and platelets (thrombocytes). Parameters of red blood cells were: total number-RBC; hemoglobin-HGB; hematocrit-HTC; red blood cell indices-MCV; mean corpuscular hemoglobin-MCH; mean corpuscular hemoglobin concentration-MCHC; red cell distribution width-RDWc. Parameters of white blood cells were: WBC-total number; LYM-lymphocytes; MID-medium size cells count; GRA-granulocytes; LY%-lymphocytes percentage; MI%-medium size cells percentage; GR%-granulocytes percentage. Parameters for platelets were: PLT-number of platelets; PCT-platelet percentage; MPV-mean platelets volume; PDWc-platelet distribution width.

Statistical evaluation. Mean values (X) and standard deviations (SD) of all the experimental data were determined. Data were evaluated using a conventional statistical procedure, the analysis of variance (ANOVA).

RESULTS AND DISCUSSIONS

Parameters of red blood cells are the main indicators of the iron status of the organism and can be modified either by the time-period of collection (Gârban et al., 1989; Pocock et al., 1989; Sanni et al., 2000) or by various factors such as: acute hemorrhage, lack of substances needed for RBC production, action of various xenobiotics a.o. The oxyphoretic capacity of RBC is important in order to prevent tissue hypoxia and the consequent disturbances. Our results on the effects of the gallium complex C(24) on erythrocyte parameters are presented in table 1 and table 2.

Table 1. Erythrocyte parameters obtained in the morning animal series

Groups	n	RBC ($\cdot 10^{12}/L$) X \pm SD	HGB (g/dL) X \pm SD	HCT (%) X \pm SD	MCV (fl) X \pm SD	MCH% (pg) X \pm SD	MCHC (g/dL) X \pm SD	RDW _C (%) X \pm SD
C _p - m	6	7.83 \pm 1.87	12.58 \pm 3.32	38.24 \pm 5.43	49.50 \pm 2.25	15.98 \pm 0.53	32.41 \pm 1.63	17.11 \pm 0.65
E - m	6	8.80 \pm 0.88	14.01 \pm 1.36	40.18 \pm 2.24	47.50 \pm 2.07	15.95 \pm 0.51	33.53 \pm 1.13	18.23 \pm 1.49
ΔX		+ 0.97	+ 1.43	+ 1.94	- 2.00	- 0.03	+ 1.12	+ 1.12

Table 2. Erythrocyte parameters obtained in the evening animal series

Groups	n	RBC ($\cdot 10^{12}/L$) X \pm SD	HGB (g/dL) X \pm SD	HCT (%) X \pm SD	MCV (fl) X \pm SD	MCH% (pg) X \pm SD	MCHC (g/dL) X \pm SD	RDW _C (%) X \pm SD
C _p - e	6	9.17 \pm 0.45	14.90 \pm 1.05	44.13 \pm 1.55	48.16 \pm 2.04	16.23 \pm 0.77	33.75 \pm 0.78	18.63 \pm 1.59
E - e	6	8.58 \pm 0.76	13.78 \pm 0.92	41.12 \pm 1.51	48.00 \pm 1.41	16.08 \pm 0.74	33.50 \pm 0.91	17.52 \pm 0.53
ΔX		- 0.59	- 1.12	- 3.01	- 0.16	- 0.15	- 0.25	- 1.11

In vivo studies using Ga compounds revealed that Ga is present mostly in blood serum and in small quantities in leukocytes (Bernstein, 2005). Parameters of white blood cells have an important role in the defending processes of the organism, e.g. phagocytosis. In table 4 and table 4 are given the obtained results regarding these parameters after C(24) injection.

Table 3. Leukocytic parameters obtained in the morning animal series

Groups	n	WBC ($\cdot 10^9/L$) X \pm SD	LYM ($\cdot 10^9/L$) X \pm SD	MID ($\cdot 10^9/L$) X \pm SD	GRA ($\cdot 10^9/L$) X \pm SD	LY (%) X \pm SD	MI (%) X \pm SD	GR (%) X \pm SD
C _p - m	6	10.70 \pm 3.12	8.15 \pm 2.15	0.32 \pm 0.18	2.21 \pm 1.02	76.83 \pm 3.05	3.23 \pm 2.91	19.93 \pm 3.11
E - m	6	13.06 \pm 3.82	10.57 \pm 3.19	0.33 \pm 0.21	2.15 \pm 0.71	81.05 \pm 3.05	3.61 \pm 2.43	17.73 \pm 3.15
ΔX		+ 2.36	+ 2.42	+ 0.01	- 0.06	+ 4.22	+ 0.38	- 2.20

Table 4. Leukocytic parameters obtained in the evening animal series

Groups	n	WBC ($\cdot 10^9/L$) X \pm SD	LYM ($\cdot 10^9/L$) X \pm SD	MID ($\cdot 10^9/L$) X \pm SD	GRA ($\cdot 10^9/L$) X \pm SD	LY (%) X \pm SD	MI (%) X \pm SD	GR (%) X \pm SD
C _p - e	6	7.66 \pm 2.76	5.51 \pm 2.52	0.34 \pm 0.18	1.80 \pm 0.89	70.58 \pm 8.09	4.67 \pm 2.98	24.75 \pm 7.72
E - e	6	9.58 \pm 4.01	6.80 \pm 2.89	0.42 \pm 0.26	2.35 \pm 1.37	71.85 \pm 5.77	4.22 \pm 2.09	23.93 \pm 5.23
ΔX		+ 1.92	+ 1.29	+ 0.08	+ 0.55	+ 1.27	- 0.45	- 0.82

Platelets or thrombocytes are small cell fragments with a short life time which circulate in the blood and are involved in hemostasis. The results obtained in this experiment are depicted in table 5 and 6.

Table 5. Parameters of platelets obtained in the morning animal series

Groups	n	PLT ($\cdot 10^9$) X \pm SD	PCT (%) X \pm SD	MPV (fL) X \pm SD	PDW _C (%) X \pm SD
C _s - m	6	503.00 \pm 379.00	0.29 \pm 0.20	6.03 \pm 0.80	30.60 \pm 1.45
E - m	6	477.00 \pm 245.00	0.27 \pm 0.13	5.91 \pm 0.79	30.51 \pm 1.89
Δ X		- 26.00	- 0.02	- 0.12	- 0.09

Table 6. Parameters of platelets obtained in the evening animal series

Groups	n	PLT ($\cdot 10^9$) X \pm SD	PCT (%) X \pm SD	MPV (fL) X \pm SD	PDW _C (%) X \pm SD
C _s - e	6	595.80 \pm 133.00	0.34 \pm 0.08	5.56 \pm 0.16	28.78 \pm 0.38
E - e	6	542.20 \pm 140.80	0.30 \pm 0.07	5.53 \pm 0.28	28.77 \pm 0.61
Δ X		- 53.60	- 0.04	- 0.03	- 0.01

Both in the morning (E-m) and in the evening (E-e) experimental groups the number of thrombocytes was decreased when compared with the control groups. The decrease was more evident in case of the evening experimental group.

CONCLUSIONS

1. The administered gallium complex C(24) on the parameters of red blood cells (RBC) showed the followings: statistically not significant increase of RBC, HGB, HCT, MCHC and RDW_C and decrease of MC and MCT in the morning series. In the evening series all the parameters were slowly decreased.
2. Regarding the effects of gallium complex C(24) on the parameters of white blood cells (WBC) an increase of values both in the morning and evening series were found with some exceptions. Thus, GRA decreased in the morning, MI decreased in the evening while GR decreased both in the morning and evening series.
3. Parameters concerning the platelets (PLT) under the action of the gallium complex C(24) revealed decrease in both animal series. More important decrease was found in case of the platelets number in the evening experimental series.

Acknowledgements. These investigations were performed with apparatus obtained by the financial support of the Romanian Ministry for Education, Research, Youth and Sports – National Authority for Scientific Research, PN-II-ID-PCCE-2008-1 (Project Nr. 2 / 2010, code CNCSIS ID-PCCE 140). Proper conditions for the animal experiments were assured by arrangements made in 2011 with the support of Prof. Dr. Eng. Stelian Acatincăi – vice-rector of the University of Agricultural Sciences and Veterinary Medicine of Banat Timișoara. The authors express thanks to Dr. Eng. Ghibu George-Daniel, Dr. Avacovici Adina-Elena and Dr. Pascu Corina for their technical assistance.

REFERENCES

1. Bernstein L.R. – in „Metallotherapeutic drugs and metal-based diagnostic agents : The use of metals in medicine” (Gielen M., Tiekink E.R.T., Eds.) , J.Wiley and Sons Ltd., New York, 2005.
2. Chitambar C.R. - *Int.J. Res. Public Health*, 2010, 7, 2337-2361
3. Gârban Gabriela, Nicola T., Baltă C., Gârban Z., Hădărugă Nicoleta, Mitar Carmen, Simiz Eliza, Ghibu G.-D., Rada Olga-Alina – pp.248-251, in *The International Symposium on*

- Analytical and Environmental Problems, with special emphasis on heavy metal ions as contaminants*", (Ed. Z. Galbacs), Publ. By SZAB Szeged, 2012
4. Gârban Z., Dancău G., Daranyi Gabriela, Erdelean R., Văcărescu G., Precob V., Eremia Iulia, Udriște C. - *Rev. Roum. Biochim.*, 1989, 26, 2, 107-117
 5. Gârban Z. - *Biochemistry: Comprehensive Treatise*. Vol. IV. Xenobiochemistry, 2nd edition (in romanian), Editura Didactică și Pedagogică R.A., București, 2007.
 6. Haiduc I., Silvestru C. - *Organometallics in Cancer Chemotherapy*, Vol I, Vol II, CRC Press Inc., Boca Raton, FL, 1989, 1990.
 7. Hayes D.K., Pauly J.E., Reiter R.J. (Eds.) – *Chronobiology : its role in clinical medicine, general biology and agriculture*, Wiley Liss, New York, 1990.
 8. Milton J.H. - *Poly(ethylene glycol) chemistry : biotechnical and biomedical applications*, Plenum Press, New York, 1992
 9. Pocock S.J., Ashby D., Shaper A.G., Walker M., Broughton P.M.G. - *J. Clin.Pathol.*, 1989, 42, 172 – 179.
 10. Sanni A.A., Oyedokun O.R., Alaka O.O. - *Afr. J. Biomed. Res.*, 2000, 3, 117–120.
 11. Schwob M. - *Les rythmes du corps: Chronobiologie de l'alimentation, du sommeil, de la santé*, Odile Jacob, Paris, 2007 <http://rhuthmos.eu/spip.php?article160>
 12. Smolinske C. Susan - *Handbook of Food, Drug and Cosmetic Excipients*, CRC Press, Boca Raton, 1992.
 13. Touitou Y., Haus E. (Eds.) – *Biologic rhythms in clinical and laboratory medicine*, Springer-Verlag, Heidelberg, 1992.
 14. Vălean Ana-Maria, Gómez-Ruiz S., Lönnecke P., Silaghi-Dumitrescu I., Silaghi-Dumitrescu Luminița, Hey-Hawkins Evamarie - *New J. Chem.*, 2009, 33, 1771-1779.
 15. *** - Council Directive 86/609/EEC of 24 November 1986 on the approximation of laws, regulations and administrative provisions of the Member States regarding the protection of animals used for experimental and other scientific purposes, *Official Journal of the European Union*, L 358 , 18/12/1986.
 16. *** - Ordonanță Nr.37/30.01.2002 pentru protecția animalelor folosite în scopuri științifice sau în alte scopuri experimentale, *Monitorul Oficial al Romaniei* Nr. 95, 2002.

ENGINE CARBON CLEANING AS THE WAY OF ENVIRONMENTAL PROTECTION

**Dragan Adamović¹, Mirjana Vojinović Miloradov¹, Vojin Močević², Jelena Radonić¹,
Maja Turk Sekulić¹, Savka Adamović³, Sabolč Pap^{1,4}**

¹ Faculty of Technical Sciences, Department of Environmental Engineering and Occupational Safety and Health, University of Novi Sad, Trg Dositeja Obradovića 6, 21000 Novi Sad, Serbia

² Hybrid Power System LLC, Zmaj Jovina 26, 21000, Novi Sad, Serbia

³ Faculty of Technical Sciences, Department of Graphic Engineering and Design, University of Novi Sad, Trg Dositeja Obradovića 6, 21000 Novi Sad, Serbia

⁴ Environmental Research Institute, North Highland College, University of the Highlands and Islands, Castle Street, Thurso, Scotland, KW14 7JD, UK
e-mail: draganadamovic@uns.ac.rs

Abstract

The paper points out the negative impact of air pollution on human health and the environment, caused by the emission of exhaust gases of motor vehicles. According to recent estimations published by the European Environment Agency, estimated traffic in Europe would be contributing more than 64% to air pollution (NO_x, NO₂, PM). Combustion chamber deposits are listed as one of the dominant causes of deterioration of the emission characteristics of motor vehicles. The primary reason for carbon deposits forming is a complex reaction that occurs between components, fuel, blow-by gas, and lubricant oil. Carbon deposit also has a negative impact on the heat transfer process in the combustion chamber, emissions, combustion and maintenance costs. The paper points out the possibility and importance of removing carbon deposits using H2E engine carbon cleaning (H2E ECC) system. The results of testing the emission characteristics of the engines on four randomly selected vehicles Euro 3 and Euro 4 classes before and after the treatment of vehicles using the H2E ECC indicate that the concentration levels of the toxic components in the mixture of exhaust gases are reduced. In this way, the emission characteristics of the treated vehicles have been improved.

Introduction

Ambient air pollution has a direct influence on human health. Air pollution alone poses the single most significant environmental risk factor in Europe today, responsible for more than 400,000 premature deaths [1]. Due to adverse health effects, air pollution has been marked as the top stressor regarding the environmental burden of disease [2]. Among various shared sources of air pollution in an urban setting, road traffic is considered to be the main contributor to pollution. According to the recent assessments published by the European Environment Agency, road traffic is estimated to contribute more than 64% to air pollution (NO_x, NO₂, PM) in Europe [3].

The primary pollutants emitted from cars and vehicles are particulate matters (PM), carbon monoxide (CO), hydrocarbon (HC), nitrogen oxides (NO_x), lead (Pb), sulfur oxides (SO_x) etc. not only are these pollutants harmful to human health, nitrogen oxides and hydrocarbons are also sources of the formation of photochemical smog and ozone [4]. In Europe, the contribution of vehicle emissions to NO_x and CO levels amounted to 40% and 26% in 2011, respectively [5]. Traffic-related emissions have become one of the significant sources of air pollution, in Chinese cities such as Beijing, Guangzhou, and Shanghai [6]. Therefore, the urban traffic problem, which encompasses exhaust emissions, congestion, and level of safety,

has become more serious. Due to their sizeable adverse impact to the environment and human health, vehicle pollutants emission reduction management has been an important topic in recent transport studies.

Regarding the environmental pollution, improving IC engine efficiency and emissions has become an important issue nowadays. Therefore, reducing vehicle pollutant emissions to improve the public's living environmental quality is a problem that government policies must deal with immediately; it is also an objective that industries and academics are working towards.

Carbon deposits

Carbon deposits (CD) can be defined as heterogeneous mixtures consisting of carbon residue, oxygenated resinous organic material and carbonaceous combinations [7]. The primary cause of CD is a complex reaction that occurs among the components, fuel, blow-by gases and lubricant oil. Most of CD originates from the fuel, while the remaining comes from the lubricant oil. The formation of CD may significantly affect the engine performance and drivability. Combustion chamber deposits are generally found on the top of pistons or the cylinder head in engines due to incomplete combustion and physical or chemical interactions between fuel or oil components and the hot chamber surface under the high-temperature, high-pressure heterogeneous mixing conditions. Carbon deposit also has a negative impact on the heat transfer process in the combustion chamber, emissions, combustion and maintenance costs.

Although fuel formulations and engine designs have both been significantly upgraded to provide the more stringent emission regulations and improve fuel economy, the formation of CD is still observed in the combustion chamber or the ring pack. The existence of CD is inescapable in internal combustion engines. Identifying the chemical composition is crucial in tracing the source of deposits. Based on statistical data and new data [8], the major elements in CD are C, O, H, N, and a small metal content level, possibly derived from the lubricating oil. Differentiating from traditional toxic and corrosive chemical substances for CD removal [9]. Mixed gas carbon removal is a new method of removing the engine carbon deposit, not only without stripping the engine, but also on the environment protection. Recently, the removing carbon deposition engine with mixed gas is widely used in engine maintenance.

Hydrogen carbon cleaning using H₂E technology

H₂E engine carbon cleaning (H₂E ECC) system in the process of water alkaline electrolysis, in the presence of potassium hydroxide (KOH), generates hydrogen and oxygen in a volume ratio of 2:1. The obtained mixture of gases is introduced into the engine cylinders through the inlet manifold, while the engine is operating in a mode set by the H₂E application during the additivation procedure. In controlled combustion conditions, degradation of CD occurs in the cylinder and the exhaust manifold.

The increased internal oxygen proportion enhances combustion, and at the same time, the catalytic properties of hydrogen make it possible for the burning of carbon to be slowly broken down to clear the internal CD.

A powerful electric current splits the water molecule into its component atoms producing an oxy-hydrogen mixture. The mixture is passed into the engine and burnt as the engine runs mixing the oxy-hydrogen with the fuel. As it passes through the induction system, combustion chamber, etc, the hydrogen reacts with the CD turning the carbon into hydrocarbons, this disposes the CD from the engine and the resulting gas exits the engine via the exhaust system. Using hydrogen technology, CD are removed from the inner workings of the engine, which naturally build up during the lifetime of the vehicle.

By removing unwanted CD, further engine deterioration and damage can be avoided.

The effect of carbon cleaning is dependent on how “dirty” the engine is. This is down to many different things: driving style, mileage, fuel used etc. If the engine doesn’t get worked high load conditions, then it will most likely have more carbon build up. Taxis and buses are the worst as they are sat idling and often short stop-start journeys at low load conditions.

Experimental

In order to assess the impact of the H2E ECC process on the emission characteristics of the tested motor vehicles. The exhaust gas analysis were performed before and after the H2E ECC treatment. H2E engine carbon cleaning treatment is shown in Figure 1.



Figure 1. H2E engine carbon cleaning treatment

The quantification of the target components in the exhaust mixtures was carried out using the gas analyser Stargas 898 Global Diagnostic System (Serial No. 3156) and the "Smokemeter 495/02."

The measurements were carried out on randomly selected used vehicles that are in regular usage and where it was possible to test the emission characteristics using the exhaust gas analysers prescribed for control on technical inspections. The measurements were included a sample of ten vehicles, four of which were with diesel engines and six vehicles were with petrol engines. The analyses were conducted at the locations in Novi Sad (Serbia) and Ystad (Sweden). Measurements of exhaust gas emissions were conducted before and after treatment with the H2E ECC system, for each vehicle. Exhaust gas emission measurements were carried out according to the method described in the instructions of the exhaust gas analysers, while the treatments were carried out according to the procedure described in the directions of the H2E ECC system.

Results

The results of testing the emission characteristics of the engines on four randomly selected vehicles with diesel engines that fulfil the Euro 3 and Euro 4 standards indicate a decrease in the opacity by an average of 60%.

The results of the emission test for six randomly selected petrol engines that fulfil Euro 3, Euro 4 and Euro 5 standards indicate a decrease in carbon monoxide (CO) concentrations for an average of 77% and total hydrocarbons (HC) for an average of 84% in the exhaust gas stream.

Conclusions

It can be concluded that for all tested vehicles, emissions of exhaust gases (opacity on diesel engines) have dropped significantly, which is the result of more efficient combustion after performed the H2E ECC procedure.

The reduction in the concentration levels of CO and HC in the exhaust gas stream is the result of providing more favourable conditions for combustion of the air-fuel mixture after the treatment with H2E ECC system. This claim is supported by the data on the slight increase in carbon dioxide (CO₂) content, which generates as a result of complete combustion at the expense of the disappearance of HC and CO.

The significantly reduced CO and HC emissions in the petrol engine provide higher overall efficiency and longer service life of the catalyst in the exhaust system of the vehicle.

Reduced opacity in the diesel engine indicates on reduced particulate intake intensity within the particle filter (DPF), which diminishes many automatic regenerations of the filter, thereby providing a longer service life and higher efficiency of the catalytic converter of exhaust gases and particulate filters.

The reduced emission of gases in the exhaust section results in reduced accumulation of deposits in the inlet manifold to which it comes through the exhaust gas recirculation system (EGR)

Acknowledgements

This research was supported by Ministry of Education, Science and Technological Development, Republic of Serbia (III46009).

References

- [1] European Environment Agency (EEA). Trends and projections in Europe 2015: Tracking progress towards Europe's Climate and energy targets. 2015. doi:10.2800/985234.
- [2] O. Hänninen, A.B. Knol, M. Jantunen, T-A Lim, A. Conrad, M. Rappolder, et al. Environmental Burden of Disease in Europe: Assessing Nine Risk Factors in Six Countries. *Environ Health Perspect* 2014. doi:10.1289/ehp.1206154.
- [3] EEA. Climate change, impacts and vulnerability in Europe 2012: an indicator-based report. 2012. doi:10.2800/66071.
- [4] D. Brugge, J.L. Durant, C.Rioux Near-highway pollutants in motor vehicle exhaust: A review of epidemiologic evidence of cardiac and pulmonary health risks. *Environ Heal A Glob Access Sci Source* 2007. doi:10.1186/1476-069X-6-23.
- [5] Eea. Air quality in Europe — 2013 report. 2013. doi:10.2800/92843.
- [6] C.K. Chan, X.Yao, Air pollution in mega cities in China. *Atmos Environ* 2008. doi:10.1016/j.atmosenv.2007.09.003.
- [7] A.K. Hasannuddin, W.J. Yahya, S. Sarah, A.M. Ithnin, S. Syahrullail, D.A. Sugeng, et al. Performance, emissions and carbon deposit characteristics of diesel engine operating on emulsion fuel. *Energy* 2018;142:496–506. doi:10.1016/j.energy.2017.10.044.
- [8] C.J. Powell, A. Jablonski Microcharacterization of heavy-duty diesel engine piston deposits. *Surf Interface Anal* 2002. doi:10.1002/sia.1209.
- [9] S.P. Yu, M.W. Lai, C.Y. Chu, C.L. Huang, C.Y. Lin, V.I. Borzenko, et al. Integration of low-pressure hydrogen storage cylinder and automatic controller for carbon deposit removal in car engine. *Int J Hydrogen Energy* 2016. doi:10.1016/j.ijhydene.2016.07.191.

ANTIOXIDANT CAPACITY AND ANTIBACTERIAL ACTIVITY OF SEA BUCKTHORN (*HIPPOPHAE RHAMNOIDES* L.)

Viola Zsuzsanna Angyal^{1,2}, Éva Stefanovits-Bányai¹, Mónika Kovács²

¹Department of Applied Chemistry, Szent István University, 1118 Budapest, Villányi street 29-43., Hungary

²Department of Microbiology and Biotechnology, Szent István University, 1118 Budapest, Somlói street 14-16., Hungary
e-mail: angyalviolazs@gmail.hu

Abstract

Consumer behavior changed a lot in the last few years. The chemicals used in food production discourage consumers, but protection against spoilage and pathogenic microorganisms is crucial, because they are important from medical and economic perspectives. Among research topics related to novel, minimally processed techniques using natural components, sea buckthorn is less studied. In spite of its widespread application and beneficial effects the potential of sea buckthorn is not completely explored.

Antioxidant capacity and antibacterial activity of commercially available sea buckthorn products (sea buckthorn instant tea, sea buckthorn tea, sea buckthorn powder, berry and juice) were determined. FRAP (Ferric Reducing Ability of Plasma) method, and TPC method with Folin-Ciocalteu reagent (Total Polyphenol Content) were applied for antioxidant capacity measurements. Antibacterial activity was tested against *Escherichia coli*, *Enterococcus faecalis*, *Listeria innocua*, *Listeria monocytogenes*, *Pseudomonas aeruginosa* and *Staphylococcus aureus* by using agar well diffusion method.

The obtained results highlighted that not only the active substance content of products but also the preparation techniques (water temperature, time of infusion) significantly influence the antioxidant capacity and antibacterial activity. Higher water temperature in case of tea preparation resulted better antibacterial activity and higher antioxidant capacity. In case of sea buckthorn powder, longer infusion time proved to be more efficient. Products with higher antioxidant capacity showed better antibacterial activity by agar well diffusion method. In case of berry and berry juice, high antioxidant capacity and excellent antibacterial activity were determined.

Introduction

Sea buckthorn, also known as *Hippophae rhamnoides* L., is an Eurasian plant belongs to the *Eleagnaceae* family, originally found on the slopes of the Himalayas [1]. Today we can find it in the Alps and on the northern shores. This plant has a rich history in natural medicine [2], due to their high content of bioactive compounds [3]. Sea buckthorn is good sources of valuable nutrients (carotenoids, tocopherols, phytosterols, phenolic acids and flavonoids), demonstrating various useful effects (antioxidant, antimicrobial) [4-6]. The aim of this study was to find commercially available sea buckthorn products and process them under aseptic conditions while examining the antibacterial effect and antioxidant capacity of the products, to explore relationships between them. I process them by taking the preparation methods recommended by the manufacturer / distributor (time of infusion, temperature).

Experimental

FRAP method, and TPC method were applied for antioxidant capacity measurements [7-8]. FRAP was defined in ascorbic acid equivalent (μg ascorbic acid equivalent/ g). TPC was determined according to the Folin–Ciocalteu spectrophotometric method described by Singleton and Rossi. Results were specified in μg gallic acid equivalent/ g. Antibacterial activity was tested against *Escherichia coli*, *Enterococcus faecalis*, *Listeria innocua*, *Listeria monocytogenes*, *Pseudomonas aeruginosa* and *Staphylococcus aureus* by using agar well diffusion method. The commercially available products were sea buckthorn instant tea, sea buckthorn tea, sea buckthorn powder, berry and juice. I used two types of preparation for the instant sea buckthorn tea. I resolved the product in cold and in 60 °C water too. In case of the sea buckthorn tea I used cold and 90 °C water. I brewed the tea in cold water 24 hours for the first preparation and 15 minutes for the second one. The third preparation of the tea I brewed in 90 °C water for 15 minutes and then removed with filter paper. The powder were once soaked in cold water for 24 hours and the other one for 15 minutes and then removed by centrifuge.

Results and discussion

Antibacterial activity tested by using agar well diffusion method. In the case of sea buckthorn tea, the cold preparations (all 15 minutes and 24 hours of brewing) did not show complete inhibitory effect, only partially, while in the case of the tea brewed at 90 °C, I have already experienced zones of inhibition in most places. In the case of cold instant tea, there was a zone of inhibition for all bacteria, but instant tea brewed at 60 °C resulted larger zones. In case of sea buckthorn powder, 15 minutes of soaking was not enough to release the inhibitory components, only of *Listeria innocua*. The 24 hour sea buckthorn powder was better, however, inhibition was not significant (less than 10 mm).

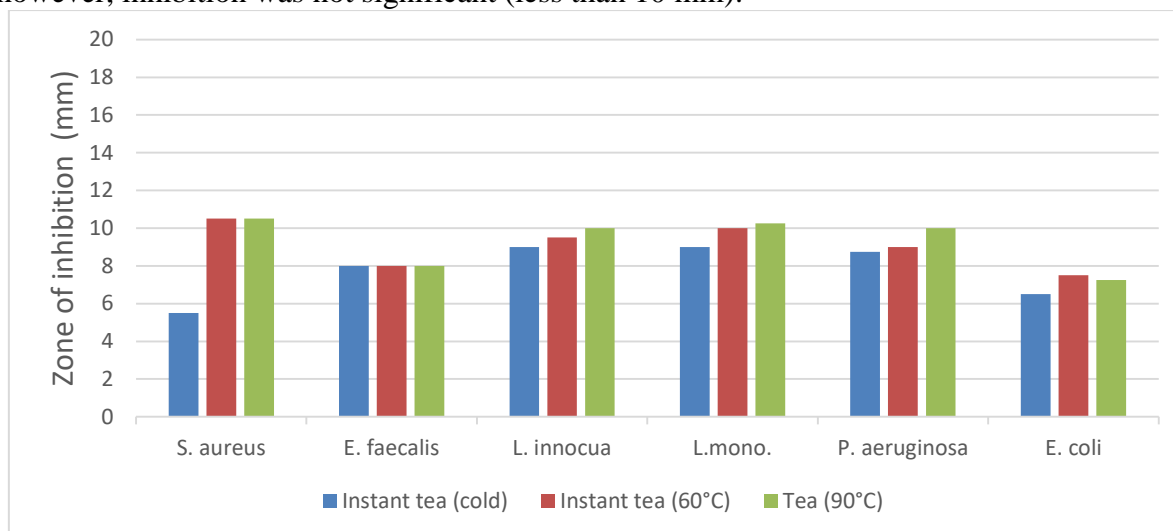


Figure 1. Inhibition zones of agar well diffusion method (tea, instant tea)

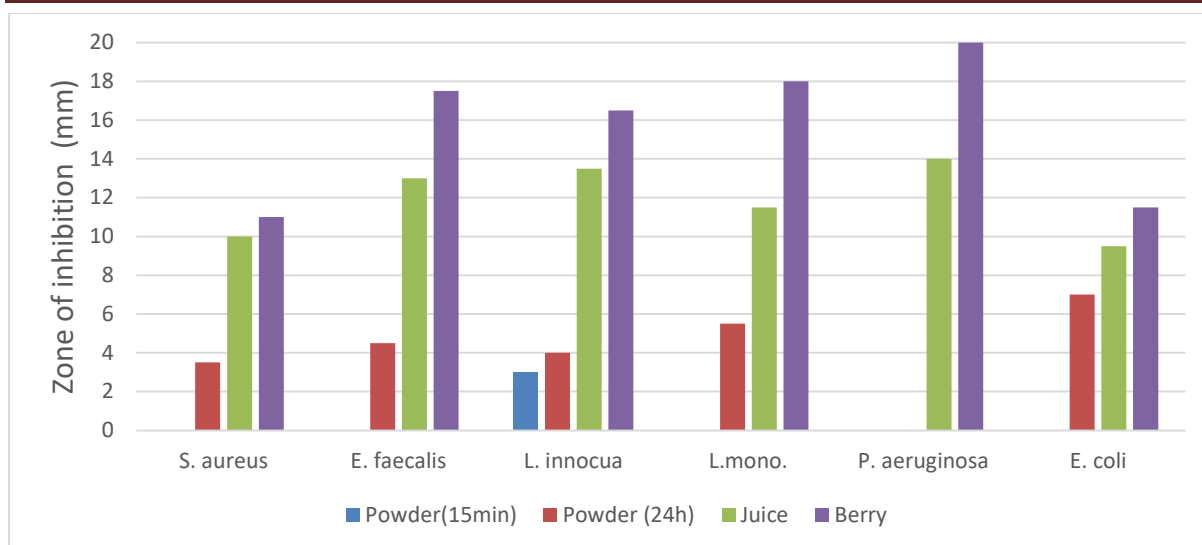


Figure 2. Figure 1. Inhibition zones of agar well diffusion method (powder, juice, berry)

FRAP method, and TPC method with Folin-Ciocalteu reagent were applied for antioxidant capacity measurements. The results show that the tea brewed at 90 °C has very good antioxidant capacity and instant teas have also high. (Figure 3.). In case of instant tea, the originally added vitamin C could have slightly influenced the result. Higher temperature affected the antioxidant compounds in a positive way, because several more components could dissolve out from the tea, that increased the antioxidant capacity. It can be seen that these three results are close to each other. This is consistent with the results of agar well diffusion method, where their antibacterial effects also closely related. The FRAP method shows that the sea buckthorn berry has remarkably good values predicted by the agar well diffusion method (Figure 3.). The results also demonstrate the high polyphenol content of sea buckthorn berry and juice. The values of the sea buckthorn powder were not particularly prominent, but it can be seen that the longer soaked powder had better results (Figure 4.).

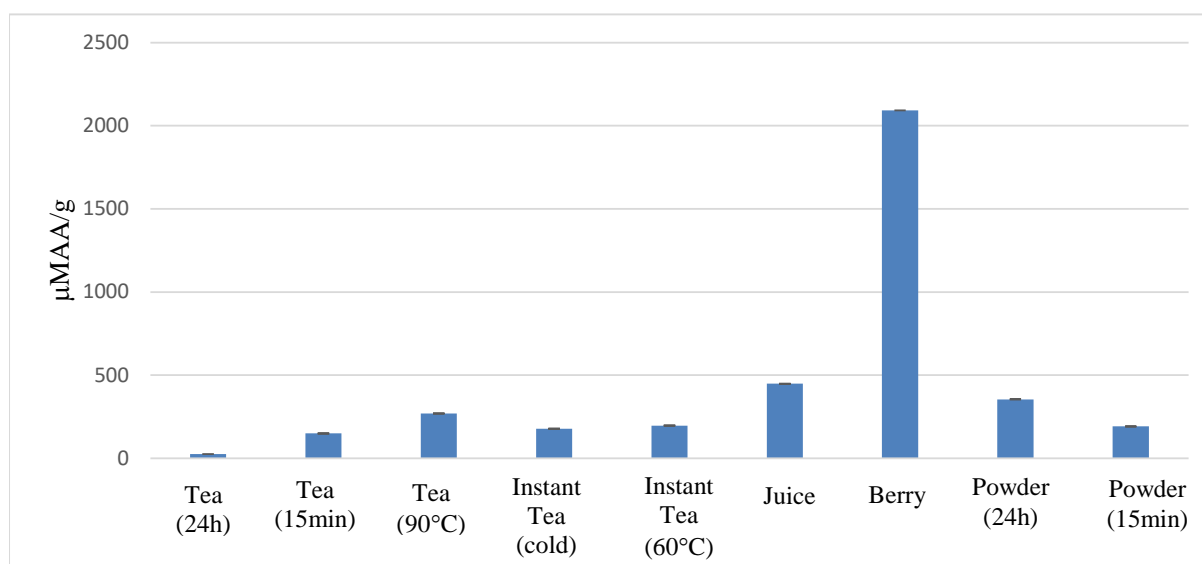


Figure 3. Ferric Reducing Ability of Plasma (FRAP), μg ascorbic acid equivalent/ g

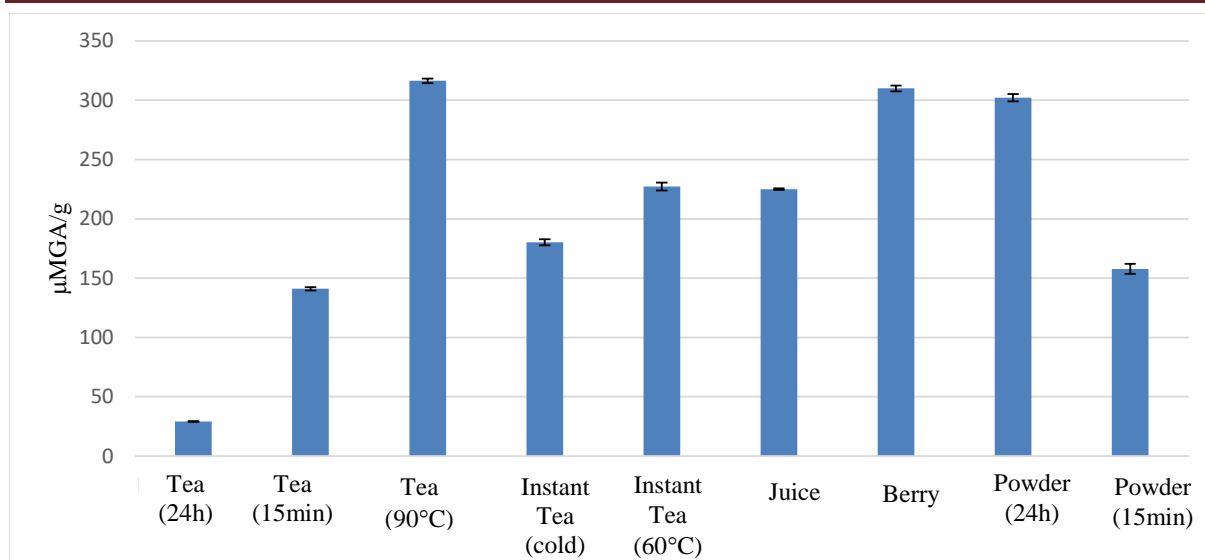


Figure 4. Total polyphenol content (TPC), µg gallic acid equivalent/ g

Conclusion

The obtained results highlighted that not only the active substance content of products but also the preparation techniques (water temperature, time of infusion) significantly influence the antioxidant capacity and antibacterial activity. Higher water temperature in case of tea preparation resulted better antibacterial activity and higher antioxidant capacity. In case of sea buckthorn powder, longer infusion time proved to be more efficient. Products with higher antioxidant capacity showed better antibacterial activity by agar well diffusion method. In case of berry and berry juice, high antioxidant capacity and excellent antibacterial activity were determined. In case of instant tea, the originally added vitamin C could have slightly influenced the result, both for bacteriocidal effect and antioxidant capacity.

Acknowledgements



SUPPORTED BY THE ÚNKP-17-1 NEW NATIONAL EXCELLENCE PROGRAM OF THE MINISTRY OF HUMAN CAPACITIES

References

- [1] Bernáth J. (szerk) (2000): Gyógy és aromanövények. Bp, Mezőgazda Kiadó, 350-354
- [2] A. Niesteruk, H. Lewandowska, Z. Golub, R. Świsłocka, W. Lewandowski, Kosmos, 4 (2013) 571-581
- [3] Olas, B. 2016. Sea buckthorn as a source of important bioactive compounds in cardiovascular diseases. Food and Chemical Toxicology 97: 199-204
- [4]. Chen, X.-M. Xu, Y. Chen, M.-Y. Yu, F.-Y. Wen, H. Zhang, Food Chemistry, 141 (2013) 1573-1579
- [5] Arora, R., Mundra, S., Yadav, A., Srivastava, R. B., Stobdan, T. 2012. Antimicrobial activity of seed, pomace and leaf extracts of sea buckthorn (*Hippophae rhamnoides* L.) against foodborne and food spoilage pathogens. African Journal of Biotechnology 11(45): 10424-10430
- [6] Chaman, S., Syed, N. I., Danish, Z., Khan, F. Z. 2011. Phytochemical analysis, antioxidant and antibacterial effects of sea buckthorn berries. Pakistan Journal of Pharmaceutical Sciences 24(3): 345-351

- [7] Benzie, I. F. F., Strain, J. J. 1996. The ferric reducing ability of plasma (FRAP) as a measure of "Antioxidant power": The FRAP assay. *Analytical Biochemistry* 239(1): 70-76
- Blois, M. S. 1958. Antioxidant determination by the use of a stable free radicals. *Nature* 4617: 1198-1200
- [8] Singleton, V. L., Rossi, J. A. 1965. Colorimetry of total phenolics with phosphomolibdicphosphotungstic acid reagents. *American Journal of Enology and Viticulture* 161: 144-158

STUDY OF THE COMPOSITION AND SIZE DISTRIBUTION OF GOLD-CONTAINING BIMETALLIC NANOPARTICLES SYNTHESIZED IN A SPARK DISCHARGE GENERATOR

**Henrik Bali¹, Albert Kéri¹, Attila Kohut², Lajos P. Villy²,
Ádám Béltéki¹, Zsolt Geretovszky², Gábor Galbács^{1*}**

¹*Dept. of Inorg. and Anal. Chem., University of Szeged, Dóm sq. 7, 6720 Szeged, Hungary*

²*Dept. of Opt. and Quant. Electron., University of Szeged, Dóm sq. 9., 6720 Szeged, Hungary*

**e-mail: galbx@chem.u-szeged.hu*

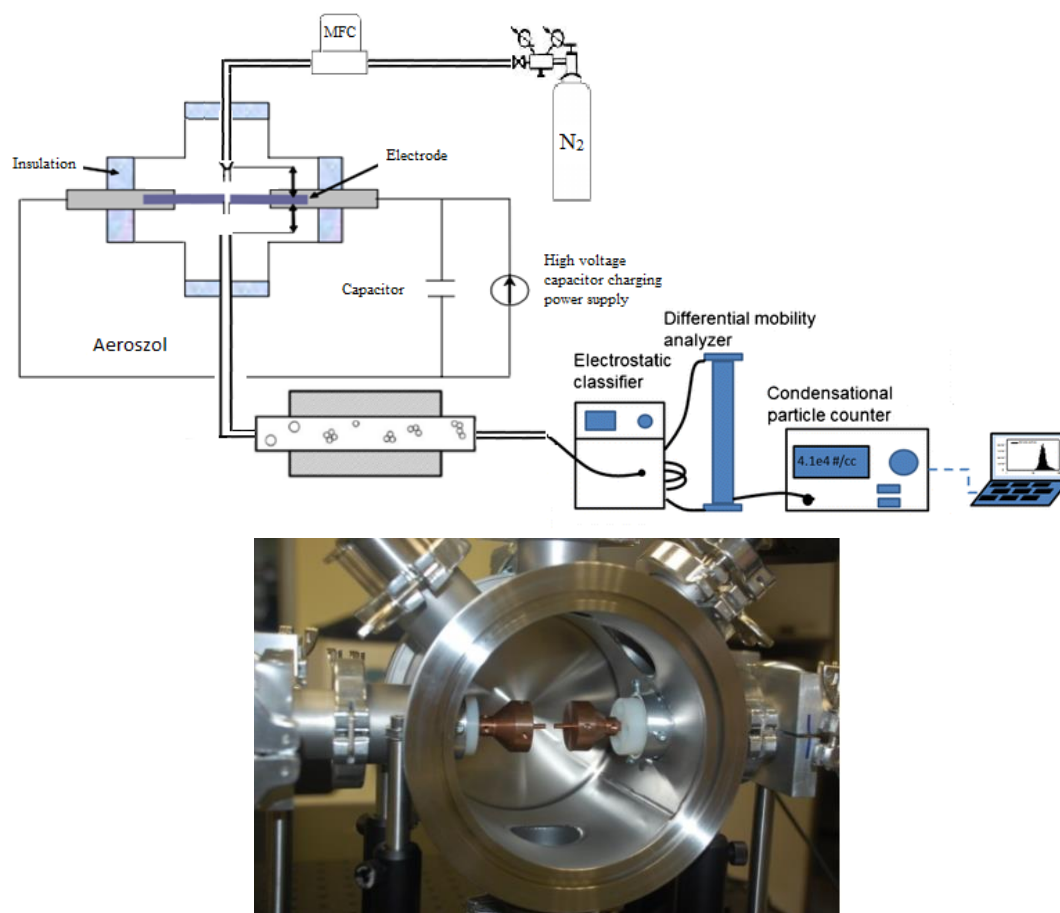
Introduction

Nanotechnology is one of the most dynamically growing fields of science, which requires the production of engineered nanoparticles (ENP) for various applications. Chemical synthesis procedures were dominating the field for many years, but physical procedures, that are based on laser or discharge ablation, are becoming more and more popular nowadays. One of these ablation-based methods is spark discharge generation, which is a versatile method for the preparation of mono- or bimetallic nanoparticles. In a spark discharge generator (SDG), a high voltage oscillating discharge is produced between two electrodes made of at least moderately conducting material. The erosion of the electrodes produce an atomic vapor in the spark gap, which is carried away by a gas flow. Nucleation and coagulation processes lead to nano-sized aggregates, which are then compacted to form spherical nanoparticles (NP). This method produces high purity NPs. SDGs can also be run continuously, thus industrial rate production is also possible. Control of the particle properties (e.g. concentration and size) can be achieved by tuning the operating conditions of the generator. The SDG method can also be considered cost-efficient and environmentally friendly.

The goal of the present work was to study how the operating parameters of SDGs influence the composition and size distribution NPs in the case of certain bimetallic particles (BNPs). In particular, we intended to study the influence of the electrode polarity, gap size and compaction on Au-Ag and Au-W particles.

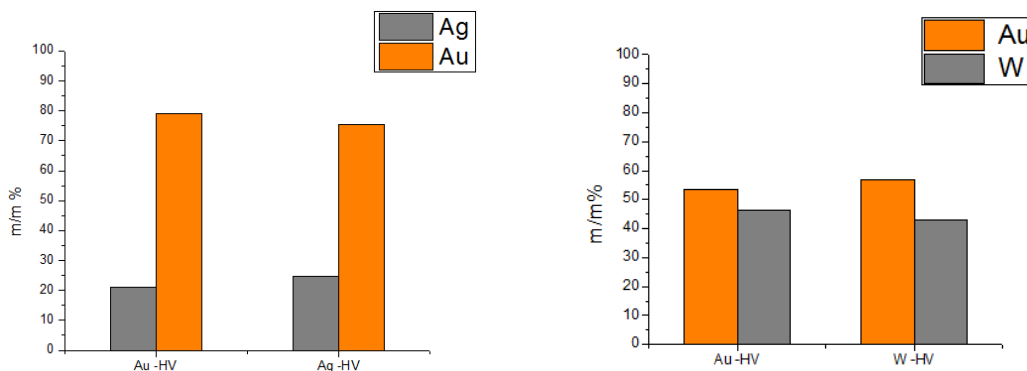
Experimental

Our SDG system is built around a gastight stainless steel chamber (DN 160). The two, 3 mm diameter, cylindrical electrodes (99.9% purity, Goodfellow Inc.) are uniaxial and positioned horizontally. The electrode gap can be controlled by two microadjusters. The carrier gas, 99.995% purity nitrogen, entered the chamber ca. 5 mm above the electrodes and flowed downwards. The flow rate was set at 5 l/min using a mass flow controller (Modell GFC16, Aalborg Inc.). All experiments were performed at atmospheric pressure (~1015 mbar). Evacuation of the chamber was done using a membrane pump (UN726TTP, KNF Neuberger Inc.). The discharge circuit consisted of an 8 nF, monolithic, high voltage capacitor (Modell 450PM980, General Atomics) and a high voltage capacitor charging power supply (HCK 800-12500, FuG GmbH). The discharge current was adjusted to keep the spark repetition rate at 100 Hz. The size distribution was monitored by an SMPS (SMPS-C, Grimm Aerosol Technik GmbH). The generated NPs were collected on glass fiber filter and then dissolved in aqua regia prior to their composition determination by ICP-MS analysis. The produced solution was then filtered on a 0.22 µm PTFE membrane syringe filter. The solution was finally measured on an Agilent 7700X ICP-MS instrument.

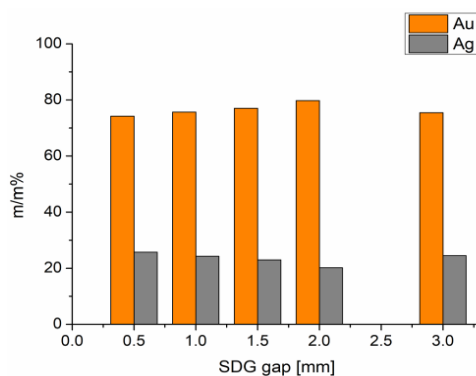


Results and discussion

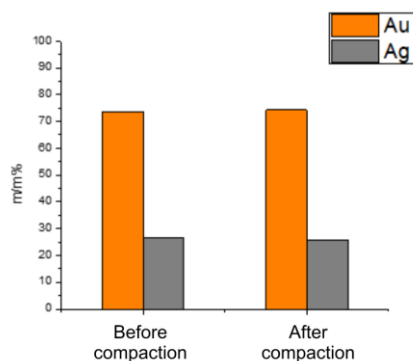
Effect of initial electrode polarity on NP composition. This parameter is expected to have only a minor influence on NP composition, since it has little impact on the extent of electrode erosion. The oscillating current will ablate always the cathode, which one of electrodes in one half-cycle and then in the next half-cycle, the other electrode gets to be the cathode and so ablated, and so on. Erosion rate is proportional to the square root of the electrical current, and since the current dampens with about a couple of percents in every half-cycle, therefore the rate of erosion will slightly (5-10%) higher for the electrode that was initially the cathode (HV). If the quality of the electrodes is different, then the erosion rate can also be different, thus this polarity-driven contribution only perturbs the already existing erosion rate difference. This translates to a slightly differing composition of NPs, as is illustrated by the graph below, which shows the case of Au/Ag and Au/W electrodes. The concentration of particles does not change significantly.



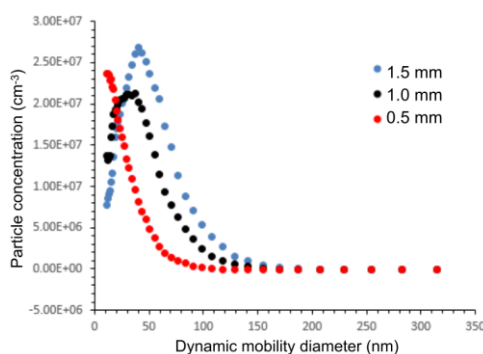
Effect of gap size on NP composition. The gap size influences the breakdown voltage, which in turn proportionally changes the spark energy. Hence, a larger gap size produces a higher energy spark, which causes more erosion. The effect of this on NP composition is such that the softer component will become slightly overrepresented in, as its erosion will increase more. Along with this, the particle concentration will typically decrease, because spark repetition rate, which primarily influences the particle yield, decreases with an increase in the breakdown voltage (assuming a constant charging current). The figure below shows the observed effect of the gap size on the NP composition for Au and Ag electrodes. It should also be added, that using extreme gap sizes, can shift the character of the discharge too – for example, at around ca. 0.5 mm gap size, a spark-to-glow transition occurs, which slightly also influences the erosion processes. As it can be seen, the total change in composition is only a few percents in the range of 0.5 to 3 mm.



Effect of compaction on NP composition. Compaction (sintering) of the particle aggregates by leading the NPs through a tube furnace is often advantageous in NP production, as it makes the particles more spherical, more uniform. The control of the process needs the optimization of the carrier gas flow rate and the furnace temperature. In the present case, we worked with a 900°C temperature, which is the highest value that can be set in our furnace. The process may result in some loss of the more volatile metal of the two, thus NP composition may be affected. In the case of Ag/Au BNPs, where there is no significant difference in the melting point (Au 1064°C, Ag 962°C), the process caused no change in the composition of particles.



Effect of gap size on NP size distribution. It is probably needless to say that the size distribution of only compacted particles can be meaningfully determined, thus we also studied this effect on compacted particles. As it turned out, the size distribution of Au-Ag BNPs shifted with an increase of gap size in such a way that the modus increased.



Conclusions

It was established that neither the initial electrode polarity, nor compaction or gap size does not significantly change the composition of the generated Au-Ag BNPs in an SDG. The effect was only a few percent. This is advantageous, since it allows the production of different concentration or size of particles of the same composition with the same set of electrodes. At the same time, the few percents change in composition caused by the polarity change can be considered as a simple and elegant means of fine-tuning the NP composition. It was also observed that the gap size strongly influences the size distribution of NPs.

At present, work is being carried out in our laboratories to extend the experiments over to other BNPs. We are also currently making attempts to assess the performance of electrode erosion models (e.g. Lwellyn-Jones and Feng et al.) in estimating the composition of BNPs.

Acknowledgments

The authors thankfully acknowledge the financial support to the project from various sources including the New National Excellence Program of the Ministry of Human Capacities (Hungary) and the EU-funded Hungarian grants EFOP-3.6.2-16-2017-00005 and GINOP-2.3.2-15-2016-00036.

SYNTHESIS OF GRAPHENE/CuGaO₂ AEROGELS FOR ADVANCED ELECTRODES

Cristina Mosoarca¹, Daniel Ursu¹, Terezia Nyari¹, Petrica Linul^{1,2}, Iuliana Serbachievici¹, Bogdan Taranu¹, Radu Banica¹

¹*National Institute for Research and Development in Electrochemistry and Condensed Matter, Dr. A. Paunescu Podeanu, no. 144, Timisoara, Romania*

²*Politehnica University Timisoara, Piata Victoriei, no. 2, Timisoara, Romania*
e-mail: radu.banica@yahoo.com

Abstract

Inorganic aerogels [1] are most often produced from silica, undergoing multiple phases of cooling and heating under high pressure (supercritical drying) or vacuum (lyophilization). Nowadays, low-cost organic aerogels such as graphene/metal oxide hydrogels are widely used in various applications (supercapacitors, oil absorption etc.) and fields like electronics, material science and aerospace engineering [2,3]. These carbon-based nanomaterials, having a nonpolar carbon structure, are useful especially for their essential hydrophobic properties [4], ultralow density, high surface area and high conductivity. Our previous work [5,6] included studies upon *p*-CuGaO₂ dye-sensitized solar cells which revealed excellent optical transparency of CuGaO₂. Also, CuGaO₂ can be used in photocatalysis for the oxidation of hydrogen sulfide, while graphene can conduct the electrons generated in the conduction band of the semiconductor to the counter-electrode closing the electrical circuit. Hybrid materials like CuGaO₂/graphene aerogels could be efficient for dye-sensitized solar cells and advanced electrodes fabrication.

Experimental

The precursor sample (P1) is a mixture of graphene oxide prepared using a modified Hummers method (conc. 0.9 mg/ml) and graphene Quattro-Type (conc. 0.05 mg/l) purchased from NanoIntegris. By centrifugation and water redispersion, the concentration of graphene increased to 0.75 mg/ml.

Further, the suspension was subjected to freeze drying and thermal treatment in a GSL-1500X Vacuum furnace (MIT Corporation) at a pressure < 1 Torr and a temperature rise rate of -4°C/minute resulting in P1T2 (Fig. 1A) and P1T3 samples.

CuGaO₂ was obtained under hydrothermal conditions at 250°C, using metal nitrates as precursors. X-Ray powder diffraction patterns of CuGaO₂ were obtained using an X'Pert PRO MPD diffractometer.

CuGaO₂ was added to P1 aqueous solution, following the protocol described above, resulting in aerogel samples S1 and S2 (Fig. 1B). Samples S1 and S2 were characterized by Scanning Electron Microscopy (SEM).

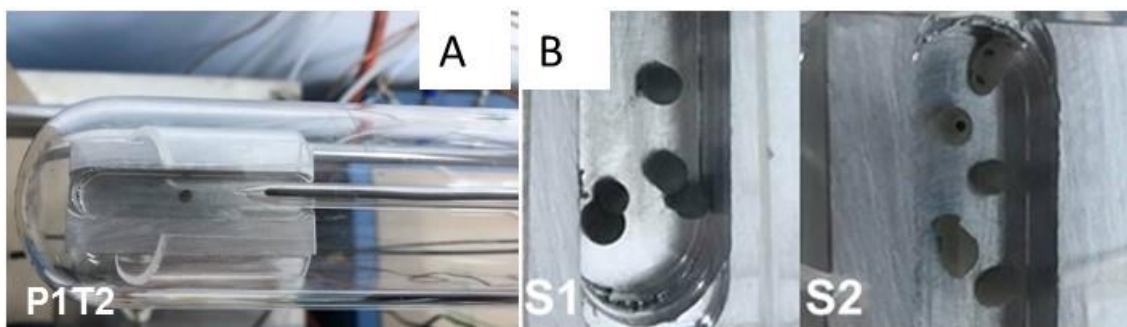


Figure 1. Photograph of (A) P1T2 aerogel sample (B) S1 and S2 aerogel samples

Results and discussion

Sample composition and processing conditions are presented in Table 1.

Sample name	CuGaO ₂ %	Treatment temperature °C
P1T2	0	240
P1T3	0	300
S1	1	300
S2	4	300

Table 1. Experimental conditions for thermal treatment and CuGaO₂ content corresponding to P1T2, P1T3, S1 and S2 samples

The sample P1T3 (Fig. 1A), resulting from the 300°C thermal treatment (Table 1), has an average pore size higher than sample P1T2 obtained at 240°C. This phenomenon is due to the lower density of hydrophilic groups as G-COOH, G-OH, G-CO, attached on the graphene sheets. A high density of functional groups leads to the adsorption of a higher quantity of atmospheric water which, in turn, leads to the loss of structural integrity and partial collapse of structures, manifested by the pore dimension decrease.

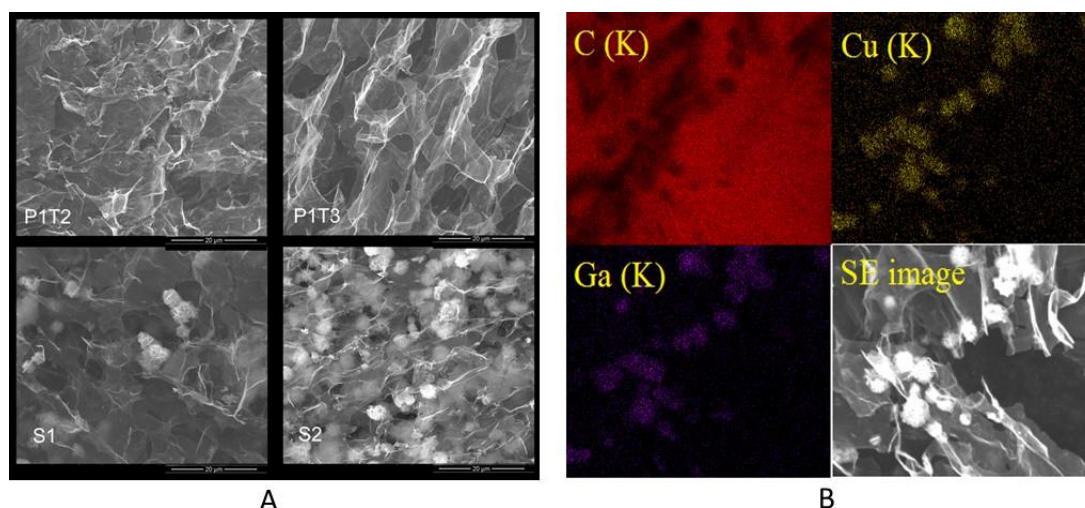


Figure 2. Graphene and CuGaO₂/graphene aerogels – (A) SEM images of P1T2, P1T3, S1 and S2 samples; (B) EDS elemental composition maps of S1 sample.

In case of S1 and S2 aerogel samples, we can see that the CuGaO_2 “flower shape” superstructures are uniformly distributed in the volume of the graphene aerogel (Fig. 2A and 2B). Due to the use of the graphite oxide and reduced graphene mixture, the S1 and S2 aerogels have both a high polar molecule absorption capacity due to the functional groups attached to the graphene oxide and, also, a high electrical conductivity due to the reduced graphene.

EDS maps (Fig. 2B) of S1 sample confirmed the homogenous distribution of Cu and Ga, which confirms the pure phase CuGaO_2 delafossite (Fig. 3) and the relative homogenous dispersion of the inorganic compound in aerogel. The use of hybrid materials like CuGaO_2 /graphene type aerogels, for dye-sensitized solar cells, electrochemical sensors and advanced electrodes will be the topic of further studies.

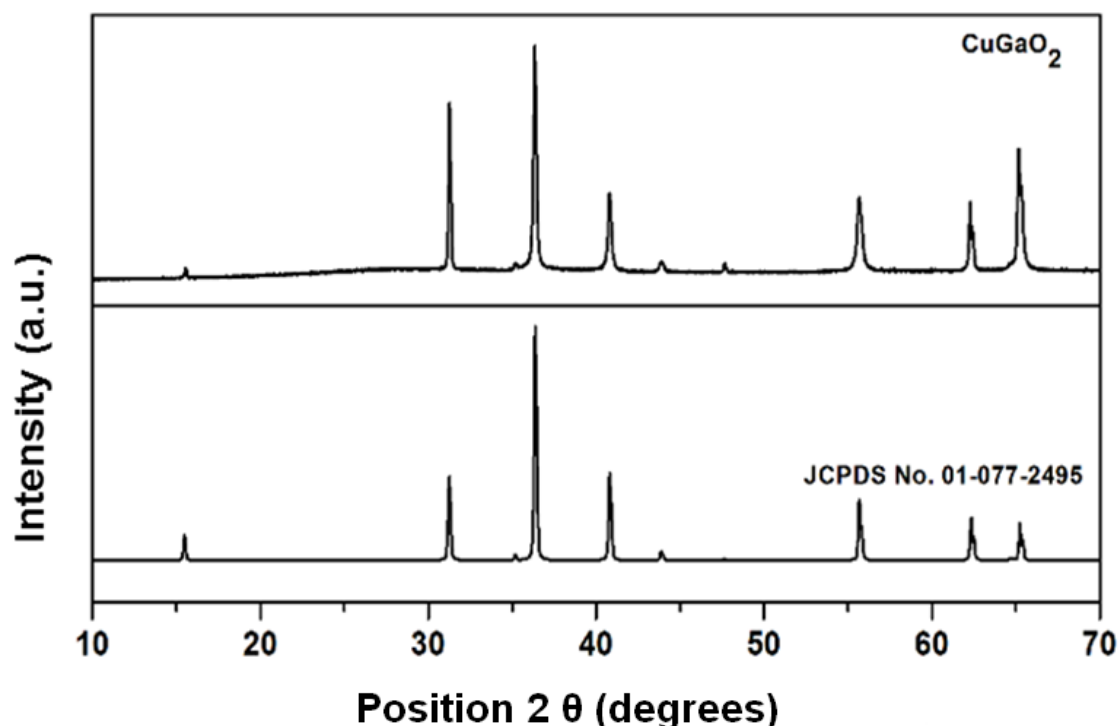


Figure 3. X-ray diffraction pattern of CuGaO_2

TEM image (Fig. 4A) suggests that $p\text{-CuGaO}_2$ semiconductor is exhibiting flat platelets. These semiconductor sheets are forming spherical superstructures coated by graphene within the aerogel. Therefore, the electrical contact between the graphene layer and the semiconductor nanoparticle is “point shaped” with reduced surface area. Further studies are required for increasing the contact surface between the semiconductor and graphene sheets.

The band gap energy value of the semiconductor (E_g) was determined from the UV-Vis diffuse reflectance spectra (Fig. 4B). Sample reflectance was transformed into absorbance using Kubelka-Munk (K-M) function. Due to the fact that CuGaO_2 has a direct inter-band transition, the E_g value was determined by extrapolating the linear part of $(K-M \cdot E)^2 = f(E)$, where K-M is the absorbance and E the reflected energy radiation (eV) [7].

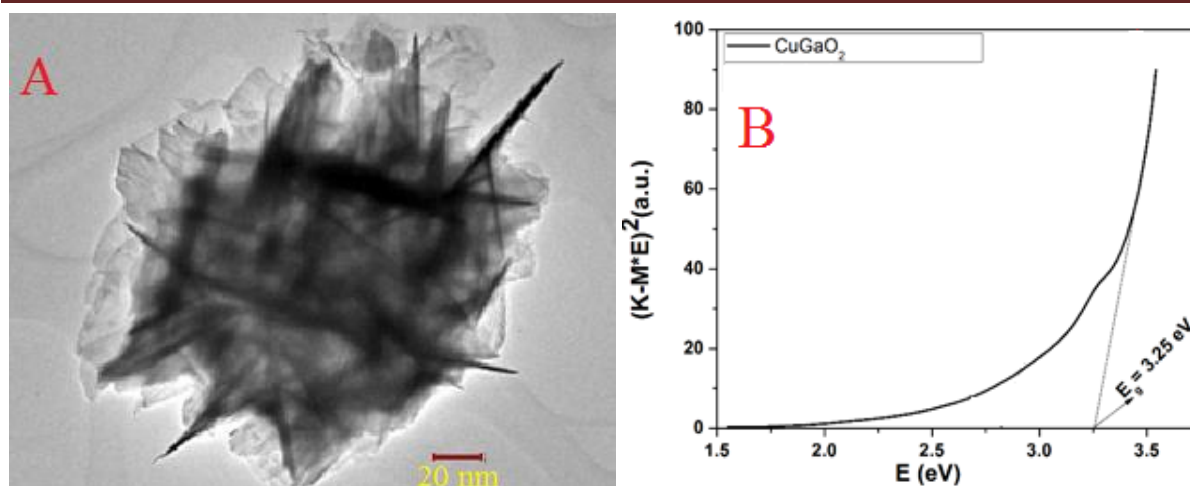


Figure 4. TEM of pure CuGaO₂ material (A) and E_g determination (B)

Conclusions

Graphene and graphene/CuGaO₂ based aerogels, with various possible nanotechnology applications, were synthesized by lyophilization followed by thermal treatment in vacuum. During the thermal treatment, the graphene oxide from precursors is partially reduced; some hydrophilic bonds are lost by condensation and decarboxylation reactions, leading to aerogel pore size change after water adsorption. An aerogel with a homogenous distribution of the semiconductor within it was obtained by mixing P1 aqueous suspension containing graphene oxide and reduced graphene with the CuGaO₂ compound, before freezing.

Acknowledgements

This work was supported by a grant of the Romanian Ministry of Research and Innovation, CCCDI-UEFISCDI, project number PN-III-P1-1.2-PCCDI-2017-0619/Contract 42/2018 “Nanostructured carbon materials for advanced industrial applications”, within PNCDI III national research program.

References

- [1] S.S. Kistler, *Nature*, 127 (1931) 741.
- [2] G. Gorgolis, C. Galiotis, *2D Materials*, 7 (2017) 032001.
- [3] G. Tang, Z.G. Jiang, X. Li, H.B. Zhang, A. Dasari, Z.Z. Yu, *Carbon*, 77 (2014) 592-599.
- [4] Y. Lin, G.J. Ehlert, C. Bukowsky, H.A. Sodano, *Appl. Mater. Interfaces*, 3 (2011) 2200–2203.
- [5] D. Ursu, M. Miclau, R. Banica, N. Vaszilcsin, *Mat. Lett.* 143 (2015) 91-93.
- [6] C. Zamfirescu, I. Dincer, G.F. Naterer, R. Banica, *Chem. Eng. Sci.* 97 (2013) 235-255.
- [7] R. Banica, T. Nyari, V. Sasca, *Int. J. Hydrogen Energ.* 37 (2012) 16489 – 16497.

SYNTHESIS OF GRAPHITE-GRAPHENE AEROGELS FOR THERMAL ENERGY STORAGE APPLICATIONS AND SENSORS

Mihai-Cosmin Pascariu, Iuliana Sebarchievici, Petrica Linul, Cristina Mosoarca, Daniel Ursu, Radu Banica*

*National Institute of Research & Development for Electrochemistry and Condensed Matter,
144 Dr. Aurel Păunescu-Podeanu, RO-300569 Timișoara, Romania*

**radu.banica@yahoo.com*

The use of graphite and graphene oxide in combination with phase change materials is a viable choice for enhancing the thermal conductivity of latent heat storage materials [1, 2]. Graphene-based aerogels attracted a lot of interest due to their fascinating properties, such as high mechanical strength, electrical conductivity, adsorption capacity and thermal resistance [3], which allow them to be used in a variety of applications like energy storage, supercapacitors and gas sensing [4].

The present study includes the preliminary results regarding the functionalization of graphite, and the chemical synthesis of graphite-graphene aerogel. The obtained carbon materials were studied using X-ray diffraction and scanning electron microscopy.

Graphite-graphene aerogel synthesis

The incorporation of surface oxygen into graphite can be achieved through a variety of methods. The *functionalization of the graphite* surface by acidic oxidation is the starting point for the vast majority of reports [5].

H₂SO₄ and HNO₃ were mixed in a 3:1 ratio to create a solution with a final volume of 160 mL. Graphite powder (2 g) was added to this solution and the mixture was heated to 70 °C with stirring for 8 h. After the oxidation process, the excess of the oxidizing agent was removed by centrifugation, followed by repeated washing, decanting and further centrifugation of the functionalized graphite in bidistilled water until the pH of the supernatant exceeded 5 (the concentration of suspension was 73.4 mg/mL).

The *graphene oxide* (prepared by the modified Hummers' method) was mixed with the functionalized graphite, in a 1:100 ratio, after which the suspension was immersed in liquid nitrogen for 2 minutes. The sample lyophilization occurred at a gas pressure of 2 Torr, and after 20 hours the gas pressure dropped to about 960 mTorr. At this point the graphite-graphene aerogel can be clearly seen inside the quartz tube (Figure 1). Finally, the aerogel was heat-treated under vacuum (GSL-1500X Vacuum furnace, MTI Corporation) at 800 °C (2 °C/min) for 60 minutes, during which the aerogel fragmented.

To also study the thermal reduction of the graphene oxide, this was heated under the same conditions. The results are compared in Figures 2 and 3.

The crystalline structure of the samples was characterized by X-ray diffraction measurements (XRD, PW 3040/60 X'Pert PRO, Cu-K α radiation), the results being presented in Figure 2.

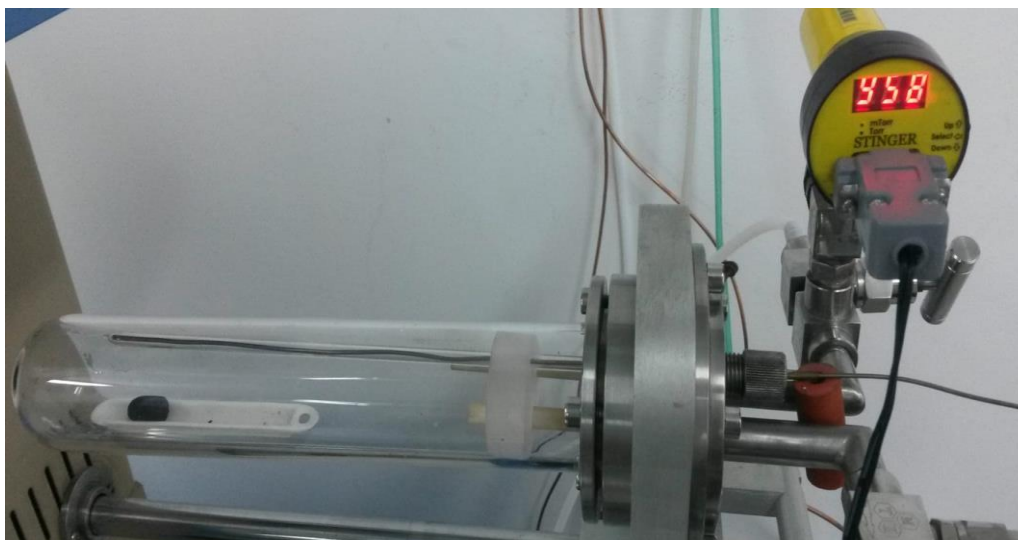


Figure 1. The graphite-graphene aerogel during its synthesis.

The crystallite size was determined using the Scherrer equation, by considering the diffraction peak located at a 2θ of 26.6 degrees, having the Miller indices (002). The obtained values were 103 nm for graphite and, respectively, 49.5 nm for the graphite in aerogel.

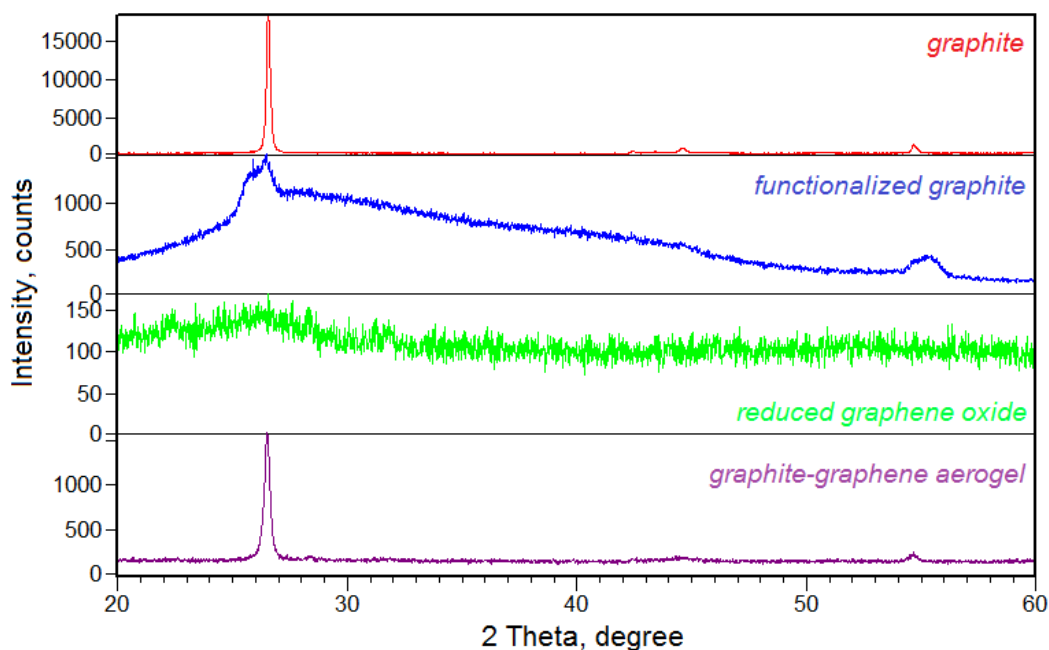


Figure 2. XRD patterns of graphite, functionalized graphite, reduced graphene oxide, and graphite-graphene aerogel.

Thus, the oxidizing mixture leads, on one hand, to the fragmentation of graphene sheets from the graphite network, and on the other hand to the intercalation of functional groups across the carbon atom layers, which is followed by the separation of sheets. The functionalized graphite is completely reduced at 800 °C.

The morphology of the samples, investigated using the scanning electron microscope (FEI Inspect S), is presented in Figure 3.

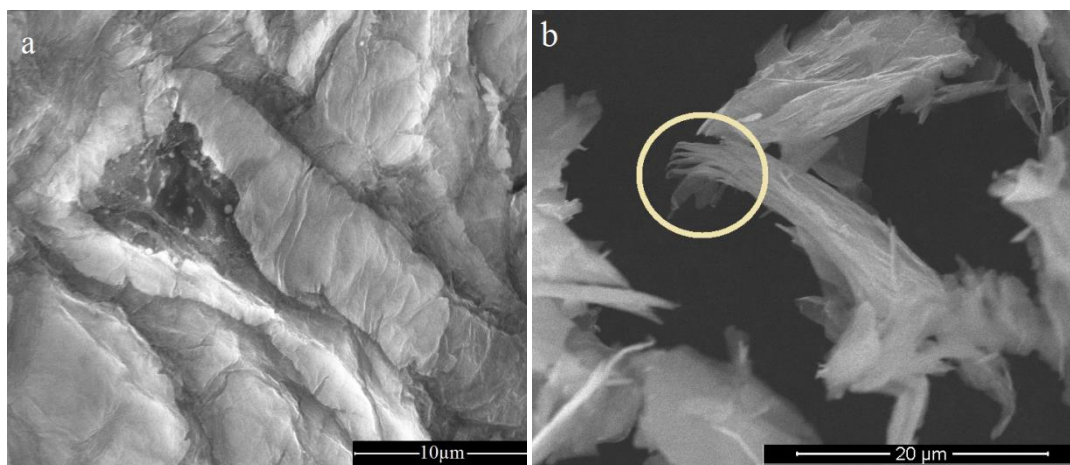


Figure 3. SEM images of (a) reduced graphene oxide and (b) graphite-graphene aerogel.

The aerogel has an interconnected porous network, the pore walls consisting of layers of stacked graphene and graphite sheets. In the SEM images (Figure 3b) we can observe the existence of individual graphite sheets, produced during the loss of oxygen through high-temperature reduction, which confirms the XRD data.

Acknowledgments

This work was supported by a grant of the Romanian Ministry of Research and Innovation, CCCDI - UEFISCDI, project number PN-III-P1-1.2-PCCDI-2017-0619 / research contract 42/2018 “Nanostructured carbon materials for advanced industrial applications”, within PNCDI III.

References

1. Z. Ge, F. Ye, Y. Ding, Composite Materials for Thermal Energy Storage: Enhancing Performance through Microstructures, *ChemSusChem*, 7, 2014, 1318 – 1325
2. N. Xie, Z. Huang, Z. Luo, X. Gao, Y. Fang, Z. Zhang, Inorganic Salt Hydrate for Thermal Energy Storage, *Appl. Sci.* 7, 1317, 2017, 1-18
3. G. Gorgolis, C. Galiotis, Graphene aerogels: a review, *2D Mater.* 4, 2017, 032001
4. M. Dragoman, L. Ghimpu, C. Obreja, A. Dinescu, I. Plesco, D. Dragoman, T. Braniste, I. Tiginyanu, Ultra-lightweight pressure sensor based on graphene aerogel decorated with piezoelectric nanocrystalline films, *Nanotechnology*, 27, 2016, 475203
5. K.A. Wepasnick, B.A. Smith, K.E. Schrote, H.K. Wilson, S.R. Diegelmann, D. Howard Fairbrother, Surface and structural characterization of multi-walled carbon nanotubes following different oxidative treatments, *Carbon*, 49, 2011, 24-36.

NOISE MEASUREMENTS AND NOISE DISTRIBUTION IN THE CITY OF SZEGED OVER A 6 YEAR TIME PERIOD

Zsolt I. Benkő¹

¹*Department of Technology, University of Szeged, H-6725 Szeged, Boldogasszony sgt. 6,
Hungary*

e-mail: bzs@jgypk.szte.hu

Abstract

Measurements were carried out on selected points of Szeged to achieve a coarse noise distribution of the city. The measurements were aimed to obtain the environmental noise load values caused by traffic mainly. The original measurements were carried out in 2012 and they were repeated on the same location spots in 2015 and 2018.

Introduction

Almost all the information a man collects is acquired through sight and hearing (83% percent through sight and 11% through the hearing). These times more and more people live in big, crowded cities. This artificial environment when compared to the natural environment is too noisy. It can be even harmful to the hearing. It is a necessity to check from time to time that our environment is still within the healthy limits.

The normal hearing of a human ranges from 20 Hz frequency to 20000 Hz.[1]

The hearing is logarithmic. The industrial tools for noise measurements are based on sound pressure level and the data are given in decibel (dB).[2] It is given by Eq.1:

$$L_p = 20 \log_{10} \left(\frac{\Delta p}{p_0} \right) \text{ dB} \quad (1)$$

where Δp is the sound pressure fluctuation, and p_0 is the reference pressure fluctuation value (audition threshold); $p_0 = 20 \text{ } \mu\text{Pa}$.

Table 1 shows some common examples for easy comparison.

L(SPL) (dB)	phenomenon
0	audition threshold; mosquito at 3 m
10	human breathing at 3 m
30	theatrical stillness
40	living area at night; stillness of nature
60	office
70	street traffic at 5 m
90	noise in factory
100	jackhammer at 1 m; disco inside
120	train horn at 10 m
130	pain threshold

Table 1. Sound pressure level examples

85 dB or higher sound pressure level over a long-term exposure can cause hearing damage. The hearing damage is cumulative throughout the entire life like e.g. radioactive dosage.

The auditory sensation depends on the frequency of the sound strongly: at the same sound pressure level a 200 Hz sound feels much weaker than a 1000 Hz sound. The equal

loudness curves are measured first by Harvey Fletcher and Wilden A. Munson in 1933. The measurements were reproduced in the time period of 2000-2003.[3][4][5][6]

The industrial noise meters use weighting curves to show similar responses to the human hearing. The A-weighting is used for auditory purposes. The C-weighting is almost flat; that can be used as the real physical sound pressure.[7]

Though +6 dB means twice the power, the human perception works in other way. If it is heard two times louder than it is +10 dB more.[8][9]

Also, in 2018, the measurements were extended to acquire samples of the CO₂ and CO levels of the air.

The atmospheric level of CO₂ is about 400 ppm by Mauna Loa Observatory, Hawaii (NOAA-ESRL) [10]; the normal value of CO₂-concentration at sea level is 250-350 ppm by industrial recommendations. [11]

Experimental

Figure 1 shows the different locations in Szeged where the measurements were carried out. Location 1, 3 and 5 are close to main roads in Szeged with heavy traffic. Location 2 and 6 are near less important roads, but sometimes they have heavy traffic. Location 4 is chosen to be far from any traffic; it is among housing blocks (sleeping area – no real daytime activity).

The measurements contain morning, mid-day and evening data for each location.

Out of curiosity the noise levels around the area of the Youth Days of Szeged (black area in the map) were measured, too. This festival is held in each August, and location 7 and 8 are used for it exclusively.

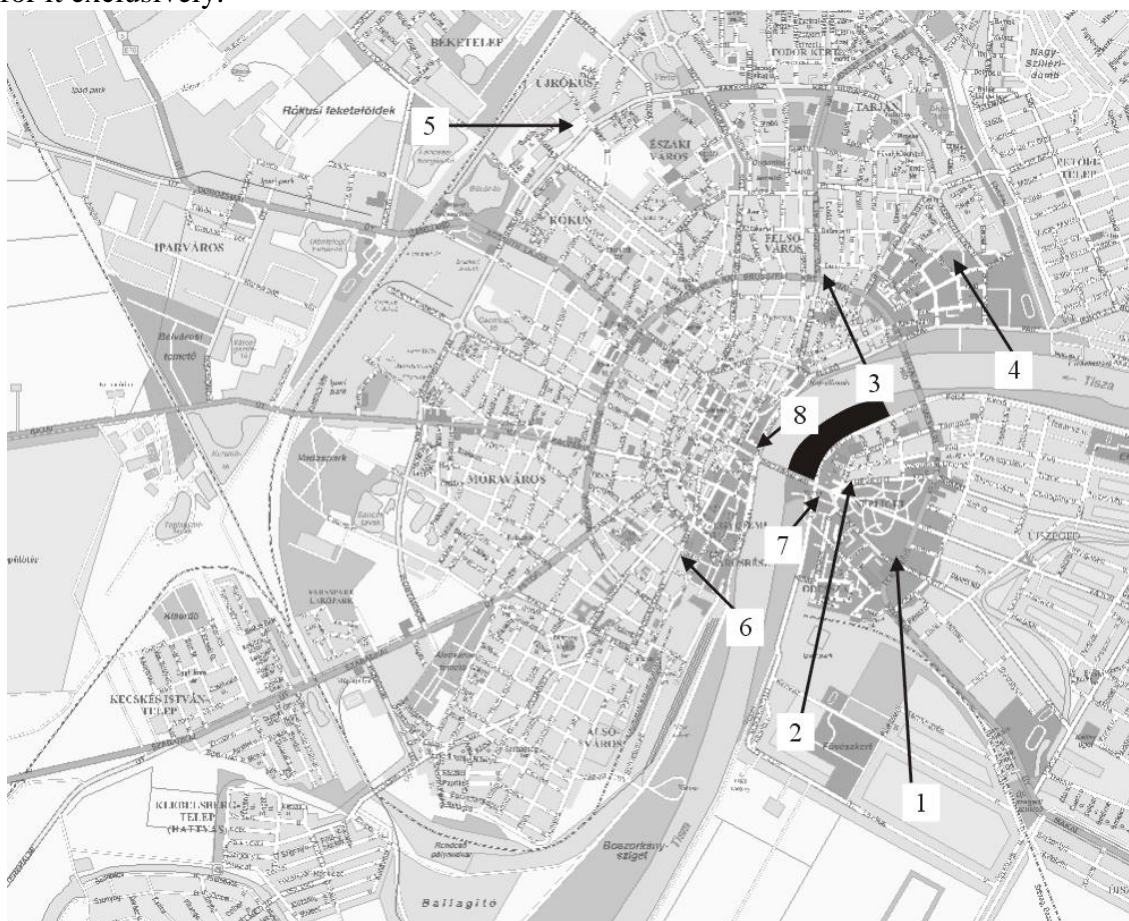


Figure 1. Locations of the measurements in Szeged

location	description (and GPS coordinates)
1	intersection of "Székely sor" and "Temesvári krt." (46° 14.728' N ; 020° 09.842' E)
2	close to the bridge (46° 14.991' N ; 020° 09.605' E)
3	intersection of "Római krt." and "József Attila sgt." (46° 15.696' N ; 020° 09.479' E)
4	near a housing block, "Csaba u. 43" (46° 15.732' N ; 020° 10.116' E)
5	school at "Rókusi krt." near Tesco (46° 16.253' N ; 020° 08.290' E)
6	school at "Boldogasszony sgt. 8" (46° 14.759' N ; 020° 09.738' E)
7	parking area at the bridge (46° 14.933' N ; 020° 09.410' E) – <i>only for YDS</i>
8	museum garden (46° 15.124' N ; 020° 09.162' E) – <i>only for YDS</i>

Table 2. Measurement location descriptions.

Results and discussion

The following tables show the current measured data for each location and all the previous values.[12] CO₂ and CO values are shown, too.

location 1	Year	workday morning (7h-8h)	workday daytime (12h-15h)	workday evening (20h-22h)
Sound level (dB)	2012	61.9 ± 5.2	55.5 ± 7.1	52.9 ± 6.8
Sound level (dB)	2015	64.6 ± 6.0	58.0 ± 8.0	52.2 ± 7.7
Sound level (dB)	2018	58.6 ± 7.6	56.1 ± 7.3	50.7 ± 7.0
CO ₂ (ppm)		286 ± 3	189 ± 9	268 ± 6
CO (ppm)		0	0	0

Table 3. Measurements on location 1.

location 2	Year	workday morning (7h-8h)	workday daytime (12h-15h)	workday evening (20h-22h)
Sound level (dB)	2012	59.2 ± 7.3	57.4 ± 7.8	54.9 ± 8.1
Sound level (dB)	2015	60.7 ± 8.5	56.9 ± 9.9	55.6 ± 7.1
Sound level (dB)	2018	59.3 ± 7.7	60.1 ± 6.0	50.1 ± 6.4
CO ₂ (ppm)		293 ± 17	193 ± 2	273 ± 20
CO (ppm)		0	0	0

Table 4. Measurements on location 2.

location 3	Year	workday morning (7h-8h)	workday daytime (12h-15h)	workday evening (20h-22h)
Sound level (dB)	2012	64.4 ± 3.4	63.4 ± 4.3	60.0 ± 4.9
Sound level (dB)	2015	67.5 ± 2.7	65.1 ± 4.0	60.1 ± 5.0
Sound level (dB)	2018	66.0 ± 3.7	64.9 ± 4.1	61.5 ± 4.7
CO ₂ (ppm)		282 ± 15	174 ± 4	258 ± 5
CO (ppm)		0	0	0

Table 5. Measurements on location 3.

location 4	Year	<i>workday morning (7h-8h)</i>	<i>workday daytime (12h-15h)</i>	<i>workday evening (20h-22h)</i>
<i>Sound level (dB)</i>	2012	43.4 ± 2.1	50.0 ± 3.5	42.9 ± 2.9
<i>Sound level (dB)</i>	2015	44.6 ± 2.1	35.3 ± 2.7	42.1 ± 4.1
<i>Sound level (dB)</i>	2018	41.4 ± 2.5	42.5 ± 2.9	41.9 ± 0.9
<i>CO₂ (ppm)</i>		270 ± 7	169 ± 20	262 ± 8
<i>CO (ppm)</i>		0	0	0

Table 6. Measurements on location 4.

location 5	Year	<i>workday morning (7h-8h)</i>	<i>workday daytime (12h-15h)</i>	<i>workday evening (20h-22h)</i>
<i>Sound level (dB)</i>	2012	57.5 ± 2.9	49.3 ± 2.5	51.4 ± 3.2
<i>Sound level (dB)</i>	2015	52.1 ± 3.3	51.0 ± 3.3	49.0 ± 3.2
<i>Sound level (dB)</i>	2018	51.2 ± 2.9	52.4 ± 3.0	49.9 ± 3.1
<i>CO₂ (ppm)</i>		285 ± 12	189 ± 12	266 ± 6
<i>CO (ppm)</i>		0	0	0

Table 7. Measurements on location 5.

location 6	Year	<i>workday morning (7h-8h)</i>	<i>workday daytime (12h-15h)</i>	<i>workday evening (20h-22h)</i>
<i>Sound level (dB)</i>	2012	64.0 ± 3.4	59.6 ± 6.2	51.9 ± 8.3
<i>Sound level (dB)</i>	2015	62.9 ± 4.7	63.8 ± 4.6	60.2 ± 4.0
<i>Sound level (dB)</i>	2018	57.4 ± 7.6	60.3 ± 6.7	60.1 ± 3.9
<i>CO₂ (ppm)</i>		279 ± 7	218 ± 14	237 ± 3
<i>CO (ppm)</i>		0	0	0

Table 8. Measurements on location 6.

The measurements to check the noise levels of the Youth Days of Szeged are shown in table 9. The samples were taken in the time period of 22h-24h.

Youth Days of Szeged	Year	<i>location 1</i>	<i>location 2</i>	<i>location 7</i>	<i>location 8</i>
<i>Sound level (dB)</i>	2012	54.2 ± 6.1	59.0 ± 4.1	59.7 ± 2.4	64.9 ± 2.5
<i>Sound level (dB)</i>	2015	53.8 ± 7.2	60.6 ± 4.4	64.2 ± 2.3	61.3 ± 2.3
<i>Sound level (dB)</i>	2018	49.4 ± 4.3	58.8 ± 5.8	62.5 ± 1.6	64.4 ± 2.0
<i>CO₂ (ppm)</i>		254 ± 2	256 ± 11	247 ± 4	255 ± 3
<i>CO (ppm)</i>		0	0	0	0

Table 9. Measurements during Youth Days of Szeged.

Conclusion

The results show that Szeged is a good city to live in. It has a rather quiet acoustical environment. Even during festivals.

Surprisingly the structure of the city is very good for the air ventilation, too. The measured CO₂ values are quite low, despite the fact, that sometimes the measurements were carried out in *1 m* distance from the moving motor vehicles (e.g. location 2 and 6).

This work aims to measure the environmental load caused mainly by the traffic. Currently there is no real tendency in the data. Maybe later, when more and more electric vehicles will

take part in the transportation some decrease could be found.

References

- [1] Rossing, T., Springer Handbook of Acoustics, Springer (2007), ISBN 978-0387304465, pp. 747-748
- [2] Thompson, A. and Taylor, B. N. sec 8.7, "Logarithmic quantities and units: level, neper, bel", Guide for the Use of the International System of Units (SI) 2008 Edition, NIST Special Publication 811, 2nd printing (November 2008)
- [3] Suzuki, Yôiti, et al. "Precise and full-range determination of two-dimensional equal loudness contours." Tohoku University, Japan (2003)
- [4] <http://www.mp3-tech.org/programmer/docs/IS-01Y-E.pdf>
- [5] ISO 226:2003
- [6] http://en.flossmanuals.net/csound/ch008_c-intensities/_book/csound/static/Fletcher-Munson.png
- [7] <http://en.wikipedia.org/wiki/A-weighting>
- [8] Stanley Smith Stevens: A scale for the measurement of the psychological magnitude: loudness. See: Psychological Review. 43, Nr. 5, APA Journals, 1936, pp. 405-416
- [9] <https://en.wikipedia.org/wiki/Sone>
- [10] <https://www.co2.earth/> (accessed: Sep.19.2018)
- [11] Bonino, S., "Carbon Dioxide Detection and Indoor Air Quality Control", Occupational Health & Safety (April 2016) {<https://ohsonline.com/articles/2016/04/01/carbon-dioxide-detection-and-indoor-air-quality-control.aspx>}
- [12] Benkő, Zs. I., "Noise Measurements and Noise Distribution in the City of Szeged", Proceedings of the 21st International Symposium on Analytical and Environmental Problems (September 28, 2015), ISBN 978-963-306-411-5, pp. 325-328

ADSORPTIVE REMOVAL OF ANTI - EPILEPTIC DRUG - CARBAMAZEPINE BY ACTIVATED CARBON

V. Bežanović¹, M. Novaković¹, M. Petrović¹, D. Milovanović¹, M. Živančev¹, S. Kovačević¹, D. Adamović¹

¹ *Department of Environmental Engineering and Occupational, Safety and Health, Faculty of Technical Sciences, University of Novi Sad, Trg Dositeja Obradovića 6, 21000 Novi Sad, Serbia*
e-mail: veselin.bezanovic@gmail.com

Abstract

This work describes the adsorption process of one of the most dominant pharmaceuticals detected in water sources, carbamazepine (CBZ), from aqueous solutions with commercially available activated carbon (AC). Adsorption studies were performed on powdered activated carbon Norit SA2, in ambient temperature, on pH value between 2 – 10, with different masses of adsorbent (6 – 20 mg), time intervals (5 – 60 min). The CBZ adsorption is explained by chemisorption which involves chemical reaction between surface and adsorbate. The results show that commercial activated carbon Norit SA2 can be applied in the process of adsorption for the purpose of removing carbamazepine from aqueous solution.

Keywords: adsorption, pharmaceuticals, carbamazepine, activated carbon, pH value.

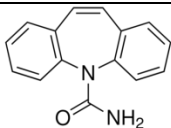
Introduction

During the last decades the phenomenon of drugs detection and classification as emerging substances in aquatic environment has been recognized as one of the most important environmental issues [1]. Among the chemicals, pharmaceuticals present large and diverse group of compounds designed to prevent, cure and treat diseases and improve health. Only in the European Union (EU) around 3000 different pharmaceutically active compounds (PhACs) are approved for use in human medicine. Furthermore, the increasing consumption of these compounds has resulted in significant concentrations in groundwater, surface water and treated wastewater effluents [2], [3], [4]. Mostly, pharmaceuticals cannot be completely eliminated from living organisms' bodies and they are excreted, causing their constant release in aqueous compartment. The widespread occurrence of pharmaceutical active compounds in surface water could be explained by their presence in domestic and industrial wastewater released into water media without adequate treatment [5]. There are currently no legally regulated maximum permitted concentrations of pharmaceuticals in the environment, despite their unknown impact on the environment and human health [6].

Carbamazepine (CBZ) (5H-Dibenz(b,f)azepine-5-carboxamide) (Table 1) as a neutral antiepileptic drug is among the most frequently reported pharmaceuticals in surface waters observed at a concentration more than 10 times higher than other micropollutants due to its high persistency [7]. Major quantity of research focusing on the removal of pharmaceuticals from wastewaters revealing that the existing conventional available treatment options are not beneficial in the elimination of these compounds [8]. Various treatment technologies have been introduced for removal of micropollutants from effluents such as coagulation - flocculation, chemical oxidation, and adsorption. With a low value of the distribution coefficient ($K_d = 1.2 \text{ L g}^{-1}$), carbamazepine can't be removed in treatment processes like anaerobic digestion. Therefore, discharge of effluents from urban wastewater treatment plants to environment could lead to occurrence of CBZ in the aquatic environments, and

subsequently in drinking water. Finding solution in the efficient post treatment could be of great importance to reduce the release of carbamazepine into surface waters.

Table 1. The physico chemical properties of CBZ

	Chemical structure	Molecular weight	pKa	logK _{ow}
Carbamazepine		236.27	2.3	2.45

Among the various treatment technologies that have been introduced for the purification and wastewater treatment, adsorption is one of the most effective methods of removing various micropollutants. Benefits of adsorption technology are reflected in high efficiency, easy handling, availability and cost-effectiveness of various adsorbents [9]. Activated charcoal, natural clays, modified clays and industrial waste, were used as adsorbents for the removal of wide range of micropollutants from wastewater solution [10], [11], [12]. Among them, natural clays showed good results as adsorbents to remove various metals, organic compounds and color.

However, some adsorbents such as carbon nanotube, graphene oxide, and functionalized materials showed a low potential for large-scale applications for the removal of organic burden [1].

Activated carbon (AC) is one of the well-known adsorbent which has great specific surface area, pore structure and one of the main advantages of using activated carbon to remove pharmaceuticals is that it does not generate toxic or pharmacologically active products [6]. High availability of AC in the market and considerable amount of research that has been published, define AC in a group of materials that can be used in the process of pharmaceuticals removing.

The aim of this study was to comprehensively evaluate the adsorption of carbamazepine onto activated carbon made from peat materials. In order to optimize processes of adsorption, influence of operational parameters was investigated. The operational parameters such as adsorbent dosage, pH value, contact time and initial concentration were changed in different experiments.

Experimental

Chemicals and reagents

Carbamazepine (CBZ, purity $\geq 99.0\%$) was purchased from Sigma Aldrich, Germany and used without further purification. Acetonitrile and formic acid (HPLC grade) were also obtained from Sigma Aldrich. The powdered activated carbon (Norit SA2) was obtained from Thermo Fisher Scientific, USA. The stock solution was prepared by dissolving 5 mg of analytical standard in 25 ml of acetonitrile (final concentration of 200 mgL^{-1}) and the working solutions were obtained by diluting the stock solution with distilled water. As aqueous matrix, distilled water was used. For pH adjustment, solution of 0.1% HCl and 1% of NaOH were used. All chemicals used in experiments were of analytical grade.

Adsorption experiments

Adsorption assays were performed in batch mode at room temperature (25°C). In order to analyze influence of pH value, five different pH values were used (2, 5, 7, 9 and 10). The initial concentration of CBZ was 5 mgL^{-1} , prepared in 50mL Erlenmeyer flasks. After pH adjustment, samples were agitated at mechanic shaker at 140 rpm. The contact time between adsorbent and pharmaceutical was 30 minutes. After stirring, all samples were filtered

through filter paper in order to remove activated carbon from solution. After performed experiment, 1 mL of samples were transferred into 2 mL vials.

The influence of mass dosage on adsorption processes was performed in 50 mL aqueous solution of carbamazepine with different masses of adsorbent (6, 8, 10, 12 and 20 mg). Kinetic studies were investigated in different time intervals (5-60 minutes). The initial concentration of carbamazepine was 5 mgL^{-1} .

Analytical procedure

For determination of remaining pharmaceutical residues, HPLC with diode array detector (Agilent 1260 series) was applied. Chromatography separation was performed at reverse stationary phase Eclipse XDB-C18 (150 x 4.6, particle size $5\mu\text{m}$) at flow rate of 0.2 mL min^{-1} and injection volume of $10 \mu\text{L}$ at room temperature. Mobile phases were consisted of: A – 0.1 formic acid and B – acetonitrile. Gradient elution mode was as follows: 20% of B for 3 min, 45% of B at 25 min, for 30% of B at 27 min and in 30-minute initial conditions were applied. The maximum absorbance for observed pharmaceutical is 290 nm.

Results and discussion

Influence of pH value

The pH value represents one of crucial parameters which have influence on adsorption capacity. Changes in the pH affect the ionization degree and the solubility of the solute as well as the surface charge of the adsorbent. Figure 1. shows the effect of pH value on CBZ adsorption.

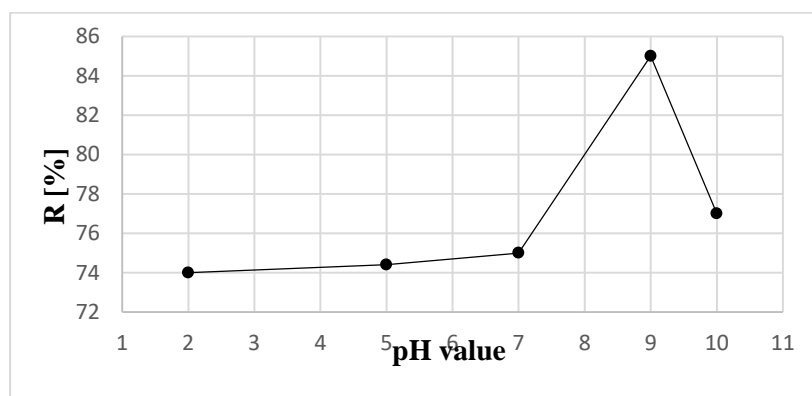


Figure 1. The effect of pH value

Intensity of interactions remains almost constant at acid and neutral conditions. Although carbamazepine molecule acts like neutral component, according to obtained results, the maximum removal efficiency (85%) was achieved in base medium, at pH 9. After performed the first set of experiments, pH 9 was adopted as optimal.

Influence of mass dosage

It is necessary to investigate what is the optimal mass of activated carbon in order to achieve satisfactory removal efficiency. By increasing the amount of activated carbon, the number of available sorption sites on its surface area will increase causing increase in removal efficiency. Figure 2. shows the impact of activated carbon dosage on CBZ adsorption.

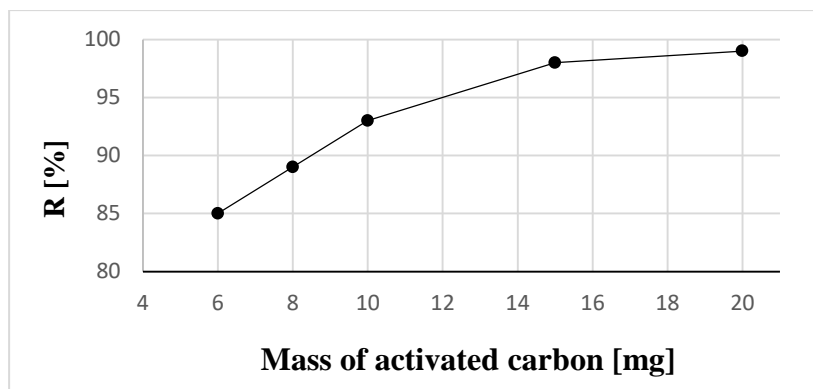


Figure 2. The influence of activated carbon mass

According to Figure 2, the maximum removal efficiency was archived at 20 mg dosage. For further investigation, 10 mg of activated carbon was used as optimal mass of AC.

Influence of contact time

The time in which activated carbon and target pollutant are in contact is essential for the theoretical modeling which can explain the nature of the adsorption process. Figure 3. shows the effect of contact time on CBZ adsorption. Contact time of 30 min was used as optimal for adsorption of CBZ on AC.

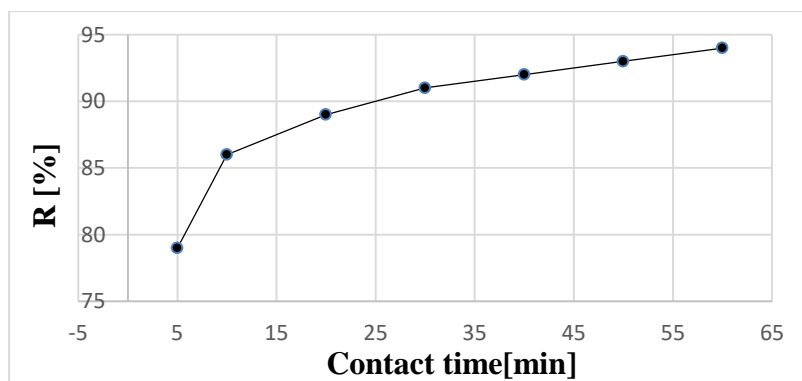


Figure 3. The influence of contact time

Conclusion

The possibility of applying the adsorption for removal of one of the most persistent organic microcontaminants in water matrices, carbamazepine, was investigated. The obtained results revealed that adsorption onto the commercially available activated carbon Norit SA2 are effective for the removal of anti – epileptic drug - carbamazepine from water. According to provided experiments, pH value of 9, mass of 10 mg, contact time of 30 minutes are the most suitable for efficient CBZ removal. The CBZ adsorption is explained by chemisorption which involves chemical reaction between surface and adsorbate. Pharmaceutical products and their degradation products are increasingly detected in the environment and still their fate and transformation pathways are largely unknown. The further development of effective methods for removal of pharmaceuticals will be a great challenge.

Acknowledgements

This study has been supported by Projects of Ministry of Education, Science and Technological Development, Republic of Serbia (Project III46009 and Project TR34014) and Project of the Government of Vojvodina “Synthesis and application of new nanostructured

materials for the degradation of organic pollutants from municipal landfill leachate in Vojvodina“, no. 114-451-1821/2016-03.

References

- [1] Baghdadi, M., Ghafari, E., Aminzadeh, B., Removal of carbamazepine from municipal wastewater effluent using optimally synthesized magnetic activated carbon: Adsorption and sedimentation kinetic studies, in *Journal of Environmental Chemical Engineering*, No. 4, 2016, pp 3309 – 3321.
- [2] Stackelberg, P.E., Furlong, E.T., Meyer, M.T., Zaugg, S.D., Henderson, A.K., Reissman, D.B., Persistence of pharmaceutical compounds and other organic wastewater contaminants in a conventional drinking-water-treatment plant, in *Science of The Total Environment*, No. 329, pp 99–113.
- [3] Alonso, S.G., Catala, M., Maroto, R.R., Gil, J.L.R., Gil de Miguel, A., Valcarcel, Y., Pollution by psychoactive pharmaceuticals in the Rivers of Madrid metropolitan area (Spain), in *Environmental International*, No. 36, 2010, pp 195 – 201.
- [4] Cabrera – Lafaurie, W.A., Roman, F.R., Hernandez – Maldonado, A.J., Removal of salicylic acid and carbamazepine from aqueous solution with Y-zeolites modified with extraframework transition metal and surfactant cations: Equilibrium and fixed-bed adsorption, in *Journal of Environmental Chemical Engineering*, No. 2, 2014, pp 899 – 906.
- [5] Novaković, M., Pap, S., Bežanović, V., Mihajlović, I., Đogo, M., Radonić, J., Turk Sekulić, M.: Efficacy Evaluation of Biosorption of Anti - Epileptic Drug –Carbamazepine onto Low – Cost Adsorbent Prepared From Apricot Stones, in *Proceedings of the IWA 8th Eastern European Young Water Professionals Conference*, Gdansk, Poland, 2016, pp. 234 – 240.
- [6] Rivera – Utrilla, J., Sanchez – Polo, M., Ferro – Garcia, M.A., Prados – Joya, G., Ocampo – Perez, R., Pharmaceuticals as emerging contaminants and their removal from water. A review, in *Chemosphere*, No. 93, 2013, pp 1268 – 1287.
- [7] Kleywegt, S., Pileggi, V., Yang, P., Hao, C., Zhao, X., Rocks, C., Thach, S., Cheung, P., Whitehead, B., Pharmaceuticals, hormones and bisphenol A in untreated source and finished drinking water in Ontario, Canada — Occurrence and treatment efficiency, in *Science of The Total Environment*, No. 409, 2011, pp 1481 – 1488.
- [8] Calisto, V., Ferreira, C.I.A., Oliveira, J.A.B.P., Otero, M., Esteves, V.I., Adsorptive removal of pharmaceuticals from water by commercial and waste-based carbons, in *Journal of Environmental Management*, No. 152, 2013, pp. 83 – 90.
- [9] Nadaroglu, H., Kalkan, E., Demir, N., Removal of copper from aqueous solution using red mud, in *Desalination*, No. 251, 2010, pp 90 – 95.
- [10] Tahir, S.S and Rauf, N., Removal of a cationic dye from aqueous solutions by adsorption onto bentonite clay, in *Chemosphere*, No. 63, 2006, pp 1842 – 1848.
- [11] Yuan, S., Jiang, X., Xia, X., Zhang, H., Zheng, S., Detection, occurrence and fate of 22 psychiatric pharmaceuticals in psychiatric hospital and municipal wastewater treatment plants in Beijing, China, in *Chemosphere*, No. 90, 2013, pp 2520 – 2525.
- [12] Dhodapkar, R., Rao, N.N., Pande, S.P., Kaul, S.N., Removal of basic dyes from aqueous medium using a novel polymer: Jalshakti, in *Bioresource Technology*, No. 97, 2006, pp 877 – 885.

REMOVAL OF COPPER IONS FROM AQUEOUS SOLUTIONS BY SUGAR BEET SHREDS AND POPLAR SAWDUST IN A FIXED-BED COLUMN

Nevena Blagojev¹, Dragana Kukić¹, Vesna Vasić¹, Marina Šćiban¹, Jelena Prodanović¹, Oskar Bera¹

¹*Faculty of Technology, University of Novi Sad, Bul. cara Lazara 1, Novi Sad, Serbia
e-mail: nevenan@uns.ac.rs*

Abstract

The potential use of sugar beet shreds and poplar sawdust for copper ions removal from aqueous solution in a fixed-bed column was investigated. Experiments were performed in a glass column (inner diameter 2.204 cm and length 50 cm), in the down-flow mode with a flow rate set to approximately 12 mL/min. Concentration (C_0) and the pH of the inlet solution were 100 mg/L and 4.5, respectively, and 10 g of the adsorbent were used to form a bed of nearly 19 cm in length. Sugar beet shreds and poplar sawdust were milled and sieved through the set of sieves, and the fraction of 400 to 600 μm was used for the adsorption experiments. The consecutive aliquots of 50 to 150 mL were collected at the bottom of the column, and they were analyzed for the content of the Cu(II) ions (C), according to the standard method of complexometric titration [1]. The column adsorption process is described regarding the effluent concentration-volume profile, or the breakthrough curve, obtained from the plot of C/C_0 versus volume of the effluent. The shape of the curve gives an insight into the dynamic behavior of the process [2, 3]. Various mathematical models can be used to describe fixed-bed adsorption [4, 5]. In this research, the novel two-stage approach for the breakthrough curve modelling was applied. The fit quality, expressed as coefficient of determination (R^2) and the sum of squared errors (SSer), showed that this model fits the experimental data more accurately than any other commonly used one-stage model. Namely, R^2 and SSer for sugar beet shreds were 0.9984 and $9.69 \cdot 10^{-3}$, respectively, while for the poplar sawdust they were 0.9999 and $2.87 \cdot 10^{-4}$, respectively. The characteristic value that describes this two-stage phenomenon is moiety of each stage, p . In the case of sugar beet shreds it was 0.43, while for the poplar sawdust it was 0.85. These results suggest that the adsorption of the copper ions onto examined biosorbents occurs under multiple mechanisms, occurring simultaneously but shifting in the dominance. When using sugar beet shreds as an adsorbent, these mechanisms are nearly equal in their dominance (0.43 to 0.57). In the case of the poplar sawdust one mechanism is significantly more dominant than other (0.85 to 0.15), and the misuse of one-stage models is usual and more likely. However, the extensive mathematical and statistical analysis confirmed the validity of the two-stage modelling approach for the copper biosorption onto sugar beet shreds and poplar sawdust.

Acknowledgements

This research was supported by the grants III43005 and III46009 (Ministry of Education, Science and Technological Development, Republic of Serbia).

References

- [1] R. Pribil, Chelometry, basic determination, Chemapol, Praha, Czechoslovakia, 1961.
- [2] A.L.P. Xavier, O.F.H. Adarme, L.M. Furtado, G.M.D. Ferreira, L.H.M. da Silva, L.F. Gil, L.V.A. Gurgel, J. Colloid Interface Sci. 516 (2018) 431–445.
- [3] O. Hamdaoui, J. Hazard. Mater. (2009). 737–746.
- [4] G. Yan, T. Viraraghavan, M. Chen, Adsorpt. Sci. Technol. 19 (2001) 25–43.
- [5] Z. Mahdi, Q.J. Yu, A. El Hanandeh, J. Environ. Chem. Eng. 6 (2018) 1171–1181.

ALTERATIONS IN SOIL FERTILITY AFTER USED LUBRICATING OIL BIOREMEDIATION

Attila Bodor^{1,2}, Tibor Sipos¹, György Erik Vincze¹, Péter Petrovski¹, Gábor Feigl³, Naila Bounedjoum¹, Krisztián Laczi¹, Árpád Szilágyi¹, Gábor Rákhely^{1,2,4}, Katalin Perei^{1,2}

¹*Department of Biotechnology, University of Szeged, H-6726 Szeged, Közép fasor 52, Hungary*

²*Institute of Environmental and Technological Sciences, University of Szeged, H-6726 Szeged, Közép fasor 52, Hungary*

³*Department of Plant Biology, University of Szeged, H-6726 Szeged, Közép fasor 52, Hungary*

⁴*Institute of Biophysics, Biological Research Centre, H-6726 Szeged, Temesvári krt. 62, Hungary*

e-mail: bodor.attila@gmail.com

Abstract

Regardless of the outcome of any environmental rehabilitation technique applied, subsequent monitoring is indispensable to assess information about soil toxicity after the treatment. Various bioremediation methods (natural attenuation, biostimulation, bioaugmentation and the usage of an organic additive) were previously performed to decontaminate soil samples taken from a railway station area polluted with used lubricating oils. In this study, ecotoxicological responses revealed that seed germination and primary root length of Indian mustard (*Brassica juncea*) were decreased in each remediated soil presumably by inhibiting breakdown products due to the biodegradation of used lubricants, while viability of root tips increased significantly indicating more vital mustard seedlings grown in remediated soils.

Introduction

Lubricating oils (LOs) are mostly produced for reducing friction in engines of motorized vehicles such as cars, motorcycles or locomotives. Therefore, used lubricating oils (ULO) containing long chain hydrocarbons, additives and heavy metals are considered as widespread, hazardous pollutants and hence potential targets of different rehabilitation processes [1-3]. Several physicochemical and biological waste management techniques are available for neutralizing oil-related pollutants in the environment [4-6]. Bioremediation, using plants and/or microorganisms for this purpose [7-8], is one of the most promising approach, since it is an environmentally friendly and cost effective technology [9-11]. Remediation treatments always need to be followed by further monitoring including ecotoxicology assays, since reduction in the concentration of the original pollutants alone does not necessarily decrease toxicity as well [12-14].

Experimental

Soil samples from a railway station area long-term contaminated with ULOs were previously rehabilitated applying different bioremediation methods such as natural attenuation (NA, soil moisture was set with water only), biostimulation (BS, soil moisture was set with the addition of water and inorganic nutrients containing nitrogen and phosphorus) and bioaugmentation combined with biostimulation (BAS, in addition to stimulation, oil-degrader *Rhodococcus erythropolis* PR4 and *Rhodococcus* sp. C strains were introduced into the polluted soil). In addition to BS and BAS treatments, samples named BS+OA and BAS+OA were supplied with an organic additive, which stimulates cellular activity of certain bacteria.

Indian mustard (*Brassica juncea* L. Czern. Var. 'Negro Caballo') was used as a model organism for soil ecotoxicology assays. In order to assess soil condition after different bioremediation treatments, seed germination [13], primary root length [14-15] and cell viability in root tips [16-17] were measured at the beginning and at the end of the 60 days long remediation experiments. Mustard seeds germinated for 4 days at 25 °C in darkness before processing [13]. Data are expressed as mean \pm SE (standard error). Statistical significance was analyzed using one way analysis of variance (ANOVA) and Duncan's test.

Results and discussion

Even in the non contaminated soil (taken from the vicinity of the polluted site) reduced seed germination (80%) could be observed confirming our preliminary data regarding its poor quality. Results were normalized using this soil as control. Seeds germinated similarly in untreated, ULO-contaminated soil (t_0), and each treatment (t_{60}) further caused significant decrease (Fig. 1.), especially in the case of BS and BS+OA samples.

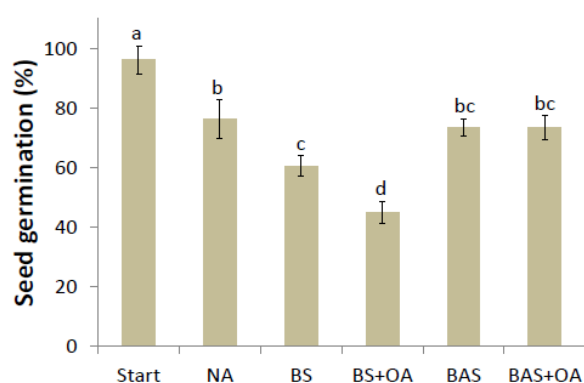


Figure 1. Seed germination at the onset and after 60 days for each bioremediation treatment. Different letters indicate statistical differences among treatments ($n \geq 4$, $p \leq 0.05$).

Significant decrease in primary root lengths was also observed in treated samples coinciding with seed germination results (Table 1.).

Table 1. Root length of Indian mustard seedlings grown in non contaminated soil and soils at the onset and after 60 days for each bioremediation treatment. Different letters indicate statistical differences among treatments ($n \geq 20$, $p \leq 0.05$).

Soil sample	Root length (mm)
Non contaminated (NC)	$22.99 \pm 0.80a$
Start (t_0)	$10.23 \pm 0.32bc$
Natural attenuation (NA, t_{60})	$10.75 \pm 0.49b$
Biostimulation (BS, t_{60})	$9.04 \pm 0.48cd$
Biostimulation supplied with organic additive (BS+OA, t_{60})	$6.50 \pm 0.42f$
Bioaugmentation combined with biostimulation (BAS, t_{60})	$7.98 \pm 0.33de$
Bioaugmentation combined with biostimulation supplied with organic additive (BAS+OA, t_{60})	$7.43 \pm 0.38ef$

The greatest degrees of growth inhibition were measured in BS+OA and BAS+OA samples. Based on root length and seed germination, we suppose that inhibition might be caused by

increased quantity or bioavailability of intermediers and breakdown products due to ULO-biodegradation in treated samples.

Fluorescent staining (fluorescein diacetate for viable root meristem cells [15] and propidium iodide for dead cells [16]) revealed that each bioremediation treatment caused increased vitality of mustard seedlings (Fig. 2.).

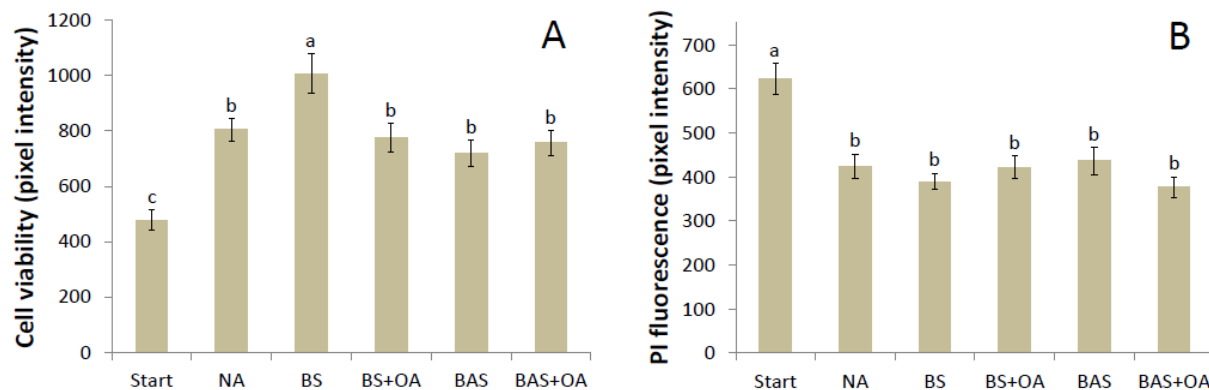


Figure 2. Cell viability (A) and propidium iodide (PI) fluorescence (B) of root meristem at the onset and after 60 days for each bioremediation treatment. Different letters indicate statistical differences among treatments ($n \geq 14$, $p \leq 0.05$).

Conclusion

Although intermediers or breakdown products from ULO-biodegradation can inhibit seed germination and root growth, we found that seedlings become more viable and vital grown in remediated soils. Our results further support previously reported suggestions by other authors [13] that decreased hydrocarbon concentration and reduced soil toxicity not necessarily have direct correlation.

Acknowledgements

The project was supported by the European Union and Hungarian State (grant agreement no. EFOP-3.6.2-16-2017-00010) and by the Norway Grant (grant agreement no. HU09-0044-A1-2013).

References

- [1] Lee, S.H., Lee, S., Kim, D.Y. and Kim, J.G., 2007. Degradation characteristics of waste lubricants under different nutrient conditions. *Journal of hazardous materials*, 143(1-2), pp.65-72.
- [2] Meeboon, N., Leewis, M.C., Kaewsuwan, S., Maneerat, S. and Leigh, M.B., 2017. Changes in bacterial diversity associated with bioremediation of used lubricating oil in tropical soils. *Archives of microbiology*, 199(6), pp.839-851.
- [3] Lee, S.H., Ji, W., Kang, D.M. and Kim, M.S., 2018. Effect of soil water content on heavy mineral oil biodegradation in soil. *Journal of Soils and Sediments*, 18(3), pp.983-991.
- [4] Chmielewska, E., Nussbaum, M.T. and Szytencelm, R.A.Y.M.O.N.D., 1997. An attempt to implement soil washing for central-europe cleanup activities. *Chemické listy*, 91(6), pp.438-443.
- [5] Jones, D.A., Lelyveld, T.P., Mavrofidis, S.D., Kingman, S.W. and Miles, N.J., 2002. Microwave heating applications in environmental engineering—a review. *Resources, conservation and recycling*, 34(2), pp.75-90.

- [6] Paria, S., 2008. Surfactant-enhanced remediation of organic contaminated soil and water. *Advances in colloid and interface science*, 138(1), pp.24-58.
- [7] Fuentes, S., Méndez, V., Aguila, P. and Seeger, M., 2014. Bioremediation of petroleum hydrocarbons: catabolic genes, microbial communities, and applications. *Applied microbiology and biotechnology*, 98(11), pp.4781-4794.
- [8] Kang, J.W., 2014. Removing environmental organic pollutants with bioremediation and phytoremediation. *Biotechnology letters*, 36(6), pp.1129-1139.
- [9] Kis, Á.E., Laczi, K., Zsíros, S., Kós, P., Tengölics, R., Bounedjoum, N., Kovács, T., Rákhely, G. and Perei, K., 2017. Characterization of the *Rhodococcus* sp. MK1 strain and its pilot application for bioremediation of diesel oil-contaminated soil. *Acta microbiologica et immunologica Hungarica*, 64(4), pp.463-482.
- [10] Bodor, A., Laczi, K., Kis, Á., Mészáros, S., Rácz, N., Rákhely, G. and Perei, K., 2015. Microbial degradation of hydrophobic compounds under various environmental conditions. *Proceeding of the 21st International Symposium on Analytical and Environmental Problems*, pp.332-335.
- [11] Bodor, A., Rácz, N., Mészáros, S., Petrovszki, P., Laczi, K., Kis, Á.E., Rákhely, G. and Perei, K., 2017. Effect of adaptation on hexane biodegradation by a *Rhodococcus* strain capable of hydrocarbon utilization. *Proceeding of the 23rd International Symposium on Analytical and Environmental Problems*, pp.380-384.
- [12] Coulon, F., Pelletier, E., Gourhant, L. and Delille, D., 2005. Effects of nutrient and temperature on degradation of petroleum hydrocarbons in contaminated sub-Antarctic soil. *Chemosphere*, 58(10), pp.1439-1448.
- [13] Jiang, Y., Brassington, K.J., Prpich, G., Paton, G.I., Semple, K.T., Pollard, S.J. and Coulon, F., 2016. Insights into the biodegradation of weathered hydrocarbons in contaminated soils by bioaugmentation and nutrient stimulation. *Chemosphere*, 161, pp.300-307.
- [14] Nwankwegu, A.S., Orji, M.U. and Onwosi, C.O., 2016. Studies on organic and in-organic biostimulants in bioremediation of diesel-contaminated arable soil. *Chemosphere*, 162, pp.148-156.
- [15] Graj, W., Lisiecki, P., Szulc, A., Chrzanowski, Ł. and Wojtera-Kwiczor, J., 2013. Bioaugmentation with petroleum-degrading consortia has a selective growth-promoting impact on crop plants germinated in diesel oil-contaminated soil. *Water, air, & soil pollution*, 224(9), p.1676.
- [16] Feigl, G., Kolbert, Z., Lehotai, N., Molnár, Á., Ördög, A., Bordé, Á., Laskay, G. and Erdei, L., 2016. Different zinc sensitivity of *Brassica* organs is accompanied by distinct responses in protein nitration level and pattern. *Ecotoxicology and environmental safety*, 125, pp.141-152.
- [17] Tsukagoshi, H., Busch, W. and Benfey, P.N., 2010. Transcriptional regulation of ROS controls transition from proliferation to differentiation in the root. *Cell*, 143(4), pp.606-616.

TOPOLOGICAL MAPS OF KOHONEN SELF-ORGANIZATION (SOM) APPLIED TO THE STUDY OF SEDIMENTS CONTAMINATED WITH PBDEs: SUPPORT FOR CLIMATE EXTREMES RISK ASSESSMENT

Maja Brborić¹, Branislav Vrana², Jelena Radonić¹, Mirjana Vojinović Miloradov¹,
Dragan Adamović¹, Maja Turk Sekulić¹

¹*Department of Environmental Engineering and Occupational Safety and Health, Faculty of Technical Sciences, University of Novi Sad, Serbia*

²*Faculty of Sciences, Research Centre for Toxic Compounds in the Environment RECETOX, Masaryk University, Brno, Czech Republic*
e-mail: turksekulic@uns.ac.rs

Abstract

Riverine sediments, collected during 2012 from ten sites in a mixed land use region of the Serbian were analysed for seven emergent PBDE congeners. All PBDEs were detected in sediments with the total concentrations range from 0.52 µg/kg (Ratno Ostrvo) to 31.19 µg/kg (Neštin) with mean levels of 8.08 µg/kg and median of 3.14 µg/kg. The classification of data by Kohonen's self-organizing maps (SOM) allowed understanding and visualizing the spatial distribution of samples. Principal component analysis (PCA) was used for validating the obtained results. Correlations and relationships between the samples and the variables can be easily visualized using the viewing of SOM planes of components. The results have highlighted the dependencies between the different PBDEs and the classification of studied sediments into three classes into function of ten stations coring and their pollution levels.

Keywords: polybrominated diphenyl ethers, emergent substances, sediment, self-organizing maps Kohonen, Danube River

Introduction

Emerging contaminants (ECs) are chemicals that have been detected in aquatic ecosystems at trace levels and for which the risk to human health is not yet known. Due to the relatively new introduction or detection of these pollutants, there exists a gap in the knowledge on their fate, behaviors and effects, as well as on treatment technologies for their efficient removal [1, 2, 3]. Furthermore, despite the advances in treatment technologies, the design of existing treatment plants is not suited to remove these ECs, in addition to there being a lack of published health standards that provide guideline in treating these pollutants. Many new ECs are being introduced into the environment without detection. In that context, this paper reviews existing research that provide reliable and quantitative information on PBDEs in aquatic sediment of Danube River.

Also, in this paper will be considered the application of self-organizing maps of Kohonen using an artificial neural network based on unsupervised learning algorithms for data classification and visualization of the spatial distribution of the content into PBDEs of sediments from 10 sampling sites along the river Danube in Serbia. The expected results should lead to a definition of existing relations between the PBDE congeners content of the sediments studied as a function of the situation of stations and sources of contributions. To confirm the results obtained by SOM, these analyzes are completed by a principal component analysis (PCA).

In addition, floodwaters are usually contaminated with infectious microorganisms, agricultural or industrial chemicals and hazardous agents present. Water and sediment contaminated with organic/inorganic chemicals and trace pollutants can heavily affect wastewater treatment plants, residential septic systems and municipal sanitary sewer systems during and after the flood event. For this reason, ensuring their climate resilience (that their capacity and

technology is adapted to possible extreme events and specific pollution under current and climate change conditions) is essential.

Experimental

Sediment sampling and preservation

The sampling was performed during October, 2012. For this investigation, ten samples of bottom sediment from different sites of Danube River (Apatin (D1), Labudnjača (D2), Neštin (D3), Begeč (D4), Ratno Ostrvo (D5), Šangaj (D6), Knićanin (D7), Belegiš (D8), Ritopek (D9), Dubravica (D10)) (Fig. 1)) were collected using a grab sampler in order to obtain representative composite samples. All sediment samples were analyzed in the laboratory of Research Centre for Toxic Compounds in the Environment - *RECETOX* (Brno, Czech Republic) after two days. Prior to analysis wet sediment samples were sieved through 2 mm sieve to remove leaves, stones and roots and the lower particle size fraction ($<63 \mu\text{m}$) was retained and analyzed. Sediment samples were extracted with toluene in a Soxhlet extractor with toluene in a B-811 extraction unit (Büchi, Switzerland). Prior to extraction, the samples were spiked with ^{13}C BDEs (47, 99, 100, 153, 154, 183, 209). PBDEs were analysed using 7890A gas chromatography–mass spectrometry (Agilent, USA).

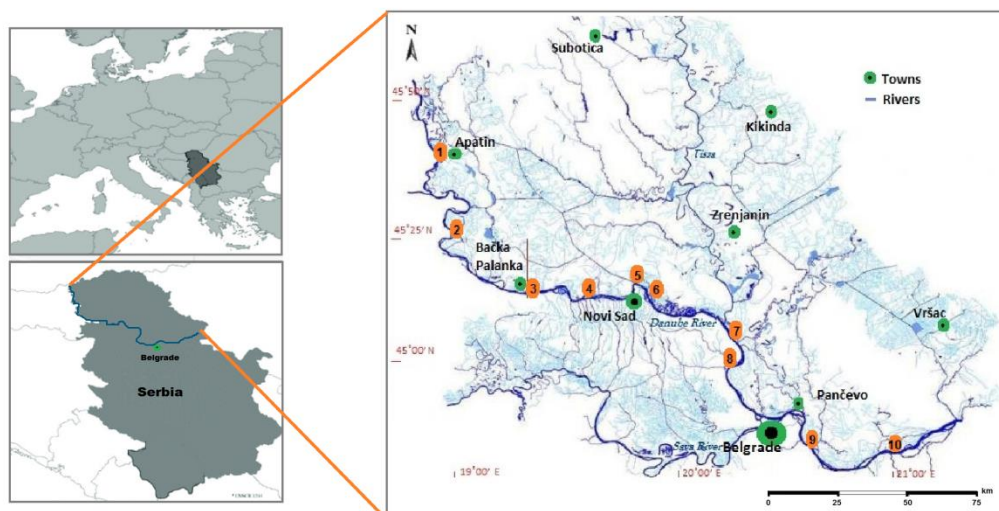


Figure 1. Map of the sampling sites

Data analysis

The artificial neural network (ANN) used in this study was the Kohonen Self-Organizing Map (SOM) [4]. SOM is an unsupervised artificial neural networks technique, which has been successfully applied in the classification of aquatic pollution [5,6,7]. These networks are composed of a grid of neurons (also called nodes); each unit of the grid is connected to the input vector through the N synapse weight W_{ij} . In fact, at each unit is associated with a vector of dimension N that contains the weight W_{ij} (Fig. 2). Therefore, sediment samples within the same node have more similarity in terms of sediment variable patterns, while more distinct patterns will be positioned at larger distances in the map [5, 6].

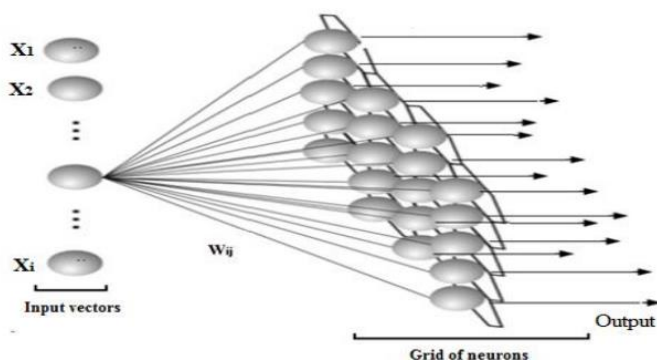


Figure 2. Scheme of a map Kohonen

In this study, the input layer (input vector) is composed of 8 neurons representing an 7 polybrominated diphenyl ethers that are BDE 47, 99, 100, 153, 154, 183, 209. These neurons are associated with every 10 neurons that represent 10 samples studying sediments. All values in the database are normalized in the range [0,1] in order to adapt to the transmission requirements function used by neural networks.

Results and discussion

Spatial distribution of PBDEs

The concentrations and distribution of PBDE congeners (BDE 47, 99, 100, 154, 153, 183, 209) were investigated in ten bottom sediment samples. The results showed that all these pollutants were detected in sediments and the mean levels of Σ_7 PBDE compounds were ranged from 0,52 $\mu\text{g/kg}$ (site D5) to 31.19 $\mu\text{g/kg}$ (site D3) (Fig. 3.). Among the PBDE congeners, BDE 209 was predominant, with contributions to the total PBDEs ranging from 22.9% (site D3) to 99.3% (site D10) in sediment samples. For the lowly brominated congeners (tri- to penta-BDEs), BDE 100 were the most abundant at the sampling site Neštin.

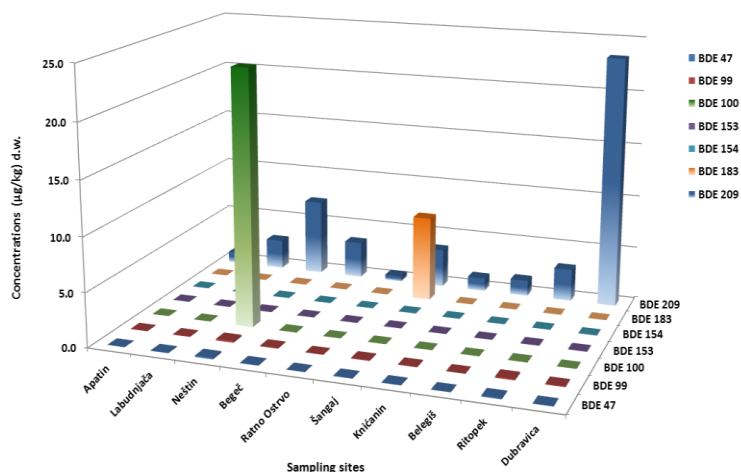


Figure 3. PBDEs concentrations ($\mu\text{g/kg}$ d.w.) in sediment of Danube River, Serbia.

Self-organizing maps of PBDEs in the sediment profiles

The plans SOM components of the dataset are shown in Figure 4. The identical colour patterns between the variables correspond to a positive correlation; this can be considered among the variables BDE 47, BDE 99, BDE 100, BDE 153 and BDE 154. There were no negative correlations between the variables. The other variables are neither positive nor

negative correlations in particular those relating to the BDE 100, BDE 183 and BDE 209 that vary independently of the others (Fig. 4).

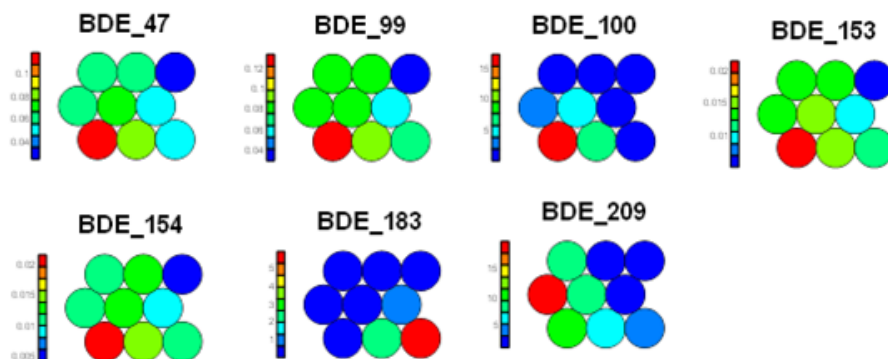


Figure 4. SOM component planes for the seven input variables

Principal component analysis (PCA)

The result of PCA with varimax rotation shows the route of score formed by the two components PC1 and PC2, which are considered the most informative since they account for the largest proportion of the variance. In our case, three principal components (PC1, PC2 and PC3) were extracted, accounting for 93.85% of the total variances, with 64.24%, 14.85% and 14.76% for PC1, PC2 and PC3, respectively. Figure 5 shows the component plot of correlations between variables on the factorial design.

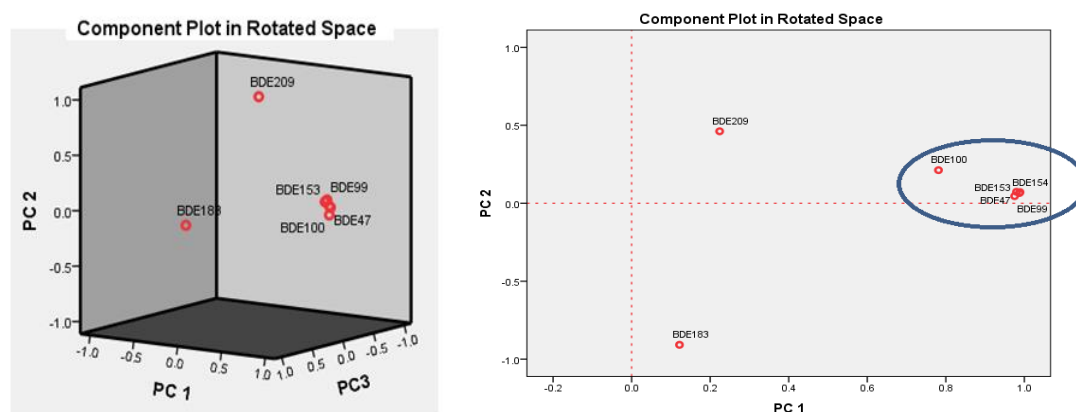


Figure 5. Component plots for PBDE congeners

The component plot of correlations between variables on the factorial design (PC1 X PC2) shows that the BDE 47, BDE 99, BDE 100, BDE 153 and BDE 154 correlate positively with the PC1 axis with respective coefficients of 0.99, 0.98, 0.78, 0.96 and 0.99. However the BDE 183 and BDE 209 correlate positively and are very poorly correlated with PC1, with respective coefficients of 0.13 and 0.22.

Conclusion

In conducted study we are presented the concentration levels of ten PBDE congeners in the Danube sediment at 10 locations. The highest level of PBDEs was recorded at the locality D5, while the lowest at the locality D3. The results obtained within our study suggest the dominance of the deca-BDE congener.

The self-organizing map SOM was used in this study for distribution of seven emerging PBDEs in sediments samples collected from Serbia's stretch of the Danube River. The

comparison with the Principal component analysis (PCA), showed, therefore that the results obtained with the self-organizing map SOM were generally similar to those of these statistical method. But, the SOM method has also provided more detailed classification of PBDE congener from sediments of the Danube River.

Despite the extensive investigations that have been done globally on persistent organic pollutants, there is a lack of information about BFRs in the Serbian environment. This study addresses a knowledge gap by providing the data on contamination status of aquatic body by PBDEs, which is an important contribution regarding environmental matters on new emerging contaminants. A more comprehensive understanding would be achieved by further studies on the dynamic pollution mechanism and the status of aquatic biota in this region. Systematic ecological and ecotoxicological effects of BFRs and associated contaminants on aquatic biota would provide a significant indication of the bioavailability of these new emerging contaminants.

At the end, obtain results will be very useful for the risk assessment, vulnerability functions and exposure database of the Danube regional multi-hazard and multi-risk model.

Acknowledgements

This research was supported by City administration for environmental protection, Novi Sad, Republic of Serbia, Ministry of Education, Science and Technological Development, Republic of Serbia (III46009) and the Czech Ministry of Education (LO1214 and LM2011028).

References

- [1] M. Vojinović Miloradov, M. Turk Sekulić, J. Radonić, N. Milić, N. Grujić Letić, I. Mihajlović, M. Milanović, Industrial emerging chemicals in the environment, *Hemijaska industrija* 68, 2014, 51-62.
- [2] N. Milic, I. Spanik, J. Radonic, M. Turk-Sekulic, N. Grujic, O. Vyviurska, M. Milanovic, M. Sremacki, M. Vojinovic-Miloradov, Screening Analyses of Wastewater and Danube Surface Water in Novi Sad Locality, Serbia, *Fresenius environmental bulletin* 23(2), 2014, 372-377.
- [3] N. Grujić-Letić, M. Milanović, N. Milić, M. Vojinovic-Miloradov, J. Radonić, I. Mihajlović, M. Turk-Sekulic Quantitative determination of caffeine in different matrices, *Macedonian pharmaceutical bulletin*, 62(1), 2016, 77 - 84.
- [4] T. Kohonen, *Self-organizing maps*, Springer, Berlin, 2001.
- [5] M. D. Subida, A. Berihuete, P. Drake, J. Blasco, Multivariate methods and artificial neural networks in the assessment of the response of infaunal assemblages to sediment metal contamination and organic enrichment, *Science of the Total Environment* 450–451, 2013, 289–300.
- [6] Y. Yang, Q. Xie, X. Liu, J. Wang, Occurrence, distribution and risk assessment of polychlorinated biphenyls and polybrominated diphenyl ethers in nine water sources, *Ecotoxicol. Environ. Saf.*, 115, 2015, 55-61.
- [7] Y. Huang, M. Liu, R. Wang, S.K. Khan, D. Gao, Y. Zhang, Characterization and source apportionment of PAHs from a highly urbanized river sediments based on land use analysis. *Chemosphere* 184, 2017, 1334-1345.

EFFECT OF CALCINATION TEMPERATURE ON THE PHOTOACTIVITIES OF ZnO NANOPARTICLES FOR DEGRADATION OF THE HERBICIDE CLOMAZONE

Vesna Despotović¹, Daniela Šojić Merkulov¹, Nina Finčur¹, Marina Lazarević¹, Goran Bošković², Sanja Panić², Biljana Abramović¹

¹*University of Novi Sad, Faculty of Sciences, Department of Chemistry, Biochemistry and Environmental Protection, Trg Dositeja Obradovića 3, 21000 Novi Sad, Serbia*

²*University of Novi Sad, Faculty of Technology, Bulevar Cara Lazara 1, Novi Sad, Serbia
e-mail: vesna.despotovic@dh.uns.ac.rs*

Abstract

The introduction of huge amount of organic pollutants such as dyes, pharmaceuticals, pesticides, etc. to the environment has caused many diseases to both aquatic and terrestrial lives due to their carcinogenic, toxic, and mutagenic poisonous nature. As environmental friendly and easy operational techniques, photocatalysis with semiconductors has been regarded as the most advanced and effective technique to replace the traditional methods used for the removal of organic pollutants [1-4]. Calcination temperature plays a key role in the crystallinity and photocatalytic activities of semiconductor photocatalysts [1]. The aim of this work was to investigate removal of the herbicide clomazone from double distilled water in the presence of novel ZnO nanoparticles under simulated sunlight. The ZnO photocatalysts were synthesized by precipitation method from the water and ethanol solutions of the acetate precursor and calcinated at 300–700 °C. The performances of the applied photocatalysts were correlated with their physic chemical properties. The efficiency of elimination the herbicide from double distilled water was monitored by UFLC–DAD technique.

Acknowledgments

This work was supported by the Ministry of Education, Science and Technological Development of the Republic of Serbia (Projects No. 172042 and 172059).

References

- [1] W. Ali, H. Ullah, A. Zada, M.K. Alamgir, W. Muhammad, M.J. Ahmad, A. Nadhman, Mater. Chem. Phys. 213 (2018) 259.
- [2] Z. Yanga, C. Denga, Y. Ding, H. Luo, J. Yin, Y. Jiang, P. Zhang, Y. Jiang, J. Solid State Chem. 268 (2018) 83.
- [3] M. Cantarella, A. Di Mauro, A. Gulino, L. Spitaleri, G. Nicotra, V. Privitera, G. Impellizzeri, Appl. Catal. B: Environ. 238 (2018) 509.
- [4] D.V. Šojić Merkulov, V.N. Despotović, N.D. Banić, S.J. Armaković, N.L. Finčur, M.J. Lazarević, D.D. Četojević-Simin, D.Z. Orčić, M.B. Radoičić, Z.V. Šaponjić, M.I. Čomor, B.F. Abramović, Environ. Pollut. 239 (2018) 457.

DEVELOPING OF ANTIOXIDANT-ENRICHED APPLE JUICE WITH ELDERBERRY (*SAMBUCUS NIGRA* L.) POMACE

**Diána Furulyás¹, Zsanett Szabó¹, Lilla Szalóki-Dorkó¹, Dóra Székely¹,
Mónika Stéger-Máté¹, Éva Stefanovits-Bányai²**

¹Department of Food Preservation, Szent István University, H-1118 Budapest, Villányi út 29-43. Hungary

²Department of Applied Chemistry, Szent István University, H-1118 Budapest, Villányi út 29-43. Hungary

e-mail: Furulyas.Diana@etk.szie.hu

Abstract

The aim of this study to develop a healthy enriched apple juice and utilization of by-product of elderberry pomace. The elderberries and their pomace contain high biological activity components, primarily polyphenols, anthocyanins, flavanols which compounds are known to have potential antioxidant properties. In this study the most efficiently extraction method was explored by using different solvents and using the chosen best method, our goal is to develop a delicious enriched apple juice with contain this pomace extracts.

Introduction

The food waste is a very important subject in the food industry, especially since in many cases by-products should not be considered as waste [1-3]. Our aim is that we are looking for an alternative to the use of fruit pomace to open new opportunities for the food industry. The chosen cultivar, Haschberg is from Hungary. Black elderberry (*Sambucus nigra* L.) is from Adoxaceae family, its shrubs are multi stemmed, they have weak, grey coloured branches on which fruit clusters develop with 5-9 mm (d) glossy, dark purple berries [4-5]. These elderberries contain high biological activity components which compounds are known to have potential antioxidant properties [6-8]. The berries can be utilized as coloring food, jam, or, because of its favorable composition, as dietary supplements [9]. Processing of elderberry fruit produces high amount of pomace, which are utilized rather inefficiently or discarded as a waste, so considerable amounts of nutrients are lost [10]. The pomace, which is left when elderberry is pressed, is also a good source of vitamins and contains compounds that show antioxidant effects like anthocyanins, flavonols, and phenolic acids are bioactive compounds present in the elderberry. There is a growing interest in the utilization of antioxidant-rich plant extracts as dietary food supplements [11-12]. Our goal, when conducting this experiment, was to find the right extraction method for extracting the antioxidant compounds from black elderberry pomace and produced apple juice were improved by using the extract of pomace which contain high biological active compounds.

Experimental

The “Haschberg” elderberry was collected from agricultural plots of Hungary at 2017. Chemicals were purchased by Sigma-Aldrich Chemie Ltd. All reagents used were of analytical grade.

Elderberry was destemmed, and then heated to 80°C, to inactivate enzymes. The material was squeezed, resulting in juice and pomace. Drying the pomace was the next step by atmospheric dryer (LMIM, Esztergom, Hungary) at 80°C until moisture content became lesser than 10%. After this step the pomace was grinded. All samples were sealed in bag and stored in a freezer at -20 °C until ready for extraction, which was performed at room temperature.

The optimum conditions for the extraction of antioxidants, anthocyanins and phenolics components from dried elderberry pomace was determined using water, ethanol and acetone as solvents, applied in different concentration (in case of ethanol and acetone: 20 (m/m) % and 40 (m/m) %) (the ratio between pomace and solvent was 1:30 proportions). After half-an-hour of extraction, supersonic bath was used for another 30 minutes, to intensify the process. The tube is centrifuged at 2500g for 10 min to the phases separate and the supernatant is recovered. After the solvents were removed (by heating at 60°C) and replaced with water, the evaporated and back diluted sample was treated with bentonite to give a translucent, completely clear liquid. Various spectrophotometric measurements were performed to select the highest antioxidant content of pomace extracts. All measurements were performed in triplicate.

- The antioxidant capacity of samples was estimated according to the procedure described by Benzie and Strain [13]. Ferric reducing antioxidant power assay (FRAP) was defined in ascorbic acid equivalent (mg ascorbic acid equivalent/ 100 g dried pomace – mg AA/100g).

- The samples were measured in terms of hydrogen donating or radical scavenging ability using the stable radical DPPH (2,2-Diphenyl-1-picrylhydrazyl) [14]. The results were expressed as millimoles of Trolox equivalents (TE) per 100g dried pomace (mM TE/100g). Higher absorbance of the reaction mixture indicates lower free radical scavenging activity.

- The free radical-scavenging activity was determined by ABTS radical cation decolorization assay described by Re et al. [15]. The results were corrected for dilution and expressed as millimoles of Trolox equivalents (TE) per 100 grams of dried pomace (mM TE/100g).

- Total Polyphenol Content (TPC) was evaluated using a method by Singleton and Rossi [16]. Results were specified in mg gallic acid equivalent/ 100 g dried pomace (mg GA/100g).

- Total Anthocyanin Content (TAC) measurement was based on Lee's pH differential method [17], results are given in mg/ 100 g dried pomace (mg/100g).

Table 1. Ingredients and name of juices

(in case of TPC, TAC and FRAP the results were expressed as mg/100g dried pomace, in case of DPPH and TEAC method, they were given is mM/100g dried pomace)

Sample name		Apple juice	Water	Pomace extract
Control apple juice	CA	70 Brix°	100%	0%
50% - enriched apple juice	EA1		50%	50%
100% - enriched apple juice	EA2		0%	100%

With the best extraction method, three types of apple juice (12 Brix°) were made from apple concentrate (70 Brix°) by diluting it to minimum 11,2 Brix° [according to Hungarian regulation of 152/2009] with different mixture of water and pomace extracts (Table 1.). The spectrophotometry methods were carrying out also for the juices sample, the results expressed per milliliter juice. Acceptability of enriched juices was determined by sensory evaluation and short market research. The sensory evaluation has been carrying out with lay judges, the samples were coded with three-digit numbers. The evaluation was based on 100-point system, during the analysis the attributes were as follows: color (max. 20 point) turbidity (max. 10 point) flavored (max. 10 point) taste (max. 40 point) elderberry taste (max. 10 point) of juices and overall impression. Evaluations of the samples were carried out separately and independently without any influence.

Results and discussion

Dried elderberry pomace was extracted with different solvents (water, 20 and 40 (m/m)% ethanol and acetone), the samples were analyzed to define total anthocyanin and polyphenol content, as well as their antioxidant capacity (FRAP, DPPH, TEAC), in order to find the most effective method of extraction to achieve an extract rich in biological activity components (Table 2.).

Table 2. The average results of the spectrophotometry measurements of the pomace extracts (in case of TPC, TAC and FRAP the results were expressed as mg/ml, in case of DPPH and TEAC method, they were given in mM/ml)

Extraction solvents		TAC	TPC	FRAP	TEAC	DPPH
Water		54.21	1166.33	1570.27	2645.50	34100.02
Acetone	20 %	411.70	1400.13	1927.75	3424.85	38155.56
	40 %	418.22	1305.67	1992.08	3841.21	40322.22
Ethanol	20 %	390.64	1207.83	1736.73	227.39	21100.03
	40 %	401.17	1323.38	2066.15	1663.32	28988.88

Based on the results the water as a solvent was not efficiently, these results of antioxidant measurements were the lowest value in most cases. The optimum extraction agent is acetone to the highest antioxidant content of pomace extracts. Between the extraction efficient of two concentration of acetone was not significantly difference. For economic and health considerations the lower concentration of solvent (20% acetone) was recommended to use for extracting the valuable components from the pomace.

Table 3. The average results of the spectrophotometry measurements of the juice samples

	TAC	TPC	FRAP	TEAC	DPPH
CA	0.04	0.37	4.34	0.22	0.73
EA1	12.77	0.39	7.12	0.20	0.62
EA2	21.70	0.44	11.07	0.25	0.86

Based on the results of juices (Table 3.), our desired goal - the enrichment of apple juice - was met, the antioxidant compounds, the FRAP value, polyphenol and anthocyanin content greatly increased by added the pomace extract. Most of the measurements showed outstanding results compared to the control sample. The antioxidant content of the sample increases in direct proportions with the amount of added pomace extract. The sample EA2 (Enriched apple juice, with 100% pomace extract) had the most antioxidant content.

The enriched apple juices had beneficial sensory properties (Fig.1), the tasters were satisfied with finished products. The most of them are happy to buy the finished products. During product development, the smell and the clearly of the juices should be improved as the participants were the least satisfied with these parameters. According to the sensory analysis, fruit concentrates dilute with only pomace extract without water (EA2 sample) is the most optimum according to evaluators. The results of the

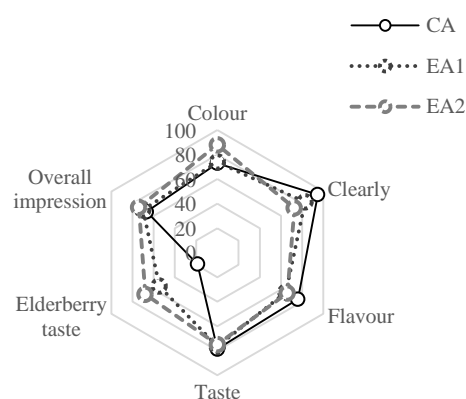


Figure 1. Results of sensory analysis

market research showed that there is a demand for the consumption of enriched juice. Overall, according to market research data, consumers are open to new products, especially if they have a health benefit and are made up of natural materials.

Conclusion

We have successfully recovered and recycled the antioxidant compounds from pomace of elderberry to produce more valuable and special apple juice. These new aspects concerning the use of the pomace as by-products for further exploitation on the production of food additives with high nutritional value, their recovery may decrease quantity of a waste of valuable components and may be economically attractive.

Acknowledgements

This work was supported by the Hungarian Government through project No. EFOP-3.6.3-VEKOP-16-2017-00005.

References

- [1] A. Mirzaei-Aghsaghali, N. Maheri-Sis, *World Journal of Zoology*, 3 (2008) 40-46.
- [2] K. Kónya, Szarvas, 5-6. (2000) 63-64.
- [3] K. Brønnum-Hansen, F. Jacobsen, J. Flink, *International Journal of Food Science & Technology* 20, (1985) 703–711.
- [4] D. Topolska, K. Valachova, P. Raptá S. Silhár, E. Panghyová, A. Horváth, L. Soltés, *Chemical Papers* 69 (2015) 1202-1210.
- [5] E. Mudge, W.L.Applequist, J. Finley, P. Lister, A.K. Townesmith, K.M. Walker, P.N. Brown, *Journal of Food Composition and Analysis* 47 (2016) 52-59.
- [6] I. Ochmian, J. Oszmianski, K. Skupien, *Journal of Applied Botany and Food Quality* 83 (2009) 64-69.
- [7] A. Sidor, A. Gramza-Michalowska, *Journal of Functional Foods* (2014) 941-958.
- [8] M. Oroian, I. Escriche, *Food Research International*, 74 (2015) 10-36.
- [9] C. Chen, X.-M. Xu, Y. Chen, M.-Y. Yu, F.-Y. Wen, H. Zhang, *Food Chemistry*, 141 (2013) 1573-1579.
- [10] C.M. Galanakis, *Trends in Food Science & Technology*, 26 (2012) 68-87.
- [11] C. Eccleston, Y. Baoru, R. Tahvonen, H. Kallio, G.H. Rimbach, A.M. Minihaue, *The Journal of nutritional biochemistry*, 13(6), (2002) 346-354.
- [12] B. Yang, H.P. Kallio, *J. Agric. Food Chem*, 49 (2000) 1939–1947.
- [13] I.I.F. Benzie, J.J. Strain, *Annalitical Biochemistry*, 239. (1966) 70-76
- [14] M.S. Blois, *Nature*, 181 (1958) 1199-1200.
- [15] N.J. Miller, C. Rice-evans, M.J. Davies, V. Gopinathan, A. Milner; *Clinical Science*, 84 (1993) 407-412.
- [16] V.L. Singleton, J.A. Rossi, *American Journal of Enology and Viticulture*, 16 (1965) 144–158.
- [17] J. Lee, R. Durst, R. Wrolstad, *Journal of AOAC International*, 88, (2005) 1269-1278.

DEVELOPMENT OF TARGETED LC-MS/MS METHOD FOR ANALYSIS OF DICLOFENAC AND ITS MAIN METABOLITES IN RAT LIVER PERFUSION SOLUTION OBTAINED BY NEW TYPE OF EX VIVO PERFUSION SYSTEM

Aya Dweny¹, Tímea Körmöczi¹, Orsolya Kovács², Reza Samavati³, Róbert Gáspár², Róbert Berkecz¹

¹*Department of Medical Chemistry, University of Szeged, H-6720 Szeged, Dóm tér 8, Hungary*

²*Department of Pharmacology and Pharmacotherapy University of Szeged, H-6720 Szeged, Dóm tér 12, Hungary*

³*Department of Pharmacodynamics and Biopharmacy, University of Szeged, H-6720 Szeged, Eötvös utca 6, Hungary*
e-mail: berkecz.robert@med.u-szeged.hu

Abstract

Isolated perfused rat liver (IPRL) is used as ex vivo simulation for more accurate evaluation of pharmacokinetic parameters of target drugs, production of their metabolites and their excretion in the bile. Compared to in vivo systems, IPRL avoids the clearance of any other organ and permits the control over the factors that may affect the hepatic metabolism, for example, the flow rate of the perfusate, pH, pressure, and concentration of chemicals.

This simple experimental technique, unlike the cultured cells, keeps the intactness of the liver, in other words, cells other than hepatocytes, drug transporters' distribution, as well as enzymes, are still affecting the metabolism which gives a realistic picture [1-2].

The portal vein of the anesthetized rat was cannulated and the perfusion solution saturated with carbogen (95% O₂ and 5% CO₂) was pumped through it. The solution was directed through the transected abdominal vein to the waste. A cannula was inserted into the inferior vena cava through the right heart atrium through which the perfusate leaved the liver after the ligation of the abdominal vein. The isolated liver was then placed into the buffer vapour chamber of the recirculated perfusion system and the perfusate samples were collected during different time intervals.

The main goal of our work was the development of targeted reversed-phase LC-MS/MS analytical method for the analysis of diclofenac (DF) and its main metabolites namely diclofenac-O-acyl glucuronide (Glu-DF) and 4-hydroxydiclofenac (4'-OH-DF) in the perfusion solution of rat liver. We are planning to use diclofenac as a reference compound in the future investigation of metabolism of designer drugs.

DF and its metabolites were extracted by the optimized liquid-liquid extraction procedure. LC separation was achieved by gradient elution of the mobile phase consisted of 0.1% formic acid in water and 0.1% of formic acid in acetonitrile on a Luna Phenyl-Hexyl column at 50° C with a run time of 10 minutes. The Agilent 1100 LC system was coupled to the triple quadrupole TSQ 7000 mass spectrometer. The appropriate transitions were monitored during the region of elution of each analyte. The linearity range of DF was between 100 ng/mL and 40 µg/mL. The related matrix effect, recovery and process efficiency were successfully evaluated.

Acknowledgements

This research was supported by the EU-funded Hungarian grant EFOP 3.6.1-16-2016-00008.

References

- [1] Pastor, Catherine M. "Isolated Perfused Rat Livers to Quantify the Pharmacokinetics and Concentrations of Gd-BOPTA." *Contrast media & molecular imaging* 2018 (2018).
- [2] Bounakta, Sara, et al. "Predictions of bisphenol A hepatic clearance in the isolated perfused rat liver (IPRL): impact of albumin binding and of co-administration with naproxen." *Xenobiotica* 48.2 (2018): 135-147.

**A COMPARATIVE STUDY ON CATALYTIC CARBON DIOXIDE
HYDROGENATION AND CARBON DIOXIDE METHANATION OVER Pt/SBA-15,
NiO, Pt/NiO, Co₃O₄ CATALYSTS**

Anastasiia Efremova¹, András Sági¹

¹*Department of Applied and Environmental Chemistry, University of Szeged, H-6720 Szeged,
Dóm tér 7, Hungary
e-mail: efrisso@yandex.ru, sapia@chem.u-szeged.hu*

Abstract

Nowadays, more and more attention of researchers is attracted to the reactions that allow to involve CO₂ in chemical transformations with the purpose of its utilization. In this study, carbon dioxide activation was performed by two heterogeneously catalyzed processes: hydrogenation and methanation. The activities of synthetically obtained 0.5% Pt/SBA-15, NiO, 0.5% Pt/NiO as well as of commercial Co₃O₄ catalysts were studied in continuous flow fixed-bed reactor with He and Ar carrier gases at varying reaction temperatures (373K-1073K). Prior to catalytic measurements, all the samples were oxidized for 30 minutes at 573 K with oxygen and reduced with hydrogen at different temperatures (373K-1073K). SBA-15 as a reference measurement, demonstrated low carbon dioxide consumption rates. At the same time, mesoporous NiO was very active. Surprisingly, derivation of NiO with Pt nanoparticles did not provide big effect on NiO catalytic performance, consequently, under established reaction conditions Ni-NiO phase was formed where metallic Ni was active. In addition, 100% carbon oxide selectivity was associated with Pt/SBA-15 as opposing to NiO based catalysts, which were highly methane selective. Concerning methanation reaction, Pt/SBA-15 catalyst was inactive up to 1073K. Nickel oxide based catalysts were active from 673K and demonstrated high CO/H₂ ratios. Impact of Pt nanoparticles on mesoporous NiO activity was also insignificant in this reaction. Commercial Co₃O₄ was subjected to carbon dioxide hydrogenation and methanation reactions under three reduction temperatures: 473K, 573K, 673K and being reduced at 473K, showed the highest conversion values in hydrogenation reaction. All three catalytic systems demonstrated high percentage of methane selectivity. However, they turned out to be inactive in methanation reaction and unwanted high ratios of CO/H₂ were observed.

DETERMINATION OF VALINE AND LEUCINE ISOMERS IN PEPTAIBOLS

**Gábor Endre^{1,2}, Tamás Marik¹, László Kredics¹ Mónika Varga¹, Csaba Vágvölgyi¹,
András Szekeres^a**

¹*University of Szeged, Faculty of Science and Informatics, Department of Microbiology,
Közép fasor 52. Szeged H-6726*

²*Doctoral School in Biology, Faculty of Science and Informatics, University of Szeged,
Szeged, Hungary
e-mail: egabcy@gmail.com*

Abstract

Peptaibols are oligomers, containing non-proteogenic amino acids. Some of them are considered as antifungal and antibiotic agents, therefore the elucidation of their structure is important. There have been a lot of efforts determining their amino acid sequences via mass spectrometry, but isobaric components cannot be determined using this technique.

In this work, a HPLC method development was carried out for the determination of leucine, isoleucine, valine and isovaline in one chromatographic run. Furthermore, a chiral separation of the optical isomers of these compounds has been also solved.

Introduction

Peptaibols are peptid-like oligomers produced as extracellular secondary metabolites by *Trichoderma* species. Some peptaibols function as antibiotic and antifungal agents [1]. They are amphiphilic, which allows them to form voltage-dependent ion channels in cell membranes, making them leak and leading to the cell death. These compounds contain non-coded, non-proteinogenic amino acids, like α -aminoisobutyric acid, ethylnorvaline, isovaline and hydroxyproline. Their N-terminus is acetylated, and the C-terminal amino acid is hydroxylated into an acid alcohol [2]. Due to their diverse nature, the structure elucidations of newly discovered peptaibols are important.

There have been a lot of efforts to determine their amino acid sequence by mass spectrometry [3-5], however, isobaric amino acids could not be specified, and no configuration of the compounds could be observed. To apply liquid chromatography, problems could be solved-, e.g. isobaric amino acids could be separated and detected, as well as the D-, and L-isomers could be distinguished due to the proper chiral derivatisation.

For the chiral determination of the desired amino acids, Marfey's reagent can be used. The reaction was carried out by adding the chiral reagent into the amino acid sample forming two products, depending on the configuration of the connecting amino acid. When the reagent is reacting with an L-amino acid, the product could form an intramolecular H-bond that results in a ring-like system. In the case of D-amino acids reaction partners, another product occurs, that cannot form any H-bonds intramolecularly. This slight difference between these two products led to their baseline separation on the applied chromatographic column.

Experimental

Trichoderma pleuroti (SZMC 12454) was cultivated on solid medium. Peptaibols were extracted using $\text{CHCl}_3/\text{MeOH} = 3/1$ and the crude extract was separated on a normal phase column in a $\text{CHCl}_3/\text{MeOH}$ gradient. One selected fraction was evaporated and hydrolysed in cc. HCl overnight, to release the amino acids. After setting the pH to 7, the achiral and chiral derivatisations were applied.

Derivatising agents, amino acid standards and other chemicals were purchased from Sigma Aldrich Inc. (Saint Louis, MO, USA). The achiral derivatisation of amino acids was done by

adding 125 μl of borate buffer ($\text{pH} = 10.2$) to 50 μl of amino acid solution. After mixing vigorously, 25 μl of OPA solution and 20 μl of FMOC solution were added. The solution was diluted with 780 μl HPLC water and mixed. The resulted solution was injected into a HPLC-UV system. Chiral derivatisation of amino acids was done by Marfey's reagent (Thermo Fischer Scientific, Waltham, MA, USA). To 50 μl of amino acid solution, 100 μl of Marfey's reagent's solution (1 w% in acetone) and 20 μl solution of NaHCO_3 (1 M) were added. After mixing, the reaction mixture was thermostated at 35°C for 60 minutes, which was followed by neutralisation by 10 μl of HCl solution (2 M). The mixture was evaporated to dryness and was dissolved in 500 μl HPLC grade DMSO. The resulted solution was diluted ten times and injected into a HPLC-UV system.

HPLC method development and measurements were done using a Dionex Ultimate 3000 UHPLC instrument (Thermo Fischer Scientific, Waltham, MA, USA). The instrument was equipped with a quaternary pump, a degasser, a well plate sampler, a column thermostat and a UV-VIS detector. Separation of achirally derivatised amino acids was performed using a Phenomenex Ez:faast AAA-MS 250 x 2 mm, 4 μm column (Phenomenex Inc., CA, USA). The mobile phase was the following: A: H_2O + 41 mM acetate buffer ($\text{pH} = 4$), B: MeOH + 41 mM acetate buffer ($\text{pH} = 4$). The elution was isocratic with the ratio of A/B = 45/55 for 33 minutes, while the flow rate was 0.35 ml/min at 45°C . The injection volume was 1 μl and peaks were detected at $\lambda = 338 \text{ nm}$ and $\lambda = 262 \text{ nm}$. Separation of chirally derivatised amino acids was performed using same column as above and the mobile phase was the following: A: H_2O + 25 mM HCOONH_4 , B: MeOH + 25 mM HCOONH_4 . During the gradient elution the B % increased from 35% to 70 % for 30 minutes. The flow rate was 0.25 ml/min at 35°C during analyses and the injection volume was 5 μl and peaks were detected at $\lambda = 340 \text{ nm}$ and $\lambda = 254 \text{ nm}$.

Results and discussion

In the first stage of our work, standard amino acid solutions were derivatised with o-phthalaldehyde (OPA) and 9-fluorenylmethyloxycarbonyl chloride (Fmoc). A non-chiral HPLC-UV method was developed for the separation of leucin, isoleucin, valine and isovaline. The components were separated in an isocratic elution within 33 minutes. The chirally derivatised L-, and D-amino acids were also separated, but in this case, a gradient elution from 35 % B to 70% B was used. After the separation method optimization, the *Trichoderma pleuroti* (SZMC 12454) strain was cultivated. At the end of the fermentation the mycelia were extracted and the crude peptaibol mixture was purified by flash chromatography using $\text{CHCl}_3/\text{MeOH}$ gradient. The peptaibol containing fractions eluted from 40% to 60% of MeOH and a fraction was selected from the collected ones contained the most amount of peptaibols. The oligomers were hydrolysed and the liberated amino acids derivatised achirally. The achiral amino acid separation resulted, that the peptaibol mixture contains valine and isovaline in 1 to 1 ratio and leucine and isoleucine in 1 to 1 ratio also as well. This peptaibol fraction was also chirally derivatised and analysed. Altogether L-isoleucine, D-isovaline and L-leucine were found, none of the two valine isomers could be detected.

Conclusion

Two successful HPLC-UV methods were developed to analyse isobaric amino acids and to define their configuration. Group of peptaibols were successfully purified, hydrolysed and analysed. After analysing the real samples, it could be concluded that further purification of the peptaibols is needed to have the pure compounds hydrolysed and analysed.

Acknowledgements

This work was supported by the Hungarian Scientific Research Fund by grants NKFI-128659 and this work was connected to the project GINOP-2.3.2-15-2016-00012.

References

- [1] N. Stoppacher, B. Reithner, M. Omann, *Rapid. Commun. Mass Sp.* 21 (2007) 3963.
- [2] J. K. Chugh, B. A. Wallace, *Biochem. Soc. T.* 29 (2001) 565.
- [3] T. Marik, P. Urbán, C. Tyagi, *Chem. Biochem.* 14 (2017) e1700033.
- [4] J. Kirschbaum, C. Krause, R. K. Winzheimer, *J. Peptide Sci.* 9 (2003) 799.
- [5] T. Marik, Cs. Várszegi. L. Kredics, *Acta Biol. Szegediensis* 57 (2013) 109.

THE EFFECT OF DIFFERENT VERTICAL ZINC DISTRIBUTION ON THE EARLY ROOT DEVELOPMENT AND ZINC ACCUMULATION OF *BRASSICA NAPUS*

Gábor Feigl¹, Árpád Molnár¹, Jolán Krajner¹, Dóra Oláh¹, Zsuzsanna Kolbert¹

¹*Department of Plant Biology, University of Szeged, H-6726 Szeged, Közép fasor 52, Hungary
e-mail: feigl@bio.u-szeged.hu*

Abstract

The early development of the root system is highly important for the plants' whole life; it is regulated by a complex system which integrates endogenous and environmental signals. Heavy metals (HMs) as exogenous factors have a different, concentration-dependent effect on the developing root: low concentrations cause stress-induced morphogenic response (SIMR, adaptation mechanism, more branched, shallower roots), while higher concentrations inhibit growth. Plants encounter heavy metals in many different ways, not only the widely studied homogenous distribution. Thus investigation of the effect of vertical distribution of HMs on the root development of crops has a great importance. In our experiments, to be able to determine and characterise the exact effect of excess zinc (Zn) on the root growth of *Brassica napus* L., several different layouts were used in soil-filled rhizotrons. This setup allowed us to examine the root growth of rapeseed in a practically 2D system, submitted to heterogeneously layered Zn-contaminated soil.

Introduction

The early development of the root system is crucial in terms of the life of a plant; besides ensuring physical stability for the whole plant, it is responsible for water and nutrient uptake and also might be practically (phytoremediation) relevant. It has a noteworthy plasticity: due to different stress conditions its architecture can change to favour seedling vigour and yield stability.

The delicate balance of the endogenous signal system responsible for the development of the root can be affected by various environmental stimuli, such as the excess of essential or non-essential HMs. Heavy metal contamination of soils and water is an existing and growing problem. This has partly originated from agricultural processes, such as excessive use of fertilisers or application of sewage [1].

HMs at low concentrations are able to induce the morphological and physiological adaptation of the root system called stress-induced morphogenic response. SIMR is a special combination of inhibition of primary root growth and induction of lateral root development, resulting in a shallower but horizontally more extensive root architecture, which most likely provides an enhanced stress tolerance [2-3], however this conjecture needs further investigations. On the other hand, HMs at high concentration lead to growth inhibition due to their phytotoxic effect by altering the most important plant physiological and metabolic processes [4]. The effect of HM excess on plants depends on numerous factors, including their mobility and their capability of bioaccumulation. Zn is a redox inactive essential microelement, with low mobility and accumulation capability in plants [5]. Zn, in low quantities as a micronutrient is essential for the normal development of plants, however in excess it might be toxic for plants and other eukaryotic organisms as well. Zn stress causes growth alterations and cell wall modifications, together with loss of functionality of enzymes and decreased photosynthesis.

Plants encounter heavy metals in many different ways, not only in the widely studied homogenous distribution. Thus investigation of the effect of vertical distribution of Zn on the root development of crops has a great importance.

Experimental

Custom-made plexi panels were ordered and assembled into 15 cm wide, 30 cm tall and 1,6 cm thick rhizotrons, using polifoam sheets and screws with wing nuts. The front panel is made of 3 mm thick, anti-glare, 100% transparent plastic, while the back panel is a 3 mm thick non-transparent black sheet; the thickness of the soil layer inside the rhizotron is 1 cm.

The rhizotrons are filled with Klamann Potgrond P blocking substrate (100% frozen through black peat with a fine structure of maximum 8 mm size, pH 6,0; 210 mg N/l; 240 mg P₂O₅/l) mixed with 20% sand; the initial water content is set to 70%. According to preliminary experiments 10 and 500 ppm Zn supplementation as treatment were chosen as SIMR-inducing and growth-inhibiting concentrations, respectively. Several heterogeneous setups were assembled (top/bottom half or top/middle/bottom third, respectively): control/10 ppm Zn (layout 1); 10 ppm Zn/control (layout 2); control/10 ppm Zn/control (layout 3); control/500 ppm Zn (layout 4); 500 ppm Zn/control (layout 5); control/500 ppm Zn/control (layout 6); 500 ppm Zn/10 ppm Zn/control (layout 7). *Brassica napus* L. (rapeseed) seeds were pre-germinated for 24 hours on 26°C and then transferred to the soil surface of the pre-filled rhizotrons. In the first 48 hours after the seeding, the young seedlings were covered with transparent plastic foil to provide optimal humidity, then the growing plants were supplemented with 10 ml distilled water in every two days. Seedlings were grown for 10 days, then the rhizotrons were scanned, disassembled and the roots were cleaned for further examination.

For visualisation of Zn, root tips were equilibrated in PBS buffer (137 mM NaCl, 2,68 mM KCl, 8,1 mM Na₂HPO₄, 1,47 mM KH₂PO₄, pH 7,4) then incubated with 25 µM Zinquin (ethyl (2-methyl-8-p-toluenesulphonamido-6-quinolyloxy)acetate) in PBS, for one hour at room temperature, in darkness, as described by Sarret et al. [6]. Roots dyed with Zinquin were investigated under a Zeiss Axiovert 200M inverted microscope (Carl Zeiss, Jena, Germany) equipped with a high resolution digital camera (Axiocam HR, HQ CCD, Carl Zeiss, Jena, Germany) and filter set 49 (exc.: 365 nm, em.: 445/50 nm). Fluorescence intensities (pixel intensity) in the meristematic zones of the root tips were measured on digital images using Axiovision Rel. 4.8 software within circles of 50 µm radii.

The results are expressed as mean ± SE by using Microsoft Excel 2016 and Student's t-test were used (*P≤0.05, **P≤0.01, ***P≤0.001). All experiments were carried out at least two times. In each treatment at least 10 samples were measured.

Results and discussion

Roots grown in layout 1 and 2 showed approximately the same growth and Zn-contents, the low Zn-treatment did not alter the morphology significantly. In layout 3 root morphology did not differ between the zones; however, Zn-content of the root tips were higher in the 10 ppm Zn supplemented zone. The difference between the Zn-accumulation capacity of the plants grown in the two- and three-layered systems can be explained by that in the layout 3 the growing root met with the Zn supplement in a younger developmental state; it is known that the HM accumulation capacity of the young, metabolically more active plant organs are high.

Upon encountering the growth-inhibiting Zn treatment the rapeseed roots showed different behaviour in the different layouts. When the germinating seedling faced the control soil at first (layout 4), it was able to develop a longer root system, and it also penetrated the 500 ppm Zn supplemented zone; however, there the growth stopped soon. In the opposite scenario, upon confronting the high Zn treatment zone first inhibited root growth in a much higher degree, the root could only slightly enter the lower control zone. Zn content of the root tips changed according to the soil Zn content, though there was a difference between the Zn-accumulation of the two layouts: in layout 4 the difference between the Zn accumulation of the control and 500 ppm zones were bigger than in layout 5. A possible explanation behind this difference can be that in layout 4 the growing root met with the control soil at its younger age and remained more active metabolically, while in layout 5 the growing root was in a stressed state and tried to exclude Zn.

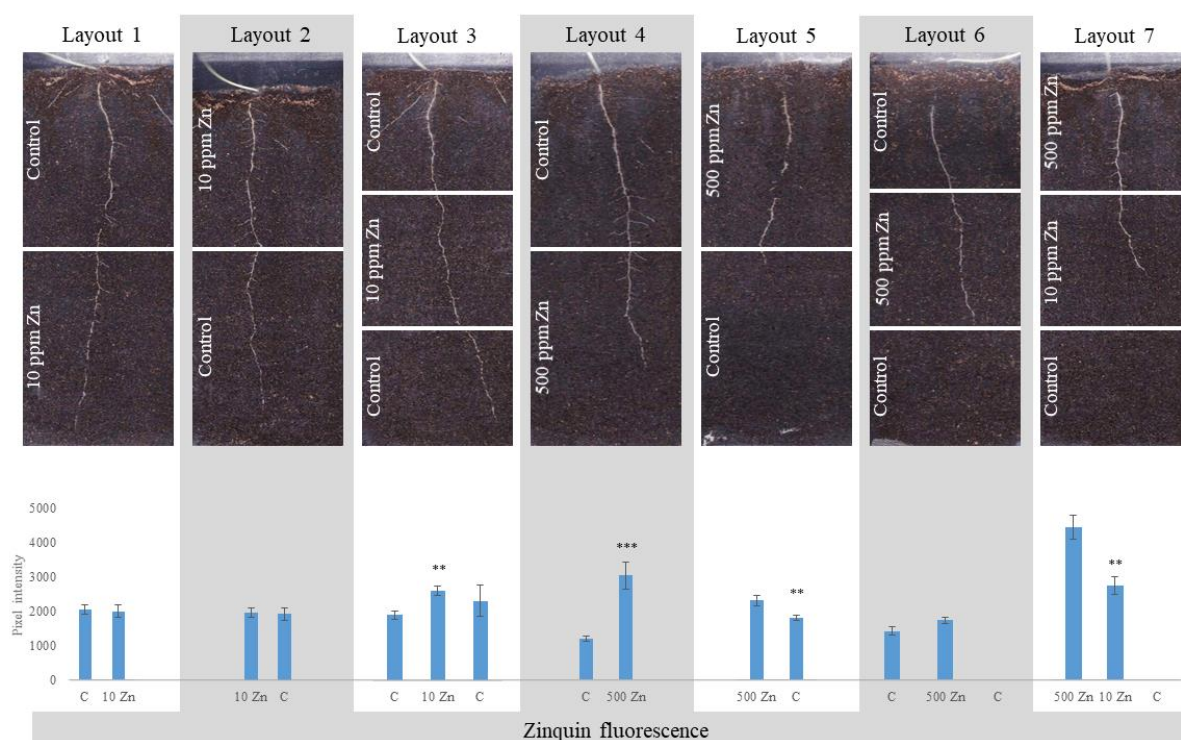


Figure 1. Representative images of the root growth in the different heterogeneous rhizotron system layouts and the Zn content-dependent Zinquin-fluorescence values in the root tips of the corresponding soil zone. Significant differences according to Student's t-test ($n = 10$, $*P \leq 0.05$, $**P \leq 0.01$, $***P \leq 0.001$) between each layouts' control and Zn-containing zones are indicated.

Layout 6 can be considered as the combination of the previous two, and the developing roots showed mixed growth characteristic: since the emerging root met the control soil at first it was able to penetrate and grow in the high Zn containing zone, though it did not enter the lower control layer. While in layout 5 the "young" root was able to grow through the high-Zn-zone, in layout 6 the growing root was relatively older upon encountering the same layer, resulting in the arrest of root growth and exclusion of Zn from its root tips.

In layout 7 we wanted to simulate a real-life Zn-contaminated soil, where the upper layer contained high amount of Zn, decreasing until control level in the lower zones. Similar to layout 5, the root system was able to grow through the 500 ppm Zn layer and entered the 10

ppm Zn zone, but could not reach the control at the bottom of the rhizotron. The roots accumulated far the highest amount of Zn in the entire experiment, and while the Zn content of the root tips grown in the 10 ppm layer were lower, it was still relatively high compared to the control levels. Seedlings in their early developmental stage receive plenty of nutrients from the seed, the root has a high metabolic activity and growth rate, which enabled the developing root to grow through the 500 ppm Zn zone, but the high Zn concentration ultimately caused the inhibition of root development in the subsequent, low-Zn-containing soil layer.

Conclusion

Results obtained from the heterogeneous Zn distribution experiments point towards the presumption that the growth inhibiting effect of the 500 ppm Zn treatment depends on the developmental stage of the rapeseed seedlings. When the root encountered the high Zn dose in a younger stage, it did not suffer growth inhibition, while the toxic effect of Zn is more pronounced on older roots. Considering the Zn accumulation, there was no close connection between the applied treatment and the Zn content of the root tips in all applied layouts.

Acknowledgements

Project no. PD 120962 and K 120383 has been implemented with the support provided from the National Research, Development and Innovation Fund of Hungary, financed under the PD-16 and K-16 funding scheme. *Brassica napus* seeds (GK Gabriella) were provided by the Cereal Research Non-Profit Ltd., Szeged, Hungary.

References

- [1] G. Tóth, T. Hermann, M.R. Da Silva, M. Montanarella (2016) Heavy metals in agricultural soils of the European Union with implications for food safety. *Environ Int* 88:299-309
- [2] G. Potters, T.P. Pasternak, Y. Guisez, K.J. Palme, M.A.K. Jansen (2007) Stress-induced morphogenic responses: growing out of trouble? *Trend Plant Sci* 12:98-105
- [3] Zs. Kolbert (2016) Implication of nitric oxide (NO) in excess element-induced morphogenetic responses of the root system. *Plant Physiol Biochem* 101:149-161
- [4] D. Kalaivanan, A.N. Ganeshamurthy (2016) Mechanisms of heavy metal toxicity in plants. *Abiotic Stress Physiology of Horticultural Crops*, pp 21, Ed: N.K. Srinivasa Rao, K.S. Shivashankara, R. H. Laxman
- [5] I. Kádár (2012) A főbb szennyező mikroelemek környezeti hatása. Magyar Tudományos Akadémia Agrártudományi Kutatóközpont Talajtani és Agrokémiai Intézete
- [6] G. Sarret, E. Harada, Y.E. Choi, M.P. Isaure, N. Geoffroy, S. Fakra, ... & A. Manceau (2006) Trichomes of tobacco excrete zinc as zinc-substituted calcium carbonate and other zinc-containing compounds. *Plant Physiology*, 141(3), 1021-1034.

HETEROGENEOUS PHOTOCATALYSIS OF IMIDACLOPRID THE EFFECT OF REACTION PARAMETERS

**Tamás Hlogvik¹, Máté Náfrádi¹, Abhimanyu Rampal², Sheema Garg², Klára Hernádi³,
Tünde Alapi¹**

¹*Department of Inorganic and Analytical Chemistry, University of Szeged, H-6720 Szeged,
Dóm tér 7, Hungary*

²*Department of Chemistry, Amity Institute of Applied Science, Amity University, Noida, Uttar
Pradesh, India*

³*Department of Applied and Environmental Chemistry, University of Szeged, H-6720 Szeged,
Rerrich Béla tér 1, Hungary
e-mail: alapi@chem.u-szeged.hu*

Abstract

The heterogeneous photocatalytic transformation of a harmful neonicotinoid insecticide, imidacloprid using TiO₂ photocatalyst was the aim of the present work. The optimal TiO₂ concentrations in oxygenated, aerated and oxygen-free suspensions were determined. However the dissolved oxygen enhanced the transformation rate of imidacloprid that was occurred in oxygen-free suspensions too. This can be explained by the relative high reactivity of imidacloprid towards hydrated electron, thus the relative contribution of direct charge can be significant. The effect of different additives was investigated to prove this assumption: NaF, methanol, *t*-butanol, chloroform, EDTA and KI. The pH and ionic strength of the solution have also significant effect, most likely by modifying the surface properties of TiO₂. The results showed, that beside HO• based reaction the direct charge transfer must have significant role in the transformation of imidaclopride.

Introduction

Imidacloprid is an insecticide belonging to the neonicotinoids, a class of chemicals which attack the nervous system of insects. It is a widely used insecticide in agriculture, although - along three other neonicotinoids - the European Union banned its use in 2018, due to its harmful effects on beneficial insects, like honeybees. [1]

Heterogeneous photocatalysis is a possible supplementary water treatment method for the removal of imidacloprid from waters. During the irradiation of the photocatalyst with light having higher energy than the band gap of the catalyst, the separation of charges creates an electron (e_{cb}⁻), and a positively charged hole (h_{vb}⁺). To avoid the recombination of charges, the e_{cb}⁻ must be trapped using an effective electron scavenger, usually dissolved oxygen takes this role. The most reactive species during heterogeneous photocatalysis are the hydroxyl radicals (HO•). They may form via their reaction of the h_{vb}⁺ with water or HO⁻ (1-2), or due to the reaction of e_{cb}⁻ with oxygen, resulting in O₂^{-•}. The further transformation of O₂^{-•} produces H₂O₂, and finally HO• (3-5) [2]. During the heterogeneous photocatalysis of imidacloprid, it is reported, that HO• has an important role. [4]



The goal of our work was to determine the dissolved oxygen and TiO_2 concentration dependency of the photocatalytic process efficiency. Moreover the effect of various additives was determined to get information about the relative contribution of the $\text{HO}\cdot$ and direct charge transfer based reactions to the transformation of imidacloprid. We used ionic compounds, such as NaCl (Cl^- has no special affinity to the TiO_2 surface) and NaF (F^- can replace $-\text{OH}$ of TiO_2 surface and consequently change the surface properties, such as adsorption capacity). Methanol and *t*-butanol were applied as $\text{HO}\cdot$ scavengers, while chloroform was used as $\text{O}_2^{\bullet-}$ scavenger. KI (I^-) and EDTA are able to decrease significantly the contribution of both direct charge transfer (through the reaction with h_{vb}^+) and $\text{HO}\cdot$ based reactions via competition with imidacloprid for these reactive species. Additives were applied in 1:1, 10:1, 50:1 molar ratios to the imidacloprid. We also investigated the effect of pH (3.0, 6.5, 9.0).

Experimental

Aqueous solutions of imidacloprid ($1.0 \times 10^{-4} \text{ mol dm}^{-3}$) were irradiated using a fluorescent UV light source (300-400nm). TiO_2 (Degussa P25 Aeroxide) were used in different concentrations ($0\text{--}1.5 \text{ g dm}^{-3}$), the suspension was sonicated before the irradiation. During the measurement, the suspension was stirred and circulated in a thermostated glass reactor. The suspension was saturated with oxygen, air or nitrogen. NaCl , NaF , methanol, *t*-butanol, chloroform, KI , and EDTA were added in $1.0 \times 10^{-4} \text{ mol dm}^{-3}$, $1.0 \times 10^{-3} \text{ mol dm}^{-3}$ and $5.0 \times 10^{-3} \text{ mol dm}^{-3}$ concentrations (1:1, 10:1, 50:1 molar ratios to the imidaclopride). The pH was adjusted with HCl and NaOH .

The samples were centrifuged and filtered before analysis using $0.22 \mu\text{m}$ syringe filters. The degradation rate of imidacloprid was determined using an Agilent 1100 series HPLC equipped with a LiChrospher® 100 RP-18 column and a diode array detector ($\lambda=270 \text{ nm}$). The eluent was a mixture of methanol and water (40:60 ratio).

Results and discussion

Imidacloprid does not adsorb significantly on the TiO_2 surface: using $1.0 \times 10^{-4} \text{ mol dm}^{-3}$ imidacloprid addition of 1.0 g dm^{-3} TiO_2 had no effect on the imidacloprid concentration in the aqueous phase. The optimal TiO_2 concentration in suspensions bubbled through with oxygen, nitrogen (oxygen-free suspension) and air were also determined.

Without TiO_2 there is a slow transformation of imidacloprid due to the small overlap of the spectrum of imidacloprid and the emitted light of the lamp. Dissolved oxygen concentration has no effect in these cases, when the transformation of imidacloprid takes place via direct photolysis. Increasing the TiO_2 dosage the competitive light absorption between imidacloprid and TiO_2 particles became more important, and direct photolysis is fully suppressed by the absorption of photons by TiO_2 particles above 0.50 g dm^{-3} . In oxygen containing suspensions the transformation rate increased with TiO_2 dosage and there was not found significant difference in the transformation rates using air or oxygen. The optimal dosage of TiO_2 was about 0.50 g dm^{-3} .

In oxygen-free suspensions the optimal TiO_2 dosage was lower, between 0.25 and 0.50 g dm^{-3} and the dose dependence of the transformation rate was found to be different than in oxygen-containing ones. Effective transformation via heterogeneous photocatalytic way requires the presence of effective e_{cb}^- scavenger, which is generally dissolved oxygen. In most cases there is no transformation of organic substances in oxygen-free suspensions. However in the case of heterogeneous photocatalysis of imidacloprid the transformation rate showed maximum between 0.25 and 0.50 g dm^{-3} , and reached a plateau above 0.75 g dm^{-3} TiO_2 dosage. The value of the transformation rate above this photocatalyst dosage is less than the half of that determined in oxygen containing suspension. At lower TiO_2 dosage the transformation takes

place by direct photolysis and heterogeneous photocatalysis. The relative contribution is depend on the TiO_2 dosage. The increase in the TiO_2 dosage reduces the importance of direct photolysis, and the overall effectiveness decreases. The efficiency of heterogeneous photocatalysis without oxygen can be explained by the relative high reactivity of imidacloprid toward e_{aq}^- . Thus imidacloprid is able behaves as e_{cb}^- scavenger instead of dissolved oxygen. In this case the transformation must take place mainly by direct charge transfer.

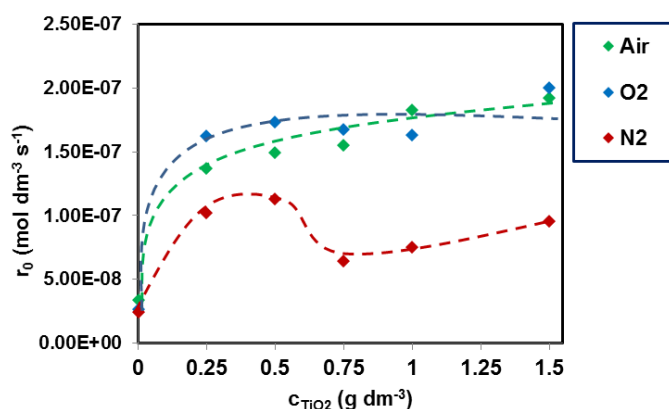


Figure 1. Transformation rates of imidacloprid using different concentrations of TiO_2 and dissolved oxygen

For further experiments we used 1.0 g dm^{-3} TiO_2 concentration to avoid direct photolysis and suspensions were bubbled with oxygen to optimize the formation rate of $\text{HO}\cdot$. The role of direct charge transfer and $\text{HO}\cdot$ based reactions were investigated via effect of various additives. Inorganic ions affect the photocatalytic process by increasing ionic strength, changing the surface charge and the adsorption properties of target compounds on TiO_2 particles. We used NaCl to investigate the effect of ionic strength increase, since Cl^- has no any kind of specific interaction with TiO_2 surface. Addition of NaCl has no significant effect on degradation rate.

F^- has a special affinity for the TiO_2 surface, replacing surface $-\text{OH}$ groups with $-\text{F}$ groups. Addition of NaF affects the efficiency of photocatalytic transformation in many cases by various ways. It is accepted, that F^- increases the $\text{HO}\cdot$ concentrations in the bulk solution by improved electron transfer capabilities, decreasing charge recombination, and increasing the possibility of h_{vb}^+ based reactions. [5] NaF addition to the imidacloprid solution did not change its adsorption, but slightly increased the degradation rates when compared to the effect of NaCl , indicating the importance of $\text{HO}\cdot$ during the transformation process. It was also confirmed by the results of methanol and *t*-butanol addition. Both alcohol is effective $\text{HO}\cdot$ scavenger and significantly decreased the transformation rate of imidacloprid when used in higher concentrations.

Dissolved oxygen reacts with the photogenerated e_{cb}^- , forming $\text{O}_2^{\cdot-}$, which may also react with certain compounds. Chloroform was used, as a $\text{O}_2^{\cdot-}$ scavenger to investigate its possible effect. Chloroform did not hinder the transformation of imidacloprid, proving the negligible effect of $\text{O}_2^{\cdot-}$.

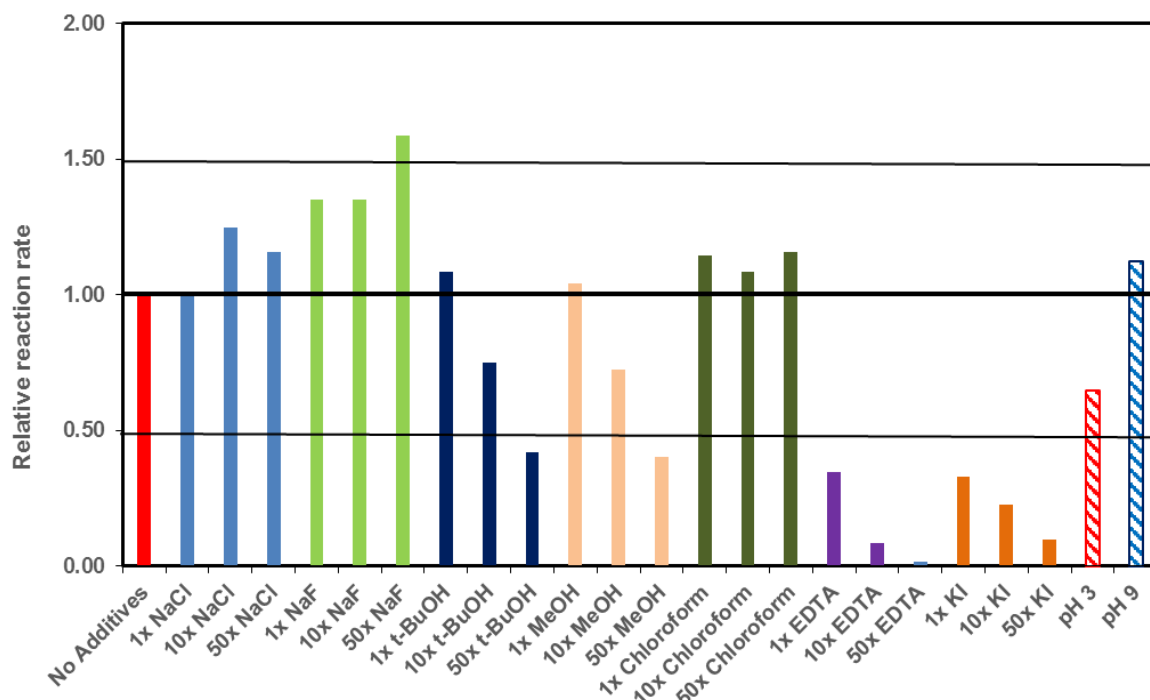


Figure 2. Relative transformation rates of imidacloprid in the case of different additives, compared to the reaction rate when no additives were used

Imidacloprid transformation is assumed partly by direct charge transfer reactions. To prove this assumption, the effect of EDTA and KI as a scavenger of $h_{\nu b}^+$ was determined. EDTA adsorbs well on the TiO_2 surface, where it can easily react with $h_{\nu b}^+$, hindering not only the transformation of other compound via direct charge transfer, but also the formation of $HO\bullet$ and other hole-induced reactions. Addition of EDTA even at 1:1 molar ratios had a more significant effect than alcohols at 50:1 ratios. At higher concentrations, EDTA nearly completely inhibits the transformation of imidacloprid (10:1 and 50:1 ratio). Similar effect of I^- (KI), which is a well-known scavenger of both $h_{\nu b}^+$ and $HO\bullet$ was experienced. Its effect is slightly less pronounced at higher dosages than EDTA, most likely because of its less significant adsorption. These results prove both the importance of surface accessibility during the photocatalytic degradation of imidacloprid, and the possibility of the direct charge transfer despite the negligible adsorption of imidacloprid on the TiO_2 surface.

We also investigated the effect of the pH, performing experiments on pH 6.5, on the estimated point of zero charge (PZC) of TiO_2 , on pH 3.0 and pH 9.0. Changing the pH has several complex effects: changes the surface charge of TiO_2 from neutral to positive (acidic conditions) or to negative (basic conditions). This may influence the adsorption on the TiO_2 surface, and other surface properties, and also the formation of reactive species. We found that on pH 3.0 the transformation rate of imidacloprid significantly lowered, while on pH 9.0 it slightly increased.

Conclusion

- The transformation rate of a harmful pesticide, imidacloprid using heterogeneous photocatalysis was investigated.
- The TiO_2 dosage was optimized under oxygen saturated and oxygen free conditions.
- Effect of $HO\bullet$ radical scavengers (methanol, *t*-butanol, chloroform) proved the significant role of $HO\bullet$ in the transformation of imidacloprid.

- The effect of EDTA and KI proved the importance of direct charge transfer beside HO• based reaction in the transformation of imidacloprid

Acknowledgements

T. Alapi acknowledge German Academic Exchange Service (DAAD) and Tempus Foundation for financial support (project number: 151955). Thanks for the financial help of the Industrial Research and development Projects of Hungarian-Indian cooperation (TÉT_15_IN-1-2016-0013))

References

- [1] E.C. Yang, Y.C. Chuang, Y.L. Chen, L.H. Chang, , J. Economic Entomology 101 (2008) 1743-1748
- [2] Nurul Aiin Ab Aziza, Puganeshwary Palaniandya, Hamidi Abdul Aziza and Irvan Dahlanb, Journal of Chemical Research. 40 (2016) 704–712
- [3] Yoshio Nosaka, Masami Nishikawa, Atsuko Y. Nosaka, Molecules. 19 (2014) 18248-18267
- [4] S. Malato, J. Caceres, A. Agüera, M. Mezcua, D. Hernando, J. Vial, A.R. Fernández-Alba, Environ. Sci. Technol. 35 (2001) 4359-4366
- [5] C. Minero, G. Mariella, V. Maurino, E. Pelizzetti, Langmuir 16 (2000) 2632-2641

INVESTIGATION OF INTERACTIONS ON CHIRAL ZWITTERIONIC STATIONARY PHASES IN ENANTIOMER SEPARATION USING HPLC AND SFC METHODS

Éva Horváth¹, Csanád Rédei¹, Borbála Boros¹, Attila Felinger^{1,2,3}

¹*Department of Analytical and Environmental Chemistry, University of Pécs, H-7624 Pécs, Ifjúság útja 6., Hungary*

²*MTA-PTE Molecular Interactions in Separation Science Research Group, 7624 Pécs, Ifjúság útja 6., Hungary*

³*Institu of Bioanalysis, University of Pécs, 7624 Pécs, Honvéd u. 1., Hungary
e-mail: eva.horvath@gamma.ttk.pte.hu*

Abstract

Most biologically and pharmacologically important molecules (amino acids, carbohydrates, pharmaceuticals, etc.) are chiral compounds that may cause various biological effects; therefore increased attention is placed on their separation, qualitative and quantitative analysis. As a result of this knowledge, in this work the theoretical background of chiral chromatographic separation was investigated by high performance liquid chromatography (HPLC) and supercritical fluid chromatography (SFC). For our measurements, a new generation chiral zwitterionic stationary phase (Zwix (-) column) was used to separate the enantiomers one of the antimalarial drugs, mefloquine.

According to the stochastic model of chromatography [1,2], the peak formed during separation is a combination of the random walk of a molecule through the column and the slow adsorption-desorption processes. Using this theory, it is possible to determine the residence time of the molecules in the stationary phase and the average number of adsorption steps from which the retention factor can be calculated.

For chromatographic measurements, van 't Hoff plot [3] is used to explain the retention mechanism. In our case, the values of the retention factors were determined in two ways, on the one hand by classical calculations, on the other hand with stochastic model, which assumes multiple binding.

Finally, the thermodynamic parameters were compared for the two chromatographic methods, high performance liquid chromatography (HPLC) and supercritical fluid chromatography (SFC).

References

- [1] A. Felinger, LCGC North America, 22 (2004) 647.
- [2] A Felinger, A. Cavazzini, F. Dondi, J. Chromatogr. A., 1043 (2004) 157.
- [3] L. D. Asnin, M. V. Stepanova, J. Sep. Sci. 41 (2018) 1337

MICROWAVE-ASSISTED Pd-CATALYZED C-P OR C-C CROSS COUPLINGS ON 13 α -ESTRANE CORE

Rebeka Jójárt¹, Péter Trungel-Nagy¹, Szabolcs Pécsy¹, Márton Szlávik¹, Gergely Horváth¹, Henrietta Ágoston¹, Erzsébet Mernyák¹

¹*Department of Organic Chemistry, University of Szeged, H-6720 Szeged, Dóm tér 8, Hungary*

Abstract

Novel 2- or 4-substituted 13 α -estrone derivatives were synthesized via Hirao or Suzuki reaction. Transformations of 2- and/or 4-halogenated derivatives of 13 α -estrone and its 3-benzyl or -methyl ether were carried out in a microwave (MW) reactor. Facile and efficient C-C or C-P coupling procedures were established using Pd or Ni catalysts. The newly synthesized compounds might have promising antitumoral properties.

Introduction

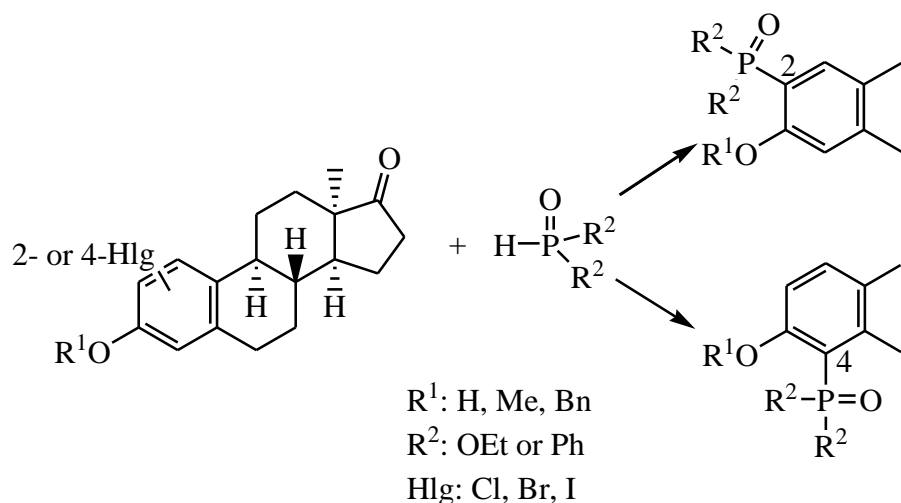
Introduction of large apolar substituents onto C-2 of estrane core may lead to compounds possessing substantial antitumoral activity. The functionalization of the aromatic ring A of estrone might be achieved via Pd-catalyzed cross coupling reactions. Hirao reaction is a powerful tool for the synthesis of aryl phosphonates from aryl bromides or iodides using dialkyl phosphites (H-phosphonates) as the reagents, Pd(PPh₃)₄ as the catalyst and Et₃N as the base.^{1,2,3} Suzuki reaction is a cross coupling reaction between aryl/alkyl halides with organoboronic acids and Pd(PPh₃)₄ as the catalyst.⁴ Our aim was to develop facile and effective C-C and C-P cross coupling methods for the preparation of 2- or 4-substituted 13 α -estrone derivatives by MW irradiation. We planned to use “green” methodologies by replacing the Pd catalyst with Ni under P-ligand- and solvent-free conditions.

Experimental

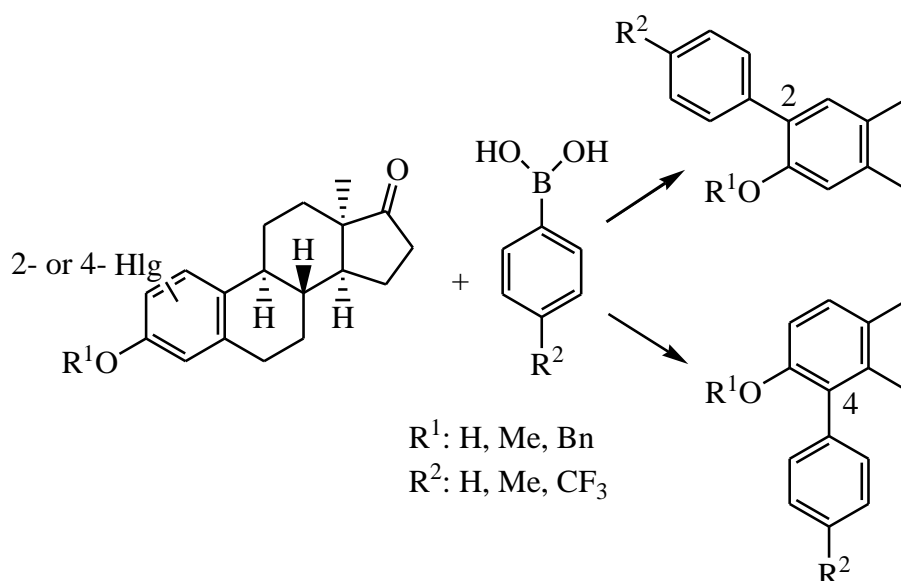
The optimization of the Hirao reaction conditions was carried out using 2-bromo- or 2-iodo-13 α -estrone 3-methyl ether as starting compounds and diethyl phosphite as a reagent. Pd(OAc)₂ or Pd(PPh₃)₄ catalysts were used without addition of any P-ligand. The Suzuki couplings were optimized using 2-bromo- or 2-iodo-13 α -estrone 3-methyl ether as starting compounds, phenylboronic acid as a reagent and Pd(PPh₃)₄ catalyst. The structures of the new compounds were confirmed by ¹H and ¹³C NMR measurements.

Results and discussion

The optimal conditions were selected for extension of C-P couplings to other steroidal scaffolds, which differ in position and nature of the halogen and/or nature of the C-3 substituent (Scheme 1). All the couplings resulted in the desired product with high yields. Couplings with NiCl₂ as the catalyst required higher reaction temperatures and longer reaction times.

Scheme 1. C-P couplings at C-2 or C-4 in the 13 β -estrone series

Suzuki reactions were efficiently performed with different para-substituted phenylboronic acids (Scheme 2). The couplings of C-2 or C-4 regioisomers could be achieved under different conditions. It can be stated that transformations at more hindered C-4 required harsher reaction conditions.

Scheme 2. Suzuki cross couplings in the 13 β -estrone series

Conclusion

We have developed efficient microwave-assisted, P-ligand-free, Pd- or Ni-catalyzed cross coupling procedures. Certain reactions proved to be effective under solvent solvent-free conditions too.

Acknowledgements

This work was supported by ÚNKP-18-4-SZTE-45 „New Excellence Program of the Ministry of Human Capacities” and by National Research, Development and Innovation Office-NKFIH through project OTKA SNN 124329.

References

- [1] T. Hirao; T. Masunaga; Y. Ohshiro; T. Agawa. *Tetrahedron Lett.* **1980**, *21*, 3595–3598.
- [2] G. Keglevich; E. Jablonkai; B. B. László. *RSC Adv.* **2014**, *4*, 22808–22816.
- [3] Jablonkai, E., G. Keglevich, B. B. László. *C. Org. Chem.* **2015**, *19*, 197-202.
- [4] V. Ahmed, Y. Liu, C. Silvestro, S. D. Taylor. *Bioorg. & Med. Chem.* **2006**, *14*, 8564-8573.

TOTAL PHENOLIC CONTENT, ANTIOXIDANT CAPACITY AND MINERAL CONTENT OF SELECTED FRUITS FROM NORTHEASTERN HUNGARY

**Fatjona Fejzullahu¹, Zsuzsa Jókai¹, Marta Uveges¹, István Mórucz²,
Éva Stefanovits- Bányai¹**

¹*Szent István University, Faculty of Food Science, Department of Applied Chemistry,
H-1118 Budapest, Villányi út 29-43, Hungary*

²*Panyolium Kft, Hungary*

e-mail: jokaine.szatura.zsuzsanna@etk.szie.hu

Abstract

Fruits have been very essential in the growth and development of human life. Therefore, the present study was designed to evaluate the chemical composition of cherry, plum and pear cultivars grown in northeastern part of Hungary. Twelve fruit species were screened for their total phenolic content, antioxidant capacity and mineral content. The results show that the chemical composition and antioxidant capacity of the investigated fruits varies significantly. Total phenolic contents of the selected fruit cultivars (cherries, plums and pears) were investigated according to the method of Singleton and Rossi, while the antioxidant activity of the fruits was determined using the ferric reducing antioxidant power (FRAP) assay. Positive correlation was found between the total phenolic content and antioxidant activity that means the phenolic content of these fruits contributes to antioxidant capacity. Mineral contents varied greatly between the species. Cherry was found to be the richest source of minerals. The most abundant mineral detected was potassium, followed by calcium and phosphorus. The trace elements were detected in lower amounts. Results showed that these fruits contain considerable amounts of minerals and phenolics, resulting also in significant antioxidant activity. They strongly support the evidences that fruits promote health benefits. These fruits, especially cherries could be potential rich resources of natural antioxidants and could be developed into functional foods or drug for the prevention and treatment of diseases caused by oxidative stress.

Introduction

Fruits have historically held a place in human diet because of their immense nutritional values. They are natural sources of beneficial components that play an important role in human nutrition and health. Fruits are particularly recognized as a source of vitamins, dietary fibre and other antioxidant compounds, such as phenolics, vitamins, carotenoids and minerals, which contribute to their chemo-preventive potential [1,2].

Phenolics are bioactive non-nutrient compounds that attribute to the sensory qualities (color, flavour, taste) of fresh fruits. In addition, many phenolic phytochemicals have antioxidative, anticarcinogenic, antimicrobial, antiallergic, antimutagenic and inflammatory activities [3,4]. Therefore, the role of fruits in disease prevention is partly associated with the antioxidant properties of their constituent phenolics [5,6]. Antioxidants are compounds that retard or inhibit the oxidation of molecules that can occur by the presence of reactive free radicals, thus protecting the body from several diseases [7]. Other health benefits of eating fruit are attributed to minerals, they are inorganic substances required by the organism in very small amount for maintenance of vital processes essential for life [8]. Epidemiological studies have found that the intake of fruits has a strong inverse correlation with the risk of developing many chronic diseases, such as cardiovascular diseases and cancer [9,10,11]. In this manner, the present research was designed to shade some light on the composition of plums, pears and

cherries grown in north-eastern part of Hungary. Particularly, mineral content, total phenols and the effect related to antioxidant capacity were determined.

Experimental

Sample collection

Fresh fruits were collected at commercial maturity during the 2017. harvest season (July, August and September). All samples originated from Szabolcs-Szatmár-Bereg country near Nyíregyháza city in north-eastern part of Hungary. From these fruits, 3 were cherry cultivars, 1 pear cultivar, and the rest were plum cultivars, respectively 8.

Sample preparation

The whole edible part of the fruit was used in the study. The fruits were washed, then they were cut in halves and pits were removed. Samples were cut into small pieces, weighed accurately (~ 40 gram), and freeze-dried immediately, since chopped material is much more unstable and may result in enzymatic browning, as well as undesirable molecular, biochemical and physiological changes. After freeze drying the samples were weighed again to determine the dry matter without water. The 250 mg/10 ml solutions were centrifuged (6000 rpm, 20 min, 4 C°) and the clean supernatants were analysed.

Determination of antioxidant capacities by FRAP (Ferric Reducing Antioxidant Power) method

Measurement of ferric reducing antioxidant power of the fruit extracts was carried out based on the procedure of Benzie and Strain [12], at 593 nm. (Spectronic Helios Gamma UV Visible Spectrophotometer Thermo Fisher Scientific.) Ascorbic Acid was used as a standard to prepare the calibration solutions. Results were expressed as $\mu\text{MAA/g}$ of dry plant material.

Determination of total phenolic contents by Folin-Ciocalteu method

The Folin - Ciocalteu method is an electron transfer based assay and gives reducing capacity which is expressed as phenolic content. Total phenolic content of the fruit extracts was determined with the Folin-Ciocalteu reagent according to a procedure described by Singleton and Rossi [13], at 760 nm.

Gallic acid was used to prepare the standard curve. The results were expressed as mMGA/g of dry plant material.

Mineral content analysis using ICP-OES

The presence of the following minerals: Ca, Mg, K, Na, Fe, Cu, Zn, Mn and P was investigated by inductively coupled plasma optical emission spectrometry (ICP-OES). All the previously freeze-dried samples were prepared for the analysis via microwave digestion method by using concentrated nitric acid and hydrogen peroxide.

After mineralization, the resulting solutions were cooled to room temperature, then they were transferred to autosampler tubes and diluted to a final volume of 25 mL with Milli-Q water. The determination of mineral contents in this clear solution was carried out by ICP-OES. The concentrations of the calibration solutions were in the range from 1 to 100 mg/kg (1,5,10,100 mg/kg, respectively) to match the amount of the elements possibly present in the samples.

Results and discussion

Total Phenolic Content

The results from the study showed a variation of total phenolic (TP) contents between the fruits tested. The TP content ranged from 13.87 ± 0.18 to 76.60 ± 9.23 mMGA/g of dry weight. Among the fruits that were used in the study, the highest content of phenolics resulted from cherry cultivars, two to three times higher than the phenolic contents of plums and pear cultivars. The results showed that Oblacsinszka species (cherry cultivar), were the richest source of phenolics with a total phenolic content of 76.60 ± 9.23 mMGA/g of dry weight. The lowest content of phenolics among all tested fruits was recorded for Vilmos species (pear cultivar), only 13.87 ± 0.18 mMGA/g of dry weight. TP content of 8 plum samples shows variation, the highest TP content was found in Unknown C plum sample.

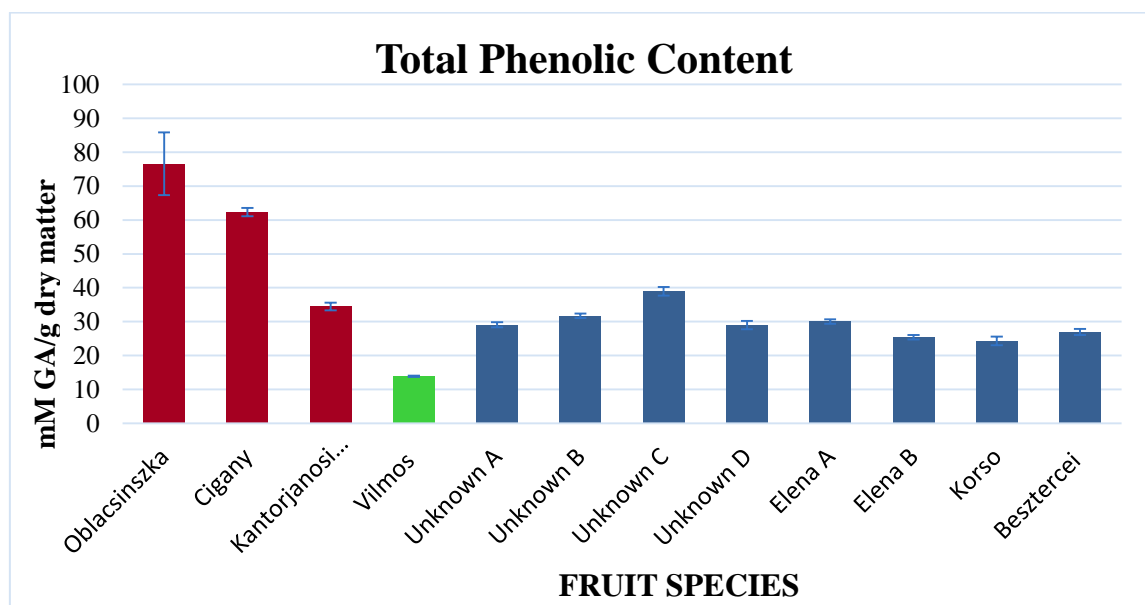


Figure 1. Total phenolic content of the investigated fruits

The total phenolic contents of the cherry species tested in the present study (118.72 – 233.01 mg GAE/100 g fw) were similar to those reported in the literature. The phenolic contents of sweet and sour cherries were investigated by Prvulovic et al. [14], the results showed that the lowest TPC was 76.05 while the highest was up to 301.19 mg gallic acid equivalents/100 g fresh fruit weight.

Antioxidant Capacity

FRAP values of the tested fruits varied significantly among each other, starting from 4.89 ± 0.14 to 52.58 ± 0.50 μ MAA/g of dry weight. Cherry cultivars resulted to have the highest antioxidant capacity among the studied fruits, followed by plum cultivars and lastly, the pear cultivar.

In descending antioxidant activity, the order was: cherry > plum > pear.

Correlation between Antioxidant Capacity and Total Phenolic Content

Despite the presence of a wide range of the antioxidant capacities and total phenolic contents among the selected fruits, the results showed a positive linear correlation between the antioxidant capacity and total phenolic content ($R^2 = 0.9176$) Figure 2. Moreover, an increase in antioxidant capacity corresponds to the increase in the total phenolic content. These results

indicate that the phenolic compounds could be the main contributor of the antioxidant activities of these fruits. These results were in agreement with many previous studies [15].

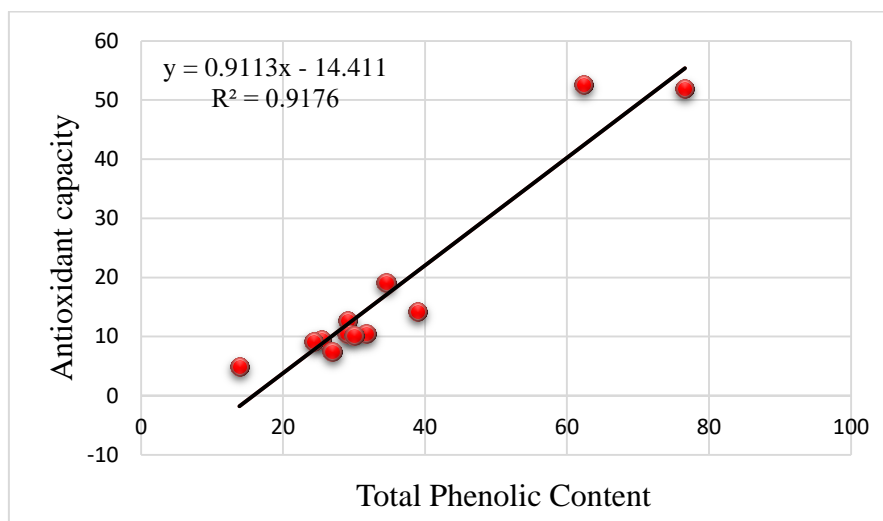


Figure 2. Correlation between the total phenolic content and antioxidant capacity of the selected fruits. Antioxidant capacity was measured by the FRAP assay and TPC by Folin-Ciocalteu method

Mineral contents

The concentrations of Na, K, Ca, Mg and P (major elements) as well as Fe, Mn, Cu and Zn (minor elements) were determined in 12 fruit samples using inductively coupled plasma optical-emission spectrometry (ICP-OES). The results are shown in table 1.

Fruit species	Concentration of minerals (mg/kg dry weight)								
	Ca	Cu	Fe	K	Mg	Mn	Na	P	Zn
Oblacsinszka	1520	11	17	14000	780	6.3	8.2	1300	3.5
Cigany	1500	13	15	13000	720	3.7	3.4	1500	4.5
Kantorjanosi Cigany	1200	4.6	11	12000	560	2.4	5.6	950	3.3
Vilmos	660	4.1	16	6400	270	2.1	11	450	4.2
Unknown A	690	3.5	7.5	9100	442	2.8	2.8	710	3.7
Unknown B	740	3.9	8	11100	430	2.6	7	740	3.9
Unknown C	540	4.7	49	11000	410	5.4	3.8	670	5.2
Unknown D	590	3.2	6.4	10000	390	3.1	5.3	715	4.2
Elena A	670	3.6	9.6	11300	490	4.1	3.6	980	4.9
Elena B	520	5.3	9	15000	470	5.6	2.6	970	5.8
Korso	560	3.7	9.4	12100	520	4.5	5	870	7.3
Besztercei	540	2.2	16	9000	340	2.3	1.6	720	3.4

Table 1. Mineral content of the investigated fruits (mg/kg dry weight)

The results listed in Table 10. shows that the most abundant mineral among the analysed fruit cultivars was potassium, followed by calcium, phosphorus and magnesium. Other microelements such as iron, manganese, zinc, copper and sodium were detected in much lower amounts.

Conclusion

The chemical composition and antioxidant capacity of the investigated fruits varies significantly due to many factors (genetics, soil composition etc.). There was a positive correlation between the total phenolic content and antioxidant activity, showing that the phenolics from these fruits may supply substantial antioxidants, which gives health-promoting advantages to the consumer.

With this study we proved that these fruits are rich sources of potassium, cherries contain the highest concentrations of all the minerals, leaving behind plums and pears. It was reported that in general fruits are not good sources of calcium. In this study, it was found that some fruits contained significant amount of calcium. In general, the elemental concentration in all samples decreased in the following order: K > Ca > P > Mg > Fe > Na > Cu > Mn > Zn. The difference in the elemental concentration between the samples can be a result of variations in the geographic origin and cultivation conditions.

Acknowledgements

The support of the European Structural and Investment Funds (grant agreement no. VEKOP-2.3.3-15-2017-00022) is also acknowledged.

References

- [1] M.J. Wargovich, HortScience 35(4) (2000) 573-575.
- [2] M.M.B. Almeida, P.H.M. Sousa, A.M.C. Arriaga, G.M. Prado, C.E Carvalho Magalhaes, G.A. Maia, T.L. Lemos, Food Research International 44(7) (2011) 2155-2159.
- [3] Y. Cao, R. Cao, Nature 398(6226) (1999) 381.
- [4] M.V. Eberhardt, C.Y. Lee, R.H. Liu, Nature 405 (2000) 903-904.
- [5] A. Scalbert, G. Williamson, Journal of Nutrition, 130(8S Suppl) (2000) 2073S-2085S.
- [6] A.M. Najafabad, R. Jamei, Avicenna Journal of Phytomedicine 4(5) (2014) 343-353.
- [7] D.O. Kim, Y.J. Kim, H.J. Heo, J. Freer, O.I. Padilla-Zakour, C.Y. Lee, New York Fruit Quarterly 12(4) (2004) 9-12.
- [8] D.K Paul, R.K. Shaha, Pakistan Journal of Biological Sciences 7(2) (2004) 238-242.
- [9] G. Block, B. Patterson, A. Subar, Nutrition and Cancer 18(1) (1992) 1-29.
- [10] J.H. Cohen, A.R. Kristal, J.L. Stanford, Journal of the National Cancer Institute 92(1) (2000) 61-68.
- [11] N. Lunet, A. Lacerda-Vieira, H. Barros, Nutrition and Cancer 53(1) (2005) 1-10.
- [12] I.F.F. Benzie, J.J. Strain, Analytical Biochemistry 239 (1966) 70-76.
- [13] V.L. Singleton, J.A. Rossi, American Journal of Enology and Viticulture, 16 (1965). 144-158.
- [14] D. Prvulovic, D. Malencic, M. Popovic, V. Studia Universitatis Babes-Bolyai, Chemia 57(4) (2012) 175-181.
- [15] N. Miletic, B. Popovic, O. Mitrovic, M. Kandic, Australian Journal of Crop Science 6(4) (2012) 681-687.

This research was supported by the Higher Education Institutional Excellence Program (1783-3/2018/FEKUTSTRAT) awarded by the Ministry of Human Capacities within the framework of plant breeding and plant protection researches of Szent István University.

ENVIRONMENTAL MAGNESIUM SUPPLY, MUTATION OF ION CHANNELS AND TRANSPORTERS

Zoltan Kiss

Department of Medicine CSMEK Hódmezővásárhely-Makó H6900 Makó, Kórház u. 2.

Abstract

Decreasing Mg-content of soil and foods aren't an isolate phenomenon. It is inseparable from the effect of other ions (1). Beside deterioration of ion equilibrium, the property of accumulation of toxic metals due to global environmental pollution is very disadvantageous, because these can substitute vital, essential macro- and microelements and can competitively block transporters and channels. The unfavorable effect are strengthened by mutations of transporters and channels, which may be the causes of severe immunodeficiencies, life-threatening arrhythmias as background of frequent diseases and do have significant public health impact via widespread use and results of genetic tests.

Introduction

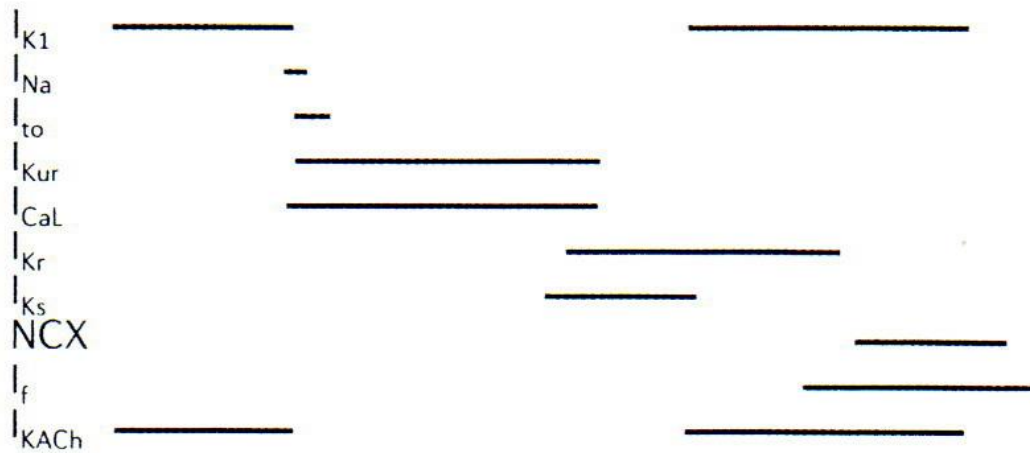
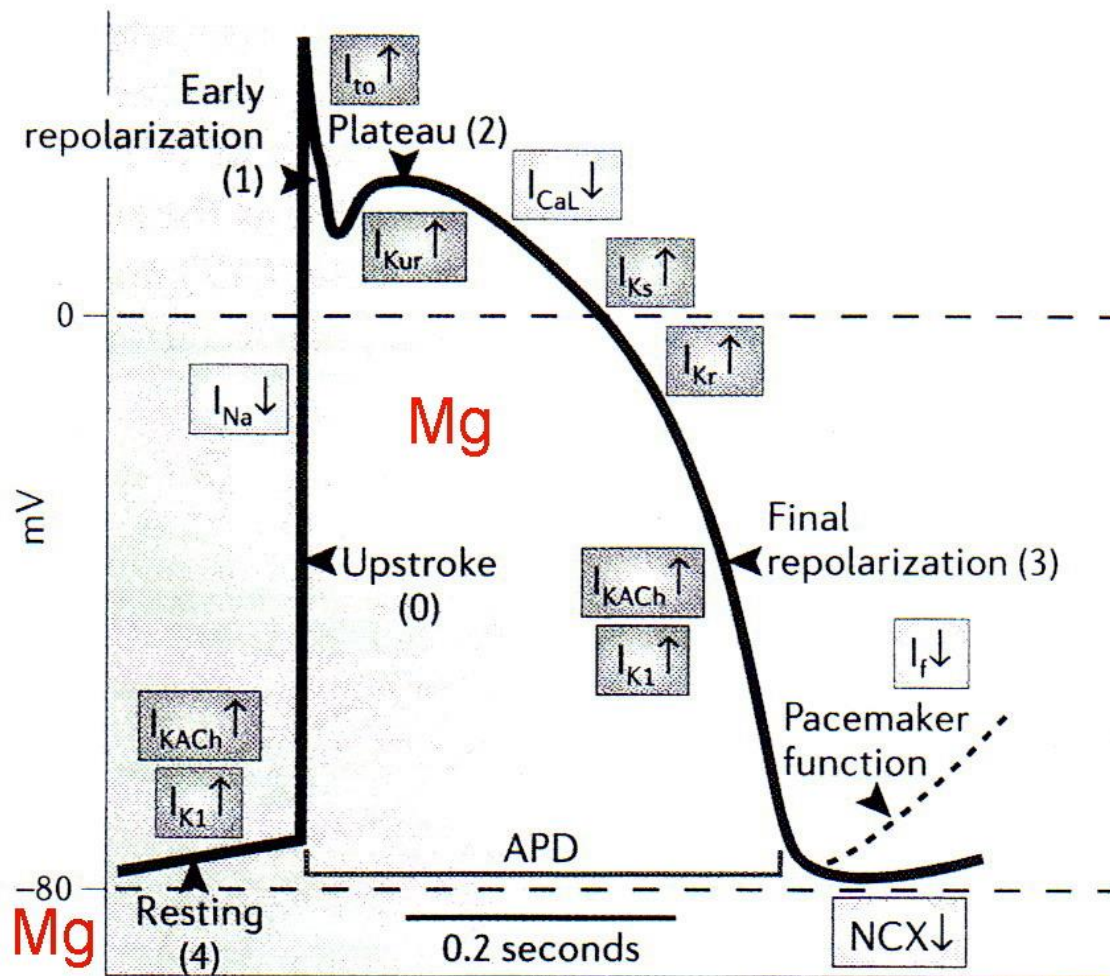
Decreasing Mg-content of soil and foods isn't an isolate phenomenon. It is inseparable from the effects of other ions, which are important signaling cations in immun system (2).

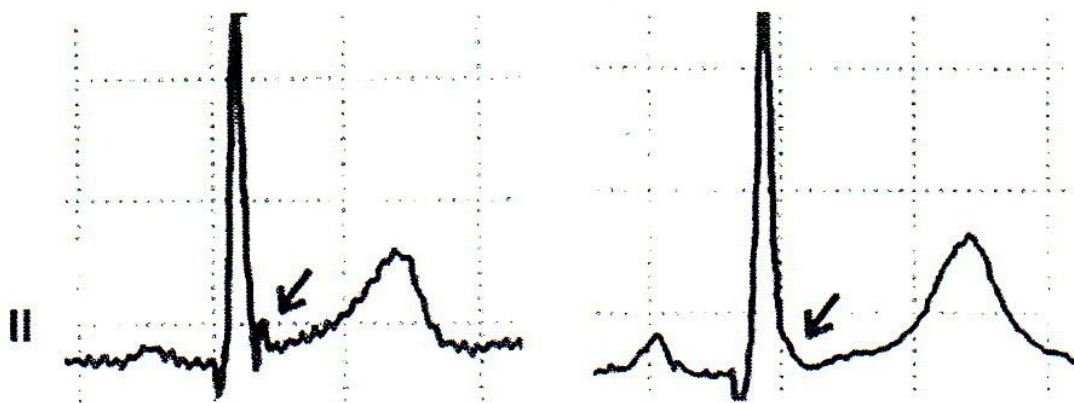
Beside deterioration of ion equilibrium, the property of accumulation of toxic metals due to global environmental pollution is very disadvantageous, because these can substitute vital, essential macro- and microelements and can competitively block transporters and channels.

Human and experimental data

Loss of function mutations in the gene encoding in MAGT1-as a critical regulator of intracellular free Mg^{++} level- cause XMEN disease with X-linked combined immunodeficiency with magnesium defect. It's characterised by CD4 lymphopenia, chronic Epstein-Barr virus (EBV) infection and related lymphoproliferative disorders (e.g lymphoma). Oral magnesium L-threonate led to better control of EBV infection. There are mutations in SCN5A sodium channel and A109A genes (3) increases the outward transient K-flux (Ito), which regulated by magnesium (4). The early repolarization was experimentally evoked by us (5).

Fig.1 demonstrates the action potentials of myocardial fiber with early transient K-efflux (a), spike and dome and early ventricular repolarization signs (b) on human surface ECG unipolar leads (arrows).





In J-wave syndromes with episodes of ventricular fibrillation (Brugada and early repolarisation syndrome, (6), was no association between serum K^+ or Ca^{++} and repolarisation, but there was a significant negative correlation between serum Mg^{++} and repolarisation dispersion (7).

The non-selective calcium-activated transient receptor potential channels are activated by receptor, ligand or direct mode and one of them (TRPM7) is taking part in the regulation of Mg-homeostasis (8). TRPM6 gene mutation leads to autosomal recessive hypomagnesemia and hypocalcemia (9). At the same time, Mg blocks the excessive Ca and environmental toxic metals' (Zn, Co, Ni, Ba, Pb, 10) influx. In the case of mutation, the intracellular Ca-influx increases in malignant tumors, supporting progression.

Discussion

There is an overlap in phenotype and electrophysiological similarities between Brugada syndrome and early repolarization (11). The presence of a prominent I_{to} -mediated action potential notch (spike and dome) in the epicardium, but not the endocardium, generates a transmural voltage gradient during the early phase of repolarization, which manifests J-wave and J-point elevation in the surface ECG in both ERP and Brugada syndrome. Heterogeneous loss of the action potential dome produces phase 2 reentry, leading to polymorphic ventricular tachycardia/ventricular fibrillation. Mutation of paracellin-1 manifests in hypomagnesemic-hypercalcaemic syndrome. Mg homeostasis plays a very important role in prevention of serious consequences of hypomagnesemia. It is inseparable from the actions of other ions.

Conclusion

The above-mentioned mutations may be the causes of severe immunodeficiencies, life-threatening arrhythmias as background of frequent diseases (recurrent sinopulmonary infections, pneumonias, syncope) and do have significant public health impact via widespread use of genetic tests in the future. Of note that blocking the intracellular influx of toxic environmental metals may have a role in the planning of medicines that will be developed for the treatment of civilization disorders, e.g. hypertension, neurodegenerative disorders.

Acknowledgements: none

References

- [1] A. Tompa, Orvostovábbk.Sz. (2018)69.(in Hungarian)
- [2] B. Chaigne-Delalande, M.J. Leonardo, Trends Immunol. 35(2014)332.
- [3] Chaigne-Delalande, B,F.J. Li et al, Science. 341(2013)186.
- [4] D.Y. Zang, C.P. Lau, G.R .Li, Pflugers Arch. 457(2009)1275.
- [5] Z. Kiss, Cardiol.Hung.13 (1984)61.(in Hungarian)
- [6] C. Anttzelevitz, Circ.J. 76(2012)1054.
- [7] N. Sato, R. Sasaki et al.Magn.Res. DO I:10.1684/mrh.2015.0379.
- [8] T. Voets, B. Nilius et al.J., Biol.Chem. 279(2004)19.
- [9] R.Y. Walder, D. Landau et al., Nat.Genet. 31(2002)171.
- [10] S. Ptoczki et al., Curr.Med.Chem. 16(2012)2738.
- [11] W.F. McIntyre, A.R. Pérez-Riera et al., J.Electrocardiol .45(2012)195.

ANTIOXIDANT CAPACITY OF CAPSICUM GENOTYPES EXHIBITING DIFFERENTIAL LILAC COLOURATION DURING MATURITY

Zsófia Kovács¹, Gábor Csilléry², Mihály Kondrák¹, Anikó Veres¹, Janka Bedő¹, Antal Szőke¹, Erzsébet Kiss¹, Éva Stefanovits-Bányai³

¹Szent István University, Institute of Genetics, Microbiology and Biotechnology, H – 2100 Gödöllő, Páter Károly str 1., Hungary

²PepGen Ltd., H- 1114 Budapest, Bartók Béla str 41. Hungary

³Szent István University, Department of Applied Chemistry, H-1118 Budapest, Villányi str 29-43.

e-mail: veres.aniko@mkk.szie.hu

Abstract

Total phenolic content (TPC) and antioxidant activity of 7 coloured *Capsicum* genotypes in four different maturity stages were investigated. The total phenolic content of the genotypes determined by the Folin-Ciocalteu method was in average higher in the early phenophases than in the fully ripe phase. Among the genotypes the extreme lilac exhibited the highest amount of TPC as a result of the putative additive effect of the high levels of anthocyanins. On dry weight basis there was a 4.5-fold difference at the ripe stage in between the extreme lilac and the white berry genotypes. Antioxidant capacity of the samples during ripening followed a similar pattern than the TPC and the values showed positive correlation from green stage 2 onwards. The study indicates that anthocyanin pigmentation could add up to the functional properties of the peppers.

Introduction

Pepper (*Capsicum annuum* L.) is one of the most commonly used spice and vegetable crops worldwide. Besides its shape and pungency, colour is a commercially important attribute as well [1, 2]. Fruit colour is of utmost importance since the pigments affecting the colouration further contribute to nutrition and flavour. The main determinants of pepper fruit colour are the chlorophyll, carotenoid and anthocyanin pigments [3]. Anthocyanins comprise a major branch of the phenylpropanoid pathway and were proved to possess - beside numerous other pharmaceutical applications to human health - antioxidant qualities. From nutraceutical aspects, various pepper fruits' carotenoid accumulation is among the highest in plants [4]. A teaspoon of its powder provides the Recommended Dietary Allowance for vitamin A of an adult person after the conversion of the precursor carotenoids to vitamin A [5]. In addition, they also act as antioxidants and free-radical scavengers, thus reducing the risk of several diseases such as cardiovascular or neurological disorders [6]. Besides phenolic compounds and various carotenoid pigments, peppers are also an excellent source of ascorbic acid.

Colour of the immature pepper fruits varies from ivory to green, with different shades of violet to nearly black [7]. Whereas the colouration of mature fruits of cultivated peppers ranges from white through yellow, orange and red to even brownish hue [8]. In most cases the presence of both chlorophylls and anthocyanins in the berry is transient as they are gradually degraded during ripening as the level of carotenoids rises [9]. Just like the extent of pigmentation, the level of antioxidants can vary with plant parts, phenophase and with post-harvest handling [10].

Since these compounds exhibit antioxidant activities it is supposed that different genotypes at different phases of maturation have distinct antioxidant capacity. Here we

describe the total phenolic content and the antioxidant activity of 7 genotypes displaying differing degrees of anthocyanin pigmentation.

Material and methods

Plant material

Seven mutant genotypes of *Capsicum* species were obtained from PepGen Ltd. All plants received similar water and fertilizer dosages and were kept under greenhouse conditions. Samples were collected at four different stages of ripening, 2 unripe stages, turning phase and at biological ripe phase. Samples were stored at -70°C until analysed (Tab. 1, Fig. 1).

Tab. 1 Genotype colour changes during maturity

Genotype	Unripe colour	Ripe colour
Sample 1	Purple	Purple
Sample 2	Lilac	Red
Sample 3	Lilac	Yellow
Sample 4	Striped lilac	Red
Sample 5	White	Red
Sample 6	White	Red
Sample 7	White	Red



Fig 1 Examples of the genotypes used, upper left: sample 4, upper right: genotype 7, lower left: genotype 3, lower right: genotype 2

Antioxidant activity

The plants antioxidant capacity was measured by the FRAP (Ferric Reducing Ability of Plasma) assay according to Benzie and Strain (1996) at $\lambda=593$ nm. Peppers were crushed and homogenized in liquid nitrogen, the extraction was carried out with $\text{MeOH}:\text{water}:\text{HCOOH}$ (60:39:1 v/v %). Samples were centrifuged at 4°C for 20 minutes resulting the supernatant that was used for the analyses. The results are expressed as mmol ascorbic acid equivalent per 1 g dry weight.

Total phenol content (TPC)

Total soluble phenols were measured with Folin-Ciocalteu reagent according to Singleton and Rossi (1965) at $\lambda=760$ nm. Sample preparation was the same as above. The results are expressed as mmol gallic acid equivalent per 1 g dry weight. For both assays laboratory duplicates from each sample were used.

Results and Discussion

The nutraceutical properties make phenolics an indispensable element of any healthy diet. There is an increasing trend towards the breeding of genotypes with elevated nutrient content, therefore the quantification of phenolics in different genotypes in different phenophases could aid the breeding works of functional foods. Peppers are an optimal source of nutraceutical compounds which are mainly localized in their peels thus through the examination of various berry colours a link between the colouration and TPC, FRAP could be sorted out. Since the extraction was carried out using $\text{MeOH}:\text{water}:\text{HCOOH}$ therefore the effect of carotenoids on the free radical scavenging was not measured. Although these compounds also greatly contribute to the overall antioxidant capacity, peppers contain numerous other antioxidants such as ascorbic acid, capsaicin and polyphenols. All the given data are expressed on dry weight basis (dw), the moisture content of the plants at different phenophases were around 91% and not significantly different from one another.

Phenophase and genotype effect on TPC and on FRAP values

The results of TPC when expressed on dw in the tested genotypes ranged between 35 mmol gallic acid equivalent/g in genotype 6 and 88 mmol gallic acid equivalent/g in genotype 1 at green stage 1. At green stage 2 however, a 4-fold variation was observed between genotype 1 and 3. Even higher differences were detected at the turning phase between the same genotypes and these proportions remained the same at ripe stages as well (Fig. 2).

Except for genotype 1 and 6, all peppers showed higher TPC values at both green stages than in their fully ripe phase, which is in line with Deepa et al. (2007) study [10]. Numerous reasons could account for these elevated values i.e.: plant tissues used, genotype effect, biotic or abiotic stresses etc. However, in case of genotype 2, 3, and 4 the additive effect of the anthocyanins in the unripe berries could also cause higher TPC values. As of genotype 1, although it has a purple berry at its unripe stages, it remains purple throughout ripening building anthocyanins up until its turning phase. Sample 1 was the single genotype with significantly higher TPC levels at nearly all stages of maturity. However, sample 7 also exhibited high values at green stage 1, 84.57 mmol gallic acid equivalent/g, while the extreme lilac sample 1 had 88.74 mmol gallic acid/g. An overall decreasing trend is visible from the TPC values during ripening which is in correlation with Marin et al. (2004) findings [11].

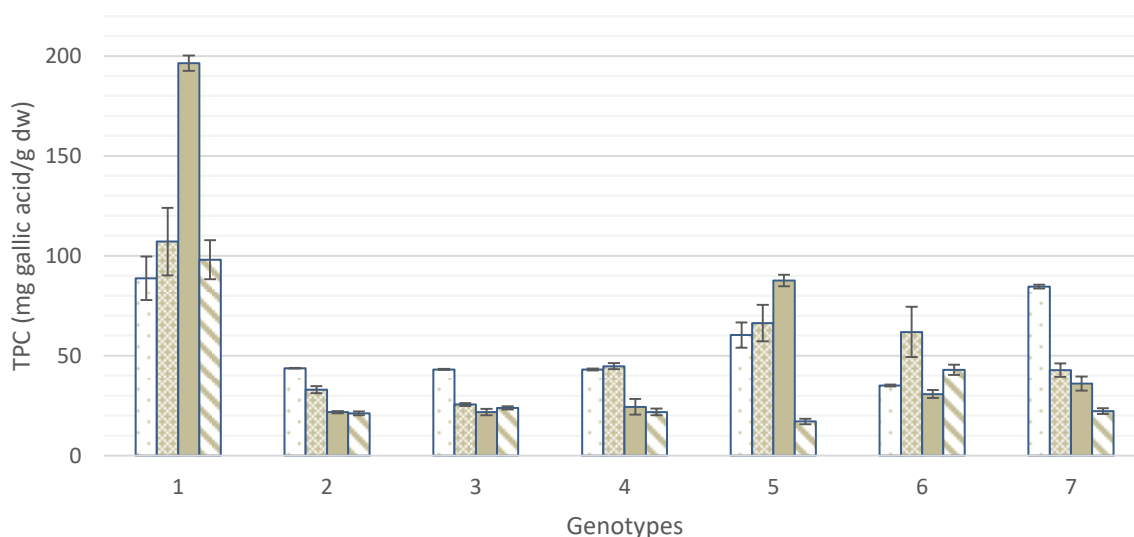






Fig. 2 TPC of seven mutant *Capsicum* genotypes in four stages of ripening. Green stage 1: , Green stage 2: , Turning phase: , Biological ripe phase: 

As of their antioxidant capacity, it was measured against their iron reducing capacity by the FRAP assay. A similar trend was observed during maturity as in the case of TPC which is supported by a line of researches. All genotypes – except for sample 1 – showed high values of antioxidant capacity at green stage 1, then a decline phase at their intermediate stages, followed by a slight increase at biological ripeness (Fig. 3). Genotype 1, in addition to containing high levels of anthocyanins throughout maturation, it also contains compounds responsible for the pungency of the berry, therefore the capsaicin could also add to the overall higher values of antioxidant capacity. At their ripe phases there is a 5.5-fold difference between the extreme lilac (genotype 1) and the plant that never turns purple (genotype 7).

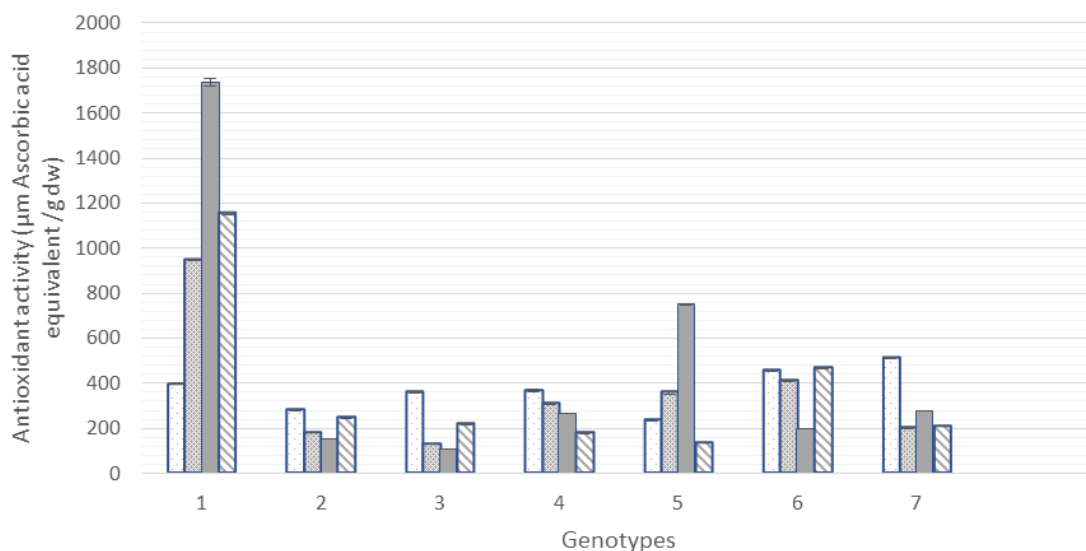


Fig. 3 Antioxidant power of seven mutant *Capsicum* genotypes in four stages of ripening. Green stage 1: □, Green stage 2: ■, Turning phase: ■, Biological ripe phase: ▨

Both the genotype and the ripening stage had a significant effect on both the TPC and on the FRAP value. The correlation between the phenolic content and scavenging free radical activity of the peppers when expressed on dry weight basis were significant in every stage examined, except for the green stage 1 where only 9% of the antioxidant activity is explained by the phenolic content. Numerous studies arrived at the same conclusion that TPC and FRAP values are closely correlated, our results show $R^2=0.89$ at green stage 2, $R^2=0.99$ at turning just like at the ripe stage [12, 13].

Conclusion

Significant variations in both TPC and FRAP values in between genotypes and phenophases indicate that the nutritional composition of the berries changes during maturation in different genotypes. The extreme lilac sample (genotype 1) exhibited outstanding results for both TPC and FRAP, indicating that the presence of anthocyanins could lead to a rich dietary composition. Although studies indicate that the ripe – yellow, orange or red coloured – berries exhibit higher values for both assays, our hypothesis that the anthocyanin build-up at the early stages of the ripening together with the genotype effect would lead to higher values in the green stages appears accurate [12].

The work/publication is supported by the EFOP-3.6.3-VEKOP-16-2017-00008 project. The project is co-financed by the European Union and the European Social Fund.

References

- [1] Lang Y-Q, Yanagawa S, Sasanuma T, Sasakuma T. Orange fruit color in *Capsicum* due to deletion of capsanthin-capsorubin synthesis gene. *Breeding Science* 2004;54:33-9.
- [2] Paran I, Fallik E. Breeding for fruit quality in pepper (*Capsicum* spp.). *Breeding for fruit quality* 2011:307-22.
- [3] Aza-Gonzalez C, Herrera-Isidrón L, Núñez-Palenius H, De La Vega OM, Ochoa-Alejo N. Anthocyanin accumulation and expression analysis of biosynthesis-related genes during chili pepper fruit development. *Biological Plantarum* 2013;57:49-55.

- [4] Kilcrease J, Collins AM, Richins RD, Timlin JA, O'connell MA. Multiple microscopic approaches demonstrate linkage between chromoplast architecture and carotenoid composition in diverse *Capsicum annuum* fruit. *The Plant Journal* 2013;76:1074-83.
- [5] Kilcrease J, Rodriguez-Urbe L, Richins RD, Arcos JMG, Victorino J, O'Connell MA. Correlations of carotenoid content and transcript abundances for fibrillin and carotenogenic enzymes in *Capsicum annuum* fruit pericarp. *Plant Science* 2015;232:57-66.
- [6] Ha S-H, Kim J-B, Park J-S, Lee S-W, Cho K-J. A comparison of the carotenoid accumulation in *Capsicum* varieties that show different ripening colours: deletion of the capsanthin-capsorubin synthase gene is not a prerequisite for the formation of a yellow pepper. *Journal of Experimental Botany* 2007;58:3135-44.
- [7] Stommel JR, Griesbach RJ. Inheritance of fruit, foliar, and plant habit attributes in *Capsicum*. *Journal of the American Society for Horticultural Science* 2008;133:396-407.
- [8] Li Z, Wang S, Gui X-L, Chang X-B, Gong Z-H. A further analysis of the relationship between yellow ripe-fruit color and the capsanthin-capsorubin synthase gene in pepper (*Capsicum* sp.) indicated a new mutant variant in *C. annuum* and a tandem repeat structure in promoter region. *PloS one* 2013;8:e61996.
- [9] Lightbourn GJ, Griesbach RJ, Novotny JA, Clevidence BA, Rao DD, Stommel JR. Effects of anthocyanin and carotenoid combinations on foliage and immature fruit color of *Capsicum annuum* L. *Journal of heredity* 2008;99:105-11.
- [10] Deepa N, Kaur C, George B, Singh B, Kapoor H. Antioxidant constituents in some sweet pepper (*Capsicum annuum* L.) genotypes during maturity. *LWT-Food Science and Technology* 2007;40:121-9.
- [11] Marín A, Ferreres F, Tomás-Barberán FA, Gil MI. Characterization and quantitation of antioxidant constituents of sweet pepper (*Capsicum annuum* L.). *Journal of agricultural and food chemistry* 2004;52:3861-9.
- [12] Sun T, Xu Z, Wu CT, Janes M, Prinyawiwatkul W, No H. Antioxidant activities of different colored sweet bell peppers (*Capsicum annuum* L.). *Journal of Food Science* 2007;72:S98-S102.
- [13] Howard L, Talcott S, Brenes C, Villalon B. Changes in phytochemical and antioxidant activity of selected pepper cultivars (*Capsicum* species) as influenced by maturity. *Journal of Agricultural and Food Chemistry* 2000;48:1713-20.

ENZYME PRODUCTION IN SUBMERGED FERMENTATION BY *ASPERGILLUS NIDULANS*

Etelka Kovács¹, Csilla Szűcs¹, Zoltán Bagi¹, Kornél L. Kovács^{1,2,3}

¹Department of Biotechnology, University of Szeged, Szeged, 6726, Hungary,

²Department of Oral Biology and Experimental Dentistry, University of Szeged, Szeged, 6726, Hungary,

³ Hungarian Biogas Association, Szeged 6726, Hungary
kovacs.etelka@bio.u-szeged.hu

Abstract

The planet has limited resources of farmland nutrients and fossil energy. Traffic emissions will have to be reduced significantly in the coming years to help abate climate change. In these days, when humankind must face these problems, biogas is considered as one of the most important natural energy sources. Plant biomass is the largest reservoir of environmentally friendly renewable energy on Earth (1-3). However, the complex and recalcitrant structure of the lignocellulose-rich substrates is a severe limitation of biogas production. Agro-industrial processes produce large quantities of corn stalk and wheat straw as plant-waste materials each year. The production of cellulase has been reported from a wide variety of bacteria and fungi. *Aspergillus nidulans* was isolated from cattle rumen under anaerobic conditions. The extracellular enzymes of *A. nidulans* were well represented in the culture media because the specific activity of endoglucanase and β -glucosidase was high.

Introduction

Filamentous fungi are preferred for commercial enzyme production, because the level of the enzymes produced by these cultures is higher than those obtained from bacteria. Almost all fungi of genus *Aspergillus* synthesize cellulase (4), therefore this genus has the potential to dominate the enzyme industry. Industrially important enzymes have traditionally been obtained from submerged fermentation (SmF) because of the ease of handling and greater control of environmental factors such as temperature and pH. There are several articles describing use of agro industrial residues for the production of cellulose such as wheat straw, wheat bran and rice straw as substrates for fungi growth. From this point of view, the organism was isolated from cattle rumen and demonstrated for its improved efficiency in SmF for the production of cellulase using agro-industrial waste as raw material.

Experimental

Aspergillus nidulans was isolated from cattle rumen (Fábiánsebestyén, Hungary) under anaerobic conditions. The isolate was grown on CMC agar medium. The isolated fungal colony was subcultured and maintained on Czapek-Dox-agar plates and stored at 4°C in a refrigerator, until needed. The cellulosic substrates such as corn stalk and wheat straw were chopped to 3-4 mm pieces. The inoculum was prepared by growing the organism in 250 ml Erlenmeyer flask with 50 ml of Czapek-Dox broth containing 30 g/l of α -cellulose, 3 g/l NaNO₃, 1 g/l K₂HPO₄, 0.5 g/l MgSO₄, 0.5 g/l KCl, 0.5 g/l FeSO₄, 15 g/l agar. The medium was inoculated from the Czapek-Dox agar plates and incubated at 37°C for 3 days in a shaker (200 rpm) before it was used for the fermentation process.

Enzyme activity

Assay of *endo*-(1,4)- β -D-glucanase activity was conducted using 3,5-dinitrosalicylic acid (DNS) method by using carboxymethyl cellulose (CMC) as a specific substrate (5). Measurement of β -glucosidase activity was assayed using *p*NPG method (6).

Results and discussion

Cellulase enzymes of *Aspergillus sp.* have traditionally been obtained from submerged fermentation. Microscopic observations of enrichment cultures revealed cellulose fibers, which presumably were released from corn or wheat straw disintegrated by cellulolytic enzymes, surrounded by fungal hyphae (Fig.1.).

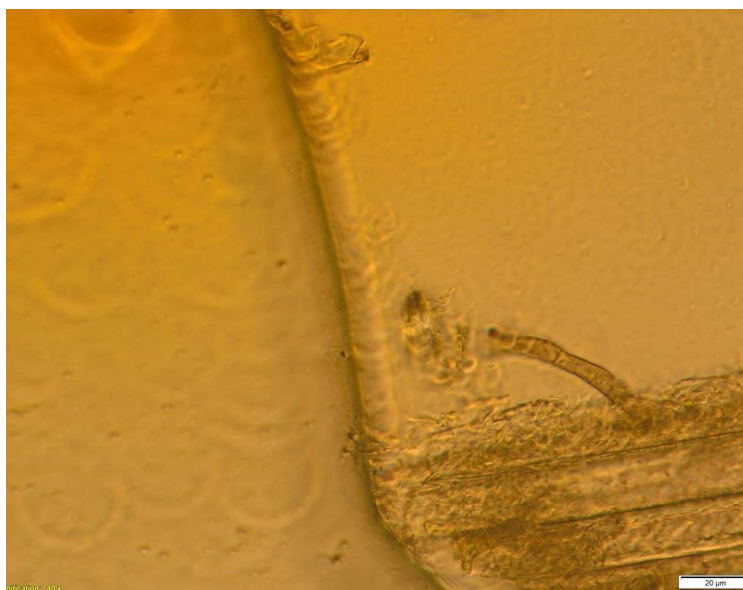


Figure 1. Cellulose fiber surrounded by fungal hyphae

It was established that an optimal inoculum concentration could increase significantly the cellulase production in submerged fermentation. With an increase in substrate concentration from 5 to 25% a rapid growth of fungi was observed which occurred together with increase of enzyme activity. 15-20% substrate concentration was found optimal. Higher or lower substrate ratio resulted in a significant decrease in endoglucanase production (Fig.2). In contrast, β -glucosidase activity showed constant increase between the lowest and the highest concentrations.

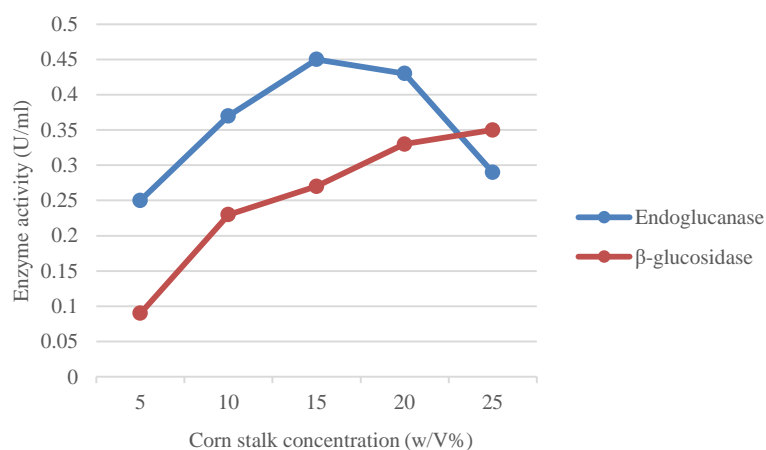


Figure 2. Effect of substrate concentration on cellulase production

Among the tested substrates, the cultivation of the fungus *A. nidulans* on α -cellulose and corn stalk provided the highest endoglucanase and β -glucosidase production (Fig.3.).

Carbon source	Enzyme activity (U/ml)	
	Endoglucanase	β -glucosidase
CMC	0.11	0.02
α -cellulose	0.23	0.45
Microcrystalline cellulose	0.10	0.02
Corn stalk	0.21	0.35
Wheat straw	0.19	0.28

Figure 3. Endoglucanase and β -glucosidase production in different laboratory and agroindustrial substrates

Conclusion

Our results indicated that the extracellular enzymes of *A. nidulans* were well represented in the culture media because the specific activity of endoglucanase and β -glucosidase was high. This result is promising because β -glucosidase is essential for the increased production of glucose from cellulosic substrates as it acts on oligosaccharides and dimers derived from the initial hydrolysis of cellulases and releases monomers from reducing sugars. Test results exploiting the stability of endoglucanases and β -glucosidases at the optimum temperature of biogas fermentation will be presented.

Acknowledgements

This work was supported by the Hungarian National Research, Development and Innovation Fund (grant number NKFI-PD 128345), the domestic grant GINOP-2.2.1-15-2017-00081 and the EU Horizon 2020 research and innovation programme, BIOSURF project (contract number 646533).

References

1. Pauss A, Nyns EJ (1993) Past, present and future trends in anaerobic digestion applications. *Biomass Bioenerg* 4:263–270
2. Gijzen HJ (2002) Anaerobic digestion for sustainable development: a natural approach. *Water Sci Technol* 45 (10): 321–328
3. Bolzonella D, Battistoni P, Mata-Alvarez J, Cecchi F (2003) Anaerobic digestion of organic solid wastes: process behaviour in transient conditions. *Water Sci Technol* 48(4):1–8
4. de Vries RP, Visser J (2001) *Aspergillus* enzymes involved in degradation of plant cell wall polysaccharides. *Micr. and Mol Bio Rev.* 65(4):497-522
5. Ahmed I, Zia M.A, Iqbal H.M.N. (2010) Bioprocessing of proximally analyzed wheat straw for enhanced cellulase production through process optimization with *Trichoderma viridae* under SSF. *Int. J. Biol. Life Sci.* 6:3.
6. Han S.J, Yoo Y.J, Kang H.S. (1995) Characterization of a bifunctional cellulase and its structural gene. The cell gene of *Bacillus* sp. D04 has exo- and endoglucanase activity. *J. Biol. Chem.* 270(43):26012–26019.

IDENTIFICATION OF THE MAIN METABOLITES OF THREE SYNTHETIC CANNABINOIDS USING LC-MS/MS TECHNIQUE

Tímea Körmöczi¹, Éva Sija², Róbert Berkecz¹

¹*Department of Medical Chemistry, University of Szeged, H-6720 Szeged, Dóm tér 8, Hungary*

²*Institute of Forensic Medicine, University of Szeged, H-6724 Szeged, Kossuth Lajos sgt. 40, Hungary*

e-mail: kormoczi.timea@med.u-szeged.hu

Abstract

The consumption of designer drugs today is a serious problem, especially among young people involvement. ‘Herbal mixtures’ containing synthetic cannabinoids (SCs) that mimic the effect of marijuana and there are easily available via the Internet. For analysis of urine samples, knowledge of the main metabolites is necessary as the mother compounds are usually not found in urine after using, due to their fast metabolism. The aims of this study were the in vitro identification of metabolites of ADB-FUBINACA, 5F-MDMB-PICA and CUMYL-PEGACLONE and to determine which analytical targets are excreted into urine. Metabolites identified after incubation of SCs with pooled human liver microsomes (HLM). The authentic urine samples were analysed by liquid chromatography-tandem mass spectrometry (LC-MS/MS) for investigation of the major in vivo metabolites. The main metabolites were the mono-hydroxylation of ADB-FUBINACA and CUMYL-PEGACLONE in positive urine specimens. We didn’t have positive sample of 5F-MDMB-PICA.

Introduction

Synthetic cannabinoids are a group of designer drugs that mimic and magnify natural cannabinoids effect. The CB₁ and CB₂ cannabinoid receptor agonists SCs sold as ‘herbal smoking mixtures’ are promoted as legal alternative to marijuana, to circumvent drug scheduling legislation [1]. The SCs are highly potent and responsible for many acute intoxications and deaths [2, 3]. In forensic practice the SC consumption is detecting the parent molecules in urine and blood specimens. Due to their fast metabolism prior the renal extraction, in most cases the parent compounds are detectable in narrow time window in human urine. The present study aims to identify appropriate marker metabolites by investigating of *phase I* metabolism of ADB-FUBINACA as a most commonly used SC, 5F-MDMB-PICA and CUMYL-PEGACLONE as the newest SCs (Figure 1), using pooled human liver microsome (HLM), and to confirm the results in authentic human urine samples.

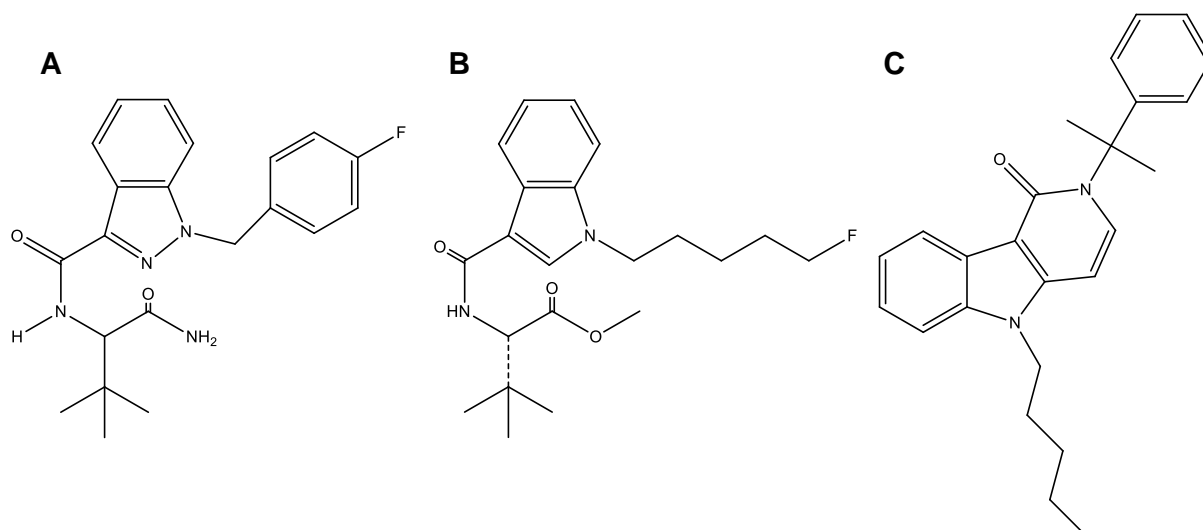


Figure 1 Chemical structure of ADB-FUBINACA (A), 5F-MDMB-PICA (B) and CUMYL-PEGACLONE (C) synthetic cannabinoids

Experimental

The LC-MS/MS method and the new sample preparation was developed for identification and analysis of metabolites in HLM and urine samples. The SCs was incubated with HLM at 37°C for 30 min. The urine samples were analysed after β -glucuronidase hydrolysis. The analysis was performed on a Q Exactive Plus hybrid quadrupole-Orbitrap mass spectrometer (Thermo Fisher Scientific, Waltham, MA, USA) coupled with a Waters Acquity I-Class UPLC™ (Waters, Manchester, UK). Compound separation was achieved using a Kinetex C18 column (150 x 2.1 mm, 2.6 μ m, Phenomenex, Torrance, CA, USA) combined with a guard column maintained at 50°C at a constant flow rate of 0.4 mL/min. Mobile phase A consisted of 0.1% formic acid, and mobile phase B was acetonitrile with 0.1% formic acid. The HLM incubates and urine samples were analyzed in positive electrospray ionization (ESI) mode. The mass spectrometer was operated in full scan and parallel reaction monitoring acquisition (PRM) modes.

Results and discussion

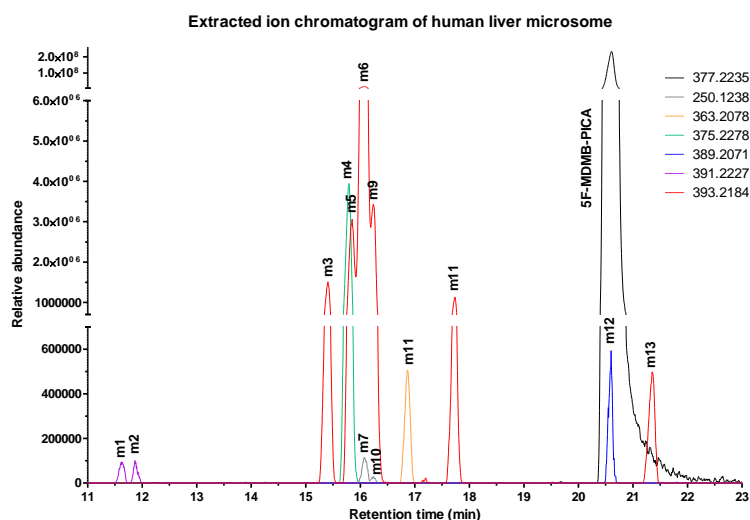
The developed analytical LC-MS/MS method provided the separation and characterization of numerous ADB-FUBINACA, 5F-MDMB-PICA and CUMYL-PEGACLONE *phase I* metabolites.

7 *phase I* metabolites of ADB-FUBINACA were detected in authentic urine sample (Table 1). The identified metabolites were assigned to 5 different biotransformations, including amide hydrolysis, dehydrogenation, monohydroxylation, formation of carbonyl derivatives and their isomers. The main metabolite of ADB-FUBINACA was the aliphatic mono-hydroxylated (M4) form [4].

Table 3 Identified metabolites of ADB-FUBINACA in HLM and authentic urine sample

	Biotransformation	Formula	Retention time (min)	[M+H] ⁺ (m/z)	Fragment ions (m/z)	Identify in urine sample	Identify in HLM
	ADB-FUBINACA	C ₂₁ H ₂₃ N ₄ O ₂ F	17.24	383.1878	109, 253, 270, 338, 366	Yes	Yes
M1	Methylenefluorophenyl loss	C ₁₄ H ₁₈ N ₄ O ₂	8.12	275.1503	145, 162, 230	No	Yes
M2	Dihydrodiol formation	C ₂₁ H ₂₅ N ₄ O ₄ F	9.22	417.1933	109, 241, 304, 372	No	Yes
M3	Amide hydrolysis + dehydrogenation	C ₂₁ H ₂₀ N ₃ O ₃ F	13.74	382.1561	109, 253, 324	Yes	Yes
M4	Aliphatic mono-hydroxylation	C ₂₁ H ₂₃ N ₄ O ₃ F	13.73	399.1827	109, 253, 354, 382	Yes	Yes
M5	Aliphatic hydroxylation + dehydrogenation	C ₂₁ H ₂₁ N ₄ O ₃ F	13.80	397.1671	109, 253, 270, 324	Yes	Yes
M6	Indazole mono-hydroxylation	C ₂₁ H ₂₃ N ₄ O ₃ F	14.32	399.1827	109, 269, 354	Yes	Yes
M7	Indazole mono-hydroxylation	C ₂₁ H ₂₃ N ₄ O ₃ F	14.84	399.1827	109, 145, 163, 269, 354	Yes	Yes
M8	Amide hydrolysis + aliphatic hydroxylation	C ₂₁ H ₂₂ N ₃ O ₄ F	14.89	400.1667	109, 253, 324, 382	Yes	No
M9	Indazole mono-hydroxylation	C ₂₁ H ₂₃ N ₄ O ₃ F	15.24	399.1827	109, 145, 269, 354	No	Yes
M10	Carbonylation	C ₂₁ H ₁₉ N ₄ O ₃ F	15.85	395.1514	109, 253, 270	Yes	Yes
M11	Amide hydrolysis	C ₂₁ H ₂₂ N ₃ O ₃ F	18.95	384.1718	109, 253, 338	No	Yes

For 5F-MDMB-PICA (Fig. 2), 13 *phase I* metabolites were identified by accurate m/z values and the fragmentation behaviour known from the literature [5].

**Figure 2** Extracted ion chromatogram of identified metabolites of 5F-MDMB-PICA in HLM

The new analytical method provided over 35 *phase I* metabolites of CUMYL-PEGACLONE in authentic urine specimens, such as formation of dehydrogenation, mono- and di-hydroxylation, dealkylation, carbonylation and carboxylation and their isomers. Fig. 3 shows

the MS/MS spectra of three di-hydroxylated metabolites of CUMYL-PEGACLONE. The biotransformation site on the structure of the molecule was determined by characteristic fragment ions. The mono-hydroxylated metabolite (M45) was identified as specific and sensitive urinary markers to proof consumption of CUMYL-PEGACLONE [6].

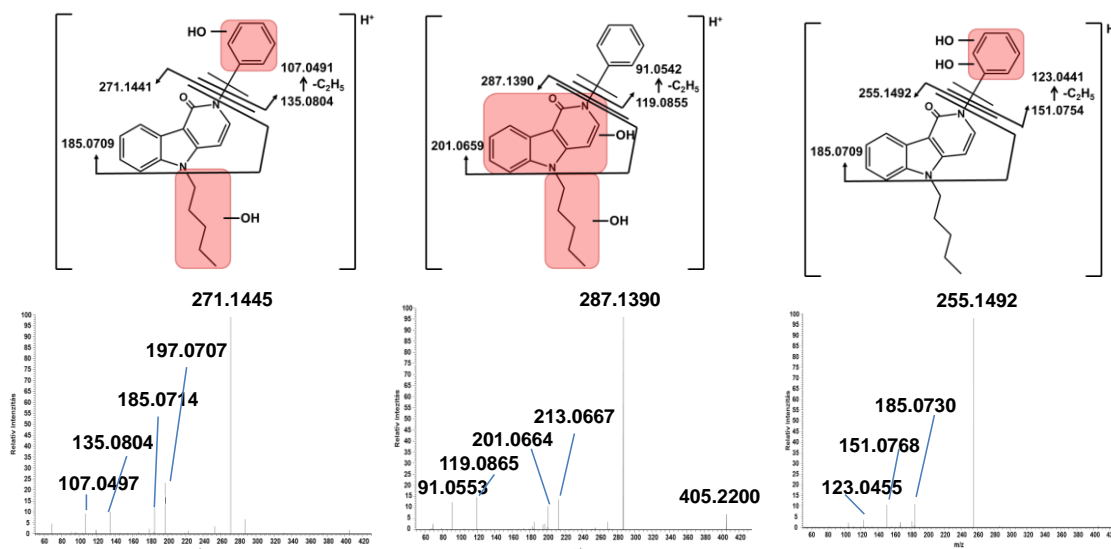


Figure 3 Di-hydroxylated metabolites of CUMYL-PEGACLONE and their MS/MS spectra in positive mode

Conclusion

The present study describes the identification of phase I metabolites of ADB-FUBINACA, 5F-MDMB-PICA and CUMYL-PEGACLONE after incubation with pooled human liver microsomes. The main metabolite of ADB-FUBINACA and CUMYL-PEGACLONE was formation of mono-hydroxylation in authentic urine specimens.

Acknowledgements

This research was supported by the EU-funded Hungarian grant *EFOP 3.6.1-16-2016-00008*.

References

- [1] W.D. Wessinger, J.H. Moran, K.A. Seely, in: P. Campolongo, L. Fattore (Eds.), *Cannabinoid Modulation of Emotion, Memory, and Motivation*, Springer, 2015, pp. 205-224.
- [2] R. Kronstrand, M. Roman, M. Andersson, A. Eklund, *Journal of analytical toxicology*, 37(8) (2013) 534-541.
- [3] A.J. Adams, S.D. Banister, L. Irizarry, J. Trecki, M. Schwartz, R. Gerona, *New England journal of medicine*, 376(3) (2017) 235-242.
- [4] J. Carlier, X. Diao, A. Wohlfarth, K. Scheidweiler, M. A Huestis, *Current neuropharmacology*, 15(5) (2017) 682-691.
- [5] L. Mogler, F. Franz, D. Rentsch, V. Angerer, G. Weinfurter, M. Longworth, S.D. Banister, M. Kassiou, B. Moosmann, V. Auwärter, *Drug testing and analysis*, 10(1) (2018) 196-205.
- [6] V. Angerer, L. Mogler, J.P. Steitz, P. Bisel, C. Hess, C.T. Schoeder, C. T., C.E. Müller, L.M. Huppertz, F. Westphal, J. Schäper, V. Auwärter, *Drug testing and analysis*, 10(3) (2018) 597-603.

MERCURY CONTAMINATION OF RAJA SPECIES FROM COASTAL SEA OF BAR REGION

Tanja Kragulj¹, Milivoje Purić², Gorica Vuković³, Vojislava Bursić⁴, Dušan Marinković⁴, Tijana Stojanović⁴, Aleksandra Petrović⁴

¹ University of Montenegro, Faculty of Natural Sciences and Mathematics, Dž. Vašingtona bb, 81000 Podgorica, Montenegro

² Agricultural Vocational School, Bjeliši bb, 85000 Bar, Montenegro

³ Institute of Public Health, Bul. despota Stefana 54a, 11000 Belgrade, Serbia

⁴ University of Novi Sad, Faculty of Agriculture, Department for Environmental and Plant Protection, Trg Dositeja Obradovića 8, 21000 Novi Sad, Serbia
e-mail: petra@polj.uns.ac.rs

Abstract

The Adriatic Sea, as other seas and oceans, have natural mechanisms to store, and in many cases, decompose natural or man made pollutants and contaminants. Mercury is a metal which is released into the environment from the natural and anthropogenic sources. Once released, mercury undergoes a series of complex transformations and cycles between atmosphere, hydrosphere and pedosphere. Methyl mercury is a chemical form of mercury which is by far, the most common form in the food chain. Fish and fish products are the dominant source of methyl mercury in food. Methyl mercury is rapidly accumulated by most aquatic biota and attains its highest concentrations in fish who are at the top of the aquatic food chain. The aim of this research was to obtain data on mercury contamination in Raja fish, that are often used as a food in coastal region. The fish were sampled from three localities in Bar region: Volujica, Bar harbour and Sutomore. The mercury contamination was tested in muscle tissue, applying Atomic Absorption Spectroscopy by the Thermo Electron S2 AA System. Two species of Raja genus were present: *Raja montagui* and *R. miraletus*. All collected fish had mercury contamination in muscle tissue near or above the proposed levels by Commission Regulation (EC) No 1881/2006.

Introduction

Considering the numerous harmful effects on the marine ecosystems and the vigorous antagonism between ecology and economy, awareness of the necessity for continuous monitoring sediment - water - organism interactions has been increased, with the aim to protect and preserve marine environment quality.

The oceans and seas are ecosystems with natural mechanisms to store, and in many cases, decompose pollutants and contaminants which have been released by the industry in restricted extent. However, this ability varies depending on numerous factors, such as: size of the sea or ocean, its currents, circulation speed, tides, temperatures, depth, freshwater flow, and even because of marine wildlife density and diversity.

The Adriatic Sea is a spacious bay of the central part of the Mediterranean Sea, of which is divided by the Apennine Peninsula. The harbor Bar is the most important Montenegrin port, located in a natural bay between the old city of Bar and Ulcinj, protected from the south by the hill Volujica, with a wide opening to the west. The total length of the operational shore is 3 km, which could host 20 ships at the same time. The closed storage area has more than 100.000 m². The harbour Bar is capable for all types of goods transshipment, especially, ores, concentrates, metallurgy products, oil and its derivatives, grain and its products, fertilizers, pesticides, cement and wood.

Mercury is a metal which is released into the environment from both natural and anthropogenic sources. Once released, mercury undergoes a series of complex transformations and cycles between atmosphere, hydrosphere and pedosphere. Methyl mercury is a chemical form of mercury which is by far, the most common form in the food chain. Fish meat is the dominating contributor to methyl mercury dietary exposure for all age classes, followed by the fish products. According to WHO (World Health Organization), the mercury content in these commodities varies widely among different fish species, and is in general higher in predatory fish. Methyl mercury contamination negatively impacts human and animal health. The response of fish methyl mercury concentrations to changes in mercury deposition has been difficult to establish, according to Harris et al. (2007), as sediment contain large pools of historical contamination. Methyl mercury is rapidly accumulated by most aquatic biota and attains its highest concentrations in fish who are at the top of the aquatic food chain (Salonen et al., 1995).

Fish with their specific diet, feeding on phyto- and zooplankton, represent a suitable and accurate bioindicator for the marine water pollution analyses. They are the natural bioindicators that could in appropriate time warn of the presence of the harmful substances in the water. As they are usually used in human nutrition, especially in the coastal regions, the harmful and dangerous substances are accumulated in their bodies in the larger quantities than those found in the water column, which directly affects human health. Recently, special attention has been paid to the presence of mercury, as the new studies have shown an increase of mercury concentrations in the tissue of marine species. Summarizing all the researches, a Global Ocean Observing System (GOOS) database was created, with all the known results so far detected throughout the world.

Raja are fish who belong to a genus of skates in the family Rajidae, which include 16 species. They have specific flat body with a rhombic shape. These bottom-dwellers are active during both day and night, and typically feed on molluscs, crustaceans and fish, which make them a secondary consumers in the food chains. Fish accumulate methyl mercury in their tissues, where it becomes strongly bound. Methyl mercury is not removed from fish tissue by any practical cooking method (Hightower & Moore, 2003).

The aim of this research was to obtain data on mercury contamination in Raja fish, that are often used as a food in coastal region.

Experimental

The fish were sampled from three localities in Bar region: Volujica, Bar harbour and Sutomore (Figure 1.). The fish were collected from the daily catch of the local fisherman by the random principal choice. The mercury contamination was tested in muscle tissue, applying Atomic Absorption Spectroscopy (AAS) by the Thermo electron S2 AA System

The standard metal solution (stock solution, 1000 mg/L) was made by dissolving 1 g of metal or its salt (calculated on 1,000 g of metal) in hydrochloric acid (1:1). Diluting the stock solution (with water), a series of lower concentration of metal were prepared.

Results and discussion

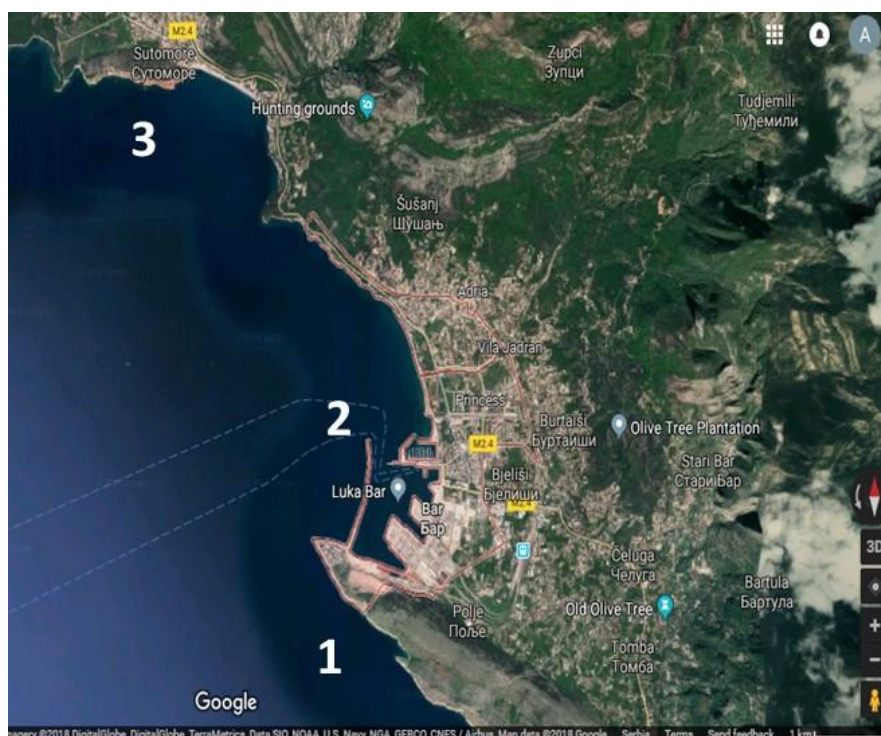
Two species of skates were present: *Raja montagui* Fowler, 1910 and *R. miraletus* Linnaeus, 1758.

All collected skate specimens had mercury contamination in muscle tissue near or above the proposed levels by Commission Regulation (EC) No 1881/2006 (Table 1.).

Table 1. Mercury concentrations in skate muscle tissues

The sample locality	Species	Average concentration of detected Hg (mg/kg)
Volujica	<i>Raja montagui</i>	1,15*
Volujica	<i>Raja miraletus</i>	0,70
Harbour Bar	<i>Raja miraletus</i>	0,85
Sutomore	<i>Raja miraletus</i>	0,50

*results above the maximum permissible concentrations (MPC) according to Commission Regulation (EC) No 1881/2006

**Figure 1.** The sample localities: 1 – Volujica, 2 – Harbour Bar, 3 - Sutomore

The prospected fish species, have had relatively high concentrations of mercury contamination, but according to Quian et al. (2001), variance among fish genera and species indicate the need for an indicator genus or species for future studies.

R. montagui is a small skate, widespreaded in the inshore waters and shallow shelf seas of the Northeast Atlantic and is common throughout the Mediterranean Sea. Juveniles tend to occur closer inshore on sandy sediments, with adults also common further offshore on sand and coarse sand-gravel substrates. Juveniles feed on small crustaceans, with larger individuals predating on larger crustaceans, and fishes (Ellis et al., 2007). *R. miraletus* is found predominantly on the shelf and appears to be one of the most abundant skates in the Mediterranean. The small maximum size of this species suggest it is likely to have a relatively short generation time and a relatively high capacity to replace numbers lost to exploitation (Smale et al., 2009). The high mercury concentration in these fish could be explained by their place in the marine food chain, as well as their preference to live at sea bottom, closely to sediment which is also contaminated.

Conclusion

Of all the heavy metals, mercury is one of the most dangerous environmental unorganic poisons, as it has no known physiological role in human metabolism. Heavy exposure to mercury, usually by food intake, causes a number of effects in the human body. Methyl mercury is absorbed on average 95% when consumed (Hightower & Moore, 2003). Methyl mercury could be accumulated, if consumed, at a greater rate than it is excreted by feces, urine and sweat. Usually, it has been accumulated in brain, muscle and kidney, not only in humans, but in all vertebrate species. Moreover, methyl mercury can cross from the maternal to fetal blood compartments, as well as it can cross the blood brain barrier, where biotransformation to inorganic mercury takes place.

At prospected localities, two Raja species were identified and in all collected specimens mercury concentrations were near or above the maximum permissible concentrations (MPC) according to Commission Regulation (EC) No 1881/2006. Fish and fish products are the dominant source of methyl mercury in food. Since Raja species are frequently found on culinary menus in the coastal region of Montenegro, the continuous monitoring of heavy metal contamination should be conducted, not only in fish body, but in sediment and water also.

References

- [1] World Health Organization – WHO: <http://www.who.int/news-room/fact-sheets/detail/mercury-and-health>
- [2] J.M Hightower, D. Moore, Environmental Health Perspectives, 11(4), pp: 604-608, 2003
- [3] R.C. Harris, J.W.M. Rudd, M. Amyot, C.L. Babiarz, K.G. Beaty, P.J. Blanchfield, R.A. Bodaly, B.A. Branfireun, C.C. Gilmour, J.A. Graydon, A. Heyes, H. Hintelmann, J.P. Hurley, C.A. Kelly, D.P. Krabbenhoft, S.E. Lindberg, R.P. Mason, M.J. Paterson, C.L. Podemski, A. Robinson, K.A. Sandilands, G.R. Southworth, V.L. St Louis, M.T. Tate, PANS, 104(42), pp: 1658616591, 2007
- [4] J.T. Salonen, K. Seppänen, K. Nyssönen, H. Korpela, J. Kauhanen, M. Kantola, J. Tuomilehto, H. Esterbauer, F. Tatzber, r. Salonen, Circulation, 91(3), pp: 645-655, 1995.
- [5] S.S. Quian, W. Warren-Hicks, J. Keating, D.R.J. Moore, R.S. Teed, Environ. Sci. Technol., 35, pp: 941-947, 2001.
- [6] Global Ocean Observing System – GOOS: <http://www.goosocean.org/>
- [7] J. Ellis, N. Ungaro, F. Serena, N. Dulvy, F. Tinti, M. Bertozzi, P. Pasolini, C. Mancusi, & Noarbartolo di Sciarra, G. 2007. Raja montagui. The IUCN Red List of Threatened Species 2007: e.T63146A12623141. <http://dx.doi.org/10.2305/IUCN.UK.2007.RLTS.T63146A12623141.en>. Downloaded on September 2018.
- [8] M.J. Smale, N. Ungaro, F. Serena, N. Dulvy, F. Tinti, M. Bertozzi, C. Mancusi, & Noarbartolo di Sciarra, G. 2009. Raja miraletus. The IUCN Red List of Threatened Species 2009: e.T161599A5461484. <http://dx.doi.org/10.2305/IUCN.UK.2009-2.RLTS.T161599A5461484.en>. Downloaded on September 2018.

OVERLOADING STUDY OF ZWITTERIONIC CHIRAL STATIONARY PHASES BASED ON CINCHONA ALKALOIDS

Renáta Kulágin^{1,*}, Ivett BacsKay², Wolfgang Lindner³, Attila Felinger^{1,2,4}

¹*Department of Analytical and Environmental Chemistry, University of Pécs, Ifjúság útja 6,
7624 Pécs, Hungary*

²*MTA-PTE Molecular Interactions in Separation Science Research Group, Ifjúság útja 6,
7624 Pécs, Hungary*

³*Department of Analytical Chemistry, University of Vienna, Währingerstrasse 38, 1090
Vienna, Austria*

⁴*Institute of Bioanalysis, University of Pécs, Medical School, Honvéd u. 1., 7624 Pécs,
Hungary*

*e-mail: rkulagin1992@gmail.com

Abstract

Nowadays, chirality has great importance in the life sciences as well as in the pharmaceutical industry. Usually the enantiomers have diverse activity in the living systems: one of the enantiomers possesses positive effect, while the other may be inactive or toxic. Thus, the separation of the enantiomers is very important.

On the *Cinchona* alkaloid-based ZWIX(+) and ZWIX(-) zwitterionic chiral stationary phases, simultaneous anion- and cation-exchange takes place. These stationary phases are good choice for the separation of the enantiomers of chiral acids, amines, amino acids and peptides.

Nonlinear chromatography was used for the investigation of the retention mechanisms. The stationary phases were overloaded by large volume injection of DL-*tert*-Leucine. *Bi-Langmuir* isotherm was used for modeling the adsorption because of the heterogeneous surface of the zwitterionic stationary phases. The isotherm parameters were determined by the *inverse method*.

In the optimization of the enantioseparation, the acid and base additives play an important role, they ensure the ionization of the selector and the selectand. Therefore, the effect of the nature and the ionic strength of the additives on the overloaded chromatographic bands were investigated.

Keywords: separation of the enantiomers, quinine- and quinidine-based chiral zwitterionic stationary phases, nonlinear chromatography, column overload, inverse method

THE IMPACT OF EXTREME WEATHER CONDITIONS AND MUNICIPAL SEWAGE DISPOSAL ON VEGETATION USING SENTINEL IMAGES, SE HUNGARY

Zsuzsanna Ladányi*, Andrea Farsang, András Gulácsi, Ferenc Kovács

Department of Physical Geography and Geoinformatics, University of Szeged, H-6720

Szeged, Egyetem u. 2-6, Hungary

**e-mail: ladanyi@geo.u-szeged.hu*

Abstract

Land application of municipal sewage can enhance the productivity of biomass production systems and can contribute to a better resistance to extremities in water supply. Understanding the impacts requires the examination of changes in soil characteristics and plant productivity. In this study (parallelly to the soil analyses) Sentinel 2B vegetation index series are assessed to monitor the biomass anomalies related to different water supply conditions and the sewage disposal in the period of 2016-2018 in a study area in SE Hungary (Újkígyós). In the humid year of 2016 there were no spatial differences in biomass production of vegetation stands, but as a result of the dry summer in 2017, biomass production deficiencies were observed on the areas of the ancient river meanders, characterised by different soil properties compared to the surrounding areas. In general, the direct impact of municipal sewage disposal could be detected on biomass by increased productivity, the response is probably related to the nutrient status of the site.

Introduction

There is a worldwide increasing interest in land application of sludge from wastewater treatment plants, since by their usage valuable components can be recycled into the soils: organic matter, nitrogen, phosphorus and other plant nutrients [1] [2]. Municipal sewage can be applied with or without treatment to increase soil organic matter and nutrient content, the conditions of which are regulated by the Government regulation Nr. 50/2001. (IV.3.) and the Decree Nr. 36/2006. (V. 18.) of the Ministry of Agriculture and Rural Development in Hungary. The disposed sewage sludge and compost can provide important macro and micro nutrients for plants, enhance soil organic matter content and adsorption capacity, improve soil structure and can contribute to more favourable soil water management [3]. Understanding the impacts requires the examination of changes in soil characteristics and plant productivity. The enhanced productivity of biomass production systems and the better resistance to extremities in water supply can be easily monitored by remote sensing techniques. The use of medium resolution satellite images provides a cost-effective way of assessing the spatial and temporal patterns of biomass productivity by extracting vegetation indices (VIs) [4] [5]. Free downloadable remote sensing data such as MODIS imagery has a higher temporal, but a lower spatial resolution and LANDSAT cannot supply good temporal resolution which hardly allow plot scale evaluation of crop development in Hungary. The Sentinel-2 satellite has a more finer resolution, however, it was launched in 2015, thus, there is no possibility for longer-term assessments.

Vegetation and soil are important carbon pools, which are significantly modified by antropogenic activities (e.g. sewage disposal). This study aims at (parallelly to the survey of the soil organic matter and nutrient content, [6] [7]) the investigation of the biomass production of a study area located in SE Hungary, where sewage disposal is regular. Productivity of areas with and without any disposal are also assessed, furthermore the spatial pattern of the anomalies is investigated concerning both disposal and changes in water supply.

Study area and methods

The study area is located in the lowland interfluvial area between the Körös and Maros River, in the territory of Újkígyós settlement (Fig. 1). It has an extent of 5.6 hectares where treated municipal sewage is disposed regularly since 2013. Chernozem and meadow Chernozem soils constitute the area, which are both of high fertility. The area, formed by fluvial and eolian processes, belongs to the Körös River Catchment. The static groundwater level was measured at 2 m below the surface during the soil sampling in March 2018. During soil sampling points were assigned where there were no disposal at all, where disposal happened in the past and on areas of disposal in autumn 2017. The field verification of satellite images were done by making a landuse map over the area in July 2018.

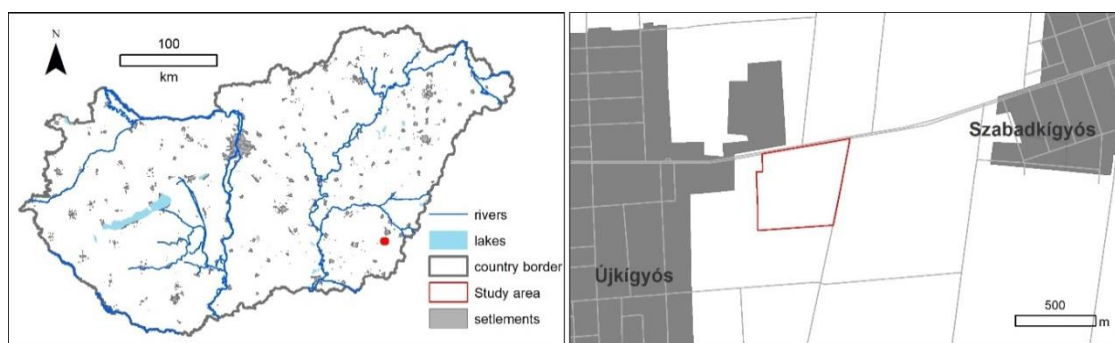


Figure 1. Location of the study area (SE Hungary, Újkígyós)

For data download, preprocessing and composite image generation, Google Earth Engine script was used, the workflow of which can be observed on Figure 2. Sentinel 2B EVI and NDVI data were selected, then images were filtered according to a max. 20% cloud cover. Cloud filtering was also applied using quality bands, and the study area was masked. Finally 32-day composite images were derived and downloaded, which were the basis of the compilation of the phenological curves and the comparison of the spatial pattern of biomass productivity. The statistical analysis and the illustration of the results were made using ArcGIS 10.2 and Microsoft Excel.

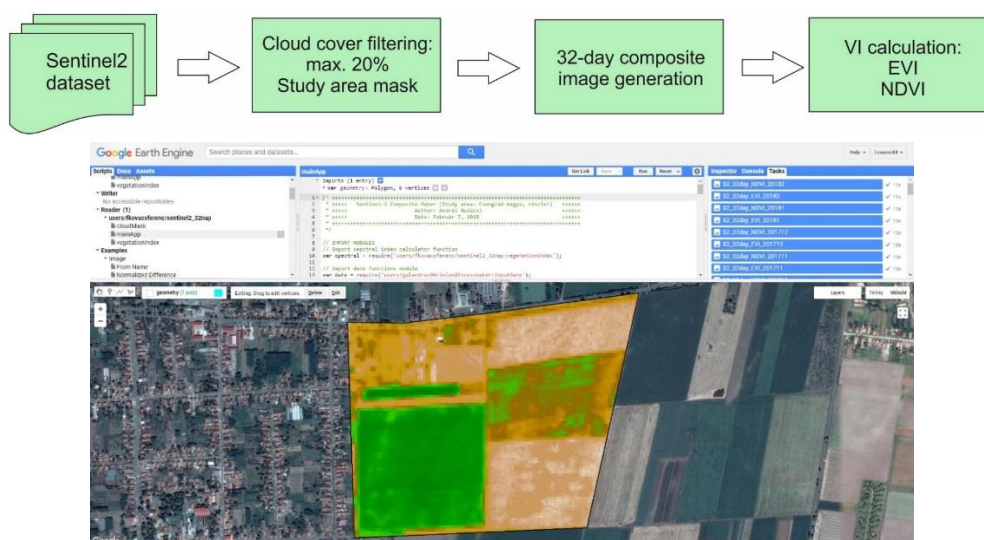


Figure 2. Workflow of vegetation index calculation for the study area using Google Earth Engine

Results and discussion

Spatial anomalies under humid and arid summer

Spatial EVI anomalies in August 2016 and 2017 were compared in the study area and its surrounding (Figure 3) to assess the differences in crop biomass production. 2016 was characterised by a precipitation amount between 600-650 mm with almost steady distribution, while in 2017 it was slightly less (500-550 mm), however, May-August (important period concerning crop growth) significantly less precipitation occurred compared to the normal distribution). As a result of the humid year of 2016, there were no significant spatial anomalies within the plots (exceptions are the pits used previously for irrigation and the surrounding forested area in the middle) and the almost bare surfaces in 2016. As a result of the dry and warm summer in 2017, significant decrease in productivity was observed on the areas of the ancient river meanders. The reason for this can be found in the different soil properties (higher ratio of finer particles) compared to the surrounding areas, resulting in less favourable water management properties, which influenced the vegetation water supply.

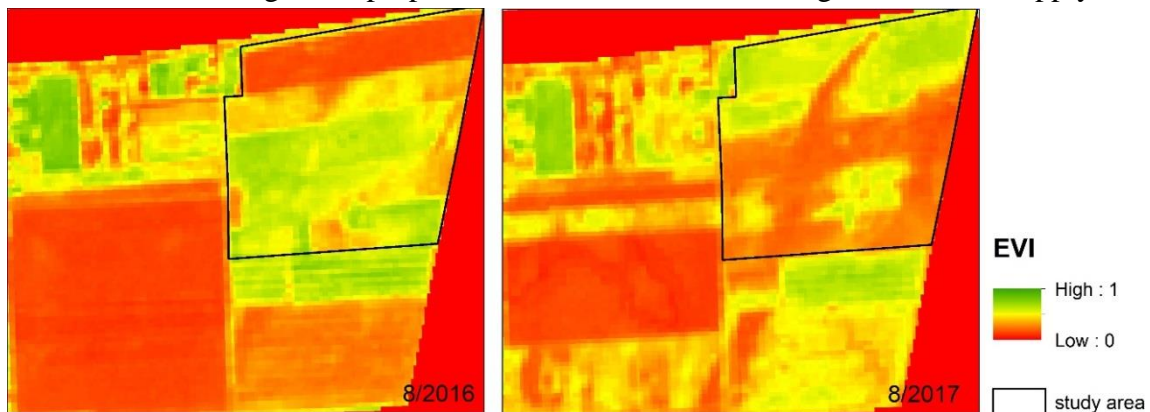


Figure 3. Spatial anomalies of crop EVI values in the study area and its neighborhood

It was difficult to compare crops with and without disposal, since the grown crops were different in the upcoming years. However, two plots could be compared where maize was grown within the study area under sewage disposal in 2016, and an other one from 2017 outside the study area without sewage disposal (Figure 4). The results show that the favourable year resulted in a somewhat earlier crop development, a wider green period in the vegetation period, and higher maximum productivity values. The 2017 maximum values are similar that of 2016, however, the dispersed values of the peak is somewhat lower. It means that a higher production in 2016 was could be observed, however, the reason for this is mostly due to the better availability of water, not the sewage disposal in this case.

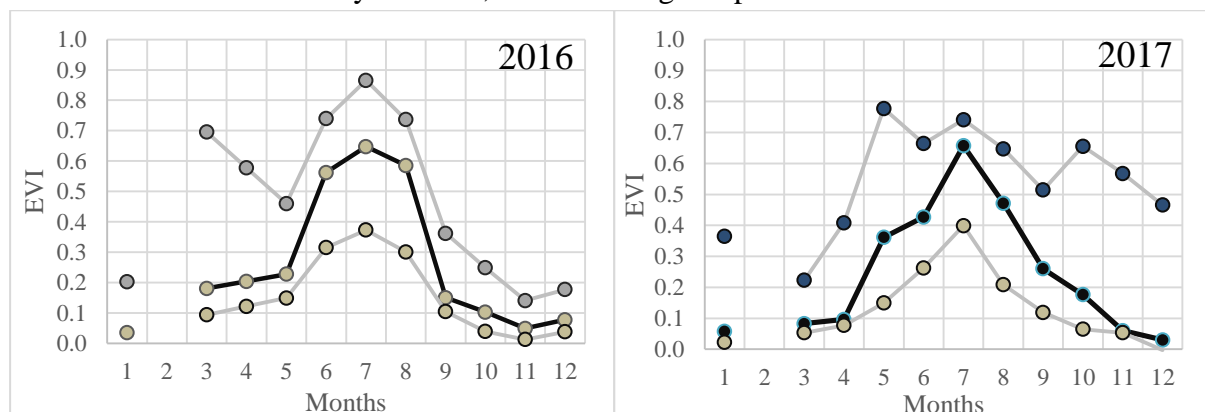


Figure 4. Maize phenological curves in 2016 (with sewage disposal, within the study area) and 2017 (without sewage disposal, outside the study area)

Differences between areas with and without disposal

Land use map of the study area in 2018 was prepared to verify the crops in the field and to surely combine VI data with them. On the study area mostly maize, cereals and oil radish

were observed on the fields (Figure 5). Comparison between the area affected by any disposal and not affected areas can be done for maize and cereals only. And the difference between VI of cereals with sewage disposal in 2018 and without disposal can be evaluated.

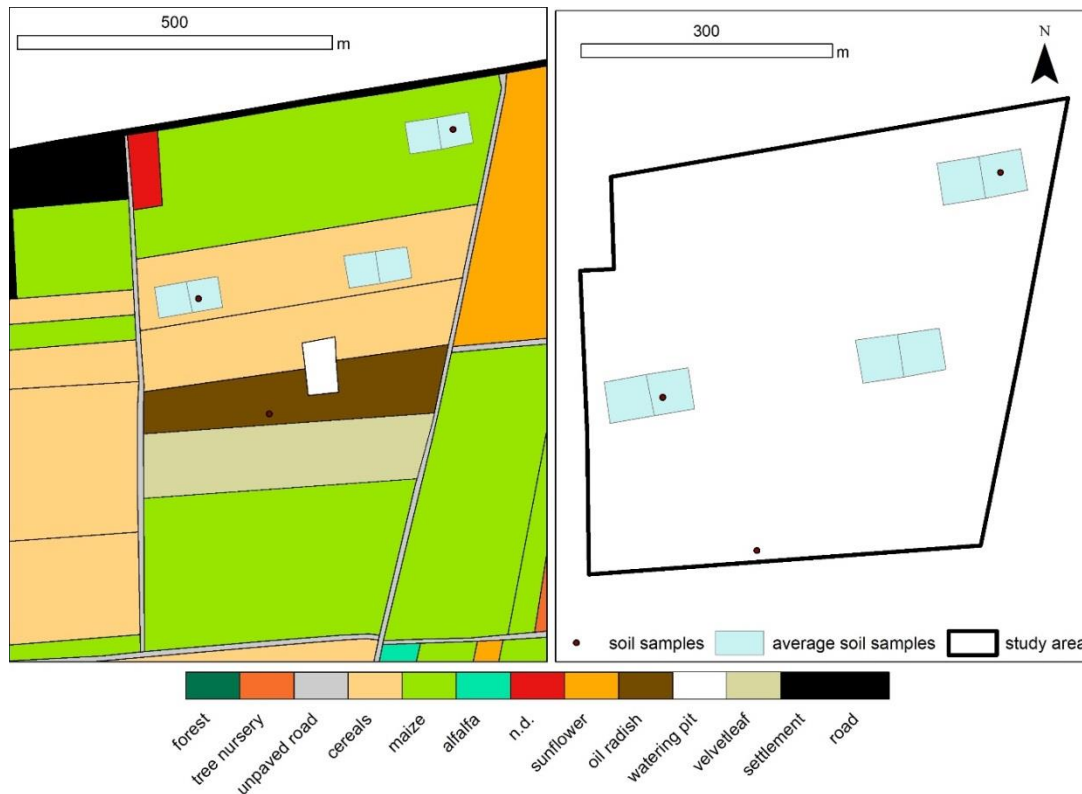


Figure 5. Land use map of the study area from 2018 marking the places of soil sampling (with, without sewage disposal and a control area in 2018)

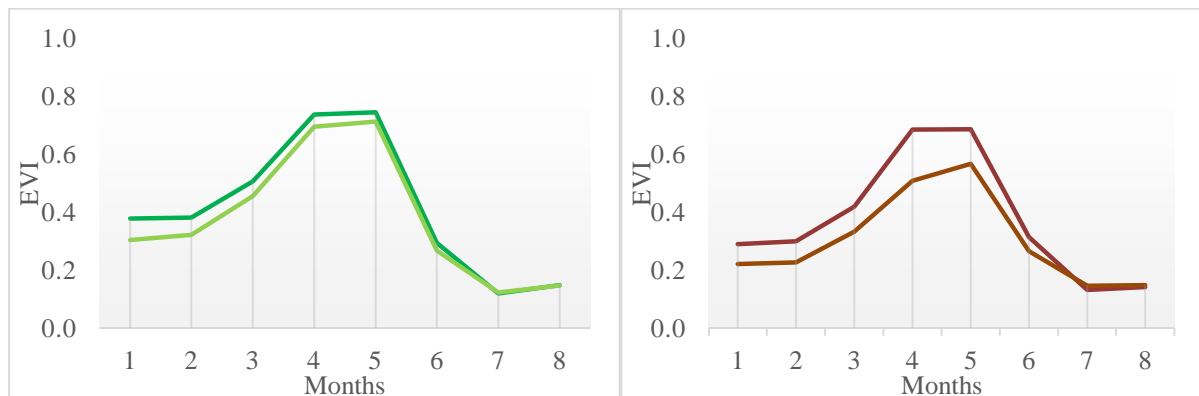


Figure 6. Winter wheat phenological curves (based on EVI) in 2018 at soil study sites with (green) and without (brown) sewage disposal in Autumn 2017

Based on the EVI phenological curves the study site (Figure 6) with sewage disposal showed increased peak values compared to the 'control' site without disposal, especially at the farthest study site, where a later peak was observed based on the average pixel values of the sample field.

Conclusion

Sentinel 2B vegetation index series were assessed to monitor the biomass anomalies related to different water supply conditions and the sewage disposal in the period of 2016-2018 in a study area composed of Chernosem soil. In the investigated humid year the vegetation indices of the crops showed an even spatial pattern, however, in the year under unfavourable, dry conditions spatial differences in biomass production could be observed. The deficiencies revealed the ancient river meanders, characterised by different soil properties compared to the surrounding areas. The direct impact of municipal sewage disposal could be detected on biomass by increased productivity, the response is probably related to the nutrient status of the site.

Acknowledgements

The research was funded by the ‘Thematic Network for the Sustainable Use of Resources – RING2017’ project (program code: EFOP-3.6.2-16-2017-00010).

References

- [1] S.R. Smith. Organic contaminants in sewage sludge (biosolids) and their significance for agricultural recycling. *Philos Trans A Math Phys Eng Sci.* 367(1904):4005-41. (2009) DOI: 10.1098/rsta.2009.0154.
- [2] A. Tomócsik, M. Makádi, V. Orosz, Gy. Füleký. Effect Of Sewage Sludge Compost Treatment On Crop Yield. *Agrofor International* Vol. 1, Issue No. 2 (2016)
- [3] I. Kádár. Szennyvizek, iszapok, komposztok, szerves trágyák a talajtermékenység szolgálatában – MTA TAKI Budapest p. 347 (2013).
- [4] A. Gulácsi, F. Kovács. Drought Monitoring With Spectral Indices Calculated From MODIS Satellite Images In Hungary. *Journal of Environmental Geography* 8 (3–4), 11–20 (2015).
- [5] L Kumar, O. Mutanga. Remote Sensing of Above-Ground Biomass. *Remote Sens.* 9(9), 935 (2017). DOI: 10.3390/rs9090935
- [6] A. Kézér Szennyvíziszap-kihelyezés hatása a talaj nehézfém-tartalmára és baktérium összetételére. Diplomamunka. Szegedi Tudományegyetem, Természeti Földrajzi és Geoinformatikai Tanszék 64 p. (2018).
- [7] B. Pálffy, A. Farsang, A. Kézér, K. Barta, K. Csányi, Zs. Ladányi. Tartós szennyvíziszap kihelyezés hatása a talaj tápanyag-, toxikus elem összetételére, valamint a baktériumaktivitásra. Talajtani vándorgyűlés, 2018.08.29-09.01. (2018).

PREPARATION OF MESOPOROUS TiO₂ BY SOL-GEL AND HYDROTHERMAL METHODS

Carmen Lazau^{1*}, Corina Orha¹, Daniel Ursu¹, Mircea Nicolaescu², Melinda Vajda²

¹National Institute for Research and Development in Electrochemistry and Condensed Matter, no 144 A. Paunescu Podeanu Street, Timisoara 300569

²“Politehnica” University of Timisoara, P-ta Victoriei, No. 2, Timisoara

e-mail: carmen.lazau@google.com

Abstract

Over the last years, there has been increasing interest in the application of TiO₂ with nanosized powders or mesoporous structure for gas sensing, photocatalysts, photoelectrodes, and solar energy conversion. In these applications, the control of morphology, particle size, distribution, phase composition, and porosity of TiO₂ is a primary factor in determining the properties of the final materials.

Mesoporous TiO₂ has a large surface area because of its confined porous structure and high surface to volume ratio, and also it should have a higher photocatalytic activity, because of the improved access to the active sites of TiO₂ [1].

To prepare TiO₂ mesoporous nanoparticles, is not such a simple work, because the raw materials, obtaining materials conditions such as the temperature, stirring rate, ionic strength, acidity, reactant ratios, and the temperature calcination influence their formation. Mesoporous TiO₂ nanoparticles can be prepared through a few methods, like hydrothermal synthesis, evaporation-induced self assembly, precipitation reaction, or the sol-gel process [2].

In this study, we report the preparation and characterization mesoporous TiO₂ by sol-gel and hydrothermal methods using hexadecylamine and Pluronic 127 like surfactant-template. The materials were characterized by X-ray diffraction (XRD), scanning electron microscopy (SEM) and BET.

Acknowledgements

This work was supported by a grant of the Roumanian Ministry of Research and Innovation CCCDI-UEFISCDI, project number PN-III-P1-1.2-PCCDI -2017-0428 (NAPOLII9, No. 40PCCDI/2017)

References

- [1] Dong Suk Kim, Seung-Yeop Kwak, Applied Catalysis A: General 323 (2007) 110–118
- [2] Rong Fu, Qianqian Yin, Xiaoling Guo, Xing Tong, Xiangdong Wang, Res Chem Intermed DOI 10.1007/s11164-017-2999-z

ROLE OF THE CONSTRUCTION AND BUILDING SECTOR IN CLIMATE CHANGE – WHAT SHOULD WE DO?

Adrienn Buday-Malik, ¹Klára Szita Tóthné^{1,2}, András Velósy¹, Anett Zajaros¹, Anita Terjék^{1,3}

1 Directorate of Development, ÉMI Nonprofit Llc, Szentendre, Hungary

2 University of Miskolc, Miskolc

3 University of Technology and Economics, Budapest

e-mail: amalik@emi.hu

Abstract

Climate change is one of the most worrying environmental issues nowadays and efforts should be made to mitigate it all over the world. Among the causes of this phenomenon there is an increasing degree of anthropogenic carbon dioxide emissions. While the world's CO₂ emissions have grown almost linearly, CO₂ emissions have dropped in Hungary: from 58,019 in 2005 to 42,086 kt in 2014. (Source: WB, 2018), but it increased in the construction sector (IEA, 2017).

Nearly 60% of the world's total carbon dioxide emissions are linked to the energy sector and 10% to buildings. Recently global cement production is the third largest source of carbon dioxide due to the use of fossil resources and change in land use, it is growing rapidly. According to statistical data, cement production is responsible for 8% of total CO₂ emissions in the world. So the responsibility of building sector in climate change is great.

In this paper we review the global situation of cement and insulating materials production, it's impact on climate change, and also investigate the domestic environmental impact of construction and building sector. This article highlights the main challenges and tries to give some proposals what we should do towards future sustainable construction and building sector.

Keywords: climate change, cement production, carbon dioxide emissions, energy quakes, zero emission, sustainability, life cycle approach

Introduction

Construction and buildings have a significant impact on the environment through several sectors of the industry. Interference with the natural environment also affects the resources of the raw material mining and the exhausted resources. Looking at a life cycle approach, one of the greatest environmental burdens is the production of building materials, in particular due to the high energy demand and carbon dioxide emissions of cement production, but also the production of clay masonry and the environmental load associated with plastics. In the maintenance of buildings, demand for cooling and heating energy and the related direct and indirect carbon dioxide emission is decisive. At the end of the life-cycle, the energy demand associated with demolition is significant. With regard to climate change, reducing wood resources is not negligible, which plays an important role in the absorption of carbon dioxide when wood is used in architecture. Due to the role of CO₂ in climate change, the article focuses primarily on cement and thermal insulating material.

Experimental

The method used in the research is to study and synthesize literature, to analyse statistics and to compare the environmental impact of individual building materials based on the life cycle software database.

Global cement production and its impact to climate

Cement production in all countries is closely related to the construction industry and economic development. Cement production has increased more than fourfold in the world over the past 40 years and is particularly significant in emerging economies. China has half of the world cement production capacity, followed by India. Producing cement requires energy intensive technology and also emits significant carbon dioxide as a result of clinker production, which is the main component of cement, due to calcination of limestone. Different types of cement (CEM I – CEM V) are commercially available, which differ in particle size, alkali content and clinker content and consequently behave differently when used. Standard Portland cement (CEM I) contains 95% clinker.

One of the key issues in the development of innovative technology for cement production is how to reduce CO₂ emissions during clinker production. Habert et al. (2010), based on Factor 4's eco-efficiency, aimed at reducing the 1990's loads by 2050. However, according to the research results so far, this can only be achieved by factor 2. Efforts to reduce emissions were aimed at decreasing the amount of heat needed to produce unit clinker and to reduce the amount of clinker needed to produce a unit of cement. The carbon emission associated with cement production is equivalent to 470-540 kg / t cement (Andrew 2017) based on various estimates. Baxter and Walton have 470 kg of CO₂ estimated at 1 ton of cement, Keeling (1973) emissivity is 0.50 t CO₂ / 1 t cement, Marland and Rotty (1984) and Olivier et al. (1999) also came to the same conclusion. The China emission factor is 0.5383 tCO₂ (t clinker)-1. India's Emission factor is 0.52 t CO₂ t /clinker. Intergovernmental Panel for Climate Change (IPCC) guide proposes less clinker content of cement to decrease the emission. According to the IPCC's more recent 2006 guidelines (Hanle et al., 2006), when using cement production data adjusted for clinker trade, the formula should be

$$E_{cem} = f_{cem} \text{clink} f_{clink} \text{CaO} \frac{Mr_{CO_2}}{M_{CaO}}$$

where $f_{cem} \text{clink}$ is the clinker ratio, and $f_{clink} \text{CaO}$ is the fraction of CaO in clinker. Mr_{CO_2} is the molecular weight of CO₂ (44.01), and Mr_{CaO} is the molecular weight of CaO (56.08). ((Andrew, 2017) Total emissions from the cement industry could therefore contribute as much as 8 % of global CO₂ emissions. (Le Quéré et al., 2016, 2017; IPCC, 2006).

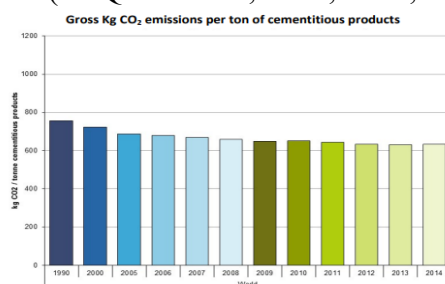


Figure 1.. Gross kg CO₂ per ton of cementitious products

Source:WBCSD, 2018

The environmental impacts of Hungarian construction sector

The impact of the construction sector on the environment and especially on the greenhouse effect could be exactly determined by material flow analysis, tracking each component of flows from cradle to grave / cradle and aggregating environmental impacts. It is a fact that from the raw material extraction to the decomposition of waste, each phase of the life cycle requires energy and is associated with carbon dioxide emissions. As detailed mass balances for the sector are not available, our analysis is confined to two main types of material in the sector and we can rely on estimated values. Building emissions based on the data of the OKIR database for 2016 are shown in the following figure. What surprising is that the CO₂ emissions of the Hungarian cement factories are not displayed in the database. It is true that

the energy needed for cement production comes from 60% of waste (car tire and tired oil, paper). (Lafarge, 2015; DDC, 2015)

According to data from the HCSO, the building industry's greenhouse gas emissions are increasing.

Table 1. CO₂ eq. emission of Construction sector 1990 - 2015 ktons

1990	1995	2000	2005	2010	2011	2012	2013	2014	2015
579,5	329,9	505,6	700,6	793,2	724,5	682,5	832,0	961,4	1 039,1

Source: KSH, 2018

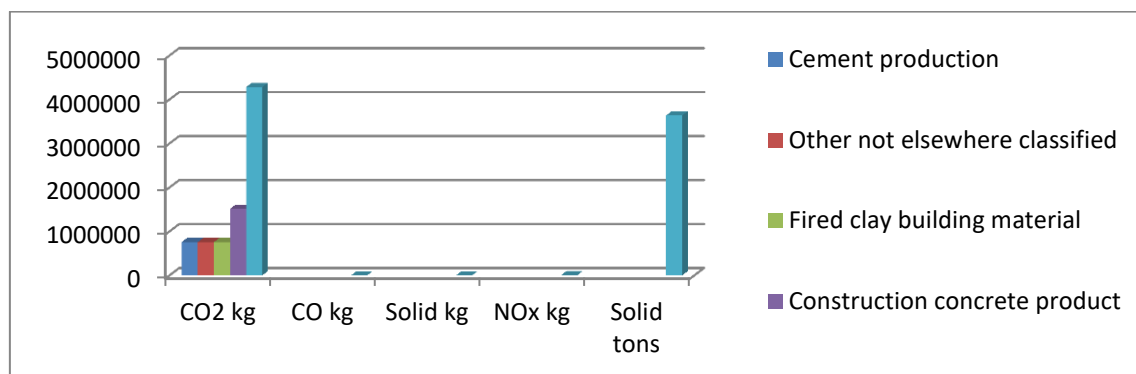


Figure 2. Emissions of Construction sector (2016)
Source: Own editing based on OKIR database (2016)

Plastic in the construction and building sector

Construction is the second largest area for the use of plastic materials. Beyond traditional applications (window frames, pipes, etc.) thermal insulating materials and composites are also applied. The volume of plastics used in construction has declined in the years of crisis, but it is growing steadily today, reaching 20 million tons in Europe. Usage of insulation materials (PUR, PS, composites) is increasing because the energy efficiency requirements of buildings have been much more. Materials utilized for thermal insulation include mineral wool, glass foam, plastic foam made of polystyrene and polyurethane. The insulating material can also be applied as a solid panel or injectable foaming fluid, which enables filling of difficult-to-reach gaps and angles. The European Association of Plastic Manufacturers of Plastic Foams are ecologically more favourable than competing materials because their production requires 16% less energy while releasing 9% less greenhouse gases. The insulation capacity of PS and PUR foams, in addition to the same thickness, is better than the competitor. The composites are mainly used to replace steel and concrete based on their excellent mechanical properties.

Life cycle approach in construction sector

A *life cycle assessment (LCA)* is an internationally accepted and useful tool to assess the environmental impact of products. The LCA methodology is based on a series of international standards and procedures, standards of environmental management called ISO 14040. LCA is a technique that aims to enable a correct assessment of the environmental aspects and potential impacts associated with a product, consisting of four distinct analysis steps (Definition of goal and scope; Establishment of life cycle inventory (LCI); Valuation of the impact of the life cycle; Interpretation of results). Most of LCA studies focused mainly for construction materials and building (Alejandro et al., 2016), does not cover all sectors. A life cycle approach can help us to make choices. It implies that everyone in the whole chain of a product's life cycle, from cradle to grave, has a responsibility and play a role taking into account all the relevant impacts on the economy, the environment and the society.

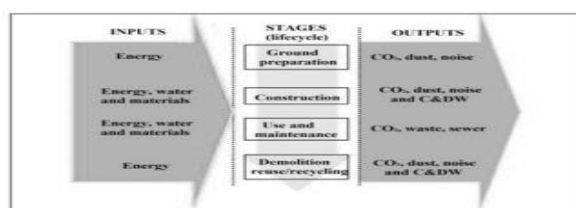


Figure 3. Environmental flows in the life cycle of a building

Source: Silva, 2003

In this paper we compare the Global Warming Potential (GWP) of different cement types and insulation materials on the base of LCA data. The used database was the construction data of SimaPro and GaBi software (CML 2001 method). The function unit is 1 kg of material and/or 1 m² wall surface. Greenhouse effect depends on clinker content, and substitute raw materials.

Table 2 Global Warming Potential [kgCO₂ eq/kg] of different concrete and cement types (CML 2001, Normalisation), GaBi Construction database

	Concrete C12_15	Ready_mix concrete C12_15	Concrete C20_25	Concrete C30_37	Ready_mix concrete C30_37	Concrete C8_10*	Ready_mix concrete C8_10*	Cement _CEM I 32_5_	Cement _CEM I 42_5_	Cement _CEM I 52_5_	Cement _CEM III 32_5_
GWP 100	0,08631	0,09074	0,09810	0,11175	0,11254	0,00014	0,00013	0,82402	0,79675	0,81889	0,30306

*It contents construction waste

Insulation materials

Rock wool and glass wool are durable, resistant, refractory and do not require maintenance. EPS and XPS based insulators are extremely sensitive to Ultra-Violet Radiation, while EPS is sensitive to condensation. Compared to their environmental effects, it can be stated that the most suitable type of insulating material per unit of mass is rock wool. But if we choose other function unit - 1 m² surface wall and that same thickness – the expanded Polystyrene has the smallest GWP.

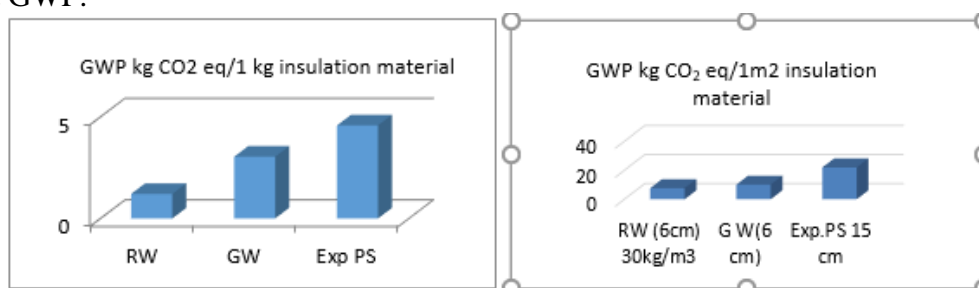


Figure 4 Comparative analysis of the environmental impact between insulation materials

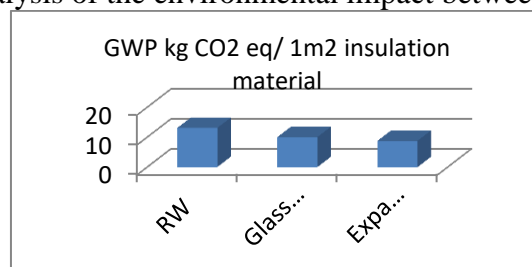


Figure 5 GWP impact of insulation (that same thickness 6 cm, Rock wool 180kg/m³)

Source: Own editing based on SimaPro 7.0 demo database

The estimated CO₂ emission of domestic plastic usage in construction sector is about 30 - 40 thousand tons.

Conclusion

Regarding the role of construction and building materials industry, also its environmental impacts on climate change, the way is to develop and follow-up a strategy that promotes the sector towards sustainability. However reliable data and material flow based life-cycle analysis can be the starting point to determine the correct target values. There is still uncertainty in the material balance of products used in the sector, in terms of inputs, but even more in terms of outputs regarding environment. The primary interest of the economy is to gather information on the supply of building materials (domestic / import), and to map the quality and environmental load characteristics of building materials available on the market. Having these data, the environmental impact of constructions in life-cycle considerations could be optimized at the design stage. These impacts include the use of resources and the contribution to the various environmental problems, such as climate change, acid rain, destruction of the ozone layer, human toxicity or depletion of resources. Increasing energy efficiency, reducing energy demand and emissions are primary sustainability aims at all stages of the life cycle. The advantage of the life-cycle method is that with detailed data analysis and evaluation loads can be more precisely defined in the different life-stages, so arising problems can be more consciously responded.

Acknowledgements

This paper supported by GINOP-2.3.4-15-2016-00004 project – “Korszerű anyagok és intelligens technológiák FIEK létrehozása a Miskolci Egyetemen”.

References

- [1] Alejandro Martínez Rocamora, Jaime Solís-Guzmán, M Marrero (2016): LCA databases focused on construction materials: A review, *Renewable and Sustainable Energy Reviews* 58(2016):565-573, DOI: 10.1016/j.rser.2015.12.243
- [2] Robbie M. Andrew (2018): Global CO₂ emissions from cement production *Earth Syst. Sci. Data*, 10, 195–217, 2018 <https://www.earth-syst-sci-data.net/10/195/2018/>
- [3] DDC (2017): Environmental measurement results for 2015
- [4] European Plastic (2017): *Plastics – the Facts 2017*
- [5] G.Habert, C.Billard, P.Rossi, C.Chen, N.Roussel (2009): Cement production technology improvement compared to factor 4 objectives *Cement and Concrete Research* 40 (2010) 820-826 <https://doi.org/10.1016/j.cemconres.2009.09.031>
- [6] IEA (2017): *Global Status Report*, UN Environment https://ec.europa.eu/energy/sites/ener/files/documents/020_fatih_birol_seif_paris_11-12-17.pdf
- [7] Lafarge Holcim (2017): *Summary report on continuous emission control* <http://www.lafarge.hu/files/18-03-06-osszefoglalo-jelentes-2017-km.pdf>
- [8] Le Quéré et al. (2016): *Global Carbon Budget 2016*. *Earth Syst. Sci. Data*, 8, 605–649, 2016
- [9] IPCC (2007): *Climate Change 2007 - Mitigation of Climate Change: Working Group III* <https://books.google.hu/books?isbn=1139468642>
- [10] Sjunnesson, Jeannette (2005): *Life Cycle Assessment of Concrete Master Thesis*, Lund University
- [11] V. Silva. (2003): *Avaliação da sustentabilidade de edifícios de escritórios brasileiros: Diretrizes e base metodológica (Evaluation of sustainability of Brazilian Office buildings: Guidelines and methodological basis)*, São Paulo, 2003, 1–16. (In Portuguese).
- [12] World Bank Statistics [13] WBCSD (2018): *Cement Industry Energy and CO₂ Performance Getting the Numbers Right (GNR)* <http://www.wbcdcement.org/pdf/GNR%20dox.pdf>

HERBICIDES APPLICATION IN SPRING ROW CROPS

Maja Meseldžija, Milica Dudić, Olga Popović, Radovan Begović

*University of Novi Sad, Faculty of Agriculture, Trg Dositeja Obradovića 8, Novi Sad, Serbia
e-mail: maja@polj.uns.ac.rs*

Abstract

The level of weed infestation of maize and sunflower differs over locations and directly affects the intensity of the competitive relationships between crops and weeds, which results in lower or greater yield losses. The experiment with tested herbicides was placed at Lipar (Serbia) during 2017. Efficacy and phytotoxicity was evaluated according EPPO/OEPP standards. The dominant weeds were: *Ambrosia artemisiifolia* L., *Chenopodium album* L., *Chenopodium hybridum* L., *Amaranthus retroflexus* L., *Datura stramonium* L., *Cirsium arvense* (L.) Scop., *Sinapis arvensis* L., *Xanthium strumarium* L., *Convolvulus arvensis* L., *Setaria glauca* L., *Sorghum halerense* (L.) Pers., *Echinochloa crus-gali* L., *Agropyrum repens* L. In the maize presence of invasive weed species *Thladiantha dubia* L., was found. Isoxaflutole, herbicide for soil application had good efficacy on weeds in maize crop. Fluorochloridone, terbuthylazine and S-metolachlor had good efficacy on all weeds in sunflower, except for broad-leaf species *Convolvulus arvensis* L.

Introduction

At the present time, maize is the most important cereal crop in the world [1]. Weed control has a major effect on the success of maize growth because the competition ability of maize is relatively low at early growth stages [2]. Maize crop is often characterized by a complex of weed flora, which consists of broad-leaf and grass weeds [3]. Weed control in maize is carried out mainly by mechanical and chemical methods, but the use of herbicide is increasing, along with increases in growing areas and production costs [4]. Because of the negative effects of weeds on the crop of corn, for their suppression is used a number of herbicides [5], most commonly, a combination of 2, 3 or more active herbicide substances, due to proven greater efficacy [6]. Different types of pre and post-emergence herbicides are used to control weeds in maize in Europe. Among post-emergence herbicides in maize, foramsulfuron is a sulfonylurea that exerts its herbicidal activity by inhibiting acetolactate synthase also known as acetohydroxy acid synthase [2], and provides adequate control of many grasses and broad-leaf weeds. Foramsulfuron can be applied in mixture with other herbicides increasing the control of some important weeds, without the risks of carry-over problems also in rotational vegetable crops [2]. Isoxaflutole is a soil and post-emergence applied herbicide that inhibits p-hydroxyphenyl pyruvate dioxygenase (HPPD), an important enzyme involved in the biosynthesis of carotene pigments in plants [7]. Recently isoxaflutole was introduced in combination with a safener, cyprosulfamide, thus allowing pre and early post application through the of field corn. Tembotrione new active substance from the group triketone. After translocation, the active substance reaches the place of growth, which causes disruption in the synthesis of carotenoids. Tembotrione was used to control broadleaf and some grass weed species in maize. The compound is sold in various mixtures and formulations [8].

Sunflower (*Helianthus annuus* L.) is the most important oil crops in Serbia [9]. Seeds have a high content (38-50%) of high-quality oil, primarily used for human consumption. Additionally, sunflower oil can be used in a wide range of products in pharmaceutical, cosmetic and chemical industries, in floriculture, honey production and also for biodiesel production [10]. The sunflower is a thermophile plant and is usually sown in mid-spring, when a large number of weeds such as *Ambrosia artemisiifolia*, *Xanthium strumarium*,

Datura stramonium, *Amaranthus retroflexus*, have already emerged [11]. Application of appropriate selective herbicides on weeds in the early growth stage is a globally important aspect of growing sunflower, both from an economic as well as ecological and environmental aspect [12]. Rather than pre or post-emergence herbicide application alone, use of both pre and post-emergence herbicides sequentially along with cultural practices may be a viable option to control the weeds effectively right from the sowing to harvesting and to increase the productivity of sunflower [13]. Products based on flurochloridone, terbuthylazine, acetochlor, oxadiazon, oxyfluorfen, and other active ingredients have been applied in soil treatments for the suppression of some grass and annual broad-leaf weeds in sunflower [11]. Terbuthylazine, which belongs to the group of triazine herbicides, affected electron transport in photosystem II. S-metolachlor belongs to a chloroacetamide family of herbicides. The primary mode of action is not clear, but the most recent evidence suggests that it blocks the formation of very long chain fatty acids [14]. The efficacy of S-metolachlor is strongly influenced by soil moisture and delayed under dry conditions [1]. However, the success of the crop depends largely on effective weed control under weed management strategy. Chemical weed control is an alternative method that may be less expensive, but riskier because of weed becoming herbicide resistant and of concerns about an unwanted side effect of herbicides [15].

The aim of this work was to determine the efficacy of the herbicide and reduction of weed reproduction after the application of herbicides during pre-emergent and post-emergent application in maize and sunflower.

Experimental

A field experiment was conducted at the Lipar (Serbia) during 2017, in order to determine the efficiency of applied herbicides on weed species in maize and sunflower. Herbicides efficiency trial was set up by random block system. Control plot, not treated with herbicides, was also included. The experiment was set up according to the EPPO/OEPP standards [16,17,18], in order to test the efficacy and phytotoxicity of the applied herbicides. The first treatment was applied after sowing and before the emergence of crop and weeds (preemergence - pre. em.), with preparations based on active ingredient isoxaflutole in the amount of 0.4 l/ha. The second treatment was applied when maize was in the 4-5 leaf phase with a preparation based on active substance tembotrione + isoxadifen-ethyl in an amount of 2 l/ha for the control of grass and broadleaf weeds and invasive weed species *Thlandiantha dubia* Bunge. The third treatment was applied when maize was in the 6-8 and *Sorghum halepense* in 4-5 leaf phase, with a preparation based on active substance foramsulfuron + isoxadifen-ethyl, in the amount of 2 l/ha and the active substance tembotrione + isoxadifen-ethyl in the low amount of 0.5 l/ha. The second experiment was set on a plot under the sunflower crop. Preemergence herbicides flurochloridone in the amount of 0.5 l/ha, postemergence herbicides terbuthylazine in the amount of 0.5 l/ha and S-metolachlor in the amount of 0.5 l/ha were applied. The second treatment was applied when *Sorghum halepense* (L.) Pers. was in 3-5 leaf phase, with a preparation based on active substance propaquizafop in the amount of 0.5 l/ha. Based on the obtained data, the coefficient of efficiency C_e (%) of herbicides is calculated by the formula Dodel loc. cit. Janjic (1985) and represents a relative ratio between the number of destroyed weeds compared to the weeds number in the control. Visual assessment of the phytotoxicity was performed according to the European Weed Research Council (EWRC) scale (1-9).

Results and discussion

At the investigated locality of Lipar the following weed species in maize and sunflower crop were identified: *Ambrosia artemisiifolia* L., *Chenopodium album* L., *Chenopodium hybridum* L., *Amaranthus retroflexus* L., *Datura stramonium* L., *Cirsium arvense* (L.) Scop., *Sinapis*

arvensis L., *Xanthium strumarium* L., *Convolvulus arvensis* L., *Setaria glauca* L., *Sorghum halepense* (L.) Pers., *Echinochloa crus-gali* L., *Agropyrum repens* L.

Application of the pre- and post-emergence herbicides in maize, isoxaflutole (0.4 l/ha), tembotrione + isoxadifen-ethyl (2 l/ha), foramsulfuron + isoxadifen-ethyl (2 l/ha) and the active substance tembotrione + isoxadifen-ethyl in low amount (0.5 l/ha) during the assessment of efficiency gave the following results presented in table 1.

Table 1. The presence of weeds in maize crop and the herbicide efficiency

	Weed species	No/m ²	Ce (%)	Control
				No/m ²
1	<i>Amaranthus retroflexus</i> L.	0	100%	2
2	<i>Ambrosia artemisiifolia</i> L.	0	100%	4
3	<i>Chenopodium album</i> L.	0	100%	2
4	<i>Convolvulus arvensis</i> L.	0	100%	3
5	<i>Datura stramonium</i> L.	0	100%	1
6	<i>Setaria glauca</i> L.	0	100%	2
7	<i>Sorghum halepense</i> (L.) Pers.	1	88%	9
8	<i>Thladiantha dubia</i> L.	1	95%	21
9	<i>Xanthium strumarium</i> L.	0	100%	1
Total number of weeds		2		45
Total efficacy (%)		95.55		-
Phytotoxicity (EWRC scale 1-9)		1		-

The efficacy assessment of herbicide application in maize was total (Ce=100%) for the following weed species: *Ambrosia artemisiifolia* L., *Chenopodium album* L., *Amaranthus retroflexus* L., *Setaria glauca* L., *Datura stramonium* L., *Xanthium strumarium* L., *Convolvulus arvensis* L. Good efficacy (Ce= 95%) of applied herbicides was on weed that are poor in our region, *Thladiantha dubia* L., and has the status of an invasive weed species. Assessment of the efficacy of the applied herbicides of 88% in maize crop was established in weed species *Sorghum halepense* (L.) Pers. Gatzweiler et al. (2012) [8] showed that composition tembotrione+isoxadifen-ethyl at the exaggerated rate of 300+150 g a.i./ha achieves a complete crop tolerance in the vast majority of the common maize varieties. According to Radivojevic et al. (2014) [19] mesotrione has shown high efficacy in the control of the following species: *Amaranthus retroflexus* L., *Chenopodium album* L., *Chenopodium hybridum* L., *Solanum nigrum* L., *Xanthium strumarium* L., *Cirsium arvense* (L.) Scop., *Datura stramonium* L.,. For *Abutilon theophrasti*, *Ambrosia artemisiifolia* L., *Bilderdykia convolvulus*, *Polygonum aviculare* high efficacy was confirmed only in higher quantities of application (1.2 L/ha). According to Onc Jovanovic et al. (2010) [20] application of compounds of different mechanisms of action and spectrum give good results in the control of annual broadleaf weeds in maize.

Application of the pre- and post-emergence herbicides flurochloridone (0.5 l/ha), terbuthylazine (0.5l/ha), S-metolachlor (0.5l/ha) and propaquizafop (0.5l/ha) in sunflower, during the assessment of efficiency gave the following results presented in table 2.

Table 2. The presence of weed species and the efficacy of tested herbicides in sunflower crop

	Weed species	No/m ²	Ce (%)	Control
				No/m ²
1	<i>Agropyrum repens</i> L.	0	100%	3
2	<i>Ambrosia artemisiifolia</i> L.	0	100%	12
3	<i>Chenopodium album</i> L.	1	90%	11
4	<i>Chenopodium hybridum</i> L.	1	100%	17
5	<i>Cirsium arvense</i> (L.) Scop.	0	100%	2
6	<i>Convolvulus arvensis</i> L.	2	0%	2
7	<i>Datura stramonium</i> L.	0	100%	7
8	<i>Echinochloa crus-galli</i> L.	1	50%	2
9	<i>Sinapis arvensis</i> L.	0	100%	1
10	<i>Solanum nigrum</i> L.	0	100%	3
11	<i>Sorghum halepense</i> (L.) Pers.	0	100%	5
Total number of weeds		5		75
Total efficacy (%)		93.33		-
Phytotoxicity (EWRC scale 1-9)		1		-

Total efficacy Ce (100%) of applied herbicides in sunflower was on: *Chenopodium hybridum* L., *Ambrosia artemisiifolia* L., *Sinapis arvensis* L., *Datura stramonium* L., *Cirsium arvense* (L.) Scop., *Sorghum halepense* (L.) Pers., *Solanum nigrum* L., *Agropyrum repens* L. (tab. 2). Tested herbicides had low efficacy (50%) on *Echinochloa crus-galli* L., while applied herbicides did not have effect on *Convolvulus arvensis* L. In a study performed by Jursík et al. (2015) [21] efficacy of flurochloridone on *E. crus-galli*, *M. annua*, and *S. physalifolium* was not satisfactory, especially with treatments without irrigation, while S-metolachlor only controlled *A. retroflexus* and *E. crus-galli* (efficacy 93–100%). Simić et al. (2011) [11] showed that applied herbicides flurochloridone + s-metolachlor reduced the number of annual broad-leaf species *S. nigrum*, *D. stramonium*, *A. retroflexus*, *Ch. album* and *Ch. hybridum*, while the effect of the herbicides on the most dominant species, *A. artemisiifolia* and *X. strumarium*, was unsatisfactory.

Conclusion

Based on the results of research during 2017, can be made the following conclusions: 9 weed species were determined in maize, while 11 weed species were determined in the sunflower crop. The presence of invasive weed species *Thladiantha dubia* L., was found in corn. Herbicide for soil application isoxaflutole had good efficacy on weeds in maize crop. Application of herbicides flurochloridone, terbuthylazine and S-metolachlor in sunflower had good efficacy on all weed species, except for broad-leaved species *Convolvulus arvensis* L. Using the tested herbicides in maize and sunflower crops, uninterrupted growth and development has been ensured.

References

- [1] J. Andr, V. Hejnák, M. Jursík, V. Fendrychová (2014). Effects of application terms of three soil active herbicides on herbicide efficacy and reproductive ability for weeds in maize. *Plant, Soil and Environment*, 60(10), 452-458.
- [2] Pannacci, E. (2016). Optimization of foramsulfuron doses for post-emergence weed control in maize (*Zea mays* L.). *Spanish Journal of Agricultural Research*, 14(3), p.e1005.

- [3] Pannacci, E., Onofri, A. (2016). Alternatives to terbuthylazine for chemical weed control in maize. *Communications in Biometry and Crop Science*, 11, 51–63.
- [4] Kir, K., Dogan, M.N. (2009). Weed control in maize (*Zea mays* L.) with effective minimum rates of foramsulfuron. *Turkish Journal of Agriculture and Forestry*, 33(6), 601–610.
- [5] Nestorović, M.(2009). Efikasnost herbicida u suzbijanju korova u usevu kukuruza. *Savremena poljoprivreda*, vol. 58, 3-4, 87-93.
- [6] Golijan, J., Elezović, I. (2015). Ispitivanje fitotoksičnosti i efikasnosti acetohlor sa dihlormidom u kukuruzu. *Zaštita bilja* 66 (1): 38-44.
- [7] Robinson, D.E., Soltani, N., Shropshire, C., Sikkema, P.H. (2013). Cyprosulfamide safens isoxaflutole in sweet corn (*Zea mays* L.). *Hortscience* 48: 1262-1265.
- [8] Gatzweiler, E., Krämer, H., Hacker, E., Hills, M., Trabold, K., Bonfig-Picard, G. (2012). Weed spectrum and selectivity of tembotrione under varying environmental conditions. In: *Proceedings of the 25th German Conference on Weed Biology and Weed Control*. Braunschweig, Germany, 385–391.
- [9] Marković, M. (2003). *Zaštita ratarskih kultura*, Agroteka, Beograd.
- [10] Castro, C., Leite, R. (2018). Main aspects of sunflower production in Brazil. *OCL*, 25(1) p.D104.
- [11] Simić, M., Dragičević, V., Knežević, S., Radosavljević, M., Dolijanović, Z., Filipović, M. (2011). Effects of applied herbicides on crop productivity and on weed infestation in different growth stages of sunflower (*Helianthus annuus* L.). *Helia*, 34(54), 27-37.
- [12] Smatana, J., Macák, M., Ernst, D. (2014). Weed control in sunflower (*Helianthus annuus* L.) on the interface of agro-climatic conditions of maize and sugar beet growing region. *Acta fytotechnica et zootechnica*, 17(04), 115-121.
- [13] Sujith, G.M., Geetha, K.N., Shadakshari, Y.G. (2017). Effect of different herbicides and cultural practices on weed dynamics and productivity of sunflower (*Helianthus annuus* L.) Grown on alfisols of eastern dry zone of Karnataka. *International Journal of Advanced Biological Research*, 7 (3), 595-599.
- [14] Reddy, S., Stahlman, P., Geier, P., Thompson, C. (2012). Weed Control and Crop Safety with Premixed S-Metolachlor and Sulfentrazone in Sunflower. *American Journal of Plant Sciences*, 03(11), 1625-1631.
- [15] Tadavi, A.G., Chorey, A.B., Gaikwad, G.S., Sawadhkar, S.M. (2017). Integrated Weed Management in Sunflower. *Int.J.Curr.Microbiol.App.Sci.* 6(9), 1080-1088.
- [16] EPPO/OEPP Standards. (2009). Guidelines for the efficacy evaluation of plant protection products. *Phytotoxicity assessment*, 31-37.
- [17] EPPO/OEPP Standards. (2009). Guidelines for the efficacy evaluation of plant protection products. *Weed in sunflower*, 30-34.
- [18] EPPO/OEPP Standards. (2009). Guidelines for the efficacy evaluation of plant protection products. *Weed in maize*, 6-10.
- [19] Radivojević, Lj., Gajić Umiljendić, J., Marisavljević, D., Anđelković, A., Pavlović, D. (2014). Primena mezotriona u kombinaciji sa terbutilazinom, nikosulfuronom i s-metolachlorom u kukuruzu. *Zaštita bilja*, 65 (4), 290, 155-162.
- [20] Onć Jovanović, E., Marković, S., Gavrilović, Z., Dakić, P. (2010). The broadleaf weeds in corn of crop on area southwestern Banat and their control, *Banat's Journal of Biotechnology*. 1(1), 52–55.
- [21] Jursik, M., Soukup, J., Holec, J., Andr, J., Hamouzová, K. (2015). Efficacy and selectivity of pre-emergent sunflower herbicides under different soil moisture conditions. *Plant Protection Science*, 51(4), 214-222.

RESIDUAL IMPACT OF THE REDUCED AMOUNT OF MESOTRIONE AND TERBUTHYLAZINE FROM DIFFERENT PREPARATIONS

Maja Meseldžija, Milica Dudić, Miroslava Nežić, Ivana Ninić

*Department of Plant and Environmental Protection, University of Novi Sad, Faculty of Agriculture, Trg Dositeja Obradovića 8, Novi Sad, Serbia
e-mail: maja@polj.uns.ac.rs*

Abstract

The aim was to determine the sensitivity of the pea plants to the soil residues by subjective evaluation and measuring the height after application of the reduced amounts of the herbicide combination of mesotrione and terbuthylazine. The experiment with tested herbicides was placed at the location of Žabalj (Serbia). After 14 days of application the average plant height was the highest (5cm) in 1/8X of the applied amount of mesotrione 50 g/l + terbuthylazine 326 g/l and then decreased with the increase in the amount, which also applies to the amounts of mesotrione 50 g/l + terbuthylazine 125 g/l, where the highest average height was 5.54 cm. The percentage of plants damage 14 days after treatment of mesotrione 50 g/l + and terbuthylazine in a higher amount 326 g/l was in the range of 38-79%, while after 21 days the percentage of damage was 60-89%. Preparation based on active substance mesotrione 50 g/l + terbuthylazine 125 g/l caused a percentage of damage to pea plants in the range of 30% (1/8X) to 85% (4X), but when peas were in the four trifoliate leaf stage 21 days after the treatment percentage of damage was 60-98%. All treated pea plants were dried after 25 days of setting up the experiment, except the control where the height of plants was 9 cm.

Introduction

The use of pesticides is directed at controlling target organisms, and despite this fact, it is not possible to predict the environmental fate of pesticides. The widespread use, mobility, persistence, and toxicity of pesticides can lead to their dissipation to all elements of the natural environment. Thus, the excessive use of pesticides is still a major problem affecting the quality of the environment [1]. Residual herbicides are useful for long-term weed control, but problematic when the same characteristic leads to injury crops planted in rotation or to natural vegetation in uncropped areas over a long period [2]. The persistence of herbicide depends on the climatic conditions as well as the physical and chemical properties of soil, and in particular on the soil content of organic matter, which limits the transport of active ingredients of herbicides to water [3]. Soil pH affects differently on carryover of the sulfonylurea, imidazolinone, triazolopyrimidine, and triazine herbicides [4]. Herbicide persistence is an important consideration in crop production since the residue of some herbicides can persist to the next growing season and may injure sensitive crops in the rotation [5]. Side effects of pesticides, including herbicides, are a problem that needs to be discussed, especially in the time of their increasing use in the EU countries. One method used to determine if herbicide residues injurious might exist in the soil is to conduct a bioassay. A bioassay is the measurement of a biological response by a living organism to determine the presence or concentration of a chemical in a substrate. This is a direct and simple method to determine if it is safe to seed or plant into areas treated with herbicides. Unlike a chemical assay, a bioassay is unique in that it measures plant susceptibility. Chemical detection identifies a substance, not biological activity [5].

Mesotrione is a member of the triketone family of herbicides [6], and provides pre- and post-emergence control of broadleaf weed species, primarily in maize [7]. Mode of action is to inhibit the enzyme 4-hydroxyphenylpyruvate dioxygenase (HPPD), which affects carotenoid

biosynthesis [8]. Mesotrione is commonly used in formulated preparation alone or in mixture with some other herbicides, atrazine, S-metolachlor, terbuthylazine, and glyphosate. In soil is easily degradable and its biological persistence is the shortest in clay soils, followed by heavy sandy loam and sandy loam types [9]. Mesotrione can be degraded by photolysis at the soil surface and can undergo microbial degradation as it translocates deeper in the soil. Some bacterial species, including *Bacillus* sp., *Pantoea ananatis*, *Bradyrhizobium* sp., and *Escherichia coli* can completely degrade mesotrione [7]. Studies reporting dissipation time of mesotrione usually showed a low persistence in soils, with a half-life time (DT50) ranging from 2 to 34 days [9]. Terbuthylazine is a herbicide belonging to the triazines family [10] and is used for weed control in pre- and post-emergent treatment of a variety of agricultural crops as well as roads, railways, and the industrial area [11]. This chemical interferes with the photosynthesis and in particular at the level of photosystem II. Terbuthylazine has a very high soil persistence, depending on the soil characteristics, it can be present up to 17 months after the field treatments [12]. Residence times of terbuthylazine in soil and aquifer sediments are likely to be long due to slow degradation under unfavorable environmental conditions [13]. In 2011, the European Food Safety Authority (EFSA) provided an extensive peer review of data concerning the environmental behavior and fate, ecotoxicology and toxicology, and risk assessment of terbuthylazine [14]. The European Commission based on these conclusions approved the inclusion of terbuthylazine in Annex I of Council Directive 91/414/EEC and its use only as a herbicide until December 2021 [15].

The aim of this study was to assess the persistence and phytotoxicity of mesotrione and terbuthylazine in the soil or to determine the effect of their residues on the growth and development of pea (*Pisum sativum* L.) on the basis of the obtained results.

Experimental

The study was conducted at locality in Žabalj (Serbia) on 19 July and lasted 28 days. For this experiment were used two different preparations Calaris pro (50 g/l mesotrione + 326 g/l terbuthylazine) and Tvister (50 g/l mesotrione and 125 g/l terbuthylazine), water, soil taken from the area where herbicides were never applied, pots and pea seeds. All treatment were set in three repetitions, including a control with soil not treated with herbicides. The preparations were applied in 6 different amounts each separately, where 500g of soil were treated with the tested amounts of herbicides, and by mixing the resulting mixture was equally distributed in pots, in which the pea was sown. The pots were in semi-controlled conditions, they had a constant light and they were daily watered. The preparations were applied in the recommended amount (X), reduced amounts (1/8X, 1/4X, 1/2X), as well as in two and four times higher amounts (2X and 4X). The evaluation was done after 14, 21 and 28 days after treatment. Efficacy treatment was assessed by a linear subjective scale of 0 - 100%, where 0% indicates that there are no changes in the plants, while 100% indicates the complete destruction of plants.

Results and discussion

Treatment results of the assessment by linear subjective scale damage as well as by measuring the height of the pea plants 14, 21 and 28 days after the treatment with herbicides are shown in Figures 1-3.

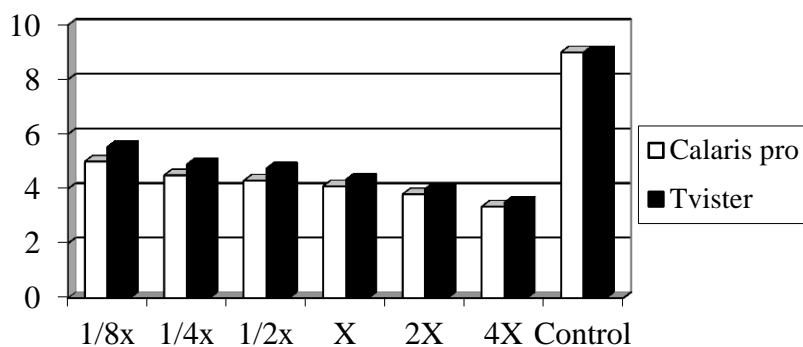


Figure 1. The average height of pea plants 14 days after treatment

Based on the results of the assessment 14 days after the application of the herbicide, the average plant height was the highest in 1/8X of the applied amount of mesotrione 50 g/l + terbuthylazine 326 g/l (5 cm), and then decreased exponentially by increasing the amount of the applied preparation, which also applies to the second preparation based on active substance mesotrione 50 g/l and terbuthylazine 125 g/l, where the highest average plant height was 5.54 cm. In the variant where 4 times higher amount than the recommended was used, the height of plants was 3.35 cm with the use of the mesotrione 50 g/l and terbuthylazine in a higher amount 326 g/l, and 3.5 cm for the application of the mesotrione 50 g/l + terbuthylazine 125 g/l. Non-treated plants had an average height of 9 cm.

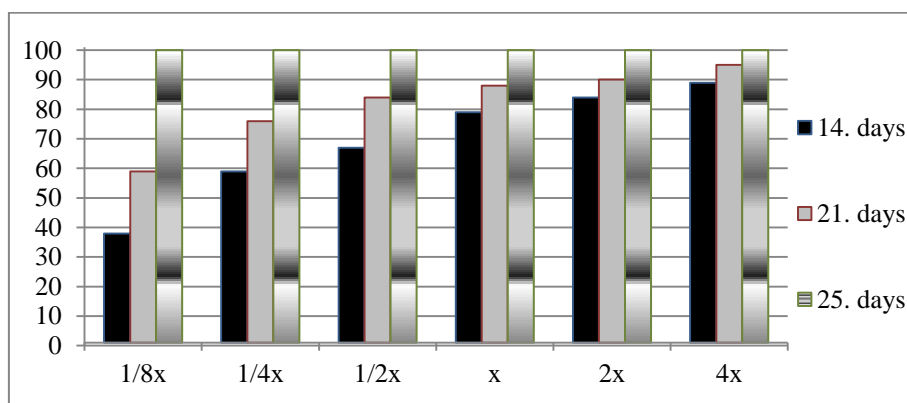


Figure 2. The percentage of plants damages 14, 21, and 28 days after application of mesotrione 50 g/l + terbuthylazine 326 g/l

From fig.2 it can be seen that 14 days after treatment with herbicides mesotrione 50 g/l + terbuthylazine 326 g/l the percentage of plants damage was in the range of 38%, with the application of 1/8X and up to 79% where four times higher amount was applied. In control, pea plants were in the 2 leaf phase. Phytotoxic effect on plants was manifested as bleaching and leaf chlorosis. When the peas were in the four trifoliate leaf stage, 21 days after treatment the increase in damage was determined and also the progressive effect of the herbicide. The percentage of damage was 59% with the application of 1/8X, and with the increase in the amount an increase in damage was also found (60-89%).

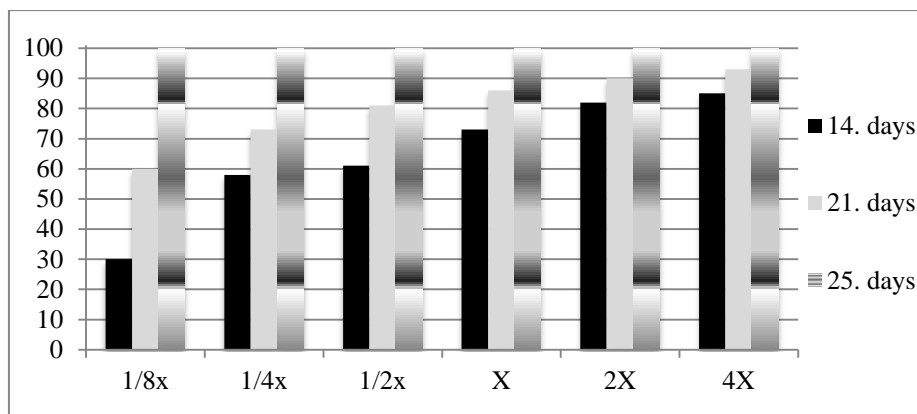


Figure 3. The percentage of plants damages 14, 21, and 28 days after application of mesotrione 50 g/l + terbuthylazine 125 g/l

The percentage of plants damage were in the range of 30% (a 1/8X application) and up to 85% where four times higher amount was applied. On the second assessment (21 days after treatment) the increase in damage was determined and also the progressive effect of the applied herbicides. Applying 1/8X amount of herbicides mesotrione 50 g/l + terbuthylazine 125 g/l, the percentage of damage was 60%, and with the increase in the amount, an increase in damage was also found (73-98%).

Conclusion

In this study, all applied amounts of both preparations showed phytotoxic effects on pea plants. The average plant height was the highest in 1/8X of the applied amount of mesotrione 50 g/l + terbuthylazine 326 g/l (5cm), and then decreased exponentially by increasing the amount, which also applies to the mesotrione 50 g/l + terbuthylazine 125 g/l where the average height was 5.54 cm. The percentage of plants damage 14 days after treatment was in the range of 38-79%, while after 21 days the percentage of damage was 60-89%. Herbicides mesotrione 50 g/l + terbuthylazine 125 g/l caused a percentage of damage to pea plants in the range of 30% (1/8X) to 85% (4X), while after 21 days percentage of damage was 60-98%. After 25 days of setting up the experiment, all treated plants were dried, except for control plants that had a height of 9 cm.

References

- [1] Baćmaga, M., Kucharski, J., Wyszowska, J. (2015). Microbial and enzymatic activity of soil contaminated with azoxystrobin. *Environmental Monitoring and Assessment*, 187(10).
- [2] Helling, C.S. (2005). The science of soil residual herbicides. Pages 3–22 in R. C. Van Acker, ed. *Soil residual herbicides: Science and management*. Topics in Canadian Weed Science. Canadian Weed Science Society, Vol. 3.
- [3] Borowik, A., Wyszowska, J., Kucharski, J., Baćmaga, M., Tomkiel, M. (2016). Response of microorganisms and enzymes to soil contamination with a mixture of terbuthylazine, mesotrione, and S metolachlor. *Environmental Science and Pollution Research*, 24(2), 1910-1925.
- [4] Sikkema, P.H., Robinson, D.E. (2005). Residual herbicides: An integral component of weed management systems in Eastern Canada. Pages 89-99 in R.C. Van Acker, ed. *Soil Residual Herbicides: Science and Management*. Topics in Canadian Weed Science, Vol.3
- [5] O'Sullivan, J. (2005). Grower-friendly bioassay for imazethapyr. Pages 81–88 in R. C. Van Acker, ed. *Soil Residual Herbicides: Science and Management*. Topics in Canadian Weed Science. Saine-Anne-de Bellevue, Quebec: Canadian Weed Science Society, Vol.3.

- [6] Milan, M., Ferrero, A., Fogliatto, S., Piano, S., Vidotto, F. (2015). Leaching of S-metolachlor, terbuthylazine, desethyl-terbuthylazine, mesotrione, flufenacet, isoxaflutole, and diketonitrile in field lysimeters as affected by the time elapsed between spraying and first leaching event. *Journal of Environmental Science and Health, Part B*, Vol. 50(12), 851-861.
- [7] Mendes, K., Martins, B., dos Reis, M., Pimpinato, R., Tornisiello, V. (2017). Quantification of the fate of mesotrione applied alone or in a herbicide mixture in two Brazilian arable soils. *Environmental Science and Pollution Research*, Vol. 24(9), 8425-8435.
- [8] Mitchell, G., Bartlett, D.W., Fraser, T.E.M., Hawkes, T.R., Holt, D.C., Townson, J.K., Wichert, R.A. (2001). Mesotrione: a new selective herbicide for use in maize. *Pest Management Science*, Vol. 57(2), 120-128.
- [9] Carles, L., Joly, M., Joly, P. (2017). Mesotrione Herbicide: Efficiency, Effects, and Fate in the Environment after 15 Years of Agricultural Use. *CLEAN - Soil, Air, Water*, 45(9).
- [10] Bartucca, M., Celletti, S., Mimmo, T., Cesco, S., Astolfi, S., Del Buono, D. (2017). Terbuthylazine interferes with iron nutrition in maize (*Zea mays*) plants. *Acta Physiologiae Plantarum*, Vol. 39:235.
- [11] European Food Safety Authority (EFSA) (2017). Peer review of the pesticide risk assessment for the active substance terbuthylazine in light of confirmatory data submitted. *EFSA Journal* (2017) 15(6):4868.
- [12] Stipičević, S., Galzina, N., Udiković-Kolić, N., Jurina, T., Mendaš, G., Dvorščak, M., Petrić, I., Barić, K., Drevenkar, V. (2015). Distribution of terbuthylazine and atrazine residues in crop-cultivated soil: The effect of herbicide application rate on herbicide persistence. *Geoderma*, Vol. 259-260, 300-309.
- [13] Johannesen, H., Aamand, J. (2003). Mineralization Of Aged Atrazine, Terbuthylazine, 2,4-D, And Mecoprop In Soil And Aquifer Sediment. *Environmental Toxicology and Chemistry*, 22(4).
- [14] European Food Safety Authority (EFSA). (2011). Conclusion on the peer review of the pesticide risk assessment of the active substance terbuthylazine. *EFSA Journal*, 9(1), 1969.
- [15] Commission Implementing Regulation (EU) No. 540/2011. (2011). Implementing Regulation (EC) No 1107/2009 of the European Parliament and of the Council as regards the list of approved active substances. *Off. J. Eur. Union*. <http://extwprlegs1.fao.org/docs/pdf/eur103357.pdf>

INVESTIGATION OF Cu_2O AS PHOTOCATHODE FOR P-TYPE DYE-SENSITIZED SOLAR CELLS

Marinela Miclau, Anamaria Dabici¹, Melinda Vajda¹, Narcis Duteanu², Daniel Ursu^{1*}

¹National Institute for Research and Development in Electrochemistry and Condensed Matter, 1 Plautius Andronescu Street, 300224 Timisoara, Romania
e-mail: danielhoratiu@yahoo.com

Abstract

In p-type dye-sensitized solar cells (p-DSSCs), NiO is the most commonly used p-type semiconductor [1]. Considering the drawbacks of NiO, alternative p-type semiconductors with better optical transparency, lower VB edge position and higher hole mobility are desired for p-DSSCs [2]. The cuprous oxide (Cu_2O) is a natively p-type semiconductor with a direct band gap of about 1.9–2.2 eV [3]. Non-toxic nature, the stability, natural abundance, low cost production, good electrical properties and a good absorption coefficient for visible light prompted to investigate the cuprous oxide as a material suitable for the realization of low cost and large scale p-DSSCs [4]. the nanoparticles have been intensively studied as photocathodes materials for DSSCs because of their larger specific surface areas to absorb more dye molecules. At the same time, the small-sized particles have shown that the inefficient ability to scatter the solar radiation which reduces the light-harvesting efficiency. Based on these premises, we propose to investigate the effect of micrometer-size structures on the photovoltaic performance of p-DSSCs based on cuprous oxide.

In this work, 3D hierarchical structure built of the micrometer dendritic rods and the porous truncated octahedrons have been successfully synthesized via a facile one-step hydrothermal methods using copper (II) acetate and ethyl cellulose as reactants. The DSSC based on the porous structure exhibits approximately 15% increase in J_{SC} and V_{OC} than 3D hierarchical structure.

XRD patterns of the Cu_2O_1 and Cu_2O_2 compound, obtained from hydrothermal method are shown in figure 1. All the diffraction peaks could be indexed as Cu_2O (cuprite) with cubic structure (space group: $Pn-3m$; JCPDS Nr. 01-074-1230), only a small amount of CuO is detected as impurity in Cu_2O_2 sample. The formation of CuO phase is determined by the time reaction which in the case of Cu_2O_2 is still small to establish completely Cu^{+1} oxidation state.

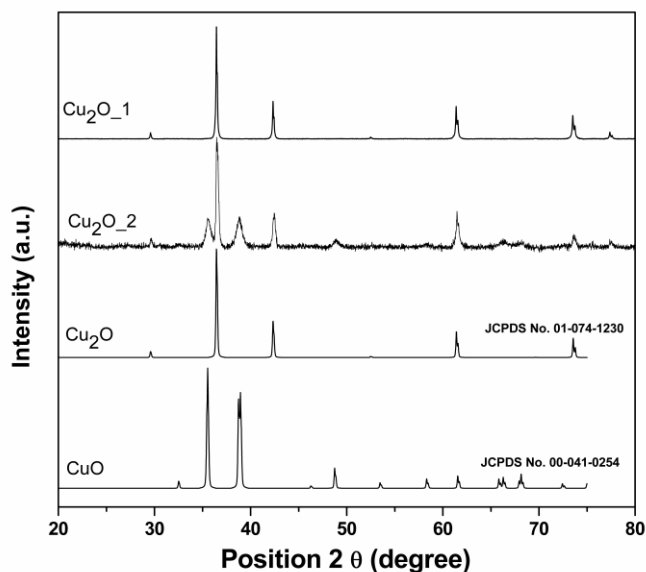


Figure 1. Room temperature X-ray diffraction patterns of Cu₂O₁ and Cu₂O₂ samples. The SEM image (figure 2a) of Cu₂O₁ powder shows the 3D hierarchical structure

The SEM image (figure 2a) of Cu₂O₁ powder shows the 3D hierarchical structure consisting of micrometer dendritic rods. In case of Cu₂O₂ sample, the SEM image (figure 2b) shows that the grains are in the shape of the porous truncated octahedron, partially covered by the microspheres.

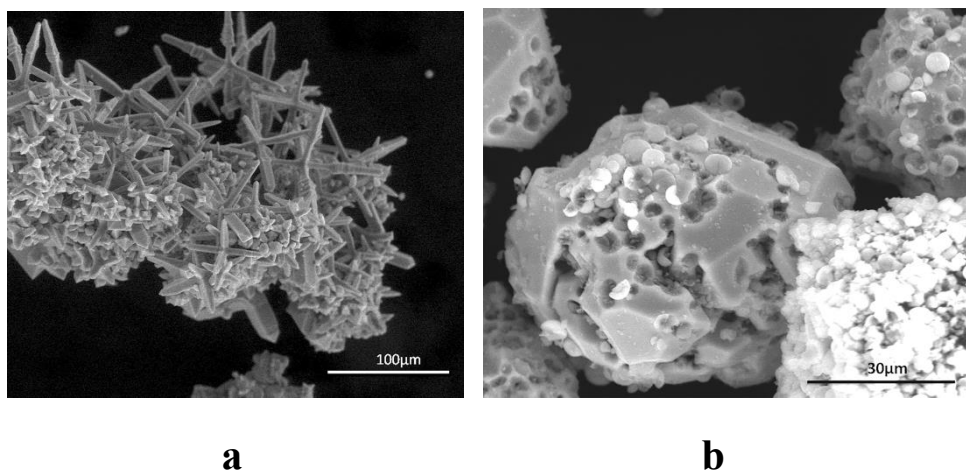


Figure 2. SEM images of Cu₂O₁ (a) and Cu₂O₂ (b) samples.

Indeed, I-V characteristics of DSSC (Fig. 3) show that the photovoltaic performance has improved in case of the porous structure, showing approximately 15% increase in J_{SC} and V_{OC} .

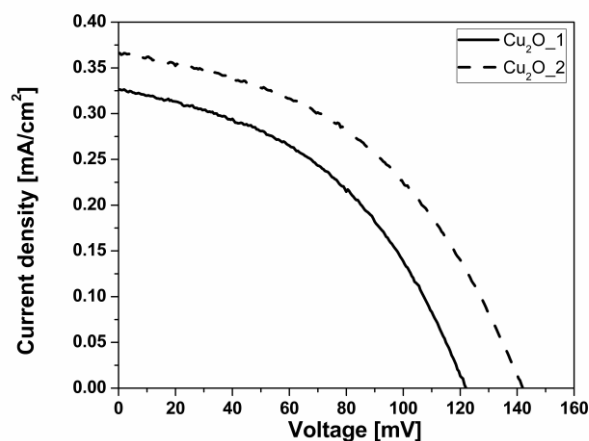


Figure 3. J-V curve of p-type DSSCs based on Cu₂O₁ and Cu₂O₂ samples.

Acknowledgements

This work was supported by a grant of the Romanian National Authority for Scientific Research and Innovation, CNCS/CCCDI - UEFISCDI, project number PN-III-P2-2.1-PED-2016-0526, within PNCDI III.

References

- [1] J. Bandara and J. Yasomanee, *Semicond. Sci. Technol.* 22 (2007) 20-24
- [2] T. Jiang, M. Bujoli-Doeuff, Y.Farré, Y. Pellegrin, E. Gautron, M.Boujtita, L. Cario, S. Jobic, F. Odobe, *RSC Adv.* 6 (2016) 112765-112770
- [3] K.H. Han, M. Tao. *Sol. Energy Mater. Sol. Cells* 93 (2009) 153-157
- [4] C. Wadia, A. P. Alivisatos, D. M. Kammen. *Environ. Sci. Technol.* 43 (2009) 2072-2079

REMOVAL OF ISOPROTURON FROM AQUEOUS SOLUTION BY ZSM-5 ZEOLITE

Ali Mohammed Hgeig¹, Mladenka Novaković¹, Maja Petrović¹, Ivana Mihajlović¹

¹University of Novi Sad, Faculty of Technical Sciences, Department of Environmental Engineering and Occupational Safety and Health, Trg Dositeja Obradovića 6, 21000 Novi Sad, Serbia

e-mail: ivanamihajlovic@uns.ac.rs

Abstract

ZSM-5 zeolite was used to remove isoproturon pesticide from aqueous solutions. The main parameters of adsorption process such as dosages of adsorbent, contact time and initial concentration of isoproturon were investigated. Adsorption equilibrium studies were carried out in batch systems. Results were modeled by adsorption isotherms: Langmuir, Freundlich and Temkin isotherms. The best correlation was achieved with Temkin adsorption isotherm. The maximum adsorption capacity of isoproturon calculated from the Langmuir isotherm was 4,12 mg g⁻¹ at room temperature. Adsorption kinetics of isoproturon has been studied by commonly used kinetic models, i.e., the pseudo-first-order model, the pseudo-second-order model and the intraparticle diffusion model. The kinetic modeling studies showed that kinetics of isoproturon on Zeolite ZSM-5 followed the model of pseudo - second order. This study proved that ZSM-5 zeolite could be used for the removal of isoproturon from aqueous media.

Introduction

Pesticides and herbicides, intentionally released into the environment, are ubiquitous in aquatic systems; they are often detected at low levels and commonly occur in the form of complex mixtures [1-2]. Leaching of chemical fertilizers and pesticides, applied to agricultural and forest land, is one of the main reasons for organic pollution in several water streams. Pesticides and herbicides are harmful to life because of their toxicity, carcinogenicity and mutagenicity [3].

Isoproturon, which belongs to phenylurea herbicides, is slowly degraded in water and quite persistent [4]. Although, there are so far no reported incidences of human poisoning, based on effects seen in animals, acute exposure to isoproturon would be expected to cause mild skin irritation and headaches, drowsiness, and lack of coordination. Thus, the efforts of many researchers have been focused on developing new and efficient remediation treatments to clean this phenylurea herbicide from the environment [4].

It has been proven that the adsorption is considered as an attractive method for the removal of different organic pollutants from environmental matrices due to its simplicity and ease of operation over other physical, biological and chemical technologies like precipitation followed by coagulation [5], membrane filtration [6-7] and photochemical degradation [8]. Natural adsorbents such as charcoal, clay minerals or zeolites are, in many instances relatively cheap, abundant in supply and have significant potential for modification of their adsorption capabilities.

The main propose of this study is to investigate the influence of factors such as contact time, mass of adsorbent ZSM-5 and initial concentration of selected pesticide isoproturon on the removal of isoproturon from aquatic media.

Material and methods

All chemicals used were of analytical grade. Stock standard solution of isoproturon (200 ppm) has been prepared by dissolving 5 mg of analytical standard in 25 mL of methanol. The stock solution was then appropriately diluted to get the test solutions.

All glassware were cleaned, then rinsed with deionised water and dried at 60 °C in a temperature controlled oven. Measurements were conducted at the room temperature (25 ± 2 °C). Zeolite ZSM-5 (manufacturer Acros Organics, Geel, Belgium) was used as adsorbent. Zeolite ZSM-5 has a very high temperature and acid stability (>1000 °C and down to pH=3, respectively). It is synthesized at high temperatures and pressures in an autoclave coated with Teflon and is characterized by low water solubility. Zeolite ZSM-5 is a type of a "high-silica"-Zeolite, which is responsible for most of its special properties. Total surface area (BET) of ZSM-5 is $390 \text{ m}^2\text{g}^{-1}$.

The experiments were carried out by varying concentrations of initial isoproturon solution, contact time and amount of adsorbent. Adsorption measurements were determined by batch experiments of known amount of the sample with 50 mL of aqueous isoproturon solutions in a series of 150 mL glass flasks. The mixtures were shaken at a constant temperature on orbital shaker at 140 rpm at room temperature for a given time. The suspensions were filtered and the filtrates were analyzed using HPLC-DAD (1260, Agilent Infinity). Separation was performed with a reversed phase column Eclipse XDB-C18 (3 x 150 mm, particle size $3.5\mu\text{m}$). The operating conditions were: the flow of 0.8 mLmin^{-1} , the temperature of the column was 25 C° and injection volume of $10 \mu\text{L}$. The isocratic separation with the ratio of mobile phases of 50:50 (water and acetonitrile) was used. The maximum wavelength of 255 nm was used for determination of isoproturon concentration. Retention time of isoproturon was 5 min.

Adsorbed amount, q_e (mg g^{-1}), was calculated via the equation:

$$q_e = \frac{(C_0 - C_f)}{m} * V \quad (1)$$

where q_e is the adsorption capacity (mg g^{-1}), C_0 and C_f are the initial and final isoproturon concentrations, respectively (expressed in mg L^{-1}), V is the solution volume (mL) and m is the adsorbent dosage (g).

The adsorption isotherms of isoproturon on zeolite were studied at room temperature, three widely used models: Langmuir, Freundlich and Temkin were applied for the fitting of the experimental data. The kinetic of the adsorption data was analyzed using three different kinetic models: the pseudo-first order, pseudo-second-order and intraparticle diffusion models.

The pseudo-first-order kinetic has been widely used to predict sorption kinetics, expressed by the following equation:

$$\log(q_e - q_t) = \log q_e - \left(\frac{k_1}{2.303}\right)t \quad (2)$$

where k_1 (1 min^{-1}) is the equilibrium rate constant of the pseudo-first order adsorption and it is determined from the plot of $\log(q_e - q_t)$ as a function of t .

The pseudo-second-order model can be represented in the following form:

$$\frac{t}{q_t} = \frac{1}{k_2 \cdot q_e^2} + \frac{1}{q_e}t \quad (3)$$

By plotting t/q_t versus t , q_e and k_2 can be determined from slope and intercept, where k_2 ($\text{g mg}^{-1} \text{min}^{-1}$) is the pseudo-second order rate constant.

The rate parameter of intraparticle diffusion can be defined as:

$$q_t = k_{id} \cdot t^{1/2} + C \quad (4)$$

where q_t is the amount of pesticide adsorbed at time t , C the intercept and k_{id} ($\text{mg g}^{-1} \text{min}^{-1/2}$) is the intraparticle diffusion rate constant.

Results and discussion

Influence of mass of ZSM-5 was studied with isoproturon concentration of 5 mgL^{-1} and contact time of 60 min. Different masses of zeolite were tested: 150, 200, 250, 300 and 350 mg. Results indicated the removal range from 90,6 to 92,7 %. There was no significant difference in removal efficiency and ZSM-5 mass of 150 mg was used for further analyses.

The adsorption kinetics of isoproturon was evaluated for the initial concentration of 5 mgL^{-1} and ZSM-5 mass of 150 mg. The mixing procedure was carried out with fixed speed (140 rpm) for the periods of 5, 10, 20, 30, 60 and 90 minutes. Removal efficiency ranged from 71.7 % to 91,2 % and increased with increasing of contact time till 60 min, then reached equilibrium. Three kinetic models were tested: pseudo first-order model, pseudo second-order model and intraparticle diffusion model (Table 1).

Table 1. Kinetic parameters for the adsorption of isoproturon onto ZSM-5

Pseudo-first order	q_e (mg g^{-1})	0.71
	k_1 (min^{-1})	0.06
	r	0.98
Pseudo-second order	q_e (mg g^{-1})	2.34
	k_2 ($\text{g mg}^{-1} \cdot \text{min}^{-1}$)	0.18
	r	0.99
Intraparticle diffusion	k_{id} ($\text{mg g}^{-1} \text{min}^{-1/2}$)	0.13
	C (mg g^{-1})	1.60
	r	0.92

From the obtained results, it could be concluded that adsorption kinetics of isoproturon on zeolite ZSM-5 could be explained by the pseudo second-order kinetic model.

Influence of initial pesticide concentration on removal of isoproturon from aqueous media was tested with concentrations of 2, 4, 5, 6, 8 and 10 mgL^{-1} , for 150 mg of zeolite and contact time of 60 min. The adsorption process was modeled by Freundlich, Langmuir and Temkin isotherms. Based on the obtained correlation coefficients, the fit of isoproturon adsorption on ZSM-5 is better with Temkin model than with Langmuir and Freundlich model. Figure 1. presents Temkin adsorption isotherm of isoproturon removal on zeolite. According to the Langmuir's model, adsorption capacity for isoproturon on ZSM-5, amounted to $4,12 \text{ mg g}^{-1}$.

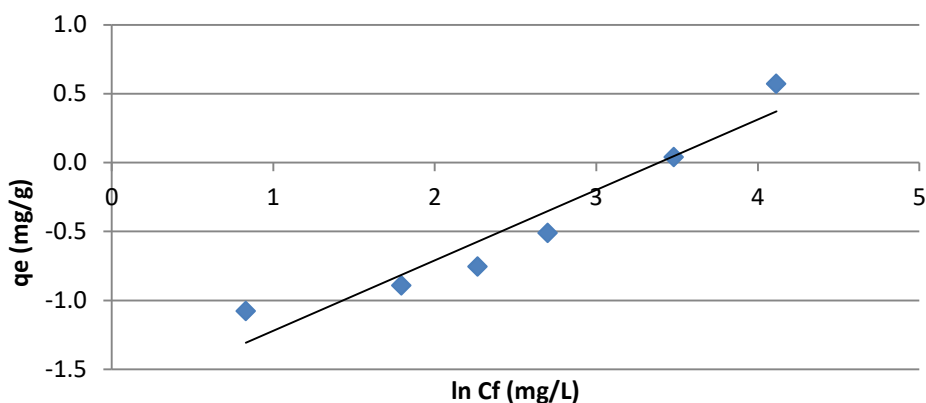


Figure 1. Temkin adsorption isotherm of isoproturon removal on ZSM-5

Conclusion

The ability of zeolite ZSM-5 to remove isoproturon from aqueous solution was investigated. In order to optimize removal process, some of main conditions were taken into account such as: initial concentration of isoproturon, contact time and mass of adsorbent ZSM-5. Those parameters were modeled by Langmuir, Freundlich and Temkin isotherms. The equilibrium studies proved that Temkin isotherm model best describes the adsorption of isoproturon on zeolite. The kinetic modeling studies showed that kinetics of isoproturon on zeolite ZSM-5 followed the model of pseudo - second order. This model includes the assumption that the binding of the particles to the adsorbent surface occurs by establishing specific chemical bonds. From the results of the present work, it can be said that ZSM5 showed quite good capabilities in removing isoproturon pesticide from water.

Acknowledgements

Authors would like to thank Ministry of Education, Science and Technological Development of the Republic of Serbia for financial support (Project No. III46009). Ali Mohammed Hgeig would like to thank the Ministry of Higher Education in Libya for his PhD grant supporting this research.

References

- [1] F. W. Shaarani, B. H. Hameed. *Desalination* 255 (1), 2010, pp. 159-164.
- [2] R.J. Gilliom, *Environmental Science and Technology* 41 (10), 2007, pp. 3408-3414.
- [3] C. Zhang, Q. Wang, J. Chen, L. Huang, X. Qiao, X. Li, X. Cai., *Environmental pollution* 159 (2), 2011, pp. 609-615.
- [4] H. Mendoza, L. Humberto, *Journal of Chemistry*, 2015.
- [5] J. Zolgharnein, S. Ali, G. Jahanbakhsh, *Clean – Soil, Water* 39 (12), 2011, pp.1105-1119.
- [6] S. Farrukh, A. Hussain, N. Iqbal, *Desalin Water Treat* 52 (2014), pp. 1833-1840.
- [7] Y.R. Qiu, L.J. Mao, *Desalination*, 329 (2013), pp. 78 -85.
- [8] V.A: Sakkas, M.A. Islam, C. Stalikas, T. Albanis, *J.Hazard. Mater* 175 (2010), pp. 33-44.

OVERVIEW OF THE PREVIOUS STUDIES ABOUT WASTE GLASS UTILIZATION IN CERAMIC BRICKS AND TILES

Zorica Miroslavljevic¹, Dragana Strbac¹

¹*University of Novi Sad, Faculty of Technical Sciences, Department of Environmental Engineering*

e-mail: zoricavojnovic@uns.ac.rs

Abstract

Paper presents a literature review relating to the potential waste glass collection and processing as glass cullet (crushed waste glass) for its use as raw material in brick and ceramic tile production. The analysis and evaluation of the vast amount of experimental research showed that glass cullet is a potentially valuable resource for the manufacture of ceramic products, such as clay fired bricks and tiles, where it can be used as substitute for expensive natural resources, improving the physical, mechanical and environmental performance of ceramic products.

Introduction

Production of ceramic – clay products, especially brickyard production, is a significant production of basic construction materials required in all spheres of constructional activities. Bricks are bonded together with mortar to yield a composite building component generally a wall. Concrete block and brick are the most common types of brickyards production. These construction materials are extensively employed worldwide both in developed and developing countries.

Construction ceramic – clay materials are very important materials for building and for them the need is constantly growing. In this respect, for the development of ceramic products with waste materials, further research and development is necessary, not only on the technical, economic and environmental features, but also public education related to waste reusing and sustainable development is required for wide production and application of ceramic product with waste materials. Clay materials are mostly used for the manufacture of bricks and ceramic tiles and waste can be added in order to enhance their properties [1]. Solid waste is a great concern among governmental agencies, and environmentalist regarding the increasing amount of waste throughout the world [2].

One waste material which has potential as a ceramic product's additive is waste glass [3]. Waste glass is not biodegradable and because of that creates a problem for solid waste disposal [4]. The disposal into landfills, also, does not provide an environment – friendly solution [5]. For example, waste glass in construction materials can be a worthy solution to the environmental problem caused by this solid waste [2]. United Nations estimates that the volume of annually solid waste amount which is disposed of over the world would be 200 million tons, and 7% of that is made up of glass [6].

Ceramic – clay materials, which are manufactured at high temperatures into non-metallic and inorganic solid products, are used in several fields of engineering, due to their specific properties. As a result of the wide range of existing ceramic applications and the manufacturing process involving high temperatures, ceramic products are ideal candidates for the incorporation of waste glass as glass cullet (crushed glass) a substitute of natural resources [1].

The main objective of this paper is to focus on the analysis and on the evaluation of the experimental research which are showed that glass cullet is a potentially valuable resource for

the manufacture of ceramic products, where it can be used as substitute for natural resources, and also improving physical, mechanical and environmental ceramic product performances.

Methodology

In the period since 2002, more recent research has been carried out around the world that have studied and summarized how to use waste glass as a potential resource in the production of ceramic products in order to improve the product's properties. The use of waste glass in various mass percentages in a mixture with clay is shown in order to prepare high quality ceramic products.

The first step in preparing the review of previous studies of using waste glass in ceramic products was collection of an initial list of publications, based on various factors, like: type of waste glass as substitute; particle size of glass cullet; application in which it was used and available data adequate for statistical analysis which are showed on Figure 1.



Figure 1. Evaluation of various factors for using waste glass in ceramic – clay products

On the basis of examination and selection of certain literature, the second step in the paper research involved the separation of the basic properties of ceramic products with glass cullet and their analysis, according to the type of waste glass and application, particle size of glass cullet and its mass percentage. It is investigate the effect of the addition of waste glass on the properties of the fired ceramic products. Considered properties of ceramic products with a certain mass percentage of glass cullet are:

1. Firing shrinkage;
2. Firing temperature;
3. Strength properties;
4. Water absorption and porosity;
5. Durability.

Recently, reviewing collected literature, several researches around the world have been carried out summarizing the use of waste glass as additives for ceramic tile and fired clay bricks to enhance its properties. The waste glass can be mixed with clay in different proportions to prepare high quality ceramic product. The addition of waste glass to ceramic product specimen range from 0.5 to 94% by mass, most studied tended to concentrate on range between 5% and 20% of glass by mass, with the glass particle size ranging from 45 to 600 μm .

Results and discussion

During the literature review, it was observed that different types of glass were used as a resource in the production of ceramic – clay products which summarized within Table 1.

Table 1. Different types of waste glass used as a resource in the production of ceramic – clay products (fired clay bricks, tiles and stoneware) by literature review

Type of waste glass	Application	Literature
Ground waste glass	Fired clay bricks	[7]; [3]; [8].
Waste glass from structural glass walls	Fired clay bricks	[9].
Container glass cullet	Fired clay bricks	[10]; [11].
Used waste broken bottles	Ceramic tiles	[12].
Non – recycled waste glass additives	Fired clay bricks	[13].
Funnel and panel glass of TV and PC waste glass	Clay bricks and roof tiles	[14].
Wastes glass from thin film transistor – liquid crystal display (TFT-LCD) optical waste glass (TVs and computers)	Eco – brick	[15].
TV/PC cathodic tube and screen glass	Typical porcelain stoneware body	[16].

Authors of literature number [17] concluded that there was no major difference between window glass and post-consumer glass being utilized in clay products, and other types of glass addition to ceramic products has also contributed to enhance their properties.

Discussion of the results of testing the properties of ceramic product with a waste glass mass fraction obtained in the considered research framework are presented in Table 2.

Results of the strength properties of specimens containing waste glass in previous studies were determined by both compressive strength and modulus of rupture testing. The range of compressive strength values varied between specimens, which may be attributed to slight variations in particle size, specimen size, and firing temperature for each testing method.

Results reported for examples of rupture demonstrate an increase in modulus of rupture with increased percentage of glass by mass ([11], [12], [14], [15], [16], [18], [19]). In the literature [18] was studied the influence of particle size, plasticity and pressing pressure on the properties of a ceramic products containing 90% by mass of recycled waste glass. The result shown that a progressive increase in the proportion of fines in the sample results in a progressive increase in the degree of sintering, as reflected in increased strength.

Table 2. Properties of ceramic bricks and tiles through the considered literature

Properties of ceramic products with waste glass	Description	Literature
Shrinkage	Shrinkage was found to increase as percentage glass by mass increased, as well as with increased firing temperature. The finer glass, particle size of 5 μm , exhibited twice the shrinkage of the coarse glass, particle size of 150 μm , in compositions.	[3]; [9]; [11]; [12]; [13]; [15]; [16]; [17]; [19].
Firing temperature	The use of 10 % by mass of waste glass and firing at 900°C yielded bricks with similar strength compared to that of normal clay brick fired at 1000°C.	[17]. [8].
Strength properties	Results indicates an increase in compressive strength with increased addition of waste glass, especially between 10% and 30% by mass. The amorphous phase of waste glass particles enhances the sintering action, which leads to achieving a better strength in bricks. Rapid increase in compression strength in samples containing glass powder with particle size of 140 – 315 μm .	[3], [7], [8], [9], [10], [13], [15], [18]. [3]. [10].
Water absorption and porosity	Decrease as percentage glass by mass increased, as well as with increased firing temperature. Water absorption as low as (2-3) % was achieved for bricks containing (15–30) % by mass of waste glass and fired at 1100°C. When the glass waste content was 45 % by weight, porosity and water absorption was rapidly increased. With smaller particle size of glass, this problem can be avoided.	[3], [7], [8], [9], [10], [11], [12], [15], [16], [17], [18], [19]. [9].
Durability	When water infiltrates into the clay brick, it decreases the durability. Results of the absorption coefficient testing, which is often a means of estimating durability, suggested an increase in durability with increasing waste glass addition.	[3]. [3], [10], [13].

Conclusion

Analyzed researches within the literature showed that lots of efforts have been done for investigating the effect of using waste glass materials as an additive in the fired clay bricks and ceramic tiles, but all of them are trying to conform to the relevant specifications in their local areas. Also, according to the literature review conclusion is that by using glass cullet, as fluxing agent, it is possible to achieve the desired shrinkage at lower temperatures, which may result in increased production rates and lower production costs. This leads to the need for more extensive research to prove it.

References

- [1] R.V. Silva, J. de Brito, C.Q. Lye b, R.K. Dhir, J. Cleaner Prod. (2017) 167, pp. 353.
- [2] H. H. Abdeen, Master Thesis: Properties of Fired Clay Bricks Mixed with Waste Glass, (2016), pp. 16.
- [3] I. Demir, Waste Manage. Res. (2009) 27, pp. 572 – 577.
- [4] H. T. Christensen, Solid Waste Technology & Management Volume 1., 1st ed. (2011) Wiley-A John Wiley and Sons, Ltd., Publisher: The Atrium, Southern Gate, Chichester, West Sussex, United Kingdom, pp. 211-213.
- [5] Z. Mirosavljević, V. Mihajlović, D. Štrbac, I. J. Eng. (2013) 3, pp. 333.
- [6] I. B. Topcu, M. Canbaz, Cem. Concr. Res. (2004) 34, pp. 267–274.
- [7] N. F. Youssef, M. F. Abadi, M. A. O. Shater, J. Euro. Ceram. Soc. (1998) 98, pp. 1721 – 1727.
- [8] N. Phonphuak, S. Kanyakam, P. Chindaprasirt, J. Cleaner Prod. (2016) 112, pp. 3057 – 3062.
- [9] V. Loryuenyong, T. Panyachai, K. Kaewsimork, C. Siritai, Waste Manage. (2009) 29, pp. 2717 – 2721.
- [10] V. A. Leshina, A. L. Pivnev, Glass Ceram. (2002) 59, pp. 356 – 358.
- [11] F. Matteucci, M. Dondi, G. Guarini, Ceram. Int. (2002) 28, pp. 873–880.
- [12] S. Mustafi, M. Ahsan, A. H. Dewan, S. Ahmed, N. Khatun, N. Absar, Bangladesh J. Sci. Res. (2011) 24, pp. 169 – 180.
- [13] S.E. Chidiac, L.M. Federico, Can. J. Civ. Eng. (2007) 34, pp. 1458 – 1466.
- [14] M. Dondi, G. Guarini, M. Raimondo, C. Zanelli, waste Manage. (2009) 29, pp. 1945 – 1951.
- [15] K. Lin, J. Cleaner Prod. (2007) 15, pp. 1755 – 1759.
- [16] M. Raimondo, C. Zanelli, F. Matteucci, G. Guarini, M. Dondi, J.A. Labrincha, Ceram. Int. (2007) 33, pp. 615–623.
- [17] J. Hwang, X. Huang, A. Garkida, A. Hein, J. Mineral. Mater. Charact. Eng. (2006) 5, pp. 119 – 129.
- [18] I. W. M. Brown, K. J. D. Mackenzie, J. Mater. Sci. (1982) 17, pp. 2171 – 2183.
- [19] A.P. Luz, S. Ribeiro, Ceram. Int. (2007) 33, pp. 761–765.

EFFECTS OF HEAVY METALS ON EARLY GROWTH OF AFRICAN MARIGOLD (*Tagetes erecta*), FRENCH MARIGOLD (*Tagetes patula*) and SIGNET MARIGOLD (*Tagetes tenuifolia*)

Dávid Mónok, Levente Kardos, György Végvári

*Department of Soil Science and Water Management, Faculty of Horticultural Science, Szent István University, Budapest, Villány út 29-43, Hungary
e-mail: monokdavid27@gmail.com*

Abstract

Heavy metals in soils cause human health and environmental risks, therefore remediation of heavy metal contaminated sites is an important issue. Marigolds have been proposed as potential plants for phytoremediation of this type of contamination. In our experiment a seed germination test was carried out to investigate the toxic effects of heavy metals (Cu, Zn and Pb) on early growth of three different marigold species (African marigold, French marigold and Signet marigold). According to our results all tested heavy metals had significant ($p < 0.05$) toxic effects on seed germination and root/shoot elongation of the three plants. Signet marigold was the most sensitive plant to heavy metals, while African marigold and French marigold were able to tolerate low concentration of metals (below 400 mg l^{-1}) without considerable decline in growth parameters. These results indicate that African marigold and French marigold could be suitable for remediating heavy metal (Cu, Zn and Pb) contaminated soils.

Introduction

Heavy metals can accumulate in the topsoil at relatively high concentrations [1,2]. Previous studies have shown that heavy metals in soil pose potential threats to the environment, because in excessive concentrations they can be toxic to living organisms and endanger the health of humans and animals through the food chain [2,3,4]. For this reason, increasing attention has been paid in recent years to the phytoremediation of heavy metal contaminated soils, which is a cost-effective, environmental friendly and sustainable technique for restoration of these sites [1,4,5,6]. Applying ornamental plants for phytoremediation could be useful, especially in contaminated urban areas, since they are apart from the food chain, and they can beautify the environment [4,6,7]. Marigolds are commonly used as ornamental plants, and have been proposed as potential plants for phytoremediation of heavy metal contaminated soil [5,7,8,9,10]. Although much research has been conducted to investigate the bioaccumulation ability of marigolds, little information is available on the toxicity of metals on these plants. However high levels of metals can reduce plants biomass, which decrease its remediation potential [4]. The aim of our study was to compare the effects of selected metals (Cu, Zn and Pb) on seed germination and shoot/root elongation of marigold species.

Experimental

Three different marigold species were used in our experiment: African marigold (*Tagetes erecta*), French marigold (*Tagetes patula*) and Signet marigold (*Tagetes tenuifolia*). Seeds were obtained from Rédei Kertimag Ltd. Heavy metal concentrations in the test solution were 0, 50, 100, 200, 400, 800, 1600, 3200, 6400 mg l^{-1} , and they were added as $\text{CuSO}_4 \cdot 5\text{H}_2\text{O}$, $\text{ZnSO}_4 \cdot 7\text{H}_2\text{O}$ and $\text{Pb}(\text{NO}_3)_2$. Chemicals were obtained from Reanal Laboratory Chemicals LLC.

The experimental procedure consisted of the following parts: 3 g cotton-wool was placed in plastic pots and twenty-five seeds were laid on each cotton-wool pads. The pads were moistened with approx. 50 ml test solution with a specific heavy metal concentration, and each pots were sealed with cellophane and set under a photoperiod of 12 h light and 12 h dark, and 25 ± 1 °C temperature. After six days, the number of germinated seeds was recorded, and root/shoot elongation were measured.

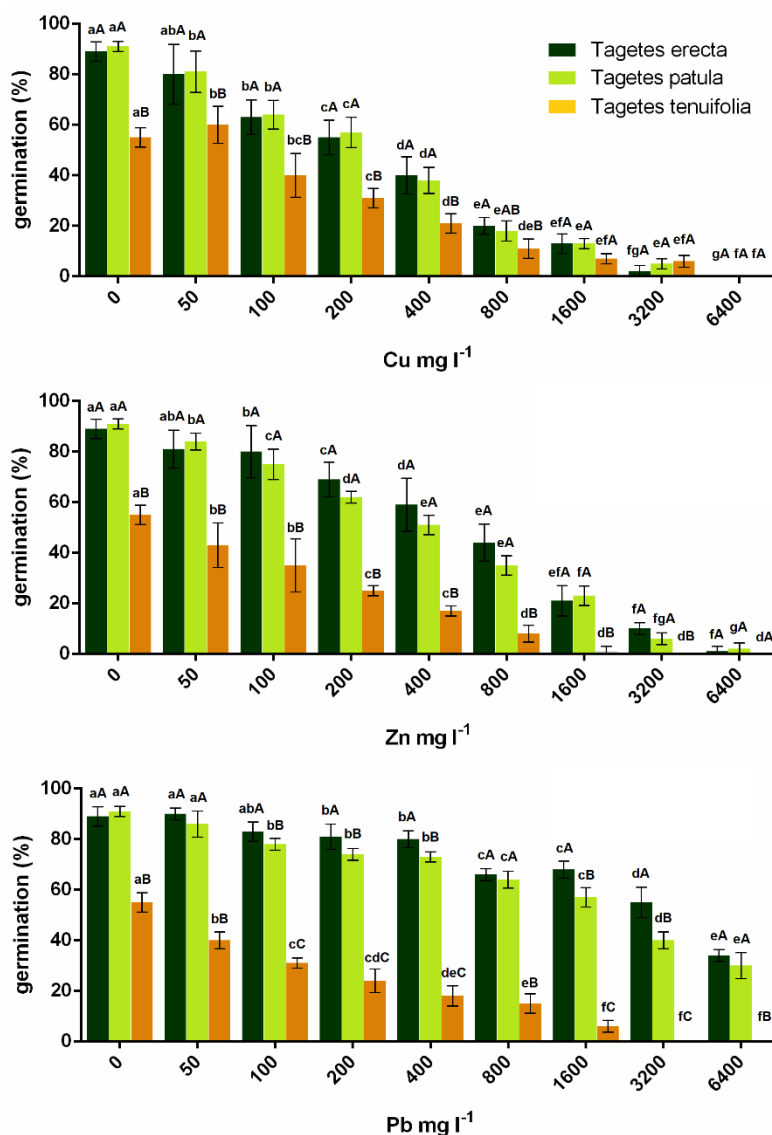
The experiment was conducted in a completely randomized design with four replications. The data were recorded as means \pm standard deviations and analyzed by Graphpad Prism 6. Two-way analysis of variance (ANOVA) and Tukey multiple comparisons were carried out to test for any significant differences (at 95% significance level) between the means. In figures the same small letter above the column means there is no significant difference at different heavy metal concentration, and the same capital letter means there is no significant difference among plants.

Results and discussion

Increasing concentration of heavy metals in the test solution significantly ($p < 0.05$) decreased the germination rates of all tested species (Fig. 1.). Signet marigold had significantly ($p < 0.05$) lower germination rates than African marigold and French marigold in all heavy metal treatments except for above 800 mg Cu l⁻¹ concentration. At 50 mg Cu l⁻¹ concentration there was a slightly increase in germination rate of Signet marigold, however all three plants had less germination rate at 100 Cu mg l⁻¹ compared with control. At 6400 mg Cu l⁻¹ germination was not observable. Zn also significantly decreased germination rates firstly at 100 mg l⁻¹ concentration, however the decline in germination rates of African marigold and French marigold was less than Cu in all concentrations. On the contrary, Zn was the most toxic heavy metal to Signet marigold. Pb had the least toxic effects on germination of African marigold and French marigold. Signet marigold was more sensitive to Pb than the other plants, and it was not germinated above 1600 mg Pb l⁻¹.

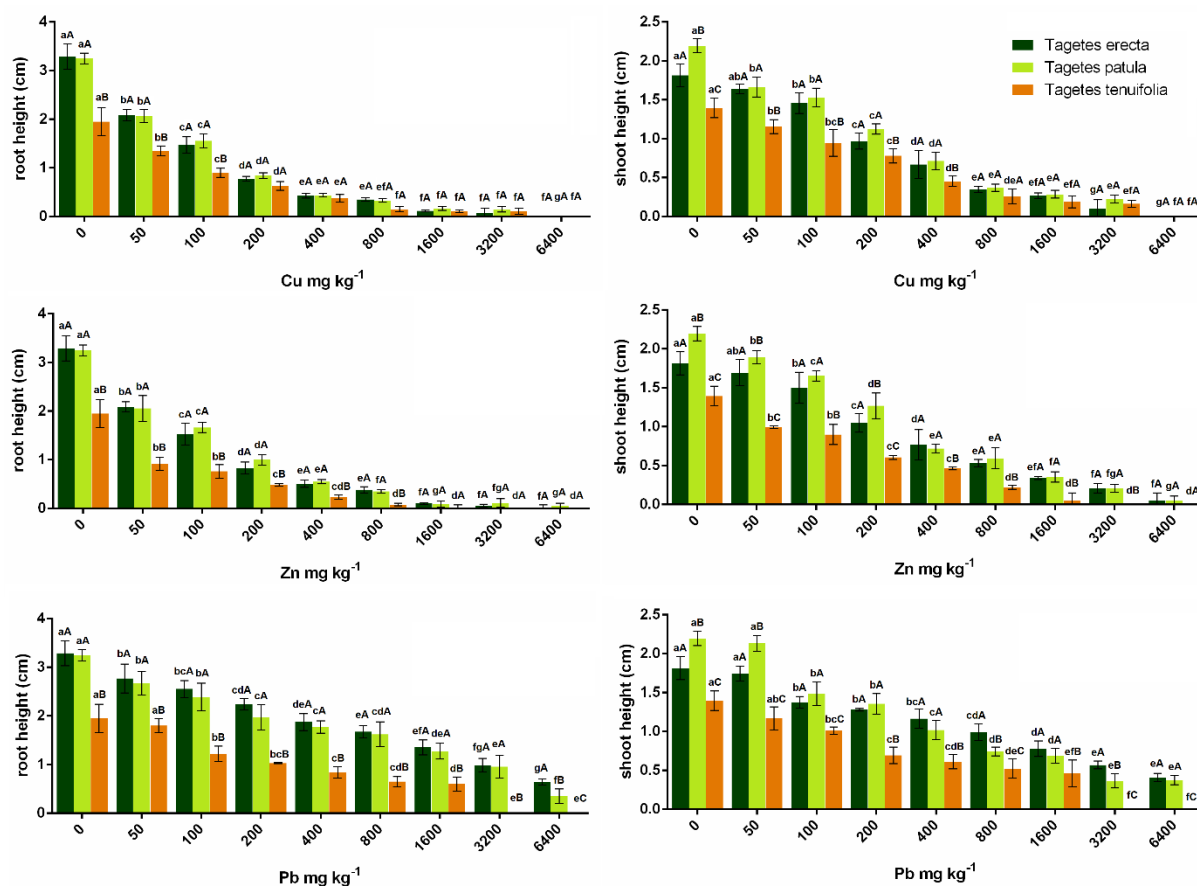
All tested heavy metals had a significant toxic effect ($p < 0.05$) on root lengths and shoot heights of the three plants (Fig. 2.). Signet marigold had significantly ($p < 0.05$) lower root lengths and shoot heights than African marigold and French marigold except for above 100 mg Cu l⁻¹ and 1600 mg Zn l⁻¹ concentrations. Toxic effects on root elongation was firstly observed at the least concentration (50 mg l⁻¹) of all tested metals. Cu was the most toxic heavy metal to root lengths, since 100 mg Cu l⁻¹ caused more than 50% decline in this growth parameter. Zn decreased root lengths by 50% at 200 mg Zn l⁻¹, while Pb decreased root lengths by 50% only at 800 mg Pb l⁻¹. Less toxic effects were observable on shoot elongation compared with the results of root elongation. Cu and Zn decreased shoot heights by 50% firstly at 400 mg l⁻¹ concentration. Shoot heights of French marigold and Signet marigold is decreased by 50% at 400 mg Pb l⁻¹, while only 1600 mg Pb l⁻¹ reduced shoot heights of African marigold at such a rate. Interestingly at 50 mg Pb l⁻¹ French marigold had significantly higher shoot heights than African marigold, however at 800 and 3200 mg Pb l⁻¹ African marigold had higher shoot heights.

Figure 1. Germination rates of marigolds.



The results showed that heavy metals caused significant ($p < 0.05$) decline in the growth parameters of the three plants. It is expected, because plant seeds were in direct contact with the toxicity of heavy metals in the test solution, and inhibition effects of heavy metals on growth parameters of African marigold has been also observed in previous studies [5,8,9,11]. Heavy metals had greater adverse effects on plant root lengths than on shoot heights. Inhibition of root elongation is known to be a more sensitive indicator to metal toxicity, since roots are the responsible for absorption and accumulation of metals [3,4,12]. Based on our results, Signet marigold is the most sensitive plant to the tested heavy metals among the three species. Between the effects of metals on African marigold and French marigold, no considerable differences were observed, however African marigold was more tolerant to high levels of Pb. Between the tested heavy metals the following series of phytotoxicity was observed in our experiment: Cu>Zn>Pb for African marigold and French marigold, and Zn>Cu>Pb for Signet marigold.

Figure 2. Root lengths and shoot heights of marigolds.



Conclusion

It was concluded that Signet marigold was very sensitive to the tested heavy metals, therefore only African marigold and French marigold can be used to remediate heavy metal (Cu, Zn and Pb) contaminated soils. These two plants can tolerate low concentration of metals (below 400 mg l⁻¹) without considerable decline in growth parameters. Marigolds may tolerate higher levels of heavy metals in natural environment, since the seeds were germinated in hydroponic solution during the experiment, which is quite different from natural soils. In soils metals could be tied up in insoluble forms, and they are less available to plants [13]. Although hydroponic experiments have very limited relevance to the natural environment, these research can be useful in demonstrating the tolerance of marigolds to Cu, Zn and Pb [14].

Acknowledgements

This research has been supported by the ÚNKP-18-3-I-SZIE-38. New National Excellence Program of the Ministry of Human Capacities, Hungary.

References

- [1] Wu, G., Kang, H., Zhang, X., Shao, H., Chu, L., Ruan, C. (2010). A critical review on the bio-removal of hazardous heavy metals from contaminated soils: issues, progress, eco-environmental concerns and opportunities. *Journal of Hazardous Materials*, 174(1-3), 1-8.
- [2] Liu, X., Song, Q., Tang, Y., Li, W., Xu, J., Wu, J., Brookes, P. C. (2013). Human health risk assessment of heavy metals in soil–vegetable system: a multi-medium analysis. *Science of the Total Environment*, 463, 530-540.
- [3] Nagajyoti, P. C., Lee, K. D., Sreekanth, T. V. M. (2010). Heavy metals, occurrence and toxicity for plants: a review. *Environmental chemistry letters*, 8(3), 199-216.
- [4] Liu, J., Xin, X., Zhou, Q. (2017). Phytoremediation of contaminated soils using ornamental plants. *Environmental Reviews*, 26(1), 43-54.
- [5] Lal, K., Minhas, P. S., Chaturvedi, R. K., Yadav, R. K. (2008). Extraction of cadmium and tolerance of three annual cut flowers on Cd-contaminated soils. *Bioresource technology*, 99(5), 1006-1011.
- [6] Liu, J. N., Zhou, Q. X., Sun, T., Ma, L. Q., Wang, S. (2008). Identification and chemical enhancement of two ornamental plants for phytoremediation. *Bulletin of environmental contamination and toxicology*, 80(3), 260-265.
- [7] Nakbanpote, W., Meesungnoen, O., Prasad, M. N. V. (2016). Potential of ornamental plants for phytoremediation of heavy metals and income generation. In *Bioremediation and bioeconomy* (pp. 179-217).
- [8] Goswami, S., Das, S. (2017). Screening of cadmium and copper phytoremediation ability of *Tagetes erecta*, using biochemical parameters and scanning electron microscopy–energy-dispersive X-ray microanalysis. *Environmental toxicology and chemistry*, 36(9), 2533-2542.
- [9] Wang, X. F., Zhou, Q. X. (2005). Ecotoxicological effects of cadmium on three ornamental plants. *Chemosphere*, 60(1), 16-21.
- [10] Bosiacki, M. (2009). Phytoextraction of cadmium and lead by selected cultivars of *Tagetes erecta* L. Part II. Contents of Cd and Pb in plants. *Acta Sci. Pol., Hortorum Cultus*, 8(2), 15-26.
- [11] Shah, K., Mankad, A. U., Reddy, M. N. (2017). Lead Accumulation and its Effects on Growth and Biochemical Parameters in *Tagetes erecta* L. *Int. J. Life. Sci. Scienti. Res*, 3(4), 1142-1147.
- [12] Araújo, A. S. F., Monteiro, R. T. R. (2005). Plant bioassays to assess toxicity of textile sludge compost. *Scientia Agricola*, 62(3), 286-290.
- [13] Ghosh, M., Singh, S. P. (2005). A review on phytoremediation of heavy metals and utilization of it's by products. *Asian J Energy Environ*, 6(4), 18.
- [14] Van der Ent, A., Baker, A. J., Reeves, R. D., Pollard, A. J., Schat, H. (2013). Hyperaccumulators of metal and metalloid trace elements: facts and fiction. *Plant and Soil*, 362(1-2), 319-334.

APPLICATION OF MOLECULAR MACHINES IN PHOTOELECTROCHEMISTRY

Mirela I. Iorga¹, Mihai V. Putz^{1,2,*}

1. Laboratory of Renewable Energies-Photovoltaics, R&D National Institute for Electrochemistry and Condensed Matter –INCEMC–Timisoara

2. Laboratory of Structural and Computational Physical-Chemistry for Nanosciences and QSAR, Biology-Chemistry Department, West University of Timisoara

() Correspondent author: MVP: mv_putz@yahoo.com, mihai.putz@e-uvr.ro*

Abstract

The paper presents an original integrated photo-electro-chemistry algorithm developed by the authors for the possibilities of application of molecular machines in photoelectrochemistry. Concerning molecular machines, five main directions have been approached: the representation of the studied system through computational programs, the calculation of reaction parameters based on HSAB principle, estimation of Coulomb blockade, predictions on the bondonic photovoltaic effect by bondonic spectral correlations, calculations of the thermodynamic indices of interconversion through the path integral formalism, and estimations about the corresponding binary logical systems.

Introduction

The current trend is to reduce as much as possible the size and weight of parts of devices and machines, with the aim of performing more and more complicated operations with much smaller pieces [1]. Through the combination between the high precision of chemical synthesis and engineering ingenuity, the "bottom-up" molecule-to-molecule approach offers unlimited opportunities for the design and construction of supramolecular nanoscale structures [2].

The design and construction of prototypes [1, 3] for molecular devices, machines and motors is based on natural processes and systems and brings together various branches of science such as supramolecular chemistry, engineering or the latest breakthroughs of synthetic chemistry. The vast majority of engineered molecular machines so far is based on interconnected molecular species such as rotaxanes, catenane and related species [4, 5, 6, 7].

The essential features of rotaxanes and catenanes derive from non-covalent interactions between their components that contain complementary recognition centers. Rotaxanes are prototypes suitable for the construction of both linear and rotary molecular machines. The typical implementation of rotaxanes for molecular machines is the development of molecular shuttles with ring translational movements [8, 9]. This type of molecular machines has a well-organized structure and has to function as multicomponent systems with a proper functional integration [3, 10].

The major importance of such systems is also confirmed by the fact that in 2016 the *Nobel Prize for Chemistry* was awarded to researchers Jean-Pierre Sauvage, Sir J. Fraser Stoddart and Bernard L. Feringa "for the design and synthesis of molecular machines" [11].

Results and discussions

In the present paper the [2]rotaxane $1H^{3+}$ [12, 13] was chosen as the working system, consisting of a dibenzo[24]crown-8 ether (DB24C8), a π -electron-donor macrocycle, and a dumbbell component containing a secondary ammonium center ($-NH_2^+$) and a 4,4'-bipyridinium (bpy^{2+}) unit. The stoppers are an anthracene moiety on one side and a 3,5-di-tert-butylphenyl group on the other side. Because the charge-transfer (CT) interaction of the p-electron-donor macrocycle with the p-electron-acceptor bpy^{2+} unit is much weaker than the

$[N^+ \cdots H \cdots O]$ hydrogen-bonding interactions between the DB24C8 macrocycle and the ammonium center, the [2]rotaxane $1H^{3+}$ will have the stable co-conformation [14] when the macrocycle surrounds the ammonium station, as represented in **Figure 1** by the $1AH^{3+}$ structure. If a base is added, in this case, tributylamine, the ammonium center is converted into an amine function, and the transient state $1A^{2+}$, after the displacement of the macrocycle onto the bpy^{2+} unit is transformed into a stable state $1B^{2+}$. The reverse process can take place if an acid is added, in this case, trifluoroacetic acid, and the system goes to the initial state through the transient state, $1BH^{3+}$. In the case of the deprotonated rotaxane, through one-electron reduction of the bipyridinium unit, the CT interactions are destroyed, and the macrocyclic ring can be displaced from the bpy^{2+} station.

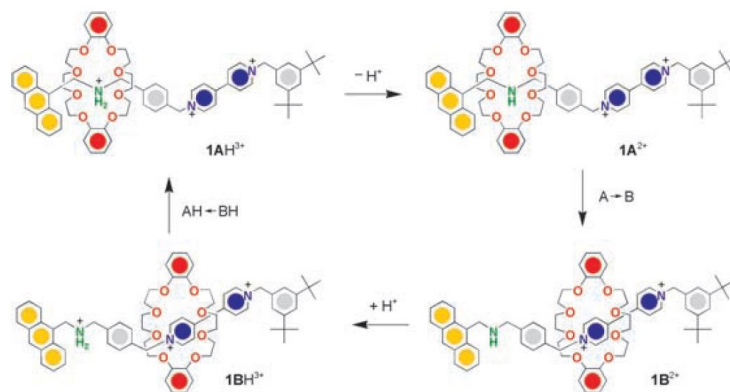


Figure 1. Schematic representation of the shuttling processes of the crown ether ring upon deprotonation and reprotonation of the ammonium site [13]

The structures of the studied rotaxane (initial, transient and final) during the molecular shuttling process were represented in HyperChem and are presented in **Figure 2**.

Based on the “Hard and Soft Acids and Bases” (HSAB) principle, chemical reactivity, transfer energy, and other parameters are calculated. HSAB principle is an important conceptual principle to treat the molecular binding and reactive processes. Writing the energy variation at transfer under the following forms:

$$\Delta E = \Delta\Omega_A + \Delta\Omega_B \quad (1)$$

$$\Delta\Omega_A = -\frac{\eta_A}{4(\eta_A + \eta_B)^2} (\Delta\chi)^2 \quad (2)$$

$$\Delta\Omega_B = -\frac{\eta_B}{4(\eta_A + \eta_B)^2} (\Delta\chi)^2 \quad (3)$$

$$\Delta\chi = \chi_A - \chi_B \quad (4)$$

the optimal energetic transfer will imply, for instance, the minimization of $\Delta\Omega_A$ respecting η_A , in conditions in which $\Delta\chi$ and η_B are maintained constant.

Therefore, the condition to achieve the optimum transfer results to be: $\eta_A = \eta_B$ implying the fact that the species with a high chemical hardness prefer the coordination with species that are high in their chemical hardness, and respectively the species with low softness (the inverse of the chemical hardness) will prefer reactions with species that are low in their softness.

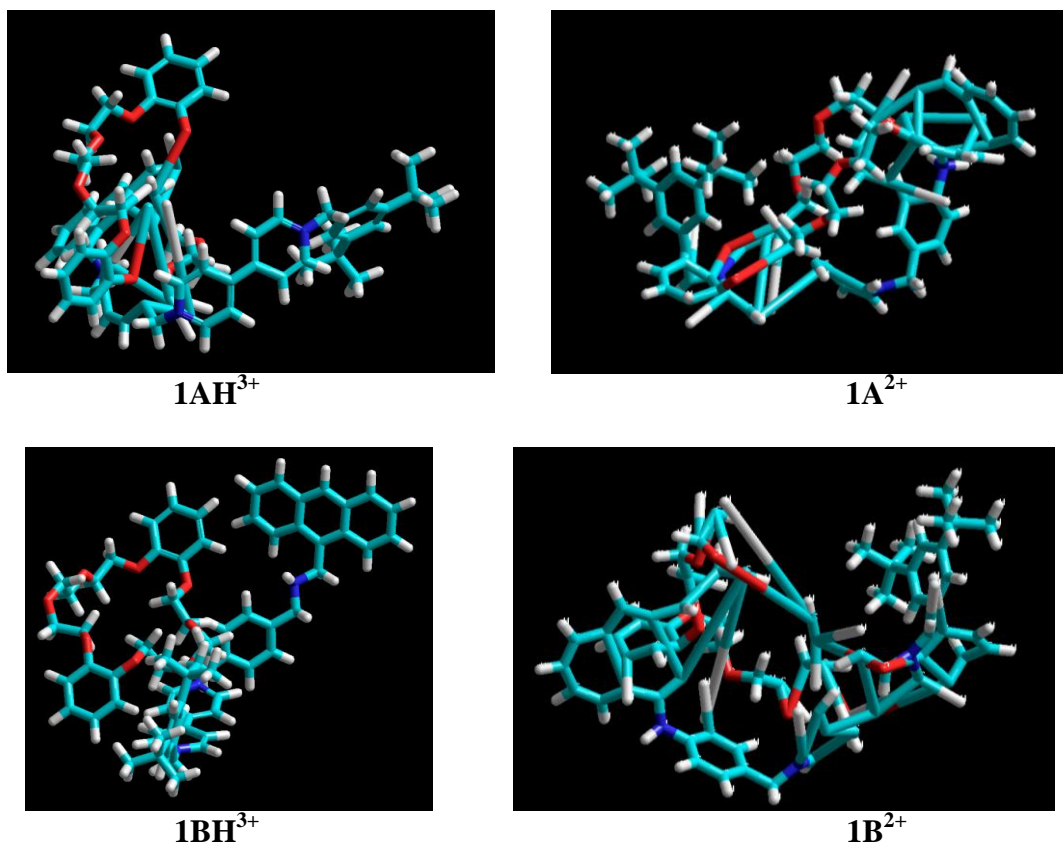


Figure 2. HyperChem representation of the structures (initial, transient and final) of the studied rotaxane during the molecular shuttling process

Coulomb blockade is estimated for these systems. A schematic representation of the Coulomb blockade is given in **Figure 3**. Tunneling/redistribution of electrical charge is expressed by a change in the electrostatic potential. Coulomb blockade allows precise control of a small number of electrons with essential applications in low power dissipation switching devices and thus an increase in the circuit integration level.

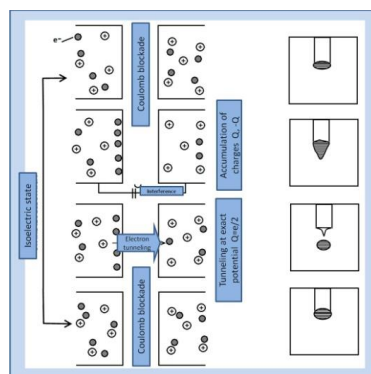


Figure 3. Schematic representation of the Coulomb blockade

Through bondonic spectral correlations, predictions are made on the bondonic photovoltaic effect. The bondonic energy in photovoltaic system due to the Planck quantification is:

$$E_B = \sqrt{hI_{SC} \times V_{OC}} = \hbar \sqrt{\frac{2\pi}{IQ}} (18.8177 \times 10^{10}) \times \Delta \tilde{\nu}_{FWHM} [cm^{-1}] \quad (5)$$

$$X_B^0[A] = \frac{4.19399 \times 10^6}{E_B[eV]} = 0.0135084 \times 10^{12} \frac{\sqrt{IQ}}{\Delta \tilde{\nu}_{FWHM} [cm^{-1}]} \quad (6)$$

and eventually rewritten into a macroscopic observable scale

$$X_B[\text{meters}] = 1.35084 \frac{\sqrt{IQ}}{\Delta\tilde{\nu}_{FWHM}[\text{cm}^{-1}]} \quad (7)$$

The PV-related bondonic quantum current will be:

$$I_B[A] = \frac{e_B}{t_B} = 1.51146 \times 10^{-7} \frac{\Delta\tilde{\nu}_{FWHM}[\text{cm}^{-1}]}{IQ^{3/2}} \quad (8)$$

Through the path integral formalism, the thermodynamic indices of interconversion (free energy, enthalpy, entropy, Gibbs energy, etc.) are calculated. The partition function is given as a simple integral:

$$Z_1 = \int_{-\infty}^{+\infty} \frac{dx_0}{\sqrt{2\pi\hbar^2\beta/m_0}} \exp[-\beta W_1(x_0)] \quad (9)$$

In terms of free energy: $F = -\beta^{-1} \log Z$ (10)

$$\Delta G = \frac{1}{\beta} \ln Z - \int \nabla V(x) dx \quad (11)$$

$$\Delta S = \frac{1}{T} \int \nabla V(x) dx \quad (12)$$

Molecular systems convert the input stimulus (optical, electrical or chemical) into output signals (which may also be of optical, electrical or chemical nature). Through the similarity between molecular machines and binary logic systems, represented in **Figure 4**, the quantum logical information is provided, and the type of logical system (AND, OR, XOR) corresponding to every state of the molecular machine during the shuttle movement could be estimated.

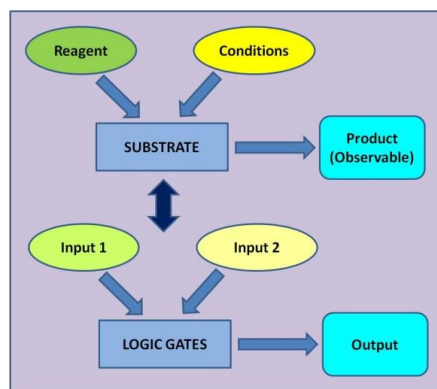


Figure 4. Schematic representation of the similarity between molecular machines and binary logic systems

Conclusion

The five main directions elaborated by the authors of the present paper lead to the development of an integrated photo-electro-chemistry algorithm of molecular machines towards moletronics and smart functionalized nano-materials.

Acknowledgments:

This contribution is part of the Nucleus-Programme under the project “Deca-Nano-Graphenic Semiconductor: From Photoactive Structure to the Integrated Quantum Information Transport” PN-18-36-02-01/2018 funded by the Romanian Ministry of Research and Innovation (MCI). The authors declare no conflict of interest.

REFERENCES

1. Balzani, V.; Credi, A.; Venturi, M. Molecular devices and machines, *Nanotoday*, **2007**, 2, 18-25.
2. Venturi, M.; Iorga, M.; Putz, M.V. Molecular Devices and Machines: Hybrid Organic-Inorganic Structures, *Current Organic Chemistry*, 2017, 21, 2731-2759.
3. Balzani, V.; Credi, A.; Venturi, M. *Molecular Devices and Machines. Concepts and Perspectives for the Nanoworld*, Wiley-VCH, Weinheim, **2008a**.
4. Balzani, V.; Credi, A.; Raymo, F.M.; Stoddart, J.F. Artificial molecular machines, *Angew. Chem. Int. Ed.*, **2000**, 39, 3348-3391.
5. Sauvage, J.P.; Dietrich-Buchecker, C. (Eds.), *Molecular Catenanes, Rotaxanes and Knots*, Wiley-VCH, Weinheim, **1999**.
6. Abendroth, J.M.; Bushuyev, O.S.; Weiss, P.S.; Barrett, C.J. Controlling motion at the nanoscale: rise of the molecular machines, *ACS Nano*, **2015**, 9, 7746-7768.
7. Venturi, M.; Credi, A. Electroactive [2]catenanes, *Electrochim. Acta*, **2014**, 140, 467-475.
8. Bissell, A.; Cordova, E.; Kaifer, A.E.; Stoddart, J.F. A chemically and electrochemically switchable molecular shuttle, *Nature*, **1994**, 369, 133-137.
9. Arduini, A.; Bussolati, R.; Credi, A.; Pochini, A.; Secchi, A.; Silvi, S.; Venturi, M. Rotaxanes with a calix[6]arene wheel and axles of different length. Synthesis, characterization, and photophysical and electrochemical properties, *Tetrahedron*, **2008**, 64, 8279-8286.
10. Balzani, V.; Credi, A.; Venturi, M. Molecular machines working on surfaces and at interfaces, *Chem. Soc. Rev.*, **2008b**, 9, 202-220.
11. ***, MLA style: "The Nobel Prize in Chemistry 2016". *Nobelprize.org*. Nobel Media AB 2014. Web. 1 Nov **2016**.
http://www.nobelprize.org/nobel_prizes/chemistry/laureates/2016/
12. Ashton, P.R.; Ballardini, R.; Balzani, V.; Baxter, I.; Credi, A.; Fyfe, M.; Gandolfi, M.T.; Gomez-Lopez, M.; Martinez-Diaz, V.; Piersanti, A.; Spencer, N.; Stoddart, J.F.; Venturi, M.; White, A.J.P.; Williams, D.J. Acid-Base Controllable Molecular Shuttles, *J. Am. Chem. Soc.* **1998**, 120, 11932-11942.
13. Garaude, S.; Silvi, S.; Venturi, M.; Credi, A.; Flood, A.H.; Stoddart, J.F. Shuttling Dynamics in an Acid-Base-Switchable [2]Rotaxane, *ChemPhysChem*, **2005**, 6, 2145-2152.
14. Fyfe, M.C.T.; Glink, P.T.; Menzer, S.; Stoddart, J.F.; White, A.J.P.; Williams, D.J. Anion-assisted self-assembly, *Angew. Chem. Int. Ed. Engl.*, **1997**, 36, 2068-2070.

DEVELOPMENT AND VALIDATION OF HIGH PERFORMANCE LIQUID CHROMATOGRAPHY METHOD FOR THE MEASUREMENTS OF BIOGENIC AMINES

Nikolett Nánási¹, Levente Hadady¹, Edina Cseh¹, Gábor Veres^{1,2}, Péter Klivényi¹, László Vécsei^{1,2}, Dénes Zádori¹

¹*Department of Neurology, Faculty of Medicine, Albert Szent-Györgyi Clinical Center, University of Szeged, Szeged, Hungary*

²*MTA-SZTE Neuroscience Research Group, Szeged, Hungary*
e-mail: nannik1026@gmail.com

Abstract

Many important biogenic amines (dopamine, noradrenaline and serotonin) are produced from amino acids by enzyme-catalysed processes and play a prominent role in neuronal functions and therefore, they serve as pharmacological target for the treatment of neurological disorders, such as Alzheimer's disease or Parkinson's disease.

The aim of the current study was to optimize a high-performance liquid chromatography method that allows selective separation of eight biogenic amines and some of their metabolites (levodopa, 3,4-dihydroxyphenylacetic acid, noradrenaline, 5-hydroxyindoleacetic acid, homovanillic acid, dopamine, serotonin and 3-methoxytyramine) using 3 internal standards with electrochemical detection. During the development of our method, we optimized the amount of ion pairing component, pH and the amount of organic phase. Several selective methods were tested, but the most effective one was used for validation process for mouse and rat brain regions, including the striatum, cortex and hippocampus.

During validation, the limit of detection, the limit of quantification, recovery, intraday and interday precisions were determined for the eight analytes. The ranges of recovery were between 87 and 120%, the intraday and interday precision were < 10% in all cases. The limit of detection and quantification ranged around 2 and 10 ng/ml, respectively.

The developed and optimized method ensures the measurement of the aforementioned biogenic amines from mouse and rat brain regions.

Introduction

Monitoring of the concentration of biogenic amines may have a great importance from several aspects [1]. The measurement of these metabolites from biological samples requires highly selective and sensitive methods because of their considerably low concentrations [1, 2]. High-performance liquid chromatography (HPLC) methods have been widely applied [3] for this purpose. HPLC combined with electrochemical detector (ECD) is one of the best alternatives for the quantitative detection of monoamines and related compounds in biological samples because of their electroactive function groups and the exceptional sensitivity of the ECD.

The aim of the current study was to optimize our latest HPLC-ECD method [3] to be able to determine 8 biogenic amines and some of their metabolites (levodopa (L-DOPA), 3,4-dihydroxyphenylacetic acid (DOPAC), noradrenaline (NA), 5-hydroxyindoleacetic acid (5-HIAA), homovanillic acid (HVA), dopamine (DA), serotonin (5-HT), 3-methoxytyramine (3-MT)) from different biological samples. It is essential to apply internal standard(s) (IS) for HPLC measurements [4, 5], therefore, based on the recommendations [4], we decided to use 3 (3,4-dihydroxybenzylamine (DHBA), isoproterenol (IPR) and N-methyl serotonin (NM-5HT)) instead of the previous one. After the successful extension of the method, we applied it to different biological samples, i.e., mice and rat brain regions and the validation process was carried out as well.

Materials and methods

L-DOPA, 5-HT and their metabolites, DA, 3-MT, DOPAC, HVA, NA and 5-HIAA were measured from the striatum, cortex and hippocampus of C57Bl/6 mice and Wistar rat animals. We used an Agilent 1100 HPLC system (Agilent Technologies, Santa Clara, CA, USA) combined with a Model 105 ECD (Precision Instruments, Marseille, France) under isocratic conditions. The brain regions were weighed and then homogenized in an ice-cold solution (striatum: 60 $\mu\text{L}/\text{mg}$; cortex: 25 $\mu\text{L}/\text{mg}$ and hippocampus: 18.75 $\mu\text{L}/\text{mg}$) containing perchloric acid (3.4 w%, Sigma Aldrich, Saint Louis, MO, USA), sodium-metabisulfite (400 μM , Fluka, Sigma-Aldrich, Saint Louis, MO, USA), ethylenediaminetetraacetic acid disodium salt (Na_2EDTA , 500 μM , Lach-Ner, Neratovice, Czech Republic), distilled water and ISs: 50 ng/ml DHBA, 200 ng/ml IPR and 100 ng/ml NM-5HT (Sigma Aldrich, Saint Louis, MO, USA). The homogenate was centrifuged at 12,000g for 30 min at 4°C. The supernatants of individual brain regions were pooled and spiked with standard solution in three different concentration levels. The working potential of the detector was set at +750 mV, using a glassy carbon electrode and an Ag/AgCl reference electrode. The mobile phase contained sodium-dihydrogenphosphate (NaH_2PO_4 ; 75 mM, Reanal, Budapest, Hungary), Na-octylsulphate (NaOS, 2.2 mM, Sigma Aldrich, Saint Louis, MO, USA) and Na_2EDTA (50 μM , Lach-Ner, Neratovice, Czech Republic) was supplemented with acetonitrile (ACN; 6.25% v/v, VWR International, Radnar, PA, USA) and the pH was adjusted to 3.0 with phosphoric acid (H_3PO_4 ; 85% w/w, Sigma Aldrich, Saint Louis, MO, USA). The mobile phase was delivered at a rate of 1.5 ml/min at 40°C onto the column (Zorbax Eclipse Plus C18, 100 x 4.6 mm, 3.5 μm particle size; Agilent Technologies, Santa Clara, CA, USA) after passage through a pre-column (SecurityGuard, 4x3.0 mm i.d., Phenomenex Inc., Torrance, CA, USA). 10 μL aliquots were injected by the autosampler with the cooling module set at 4°C.

Results

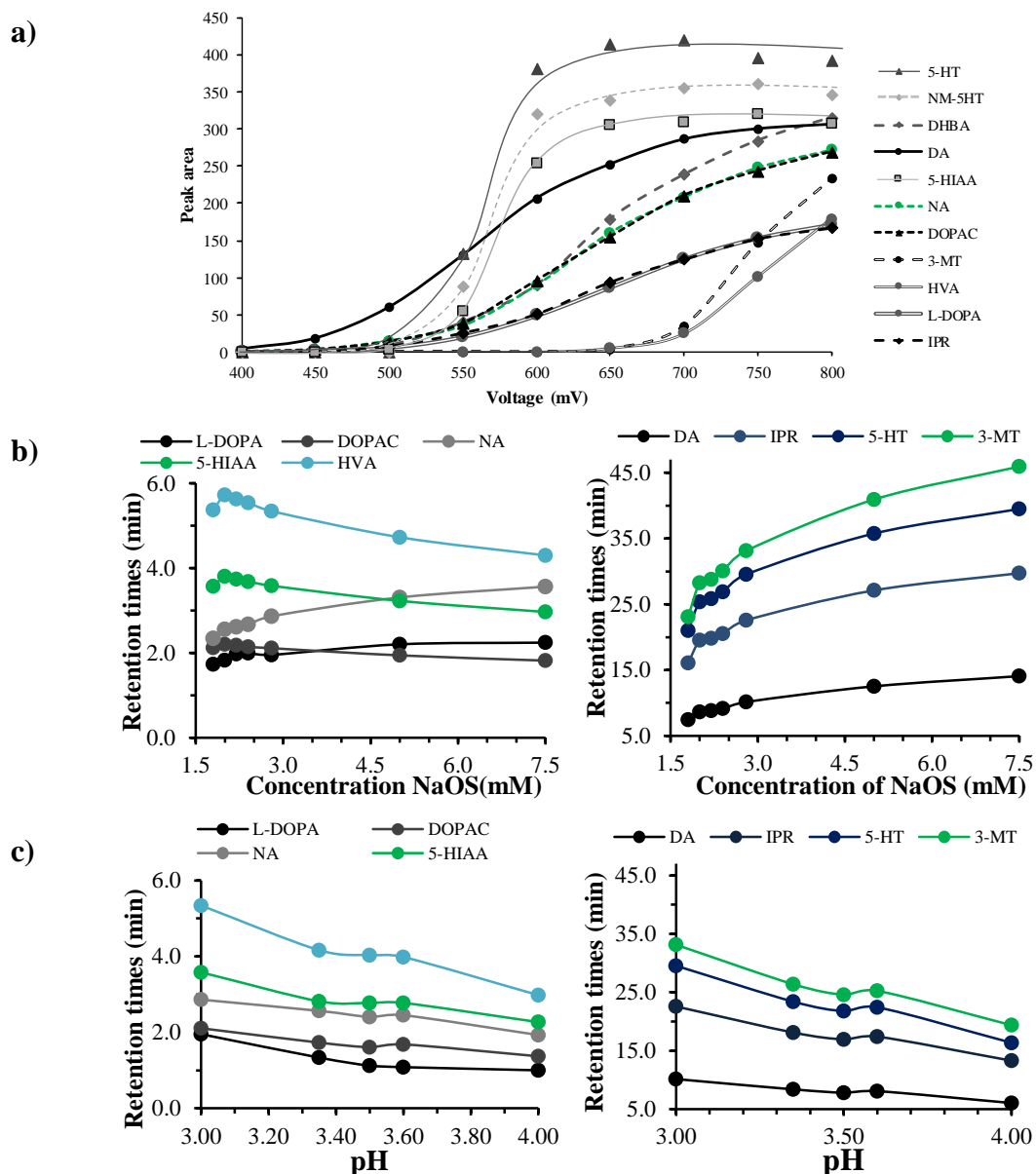
Before validation, the optimal working potential was investigated. The detector was set from 400 mV to 800 mV with 50 mV increments (**Fig 1a**). Although 800 mV would be the best working potential for HVA and 3-MT, the signal-to-noise ratio also increases with the applied working potential, so we decided to set the detector at +750 mV.

First we determined the effect of the change in NaOS concentration (**Fig.1b**) with a result that the increasing amount has ambivalent effect on analytes: increased retention times were observed in case of L-DOPA, NA, DA, 5-HT, 3-MT, IPR (IS), whereas in case of DOPAC, 5-HIAA and HVA the retention time decreased. The concentration of 7.5 mM was selective for all the compounds as well, however, the run time was more than 45 min.

Then we checked the influence of the pH value of the mobile phase (**Fig.1c**). As it can be seen, the increasing value of pH from 3.0 to 4.0 reduced the retention time of all the analytes.

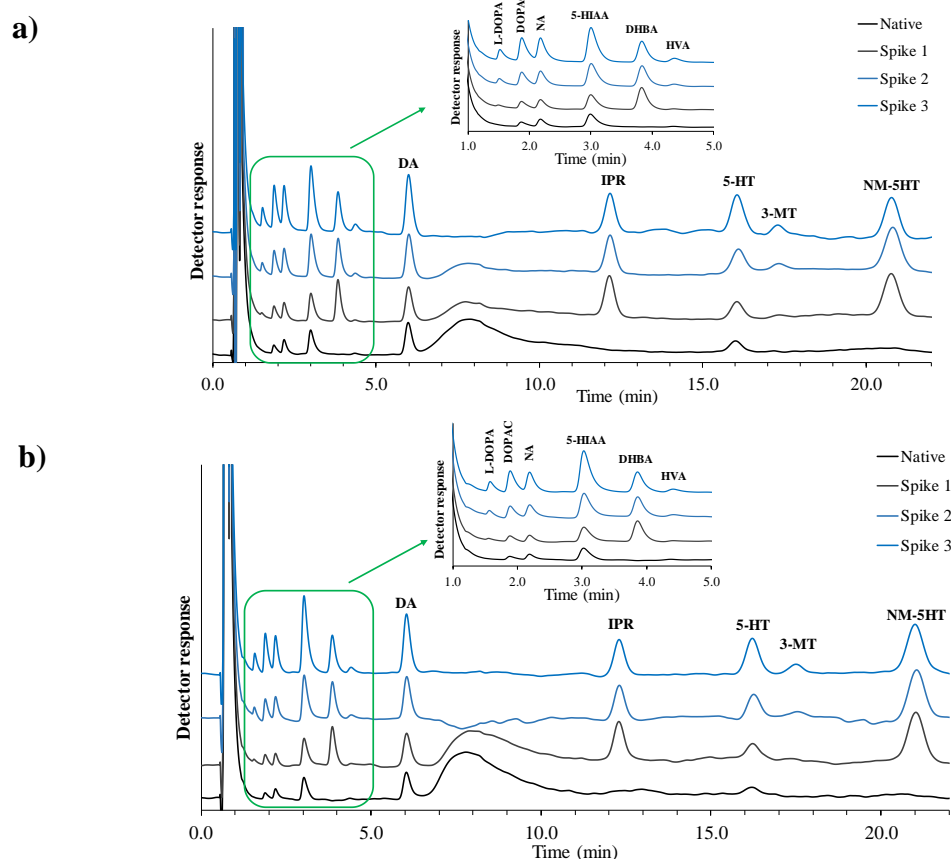
These results showed that the best choice is to keep the pH at 3.0 and NaOS in the concentration range between 2.10 mM and 2.20 mM with 5 or 6 v/v% ACN. With the 2 new internal standards (DHBA and NM-5HT), the optimal mobile phase consists of 2.20 mM NaOS, 75 mM NaH_2PO_4 , 50 μM Na_2EDTA and 6.25 v/v% ACN. Before adding ACN, the pH value of water phase was set to 3.0 with 85 w/w% H_3PO_4 . Test runs showed that mice and rat brains can be measured well with this method.

Fig. 1 Voltage vs. peak area responses of the analytes and internal standards (a) and the effect of the concentration of NaOS (b) or pH (c) in mobile phase to retention times of analytes and internal standard. The pH was set to 3.0 and ACN was 5 v/v%.



ACN acetonitrile; DA dopamine; DHBA 3,4-dihydroxybenzylamine; DOPAC 3,4-dihydroxyphenylacetic acid; HVA homovanillic acid; IPR isoproterenol; L-DOPA levodopa; NA noradrenaline; NaOS Na-octylsulphate; NM-5HT N-methyl serotonin; 3-MT 3-methoxytyramine; 5-HIAA 5-hydroxyindoleacetic acid and 5-HT serotonin.

We only demonstrate the results of the striatum from mice and rats. The results of validations are presented in **Table 1**. In **Fig. 2** the native and the spiked chromatograms are demonstrated. Native sample is from pooled mice or rat striatum, cortex, hippocampus, cerebellum and brainstem regions.

Fig. 2 Native and spiked chromatograms of pooled mice (a) and rat (b) brain regions.

DA dopamine; DHBA 3,4-dihydroxybenzylamine; DOPAC 3,4- dihydroxyphenylacetic acid; HVA homovanillic acid; IPR isoproterenol; L-DOPA levodopa; NA noradrenaline; NM-5HT N-methyl serotonin; 3-MT 3-methoxythiramine; 5-HIAA 5-hydroxyindoleacetic acid and 5-HT serotonin.

Table 1. Summary of validation parameters of HPLC-ECD method for biogenic amines in mouse and rat striatum.

Validation parameters		L-DOPA	DOPAC	NA	5-HIAA	HVA	DA	5-HT	3-MT
Linear range (ng/ml)	mouse	5-150	5-80	5-80	10-100	10-100	5-200	5-100	10-200
	rat								
Correlation coefficient	mouse	1.000	0.999	0.999	0.998	0.994	0.999	0.999	0.998
	rat	0.999	0.999	0.999	0.995	0.993	1.000	0.999	0.997
LOD (ng/ml)	mouse	1.3	0.5	0.7	5.5	7.4	2.0	3.8	9.8
	rat	3.1	3.6	7.1	7.9	8.6	2.6	3.8	12.8
LOQ (ng/ml)	mouse	3.9	1.5	2.1	16.5	22.3	6.0	11.6	29.7
	rat	9.3	10.9	21.7	23.9	26.1	7.9	11.4	38.7
Recovery (%)	mouse	100.7	108.0	110.6	108.9	104.3	109.0	104.4	102.0
	rat	108.0	104.9	106.1	109.0	95.3	106.1	103.5	97.3
Intraday precision	mouse	3.19	1.81	3.68	3.82	8.23	1.59	5.36	6.70
	rat	1.96	2.57	3.17	2.76	7.28	1.85	3.60	9.74

(CV%)									
Interday precision (bias%)	mouse	3.24	1.83	3.89	3.85	8.59	1.63	5.42	6.85
	rat	1.98	2.57	3.17	2.75	7.42	1.84	3.62	9.52

DA dopamine; DOPAC 3,4- dihydroxyphenylacetic acid; HPLC-ECD high-performance liquid chromatography with electrochemical detector; HVA homovanillic acid; L-DOPA levodopa; LOD limit of detection; LOQ limit of quantification; NA noradrenaline; 3-MT 3-methoxytyramine; 5-HIAA 5-hydroxyindoleacetic acid and 5-HT serotonin.

Discussion

We successfully extended our latest method with 5 new compounds, of which 2 are internal standards. The applied method is suitable for the measurements of brain regions of mice and rats. The validation parameters are in line with international guidelines. Based on our results, this method will be a valuable tool for multiple experiments, such as, rodent toxin models of neurological disorders.

Acknowledgements

The research was supported by GINOP-2.3.2-15-2016-00034 ('Molecular Biological Fundamentals of Neurodegenerative and Immune Diseases: Therapeutic Trials with Kynurenines') and EFOP-3.6.1-16-2016-00008 ('Development of intelligent life science technologies, methods, applications and development of innovative processes and services based on the knowledge base of Szeged').

Dénes Zádori was supported by the János Bolyai Research Scholarship of the Hungarian Academy of Sciences and by the UNKP-18-4 New National Excellence Program of the Ministry of Human Capacities.

References

1. Zhang L, Yang J, Luo Y et al (2016) Simultaneous determination of eleven compounds related to metabolism of bioamines in rat cortex and hippocampus by HPLC-ECD with boron-doped diamond working electrode. J Pharm Biomed Anal 118:41–51. <https://doi.org/10.1016/j.jpba.2015.10.020>
2. Allen SA, Rednour S, Shepard S, Pond BB (2017) A simple and sensitive high-performance liquid chromatography–electrochemical detection assay for the quantitative determination of monoamines and respective metabolites in six discrete brain regions of mice. Biomed Chromatogr 31:e3998. <https://doi.org/10.1002/bmc.3998>
3. Torok R, Salamon A, Sumegi E et al (2017) Effect of MPTP on mRNA expression of PGC-1 α in mouse brain. Brain Res 1660:20–26. <https://doi.org/10.1016/j.brainres.2017.01.032>
4. Dolan JW (2009) Calibration curves, part II: What are the limits? How are the signal-to-noise ratio and imprecision related? LC-GC N Am 27:306–312
5. ICH (1995) ICH Harmonized tripartite guideline, validation of analytical procedures. Federal Register, 60, 11260

MESOPOROUS SBA-15 AND CeO₂ CARRIED COPPER WITH A CONTROLLED SIZE THE APPLICATION OF NANOPARTICLES CO₂ IN HYDROGENATION REACTIONS

Ádám Nyitrai

Consultants: Dr. Kónya Zoltán, Dr. Sápi András

University of Szeged Faculty of Science and Informatics Department of Applied and Environmental Chemistry

Keywords: copper nanoparticle, controlled size, carbon dioxide hydrogenation

In the Earth's atmosphere the CO₂ level is growing rapidly. Researchers worldwide pioneer methods to exploit the surface properties of various materials. One of the solutions the CO₂ has catalytic transformation happening in processes may be heterogeneous. The modern nanotechnology one and surface we are capable with chemistry examination methods onto the planning of the reactions and his understanding with an atomic level in the interest of the bigger activity and selectivity. The copper based catalysts prove to be promising because of their high activity and their low price.

In this project, copper nanoparticles with a diameter of 2-20 nm were made with a controlled size and we carry them up the big one with a specific surface taken to the mesoporous CeO₂ and SBA-15 onto carriers, with a replication method. We examine the catalysts with a transmission electron microscopy, adsorption with measurements (BET), x-ray diffraction, inductive coupling plasma with mass spectrometry, we test them furthermore in CO₂ hydrogenation reactions with a continuous flow pipe reactor.

ELECTROCHEMICAL NITRIFICATION OF AMMONIUM IN SIMULATED GROUNDWATER USING BORON-DOPED DIAMOND ELECTRODES

Anamaria Baci¹, Claudia Licurici¹, Adina Pacala², Ilie Vlaicu², Katalin Bodor², Florica Manea¹

¹Politehnica University of Timisoara, P-ta Victoriei, No. 2, Timisoara, Romania, e-mail: florica.manea@upt.ro

²Aquatim SA Timisoara, Str. Gheorghe Lazăr nr. 11/A, 300081 Timișoara, Romania, e-mail: adina.pacala@aquatim.ro

Abstract

In this work, the electrochemical oxidation of ammonium from simulated groundwater on boron-doped diamond (BDD) electrodes was assessed in order to be integrated within the drinking water treatment technology. All nitrogen species, *i.e.*, nitrate, nitrite and total nitrogen, were monitored to assess the electrochemical nitrification of ammonium until gaseous nitrogen. For the simulated groundwater containing ammonium concentration of about 1 mgL⁻¹, the application of electrochemical oxidation at lab scale using BDD electrodes at the current density of 50 Am⁻² assured an efficient oxidation of ammonium resulting nitrate at the concentration below maximum allowance concentration, as main intermediate of the electrochemical nitrification.

Introduction

It is well-known that the presence of ammonium in groundwater used as source for the drinking water represents a public health issue in developing and developed countries [1]. The Romanian legislation imposes the maximum allowance concentration (MAC) for ammonium in drinking water of 0.5 mg/L and higher concentrations require its removal. The ammonium presence in groundwater influences the selection of drinking water treatment process [2-4], the conventional method consisting in the „break-point“ chlorination [2]. The drawbacks of the conventional method demand to find new technological solution for the ammonium removal from drinking water.

The electrochemical oxidation represents an advanced oxidation process studied for the removal of organic and inorganic compounds especial from wastewater [5, 6] and less from drinking water, except in disinfection stage. In general, the electrochemical oxidation actS to destroy the pollutants by direct oxidation on the electrode surface or by indirect oxidation through various powerful oxidants generated within the electrolyte depending on the electrolyte composition, *e.g.*, hydroxyl radical, Cl₂, etc.

The process performance key is given by the electrode material that besides the water composition dictates the type of direct or indirect oxidation. Boron-doped diamond (BDD) anodes have been successfully applied for advanced treatment of wastewater and also, disinfection due to its great mechanical and electrochemical properties, such as: resistance, inertness to the corrosion media, stability etc. The promising results have been reported for the application of BDD electrode for ammonium oxidation from waterwaters [7-9]. However, there are a few reports related to ammonium removal from drinking water. The results of the test applied for removal of ammonium form groundwater using an electrooxidation module integrated within the groundwater treatment pilot plant was reported by our group [10].

The aim of this paper is to study the performance of electrooxidation process using BDD electrodes at the laboratory scale to assure the electrochemical nitrification in order to remove the ammonium fROm simulated chloride containing groundwater.

Experimental

For bulk electrolysis a rectangular cell made of stipler, with intercalated vertical anodes and cathodes, was used. The cell arrangement consisted of boron-doped diamond (BDD) anodes with the active surface area of 0.021 m² intercalated with the stainless steel cathodes at the distance between anodes and cathodes of 1 cm. The electrolysis was carried out at room temperature (22-25 °C) in batch mode under galvanostatic working regime for 1 mgL⁻¹ ammonium in 250 mgL⁻¹ NaCl supporting electrolyte. The BDD/Nb electrodes (100 mm x 50 mm x 1 mm) by CONDIAS, Germany were used as anodes, and stainless steel plates (100 mm x 50 mm x 1 mm) were employed as cathodes. A regulated DC power supply (HY3003, MASTECH) was used to assure galvanostatic regime at current densities of 50 mA cm⁻² and 100 mA cm⁻².

At given time intervals, samples were drawn from the cell to monitor the performance of the electrochemical process in terms of nitrogen species concentrations. Determination of the nitrate, nitrite and ammonium concentrations was performed according to the standardized methods. For the determination of ammonium concentration, SR ISO 7150-1 / 2001 was used by the spectrophotometric method, the determination of nitrite content was carried out using the molecular absorption spectrometry method SR ISO 6777/1996 and the determination of nitrate content was performed using the method SR ISO 7890-1 / 1998 by spectrophotometric method with 2,6 dimethylphenol. Total nitrogen was determined using the total organic carbon analyzer, TOC-L CPH SHIMADZU. An Inolab WTW pH meter was used to measure the solution pH.

The specific energy consumption, W_{sp} , was calculated with the relation (1):

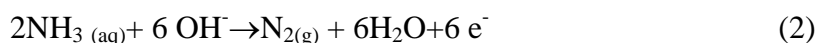
$$W_{sp} = \frac{(Q \cdot V^{-1})U}{1000} \quad (\text{kWh dm}^{-3}) \quad (1)$$

where Q represents the specific charge consumption, U is the cell voltage (V), V is the solution volume (dm³).

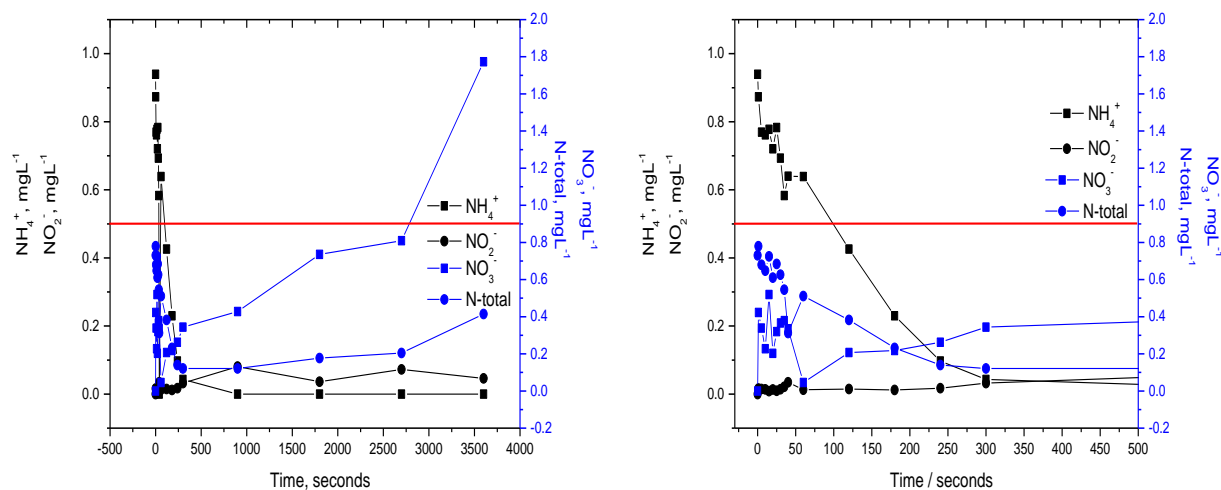
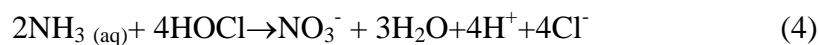
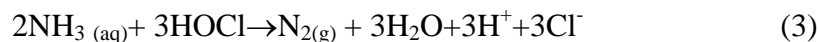
Results and discussion

Even if the ammonium conversion into nitrogen represents the main reaction characteristics to the electrochemical nitrification (eqs. 2, 3), some intermediates of nitrogen species (nitrite and nitrate) should be generated (eq. 4), which are undesired and affecting the water quality. The electrolysis process was conducted to maintain all nitrogen species below the maximum allowance concentrations (MAC) regulated by the legislation with minimum energy consumption. The evolution of the nitrogen species during the electrolysis process under conditions of applying a current density of 50 Am⁻² for a synthetic water containing 0.906 mgL⁻¹ NH₄⁺ is presented Figure 1a. It can be seen a fast decrease of ammonium concentration and after 150 seconds the ammonium concentration reached below the MAC of 0.5 mgL⁻¹ (Figure 1b). Also, during the first stage of the electrolysis the nitrate concentration increased followed by the sharp decreasing and then, a further slight increasing occurred. Total nitrogen as sum of the all nitrogen species followed the nitrate tendency characterized by the lower value, which means that the major intermediate is nitrate besides the gaseous nitrogen.

The main reactions that govern the electrochemical process are [7, 10]:

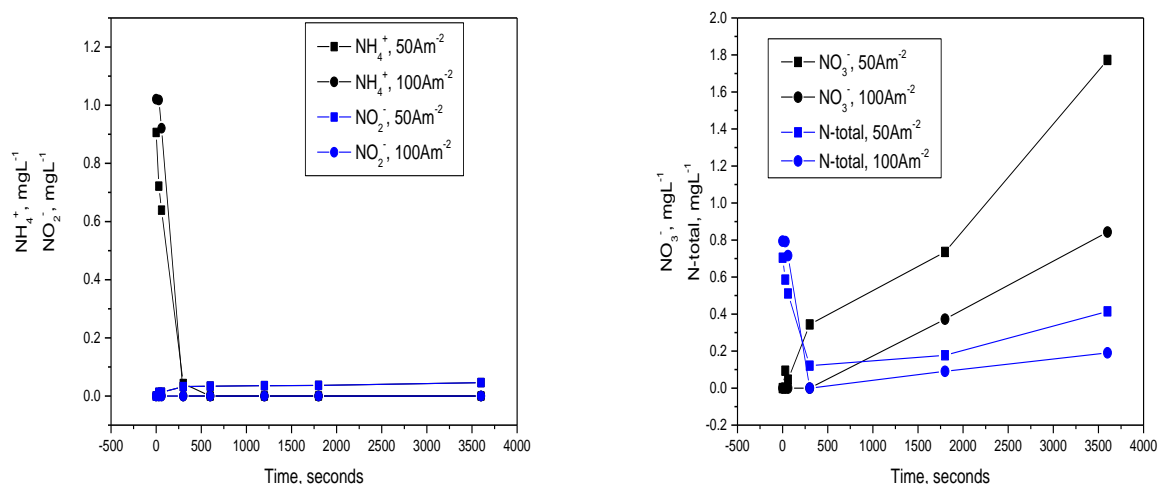


In the presence of chlorine generated electrochemically from chloride present into the water, the ammonium oxidation should occur according with equations (3) and (4).



a) b)
Fig. 1. a) Concentration profile for ammonium, nitrite and nitrate species during electrolysis on BDD operated at 50 Am^{-2} for simulated water containing 0.9 mgL^{-1} ammonium and 250 mgL^{-1} NaCl at $\text{pH}=7.7$; b) Detail of Figure 1a

A very important working parameter for the electrolysis operation is considered current density that dictates the process kinetics. Two current densities of 50 and 100 Am^{-2} were applied and the evolution of the nitrogen species are presented in Figures 2 a and b. A slight enhancement of the process performance is noticed for 100 Am^{-2} but the question that arises is given by the economic aspect.



a) b)
Fig. 2. Comparative concentration profiles for nitrogen species during electrolysis on BDD operated at 50 and 100 Am^{-2} for simulated water containing 0.9 mgL^{-1} ammonium and 250 mgL^{-1} NaCl at $\text{pH}=7.7$: a) ammonium and nitrite; b) nitrate and total nitrogen

The specific energy consumption is considered the main component of the economic aspect and its evolution is presented comparatively for both current densities in Figure 3. It is obviously that the longer electrolysis time the higher specific energy consumption and also, higher current density higher the energy consumption, thus, the electrolysis time and the current density should be selected in according with the concrete application.

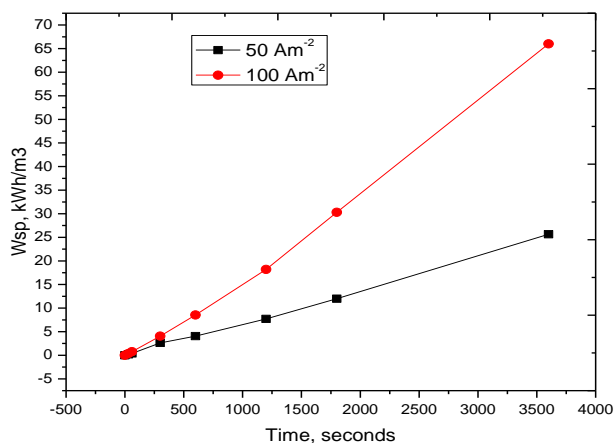


Fig.3. Specific energy consumption during electrolysis process

Conclusion

The electrochemical oxidation of ammonium from simulated groundwater on boron-doped diamond (BDD) electrodes assured the electrochemical nitrification of ammonium for both applied current densities of 50 and 100 Am^{-2} . Besides the desired conversion of ammonium into gaseous nitrogen, nitrate, nitrite and total nitrogen were identified as intermediates, nitrate being the main intermediate but under the maximum allowance concentration of 50 mgL^{-1} . Higher current density allowed the ammonium conversion of ammonium to gaseous

nitrogen more effectively in comparison with lower current density but the application of high current density is limited by the economic aspect. Thus, for the simulated groundwater containing ammonium concentration of about 1 mgL^{-1} , the application of the current density of 50 Am^{-2} assured an efficient oxidation of ammonium at short electrolysis time of 250 seconds, when the all nitrogen species intermediates were generated at the concentrations below the maximum allowance concentrations avoiding water pollution. However, the presence of nitrate within the real groundwater matrix at the concentration higher than maximum allowance concentration limited the application of this cell arrangement and operating conditions of the electrochemical process within the drinking water treatment technology.

Acknowledgements

This work was supported by a grant of the Romanian Ministry of Research and Innovation, CCCDI-UEFISCDI, project number 26PCCDI/01.03.2018, "Integrated and sustainable processes for environmental clean-up, wastewater reuse and waste valorization" (SUSTENVPRO), within PNCDI III.

References

- [1] G. Huang, F. Liu, Y. Yang, W. Deng, S. Li, *Journal of Environmental Management* 154 (2015) 1-7.
- [2] V. Patroescu, C. Jinescu, C. Cosma, I. Cristea, V. Badescu, *Revista de Chimie* 66 (4) (2015) 537-541.
- [3] G. Romanescu, E. Paun, I. Sandu, I. Jora, E. Panaitescu, O. Machidon, C. Cristian Stoleriu, *Revista de Chimie* 65 (4) (2014) 401-410.
- [4] D. Bociort, C. Gherasimescu, R. Berariu, R. Butnaru, M. Branzila, I. Sandu, , *Revista de Chimie* 63 (11) (2012) 1151-1157.
- [5] G. Perez, J. Saiz, R. Ibanez, A.M. Urtiaga, I. Ortiz, *Water Research* 46 (2012) 2579-2590.
- [6] H. Sarkka, A. Bhatnagar, M. Sillanpaa, *Journal of Electroanalytical Chemistry* 754 (2015) 46-56
- [7] A. Kapalka, L. Joss, A. Anglada, C. Comninellis, K. M. Udert, *Electrochemistry Communications* 12 (2010) 1714-1717.
- [8] V. Diaz, R. Ibanez, P. Gomez, A. M. Urtiaga, I. Ortiz, *Water Research* 45 (2011) 125-134.
- [9] W.T. Mook, M. H. Chakrabarti, M. K. Aroua, G. M. A. Khan, B. S. Ali, M. S. Islam, M. A. Abu Hassan, *Desalination* 285 (2012) 1-13.
- [10] N. Lungar, K. Bodor, I. Vlaicu, A. Pacala, F. Manea, *Proceedings of International Conference Sustainable Solutions of Water Mangement*, Bucharest 15-17 May 2017, 49-58.

CHEMICAL AND NUTRITIONAL ASPECTS OF SOME FRESH SMOOTHIE TYPES

Popescu Sofia, Velciov Ariana*, Cozma Antoanela, Catutoiu Alexandra, Poiana Mariana, Stoin Daniela, Micula Lia, Alexa Ersilia

University of Agricultural Sciences and Veterinary Medicine of Banat "King Mihai I of Romania" Timisoara

Faculty of Food Processing Technology Food Science Department 300645, Timisoara, Calea Aradului, nr. 119, Roumania

author's email address: ariana.velciov@yahoo.com, sofia.pintilie@yahoo.com

Abstract

Vegetable and fruits are foods that can be consumed either fresh or processed into juices, smoothies, syrups, jams, fruit compotes, etc. Fruit and vegetables play the important role in the people diet. Worldwide, the consumption of fresh food (fruits, vegetables, and herbs) is steadily in increasing tendency. The good looks, nice colour or taste and aromas, but especially their nutritional value, the rich content in sugars, vitamins and minerals necessary in the diet of the human body are considered to be important. The lower incidence of degenerative diseases is associated with the diet rich in fruits and vegetables.

The purpose of our study was revealing certain physico-chemical and nutritional properties of some fresh foods and the juices or smoothies that we can obtain from them. These aspects highlight their dietary and healing properties.

Keywords: fresh food, juices, smoothie, chemical characteristics, healing properties

Introduction

A diet rich in fruits and vegetables is important for its positive effects on the prevention of chronic degenerative diseases (such as heart dysfunction, cardiovascular diseases), diabetes, high blood pressure, low density lipoprotein oxidation, and associated with a lower incidence of them [1].

Fruits contain high levels of bioactive compounds (vitamin C, total phenolic content, anthocyanin, carotenoids, tannins, flavones and flavonoids), which are important to preserve in the preparation as well as purees, beverages, juices and other varieties of food products [2]. Smoothies represent a convenient and excellent alternative to enhance the daily intake of fruit and vegetables in order to obtain their health-promoting benefits. Purees, smoothies and juice of fruit and vegetable offers similar health benefits as having whole fruits and vegetables [3, 4].

Drinking smoothies have many benefits for human health [3, 5, 6, 7] such as high nutritional and energy values, increased contents of vitamins, antioxidants, polyphenol and fibres a.o.

The aim of the study was to analyse some potential health-promoting constituents from 6 different samples (fruit, vegetable and smoothies).

Experimental

Samples preparation

There are many possibilities to obtain the smoothie from raw material (fruits, vegetables, herbs). In our study, our smoothies were prepared without adding of water, sugar and citric acid. Smoothies were prepared from only one fruit or several fruits. Smoothies also used

frozen fruits (sea-buckthorn) and dried fruit infusions (cranberry). The samples necessary in our study are fresh fruit pineapple, apple, sea-buckthorn and dried fruit cranberry (infusion of cranberry fruit).

The samples (fruit, vegetable) were selected according to uniformity of shape and colour, then stored in polyethylene bags at 5 °C (up to 5days) until analysis. The samples are fresh (pineapple, apple, and cucumber), frozen (sea-buckthorn) and dried (cranberry) from a Romanian hypermarket, from Timisoara city (west of Romania).

The smoothie sample was obtained by mixing the fruits (fresh and frozen) with cucumber and infusion of dried cranberry fruits.

Analytical procedures

Humidity (moisture) of fresh food samples was evaluated thermo-gravimetrically by using Sartorius thermo-balance.

Total dry content (TSC,) can be determined from moisture content as below:

$$\text{Total dry content (\%)} = 100 - \text{Moisture (\%)}$$

The method for determination of **ascorbic acid content (vitamin C)** was by titration with 2,6-dichlorophenolindophenol until a pink colour appeared [1, 8].

All determinations were performed in triplicate, calculating their arithmetic mean of three separate determinations. The statistically data were acquired using the program Microsoft Excel.

Results and discussion

The obtained data regarding water content (HC, %) and dry content (TSC, %) in samples (fruits, vegetables and smoothies) represented in fig. 1.

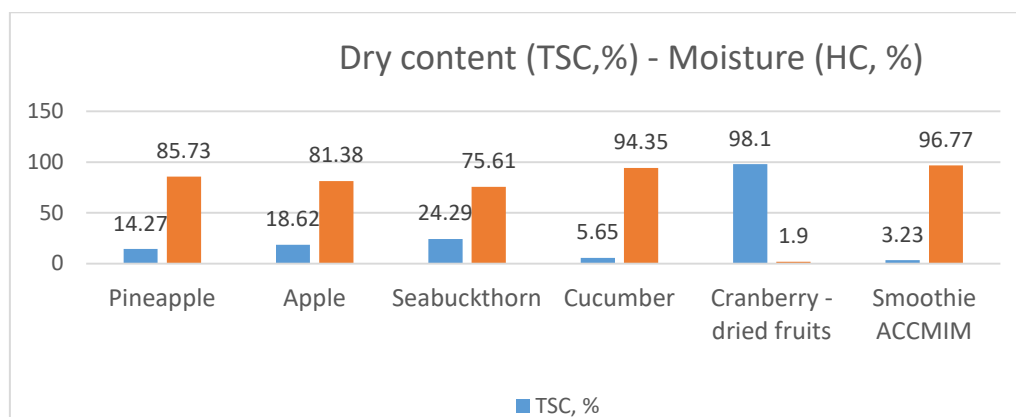


Fig. 1 Dry content (TSC, %) and humidity (HC, %) in samples

Smoothie ACCMIM is prepared from fresh pineapple, apple fruits, fresh cucumber, frozen sea-buckthorn fruit and infusion of cranberry.

Water content (humidity) is a parameter related to the maturity of fruit. In the present study water content values are between 1.9 % (in dried cranberry fruit) and 96.77 % (smoothie).

Refractive indexes of juice samples were between 1.3345 (infusion of dried cranberry fruits) and 1.3519 (pineapples juice) - see fig. 2.

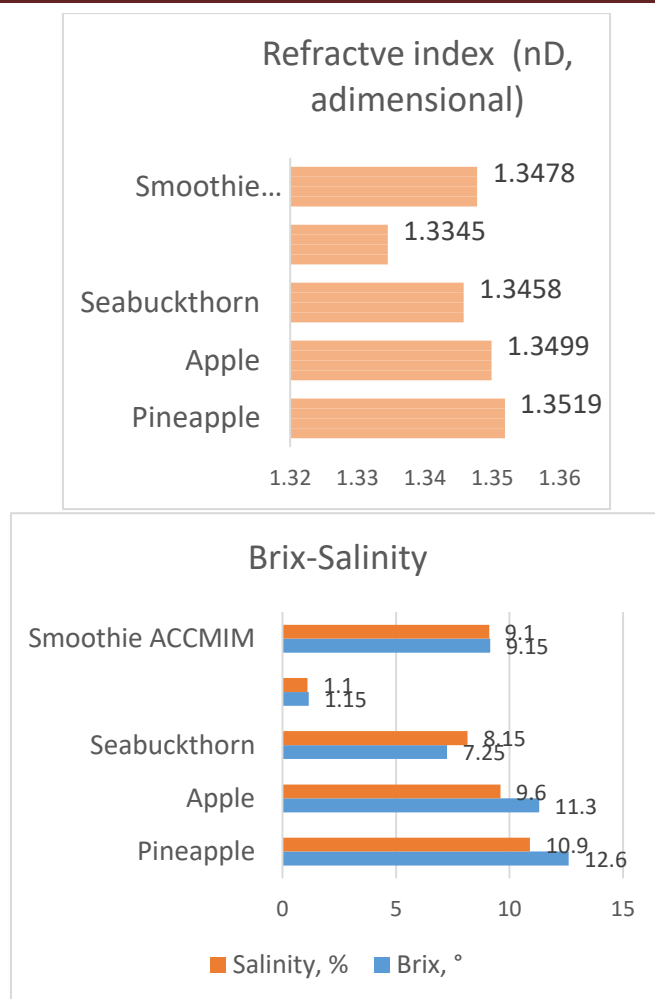


Fig. 2. a) Refractive index (nD) of sample; b) Brix and salinity of sample

The high level of brix and salinity are in pineapple, follow by apple and the low level are in infusion of dried cranberry fruit.

In fig. 3 we are presenting total mineral content (ash, %) values.

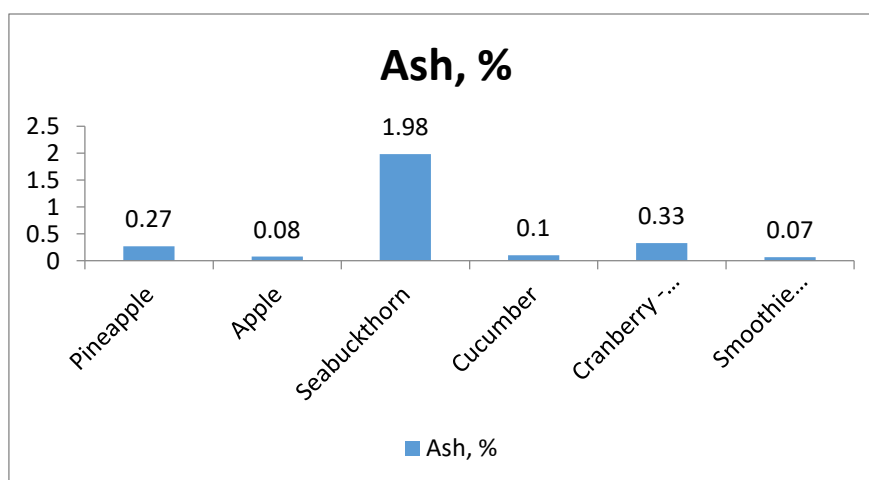


Fig. 3 Total mineral content (Ash, %) in sample

From the analysed data presented above, we can observe that the highest value (1.98 %) of the total mineral content was found in sea-buckthorn, and the lowest value were found in smoothie ACCMIM (0.07 %). The ash quantity resulting from mineralization represents the total mineral content (ash, %).

Determination of ascorbic acid content samples are presented in Fig. 4.

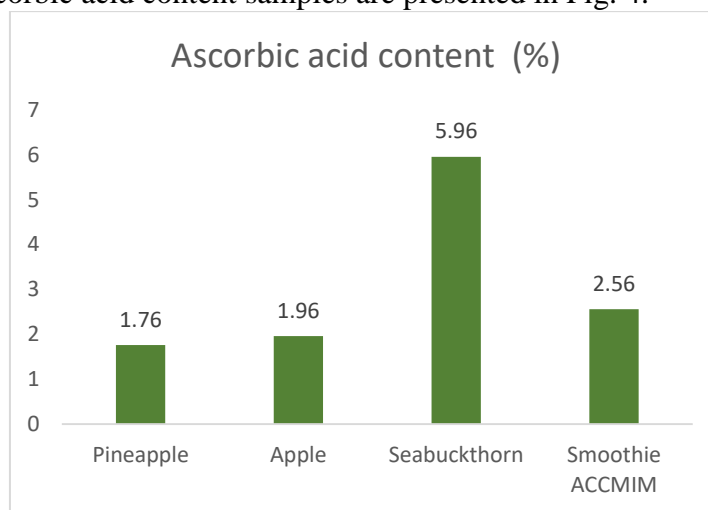


Fig. 4 Ascorbic acid content in samples

The values of ascorbic acid content were between 1.76 – 5.96 (%) (in pineapple respectively in sea-buckthorn).

Conclusions

Fresh beverages are ideal food forms to deliver bioactive compounds to consumers.

In this study, complex beverages formulas, smoothies were formulated containing green fresh food and infusion of dried fruit as medicinal tee.

The obtained results will be used for future research because this data highlighted once more the fact that minimally processed foods are important source of mineral and vitamin.

Fresh smoothies of fruits and vegetables and the tea without additives have superior quality.

References

- [1] Popescu S., Velciov A., Nicolin A., Lalescu D., Micula L., Statistical modeling of physic chemical and biochemical characterization of various smoothie types, Conference Proceedings International Multidisciplinary Scientific Geoconference SGEM, vol. 18, Issue 6.1 Micro and Nano Technologies, 2018
- [2] Park Y.S., Ham K.S., Park Y.K., Leontowicz H, Leontowicz M, Namiesnik J, Katrich E, Gorinstein S., The effects of treatment on quality parameters of smoothie-type ‘Hayward’ kiwi fruit beverages, Food Control, vol.70, pp 221-228, 2016;
- [3] Tahmassebi J.F., Kandiah P., Sukeri S., The effects of fruit smoothies on enamel erosion, Eur Arch Paediatr Dent, vol 15, pp 175–181, 2014;
- [4] Ruxton C.H.S., Gardner E.J., Walker A., Can pure fruit and vegetable juices protect against cancer and cardiovascular disease too? A review of the evidence, Int J Food Sci Nutr, vol 57, pp 249–72. 2006;
- [5] Ruxton C.H.S., Smoothies: one portion or two?, Nut Bull., vol 33, pp129–32, 2008;
- [6] Hussein I., Pollard M.A., Curzon M.E., A comparison of the effects of some extrinsic and intrinsic sugars on dental plaque pH, Int J Paediatr Dent, vol 6, pp 81–86. 1996;
- [7] Beighton D., Brailsford S.R., Gilbert S., Intra-oral acid production associated with eating whole or pulped raw fruits, Caries Resc, vol 38, pp 341–9, 2004;
- [8] AOAC, Official Methods of Analysis, AOAC, Washington, DC, USA, 16th ed., 1995;

ANALYSIS OF EMPLOYEE'S AWARENESS OF ENERGY COSTS

Nebojša M. Ralević¹, Ivana Dolga¹, Aleksandra Mihailović¹
Vladimir Dj. Djaković¹, Goran B. Andjelić²

¹*University of Novi Sad, Faculty of Technical Sciences, Department of Fundamentals
Sciences, Novi Sad, Serbia*

²*Educons University, Faculty of Business Economy, Sremska Kamenica, Serbia
e-mail: nralevic@uns.ac.rs, ivana.dolga@gmail.com, zandra@uns.ac.rs,
v_djakovic@uns.ac.rs, goran.andjelic@educons.edu.rs,*

Abstract

In this document analysis of employee awareness about energy costs in companies is given through tests of questionnaire. There were three main questions observed about other sources of energy, including fossil fuels and renewable energy as a supplementation and/or replacement for the electric energy. In the conducted research 150 respondent (employees) was included with their opinion about the importance of source of energy related to companies' energy costs. In this paper relation between companies (employees) with higher energy costs and the level of awareness about different energy source is proven.

Keywords: Electric energy, renewable energy, fossil fuels, costs of energy.

Introduction

Survey "Renewable energy sources on a test sample of 150 respondents" was conducted. It contained questions about personal data and an opinion on efficient consumption and renewable energy sources (1st competitiveness and consumption, 2nd sources of energy). Each of the questions asked consisted of answers with a scale of 5 offered responses: A - insignificant, B - less significant, C - intermediate, D - very significant, E - extremely significant.

We will consider the criterion question

Electricity consumption has a significant share in the total cost of the company.

The answer to this criterion question shows us how the respondent looks at the consumption of electricity within the work he deals with. Since this is the criterion question, it means that the entire sample is divided into 5 groups depending on their answers to it. So the sample is divided into 5 groups:

A - insignificant (0 respondents), B - less significant (5 subjects), C - intermediate (37 subjects), D - very significant (72 respondents) and E - extremely significant (36 subjects).

Based on the distribution of the answers to the criterion question, we see that the group A is minimal, we will not use it in the future because there are no respondents, while the results of group B are less significantly taken with the reserve because the group has a small number of respondents, so we can not consider the result as relevant. So our focus will be on the difference in attitudes between groups: C - medium significant (37 subjects), D - very significant (72 respondents) and E - extremely significant (36 respondents).

Methodology

Our goal is to determine whether there are differences and on which questions differences exist between the 4 groups mentioned. That is, among the respondents who consider that electricity consumption has a significant share in the total costs of the company. We will test hypotheses:

H1 – Groups defined by criteria question (CQ) have different opinion (answer) on the question “*Fossil fuels (oil, gas, coal ...) will remain the basic type of energy supply until 2020.*”

H2 - Groups defined by criteria question have different opinion (answer) on the question “*It is feasible that by 2020, renewable energy sources represent 25% of total energy sources*”.

H3 - Groups defined by criteria question have different opinion (answer) on the question “*The share of renewable energy from 25% by 2020 is at a satisfactory level*”.

From the analysis, we will use MANOVA and ANOVA analysis. The analysis was done with R-project. First, the MANOVA analysis was done where we tested whether there was a difference on all groups. If there is the difference as a result of MANOVA, later ANOVA analysis was conducted to test between which groups differences exists.

Results

First test was done on the first question in relation to the criterion question:

1. Fossil fuels (oil, gas, coal) will remain the basic type of energy supply until 2020.
2. Electricity consumption has a significant share in the total cost of the company.
(criterion question, CQ)

MANOVA results are shown in the table bellow

	Df	Sum Sq	Mean Sq	F value	Pr (>F)
CQ	3	5.41	1.804	1.576	0.198
Residuals	146	167.05	1.144		

There is no a significant difference, so hypothesis H1 is not proven.

Next analysis, ANOVA was done on questions:

1. Fossil fuels (oil, gas, coal ...) will remain the basic type of energy supply by 2020.
2. Electricity consumption has a significant share in the total cost of the company.
(criterion question, CQ)

Groups defined by criteria question	Diff	lwr	upr	p adj
(C - intermediate)- (B - less significant)	0.037838	-1.28671	1.362389	0.999853
(D - very significant) - (B - less significant)	0.033333	-1.25232	1.318987	0.99989
(E - extremely significant) - (B - less significant)	0.477778	-0.84896	1.804517	0.785607
(D - very significant) - (C - medium significant)	-0.0045	-0.56681	0.557806	0.999997
(E - extremely significant) - (C - intermediate)	0.43994	-0.21085	1.090727	0.298448
(E - extremely significant) - (D - very significant)	0.444444	-0.123	1.01189	0.179797

In all cases p value is grater then 0.05 so the conclusion is that there is no significant difference. In this case it means that between the groups defined by criteria question, there are no significant differences on the first question “*Fossil fuels (oil, gas, coal ...) will remain the basic type of energy supply by 2020.*” This means that the groups have similar opinion about the mentioned subject.

Second test was done on the third question in relation to the criterion question

3. It is feasible that by 2020, renewable energy sources represent 25% of total energy sources.
2. Electricity consumption has a significant share in the total cost of the company.
(criterion question, CQ)

MANOVA results are shown in the table bellow

	Df	Sum Sq	Mean Sq	F value	Pr (>F)
CQ	3	10.48	3.492	3.026	0.0315
Residuals	146	168.48	1.154		

In this case there is the statistically significant difference because $p = 0.0315$ which is less than 0.05. Hypothesis H2 is proven.

Next analysis, ANOVA was done on questions:

3. It is feasible that by 2020, renewable energy sources represent 25% of total energy sources.
2. Electricity consumption has a significant share in the total cost of the company.
(criterion question, CQ)

Groups defined by criteria question	Diff	lwr	upr	p adj
(C - intermediate)- (B - less significant)	-0.32973	-1.65995	1.000495	0.917422
(D - very significant) - (B - less significant)	-0.11389	-1.40505	1.177272	0.995738
(E - extremely significant) - (B - less significant)	0.4	-0.93242	1.732422	0.863331
(D - very significant) - (C - intermediate)	0.215841	-0.34888	0.78056	0.753466
(E - extremely significant) - (C - intermediate)	0.72973	0.076155	1.383305	0.022039
(E - extremely significant) - (D - very significant)	0.513889	-0.05599	1.083765	0.093028

There is a significant difference between groups E and C and between groups E and D.

In the group C for the third question 35.1% respondents answered with C – intermediate and in the group E 19.4% respondents answered with C – intermediate.

In the group C for the third question 8.1% respondents answered with E - extremely significant and in the group E 38.9% respondents answered with E - extremely significant

In the group D for the third question 16.7% respondents answered with B - less significant and in the group E 5.6% respondents answered with B - less significant.

In the group D for the third question 25% respondents answered with C – intermediate and in the group E 19.4% respondents answered with C – intermediate

Given result illustrate that the group of respondents who think that electricity consumption has significant share in the total cost of the company (answer E on the CQ), have different opinion (answer) on question “It is feasible that by 2020, renewable energy sources represent

25% of total energy sources” and for the group E characteristic answer on the same question

	A - insignificant		B – less significant		C - intermediate		D – very significant		E – extremely significant.	
Criteria group	n	%	n	%	n	%	n	%	n	%
B - less significant	0.	.0	0.	.0	3.	60.	1.	20.0	1.	20.0
C - intermediate significant	3.	8.1	4.	10.8	13.	35.1	14.	37.8	3.	8.1
D - very significant	3.	4.2	12.	16.7	18.	25.0	25.	34.7	14.	19.4
E - extremely significant	1.	2.8	2.	5.6	7.	19.4	12.	33.3	14.	38.9

E- extremely significant

On the other side respondents who think that electricity consumption has insignificant share in the total cost of the company (answer C on the CQ), have moderate opinion (answer C – intermediate) on question “It is feasible that by 2020, renewable energy sources represent 25% of total energy sources”.

Frequency distribution of answers on the question “It is feasible that by 2020, renewable energy sources represent 25% of total energy sources” in regard to criteria groups

Third test was done on the fourth question in relation to the criterion question:

4. The share of renewable energy from 25% by 2020 is at a satisfactory level.
2. Electricity consumption has a significant share in the total cost of the company. (criteria question, CQ)

MANOVA results are shown in the table below

	Df	Sum Sq	Mean Sq	F value	Pr (>F)
CQ	3	1.36	0.4547	0.383	0.766
Residuals	146	173.47	1.1881		

There is no a significant difference, so hypothesis H3 is not proven.

Next analysis, ANOVA was done on questions:

- 4 The share of renewable energy from 25% by 2020 is at a satisfactory level.
- 2 Electricity consumption has a significant share in the total cost of the company. (criterion question, CQ)

Groups defined by criteria question	Diff	lwr	upr	p adj
(C - intermediate)- (B - less significant)	0.324324	-1.02544	1.674087	0.924082
(D - very significant) - (B - less significant)	0.138889	-1.17124	1.449014	0.992666
(E - extremely significant) - (B - less significant)	0.083333	-1.26866	1.435326	0.998531
(D - very significant) - (C - medium significant)	-0.18544	-0.75845	0.387578	0.834785
(E - extremely significant) - (C - mean)	-0.24099	-0.90417	0.422184	0.780945
(E - extremely significant) - (D - very significant)	-0.05556	-0.6338	0.522691	0.994512

There is no significant difference.

Discussion

Respondents who have moderate opinion (answer C – intermediate) on the criteria question, they also usually have moderate opinion (answer C – intermediate) on the tested question “*It is feasible that by 2020, renewable energy sources represent 25% of total energy sources*”.

Reason is given by the fact that they do not feel pressure with high costs of electric energy, and so their interests for the other source of energy are small.

Respondents from the companies where costs for electric energy are intermediate, has no attention on the other sources of energy beside electric energy.

Otherwise respondents from companies with high electric energy costs, have more attention on the renewable sources of energy.

Conclusion

For hypothesis H1 and H3 results indicated that there is no significant differences between criteria groups.

For hypothesis H2 results indicate statistically significant difference between criteria groups.

This means that the group of respondents who think that electricity consumption has significant share in the total cost of the company (answer E on the CQ), have different opinion (answer) on question “*It is feasible that by 2020, renewable energy sources represent 25% of total energy sources*” and for the group E characteristic answer on the same question is E-extremely significant.

And on the other side respondents who think that electricity consumption has insignificant share in the total cost of the company (answer C on the CQ), have moderate opinion (answer C – intermediate) on question “*It is feasible that by 2020, renewable energy sources represent 25% of total energy sources*”.

Acknowledgements

The authors acknowledge the financial support of the Ministry of Education, Science and Technological Development of the Republic of Serbia, within the Project No. TR34014.

References

- [1] Martin Kaltschmitt, Wolfgang Streicher, Andreas Wiese (ed): Renewable energy. Technology, economics and environment, Springer, Berlin/Heidelberg. 2007.

COMPETITIVE ADSORPTION OF SAMPLE SOLVENT AND ANALYTE IN SUPERCRITICAL FLUID CHROMATOGRAPHY

Csanád Rédei¹, Attila Felinger^{1,2,3}

¹ Department of Analytical and Environmental Chemistry, University of Pécs,
Ifjúság útja 6., H-7624 Pécs, Hungary

² MTA-PTE Molecular Interactions in Separation Science Research Group,
Ifjúság útja 6., H-7624 Pécs, Hungary

³ Institute of Bioanalysis, University of Pécs,
Honvéd u. 1., H-7624 Pécs, Hungary
e-mail: redei.csanad@gmail.com

Abstract

Supercritical fluid chromatography (SFC) has gained increased attention in the fields of theoretical research, purification processes and separation sciences over the last few years due to the latest technological advancements. The method is well-known for being capable of faster separations and reduced solvent consumption compared to liquid chromatography (LC) while also achieving high efficiency. Due to the nature of carbon-dioxide serving as mobile phase, eluent strength is well-tunable by adjusting temperature, pressure and the amount of organic modifier. However, SFC is considered a complementary technique besides liquid and gas chromatography since there is always a trade-off in terms of the advantages [1].

Recently, Gritti experienced an anomaly in the retention behaviour of alkylbenzenes using a heavily modified Waters ACQUITY UPC² System [2]. These small molecules are ideal for studying the processes taking place in the chromatographic column. Therefore, the aim of this work is to study the retention of several *n*-alkylbenzenes on an alkylamide stationary phase using a standard UPC² System and assessing the effect of different sample solvents on chromatographic efficiency. The results show that even a small amount of methanol overloads the column and a competitive adsorption takes place between the analytes and the sample solvent. This is indicated by the changes in column efficiency, retention factors and peak widths. The selected experimental conditions guarantee that the density of the mobile phase does not change significantly along the column, so the phenomenon can be modeled as in LC. The concentration of the analytes is negligible compared to the amount of methanol – but their adsorption is influenced by the solvent – while the adsorption of methanol remains unaffected by the alkylbenzenes. The competition was described by determining the single-component adsorption isotherms for both the analytes and the solvent then competitive isotherms were calculated. The solvent effect was modeled by a numerical method created in-house where the differential mass balance equation was integrated using the Rouchon algorithm. The experimental observations were confirmed by *in silico* experiments and further cases involving hypothetical analytes were studied as well.

References

- [1] Tarafder, A.: *Trends Anal. Chem.* **81** (2016) 3-10.
- [2] Gritti, F.: *J. Chromatogr. A* **1468** (2016) 209-216

KINETICS OF AIR-BLOWING OF SOME ROMANIAN PETROLEUM OIL RESIDUES

Dan Rosu

National Institute for Research and Development in Electrochemistry and Condensed Matter, Timisoara, A.P. Podeanu no.1, 300569, Romania
e-mail: antiquitera@yahoo.ca

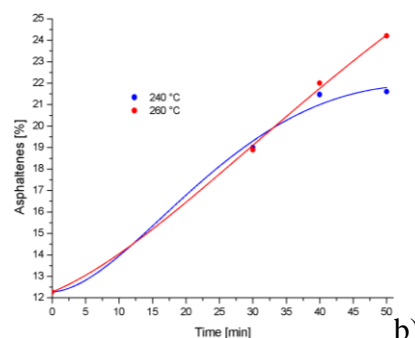
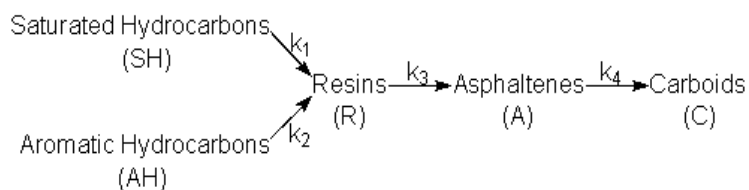
Abstract

Air blowing is the process by which compressed air is blown into a bitumen feedstock typically at 230–260°C. This process results in complex reactions which raise the softening point and viscosity of the asphalt bitumen [1].

Air blowing of bituminous materials was carried out in a static mixing gas-liquid reactor at 240° and 260 °C.

Chemical composition of feed material was: 30,08% saturated hydrocarbons; 30,26% aromatic hydrocarbons; 27,39% resins; 12,27% asphaltenes.

A reaction scheme and kinetics equations has been proposed to explain the time dependence of asphaltene contents during air blowing process.



Chemical transformation during petroleum oil residues air oxidation process (a) and the time dependence of asphaltene contents (b)

References

[1] J.G. Speight, Asphalt Materials Science and Technology, Elsevier, 2016

SYNTHESIS AND CHARACTERIZATION TiO₂ POWDERS AND THIN FILM OBTAINED BY SOLVOTHERMAL METHOD FOR APPLICATIONS IN ENVIRONMENT FRIENDLY BUILDING MATERIAL TECHNOLOGIES

Florina Ștefania Rus¹, Petru Negrea², Paulina Vlăzan¹, Ștefan Novaconi¹

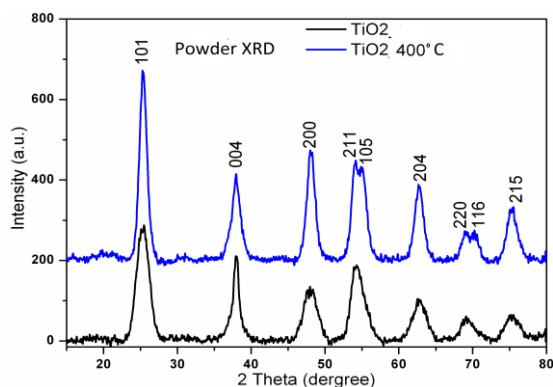
¹National Institute for Research and Development in Electrochemistry and Condensed Matter, 144 Aurel Păunescu Podeanu St, 300569, Timișoara, România

² Politehnica University Timișoara, 2 Piața Victoriei, 300006, Timișoara, România
e-mail: rusflorinastefania@gmail.com

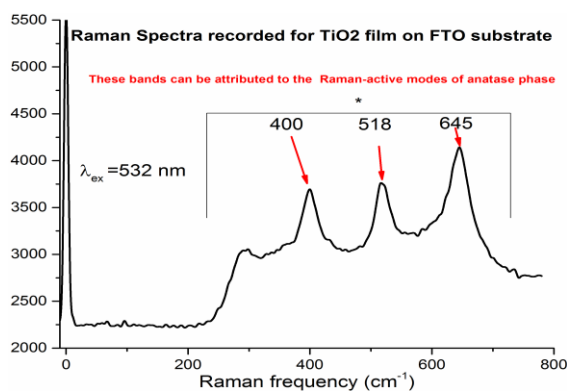
Abstract

The ability to fast obtain materials around specific application like design various new concept devices, such as gas sensors, catalysts, applications in environment friendly building material technologies with unique parameters of light absorption, solid state fuel cell, energy harvest, charge generation, and charge transport is thus vital to improving sciences and creating novel functionalities necessary for increasing implementation of photoactive materials [1].

Our research focus has been mainly on fast obtaining anatase TiO₂ in two forms: powder and film using solvothermal method. Characterization of the obtained compounds was achieved by X-ray diffraction (XRD), scanning electron microscopy (SEM), ultraviolet–visible spectrophotometry (UV-VIS), Raman Spectroscopy and Photoluminescence. Visible Raman spectra was recorded at room temperature on a Scanning Probe Microscopy (SPM) System with MultiView 1000 platform using 532 nm single-frequency laser as excitation source. The SE was carried out by Woollam VASE ellipsometer at (1.25 – 5) eV photon energy range at 55°– 75° angles of light incidence. The data analysis was performed with commercial Woollam CompleteEase software.



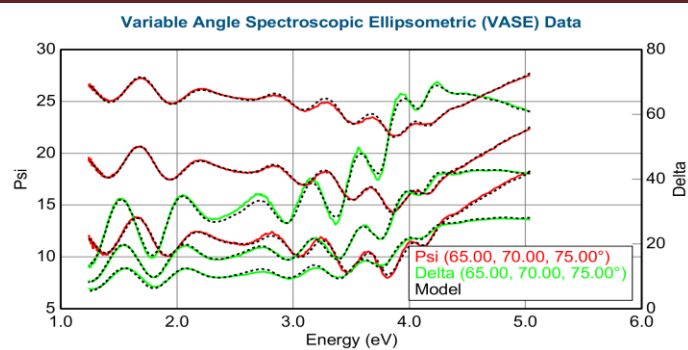
X'Ray Diffraction for TiO₂ powder



Raman spectra of TiO₂ film

Rietveld profile fitting of X-ray diffraction (XRD) pattern of the TiO₂ nanoparticles revealed highly crystalline anatase with P42/mnm structure. The anatase phases of TiO₂ could be sensitively identified by Raman spectroscopy based on their Raman spectra.

Variable angle spectroscopic ellipsometry (VASE) has been used to determine the optical properties of the TiO₂ film. The energy dependent ellipsometric angles Ψ and Δ were recorded for 3 angles. Measurement of ellipsometry was performed in the spectral range 1.24– 5 eV at incident angles of 65-70-75°. The TiO₂ layer is approximated by a Kramers-Kronig consistent B-spline.



SE spectra for the TiO_2 film

Acknowledgement

This work was supported by a grant of the Romanian Ministry of Research and Innovation, CCCDI–UEFISCDI, project number PN-III-P1-1.2-PCCDI-2017-0391/CIA_CLIM-Smart buildings adaptable to the climate change effects, within PNCDI-III

References

- [1] Elia Boonen and Anne Beeldens, Coatings, Recent Photocatalytic Applications for Air Purification in Belgium 2014, 4, 553-573

NOISE AT PUBLIC EVENT

**Selena Samardžić¹, Milka Veselinović¹, Milan Cvijanović², Uranija Kozmidis Luburić¹,
Robert Lakatoš¹, Tomas Nemeš¹, Aleksandra Mihailović¹**

¹*Faculty of Technical Sciences, University of Novi Sad, Trg Dositeja Obradovića 6, Serbia*

²*Clinical Center of Voivodina, Faculty of Medicine, University of Novi Sad, Serbia*

e-mail: sselena@uns.ac.rs

Abstract

Recent years the noise is one of the leading pollutants in working and living environment. Although in some cases the noise levels do not exceed proposed levels, people often have the opposite impression. While for the most activities noise regulation exists, for public events this is not the case. There are certain guidelines, however established levels differ from country to country. In order to determine the noise level during public events the equivalent level of noise was measured at one public event on which approximately 50,000 people was present. The results show significantly high levels of noise, especially during rock concert and firework, when certain protective measures should be implemented.

Introduction

Industrialization, fast pace of life, traffic, transport and population growth make difficult for people to find quiet place to be. Lots of studies have shown that presently the noise is one of the leading problems in the environment and the second largest environmental cause of health problems [1]. Most of the population in the cities are constantly complaining about the traffic and street noise, loud music or about some other source of irritable sounds. People react differently to noise, but generally noise has negative impact on human health.

It increases anxiety, damages hearing, and it also causes cardiovascular and other diseases [2] and disturbs body immune response [3].

There are many studies on this subject, but little information can be found about the noise on public events, such as cultural and political events. In most cases they are held in city centre and they can last for a few days. In these circumstances the presence of people alone makes certain level of noise. Often visitors of these events consume alcohol and other stimulants which together with the noise increases the negative impact on human health. Young people are especially affected when going to loud places, by using headphones and playing video games. They often complain about tinnitus and headaches, and these can last for a few days after the exposure. Considering that the effect of hearing damage is cumulative, this observation can not be negligible.

It is also very important to mention that during public events noise protective measures are rarely implemented. Legislations provide punishment for every procedure that disturbs public peace and order. However, public events are excluded. Organizers of public gatherings, amusement and sport events and of other indoor and outdoor activities, in their notifications of the gatherings and similar activities are obliged to provide data on the noise protective measures if the use of different devices exceed allowed noise levels. For example, in Britain it is strictly prescribed that during concert or any other public event continuous equivalent noise level (dBA) can not exceed 107 dBA, while the audience should stand at least 3 meters away from the source of the sound. For the noise level higher than 96 dBA there should be a warning about the health risk concerning the exposure to noise [4]. However, it is known that

noise above 115 dB sound pressure level (SPL) can damage the inner ear and can induce enduring negative functional changes recordable in the central auditory nervous system [5].

In order to determine equivalent A-level sound pressure level of noise, the noise was measured during one cultural event in city centre. Tens of thousands people were present, and along with public speaking there were cultural and artistic activities followed by the firework. L_{eq} , L_{min} and L_{max} levels of noise were measured and frequency characteristics for 1/3 octave band in places where high noise level was noticed.

The environment surrounding is similar during political events, hence it would be desirable to compare these events in some of the upcoming research.

Materials and methodes

The study was conducted at public event that was held at the city center with nearly 10,000 inhabitants. This manifestation lasted for four days from 7pm to 4am, with nearly 50,000 visitors. Rock concert, dancing and firework was organized on the stage at the event.

The noise level was measured using the TES-1358A Sound Level Meter (SLM), with RS-232 Interface. The calibration procedure of the instrument was performed before the actual measurements using standard acoustic calibrator recommended by SLM manufacturer (TES Electrical). The desired response of SLM was set at "fast". When the measurements were made, the microphone was located in such a way as not to be in the acoustic shadow of any obstacle in appreciable field of reflected waves. Noise levels were measured at the position of the visitors head. The direction of SLM was towards the source of sound. For conducting the noise survey, Serbian guidelines for noise measuring were followed (RANLWE, 1992). The A-weighted levels on L_{eq} , L_{max} and L_{min} Sound Pressure Level (SPL) in dBA were collected. L_{eq} is the equivalent continuous noise level which at a given location and over a given period of time contains the same A-weighted sound energy as the actual fluctuating noise at the same location over the same period [4].

The measurements were taken over a period of 1min [4]. At the end of experiment the data were downloaded to a personal computer. With the help of utility software, the equivalent SPL and noise spectrum at each reading was obtained. The data were statistically analysed using Microsoft Excel. This was followed by a graphic representation of the means of L_{eq} SPL-s at different octave bands.

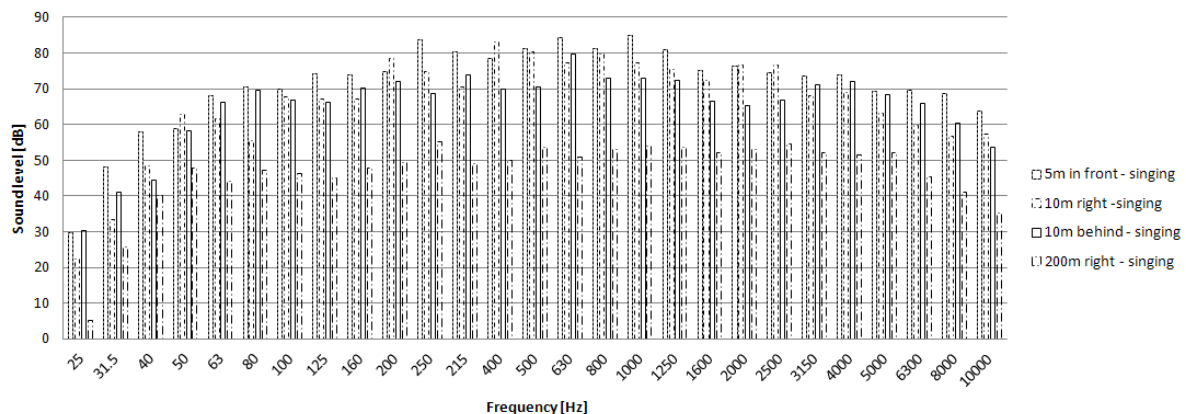
Results and discusion

Table 1. shows the results of L_{eq} , L_{min} , L_{max} measurements during one day of the festival. The maximum values of the equivalent sound pressure levels of noise were measured during the firework and the concert with values 92.5 and 101.9 dBA, respectively. It is well known that those values have a negative impact on human health [6].

Table 1. Results of the measurements for different activities held during the open space event.

	No.	r [m]	L_{Aeq} [dB]	L_{Amax} [dB]	L_{Amin} [dB]
Country dance					
	1.	5 (on the left)	76.2	83	70.3
	2.	5 (in front)	81.5	85	73.9
Speech					
	3.	5 (in front)	86.2	92.6	72.5
Fireworks					
	4.	5 (in front)	92.5	102.1	82.4
No performance					
	5.	5 (on the left)	76.1	87.9	69.7
	6.	5 (in front)	76.2	85.6	69.8
Concert					
	7.	5 (in front)	101.9	110.3	90.1
	8.	10 (on the right)	91.4	98	80.5
	9.	10 (behind)	81.9	88.5	73.9
	10.	200 (on the right)	66.4	79.9	59.5

Figure 1 shows frequency characteristics 1/3 octave of the equivalent noise level measured on 4 places which were 5 meters, 10 meters (in the centre of the venue and on the right side of the stage) and 200 meters from the stage. By looking at the Table 1 and Graphic 1 we can conclude that the further the stage is the level of the noise decreases. At 5 and 10 meters distance the levels of noise were high, above 80 dBA, for frequencies between 200 and 1250 Hz. The result is very interesting concerning that high noise levels at frequencies below 1 kHz produced interference with human communication, since much of the human speech is between 300 and 700 Hz, creating different subjective experience of the noise intensity. It can be said with certainty that at the distance of 200 meters the level of the noise on all frequencies is below values that can affects *human well-being and psychophysical condition*.

Figure 1. L_{eq} 1/3 octave band at different locations from stage

On the figure 2 frequency characteristics at 1/3 octave band for different activities on the stage was shown. Measurements were done at the distance of 5 meters. In all circumstances high levels of noise were detected, nearly and above 80 dBA, especially during the firework and concert. During speeches high levels were also detected. This situation is very similar with political events which are usually organised on stage with one or more spokesmen.

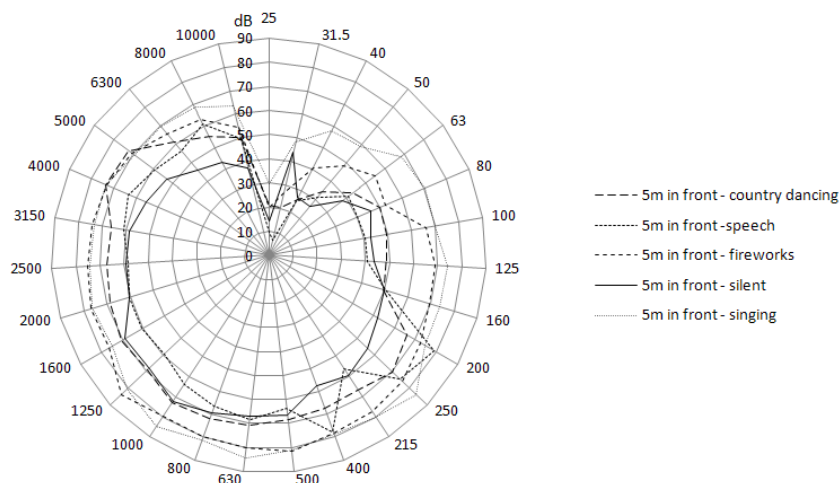


Figure 2. Frequencies analysis of L_{eq} at 5 meters from stage

In this case the noise is fluctuating with maximum level of the sound pressure level of 86.2 dBA between frequency of 200 and 400 Hz. It is interesting to mention that even during breaks, when there are no activities on the stage, the noise caused by the crowd had maximum values L_{eq} between 60 and 70 dBA for frequencies from 500 to 1600 Hz.

Conclusion

Based on the given results we can conclude that during public events people are exposed to considerable noise levels which can have impact on human health. Although these events are occasional, the protective measures must be taken against the excessive exposure to noise. Especially because its effects are cumulative and are not detected immediately. The authorities should make the organizers of such events to constantly monitor the noise during the event and, if for longer period of time the noise exceeded determined levels, to implement adequate measures. Nevertheless, along with the measurement of the noise level it is necessary to take future steps and to provide other protective measures during public events.

Acknowledgements

The authors acknowledge the financial support of the Ministry of Science and Technological Development of the Republic of Serbia, within the project No. III 43002 and TR34014.

References

- [1] World Health Organization, NIGHT NOISE GUIDELINES FOR EUROPE, Edited by Charlotte Hurtley: 2009, ISBN 978 92 890 4173 7
- [2] Davies, H. W., Teschke, K., Kennedy, S. M., Hodgson, M.R., Hetzman, C., et al. (2005). Occupational exposure to noise and mortality from acute myocardial infraction. *Epidemiology*, 16 (1), 25-32.
- [3] Iyyanki V. Murali Krishna, Valli Manickam, Noise Pollution and Its Control, Environmental Management, 2017, ISBN 978-0-12-811989-1

- [4] Guidance on the control of environmental music noise and its impact on communities close to the events, Noise Council, Code of practice on environmental noise at concerts, 1995 Chartered Institute of Environmental Health, ISBN 0 900103 51 5
- [5] Xiaoming Zhou and Michael M. Merzenich, Environmental noise exposure degrades normal listening processes, *Nature Communications*, (2012), volume 3, Article number: 843
- [6] Ron Chepesiuk, Decibel Hell: The Effects of Living in a Noisy World, *Environ Health Perspect.* 2005 Jan; 113(1): A34–A41.

ENVIRONMENTAL EFFECT ON THYROID DISFUNCTION

Krisztián Sepp¹, Andrea Serester², Zsolt Molnár², Marianna Radács³, Zsuzsanna Valkusz¹, Márta Gálfi²

¹*First Department of Medicine, Faculty of Medicine, University of Szeged, 8-10 Korányi AlleyH-6720 Szeged, Hungary*

²*Institute of Applied Sciences Department of Environmental Biology and Education, Gyula Juhász Faculty of Education, University of Szeged, 6 Boldogasszony blv. H-6725, Szeged, Hungary*

email: sepp.krisztian@med.u-szeged.hu

Abstract

The challenges of endocrinology, including those of endocrine disruption, force today's medical science to face the numerous environmental health risks. Disruption of the endocrine system, which in reality affects the unity of the psycho-neuroendocrine immune system, may play a role in the development of many diseases. In this work, one of the basic questions was whether the environmental loads can cause disease (transformation disorders and processes) in the thyroid gland. Our aim was to develop the novel diagnostic method or environment-related thyroid diseases. The endocrine disrupting compounds play an important role in inflammation and transformation of the thyroid gland. For this reason, upgrading any diagnostic method by adding environmental parameters is advised.

Introduction

The problem area of endocrine disruption in the introduction suggests that today's medical science, including the challenges of endocrinology [1] have to face numerous environmental health risks [2]. Disruption of the endocrine system, which actually affects the unity of the psycho-neuroendocrine immune system, may play a role in the development of many diseases. Thus, exploring the changing environmental conditions in the living spaces provided by society and the examining of the relationships among the health problems posed by those exposures can help us study the pathogens and pathomechanisms of certain systemic diseases. In the last half century, endocrine disruptors (ED) have caused very serious dysfunctions in the endocrine glands, especially in the thyroid [3], which have led to severe functional variations. For diseases with thyroid proliferation [4] it is a major health and therapeutic question whether the benign and/or malignant thyroid diseases should be considered in conjunction with the pathogens.

Therefore, in this work, one of the basic questions was whether the environmental loads can cause disease (transformation disorders and processes) in the thyroid gland? In order to provide an answer, recognition of the disease, diagnostic typing and exploration of anamnesis relationships became necessary.

Our aim was to develop the novel diagnostic method for environment-related thyroid diseases.

Methods

The grown thyroid-gland was classified by European Thyroid Association (ETA) and American Thyroid Association (ATA) methods (Table 1).

Table 1 Risk classification systems for thyroid diseases (SPECT/CT based)

	1	2	3
ETA 2006 guidelines	very low <i>the tumor is unifocal T1 (≤ 1 cm) N0M0 and there is no extension beyond the thyroid capsule</i>	low <i>the tumor is T1 (> 1 cm) N0M0, or T2N0M0, or multifocal T1N0M0</i>	high <i>the tumor is any T3; any T4; any T with N1 or M1</i>
ATA 2009 guidelines	low risk <i>no local or distant metastases; no tumor invasion of local regional tissues; no aggressive histology or vascular invasion</i>	intermediate risk <i>microscopic invasion of the tumor into the perithyroidal tissue; cervical lymph node metastasis are present;</i>	high risk <i>macroscopic tumor invasion; incomplete tumor resection; distant metastasis; thyroglobulinemia</i>

By these classifications of thyroid diseases were not examined in the anamneses the effects of environmental (exposure to ED compounds) medic status*. In the endocrine regulation network, the linkage of TSH, aTG, anti-TPO factors were not studied. The guide of the Endocrine Society was used for taking the patients' medical history [5]. After the first medical examination, the patients (n=35) were diagnosed with thyroid dysfunction. In general, the laboratory test contains plasma hormone levels, hormone diurnal rhythm, U-hormones and their metabolites, stimulatory/inhibitory test and standard biochemistry in the examination method of endocrine disease.

In the present work, the diagnostic protocol was supplemented with environmental health issues in which we studied occupation, workplace, place of residence, number of electric devices inside and outside the home, plastic items and exposure to chemicals.

Determination of hormone and antibodies

Whereas the usual microsomal antibody tests employ unpurified microsomes as an antigen preparation, the anti-TPO tests use a purified peroxidase. The two procedures are of comparable performance in terms of clinical sensitivity, but better lot-to-lot consistency and higher clinical specificity can be expected from anti-TPO tests due to the higher quality of the antigen used. Recombinant antigen and polyclonal anti-TPO antibodies are used in the Elecsys Anti-TPO assay. Measuring range is 5.00-600 IU/mL (defined by the lower detection limit and the maximum of the master curve). Values below the lower detection limit are reported as < 5.00 IU/mL. Values above the measuring range are reported as > 600 IU/mL.

Immunoassay for the in vitro quantitative determination of antibodies to thyroglobulin in human serum and plasma. The anti-Tg determination is used as an aid in the detection of autoimmune thyroid diseases. The Elecsys Anti-Tg assay uses human antigen and monoclonal human anti-Tg antibodies. Measuring range is 10.0-4000 IU/mL (defined by the lower detection limit and the maximum of the master curve). Values below the lower detection limit are reported as < 10.0 IU/mL. Values above the measuring range are reported as > 4000 IU/mL.

The Elecsys TSH assay employs monoclonal antibodies specifically directed against human TSH. The antibodies labeled with ruthenium complex consist of a chimeric construct from human and mouse-specific components. As a result, interfering effects due to HAMA (human anti-mouse antibodies) are largely eliminated. Measuring range is 0.005-100 μ IU/mL (defined by the lower detection limit and the maximum of the master curve). The functional sensitivity

is 0.014 $\mu\text{IU/mL}$. Values below the lower detection limit are reported as $< 0.005 \mu\text{IU/mL}$. Values above the measuring range are reported as $> 100 \mu\text{IU/mL}$ (or up to $1000 \mu\text{IU/mL}$ for 10-fold diluted samples).

TSH, Anti-TPO and anti-TG were measured from serum using electrochemiluminescence immunoassay (ECLIA) on Modular E170 analyzer (Roche, Mannheim, Germany) [6, 7].

Results

Table 2 Parameters and classification (ATA, ETA) of thyroid cancer patients

	code	age	ATA	ETA	TSH (mIU/l)	aTG (IU/ml)	aTPO (IU/ml)
control					0,27- 4,29	<115	<34
1	AE	29	1	2	4,67	3298	>600
2	BA	18	2	3	1,59	1125	242
3	BB	18	2	3	2,32	24,51	10,35
4	CSB	44	1	2	1,8	-	12,44
5	CP	66	2	3	2,44	855	-
6	DA	60	1	2	3,14	20,29	-
7	DI	64	1	2	2,46	34,1	-
8	DM	36	2	3	2,94	56,3	-
9	FI	38	1	2	3,32		23,59
10	HE	52	1	2	5,15	45,46	-
11	HL	76	1	2	1,30	21,55	8,24
12	HB	29	2	3	2,61	15,53	7,31
13	JA	23	1	2	0,85	<10,10	-
14	KS	43	2	3	3,28	704	-
15	KG	54	2	3	0,96	238	-
16	KAN	18	1	2	1,35	304,40	-
17	KI	59	1	2	0,72	28,72	-
18	MZS	50	1	2	1,38	46,16	-
19	MA	42	2	3	1,81	367,80	-
20	NN	32	1	2	1,11	-	17,87
21	NBA	22	1	2	0,97	18	-
22	RV	55	2	3	1,36	458,3	78,39
23	SA	35	2	3	11,13	-	282
24	SR	39	2	3	2,24	10,20	-
25	SZJ	61	2	3	0,45	-	8,65
26	SZI	77	1	2	0,68	10,47	-
27	SZT	27	1	2	1,52	22,48	-
28	TKM	40	1	2	1,44	38,4	-
29	TFP	48	1	2	1,05	19,71	-
30	TI	54	1	2	1,42	12,94	-
31	TT	21	1	2	0,80	-	10,76
32	TGYL	84	1	2	2,44	13,44	-
33	VSG	38	2	3	6,24	-	>600
34	VM	59	1	2	3,2	13,72	-
35	ZK	64	2	3	1,46	34,81	-

Table 3 Increased inflammatory parameters (aTG, aTPO) in thyroid cancer

	code	age	TSH (mIU/l)	aTG (IU/ml)	aTPO (IU/ml)	TSH/aTG x 10 ⁻⁶	TSH/aTPO x 10 ⁻⁶	environmental factors
control			0,27- 4,29	<115	<34	<4.29/115	<4.29/34	
median						0,0353475	0,057794	
1	AE	29	4,67	3298	>600	0,00141*	< 0,007789*	9
2	BA	18	1,59	1125	242	0,00141*	0,00657*	8
5	CP	66	2,44	855	-	0,002853*	-	8
14	KS	43	3,28	704	-	0,004659*	-	8
15	KG	54	0,96	238	-	0,004033*	-	9
16	KAN	18	1,35	304,40	-	0,004434*	-	6
19	MA	42	1,81	367,80	-	0,004921*	-	8
22	RV	55	1,36	458,3	78,39	0,002967*	0,017349*	7
23	SA	35	11,13	-	282	-	0,039468*	8
33	VSG	38	6,24	-	>600	-	< 0,0104*	6

TSH: thyroid-stimulating hormone; aTG: antithyroglobulin antibody; aTPO: thyroperoxidase antibody

*p<0.01 relation to the median

Inflammatory parameters and factors derived from TSH data were always lower than the calculated median of control. At the same time, these results can be correlated with environmental health issues.

Conclusions

It is common for endocrine disrupting compounds to play an important role in inflammation at low doses, therefore it seems worthwhile to determine the inflammatory factors (aTG, aTPO) in addition to TSH in the case of thyroid dysfunction. It could be also important to find out the patients' environmental exposition of endocrine disrupting compounds when taking anamnesis.

This work was supported: TÁMOP-4.2.4.A/2-11/1-2012-0001 "National Excellence Program," EFOP-3.6.1. 16-2016-00008 and EFOP-3.4.3-16-2016-00014.

References

- [1] K. Sepp, M.A. Laszlo, Zs. Molnar, A. Serester, T. Alapi, M. Gálfi, Zs. Valkusz, M. Radács: The Role of Uron and Chlorobenzene Derivatives, as Potential Endocrine Disrupting Compounds, in the Secretion of ACTH and PRL. International Journal of Endocrinology Article ID 7493418, 2018.
- [2] Gy. Nagyéri, Zs. Valkusz, M. Radács, T. Ocskó, P. Hausinger, M. László, F.A. László, A. Juhász, J. Julesz, M. Gálfi: Behavioral and endocrine effects of chronic exposure to low doses of chlorobenzenes in Wistar rats," Neurotoxicology and Teratology 34, 9–19, 2012.
- [3] O.E. Okosieme, I. Khan, P.N. Taylor: Preconception management of thyroid dysfunction. Clinical endocrinology, 89: 269-279, 2018.
- [4] G. Pellegriti, F. Frasca, C. Regalbuto, S. Squatrito, R. Vigneri: Worldwide increasing incidence of thyroid cancer: update on epidemiology and risk factors. Journal of Cancer of Epidemiology, Article ID: 965212, 2013.
- [5] L. Leenhardt, M.F. Erdogan, L. Hegedus, S.J. Mandel, R. Paschke, T. Rago, G. Russ: 2013 European Thyroid Association guidelines for cervical ultrasound scan and ultrasound-guided techniques in the postoperative management of patients with thyroid cancer. Eur Thyroid J. 2:147-159. 2013.
- [6] R.S. McIntosh, M.S. Asghar, A.P. Weetman: The antibody response in human autoimmune thyroid disease. Clin Sci 92:529-541. 1997.

[7] U. Feldt-Rasmussen: Analytical and clinical performance goals for testing autoantibodies to thyroperoxidase, thyroglobulin, and thyrotropin receptor. Clin Chem 42:160-163. 1996.

MODELLING OF MANAGEMENT SYSTEM OF ENVIRONMENTAL TOXICOLOGY RESEARCH LABORATORY

Andrea Serester

*Óbuda University, Doctoral School of Applied Informatics and Applied Mathematics and
University of Szeged, Gyula Juhász Faculty of Education, Institute of Applied Science,
Department of Environmental Biology and Education
e-mail: galfi@jgypk.u-szeged.hu*

Abstract

The environmental loads have serious burden both in individual and in social levels. The endocrine disruptor compounds (EDC) may cause endometriosis, fibrosis, childhood obesity, adulthood diabetes (type II.), cryptorchidism, male infertility and diminution of the levels of testosterone. Within the EU, this is approximately € 163 billion worth of specific health expenditure annually. Currently there is no standard method to examine these agents, in the environmental toxicology (Et). This issue is examined with several proceedings by environmental toxicology research laboratories (EtRL), however there are difficulties to compare the results of the laboratories. To solve this problem, the aim of this paper is to demonstrate a virtual verification method, using a solution, in which the operation of research unit is matched in the international requirement system. With the aim of providing comparable and reliable data from EtRL research and/or project results. At the same time, the safe handling of this data system is examined using the knowledge of the network studies, and this information is handled with virtual verification in a simulation model.

Based on our results, the virtual verification simulation model can enable the EtRL management system to operate at minimum risks.

Introduction

Nowadays, environmental toxicology research is at the centre of interest, because environmental pollutions have a significant health burden on individuals and societies [1].

Environmental load agents that interfere with the endocrine system are called endocrine disruptor compounds (EDC). They have high health risks [2]. The results of the EDC effects confirmed by the DELPHI method, EDC exposure to the population of Europe can manifest in intellectual effects e.g. autism, loss of skills – dysfunctions and in hyperactivity. EDC also can cause serious medical costs, because of endometriosis, fibrosis, childhood obesity, adulthood diabetes (type II.), cryptorchidism, male infertility and diminution of the levels of testosterone. Their estimated cost within the EU, 1.28 % of total domestic products (approximately € 163 billion) annually.

The above mentioned supports, that it is important to develop a standardized methodology for the study of substances with EDC activity, as soon as possible. An important aspect of this is to make the results of basic and applied research of environment toxicology research laboratories can be directly utilized at the social (sectoral) level. All this, can be ensured by matching laboratory operations with international requirements (e.g. ISO), in this context the

structure of the data system is essential and it also means the controlled operation of the resources of the activity processes that can be traced and traced back. Systematic operation, therefore, represents the development of sustainable accuracy and result security. The material resource background and the methodical stability in the standardized laboratory operation create the possibility to utilize the research results directly in the society.

Since data-based, objective parameters controlled by a research laboratory operation, is the most efficient electronically, therefore, systematic control options with virtual verification have already been required.

In the present work the main goal is to solve this task pilot: with creation of simulation models, with definition the key elements and complex processes of environmental-toxicology laboratories and with persistent activity control.

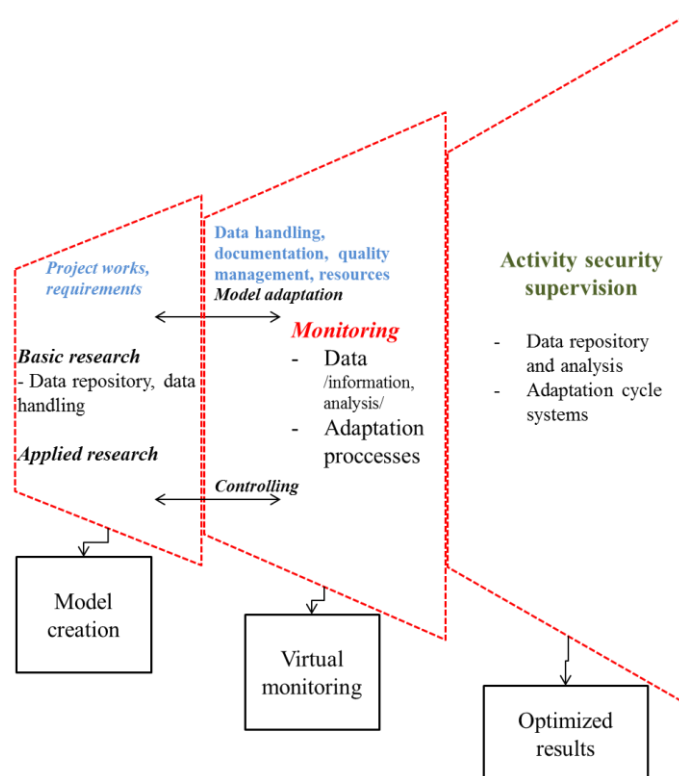


Figure 1 Environment-toxicology research laboratory operating model with requirement compliance

Research protocol

Firstly, in the research tasks, the selection of international requirements for the field of environmental toxicology (Et) research (theoretical / practical and organizational operation) was made resulting in the simultaneous adaptation of the specialized sciences, ISO, GLP and GMP requirements. In the next step, the activity target areas and the networks of resources implementing the activities have been set up. The next step was to create the target areas for action and the implementing activities of networks of resources. Then the identified system elements were defined depending on the requirements of the standard management. The junctions of the established network of connections were ranked according to graph attributes

(Figure 2) [3]. The responsibilities of human resources were assigned to the network connections, to which the appropriate powers were associated. According to this method, the personal requirements of the management system were defined. The management "pyramid" was therefore directed the methodological and resource elements of the project and research tasks, according to the criteria of the Et testing laboratory requirements. The standard requirements handle the safety of results of the environmental toxicology research laboratories (EtRL) with the safety indicators of the validated indicators of measurement and the safety of methodology; therefore they are handled by confidence intervals (Figure 3) [4,5]. Therefore virtual monitoring of the network connection system can be possible with the data from the activities of EtRL and with binary code (0, 1) of the system operation. Based on the method described above, the research and project systems of EtRL with safety code can also support independent controlling and auditing, which minimizes system certification risks (Figure 1).

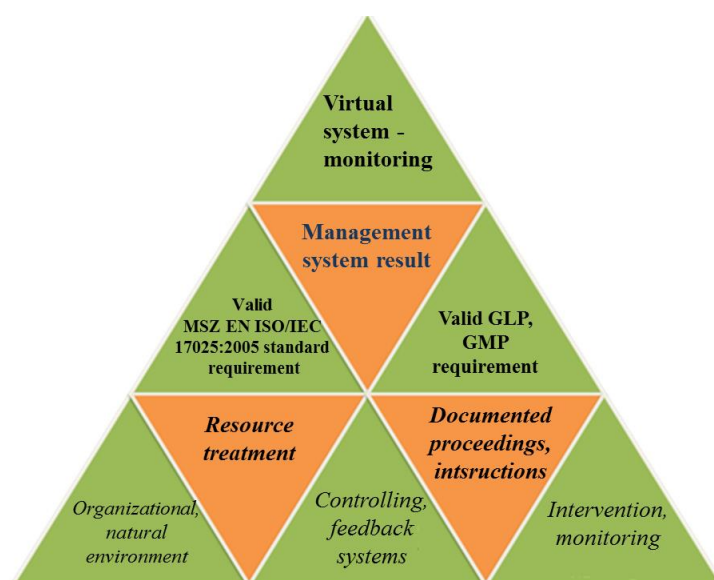


Figure 2 Environment-toxicology research laboratory hierarchical operation (according to grid-based relationships)

Results, discussion

The system operation developed as described herein can be virtually monitored because the node structure outlined a hierarchical system operation, for which the management standard requirements were well suited.

The Et testing laboratory system operated according to the presented results, which is handled by confidence intervals can be interpreted as a “hyperspace”, which means the basis of virtual verification.

Conclusion

With the help of this pilot simulation modelling, the EtRL operation management system has been designed so that international compliance can be followed by an external independent party using virtual verification.

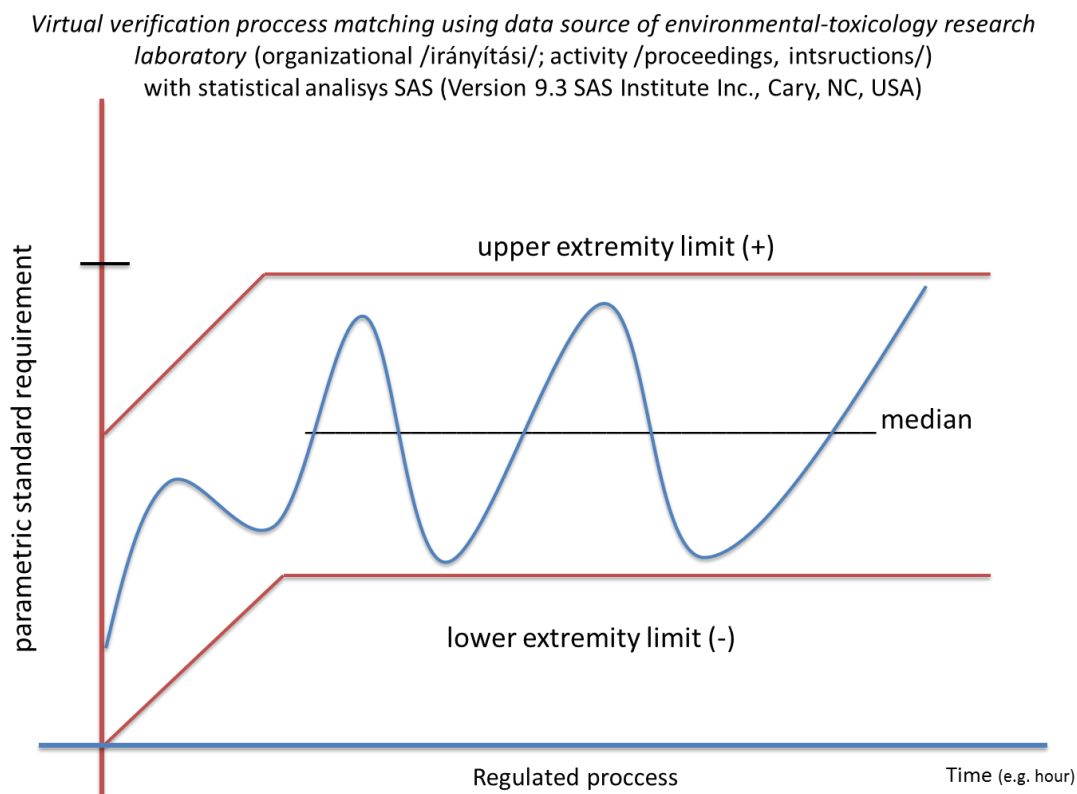


Figure 3 Validated system of Environment-toxicology research laboratory handled by confidence interval

References

- [1] Sepp K, Laszlo AM, Molnar Z, Serester A, Alapi T, Galfi M, Valkusz Z, Radacs M: The role of uron and chlorobenzene derivatives, as potential endocrine disrupting compounds, in the secretion of ACTH and PRL. *Int J Endocrinol.*, 2018, 2, 018:7493418. doi: 10.1155/2018/7493418, eCollection.
- [2] Trasande L., Zoeller RT, Hass U, Kortenkamp A, Grandjean P, Myers JP, DiGangi J, Hunt PM, Rudel R, Sathyanarayana S, Bellanger M, Hauser R, Legler J, Skakkebaek NE, Heindel JJ: Burden of disease and costs of exposure to endocrine disrupting chemicals in the European Union: an updated analysis. *Andrology*, 2016, 4: 565–572, doi:10.1111/andr.12178.
- [3] Boole, G: *The mathematical analysis of logic, being an essay towards a calculus of deductive reasoning.* 1965, Oxford, Basil Blackwell.
- [4] Chindelevitch L, Ziemek D, Enayetallah A, Randhawa R, Sidders B, Brockel C, Huang ES: Causal reasoning on biological networks: interpreting transcriptional changes. *Bioinformatics*, 2012, 28: 1114–21.
- [5] Langton CG: Artificial life. In: Langton CG, editor, *Proc. of an Interdisciplinary Workshop on the Synthesis and Simulation of Living Systems*, Los Alamos, New Mexico, 1989.

This work was supported by EFOP-3.4.3-16-2016-00014

A GREEN, FLUORESCENT LABELING OF ESTROGENS

**Vivien Szabó¹, Péter Trungel-Nagy¹, Patrik Antal¹, Andrea Liliom¹, Édua Kovács¹,
Erzsébet Mernyák¹**

¹*Department of Organic Chemistry, University of Szeged, H-6720 Szeged, Dóm tér 8,
Hungary*

Abstract

Novel 2- or 3-labeled 13 β - and 13 α -estrone derivatives were synthesized via Cu(I)-catalyzed azide-alkyne click reaction (CuAAC). The steroidal alkynes or azides were reacted with the appropriate BODIPY-based fluorescent dyes bearing the complementary functions. The newly synthesized fluorescent estrone derivatives may serve as good candidates for the development of “green” biological assays.

Introduction

Estrogens belong to a class of natural steroids, which possess estrogenic activity. Certain synthetic estrone-derived compounds are described as antitumoral compounds, but the mechanism of their action is mostly unknown [1]. In order to investigate and monitor their mechanism, their labeling is essential. Estrone-based enzymatic or receptorial assays use radioisotope labeling. It would be of particular interest to replace the harmful radioactive methods for greener fluorescent ones. The biological behavior of the fluorescent labeled biomolecules depends on the chemical structure of the conjugate. The size of the fluorescent dye, the linker between the two moieties and the nature of the coupling group may be crucial [2-4].

Results and discussion

Steroids bearing azide or terminal alkyne function and two BODIPY dyes have been synthesized. Estrone was provided with ethynyl function at C-2 via Sonogashira coupling of the steroidal aryl iodide with trimethylsilylacetylene. The steroidal azide was synthesized in a two-step procedure: by alkylation of the phenolic OH group with α,ω -dibromoalkanes and the subsequent nucleophilic substitution of the bromide with azide. Fluorescent dyes based on BODIPY-core were provided with azide or alkyne functional groups. Fluorescent labeling of estrone was efficiently achieved at the C-2 or C-3 position (Fig. 1). The *in vitro* testing of the newly synthesized labeled estrones is under progress.

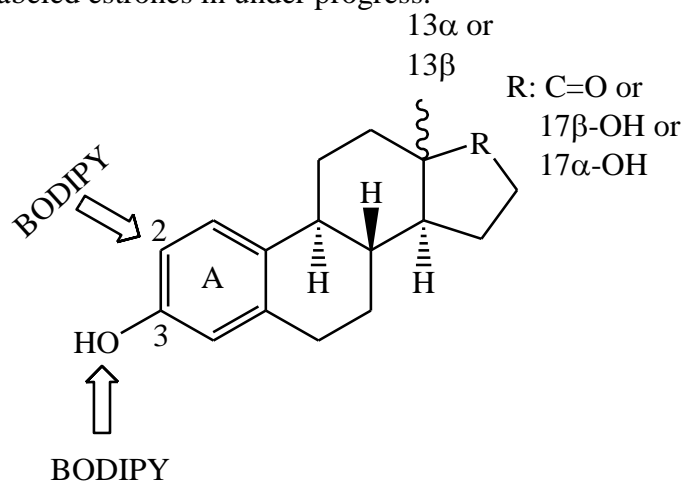


Figure 1. Fluorescent labeling of estrone at positions C-2 or C-3

Conclusion

We have developed an efficient “green” fluorescent labeling procedure for estrone derivatives using Sonogashira and/or CuAAC reactions as key steps.

Acknowledgements

This work was supported by National Research, Development and Innovation Office-NKFIH through project OTKA SNN 124329. The work of Erzsébet Mernyák was supported by János Bolyai Research Scholarship of the Hungarian Academy of Sciences.

References

- [1] S. Osati; H. Ali; B. Guerin; van J.E. Lier. *Steroids* **2017**, *123*, 27-36.
- [2] G. Ulrich; R. Ziessel; A. Harriman. *Angew. Chem. Int. Ed.* **2008**, *47*, 1184–1201.
- [3] A. Loudet; K. Burgess. *Chem. Rev.* **2007**, *107*, 4891–4932.
- [4] H. Langhals; A. Obermeier. *Eur. J. Org. Chem.* **2008**, *36*, 6144–6151.

OPTIMIZATION OF MICROFILTRATION FOR DISTILLERY WASTEWATER PURIFICATION

Vesna Vasic, Marina Sciban, Jelena Prodanovic, Dragana Kukic, Aleksandar Jokic, Nevena Blagojev

*University of Novi Sad, Faculty of Technology Novi Sad, Bul. cara Lazara 1
21000 Novi Sad, Serbia, e-mail: vesnavasic@tf.uns.ac.rs*

Abstract

In our previous work we examined the possibility of application of microfiltration for distillery stillage purification in the systems without [1] and with the presence of static mixer [2]. Feed flow rate ($Q = 40; 100$ and 160 l/h), transmembrane pressure (TMP = $0.3; 0.6$ and 0.9 bar) and feed pH ($3; 6$ and 9) were considered for design of experiments. Influence of choosen factors on permeate flux and specific energy consumption was investigated using Response Surface Methodology. The results showed that Response Surface Methodology is an appropriate model for mathematical presentation of the process. To optimize a process that has two or more responses, several methods can be applied, but the most commonly used method is the concept of the desired function (desirability function) [3]. In this work optimization of the experimental conditions was conducted using the modified Harrington method of the desired function. To optimize the microfiltration process of distillery wastewater, the following responses were selected: mean flux permeate in the static mixer system (JSM) and the relative change in specific energy consumption (ER). The goal of optimization was to select the feed flow rate and transmembrane pressure values for which the observed responses will be maximum, ie their desired functions will have a higher value.

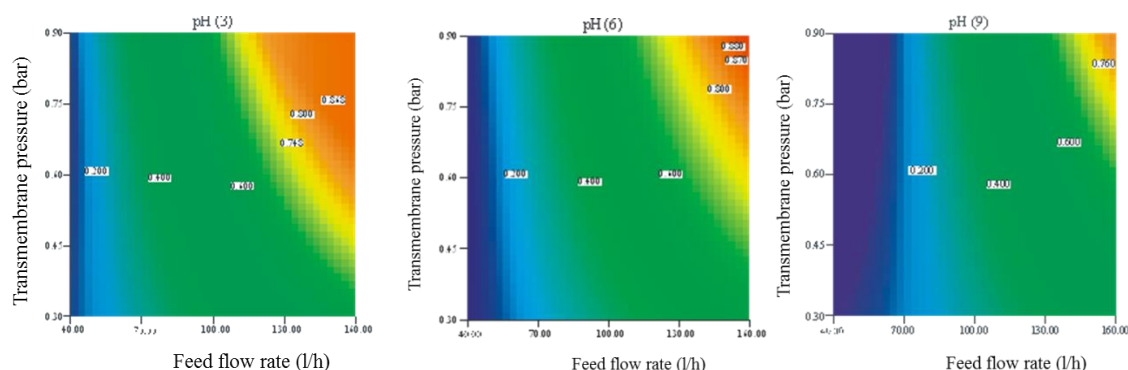


Figure 1. Dependence of total desired function from the feed flow rate and transmembrane pressure

Obtained results (Figure 1) showed that the microfiltration was best performed at maximum flow and transmembrane pressure values, at all pH values, with the fact that the value of total desired function decreases with the increase of pH. If all factors, including pH value, are used for optimization, the optimum values of the parameters for optimization showed that the microfiltration was best performed at the values of feed flow of 160 l/h and TMP of 0.9 bar, at pH value of 5.81 . Under these conditions, the total desired function had a maximum value of 0.944 , the mean permeate flux for the system with static mixer was 58.3 l/m³h, while the relative change in the specific energy consumption was 123% .

Acknowledgements

This research was supported by the grant number TR 31002 from the Ministry of Education, Science and Technological Development of the Republic of Serbias.

References

- [1] V.Vasić, A.Jokić, M.Šćiban, J.Prodanović, J.Dodić. Environ. Eng. Manag. J. 15 (2016) 2781-2788.
- [2] V.M. Vasić, A.I. Jokić, M. B. Šćiban, J.M. Prodanović, J.M. Dodić, D.V. Kukić. Acta Periodica Technologica. 48 (2017) 285-293.
- [3] M.Khayet, C.Cojocar, G.Zakrzewska-Trznadel. J. Membrane Sci. 321 (2008) 272-283.

CHEMICAL COMPOSITION OF SOME FLOUR MIXTURES WITH HIGH NUTRITIONAL VALUE

Stoin Daniela*¹, Poiana Mariana-Atena¹, Mogradean Diana¹, Cozma Antoanela¹, Jianu Calin¹, Trasca Teodor¹, Ravis Adrian¹

¹University of Agricultural Sciences and Veterinary Medicine of Banat "King Mihai I of Romania" Timisoara

Faculty of Food Processing Technology Food Science Department 300645, Timisoara, Calea Aradului, nr. 119, Roumania

author's email address: danielastoin@yahoo.com

Abstract

The objectives of this study were to optimize high nutritional blends obtained by partial substitution of white wheat flour 550 (WWF) with rye flour (RF), oat flour (OF), quinoa flour (CF) and maize flour, respectively, and assessing the impact of using these mixtures on the sensory qualities of multigrain bread. WWF has been substituted by 5%, 10%, 15%, 20% and 25% RF, OF, QF and MF, respectively. As for flours and flours mixtures, the following determinations were carried out: moisture, protein content, ash content, fat content, fiber content, and total carbohydrate content. The resulting mixtures had high protein content (11.23% at M6 and 11.91% at M3), fiber (2.71% at M6 and 3.68% at M1), ash (1.28% at M6 and 1.70% at M3) fat (2.61% at M6 and 3.42% at M1) and low carbohydrates (65.74% at M1 and 68.02% at M6) and moisture ranged between 13.77% at M1 and 14.15% at M6.

Based on the obtained results regarding the physic-chemical composition of the M1 ÷ M6 mixtures, it can be appreciated that all these mixtures are suitable for being used in obtaining bakery products (multigrain bread) according to the established substitution amounts, because all the results obtained for the nutritional and quality parameters had the values closest to the daily nutritional needs of the human body for good development and function.

Introduction

Current concerns both at national and international level in the food sector are directed towards product quality, diversification of production and the renewal of the range of products, thus aiming at obtaining high nutritional products without additives, preservatives or other compounds with a negative impact on the human organism [1, 2, 3].

The food pyramid reflects the nutritional recommendations, the quantities and types of foods to be consumed daily to maintain health and reduce the risk of developing various dietary diseases [4, 5]. The most important foods that make up the food pyramid are cereals, vegetables, and fruits as the foundation of balanced nutrition, calling them the "basis" for proper nutrition and health [5].

The flours used in this study to obtain functional multigrain bread were: white wheat flour 550 (WWF), rye flour (RF), oat flour (OF), quinoa flour (QF) and maize flour (MF). The use of these different types of flour in various amounts (RF, OF, QF, MF) in the production of multigrain bread by the partial substitution of WWF is justified on the basis of their complex chemical composition, implicitly for their food and biological value [6, 7, 8, 9, 10, 11].

The beneficial effects of rye on health are due to the high intake of fiber, protein, mineral salts (iron, calcium, phosphorus, magnesium, potassium), nitrates, starch carbohydrates, cellulose, essential amino acids, vitamins A, C, E, K, complex B, and very few fats (cholesterol free) [6, 7].

The superior nutritional value of oats is given by the high content of proteins, lipids, minerals, fibers, various other phyto-constituents such as flavonoids, flavonolignans, saponins, sterols and triterpenoids [8].

Quinoa is very rich in proteins and essential amino acids (isoleucine, methionine, lysine, thiozine, valine); vitamins A, B, C and E; calcium, iron, magnesium, omega 3; manganese, copper, magnesium, phosphorus; soluble fibers as well as insoluble fibers [9, 10].

Corn contains proteins, sugars, fats, essential fatty acids omega-3 and omega-6, vitamins (B1, B2, B3, B5, B6, B9, C, E, K), mineral salts (sodium, magnesium, phosphorus, iron, zinc, calcium, copper, selenium), antioxidants (carotene, lutein, cryptoxanthin) [11].

Starting from these observations, the purpose of this study was to optimizing some blends of high nutritional flours, establishing the optimum manufacturing recipe, and the optimal doses of RF, OF, QF and MF that can be added to the multigrain bread without affecting its quality.

Experimental

Materials

The flours analyzed in this study have been purchased from hypermarkets and specialized stores.

Steps in the preparation of flour mixtures

When determining the proportion of each flour assortment to form a mixture, account was taken of the physical, chemical and technological characteristics of these flours. Thus, due to the fact that both RF and OF, QF and MF do not contain gluten, in order to ensure the formation of the three-dimensional gluten skeleton of the dough, 40% and 60% of WWF were added.

In the obtaining of the 6 blends RF, OF, QF and MF were used in variable proportions (5%, 10%, 15%, 20% and 25%) because it is known that these flours have a high nutritional value, rich in proteins, fibers, essential amino acids, antioxidants, minerals and vitamins [6, 7, 8, 9, 10, 11].

The 6 mixtures of flours to be used in making multigrain bread are:

Mixture (M1): 40% WWF:10% RF:25% OF:20% QF:5% MF;

Mixture (M2): 40% WWF:15% RF:20% OF:20% QF:5% MF;

Mixture (M3): 40% WWF:20% RF:15% OF:20% QF:5% MF;

Mixture (M4): 60% WWF:10% RF:10% OF:15% QF:5% MF;

Mixture (M5): 60% WWF:10% RF:15% OF:10% QF:5% MF;

Mixture (M6): 60% WWF:10% RF:20% OF:5% QF:5% MF.

Analytical procedures

Proximate composition of flours and flour mixtures

For determining the average chemical composition of flours and flour mixtures, were determined: moisture, acidity, fat content, ash content, fiber content and carbohydrate content was determined according to standard method A.O.A.C. 1995 [12]; protein content was determined by the Kjeldahl method according to standard method A.A.C.C. 2000, No. 46-10 [13].

All determinations were performed in triplicate, calculating their arithmetic mean of three separate determinations. The data were statistically analyzed using the program Microsoft Excel.

Results and discussion

Proximate composition of flours and flour mixtures

Table 1 presents the results obtained from the proximate analysis of flours. The results obtained regarding the composition of the four flours (RF, OF, QF and MF) analyzed compared to WWF, highlights their nutritional potential as a result of the higher protein content, raw fiber, fats and ash. RF showed high protein levels - 12.82% compared to 10.72%

in WWF, fiber - 3.84% vs. 1.36% in WWF, ash - 2.72% vs. 0.69% in WWF, fat - 1.98% in WWF and lower carbohydrate levels - 64.42% vs. 71.24% in WWF [6, 7].

Also, the composition of OF, QF and MF was superior for all analyzed constituents compared to WWF, and confirmed by Lea J. (2009), Singh, R. et. al. (2013), Qamar S. et al. (2017) and Filho A.M. et. al. (2017). Thus, fat content ranged between 4.46% in OF and 6.16% in QF versus 1.65 in WWF; protein content ranged between 11.12% in MF and 11.36% in OF and 14.13% in QF versus 10.72% in WWF; fiber content ranged between 2.55% in MF and 5.42% in OF and 6.46% in QF vs. 1.56% in WWF; ash content ranged between 1.85% in OF and 2.62% in QF vs. 0.69% in WWF [8, 9, 10, 11].

Table 1. Proximate composition of flours studied

Analysis (%)	White wheat flour 550 (WWF)	Rye flour (RF)	Oat flour (OF)	Quinoa flour (QF)	Maize flour (MF)
Moisture	14.34±0.29	14.22±0.09	13.98±0.60	11.94±0.25	15.07±0.06
Fat	1.65±0.21	1.98±0.24	4.46±0.21	6.16±0.20	4.76±0.20
Protein	10.72±0.35	12.82±0.42	11.36±0.13	14.13±0.18	11.12±0.19
Fiber	1.36±0.16	3.84±0.15	5.42±0.19	6.46±0.41	2.55±0.21
Carbohydrates	71.24±0.23	64.42±0.41	62.93±0.32	58.69±0.33	66.44±0.18
Ash	0.69±0.27	2.72±0.22	1.85±0.24	2.62±0.16	2.06±0.21

All determinations were done in triplicate and the results were reported as average value ± standard deviation (SD).

The flour mixtures were marked as: **M1, M2, M3, M4, M5, M6.**

Table 2. Proximate composition of flour mixtures studied

Mixtures	Moisture (%)	Fat (%)	Protein (%)	Fiber (%)	Carbohydrates (%)	Ash (%)
M1	13.77±0.21	3.42±0.06	11.77±0.20	3.68±0.20	65.74±0.16	1.62±0.21
M2	13.78±0.24	3.31±0.18	11.84±0.45	3.60±0.14	65.81±0.08	1.66±0.08
M3	13.79±0.11	3.18±0.24	11.91±0.12	3.52±0.19	65.90±0.24	1.70±0.28
M4	13.95±0.32	2.78±0.47	11.50±0.33	2.81±0.41	67.61±0.28	1.35±0.22
M5	14.05±0.14	2.69±0.36	11.37±0.11	2.76±0.19	67.82±0.27	1.31±0.20
M6	14.15±0.13	2.61±0.52	11.23±0.21	2.71±0.19	68.02±0.11	1.28±0.14

All determinations were done in triplicate and the results were reported as average value ± standard deviation (SD).

In contrast, carbohydrate content is lower for all four flours compared to WWF, ranging between 58.69% in QF and 66.44% in MF compared to 71.24% in WWF, which contributes to lowering the glycemic index of the products obtained from these flours [8, 9, 10, 11, 14, 15]. As for the moisture content of the analyzed flour samples, it was lower in the case of QF (11.94%), OF (13.98%) and RF (14.22%) than that of WWF (14.34%), while moisture content in MF was 15.07% [16].

Analyzing the moisture values (Table 2) corresponding to the six mixtures of analyzed flour, it can be seen that it varied between 13.77% (M1) and 14.15% (M6), which makes the use of these blends in multigrain bread manufacturing, to require a smaller amount of water to be added to the dough [14]. It can also be noticed that the humidity of the mixtures M1 ÷ M3 (13.77 ÷ 13.79%) was lower than that for the M4 ÷ M6 mixtures (13.95 ÷ 14.15%) which makes the use of M1 ÷ M3 blends in the manufacturing technology of the multigrain bread to cause a slight extension of its freshness [14, 15]. The fat content of the analyzed mixtures varied between 2.61% (M6) and 3.42% (M1), observing that with the increase of the WWF percentage from 40% to 60% and the decrease of the QF percentage from 20% at 5% and the percentage of OF from 25% to 10%, the fat

content of the mixtures decreases linearly, thus avoiding the risk of increasing acidity of these mixtures [16].

According to the results presented in Table 2, the studied mixtures (M1 ÷ M6) can be considered important "sources of proteins, fibers and minerals", thus the protein content ranges between 11.23% in M6 and 11.77% in M1, the fiber between 2.71% in M6 and 3.68% in M1 and the ash rate between 1.28% in M6 and 1.62% in M1, results that are consistent with those obtained by Lea J. (2009), Singh, R. *et al.* (2013), Qamar S. *et al.* (2017) and Filho A.M. *et al.* (2017) [8, 9, 11]. Regarding the carbohydrate content of the analyzed mixtures (M1 ÷ M6) (Table 2), it can be observed that it increases linearly from M1 (65.74%) to M6 (68.02%) with the increase of the WWF percentage from 40% to 60% [8, 9, 11, 15].

Conclusions

Mixtures M1 ÷ M6 can be successfully incorporated into the multigrain bread obtaining recipe, resulting in a value-added functional product due to the superior protein, fiber, mineral and fat content compared to WWF.

Based on these results, we can formulate the following recommendation, namely, the use of these blends in both multigrain bread technology and in other pastry and bakery products technology. The use of RF, OF, QF and MF for the purpose of obtaining bakery products does not raise technological problems and can be processed following the model of classic production lines existing in bakery units.

The results in this research confirm that this mixture is a good source of many important nutrients that appear to have a very positive effect on human health and could be used to obtain potentially functional foods.

The recipe for multigrain bread recommended following the observations from this study is: flour mixture (60% WWF: 10% RF: 15% OF: 10% QF: 5% MF), water - 57%, yeast – 2.5%, salt – 2%.

References

- [1] Bronzwaer S., EFSA scientific forum "from safe food to healthy diets". EU risk assessment - Past, present and Future. Trends Food Sci. Technol., 19:S2–S8, 2008.
- [2] Roberts S.B., Rosenberg I., Nutrition and aging: changes in the regulation of energy metabolism with aging. *Physiol. Rev.*, 86:651–667, 2006.
- [3] Vicentini A., Liberatore, Mastrocola D., Functional Foods: Trends And Development Of The Global Market, *Ital. J L.. Food Sci.*, volume 28, pp338-351, 2016.
- [4] Chwang, L. C., "Nutrition and dietics in aged care". *Nutrition and Dietics*, vol. 69 (3), pp 203–207. doi:10.1111/j.1747-0080.2012.01617.x. Retrieved March 31, 2015.
- [5] Vitamin and mineral requirements in human nutrition: report of a joint FAO/WHO Expert Consultation, Bangkok, Thailand, 1998.
- [6] Bushuk W., Rye: Production, chemistry, and technology (2nd ed.), Amer. Assn. Cer. Chem., St. Paul, Minnesota. 2001.
- [7] Hansen H., Moller B., Andersen S., Jorgensen J., Hansen A., Grain Characteristics, Chemical Composition, and Functional Properties of Rye (*Secale cereale* L.) As Influenced by Genotype and Harvest Year, *J. Agric. Food Chem.*, vol. 52, pp 2282–229, 2004.
- [8] Singh, R., S. De, and A. Belkheir, Avena sativa (Oat), a potential nutraceutical and therapeutic agent: an overview. *Critical reviews in food science and nutrition*. **53**(2): pp. 126-144, 2013.

- [9] Filho A.M., Pirozi M.R., Borges J.T., Pinheiro Sant'Ana H.M., Chaves J.B., Coimbra J.S., Quinoa: Nutritional, functional, and antinutritional aspects, Crit Rev Food Sci Nutr., vol. 57(8), pp 1618-1630, 2017.
- [10] James Lea. Quinoa: composition, chemistry, nutritional, and functional properties. Adv Food Nut Res.; 58:1–31, 2009.
- [11] Qamar S., , Aslam M., Huyop F., Javed M. A., Comparative study for the determination of nutritional composition in commercial and noncommercial maize flours, Pak. J. Bot., 49(2): pp. 519-523, 2017.
- [12] A.O.A.C., “Official Methods of Analysis” Association Official Analytical Chemists of the 16th Ed. International, Washington, D.C., U.S.A., 1995.
- [13] AOAC (Association of Official Analytical Chemists) Official Methods of Analysis International. 17th, Ed. Washington, DC: AOAC, 2000.
- [14] Stoin D., Negrea M., Jianu C., Velciov A., Trașcă T., Evaluation of the nutritional and sensory quality of functional bread assortments obtained from wheat flour and carrot powder (*Daucus carota* L.), Journal of Agroalimentary Processes and Technologies, volume 23 (4), pp. 264-270, 2017.
- [15] Malolma S.A., Eleyinmi A.F., Fashankin J.B., Chemical composition, rheological properties and bread making potential of composite flours from bread fruit, bread nut and wheat. African Journal of Food Sciences 5: pp. 400-410, 2011.
- [16] Stoin D., Milling and Milling Technology, Publishing house Eurobit, Timișoara, pp. 396, ISBN 978-973-620-448-7, 2008.

**CHIRAL HIGH-PERFORMANCE LIQUID AND SUPERCRITICAL FLUID
CHROMATOGRAPHIC ENANTIOSEPARATIONS OF LIMONENE-BASED
BICYCLIC AMINOALCOHOLS AND AMINODIOLS ON POLYSACCHARIDE
CHIRAL STATIONARY PHASES**

**Tímea Orosz¹, Gábor Némethi¹, Attila Bajtai¹, Zsolt Szakonyi², Ferenc Fülöp², István
Ilisz¹, Antal Péter¹**

¹*Institute of Pharmaceutical Analysis, University of Szeged, Somogyi utca 4, H-6720 Szeged,
Hungary*

²*Institute of Pharmaceutical Chemistry, University of Szeged, Eötvös utca 6, H-6720 Szeged,
Hungary*

e-mail: orosz.ti@chem.u-szeged.hu

Chirality is extremely important for the modern pharmaceutical industry since many drug compounds are chiral molecules whose stereoisomers usually possess various toxicological and pharmacological properties. One of the enantiomers (eutomer) have the desired pharmacological activity, while the other isomer (distomer) is inactive or in worst cases some undesirable effects or even toxic effect can also be produced.

The investigated compounds were limonene-based bicyclic 1,3-aminoalcohols and 1,3,5- and 1,3,6-aminodiols. In recent years, these compounds have been intensively investigated due to their potential biological activity and their benefits in synthetic chemistry. Aminoalcohols and aminodiols are known to be outstanding building blocks for the synthesis of remarkable heterocyclic compounds. Aminodiol-based nucleoside analogs possess noteworthy antitumor or antiviral activity [1]. The synthesis of new, limonene-based chiral bicyclic 1,3-aminoalcohols and aminodiols from commercially available starting materials have recently been reported [2].

As a result of the pharmaceutical and biological activity of chiral 1,3-aminoalcohols and aminodiols, it is very important to have at hand enantioselective analytical methods for the identification and separation of these compounds. Enantioseparations of limonene-based bicyclic 1,3-aminoalcohols and 1,3,5- and 1,3,6-aminodiols were carried out with high-performance liquid chromatographic and supercritical fluid chromatographic (SFC) methods on commercial polysaccharide-based chiral stationary phases.

The effects of the mobile phase composition, the nature and concentration of the alcohol additive, the temperature and the structures of the studied analytes on the separations were investigated in the normal phase and SFC mode. The elution sequence was determined in all cases. The separations of the stereoisomers of the investigated analytes were optimized in both chromatographic modes.

Acknowledgements



Supported by the UNKP-18-3 New National Excellence Program of the Ministry of Human Capacities.

References

- [1] Largy E, Liu W, Hasan A, Perrin DM. A Pyrimidopyrimidine Janus-AT Nucleoside with Improved Base-Pairing Properties to both A and T within a DNA Duplex: The Stabilizing Effect of a Second Endocyclic Ring Nitrogen. *Chem-Eur J*, 1495-1499, 2014.
- [2] Le Minh T, Fülöp F, Szakonyi Z. Stereoselective Synthesis of Limonene-based Chiral 1,3-Aminoalcohols and Aminodiols. *Eur J Org Chem* 2017.

INHOMOGENITY OF THE 172 nm VUV LIGHT IRRADIATED AQUEOUS SOLUTIONS

Luca Farkas¹, Gábor Peintler², Thomas Oppenländer³, Tünde Alapi¹

¹*Department of Inorganic and Analytical Chemistry, University of Szeged, H-6720 Szeged, Dóm tér 7, Hungary*

²*Department of Physical Chemistry and Materials Sciences, University of Szeged, H-6720 Szeged, Rerrich Béla tér 1, Hungary*

³*Faculty of Medical and Life Sciences, University of Furtwangen, Villingen-Schwenningen, Jakob-Kienzle-Straße 17. 78054 VS-Schwenningen
e-mail: alapi@chem.u-szeged.hu*

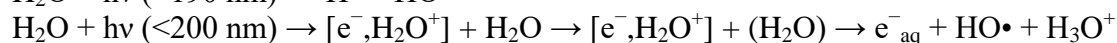
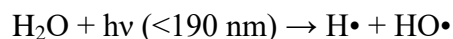
Abstract

Vacuum ultraviolet (VUV) photolysis is one of the Advanced Oxidation Processes (AOPs) for the elimination of trace pollutants from water and air. The ultraviolet (UV) radiation below 200 nm is named VUV, because it is strongly absorbed by air. Using VUV photolysis reactive species ($\bullet\text{H}$ and $\bullet\text{OH}$) can be generated directly from water without addition of any chemicals. Consequently VUV radiation is used for producing ultrapure water and often investigated as a possible method for elimination of organic pollutants from water. In the case of VUV photolysis low pressure mercury vapor lamp (emits both 254 nm UV and 185 nm VUV photons) or Xe excimer lamp (emits both 172 nm VUV photons) can be applied as light source. In latter case the absorption coefficient of water at 172 nm is 550 cm^{-1} . Consequently, the penetration depth of VUV radiation is very small, only 0.04 mm. In this work we have investigated the effect of inhomogeneity caused within this very thin VUV irradiated layer on the concentration of the primary formed reactive species, such as $\bullet\text{H}$ and $\bullet\text{OH}$, using model calculation.

Introduction

Advanced Oxidation Processes (AOPs) are based on hydroxyl radical ($\bullet\text{OH}$) initiated transformations. One of the possibilities of the $\bullet\text{OH}$ generation is the irradiation of water with light having shorter wavelength than 190 nm. Generally low-pressure mercury vapor lamp is used as light source when VUV photolysis is applied to reduce the TOC content of purified water and produce ultrapure, high quality water. Another possible light source is the Xe excimer lamp which emits quasi-monochromatic light with maximum at 172 nm. There are several benefits of this excimer lamp, such as high average specific power radiation, high energy of emitting photons, quasi-monochromatic radiation, high spectral power density, absence of visible and IR radiation, low heating of radiating surface (cold lamps), no fixed geometry, no warm up time etc. The availability of multiple-wavelength UV radiation by simultaneous excitation of several kinds of working excimer molecules is also possible. Finally, excimer lamps based on noble gases are non-hazardous and are much more environmentally friendly than mercury vapor lamps. [1-4]

In VUV irradiated aqueous systems the first step is the excitation of water molecules. Absorption of the VUV radiation results in the homolysis or photochemical ionization of water molecules. The value of quantum yield of ionization (0.05) is much smaller than the quantum yield of homolysis (0.42):



Despite the many advantages of this technology and the promising results obtained through lab scale studies, there are still some factors that stymie the wide scale application of the VUV reactors for water treatment. Lack of proper model and simulation tool for predicting and analyzing the performance of VUV irradiated systems is among the key factors hindering their practical implementation. Model calculations generally do not take care about the effect of inhomogeneity caused by the extremely short penetration depth of 172 nm VUV light.

Results and discussion

The first step of the present work was the collection of the kinetic data reported and used in the published papers related to the 172 nm irradiated solutions. The origin of these data were also checked and compared. The rate constants of the recombination of $\bullet\text{H}$ (resulting in H_2) and $\bullet\text{OH}$ (resulting in H_2O_2) were originated from experimental data obtained of gamma irradiated system. Opposite 172 nm irradiated water, the intensity of gamma photons decreases only with 10% in a few cm thin water layer. Thus gamma irradiated solution can be defined as a „homogen system“, while the 172 nm irradiated one is an „inhomogen system“.

1. Table. Rate constants of the recombination reactions of $\bullet\text{H}$ and $\bullet\text{OH}$ radicals

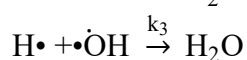
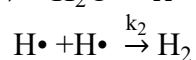
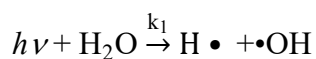
Ref.	$k_{\text{H}+\text{OH}}$ ($\text{M}^{-1}\text{s}^{-1}$)	$k_{\text{H}+\text{H}}$ ($\text{M}^{-1}\text{s}^{-1}$)	$k_{\text{OH}+\text{OH}}$ ($\text{M}^{-1}\text{s}^{-1}$)	reaction partner	method for radical generation
[10]	$1,00 \cdot 10^{10}$			$\text{Fe(II)/Ce(III)}, \text{H}_2\text{O}_2, \text{H}_2\text{SO}_4$	
[11]		$5,00 \cdot 10^9$		$\text{H}_2\text{O}_2, \text{Fe(II)}, \text{kénsav}$	Van Slyke
[12]			$8,20 \cdot 10^9$		
[4]	$1,2 \cdot 10^{10} *$	$6,00 \cdot 10^9$	$6,00 \cdot 10^9 *$	$\text{H}_2\text{O}_2, \text{H}_2\text{O}, \text{H}_2\text{SO}_4, \text{Fe(III)}$	Van De Graaff
[13]		$1,50 \cdot 10^{10} *$		Fe(II)	Van De Graaff
[5]	$7,00 \cdot 10^9 **$		$5,25 \cdot 10^9 **$		
[14]			$6,30 \cdot 10^9$	Ferro-cyanide	Osram Xe- excimer lamp
[15]		$1,25 \cdot 10^{10}$			Osram Xe- excimer lamp
[9]	$1,04 \cdot 10^9 **$	$7,75 \cdot 10^9 **$	$8,70 \cdot 10^9 **$		

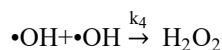
* experimental data (relative method)

** experimental data (absolute method)

The basic of the model calculation using Octave [17] program were the followings:

1. Generally about 40 various reactions take place in a VUV irradiated water. In this work we used a simplified reaction system containing only the following four main steps:





- The reaction rate constants were the average of the rate constants reported in **Table 1** ($k(h\nu) = 9 \times 10^{13} \text{ M}^{-1}\text{s}^{-1}$, $k(\bullet\text{H} + \bullet\text{H}) = 1 \times 10^{10} \text{ M}^{-1}\text{s}^{-1}$, $k(\bullet\text{H} + \bullet\text{OH}) = 1.5 \times 10^{10} \text{ M}^{-1}\text{s}^{-1}$, $k(\bullet\text{OH} + \bullet\text{OH}) = 6 \times 10^9 \text{ M}^{-1}\text{s}^{-1}$).
- The actual concentration of photon was calculated via Lambert-Beer law, using the value of the absorption coefficient of water at 172 nm 550 cm^{-1} [16].
- The diffusion constants of various species ($D(\bullet\text{H}) = 8 \cdot 10^{-5} \text{ cm}^2\text{s}^{-1}$, $D(\bullet\text{OH}) = 2 \cdot 10^{-5} \text{ m}^2\text{s}^{-1}$, $D(\text{H}_2) = 8 \cdot 10^{-5} \text{ m}^2\text{s}^{-1}$, $D(\text{H}_2\text{O}_2) = 1.5 \cdot 10^{-5} \text{ m}^2\text{s}^{-1}$) were also incorporated of the model.
- The total thin of the treated water layer was 0.2 cm, which was divided into 950 cells. In each cells, the intensity of the VUV light and concentration of primary radicals were supposed to be constant and homogenous. Near the lamp, the cells size were very small (40 nm). Farther from the wall of the light source cells size were bigger and the the biggest one were 200 nm.

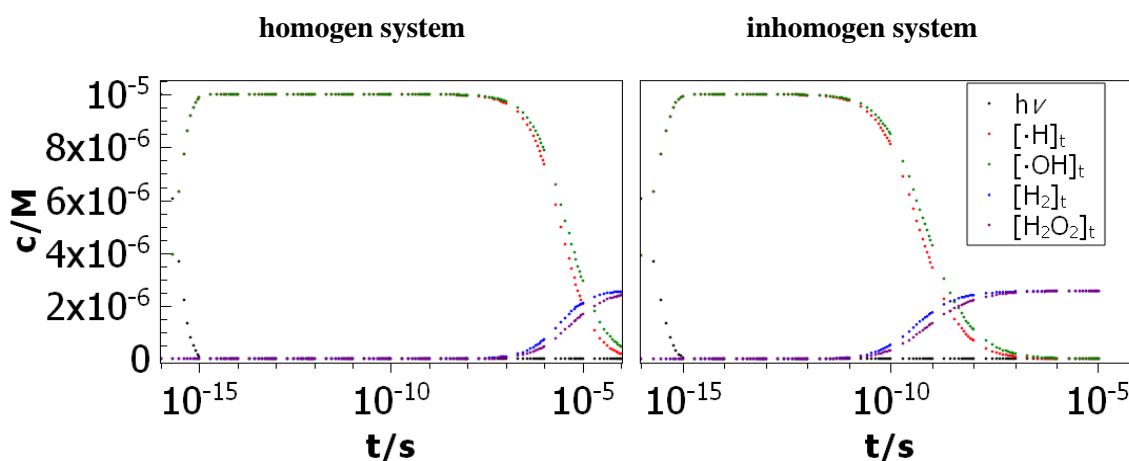
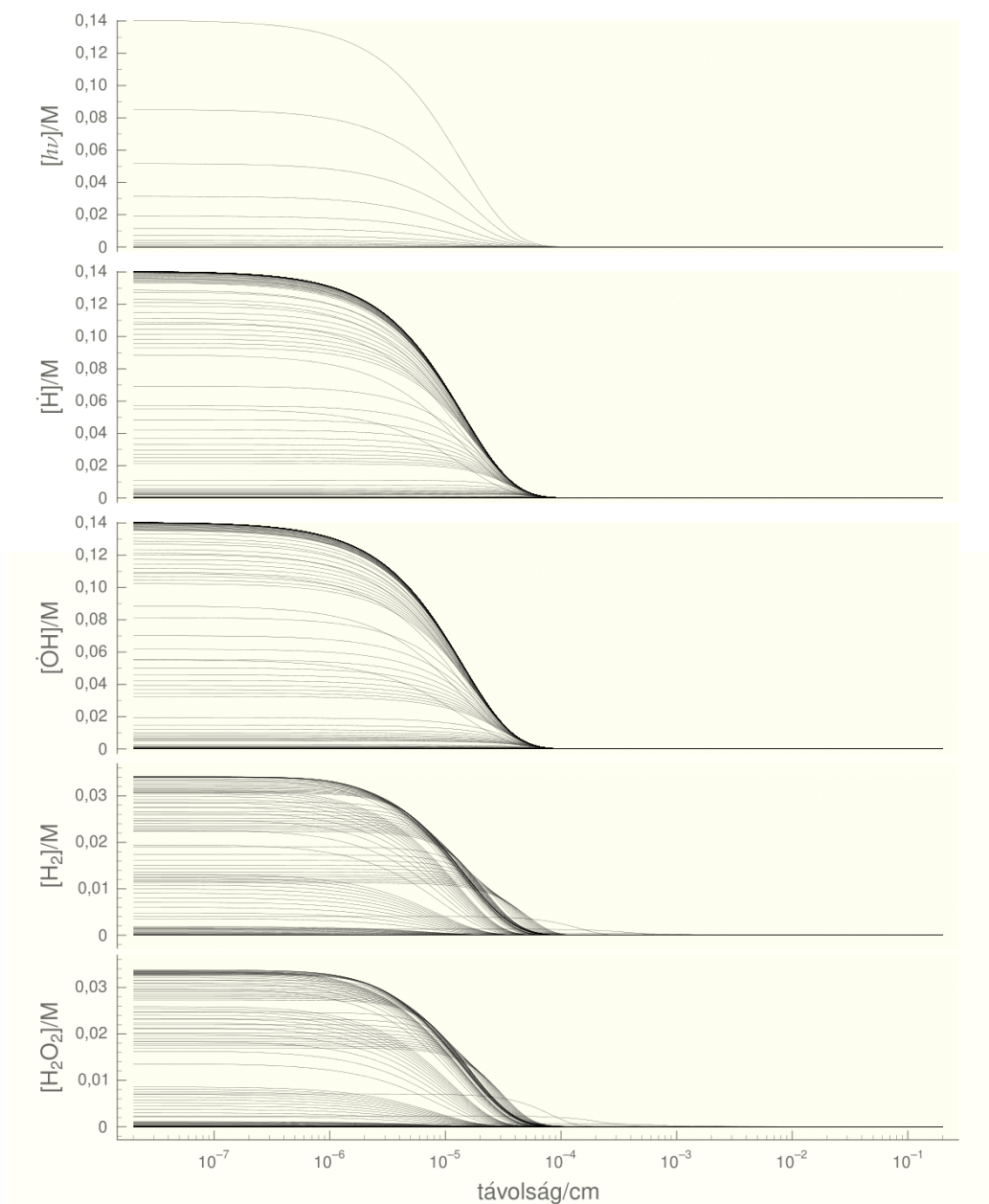


Figure 1. The time dependence of the various radicals and their recombination products in homogen and inhomogen system. Data used for modeling: $k(h\nu) = 9 \cdot 10^{13} \text{ M}^{-1}\text{s}^{-1}$, $k(\dot{\text{H}} + \dot{\text{H}}) = 1 \cdot 10^{10} \text{ M}^{-1}\text{s}^{-1}$, $k(\dot{\text{H}} + \dot{\text{OH}}) = 1.5 \cdot 10^{10} \text{ M}^{-1}\text{s}^{-1}$, $k(\dot{\text{OH}} + \dot{\text{OH}}) = 6 \cdot 10^9 \text{ M}^{-1}\text{s}^{-1}$, $D(\dot{\text{H}}) = 8 \cdot 10^{-5} \text{ cm}^2\text{s}^{-1}$, $D(\dot{\text{OH}}) = 2 \cdot 10^{-5} \text{ m}^2\text{s}^{-1}$, $D(\text{H}_2) = 8 \cdot 10^{-5} \text{ m}^2\text{s}^{-1}$, $D(\text{H}_2\text{O}_2) = 1.5 \cdot 10^{-5} \text{ m}^2\text{s}^{-1}$, $c_0(h\nu) = 1 \cdot 10^{-5} \text{ M}$, $c_0(\text{H}_2\text{O}) = 55.5 \text{ M}$.

The results obtained in the case of homogen and inhomogen system are presented on Figure 1. The time dependence of the various radicals and their recombination products in the two system show, that inhomogeneity has significant effect on the time scale. In homogen system the recombination of primary formed radicals take place within 10^{-5} sec. In the case of simulation obtained this time is decreased with 4 orders because of the reactions take place only in a very small part of the total volume of the reaction system. Within this photoreaction zone the radical concentration is much higher than in the homogen system.



2. Figure Concentration of primary radicals and their recombination products versus the distance from the light source, taking into consideration the inhomogeneity.

Using the model taking into consideration the inhomogeneity of the VUV irradiated aqueous solution, the concentration of the primary radicals and their recombination products were calculated (Figure 2.). Radicals disappear from the system within the distance, which can be reached by photons. The concentration of recombination products (H_2 and H_2O_2) decrease and increase with the time and finally reach a constant value. The effect of diffusion can be observed on the curves related to H_2 and H_2O_2 concentration versus the distance from the wall of the lamp and their concentration is much lower than the radical concentration.

Conclusion

- Inhomogeneity must be incorporated into the model calculation in the case of 172 nm irradiated aqueous solutions

Acknowledgements

T. Alapi and T. Oppenländer acknowledge German Academic Exchange Service (DAAD) and Tempus Foundation for financial support (project number: 151955).

References

- [1] T. Oppenländer: Vacuum-UV Oxidation, The H₂O-VUV AOP, in book Photochemical Purification of water and air, Wiley-VCH, 2003
- [2] Gonzalez M. C., Oliveros E., Worner M. and Braun A. *J Photochem and Photobiol C*: **5** (3), 225–246. (2004)
- [3] T. Alapi, K. Schrantz, E. Arany, Zs. Kozmér: Vacuum-UV radiation driven processes (Chapter 5), Advanced Oxidation Processes for Water treatment: Fundamentals and applications Ed.: Mihaela I. Stefan, IWA, 2017.
- [4] J.K. Thomas, The Journal of Physical Chemistry, 1963. 67(12) 2593-2595.
- [5] J.K. Thomas, Transactions of the Faraday Society, 1965. 6 702.
- [9] P. Pagsberg, P. The Journal of Physical Chemistry, 1969. 73(4) 1029-1038.
- [10] J. Rotblat and H.C. Sutton Proc. of the Royal Soc A: Math. Phys. and Eng. Sci., 1960. 255(1283) 490-508.
- [11] J.K. Thomas and E.J. Hart Radiation Research, 1962. 17(3): p. 408.
- [12] H.A. Schwarz The J. of Physical Chemistry, 1962. 66(2) 255-262.
- [13] H.A.Schwarz, H.A., The J. of Physical Chemistry, 1963. 67(12): p. 2827-2830.
- [14] J. Rabani and M.S. Matheson The J. of Physical Chemistry, 1966. 70(3) 761-769.
- [15] P.Y. Feng The J. of Physical Chemistry, 1970. 74(6) 1221-1227.
- [16] J.L. Weeks, G.M.A.C. Meaburn, S. Gordon Radiation Research, 1963. 19(3): p. 559.
- [17] J.W. Eaton, D. Bateman, S. Hauberg, R. Wehbring (2016). GNU Octave version 4.2.0 manual: a high-level interactive language for numerical computations. URL <http://www.gnu.org/software/octave/doc/interpreter/>

ANTIOXIDANT ACTIVITY AND PHENOLICS IN TOMATO LEAVES EXTRACTS INFECTED WITH LATE BLIGHT

Marijana Peić Tukuljac¹, Dejan Prvulović¹, Slađana Medić-Pap², Dario Danojević²

¹University of Novi Sad, Faculty of Agriculture, Trg D.Obradovića 8, 21000 Novi Sad, Serbia

²Institute of Field and Vegetable Crops Novi Sad, M. Gorkog 30, 21000 Novi Sad, Serbia
e-mail:marijanapeictukuljac@yahoo.com

Abstract

Tomato is one of widely cultivated vegetable food crops in the world, because of its significant importance in human nutrition. Late blight is a serious tomato disease caused by *Phytophthora infestans*, which could lead to complete crop loss. The aim of this paper was to analyse the content of bioactive compounds in leaves of tomato genotype Bizon and their connection with late blight infection rate. It was found that at the beginning of late blight infection plant generated a high amount of polyphenols and flavonoids, but their concentration and antioxidant activity were reduced with the increasing rate of infection. Statistically significant differences ($p < 0.01$) were observed between infection rate and sampling date as well as in their interaction on the measured biochemical parameters.

Introduction

Plants are constantly exposed to many abiotic and biotic stress conditions such as high temperature, drought as well as the attack of the pathogens. In these stressful conditions, the production of reactive oxygen species (ROS) is increased and induces cellular damage. Despite their ability to cause harmful oxidation, in low concentration ROS are important signalling molecules. Different enzymatic and non-enzymatic defence mechanisms, are involved in ROS scavenging and prevention of oxidative stress [1,2]. Phenolic compounds are the most important non-enzymatic antioxidants. Flavonoids are a large group of natural phenolic compounds which are capable of chelating free radicals by donating a hydrogen atom or by single-electron transfer [3].

Tomato is one of the most important vegetable cultivated throughout the world that is consumed fresh as well as processed. It has a big influence in nutrition because provide a sufficient amount of dietary antioxidants and vitamin, especially vitamin A and C [4]. *Phytophthora infestans* is an oomycete which cause one of the most serious disease of tomato known as late blight (LB). This destructive disease is responsible for significant economical losses of tomato crops [5].

The goal of this paper was to investigate the effect of the late blight intensity in tomato leaves on antioxidant capacity, by measuring the content of total phenols and flavonoids, and by using six different antioxidant assays.

Experimental

The material for this study was lower leaves of tomato genotype Bizon that was cultivated in the experimental field of the Institute of Field and Vegetable Crops, Novi Sad, Serbia, during 2014. Sowing for seedlings production in a glass house was done on 3rd of April and the plants were transplanted on 27th of May into the open field. Space between rows was 140 cm, while space between plants in the row was 50 cm. There was no fungicide application. The first sampling date was on 4th of August and the second was on 18th of August. Ten fully expanded lower leaves were taken from different plants and evaluation of infection rate was done according to the EPPO modified scale: 0-without infection, 1-less than 5% of leaf affected, 2- spots covering 5-10%, 3-spots covering 10-25%, 4- spots covering 25-50%, 5-spots covering more than 50% of the leaf.[6]

For biochemical analyses, plant material (200 mg) was milled to a fine powder and samples were prepared by extraction in 70% aqueous acetone solution (50 ml) during 24 h then centrifuged at 5000 rpm for 15 min. The supernatant was separated and kept in cold storage. The total polyphenolic content (TP) was determined according to the Folin-Ciocalteu procedure [7]. Determination of total flavonoid content (TF) was carried out using a method based on the flavonoid characteristics to build metal-complexes with aluminium chloride (AlCl_3) [8]. The calibration curve was constructed with Quercetin and the results of TP and TF were expressed as catechin equivalents in mg per g of dry weight (mg QE/g DW). The total antioxidant activity (TAA) of extracts was determined according to the phosphomolybdenum method described by Kalaskar and Surana [9]. Using the method reported by Saha et al. [8] was assayed the total reduction capacity (TRC). Determination of DPPH radicals scavenging activity was measured as described by Lai and Lim [10]. Ferric reducing antioxidant power (FRAP) of extracts was estimated with the method developed by Valentão et al. [11]. The ABTS radical scavenging assay was performed according to the method by Miller et al. [12]. The calibration curve was constructed with a standard Trolox solution and the results of TAA, TRC, DPPH, FRAP and ABTS were expressed as Trolox equivalents in mg per g of dry weight (mg Trolox/g DW). The nitroblue tetrazolium (NBT) assay was used to determine the superoxide free radical scavenging activity [9] and the results were expressed as a percentage of inhibition of superoxide anion. All experimental measurements were performed in triplicate and the results of the total polyphenols, flavonoids and antioxidant activity assayed with the total antioxidant activity, total reduction capacity, FRAP, DPPH, ABTS and NBT test were expressed as the mean \pm standard deviation (Table 1).

The data obtained were processed by applying the analysis of variance (Factorial ANOVA) using software STATISTICA ver. 13.2 (StatSoft, Inc., USA) and significant differences between the groups were determined using the Bonferroni test ($p < 0.01$). The correlation coefficients were calculated according to Spearman.

Results and discussion

The content of polyphenols, flavonoids and antioxidant activity of tomato leaves extracts are presented in Table 1. Except for the FRAP test, two-way ANOVA suggested that the rate of infection, sampling date and interaction between these two factors have statistically significant ($p < 0.01$) influence on all measured biochemical parameters.

In both sampling dates, the content of total phenols and flavonoids of analysed extracts was reduced with increasing of infection rate. *Post-hoc* Bonferroni test ($p < 0.01$) for all assays showed the most pronounced difference between non-infected plants and plants attacked by late blight in the cases when LB's infected area covering 25% and more than 50% of the leaf. At the beginning of infection, the amount of polyphenols and flavonoids is increased, since these secondary metabolites have a role in the plant response to abiotic and biotic stress [3].

Table 1. Polyphenolic compounds and antioxidant activity of tomato leaves extracts

Parametar	Infection rate	TP ¹	TF ¹	TAA ²	TRC ²	DPPH ²	ABTS ²	FRAP ²	NBT ³
Sampling date 1	0	21.91 ^{ai} ± 0.145	21.37 ^{abcdf} ± 0.298	57.93 ^{abd} ± 2.867	6.96 ^a ± 0.116	2.04 ^a ± 0,150	5.44 ^a ± 0,197	3.45 ± 0.062	54.98 ^{ad} ± 0.554
		23.36 ^a ± 0.417	22,73 ^{abcd} ± 0,428	60.94 ^{ad} ± 0.720	8.27 ^{cd} ± 0,072	3.09 ^c ± 0,196	6.32 ^c ± 0,181	4.95 ± 0.046	52.99 ^a ± 0.575
	2	13.18 ^{bc} ± 0.431	5.85 ^{bdfg} ± 0,150	51.84 ^{de} ± 0.735	7.94 ^{ac} ± 0.128	1.59 ^{ad} ± 0.225	4.92 ^{ad} ± 0.135	2.57 ± 0.050	33.85 ^{ce} ± 1.354
		12.07 ^{cb} ± 0.176	5.77 ^{fg} ± 0.348	48.57 ^{de} ± 0.960	7.44 ^{ac} ± 0.104	1.57 ^{ad} ± 0.149	4.20 ^d ± 0,379	2.54 ± 0.043	30.25 ^e ± 1.730
	4	4.57 ^d ± 0.053	0.89 ^g ± 0.030	26.97 ^c ± 1.732	3.58 ^f ± 0.492	0.75 ^d ± 0.202	2.30 ^b ± 0.478	0.81 ± 0.036	10.98 ^f ± 0.695
		59.40 ^e ± 1.357	30.44 ^{ac} ± 17.279	55.53 ^{abd} ± 0.910	11.67 ^{be} ± 0.487	5.23 ^b ± 0.227	1.75 ^b ± 0.041	8.57 ± 0.082	62.7 ^b ± 0.242
	1	67.55 ^f ± 0.421	32.04 ^{cd} ± 0.180	59.19 ^{ad} ± 1.600	10.36 ^{be} ± 0.275	5.02 ^b ± 0.362	2.07 ^b ± 0.090	6.59 ± 0.289	60.52 ^b ± 0.714
		53.35 ^g ± 2.108	23.69 ^{ad} ± 1.052	54.79 ^{ac} ± 1.342	9.89 ^e ± 0.355	3.65 ^c ± 0.223	1.46 ^{be} ± 0.069	5.70 ± 0.228	56.71 ^d ± 0.479
	3	48.72 ^h ± 0.926	13.79 ^{ae fg} ± 2.057	52.09 ^{be} ± 4.362	10.43 ^{be} ± 0.666	3.63 ^c ± 0.427	1.41 ^{be} ± 0.021	5.26 ± 0.177	52.36 ^e ± 0.905
		19.57 ⁱ ± 0.728	1.95 ^{fg} ± 0.172	25.89 ^c ± 1.145	9.50 ^{de} ± 0.160	0.774 ^d ± 0.035	0.78 ^e ± 0.060	1.31 ± 0.129	8.49 ^f ± 1.566

Value is a mean of three replicates ± standard deviation (SD)

¹Expressed as mg Quercetin/g DW ²Expressed as mg Trolox/g DW ³Expressed as % inhibitionValue without the same superscript within each row differ significantly at $p < 0.01$ (Bonferroni post-hoc test)

0-without infection, 1- infected area covering less than 5% of leaf, 2- infected area covering 5-10% of leaf, 3- infected area covering 10-25% of leaf, 4- infected area covering 25-50% of leaf, 5- infected area covering more than 50% of leaf.

This fact suggested that polyphenols and flavonoids are involved in the first response of plants to late blight attack. The results of this study are in agreement with report of other authors [12]. Taking into consideration that FRAP and ABTS tests are specific for flavonoids, and that FRAP did not show the statistically significant difference between infected plants, it is suggested that some other polyphenolic compounds, like terpenoids and flavonones, may be involved in antioxidant protection mechanisms in tomato.[13] According to other authors, the amount of polyphenols increases during the early phases of infection because the plant is generating some precursors of lignin, which also belongs to this large group of molecules. Lignin is known as a physical barrier against initial pathogen colonization [5,14,15,16]. Spearman coefficient for all measured biochemical parameters showed strong negative correlation with LB infection rate, but the only correlation with TRC was not significant (Table 2). Except for the correlation between ABTS and TP as well as TF, all used tests were in strong positive and significant correlation.

Table 2. The Correlation between biochemical parameters and leaf infection intensity

	TP ¹	TF ¹	TAA ²	TRC ²	DPPH ²	ABTS ²	FRAP ²	NBT ³
Infection rate	-0.61**	-0.76**	-0.85**	-0.27	-0.68**	-0.46**	-0.71**	-0.85**
TP ¹		0.86**	0.65**	0.84**	0.93**	-0.27	0.95**	0.86**
TF ¹			0.82**	0.58**	0.89**	0.09	0.90**	0.89**

¹Expressed as mg Quercetin/g DW, ²Expressed as mg Trolox/g DW, ³Expressed as % inhibition

**Statistically significant at $p < 0.01$ (Spearman correlation)

Conclusion

The results of this study suggested that infected tomato plant in early phase of infection with *Phytophthora infestans*, generated a higher amount of polyphenols and flavonoids. These natural antioxidant substances are involved in earlier defence mechanism against the pathogen. The results of ABTS and FRAP indicate that some other polyphenolics compounds, apart from flavonoids, are involved in mechanisms of antioxidant protection of tomato.

Acknowledgements

This research was a part of project TR 31030 "Developing vegetable varieties and hybrids for outdoor and indoor production" supported by the Ministry of Education, Science and Technological Development of Republic of Serbia.

References

- [1] B. Poljsak, D. Šuput, I. Milisav. Achieving the Balance between ROS and Antioxidants: When to Use the Synthetic Antioxidants. *Oxidative Medicine and Cellular Longevity*, 2013, 2013:11
- [2] A. Krishnamurthy, B. Rathinasabapathi, Oxidative stress tolerance in plants: Novel interplay between auxin and reactive oxygen species signaling. *Plant Signaling & Behavior*, 2013;8(10):e25761
- [3] D. Procházková, I. Bousová, N. Wilhelmová, Antioxidant and prooxidant properties of flavonoids, *Fitoterapia*, 2011;82(4):513-23.
- [4] P. Adhikari, Y. Oh, D.R. Panthee, Current Status of Early Blight Resistance in Tomato: An Update. *International Journal of Molecular Sciences*, 2017; 18(10):2019

- [5] M. Nowicki, M.R. Foolad, M Nowakowska, E.U. Kozik, Potato and Tomato Late Blight Caused by *Phytophthora infestans* : An Overview of Pathology and Resistance Breeding, *Plant Disease*, 2012, 96: 4-17.
- [6] EPPO/OEPP Standards 2013. Efficacy evaluation of fungicides PP 1/65 (3), Downy mildew of lettuce and other vegetables, 83-87
- [7] V Nagavani, Raghava Rao T, Evaluation of antioxidant potential and identification of polyphenols by RP-HPLC in *Micheliachampaca* flowers, *Advances in Biological Research*, 2010, 4 (3): 159-168
- [8] A. Saha., R. Rahman., M. Shahriar., S. Saha., N. Al Azad., S. Das, Screening of six Ayurvedic medicinal plant extracts for antioxidant and cytotoxic activity, *Journal of Pharmacognosy and Phytochemistry*, 2013, 2 (2): 181-188
- [9] M. Kalaskar, S. Surana, Free radical scavenging, immunomodulatory activity and chemical composition of *Luffa acutangula* var. *amara* (Cucurbitaceae) pericarp, *Journal of the Chilean Chemical Society*, 2014, 59(1): 2299-2302
- [10] H.Y. Lai, Y.Y. Lim, Evaluation of antioxidant activities of the methanolic extracts of selected ferns in Malaysia, *International Journal of Environmental Science and Development*, 2011, 2(6): 442-447
- [11] P. Valentão, E. Fernandes, F. Carvalho, P.B. Andrade, R.M. Seabra, M.L. Bastos, Antioxidative properties of cardoon (*Cynara cardunculis* L.) infusion against superoxide radical, hydroxyl radical, and hypochlorous acid, *Journal of Agricultural and Food Chemistry*, 2002, 50 (17), 4989-4993
- [12] D. Prvulović, S. Medić-Pap, D. Danojević, S. Tančić-Živanov, D. Latković: *Polyphenolic content and antioxidant capacity of tomato leaves extracts infected with late blight*, XXIII savetovanje o biotehnologiji sa međunarodnim učešćem, Book of abstracts, 2018, 333-338
- [13] M. Henriquez , L. Adam, F. Daayf, Alteration of secondary metabolites' profiles in potato leaves in response to weakly and highly aggressive isolates of *Phytophthora infestans*, *Plant Physiology and Biochemistry*, 2012, 57: 8-14
- [14] N. Miller, C. Rice-Evans, M. Davies, V. Gopinathan, A. Milner, A novel method for measuring antioxidant capacity and its application to monitoring the antioxidant status in premature neonates, *Clinical Science*, 1993, 84 (4): 407-412
- [15] K. Kulbat, The role of phenolic compounds in plant resistance, *Biotechnology and Food Sciences*, 2016, 80(2): 97-108
- [16] E. Miedes, R. Vanholme, W. Boerjan, A. Molina, The role of secondary cell wall in plant resistance to pathogens, *Frontiers in Plant Science*, 2014, 5: 358

SYNTHESIS AND CHARACTERIZATION OF 3D MESOPOROUS TRANSIENT METAL OXIDE FOR HIGH-PERFORMANCE CATALYSTS

Anett Gyuris, András Sági

Department of Applied and Environmental Chemistry, University of Szeged, 6723 Szeged
Rerrich Béla tér 1., Hungary,
e-mail: sapia@chem.u-szeged.hu, anett1224@hotmail.com

Keywords: Catalysts supports, Transient metal oxides, Hard template – Replica Method, Heterogeneous Catalysis

Different 3D mesoporous oxide materials (SiO_2 – KIT-6, MCF-17, SBA-15, Co_3O_4 , MnO_2 , Fe_2O_3 , NiO , CeO_2) prepared by the soft and hard template (replica) method due to the fact that the usage of the 3D mesoporous oxide supports with high specific surface area has great influence on the catalytic activity and selectivity (e.g. Co_3O_4 supported catalyst is 10 times more active compared to the SiO_2 supported Pt.).

The synthesis of KIT-6 is as follows: P123 (Pluronic-123) was homogenized in deionized water and cc. HCl and then butyl alcohol was added. This mixture was stirred for 1 hour at 35 °C. After 1 hour we were poured 58g TEOS (Tetraethyl orthosilicate) and stirred for 24 hours. After the material was dried we were filtered. The next day was calcined at 550 °C for 6 hours.

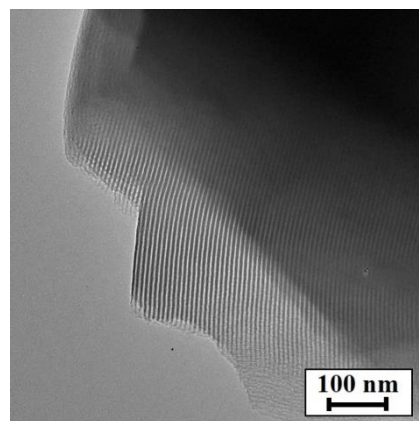


Fig. 1. TEM images of KIT-6

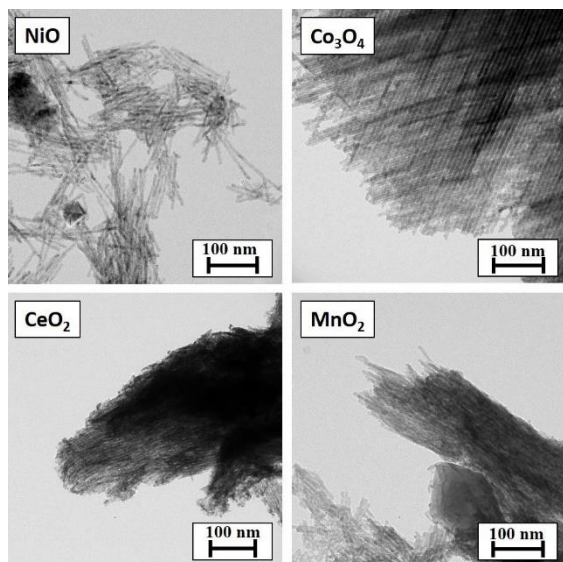


Fig. 2. TEM images of NiO (A), Co_3O_4 (B), CeO_2 (C), MnO_2 (D)

Furthermore Co_3O_4 , MnO_2 , Fe_2O_3 , NiO , CeO_2 mesoporous oxide carriers were prepared. For the synthesis metal-nitrate was dissolved in deionized water. The prepared mesoporous KIT-6 silica were dissolved in toluene and all of it was stirred at 65 °C. The material was dried at 60 °C overnight then it was calcined at 300 °C for 6 hours. After the silica template was removed with NaOH solution and we were washed several times with deionized water and dried.

The synthesis of these mesoporous oxide carriers were successful and had large surface area. This fact was supported by TEM, BET and XRD monitoring prove.